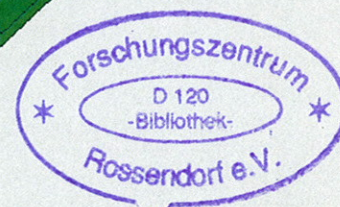
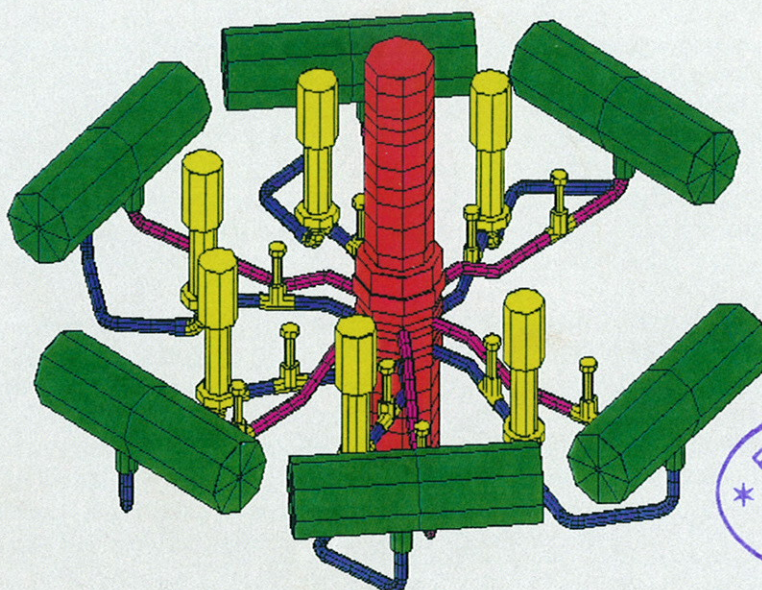


FZR-196

Oktober 1997

*E. Altstadt, F.-P. Weiß, M. Werner, V. Bulavin, V. Pavelko,
D. Gutsev, G. Anikin, A. Usanov, V. Dodonov*

**Entwicklung von theoretischen
Schwingungsmodellen für WWER-
Reaktoren auf der Grundlage der Finite-
Elemente-Methode und Justierung dieser
Modelle mit Schwingungsmessungen von
Originalanlagen**



Abschlußbericht zum BMBF-Forschungsvorhaben
Förderkennzeichen 1500999

Das diesem Bericht zugrunde liegende Vorhaben wurde mit Mitteln des Bundesministers für Bildung, Wissenschaft, Forschung und Technologie (BMBF) unter dem Förderkennzeichen 1500999 gefördert. Die Verantwortung für den Inhalt dieser Veröffentlichung liegt bei den Autoren.

Herausgeber:

FORSCHUNGSZENTRUM ROSSENDORF

Postfach 51 01 19

D-01314 Dresden

Telefon (03 51) 26 00

Telefax (03 51) 2 69 04 61

Als Manuskript gedruckt
Alle Rechte beim Herausgeber

Berichtsblatt

1. ISBN	2. Berichtsart Abschlußbericht	3.
4. Titel des Berichtes Entwicklung von theoretischen Schwingungsmodellen für WWER-Reaktoren auf der Grundlage der Finiten-Elemente-Methode und Justierung dieser Modelle mit Schwingungsmessungen von Originalanlagen		
5. Autor(en) (Name, Vorname(n)) Altstadt, Eberhard; Weiß, Frank-Peter; Werner, Matthias; Bulavin, Valeriy, V.; Pavelko, Vladimir, I.; Gutsev, Dimitriy, F.; Anikin, Gennadiy G.; Usanov, Alexendr I.; Dodonov, Valeriy, A.		6. Abschlußdatum des Vorhabens Oktober 1996
		7. Veröffentlichungsdatum Juli 1997
8. Durchführende Institution (Name, Adresse) Forschungszentrum Rossendorf e. V. Institut für Sicherheitsforschung Postfach 51 01 19 01314 Dresden		9. Ber.Nr. Durchführende Institution
		10. Förderkennzeichen 1500999
		11. Seitenzahl
		12. Literaturangaben
13. Fördernde Institution (Name, Adresse) Bundesministerium für Bildung, Wissenschaft, Forschung und Technologie (BMBF) 53175 Bonn		14. Tabellen
		15. Abbildungen
16. Zusätzliche Angaben		
17. Vorgelegt bei (Titel, Ort, Datum)		
18. Kurzfassung <p>Das Vorhaben zielte auf die Unterstützung von 6 russischen Wissenschaftlern aus drei unterschiedlichen Institutionen ab. Ihre Arbeiten zur Anlagendiagnostik / Schadensfrüherkennung dienen der Erhöhung der Sicherheit von WWER-Reaktoren.</p> <p>Das Vorhaben leistet einen Beitrag zur verbesserten Beurteilung der mechanischen Integrität von Reaktoren der russischen WWER-440 und WWER-1000 Baureihe, insbesondere zur empfindlichen Früherkennung und Lokalisation mechanischer Schädigungen an Reaktorkomponenten mit Hilfe schwingungsdiagnostischer Methoden. Zu diesem Zweck wurde das Finite-Element-Modell zur Simulation des mechanischen Schwingungsverhaltens aller Primärkreis-komponenten eines WWER-1000 erstellt. Dafür wurde das Programmpaket ANSYS® genutzt. Das Vorhaben knüpfte an das vom BMFT geförderte Vorhaben (Förderkennzeichen: 1500916) zur FE-Modellierung des Reaktortyps WWER-440 an.</p> <p>Das Berechnungsmodell zum WWER-440 wurde mit neueren Ergebnissen experimenteller Schwingungsuntersuchungen weiter justiert. Die Justierung des FE-Modells für den WWER-1000 ist durch Übergabe von Ergebnissen dedizierter Schwingungsmessungen vorbereitet wurden.</p> <p>Das Modell kann in der Hauptsache genutzt werden, um zu klären, wie sich unterstellte mechanische Defekte von Reaktoreinbauten auf die Schwingungen der Gesamtanlage auswirken. Diese Schadenssimulation ist besonders geeignet, empfindliche Meßpositionen für die on-line Überwachung zu finden und physikalisch fundierte Grenzwerte zu definieren.</p>		
19. Schlagwörter Druckwasserreaktor, Schwingung, Modalanalyse, Finite-Elemente-Methode, Schadenssimulation		
20. Veriag Forschungszentrum Rossendorf e. V. Postfach 51 01 19, 01314 Dresden		21. Preis

Document Control Sheet

1. ISBN	2. Type of Report Final Report	3.
4. Report Title Development of theoretical vibration models for VVER type reactors based on the finite element method and adjustment of these models by vibration measurements at original nuclear power plants		
5. Author(s) (Family Name, First Name) Altstadt, Eberhard; Weiß, Frank-Peter; Werner, Matthias; Bulavin, Valeriy, V.; Pavelko, Vladimir, I.; Gutsev, Dimitriy, F.; Anikin, Gennadiy G.; Usanov, Alexendr I.; Dodonov, Valeriy, A.		6. End of Project October 1996
8. Performing Organization(s) (Name, Address) Research Center Rossendorf, Inc. Institute for Safety Research PF 510119, D-01314 Dresden/Germany		7. Publication Date July 1997
		9. Originator's Report No.
		10. Reference No. 1500999
		11. No. Of Pages
13. Sponsoring Agency (Name, Address) Bundesministerium für Bildung, Wissenschaft, Forschung und Technologie (BMBF) 53175 Bonn		12. No. Of References
		14. No. Of Tables
		15. No. of Figures
16. Supplementary Notes		
17. Presented at (Title, Place, Date)		
18. Abstract <p>The project aims to support 6 Russian scientists from three different institutions. Their work on plant diagnostics /early failure detection significantly supports the increase of the safety of VVER reactors.</p> <p>The project contributes to the improved evaluation of the mechanical integrity of the soviet-type VVER-440 and VVER-1000 reactors especially, to a sensitive early failure detection and to the localization of mechanical damages of reactor components by means of vibration monitoring. For that purpose the finite element model for the simulation of mechanical vibration of all primary circuit components of a VVER-1000 was established. The modeling is based on the finite element code ANSYS® and builds up on the former project (registr.-No. 1500916) which was also funded by BMFT.</p> <p>The calculation model for the VVER-440 modelling was further adjusted using results from new experimental vibration investigations. The adjustment of the VVER-1000 model was prepared analysing dedicated vibration measurements, which were made available in the framework of this project.</p> <p>The model can be applied to clarify how hypothetical damages of reactor internals influence the vibration signature of the primary circuit. Such kind of damage simulation is an appropriate means to find sensitive measuring positions for on-line monitoring and to define physically based threshold values.</p>		
19. Keywords Pressurized Water Reactor, Vibration, Modal Analysis, Finite-Elements-Method, Failure Simulation		
20. Publisher Research Center Rossendorf, Inc. Post Office Box 51 01 19, D-01314 Dresden		21. Price

Abschlußbericht

Förderkennzeichen : 1500999

Berichtszeitraum : 01.11.1994 - 31.10.1996

Vorhabentitel :

Entwicklung von theoretischen Schwingungsmodellen für WWER-Reaktoren auf der Grundlage der Finite-Elemente-Methode und Justierung dieser Modelle mit Schwingungsmessungen von Originalanlagen

Project Title :

Development of theoretical vibration models for VVER type reactors based on the finite element method and adjustment of these models by vibration measurements at original nuclear power plants

Kurztitel : Schwingungsmodellierung von WWER-Reaktoren

Gemeinsames Vorhaben von
Forschungszentrum Rossendorf (FZR), Deutschland
und

Kurtschatov Institut Moskau (KI), Rußland
Forschungsinstitut für den Betrieb von KKW Moskau (RRINPPO), Rußland
Experimentelles Konstruktionsbüro "Gidropress" Podolsk (OKB), Rußland

Autoren :

E. Altstadt, F.-P. Weiß, M. Werner (FZR)
V. Bulavin, V. Pavelko (KI)
D. Gutsev, G. Anikin (RRINPPO)
A. Usanov, V. Dodonov (OKB)

Inhalt :

	Seite
1. Übergeordnete Zielsetzung	3
2. Einzelzielsetzungen	5
3. Methode der finiten Elemente (FE)	7
3.1. Mathematische Grundlagen	7
3.2. Vorgehensweise bei der Modellierung mit finiten Elementen	7
4. Ablauf der Arbeiten	10
5. Ergebnisse	11
6. Literatur	12
Anhang	

1. Übergeordnete Zielsetzung

Dieses Vorhaben zielte auf die Unterstützung von sechs russischen Wissenschaftlern aus drei unterschiedlichen Institutionen ab. Ihre Arbeiten zur Anlagendiagnostik und Schadensfrüherkennung sind ein wichtiger Beitrag zur Erhöhung der Sicherheit von WWER-Reaktoren. Die Betriebserfahrung mit diesen Reaktoren zeigten, daß die Einbauten der Reaktordruckbehälter durch strömungsinduzierte mechanische Schwingungen beschädigt werden können. Speziell an WWER-Reaktoren wurden folgende Phänomene beobachtet, die bereits zu ernsthaften Komponentenschäden führten:

- Strömungsinduzierte anomale Kernbehälterbewegungen infolge plastischer Deformation der Federrohrsegmente. Dabei traten Relativverschiebungen zwischen dem Reaktordruckbehälter und dem Kernbehälter mit Amplituden von bis zu 4 mm auf. An den Führungskeilen des Kernbehälters wurde bis zu 18 mm Material abgetragen.
- Strömungsinduzierte Regelelementschwingungen, die zu mechanischen Anschlägen an die benachbarten Brennelemente geführt haben. Die Mäntel der Brennelemente wurden dabei teilweise zerstört.

Als Konsequenz wurden an vielen WWER-Anlagen on-line Monitore zur Schwingungsüberwachung installiert. Ein entscheidender Nachteil dieser Schwingungsüberwachungssysteme bestand zum damaligen Zeitpunkt im Fehlen eines theoretischen Schwingungsmodells, welches eine detaillierte physikalische Interpretation der

gemessenen Signale gestattet. Hinzu kam, daß keine ausreichenden incore Schwingungsmessungen für die Validierung des Modells zur Verfügung standen. Derartige Messungen sollten bevorzugt bei nichtnuklearem Betrieb während der Inbetriebnahmephase durchgeführt werden.

Solche incore Messungen geben zunächst unabhängig vom theoretischen Modell weitreichenden Aufschluß über das gekoppelte Bewegungsverhalten der Einbauten des Reaktordruckbehälters (RDB), was mittels rein externer Messungen über die RDB-Außenwand nicht möglich ist. Insofern stellen diese Messungen schon einen gewichtigen Beitrag zur Verbesserung der Schadensfrüherkennung dar. Jedoch erst durch die Benutzung eines theoretischen Schwingungsmodells ist man umfassend in der Lage,

- die normalen Schwingungen der Komponenten zu beschreiben, insbesondere die gemessenen Schwingungsfrequenzen im Neutronenrauschen, in Druckschwankungen sowie in mechanischen Verschiebungen bzw. Beschleunigungen den Eigenschwingungsformen des gesamten gekoppelten mechanischen Systems zuzuordnen;
- physikalisch fundierte Grenzwerte für Frequenzverschiebungen und Amplitudenänderungen als Alarmschwellen für die on-line Überwachung festzulegen;
- die mechanischen Belastungen, die mit dem Ausfall einer bestimmten Komponente verbunden sind, zu bewerten. Diese Möglichkeit ist wichtig für die Untersuchung von Szenarien der Schadensausbreitung nach dem Initialversagen einer Komponente.

Damit eine möglichst genaue Beschreibung des Schwingungsverhaltens erreicht wird, müssen Finite-Elemente-Modelle unter Verwendung von Resultaten experimenteller Schwingungsuntersuchungen justiert werden.

Im Rahmen eines vom BMFT geförderten Vorhabens (Förderkennzeichen: 1500916) entwickelte das Forschungszentrum Rossendorf ein theoretisches, auf finiten Elementen (FE) basierendes Modell für den Primärkreislauf des WWER-440. Dieses Modell und gegebenenfalls auch ein entsprechendes Modell für den WWER-1000 bedürfen allerdings der Justierung und der Verifikation mit Daten aus Schwingungsmessungen an den Originalanlagen in Osteuropa.

Die Durchführung und Auswertung von Schwingungsmessungen bei Inbetriebnahmen und bei normalen Betrieb der Anlagen durch die russischen Partner war Schwerpunkt des Vorhabens. Als Ergebnis des Vorhabens steht ein validiertes Modell für den WWER-440 zur Verfügung, wobei das Schwergewicht auf dem Reaktordruckbehälter und dessen Einbauten liegt. Es ist dabei ein generelles Ziel, die justierten und validierten Modelle zur Nutzung an die osteuropäischen Partner zu übergeben, um damit die wissenschaftliche Grundlage für eine empfindliche on-line Schwingungsüberwachung zur Verbesserung der Anlagensicherheit von WWER-Reaktoren bereitzustellen.

Das Vorhaben ist in die Kooperationen im Rahmen der wissenschaftlich-technischen Zusammenarbeit (WTZ) zwischen Deutschland und Rußland auf dem Gebiet der friedlichen Nutzung der Kernenergie eingebunden. Außerdem stellt das Vorhaben eine konsequente Fortführung des bereits erwähnten BMFT-Förderprojektes Nr. 1500916 "Analytische Modellierung mechanischer Schwingungen von Primärkreis Komponenten des Druckwasserreaktors WWER-440 mit finiten Elementen" dar, welches vom Forschungszentrum Rossendorf von 1992 bis 1995 bearbeitet wurde.

2. Einzelzielsetzungen

Die Einzelzielsetzung erfolgte entsprechend den Punkten A1 bis A5 des Arbeitsplanes der Vorhabensbeschreibung.

- 2.1. Vorbereitung der Modellierung des WWER-1000 mit finiten Elementen zur Berechnung des mechanischen Schwingungsverhaltens unter Einbeziehung der Fluid-Struktur-Wechselwirkung
 - Erarbeitung eines Strukturmodells für den Primärkreislauf des WWER-1000 unter Verwendung des FE-Codes ANSYS® basierend auf der Sichtung und Bewertung der Konstruktionsunterlagen.
 - Berechnung der anfänglichen Parameter für das FE-Modell auf der Grundlage der sich aus den Konstruktionsunterlagen ergebenden Massen, Trägheitsmomente und Steifigkeiten.
 - Generierung der Eingabefiles für den FE-Code für alle Hauptkomponenten des Primärkreislaufes (Reaktordruckbehälter, Kernbehälter, Hauptkühlmittelleitungen, Hauptumwälzpumpen, Dampferzeuger).

- 2.2. Durchführung von Betriebsmessungen an WWER-440- und WWER-1000-Reaktoren sowie Auswertung dieser Messungen
 - Erstellung von Meßprogrammen für WWER-440- und WWER-1000-Reaktoren.
 - Vorbereitung der Messungen und Instrumentierung an den ausgewählten Anlagen.
 - Realisierung von Betriebsmessungen an russischen und ukrainischen WWER-Reaktoren mit Hilfe von Neutronenrauschen, Druckschwankungen, Beschleunigungen sowie Verschiebungen in Abhängigkeit davon, welche Möglichkeiten von den jeweiligen Betreibern eingeräumt werden.

- 2.3. Durchführung experimenteller Schwingungsuntersuchungen an einem WWER-1000-Reaktor während der Inbetriebnahme und die Auswertung dieses Experimentes
- Realisierung von Schwingungsexperimenten an einem ausgewählten WWER-1000-Reaktor während der Inbetriebnahme oder im Ausnahmefall während der Umladung.
 - Auswahl geeigneter Typen, Positionen und Signale für die Erregung.
 - Auswahl von Meßpositionen und geeigneten Meßsignaltypen (einschließlich von Signalen des RDB und seiner Einbauten).
 - Technische Vorbereitung und Durchführung des Experimentes.
- 2.4. Weitere Justierung des FE-Modells für den WWER-440 und Vorbereitung der Justierung des FE-Modells für den WWER-1000 anhand der experimentellen Daten
- Justierung des Modells für den WWER-440 und Aufbereitung der Meßdaten vom WWER-1000 für eine spätere Justierung nach Vorliegen des Modells.
 - Verarbeitung, Analyse und Auswahl der experimentellen Daten für die Justierung.
 - Vergleich der Eigenfrequenzen und Schwingungsformen aus der Messung mit denen der numerischen Rechnung zum WWER-440.
 - Sichtung von vorhandenem Datenmaterial aus älteren Messungen und Prüfung der Verwendbarkeit.
 - Korrektur der Parameter des FE-Modells des WWER-440, um Übereinstimmung zwischen Experiment und Rechnung zu erhalten.
- 2.5. Vorbereitende Arbeiten zur Durchführung von Schadenssimulation und Sensitivitätsstudien
- Erstellung eines Kataloges der zu untersuchenden mechanischen Schäden.
 - Erarbeitung von ersten Empfehlungen für die on-line Schwingungsüberwachung.

3. Methode der finiten Elemente (FE)

3.1. Mathematische Grundlagen

Statische und dynamische Verformungen elastischer Strukturen werden durch partielle Differentialgleichungen (DGL) beschrieben, die nur in einfachen Sonderfällen geschlossen lösbar sind. Die Methode der FE ist ein bereichsweise angewandtes numerisches Näherungsverfahren zur Lösung dieser DGLn. Für die charakteristische Funktion der DGL, die Verschiebung $u(x,y,z,t)$, werden Ansatzfunktionen (i.a. Polynome) eingeführt, die in einem Teilbereich des DGL-Gebietes (der mechanischen Struktur) definiert sind. Diese Teilbereiche bezeichnet man als FE, wobei die Menge aller FE das gesamte DGL-Gebiet überdeckt. Die Verbindungsstellen zweier benachbarter FE sind die Knoten. Die noch unbekanntenen Knotenverschiebungen u_x , u_y , u_z und ggf. auch die Rotationen rot_x , rot_y , rot_z dienen als Gewichte für die Ansatzfunktionen und bestimmen so den Verlauf der Verschiebung im FE. Setzt man den so gewonnenen Näherungsansatz in die Integralform (oder schwache Form) der DGL ein, führt das auf ein algebraisches Gleichungssystem für die Knotenverschiebungen (GALERKIN-Verfahren), welches bei linearer DGL ebenfalls linear ist und in Matrixschreibweise formuliert wird. Damit ist eine Näherungslösung für die charakteristische Funktion $u(x,y,z,t)$ gewonnen worden.

Aus den bekannten Knotenvariablen lassen sich über die Verschiebungs-Verzerrungs-Beziehungen auch die elastischen Dehnungen und daraus wiederum über das Materialgesetz die Beanspruchungen (Schnittkräfte und Spannungen) ableiten. Die Genauigkeit der FE-Lösung ist i.a. um so höher, je feiner die Vernetzung, d.h. je kleiner die Elementgröße, gewählt wird /1/.

Die FE-Methode ist nicht auf den klassischen Anwendungsfall der Elastizitätstheorie beschränkt, sondern auch auf andere DGL der Physik übertragbar (Wärme- und Magnetfeldberechnungen, Akustik, Strömungsvorgänge etc.).

3.2. Vorgehensweise bei der Modellierung mit finiten Elementen

Die praktische Anwendung der FE-Methode erfordert also eine gedachte Zerlegung der zu analysierenden realen Struktur in Teilstücke, die den FE des Berechnungsmodells zugeordnet werden. Entsprechend den konkreten geometrischen Dimensionen und Materialeigenschaften ergeben sich aus dieser Diskretisierung die Parameter der FE, d.h. die Elementsteifigkeitsmatrizen, Elementmassenmatrizen und ggf. Elementdämpfungsmatrizen. Die Belastung der Struktur (Kräfte, Drücke, Verschiebungen usw.) wird dabei von der rechten Seite des zu lösenden algebraischen Gleichungssystemes geliefert.

Die allgemeine Vorgehensweise läßt sich in drei Hauptphasen unterteilen: *Pre-processing*, *Lösungsphase* und *Postprocessing*.

- *Preprocessing*

Der erste Schritt der Diskretisierung der Struktur ist die Auswahl geeigneter Elementtypen. Prinzipiell stehen dem FE-Anwender zur Verfügung: Punktelemente (Punktmassen, Einzelfedern und -dämpfer etc.), Linienelemente (Stäbe, Biegebalken, Seile etc.), Flächenelemente (Schalen, Scheiben, Platten etc.) und Volumenelemente (Massivbauteile). Mit der Wahl von Punkt-, Linien- oder Flächenelementen ist jeweils eine gewisse Idealisierung verbunden, die durch die Problemstellung gerechtfertigt sein muß. Andererseits ist aus Speicherplatz- und Rechenzeitgründen eine möglichst einfache Modellierung anzustreben.

Eine weitere festzulegende Modelleigenschaft ist die Dimension der Verformung und damit verbunden die Anzahl der Freiheitsgrade (DOF) eines Knotens. Eine ebene Verformung in der x-y-Ebene beispielsweise ist durch die drei Knoten-DOF u_x, u_y, rot_z gekennzeichnet, während eine räumliche Verformung 6 DOF pro Knoten ($u_x, u_y, u_z, \text{rot}_x, \text{rot}_y, \text{rot}_z$) aufweist.

Die Lage der Knoten und die Anzahl der Elemente hängen einerseits von der gewünschten Feinheit des FE-Netzes ab, andererseits müssen auch die in der Struktur vorhandenen Diskontinuitäten berücksichtigt werden (Materialwechsel, geometrische Übergänge, eingeprägte Belastungen etc.).

Nachdem Elementtypen und Knoten-DOF sowie Elementgrößen und Knotenpositionen festgelegt sind, erfolgt die Parametrisierung der FE. Diskretisiert man z.B. einen Strukturabschnitt mit Balkenelementen, so müssen für jedes FE die Flächenträgheitsmomente, der Querschnitt, die Massenbelegung sowie die Materialwerte ermittelt werden. Die Parametrisierung der FE erfolgt auf der Grundlage der Konstruktionsunterlagen und anderer Informationsquellen (z.B. Messungen oder Wägungen).

Die Lagerung auf dem Fundament, die Verbindung von einzelnen Teilstrukturen und sonstige kinematische Einschränkungen werden bei der FEM über Rand- und Zwangsbedingungen realisiert. An den entsprechenden Knoten werden dazu bestimmte DOF festgesetzt bzw. mit DOF anderer Knoten über lineare Beziehungen verbunden.

Schließlich ist für die komplette FE-Modellierung auch die Einarbeitung der Erregung erforderlich, sofern die Art der Analyse (statische Analyse, harmonische Analyse oder transiente Analyse) ein Gleichungssystem mit rechter Seite verlangt. Die Erregung (oder die Last) kann in Form von Knotenkräften oder Knotenverschiebungen bzw. durch verteilte Elementlasten (Drücke, Streckenlasten) aufgebracht werden.

- *Berechnungs- oder Lösungsphase*

Aus den parametrisierten FE werden die Systemmatrizen für das zu lösende Gleichungssystem gebildet. Handelt es sich um eine statische Analyse, gibt es nur eine

Steifigkeitsmatrix **C**, während bei dynamischen Berechnungen noch die Massenmatrix **M** und ggf. die Dämpfungsmatrix **B** hinzukommen. Die rechte Seite **f** des Gleichungssystems wird aus der Erregung gebildet. Die allgemeine transiente Gleichung für eine elastische Struktur ist

$$\mathbf{M}\ddot{\mathbf{q}}(t) + \mathbf{B}\dot{\mathbf{q}}(t) + \mathbf{C}\mathbf{q}(t) = \mathbf{f}(t) \quad (3.1)$$

Der Vektor **q** enthält die unbekanntenen Knotenverschiebungen und entspricht damit dem räumlich diskretisierten Verschiebungsfeld der Struktur. Bei einer statischen Analyse entfällt die Zeitabhängigkeit von **q** und **f**, so daß ein einfaches lineares Gleichungssystem vorliegt.

$$\mathbf{C}\mathbf{q} = \mathbf{f} \quad (3.2)$$

Bei der Modalanalyse (Ermittlung von Eigenfrequenzen und Eigenschwingungsformen) entfällt der Erregervektor (**f = 0**), und aus Gl. (3.1) wird ein Eigenwertproblem:

$$(\lambda^2 \mathbf{M} + \lambda \mathbf{B} + \mathbf{C}) \cdot \hat{\mathbf{q}} = \mathbf{0} \quad (3.3)$$

Die harmonische Analyse ist durch einen Erregervektor der Form $\mathbf{f} = \mathbf{f}_0 \sin \Omega t$ charakterisiert. Der Amplitudenvektor $\hat{\mathbf{q}}$ ergibt sich aus

$$(-\Omega^2 \mathbf{M} + j\Omega \mathbf{B} + \mathbf{C}) \cdot \hat{\mathbf{q}}(\Omega) = \mathbf{f}(\Omega) \quad (3.4)$$

Für jede dieser Analysearten existieren spezielle Lösungsverfahren /2/. Die Lösung von Gl. (3.1) (transiente Analyse) ist dabei am aufwendigsten hinsichtlich Rechenzeit und Speicherbedarf, da das Gleichungssystem auch bzgl. der Zeit diskretisiert werden muß. Charakteristisch für die FEM ist, daß es sich bei den Gln. (3.1)-(3.4) um Gleichungssysteme hoher Dimension handelt. Je feiner die Diskretisierung der Struktur mit FE erfolgt, um so größer werden die Gleichungssysteme.

Die Modalanalyse und die harmonische Analyse sind nur für lineare Strukturmodelle möglich, während die statische und transiente Analyse auch nichtlinear sein können. Bei nichtlinearen Strukturmodellen sind die Systemmatrizen **M**, **B**, **C** nicht konstant sondern vom Verschiebungsvektor **q** oder von der Zeit **t** abhängig. Nichtlinearitäten können geometrisch bedingt sein (große Verformungen, Anschläge) oder durch das Materialverhalten (Plastizität, Kriechen, nichtlineares Spannungs-Dehnungsverhalten). In diesen Fällen kommen iterative Algorithmen zur Lösung der Gleichungssysteme zum Einsatz (NEWTON-RAPHSON-Verfahren /2/).

- *Postprocessing*

Im Postprocessor des FE-Codes wird die Lösung für die im Vektor q enthaltenen Primärvariablen (Knotenverschiebungen bzw. -verdrehungen) weiterverarbeitet. Einerseits kann man aus den Primärvariablen abgeleitete Größen wie Dehnungen, Spannungen und Schnittkräfte berechnen, andererseits kann eine Signalverarbeitung durchgeführt werden (Fouriertransformation, Differenzierung etc.), wenn die Primärdaten als zeitabhängige Größen vorliegen. Mit Hilfe vielfältiger graphischer Funktionen werden die Informationen aus dem Lösungsvektor bzw. aus den daraus abgeleiteten Größen verdichtet und übersichtlich dargestellt, so daß eine Bewertung der durchgeführten Analyse besser möglich ist.

4. Ablauf der Arbeiten

- Nach dem offiziellen Vorhabensbeginn fand vom 12.-16. Dezember 1994 ein Workshop /3/ im Forschungszentrum Rossendorf statt, der die Ausarbeitung der konkreten Arbeitsprogramme zu den Einzelzielsetzungen Punkte 2.1. bis 2.3. des Vorhabens zum Gegenstand hatte. Dabei wurden für die Betriebsmessungen der 4. Block des WWER-440 in Novovoronesh und für die Schwingungsuntersuchungen bei Inbetriebnahme der 2. Block des WWER-1000 in Balakovo ausgewählt. Art und Umfang der Instrumentierung für diese Meßaufgaben sowie die Verantwortlichkeiten wurden festgelegt. Die entsprechenden Protokolle sind im Anhang Teil 7 dieses Berichtes zu finden.
- Die laufenden Arbeiten wurden bei dem Arbeitstreffen vom 1.-3. November 1995 im Forschungszentrum Rossendorf erörtert (siehe Protokoll im Anhang Teil 7). Die russischen Partner übergaben dazu einen Zwischenbericht, der den Stand der Arbeiten entsprechend dem wissenschaftlichen Arbeitsprogramm repräsentierte. Probleme bereitete vor allem die Erfüllung des Punktes 2.3. der Einzelzielsetzung, da aufgrund der besonderen Lage in Rußland keine Inbetriebnahme eines neuen WWER-Blockes während der Projektlaufzeit mehr vorgesehen war. Als Alternativen sollten sowohl die Möglichkeit von Messungen in einem Kraftwerk außerhalb Rußlands (KKW Khmelnitzkij, Ukraine), wie auch die Überprüfung von bereits vorhandenen Meßdaten auf Eignung zur Modelljustierung untersucht werden. Ähnliche Schwierigkeiten bereitete die Abarbeitung des Punktes 2.2. Auch hierzu wurden alternative Lösungen erörtert. Die Arbeiten zum Punkt 2.1. der Einzelzielsetzungen verliefen planmäßig. Die Arbeitsprogramme zu den Punkten 2.4. und 2.5. der Einzelzielsetzungen wurden entsprechend dem vorgesehenen Zeitplan für das Jahr 1996 abgestimmt.
- Ein zweiter Zwischenbericht der russischen Seite vom 27. März 1996 (siehe Begleitschreiben im Anhang Teil 7) lieferte eine umfangreiche Aufstellung aller bereits früher durchgeführten Messungen an WWER-1000-Reaktoren während der Inbetriebnahme wie auch während der Betriebsphase. Eine Einschätzung der

Daten hinsichtlich Qualität und Eignung zur Modelljustierung konnte vorgenommen werden.

- Bei dem Arbeitstreffen vom 5.-7. November 1996 im Forschungszentrum Rossendorf konnte die Erfüllung des Arbeitsprogramms konstatiert werden. Die Arbeiten zu den Planpunkten des Vorhabens konnten abgeschlossen werden. Das entsprechende Abschlußprotokoll ist im Anhang Teil 7 beigefügt.

5. Ergebnisse

Die Ergebnisse zu den einzelnen Arbeitsplanpunkten sind im Anhang in den Abschnitten Teil 1 bis Teil 6 detailliert dargestellt.

Teil 1 enthält die Eingabedaten aller Hauptkomponenten des Primärkreislaufs des WWER-1000 für die Berechnung mit dem FE-Code ANSYS. Dies umfaßt sowohl die Einbauten des Reaktordruckbehälters wie auch die Kreislaufkomponenten (Hauptumwälzpumpen, Dampferzeuger, Hauptkühlmittelleitungen). Weiterhin enthält dieser Berichtsteil die Meßprogramme für die Schwingungsmessungen an den WWER-440- und WWER-1000-Reaktoren sowie die wesentlichsten Ergebnisse bereits vorliegender Schwingungsmessungen an beiden Reaktortypen. Speziell mit den experimentellen Daten zum WWER-440 war eine weitere Justierung des FE-Modellen zu diesem Reaktortyp vorgenommen werden. Die Ergebnisse der Rechnungen mit dem validierten Modell für den WWER-440 sind im Abschlußbericht zum Projekt 1500916 dargestellt.

Teil 2 hat eine detaillierte konstruktive Beschreibung des oberen Blocks und der Hauptumwälzpumpen des WWER-1000 zum Inhalt. Mögliche Fehlfunktionen im Bereich der Kerneinbauten werden im Hinblick auf Arbeiten zur Schadenssimulation und für Sensitivitätsstudien erörtert. Experimentelle Daten von Schwingungsmessungen und Messungen von Druckfluktuationen sowie von incore- und excore-Neutronenrauschen am Block 1 des KKW Kalinin (WWER-1000) werden analysiert. Dieser Berichtsteil enthält auch die Resultate von Schwingungsmessungen während der Kalt-Warm-Erprobung eines WWER-1000.

Die Teile 3 bis 5 stellen die Ergebnisse weiterführender Untersuchungen zur Ausbildung von stehenden akustischen Wellen vor. Diese Untersuchungen wurden am Block 1 des KKW Kalinin durchgeführt und beschäftigten sich vor allem mit der Ursache und der Auswirkung von Resonanzanregung auf die Schwingungen von Kerneinbauten.

Bei Schwingungsmessungen während der Inbetriebnahme von Block 1 des KKW Khmelnitzkij, wurde u.a. ein abnormes Schwingungsverhalten der Reaktoreinbauten festgestellt. Der wesentliche Befund äußerte sich in einem signifikanten Anstieg der Schwingungsamplituden im Frequenzbereich zwischen 5.0 und 10.0 Hz. In diesem Frequenzbereich liegen die Eigenfrequenzen typischer Schwingungsformen des

Kernbehälters. Der Verdacht auf einen Montagefehler konnte bei einer visuellen Inspektion bestätigt werden. Es wurden zu große Einbautoleranzen im Bereich des oberen Kernbehälterflansches festgestellt. Diese hatten zur Folge, daß der Kernbehälter selbst sowie seine Einbauten nur mit unzureichender Niederhaltekraft im Reaktor-druckbehälter fixiert waren, was sich naturgemäß in einem veränderten Schwingungsverhalten abbildete.

Teil 6 legt den Entwicklungsstand des FE-Modells zum WWER-1000 mit dem ANSYS-Code dar. Als Ergebnis stehen lokale FE-Modelle von Reaktordruckbehälter, Kernbehälter, Hauptumwälzpumpen, Oberem Block und Dampferzeuger zur Verfügung. Auch ein globales Modell des gesamten Primärkreislaufs, welches auf den lokalen Modellen basiert, konnte vorgelegt werden. Theoretische Eigenfrequenzen und Schwingungsmodi für die einzelnen Komponenten werden angegeben.

6. Literatur

- / 1 / Zienkiewicz, O.C., Whiteman, J.R.: Finite Elements - The Mathematics of Finite Elements and Applications, Academic Press, London 1973
- / 2 / ANSYS User's Manual for Rev. 5.0 Vol. 4: Theory. Swansons Analysis Systems, Inc. (1993)
- / 3 / Protocol of the Workshop on Vibrational Modelling of VVER Type Reactors, held at Research Center Rossendorf, Institute for Safety Research, Dec. 12-16 1994

Anhang

Teil 1

APPROVED
Director General
of Diagnostic Center
"DIAPROM"

 Gutsev D.F.

" 3 " 08 1995

**ELABORATION of NUMERICAL VIBRATION
MODELS of the VVER TYPE REACTORS**

**A set of data for elaboration and adjusting the
finite-element-based model of the VVER-1000 plant**

Intermediate Report

320 - O.211 - 003

1995

CONTENTS

	Page
1. Introduction.....	4
2. Initial data for elaboration of finite-element model of V-320 reactor internals.....	5
3. Initial data for elaboration of V-320 plant primary circuit.....	8
4. Experimental procedures of noise vibrational measurements at VVER plants.....	9
4.1. VVER-1000 plant.....	9
4.2. VVER-440 plant.....	10
5. Main results of noise vibrational measurements at VVER NPP.....	11
5.1. VVER-1000 plant.....	11
5.2. VVER-440 plant.....	14
6. References.....	20
List of abbreviations adopted.....	22

1. INTRODUCTION

1.1. Theoretical vibration models of VVER type reactors should be an integral part of special software of the diagnostic systems. When applied, such models are to calculate eigenfrequencies and corresponding mode shapes of equipment for different fastening conditions including abnormal ones: the wear of internal clamping, the degradation of spring elements and so on. So results of modelling may be used for early detection of an abnormal vibration behaviour of the reactor plant.

By now some programs are developed for calculation of VVER reactors eigenfrequencies and some results are available (see, for example, [1, 2]). But such works were tentative ones and were aimed at development of the mathematic basis.

It's clear that the following steps should be sequentially done to elaborate the representative vibration model:

- preparation of an initial parameter set for the finite-element model based on masses, momenta of inertia, stiffness matrices gained from construction drawings;
- generation of input files for the finite-element-code and coupling of the main components;
- adjusting the theoretical models using experimental data on vibration behaviour of VVER plants during commissioning and operation the NPP;
- elaboration of the tables of mechanical damages reactor plants to be detected by the changes vibration characteristics;
- calculation on the basis of the previous steps, of eigenfrequencies and mode shapes of main equipment;
- creation of base data on vibration behaviour of VVER plants.

1.2. The report under discussion contains initial parameters set for elaboration of numerical model of VVER-1000 plant on the basis of data from technical project V-320.

With the spotlight fixed on the damages of reactor internals, the particular emphasis has been placed on initial parameters of this component of VVER plant. A set of data on primary circuit equipment provides the coupling of the main components of the plant.

Experimental procedures and main results of vibration measurements at unit 1 of Kalinin NPP are also presentid. These data are necessary for the first step of model adjustment. The second one can be done after performance of special vibration tests at selected VVER. The working prosedures of such tests also presented in the report.

Taking into account that vibration measurements on VVER-1000 only begun last year and were applied to the reactor, some results of vibration measurements on VVER-440 plants (including primary circuit equipment) also presented. They can be used for having a general grasp on vibration behaviour of VVER type reactors as well as for adjustment VVER-440 model in the future.

1.3. The ultimate result of the work in the form of verified VVER vibrational models should be used as an integral part of the software at Russian Diagnostic Center

"DIAPROM".

2. INITIAL DATA FOR ELABORATION of FINITE-ELEMENT MODEL of V-320 REACTOR INTERNALS

Mutual location of internals and reactor vessels shown in fig.1. The fit diameters in the separating ring assembly are:

core barrel - \varnothing 3625 - 1,1 ; reactor vessel - \varnothing 3620 A₃
- 2,2

Core barrel (fig. 2 - 7)

Outer diameter: 3630 (above the separating ring);

3620 (below the separating ring);

Inner diameter: 3500 (above the inlet nozzles);

3490 (below the inlet nozzles).

Small semiaxis of elliptical bottom - 1100 mm.

Upper part of the core barrel (above the separating ring) is perforated by 278 holes \varnothing 180 and two holes \varnothing 300.

The core barrel has fastening in three cross-section:

on vessel support shoulder in cross-section of main reactor joint;

in cross-section of coolant flow separator (separating ring);

in lower support assembly made of 8 keys on cantilevers.

The core barrel clamping at the upper cross-section is provided by means of elastic tubular elements 63×5 (three sectors), which are located between reactor head and core barrel flange, as well as by means of 126 keys located at the reactor flange. Upon tightening of reactor main joint the tubular elements became deformed providing thrust effort between the reactor head and the core barrel.

Core barrel clamping at the middle cross-section is provided by clamping of the separating ring to core barrel at the operation temperature.

Core barrel splines ensure its fixing in vessel and make axial radial movements with respect to vessel possible in the case of reactor heating-up.

Protective tubes unit (PTU), fig. 8 - 11.

The perforation and the weight are:

Element	n1	n2	n3	n4	n5	Weight (Kg)
	d1	d2	d3	d4	d5	
P Supporting plate	72	78	12	168	182	8400
L Average	108	120	92	133	122	
A plate	90	30	42			9300
T Upper plate	90	22,5	100			
E Supporting	36	6				3600
S shell (between average and supporting plates)	200	145				
	2148	780	40			12500
	40	32	60			

Where n_i is the number of holes with d_i as diameter (mm)

The weight of the shell between average and upper plates is 6185 kg.

Core baffle (fig. 12 - 16)

Core baffle represents a cylinder consisting of five rings in height. Rings are connected with each other with the help of studs and fixed with respect to each other in plan with the help of pins.

The bottom part of core baffle is fixed by means of three pins at the height of 60 mm. Core baffle is held against belt line of core barrel by 6 threaded tractions installed in the longitudinal channels (fig. 13).

Keys

1. Vessel keys and respective core barrel grooves in the upper cross-section:

12 pieces $\varphi_i = 22^\circ + (i - 1) * 30^\circ$ ($i = 1 \div 12$) (fig. 3, 17)

width is 100 mm;

height is 80 mm (interaction length is 40 mm)

2. PTU keys and respective core barrel grooves (fig. 9, 18)

2 pieces with a width 60 mm

$\varphi_i = 52^\circ + (i - 1) * 120^\circ$ ($i = 1, 2$)

one piece with a width 70 mm $\varphi = 292^\circ$

height is 310 mm (interaction length is 260 mm)

3. Core barrel keys and respective grooves in the supporting plate of PTU (fig. 19)

$$6 \text{ pieces } \varphi_i = (i - 1) * 60^\circ \quad (i = 1 \div 6) \quad (\text{fig. 8})$$

width is 70 mm

height is 280 mm (interaction length is 80 mm)

4. Core barrel keys and respective core baffle grooves (fig. 12, 13)

$$6 \text{ pieces } \varphi_i = (i - 1) * 60^\circ \quad (i = 1 \div 6)$$

width is 80 mm

height is 180 mm (interaction length is 80 mm)

5. ^{Upper} Lower support assembly of core barrel (fig. 5 ÷ 7)

Tubular elements 63x5 (fig. 4) are fixed at the core barrel flange by three sections (fig.

3)

overall length is 7300 mm

linear load 29 kg/mm under tightening upon 3 mm

maximum pressing effort accords with displacement 19 mm

Notes.

1. Presented data accord with technical project of VVER-1000

2. Reactor internals are made of steel 08X18H10T

$$E_{T=20} = 2,01 * 10^5 \text{ MPa} \quad \alpha_{T=50} = 16,4 \text{ mkK}^{-1}$$

$$E_{T=300} = 1,8 * 10^5 \text{ MPa} \quad \alpha_{T=300} = 17,4 \text{ mkK}^{-1}$$

$$\rho = 7800 \text{ kg/m}^3$$

3. INITIAL DATA for ELABORATION of V-320 PLANT PRUMARY CIRCUIT

Reactor (fig. 20) comprises the following assembly units: internals (see section 2), pressure vessel (RPV) and upper unit.

Pressure vessel (fig. 21) consists of flange, upper shell of nozzle area, support shell, cylinder part and elliptical bottom. The support belt is located at the outer surface of support shell to fix the reactor at the supporting ring (fig.22) which, in turn, is fixed at the supporting truss. The last comprises weld construction which consists of radial chest beams. The thrust ring is used to endure seismic loads. Pressure vessel and reactor head are made of steel 15XHMΦA.

$$E_{T=20} = 2,1 \cdot 10^5 \text{ MPa}, \quad E_{T=300} = 1,95 \cdot 10^5 \text{ MPa}.$$

Pressure vessel mass is 323 t.

Upper unit (fig.23) consist of reactor head with nozzles, metal structure and CPS drives. Reactor head mass is 90,3 t, metal structure mass is 31,2 t, CPS drives mass - 41,25 t.

Steam generator (fig. 24) consist of cylinder shell generator is installed at two supporting constructions consisted of support bedding, roller bearing and connecting tractions.

The hydroshock-absorber system is used to enduce seismic loads.

At the upper part of steam generator there are nozzles for steam collector and for feedwater lines.

The steam generator mass is 506 t.

Main coolant pump (fig. 25) is installed on three dovetailes with roller supports which provide free displacements in the horizontal direction. The hydroshock-absorber system is used to enduce horizontal seismic loads. MCP mass is 140 t.

Main coolant pipelines (fig. 26 - 28) is a component of the circulating loops and consist of the tube units connecting the loop equipment - a reactor, a steam generator and coolant pump. Main coolant pipelines are made of steel 10ГН2МΦА with inner diameter 850 mm and wall thickness 70 mm. The pipelines are connected with such systems as pressurizer system, high-pressure and low-pressure injection systems, make-up and blowdown system, active and passive parts of the emergency core cooling system.

4. EXPERIMENTAL PROCEDURES of NOISE VIBRATIONAL MEASUREMENTS at VVER PLANTS

4.1. VVER-1000 plant.

4.1.1. Measurement objective.

The objective in measurements is to obtain vibration characteristics of VVER-1000 internals and FA (eigenfrequencies and mode shapes) using signals of SPD's, IC, PFS TC as well as to develop diagnostic methods for early detection of core and internals damages.

4.1.2. Using means.

The following means are used:

- measuring channels of pressure fluctuation sensors (PFS), three pieces;
- self-powered detectors (SPD);
- ex-core ionization chambers (IC) of an intermediate range (N7, 14, 21);
- thermocouples (TC) of in-core instrumentation system;
- detector units of noise diagnostic system "KAZMER";
- units for separation of variable components of IC signals;
- a set of filters;
- analog magnitograph.

Measurement scheme is shown in fig. 29, 30, 31.

Communication must be used between "KAZMER" and in-core instrumentation system "Hindukush" during measurements to fix the following technological parameters:

- thermal output;
- coolant pressure at the core outlet;
- coolant temperature at the reactor inlet and outlet;
- pressure difference through the core;
- water level in the pressurizer;
- current boric acid concentration;
- poison of group X of SUZ control members.

4.1.3. Measurements procedure.

Measurements are carried out at the nominal operation of the plant as well as at intermediate levels of output.

The list of the measuring channels commutation and sequence of sensors integration are shown in tables 1, 2.

Initial time realisations of detectors are digitized by 16-channel ADC of "KAZMER" and written at the magnitograph cocurrently.

Signal processing are carried out in two frequency ranges: 0,1 - 20,0 Hz.

4.1.4. Data processing.

The following tasks should be solved to define vibration parameters:

- identification of frequency components which deal with mechanical oscillations of FA and internals;
- isolation of frequency components which deal with reactivity effects (temperature and flow fluctuations, barometrical and hydroulic effects etc.);
- estimation of local effects contribution in the point of sensors.

As a result of processing the following characteristics must be obtained:

eigenfrequencies and cooresponding mode of shapes of FA and internals;

eigenfrequencies and corresponding mode of shapes of acoustic standing waves in the primary circuit of VVER-1000 plant.

4.2. VVER-440 plant.

4.2.1. Measurement objective.

The objective in measurements is to obtain real vibration characteristics of VVER-440 plant and its individual components with identification of eigenfrequencies.

To identify vibration behavior of the plant signals of different sensors are recorded: ex-core IC, relative displacement sensors, absolute displacement sensors, pressure fluctuation sensors and accelerometers.

4.2.2. Using means.

Diagnostic system SUS is used as a base for data collection and processing.

The system comprises:

- 4 absolute displacement sensors at the reactor head;
- 24 relative displacement sensors at MCP and SG;
- 4 pressure fluctuation sensors installed directly in the main coolant pipelines;
- registrating and processing units which provide to obtain digital time realization with the duration 4 sec.

Sensor arrangement at plant equipment is shown in fig. 32.

During measurement additional devices will be used:

- apparatus for separation of variable components of neutron flux;
- 2 accelerometers at outer surface of reactor vessel in the nozzle area together with units for signal preparations;
- analog magnitograph.

3 ionization chambers KNK-57 type will be additionally used during measurements at the start-up and at the full output of the reactor. Instrumentation and control system should be used for fixing the following parameters:

- thermal output;
- coolant pressure;
- coolant temperature at the reactor inlet and outlet;
- pressure difference through the core;
- water level in the pressurizer;
- current boric acid concentration;
- position of control device for ARK drives.

4.2.3. Measurements procedure.

Measurements are carried out at the different working parameters of the plant beginning from heating-up and finishing at its nominal output.

Sensor signals are fixed at the magnitograph through each 10° C during heating-up of the plant. Ionization chambers will be used from start-up of the reactor.

Then measurements are carried out at 10, 30, 50, 75 and 100% of plant output.

Using SUS system it's possible to record sensor signal with duration 4 sec. The magnitograph provides signal recording up to 15 minutes.

4.2.4. Data processing.

Processing and analysis of records will be carried out upon finishing experimental program using special software. Identified eigenfrequencies of plant components, including internals, must be obtained.

5. MAIN RESULTS of NOISE VIBRATIONAL MEASUREMENTS AT VVER NPP

5.1. VVER-1000 plant.

The vibration characteristics of reactor internals and fuel assemblies at Kalinin-1 were studied using experimental system that includes (fig. 29, 31):

- * in-core self-powered detectors (SPD), installed in seven points along height of any of 64 fuel assemblies;
- * three ex-core ionization chambers (IC) installed at 120° angle about one another at the middle of core height;
- * three pressure pulsation sensors installed in piping of two adjacent loops using short surge lines of 50 cm length.

While proceeding to consideration of RI and FA vibration measurements done at Kalinin NPP, Unit 1 under nominal power operation it should be pointed out that analysis of vibration by neutron noise hindered by some effects masking vibration, namely:

- a) transfer effects;
- b) global neutron noise;
- c) acoustic standing waves.

Transfer effects occur due to transfer of coolant non-uniformity, for example, temperature fluctuations from core inlet along the fuel channel (fig. 33, 34). These broadband effects results in the delay of the SPD signal with respect to another signal that forms linear dependency of noise signal phase on frequency. If any frequency of RI and FA vibration falls within this frequency band, expected in-phase or antiphase state between signals of two neutron detectors would not occur. To eliminate this type of masking, phase characteristic has to be adjusted by linear dependency.

Another known type of masking is global component of neutron noise with intensity rising as frequency falls off. Global component also results in biasing of phase estimate. At low frequencies biasing can be so considerable that none phases expert for zero phase would be observed.

Acoustic standing waves can mask RI and FA vibration owing to oscillating loads both by azimuth and axially because of certain distribution of nodes and antinodes of standing waves and their harmonics. Rather complicated conditions of standing waves generation with nodes and antinodes in reactor flow path and being realized as 3D geometrical structure have been revealed by results of theoretical analysis of frequencies and mode of coolant acoustic waves at VVER reactor [3].

Than, total set of candidate resonance was checked for same criteria:

- a) amplitude features;
- b) phase features;
- c) harmonic and subharmonic features;
- d) features of multidimensional autoregression analysis (MAR-criteria).

It is shown below how this criteria could be applied to identify any characteristics of RI and FA vibration.

Amplitude features

In the ideal case the variance of SPD noise normalized by zero-frequency component at the first harmonic frequency of FA with two fixed ends as a function of height Z shall coincide with the first mode of vibration, i.e. be in the form $\text{const.} \sin(\frac{Z}{H})$, where H is a distance between upper and lower points of FA fixation. The variance of SPD signals at the second harmonic frequency (both ends of FA are fixed) as a function of height shall be in the form $\text{const.} \sin(\frac{2Z}{H})$, etc.

In this experiment the first mode of FA and CB vibration was identified by amplitude features (see fig. 35 where amplitudes of ASPD resonances are given in relative units depending on SPD number).

Phase features

Phase pattern can be obviously used to identify reactor barrel vibration by phase ratio of IC signals. In such a case, under three ex-core neutron detectors at frequency of combined vibration a certain pair of signals would be in the phase, while other two pairs of signals would be in antiphase state. In-phase state at vibration frequencies will be identified for SPD signals in different FAs but within gradient of neutron field of the same sign. On the contrary, antiphase state is typical for FA being in different sign gradients (fig. 36, 37). These correlations can be regarded as second criteria for FA combined vibration due to vibration of barrel, STA, etc.

The application of phase ratio for pairs "SPD-SPD" is not too obvious. In particular, low-frequency band of these signal pairs is completely masked by global effects and transfer effects, therefore it could not be used to confirm frequency of the first mode of FA vibration.

Nevertheless, phase ratio of "SPD-SPD in the same channel" enable to reveal the second mode of FA vibration. That frequency, which was roughly estimated by calculations and rig testing, shall be found within the bend of masking effects. It can be however revealed by thorough spectral analysis when low coherence of signals is compensated by the large number periogram averaging (up to 2000).

Fig. 38 shows schematically phase estimation for two series of coherence functions: 7 - 2, 7 - 3, ... 7 - 6 and 4 - 2, 4 - 3, ... 4 - 7 at 7.6 Hz frequency.

Next come phase ratio of "SPD-IC" couples. The most reliable are phase patterns of FA combined vibration for couple "SPD-distant IC". For these couples two resonances (fig. 39) are pronounced within frequency band 2 - 3 Hz. Antiphase state is observed there irrespective of SPD number. This phenomenon agrees with the conclusions on FA combined vibrations.

Harmonic features

Appearance of harmonics or subharmonics of signals in question is caused by non-linear phenomena. In particular, displacement of SPD due to FA vibration (Fig.40) results in non-linear phenomena. As a result, harmonic series $f, 2f, 3f, \dots$ in SPD signals appears simultaneously with joint vibration of FA and SPD at frequency f . Significantly, the above series is the series of accurate harmonics. Therefore, harmonic features can be in additional confirmation when the different modes of FA vibration are to be identified. Under this experiment harmonic features were used in addition to amplitude and phase features to find out frequency of FA vibration at first and second modes.

It is worthy to point out that harmonic features can be very helpful to identify such non-linear phenomena as RI collision interactions. If they are present, harmonics and subharmonics of amplified forces shall be found in spectra: MCP frequencies, and frequency of coolant acoustic oscillations (Table 3, 4).

Table 3. Subharmonics F_{mcp} (coherence SPD-SPD N08-17)

N Subharm.	1/4	1/2	3/4	1	5/4	3/2	2
Hz	4.050	8.301	12.480	16.600	20.750	24.960	33.200

Table 4. Subharmonics ASW (coherence SPD-SPD N08-17)

N Subharm.	1/4	1/3	1/2	2/3	1	4/3	2	8/3
Hz	2.197	2.954	4.443	5.908	8.862	11.820	17.680	23.560

MAR-criteria

MAR-analysis enables to distinguish RI vibration under joint consideration of neutron field fluctuations and coolant pressure field fluctuations. Judging by mutual contributions of one signal to another one, this analysis provides information of primary sources of any particular resonance.

For the purpose of described experiment 3D MAR-model been used. It was consisted of signals of SPD, IC and PPD places far from each another (fig. 41). The simplified scheme is given in fig. 42 with data of mutual contribution of signals at some characteristic frequencies. Out of them, the most interesting frequencies are 2.3 and 4.5 Hz. SPD signal affects resonance 2.3 Hz. IC is responsible for resonance 4.5 Hz. One may argue therefore that these frequencies are frequencies of FA and reactor barrel natural oscillations, respectively.

Successive application of all above mentioned criteria permits to analyze step-by-step primary sources of resonances with the specified spectral characteristics. As a result, rather comprehensive information on FA and RI vibration state has been obtained.

Summing up fig. 43 - 46 present the specified spectral characteristics and identify the most intensive frequency components of FA and RI vibrations.

To conclude, two important aspects have to be underlined.

Firstly, measurements of FA and RI vibration at Kalinin NPP provided positive results: no abnormal modes (e.g., vibration of FA with end being fixed) were identified; change of FA vibration frequency during its service was not observed.

Secondly, data presented show rather good agreement with the design analysis of FA and RI vibration characteristics as well as with the results of start-up and adjusting measurements. That proves efficiency of the approach applied to FA and RI vibration analysis by neutron noise and enables to replicate this approach at other VVER reactors.

5.2. VVER-440 plant

In last years specialists of Diagnostic Centre "DIAPROM" have amassed significant experimental data on vibration behaviour of VVER-440 plant using diagnostic systems at Kola NPP and Novovoronezh NPP.

These systems use sensors installed at the different components of primary circuit (see fig. 32). It enables to analyse vibration behaviour of the plants as a whole.

Omitting methodical peculiarities of the vibration analysis (which are similar to ones in the previous section and are oriented to using cross spectral analysis, MAR-analysis and spectrum decomposition) let's discuss main data on vibrational characteristics of VVER-440 plant.

Pressure fluctuation

Fig. 47 presents autospectral power density (ASPD) of pressure fluctuations in the hot leg of Kola NPP (unit 2) loop in the frequency range 0 - 50 Hz. One can see that ASPD of all sensor are practically similar. The frequencies 0,6 - 0,7; 6,5 - 7,0; 19,0; 24,5; 30,5; 32,0; 39,0; 40,5; 47,0 and 49,0 Hz are standed out sharply in the bigures. Besides of that, there are frequencies 2,6; 3,5; 4,8; 5,1; 8,5 - 9,0; 10,5; 11,5 - 12,3 Hz which have rather small amplitudes but exist stable. Some of them couldn't be seen distinctly because of the neighbourhood with the most intensive and broad frequencies.

Analysing coherence and phase functions between different pairs of sensors 2P1, 2P2, 2P3 and 2P4 we can do the following conclusions.

First, phase difference between 2P3 and 2P4 signals at above mentioned frequencies 5,1; 11,8; 30,5; 40,5 Hz is $+110^\circ$, -60° , -40° and $+40^\circ$ respectively. These phase values are unlike 0° or 180° .

From the above reasoning it's clear that frequencies 5,1; 11,8; 30,5 and 40,5 Hz deal with running pressure waves. This conclusion is confirmed by experimental results, which were obtained at unit 2 at coolant temperature 190°C and coolant pressure 30 bar. ASPD of PFS signals for these conditions is shown in fig. 48. One can see that peaks at the frequencies 5,1; 11,6; 30,5 and 40,5 Hz are still retained. More of that, the peak at the frequency 5,1 Hz broke free from neighbouring peak at the frequency 6,5 - 7,0 Hz and became more apparent. It took place because of that peak at the frequency 6,5 - 7,0 Hz are shifted to the meaning $\sim 10,2$ Hz in accordance with changing of coolant temperature. Just the same happened with above mentioned peak at the frequency 8,5 - 9,0 Hz, whose meaning became $\sim 12,0$ Hz. That measurement indicated that frequencies 6,5 - 7,0 and 8,5 - 9,0 Hz deal with acoustic standing waves.

Internal vibrations

Fig. 49, 50 present spectral characteristics of three ionization chambers N1, N2, N3 of Kola NPP (unit 2) in the frequency range 0 - 6 and 0 - 50 Hz respectively.

Table 5 contents values of the frequencies also presents components of coherence and phase function for different pairs of IC signals. Presented data were obtained while all MCP were in operation at the 50% of plant output. Data outlined in table 5 indicate that N1, N2, N3 signals have significant noncorrelative noise components. It results in low values of coherence function between these signals as well as inaccurate estimations of phase values. The coherence function is significantly higher than 0,1 only for frequencies 0 - 1,0 and 30,7 Hz.

Distinct peak at the frequency 0,92 - 0,98 Hz (see fig. 49) seems to be produced by pendulum oscillations of SUZ control member. nearby resonance has been surveyed in IC signals at one of the units "Paks" NPP and has been identified by Hungary specialists as being dealt with above mentioned reason.

Let's take a brief look at peaks at 5,1 and 11,5 Hz, which were observed in the PFS spectrums (see fig. 47) and were qualified as running waves caused by internal oscillations.

To understand the reason of its appearance let's call attention to information of ADS signals. Tables 6 and 7 present coherence and phase functions for different pairs of ADS at $\sim 5,1$ and $\sim 11,5$ Hz.

Table 6

Function	Sensor pair					
	2A1- 2A2	2A1- 2A3	2A1- 2A4	2A2- 2A3	2A2- 2A4	2A3- 2A4
Coherence at $\sim 5,1 \Gamma_{\text{ц}}$	0,175	0,06	0,19	0,01	0,8	0,025
Phase at $\sim 5,1 \Gamma_{\text{ц}}$	$\sim 150^\circ$	$\sim 165^\circ$	0°	130°	180°	$\sim 80^\circ$

Table 7

Function	Sensor paire					
	2A1- 2A2	2A1- 2A3	2A1- 2A4	2A2- 2A3	2A2- 2A4	2A3- 2A4
Coherence at $\sim 11,5 \Gamma_{\text{ц}}$	0,5	0,9	0,5	0,4	1,0	0,4
Phase at $\sim 11,5 \Gamma_{\text{ц}}$	$\sim 180^\circ$	$\sim 110^\circ$	0°	50°	180°	$\sim 120^\circ$

In analysing information of tables 6, 7 let's take into account data of 2A1, 2A2 and 2A4 only without 2A3. In this case we can do the following contention. From phase functions it will be noticed that reactor head executes two types oscillations at 5,1 and 11,5 Hz in the same direction or in the directions close to each other. Components at 5,1 and 11,5 Hz for 2A3 disrupt the picture of reactor head oscillations. This circumstance shows that quality of 2A3 signal was inadequate.

The reactor head oscillations at cited frequencies could take place for a number of reasons. They may be caused by oscillation of RPV or internals at the eigenfrequencies. To detect the real reason of oscillations at 5,1 and 11,5 Hz it's necessary to enlist additional information on construction peculiarities of the plant and information on eigenfrequencies for different mode shapes.

It may be supposed that two types of oscillation at 5,1 and 11,5 Hz are stipulated by inherent pendulum (beam) vibrations of the core barrel which is fixed at upper flange. It's supposed that oscillations at 5,1 Hz may be realized in the case when the bottom end of the core barrel is free. Such type of vibration can presumably occur in the case of the wear of the keys in bottom clamping assembly.

Beam oscillations at 11,5 Hz can take place if the core barrel is fixed at upper and bottom clamping assemblies.

RPV vibrations

The analysis of RPV vibrations will be done using ADS and IC signals at units 1, 2 Kola NPP.

Of significant resonances totality observed in cross spectral characteristics of ADS at unit 2, in table 8 picked up 35 resonances. The table doesn't include harmonics line

6,64x π Hz connected with acoustic standing waves. Out of interest also are the frequencies 1,95; 4,88; 8,00; 14,45 Hz which haven't characteristic phase values (+90, -90, 0, 180°).

Similar actions can be done with spectral characteristics of ADS signals obtained at unit 1. Some of them are presented in fig. 51 - 54. Table 9 included the most representative data (similar to table 8) on cross spectral characteristics of ADS signals.

For further analysis of the signals it's necessary to carry out spectrum decomposition for different types of RPV and core barrel vibrations [4]. It's results present in fig.55 for ADS of unit 1. Using these data we can compile the table for dominating frequency components (table 10).

Analysis of presented data allows to do the following conclusions.

Different types of RPV oscillations (circular, pendulum, vertical) took place at 4,88 and 5,76 Hz. Stochastic component also took place at 4,88 Hz.

There is the resonance frequency 10,35 Hz at unit 1 of Kola NPP which corresponds closely with the frequency 10,94 Hz at unit 2. The last also deals with pendulum oscillations although their amplitudes are one order smaller. The frequencies 10,34 and 10,94 Hz seem to be eigenfrequencies of pendulum oscillations of RPV at unit 1 and 2.

From the proximity of the frequencies it's safe to assume that 5,94 Hz at unit 2 and 5,76 Hz at unit 1 are eigenfrequencies associated with circular motion.

The automatic spectrum decomposition allows to pick out frequencies 1,86; 2,93; 3,71; 4,10 Hz which have "loop" origin. As it will be shown below, inherent oscillations of different loop components take place at these frequencies. Table 10 shows that their integral influence on RPV result in predominance of pendulum oscillations.

Now let's discuss the origin of 10,74; 17,29 and 30,66 Hz. Two first of them are clearly defined, have a good time reproducibility and absence of phase difference for neutron signal pair N3 - N4 (fig. 18 - 24). Coherence function at 10,74; 17,29 Hz is close to zero for all pairs of IC - APS. These facts are necessary conditions for shell models for whom ADS are insensitive. To confirm this assumption it's necessary to extend neutron channels in four at least.

At the frequency 30,66 Hz all six pair of signals have no any phase shift. It seems to be the case when RPV amplitude is quite enough to be manifested in IC signals. Just the same frequency was mentioned at unit 2 of Kola NPP as eigenfrequency of core barrel vertical oscillations.

To identify the other frequency components of APS and IC signals let's use three-dimensional MAR-model, which includes: pressure fluctuations (P), radial MCP vibrodisplacements (R_{MCP}) and absolute displacements of RPV (A). Such model allows to clarify "RPV" or "loop" origin of those or another frequencies. The data on mutual contribution of signals are given in fig. 56 - 58. The scheme in fig. 59 presents results of decomposition at some characteristic frequencies. The dominating source is marked by double frame.

Main results of MAR-analysis are:

- the frequencies 1,55; 3,52; 7,52 Hz have a "loop" origin that is they derive from loops oscillations;
- 2,19; 5,28; 10,93; 12,16 Hz have a "RPV" origin;
- 6,29 and 8,64 Hz derive from pressure fluctuations.

In conclusion let's compare presented data with results of similar noise measurements at unit 3 of Novovoronezh NPP. The lasts are presented by table 11 with the most characteristic frequencies.

The following conclusions may be done.

Some resonances conceptually agree closely with resonances detected at Kola NPP by neutron detectors:

4,00 - 4,84 Hz - pendulum oscillations of core barrel;

31,93 - 32,37 Hz - vertical oscillations of core barrel.

The following reconances conceptually agree closely with ones detected at Kola NPP by ADS:

10,25 - 10,33

11,87 - 12,16 - RPV motion together with the core in an elliptical (including circular)

12,67 - 12,89 trajectories

13,62 - 13,99

Primary circuit vibrations

The definition of vibration peculiarities of primary circuit equipment at unit 2 Kola NPP which are presented here, was founded on analysis of noise signals using ADS and RDS. Measurements were carried out at 50% plant output with all MCP in operation. Two RDS at each MCP and each SG control their motion in horizontal perpendicular directions (TG_{MCP} , R_{MCP} , TG_{SG} , R_{SG}). In doing so, one RDS (R_{MCP}) at MCP controls its vibration along coolant pipeline. All of ADS allow to control vertical vibration of RPV.

The most illustrative spectral characteristics are shown in fig. 60 - 61. Descriptive MAR-models which were used to analyse signals of sensors at different equipment are shown in fig. 62. Analysis results present in table 12.

Referring to table 12 it will be observed that the following modes were identified:

0,9 - 1,5 Hz - pendulum SG oscillations around reactor vertical axis;

1,8 - 2,2 Hz - pendulum SG oscillations around itself vertical axis;

2,7 - 3,4 Hz - pendulum MCP oscillations around inlet pipe axis;

6,2 - 6,6 Hz - first harmonic of acoustic standing wave;

8,7 - 9,0 Hz - pendulum oscillations of MCP motor.

REFERENCES

1. E. Altstadt, m. Scheffler, F.-P. Weis. Component Vibration of VVER reactors-Diagnostic and Modelling, "Progress in Nuclear Energy", Vol.29, №3/4, 1995.
2. V.Kinelev, S.Perov, V.Sulimov. Mathematical modelling of VVER-1000 primary circuit eigenfrequencies for equipment diagnostics, SMORN-VII,1995.
3. V.V.Bulavin, D.F.Gutsev, V.I.Pavelko. The experimental definition of the ASW series shapes, formed in the coolant of the primary circuit of VVER-440 type reactor, "Progress in Nuclear Energy", Vol. 29,№3/4,1995.
4. V.V. Bulavin, D.F.Gutsev, V.I.Pavelko. Some results of the vibration analysis on the VVER-440 type reactor vessel top head and on the facilities of its primary circuit six loops, SMORN-VII, 1995.

LIST OF ABBREVIATIONS ADOPTED

ADS - absolute displacement sensor
ASPD - autospectral power density
FA - fuel assembly
IC - ionization chamber
MAR - multidimensional autoregression analysis
MCP - main coolant pump
NPP - nuclear power plant
PFS - pressure fluctuation sensor
PTU - protective tube unit
RDS - relative displacement sensor
RI - reactor internals
RPV - reactor pressure vessel
SG - steam generator
SPD - self-powered detector
SUZ - control and protective system
TC - thermoconple
VVER - water-cooled, water-moderate power reactor

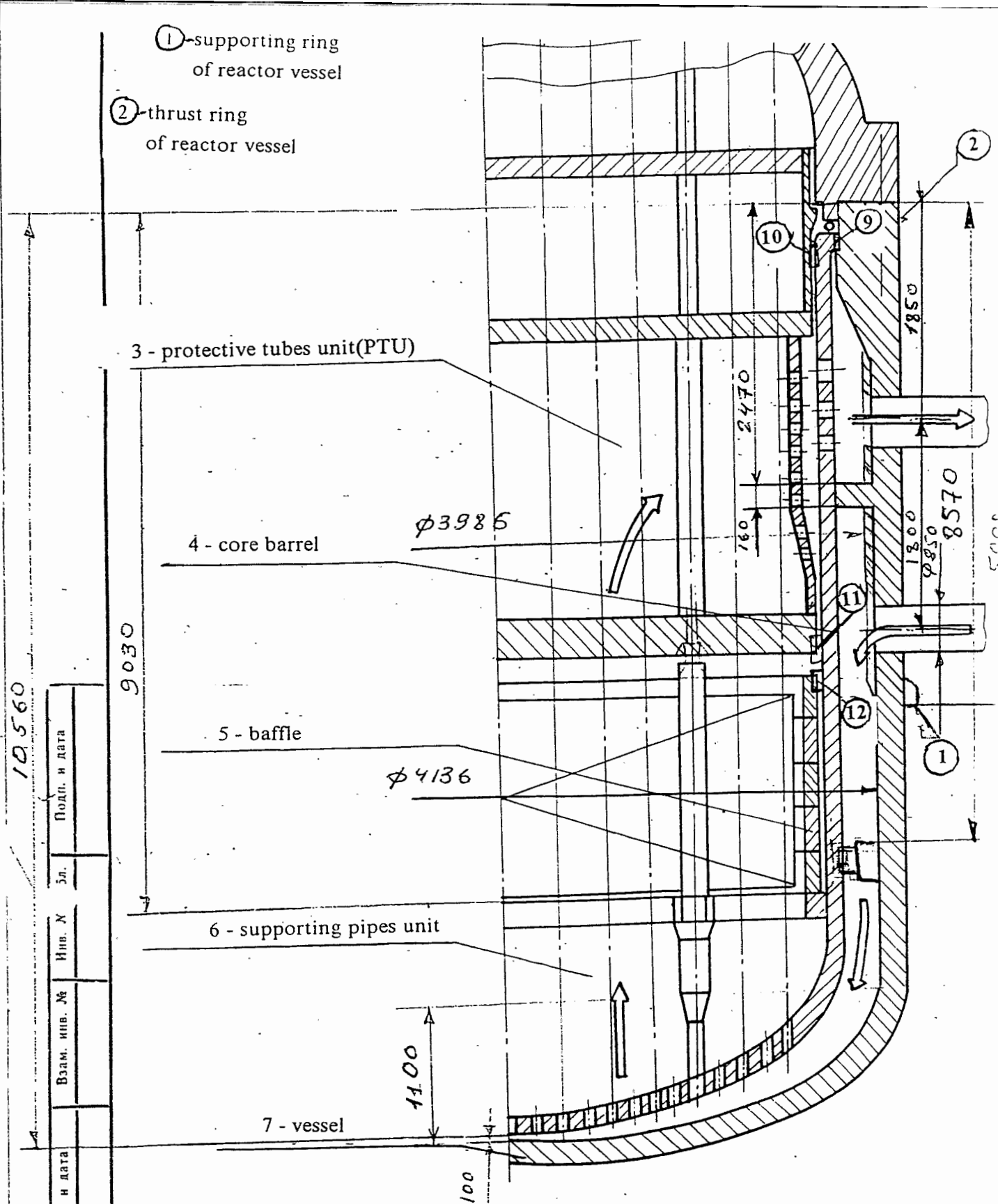


Fig. 1. Mutual location of reactor internals

- ⑨- reactor vessel keys
- ⑩- PTU keys
- ⑪- core barrel keys for PTU
- ⑫- core barrel keys for baffle

Подп. и дата	Взам. инв. №	Инв. №	Эл.	Подп. и дата

Рис. 2
Fig.

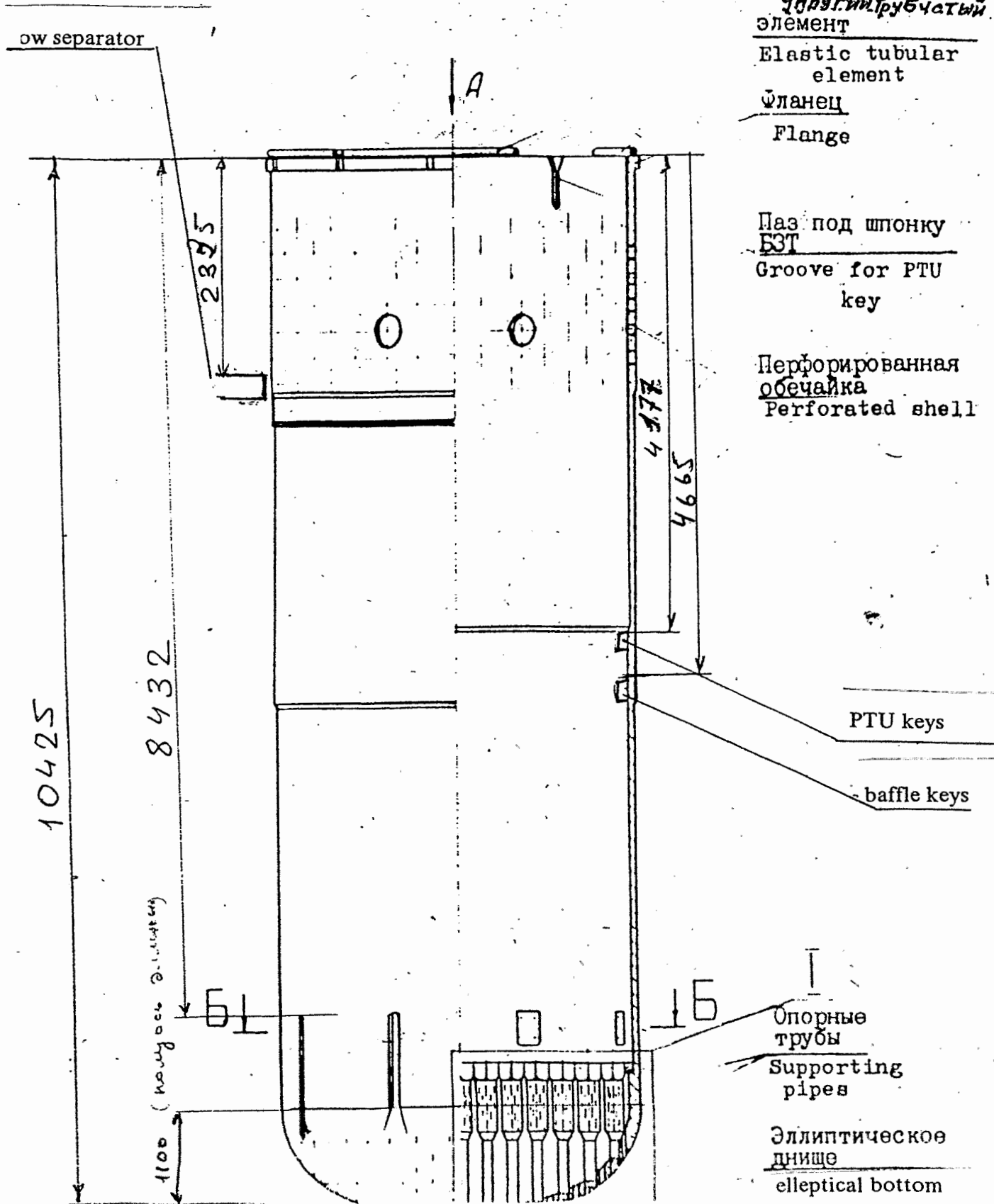
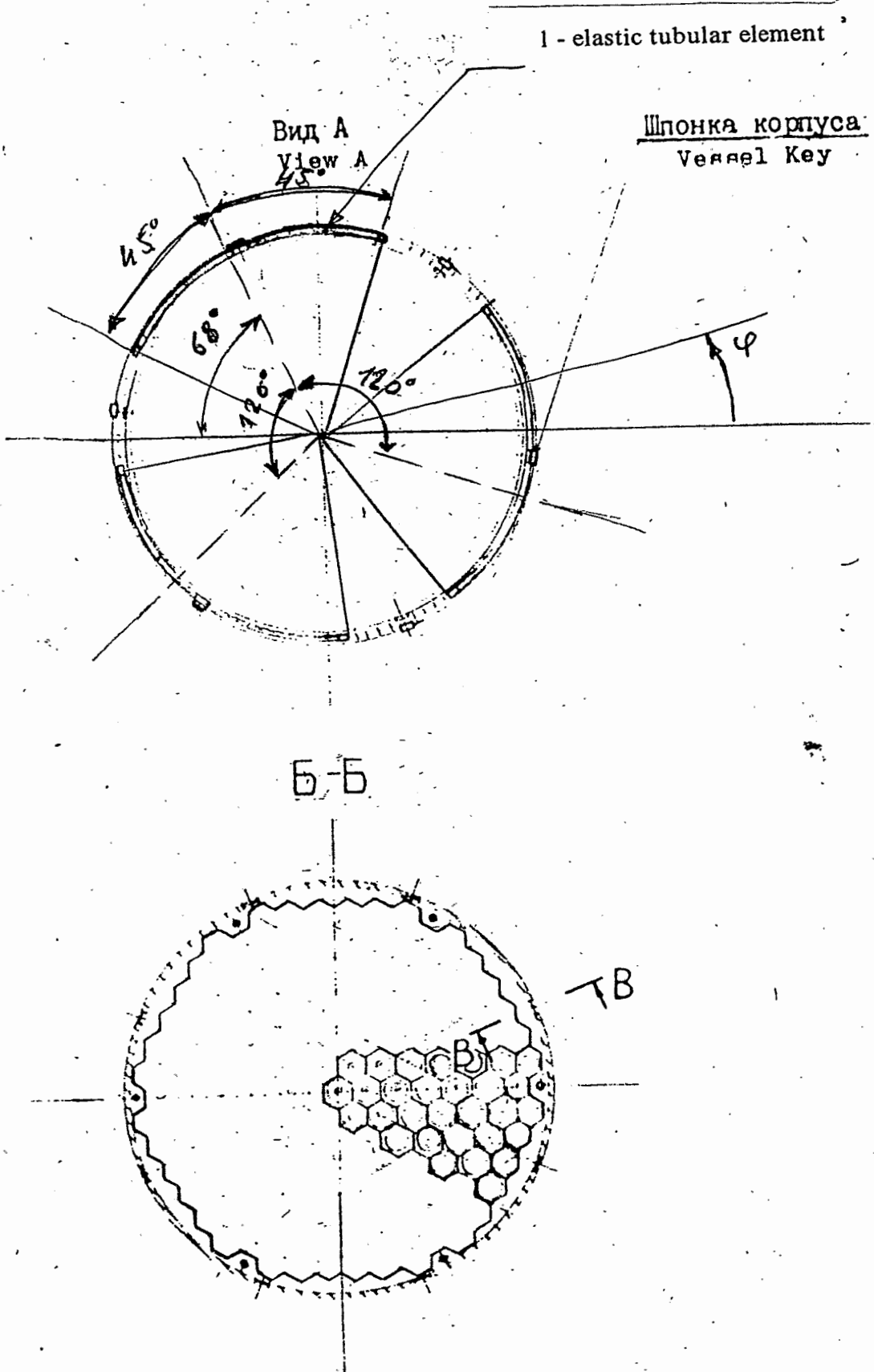
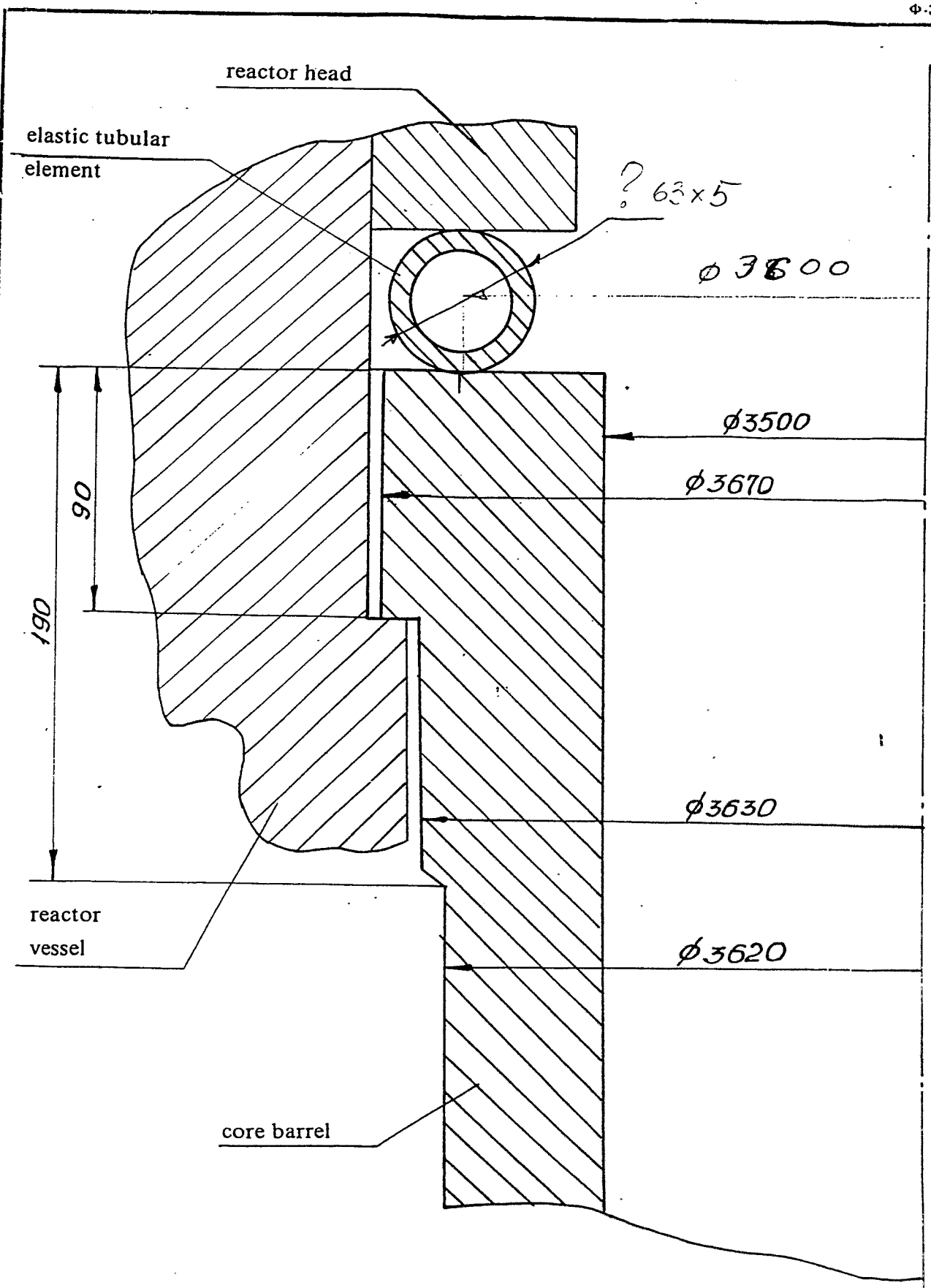


Fig. 3





Подп. и дата	
Взам. инв. №	Инв. №
Взам. инв. №	Инв. №
Подп. и дата	

Fig. 4. Upper support assembly of core barrel

№ докум.	Подп. и дата	Взам. инв. №	Изм. № дубл.	Подп. и дата

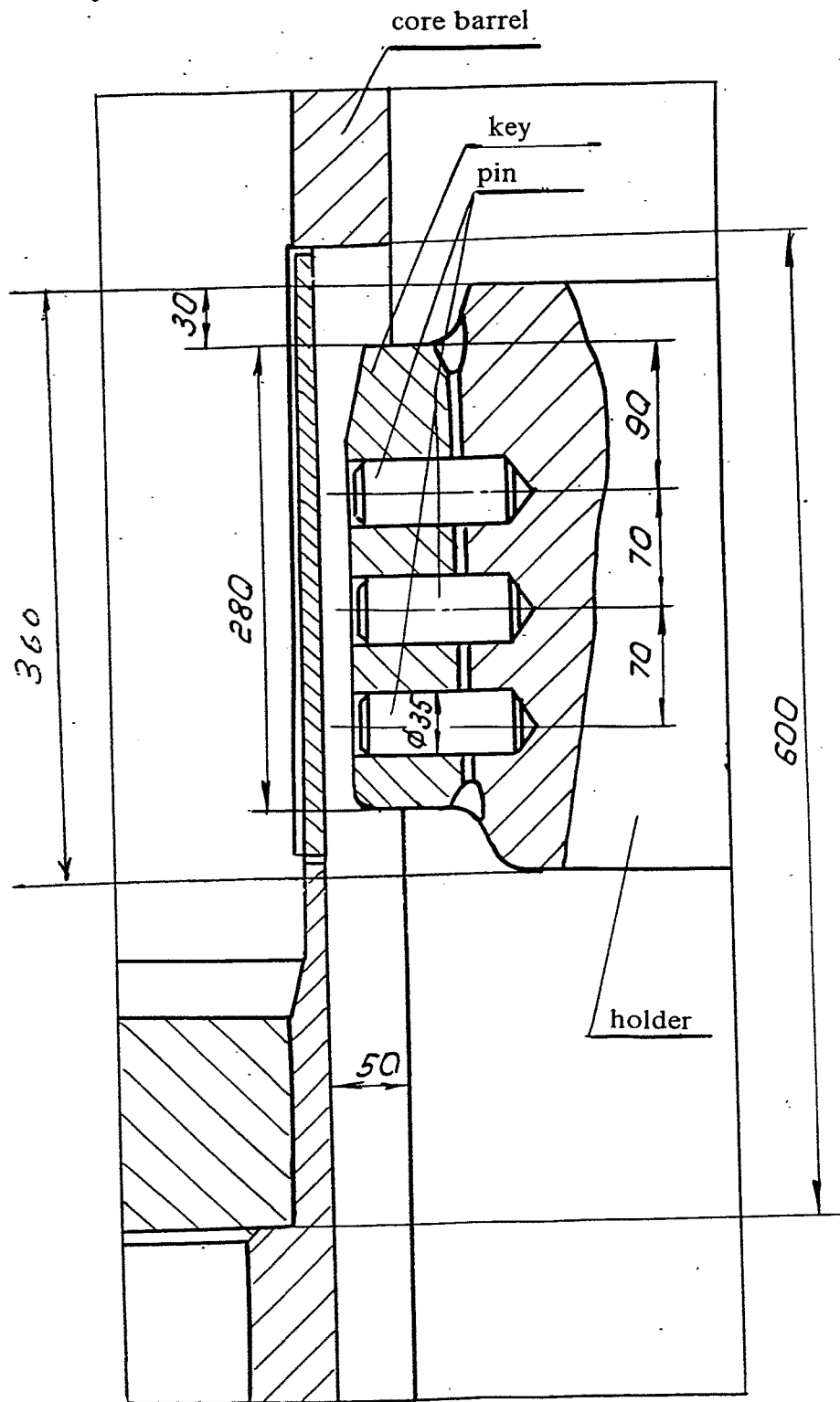


Fig. 5. Lower support assembly of core barrel
(vertical section)

эл.	Подп. и дата	Взам. инв. №	Инв. № дубл.	Подп. и дата

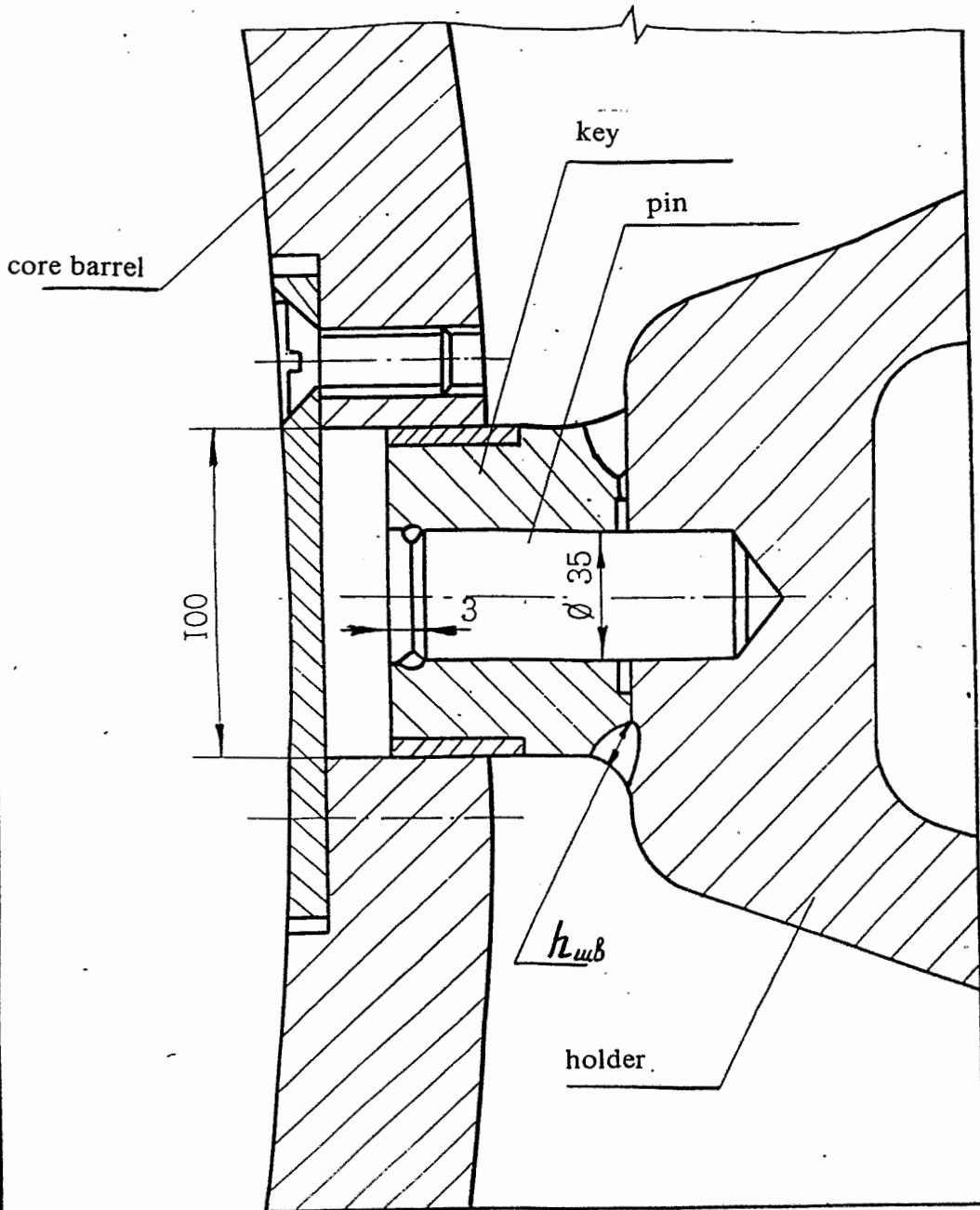


Fig. 6. Lower support assembly of core barrel
(horizontal section)

подл.	Подп. и дата	Взам. инв. №	Инв. № дубл.	Подп. и дата

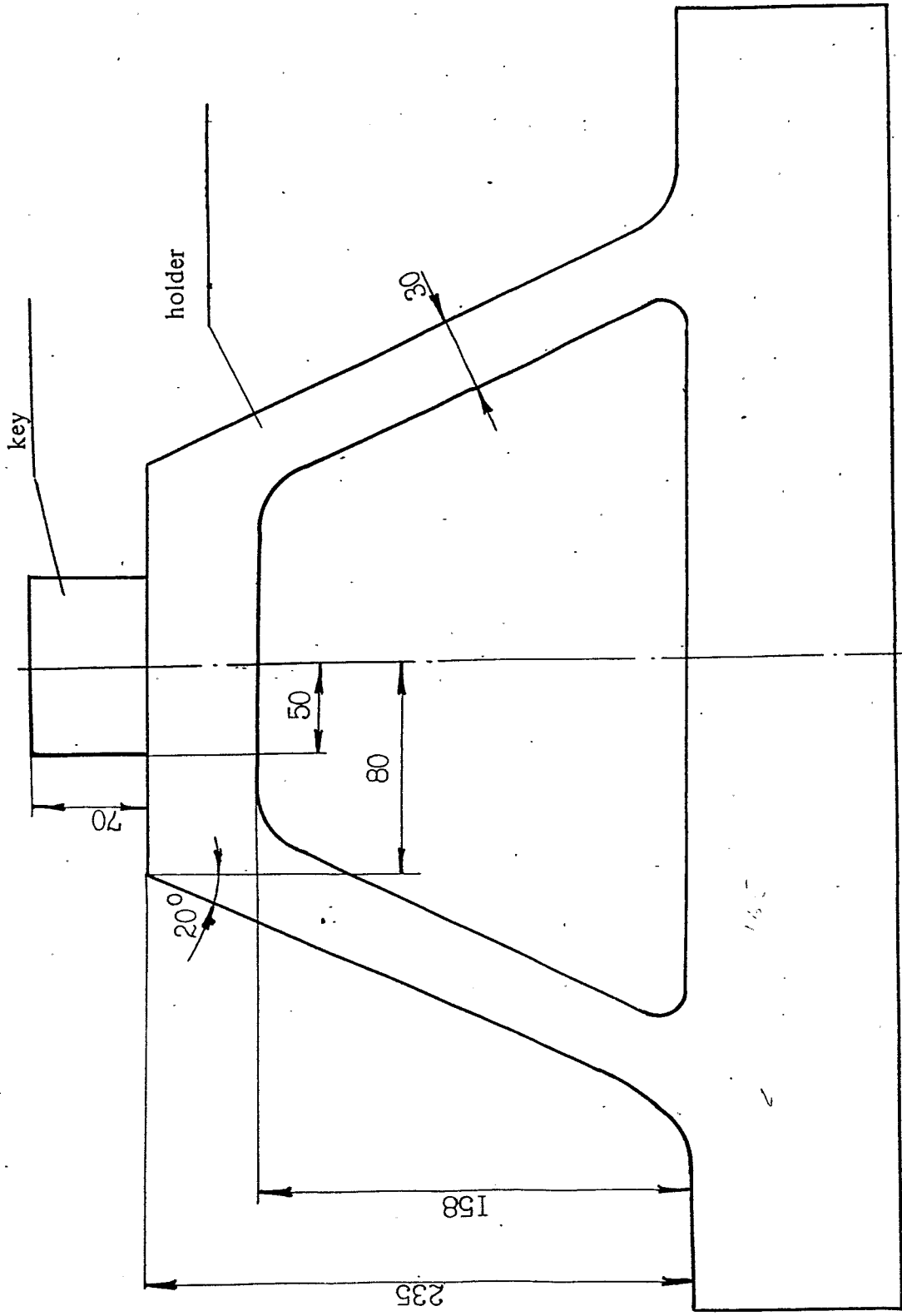


Fig. 7. Holder's cross section

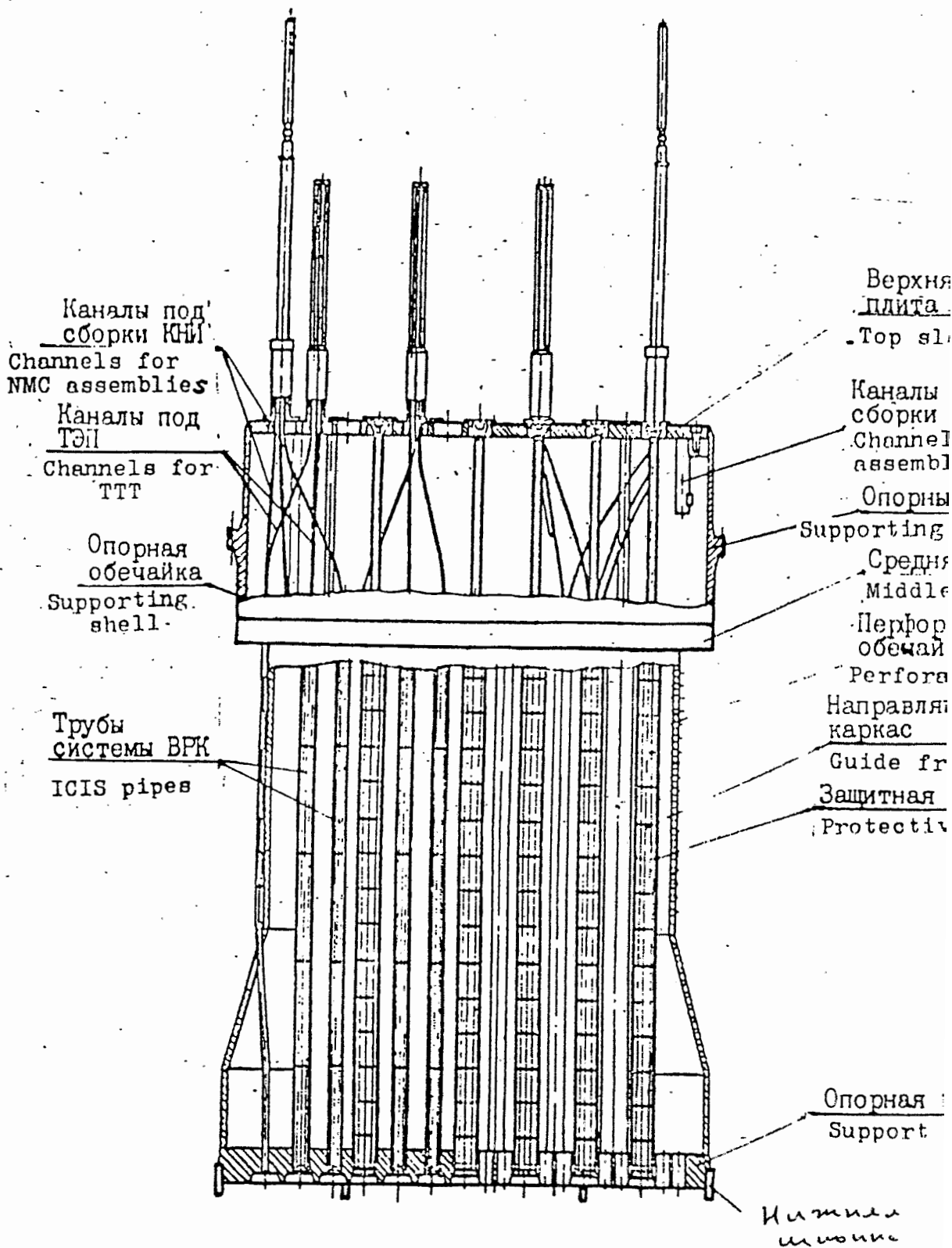


Fig. 8

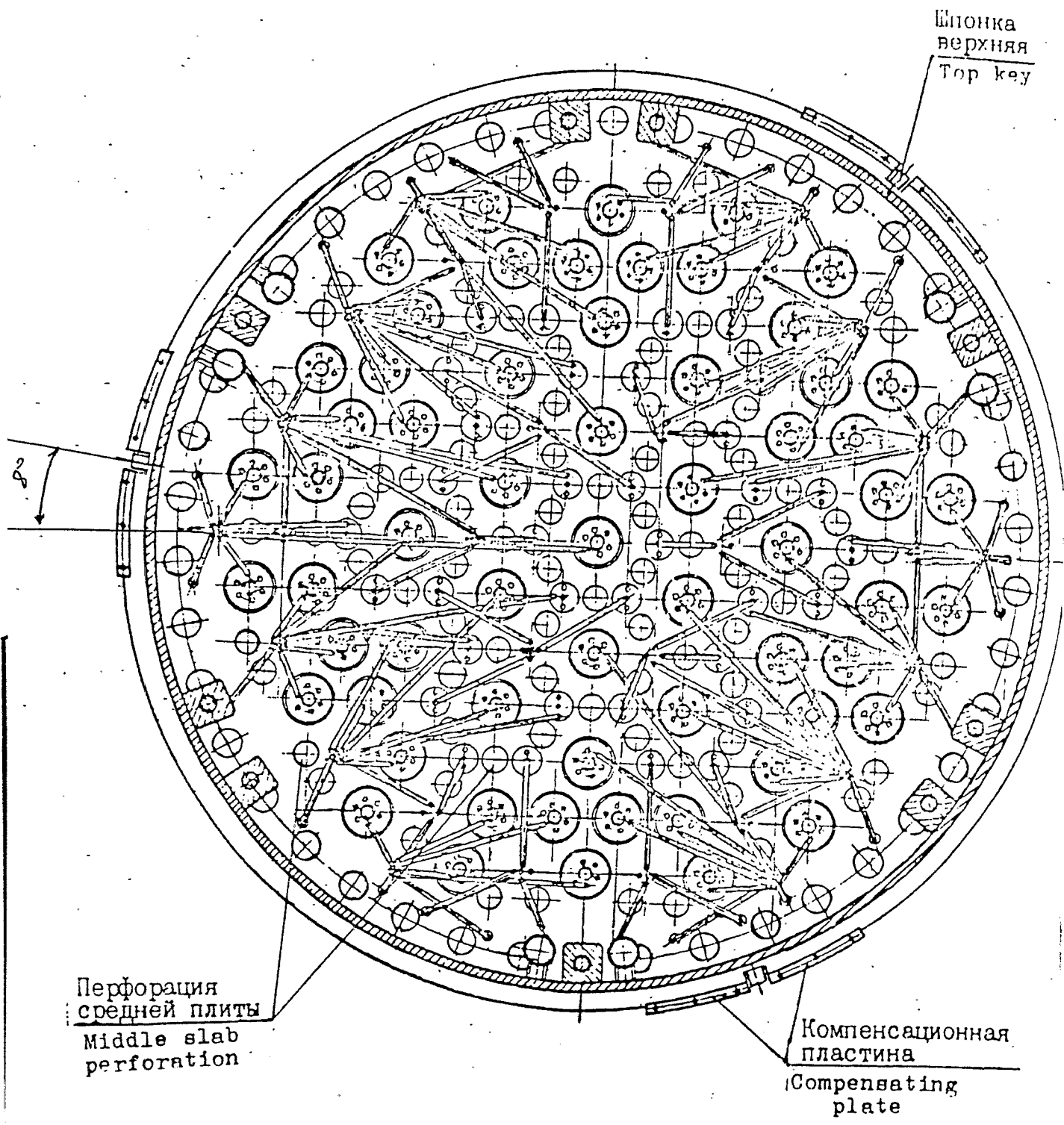


Рис. 9
Fig. 9

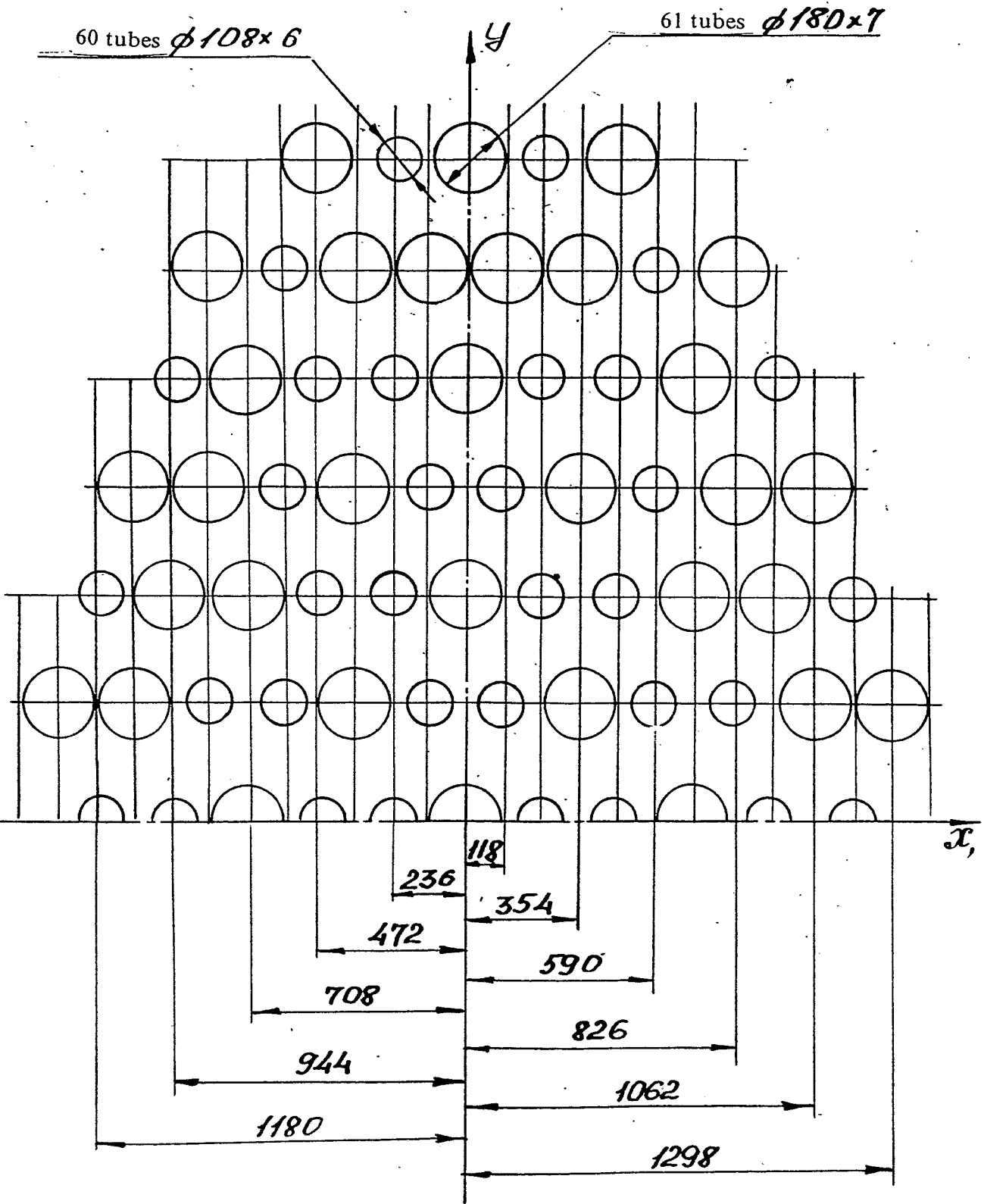
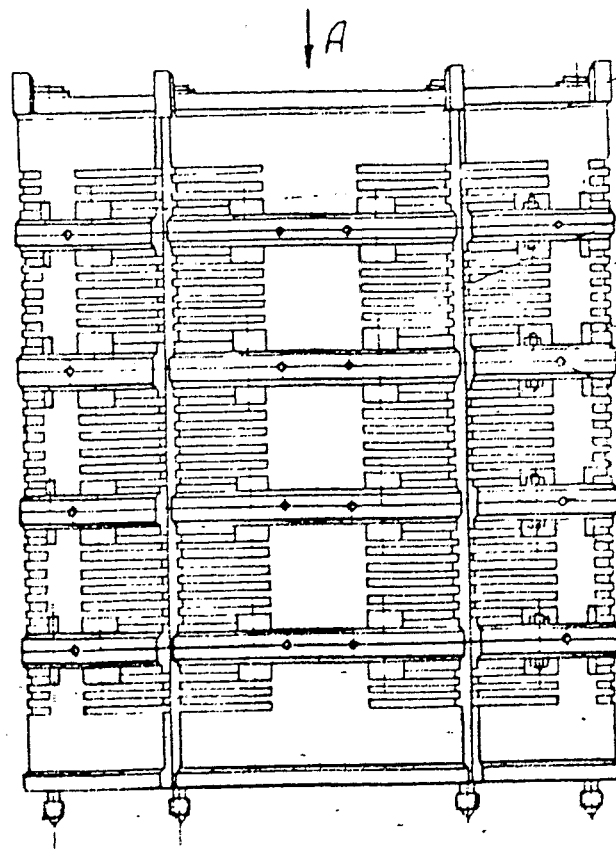


Fig. 11. Scheme of PTU location relatively of symmetry axis



Шпилька

Key.

Продольные каналы

Longitudinal channels

Поперечные каналы

Transverse channels

ШТИФТЫ

Pins

Шпилька

Stud

Кольцо

Ring

Вид А
View A

Места под сборочные образцы-свидетельства

Places for witness specimens

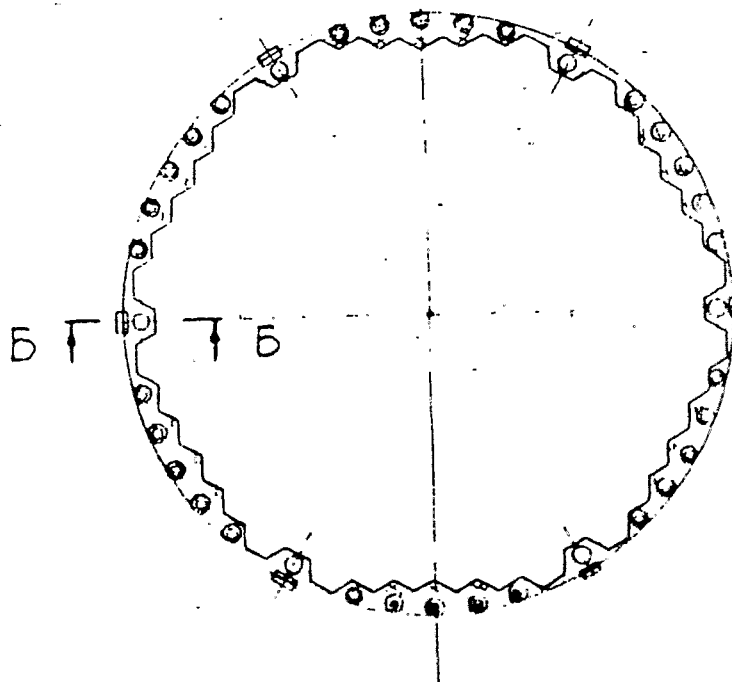


Fig. 12

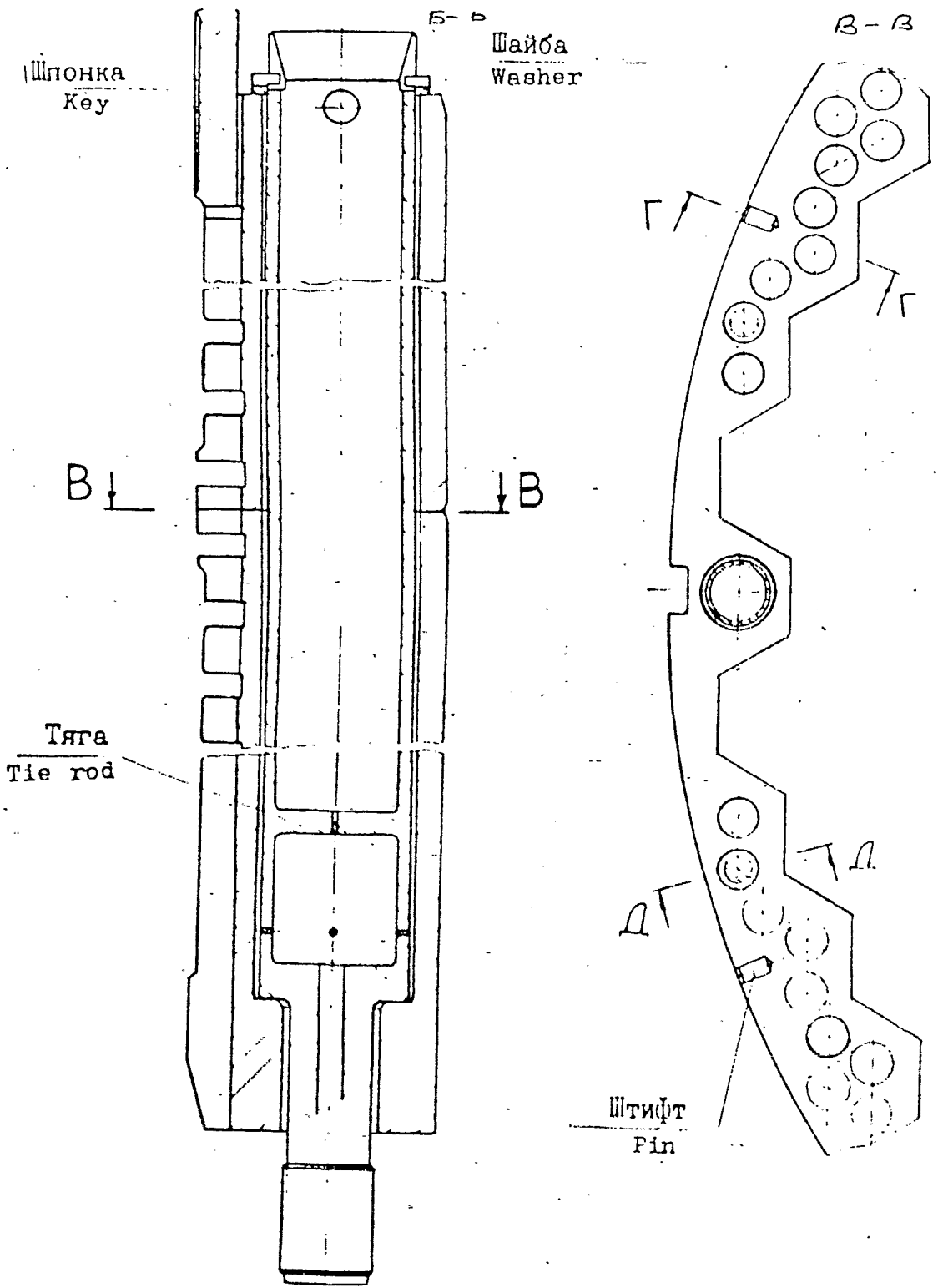
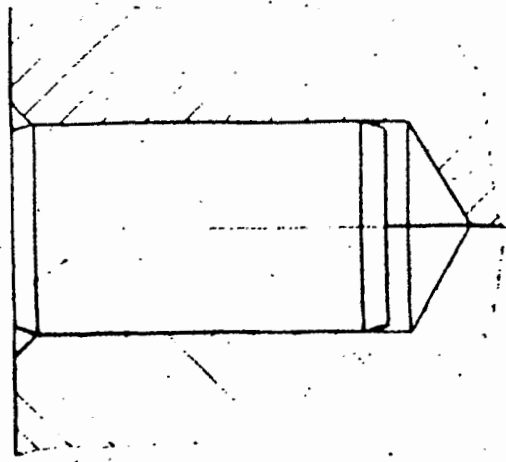


Рис.
Fig. 13.

ШТИФТ
Pin



A-A

Шпилька
Stud

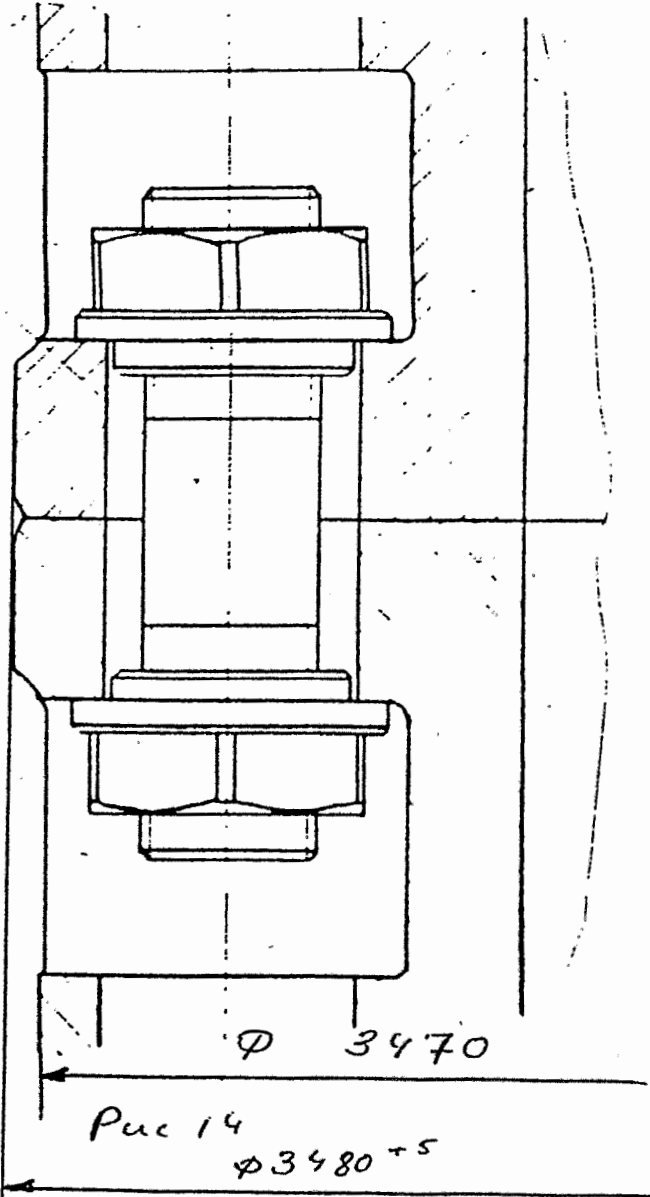


Рис 14
 $\varnothing 3480 \pm 5$

Fig. 14

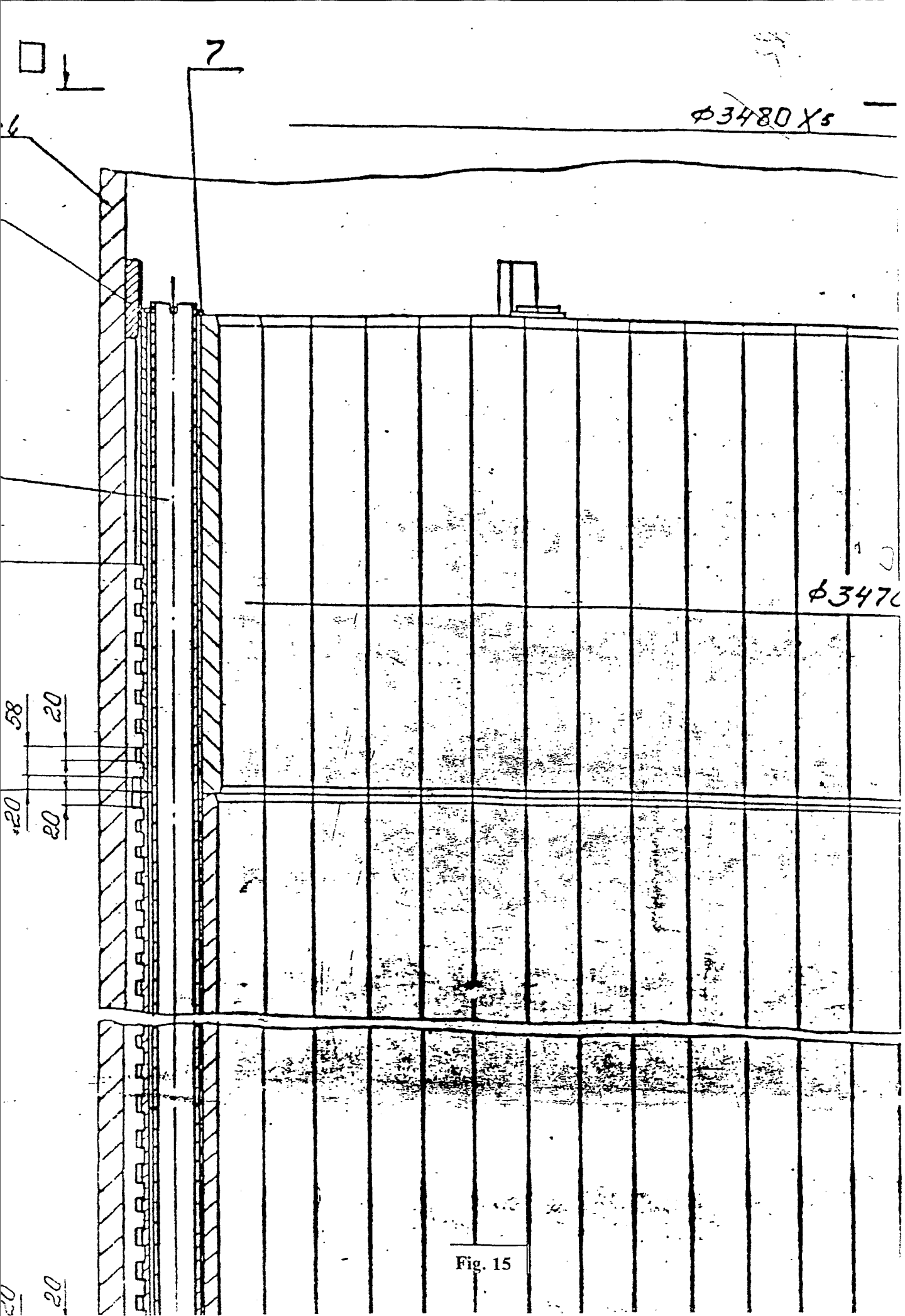
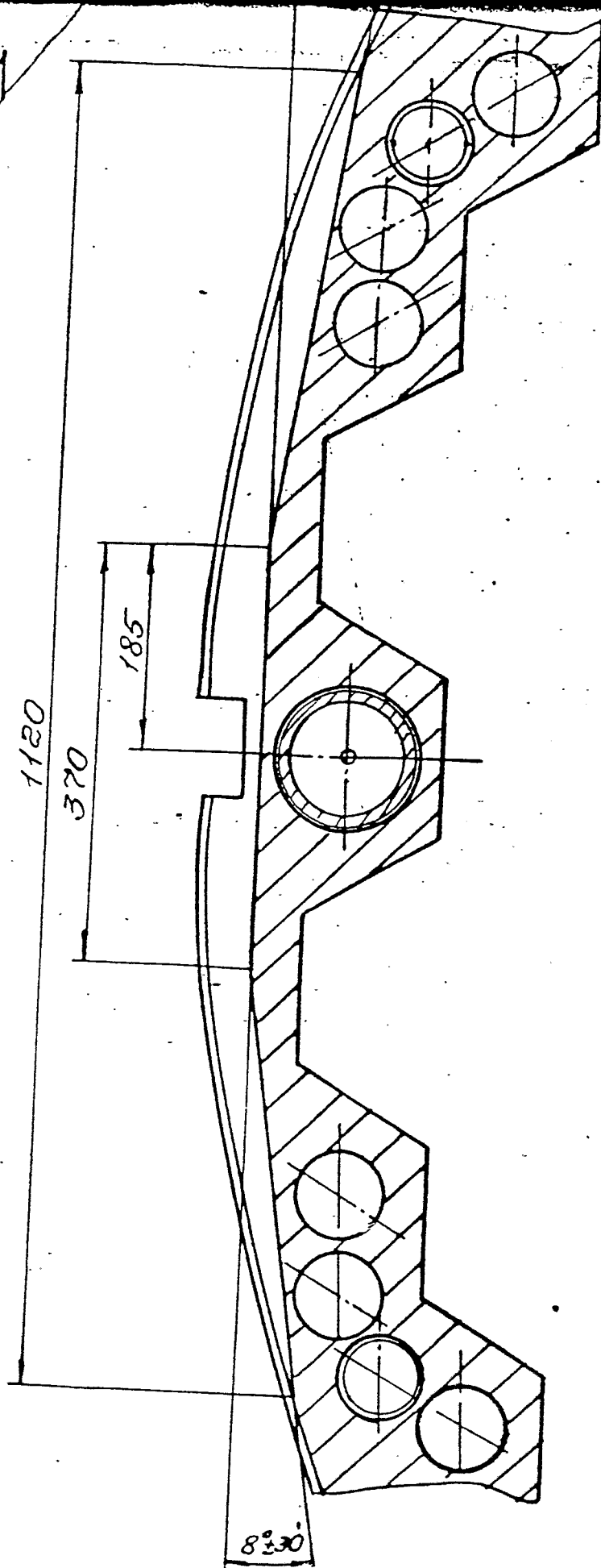


Fig. 15



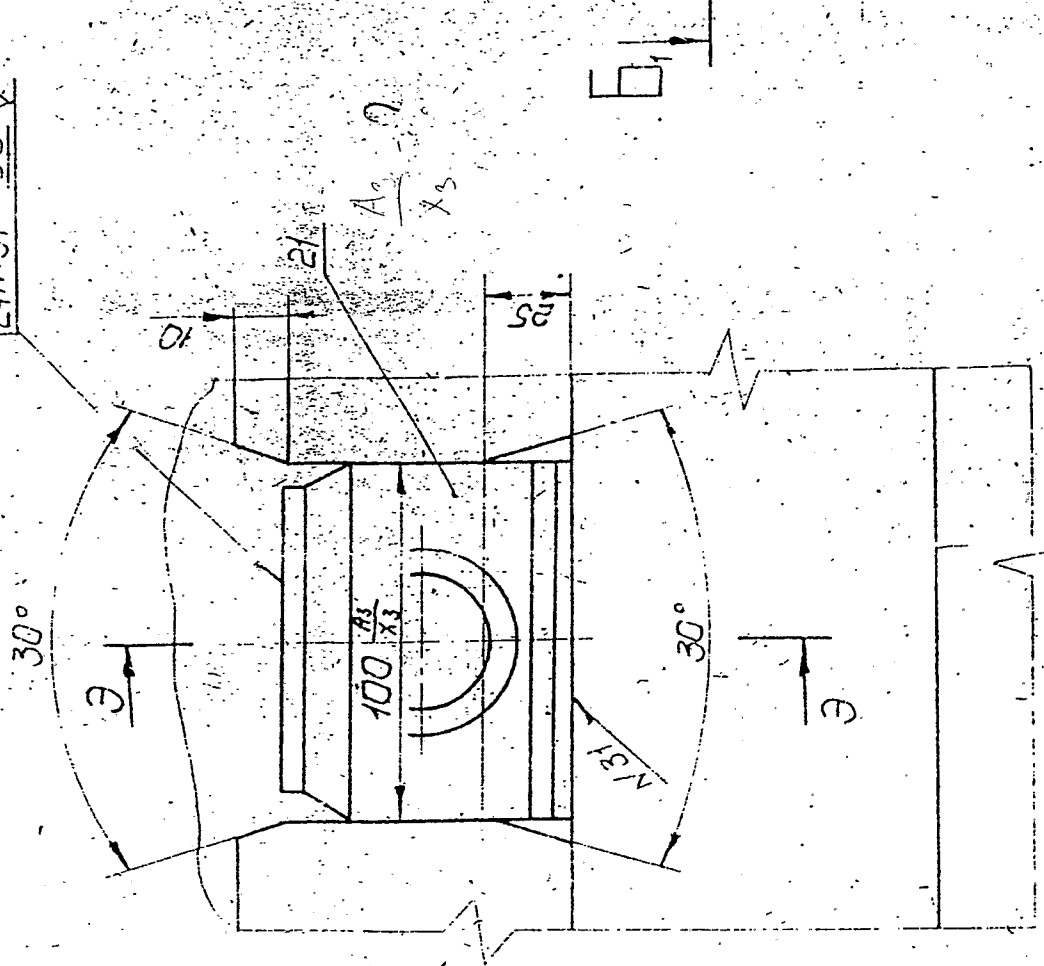
8^{±0.30}

Fig. 16

Вид В
View
M 1:2

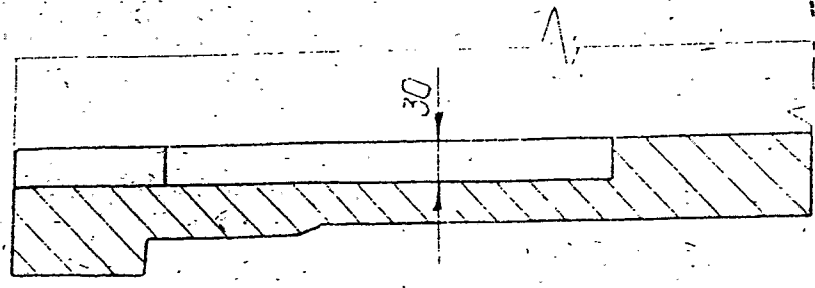
повернуто зона B14
turned zone B14

24N.31 R20



2 - reactor vessel's keys in the core barrel's flange

30HC B29
zone
M 1:5



1 - core barrel's grooves for PTU keys

Fig. 17

30HC зона B14
zone B14

Вид
View

H

поверхность
turned
30H8
zone B14

M 1:5

Вид
View

□

поверх
tur

M 1:5

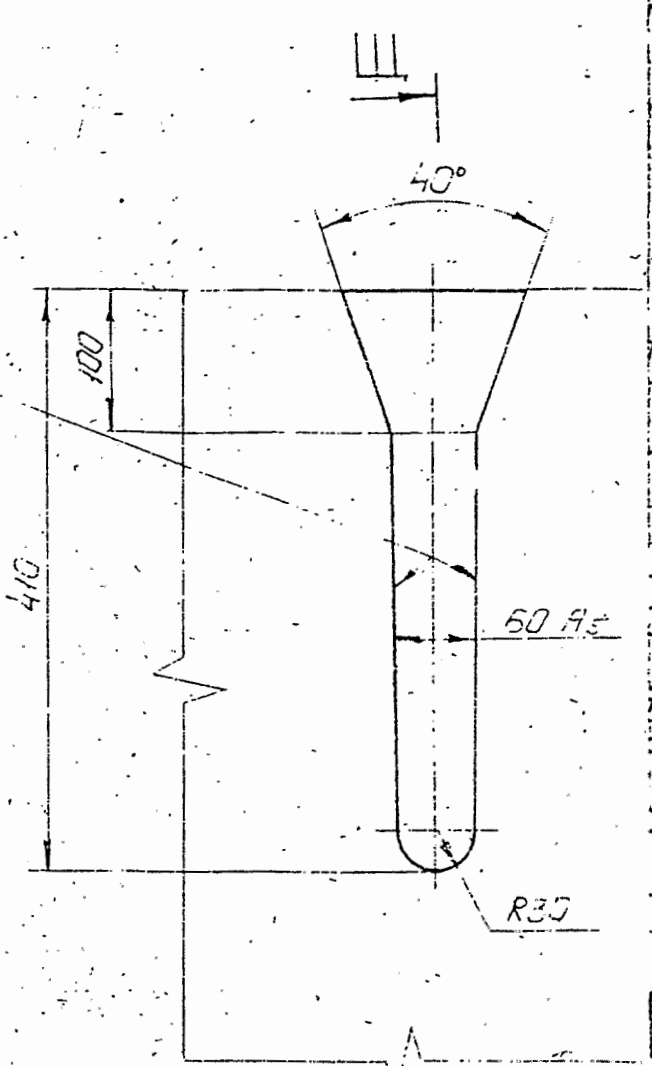
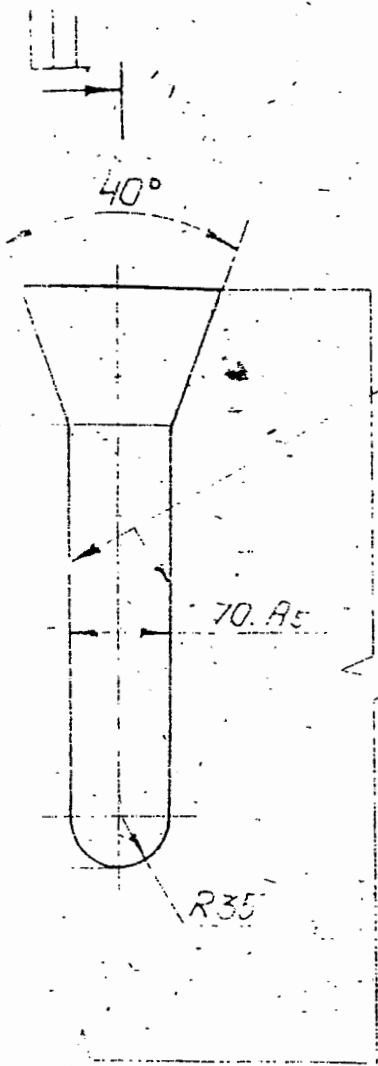


Fig. 18. Core barrel's grooves for PTU keys

30H8
zone A31

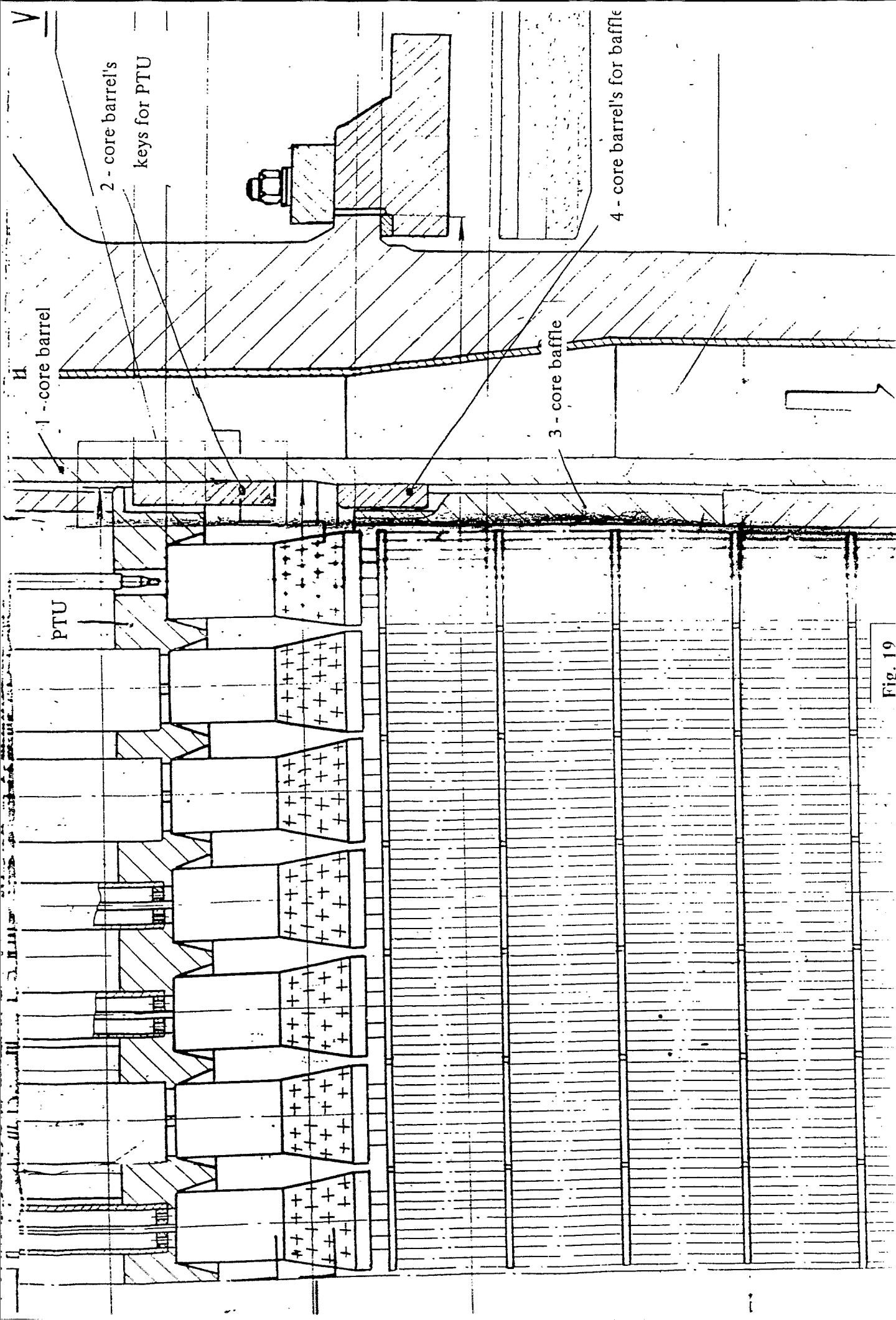
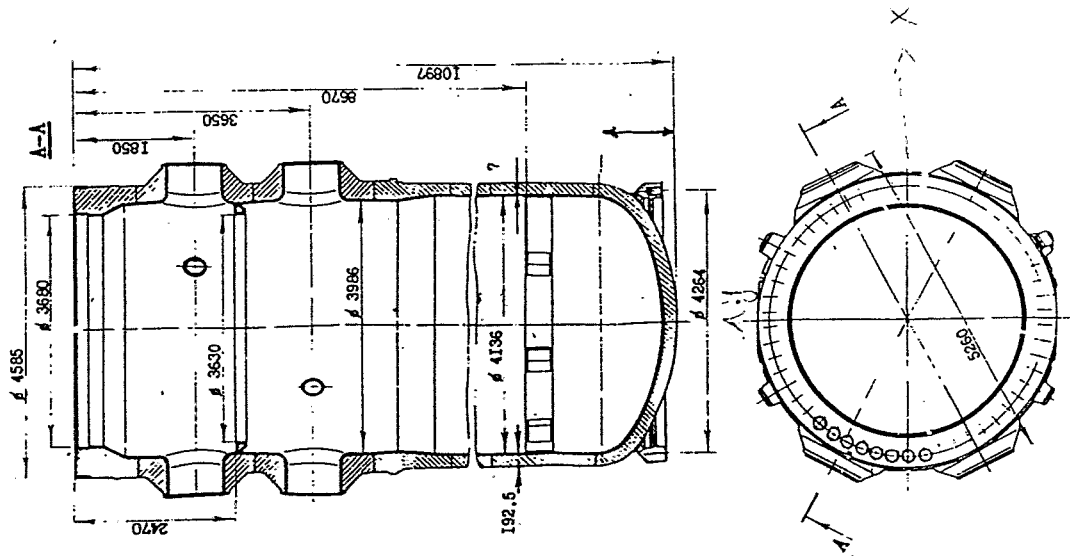
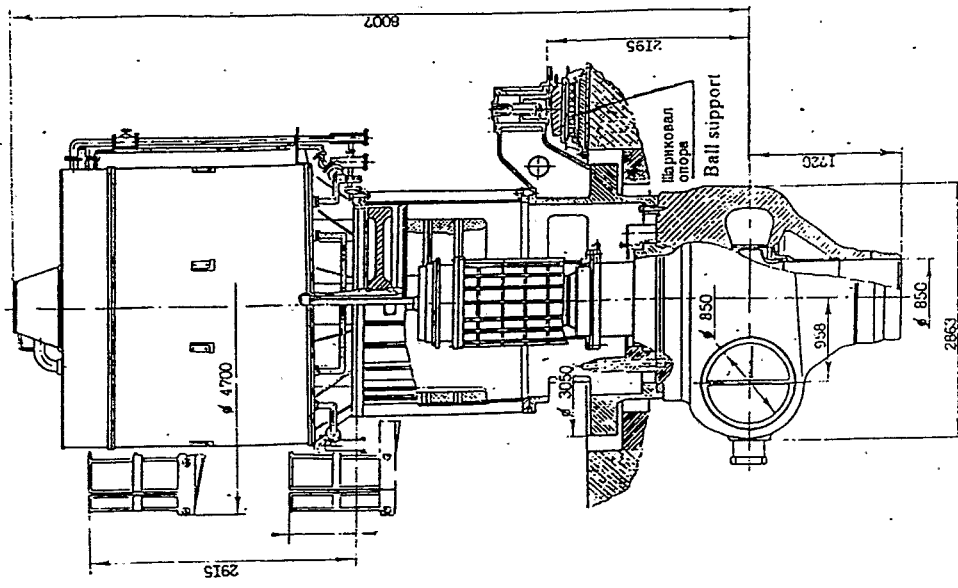


Fig. 19



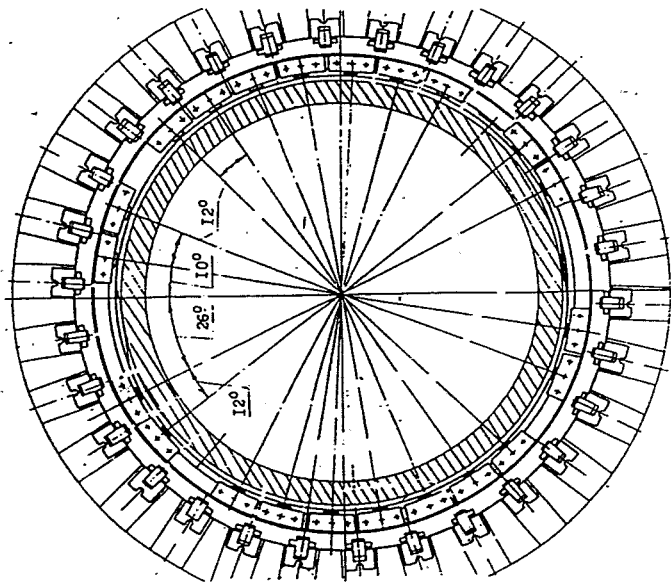
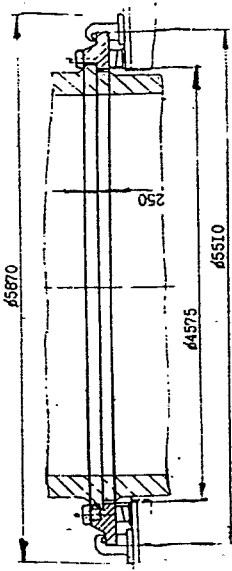
Корпус реактора
Reactor vessel

Fig. 21



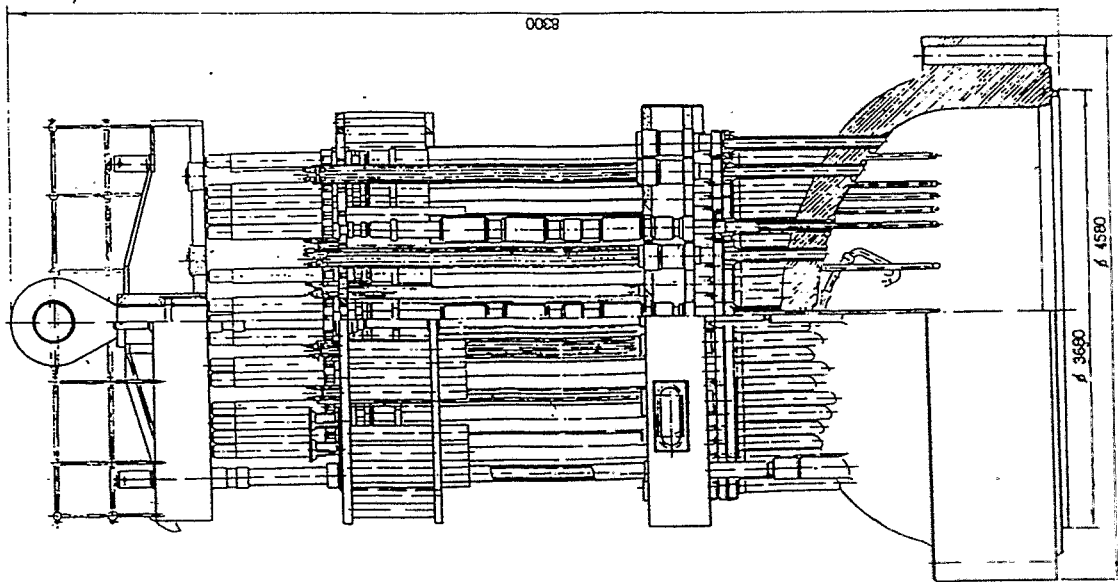
Главный циркуляционный насос ГЦН-195М
Primary coolant pump

Fig. 25



Кольцо опорное
Supporting ring

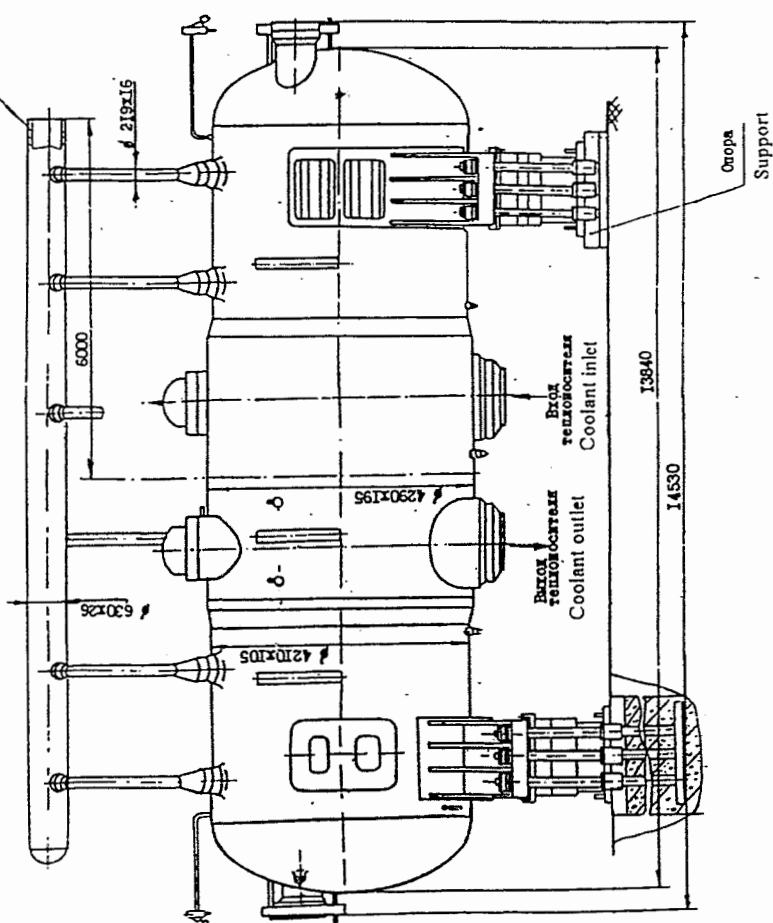
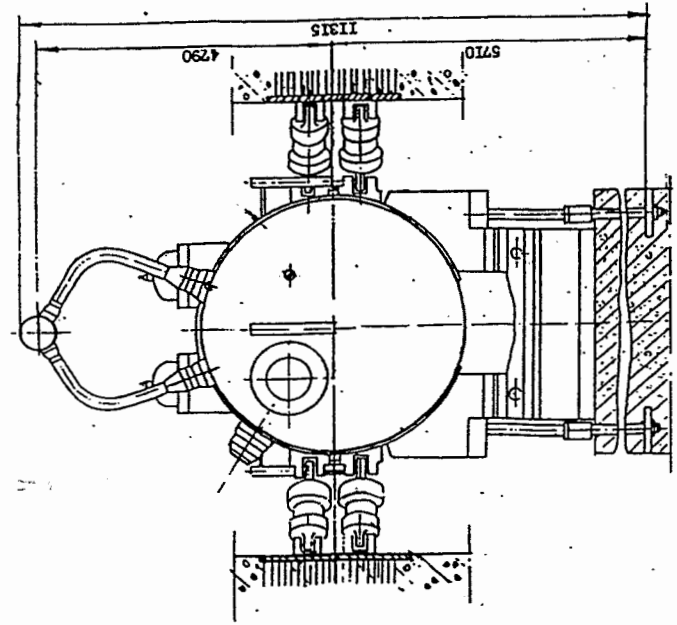
Fig. 22



Верхний блок
Upper controlling block

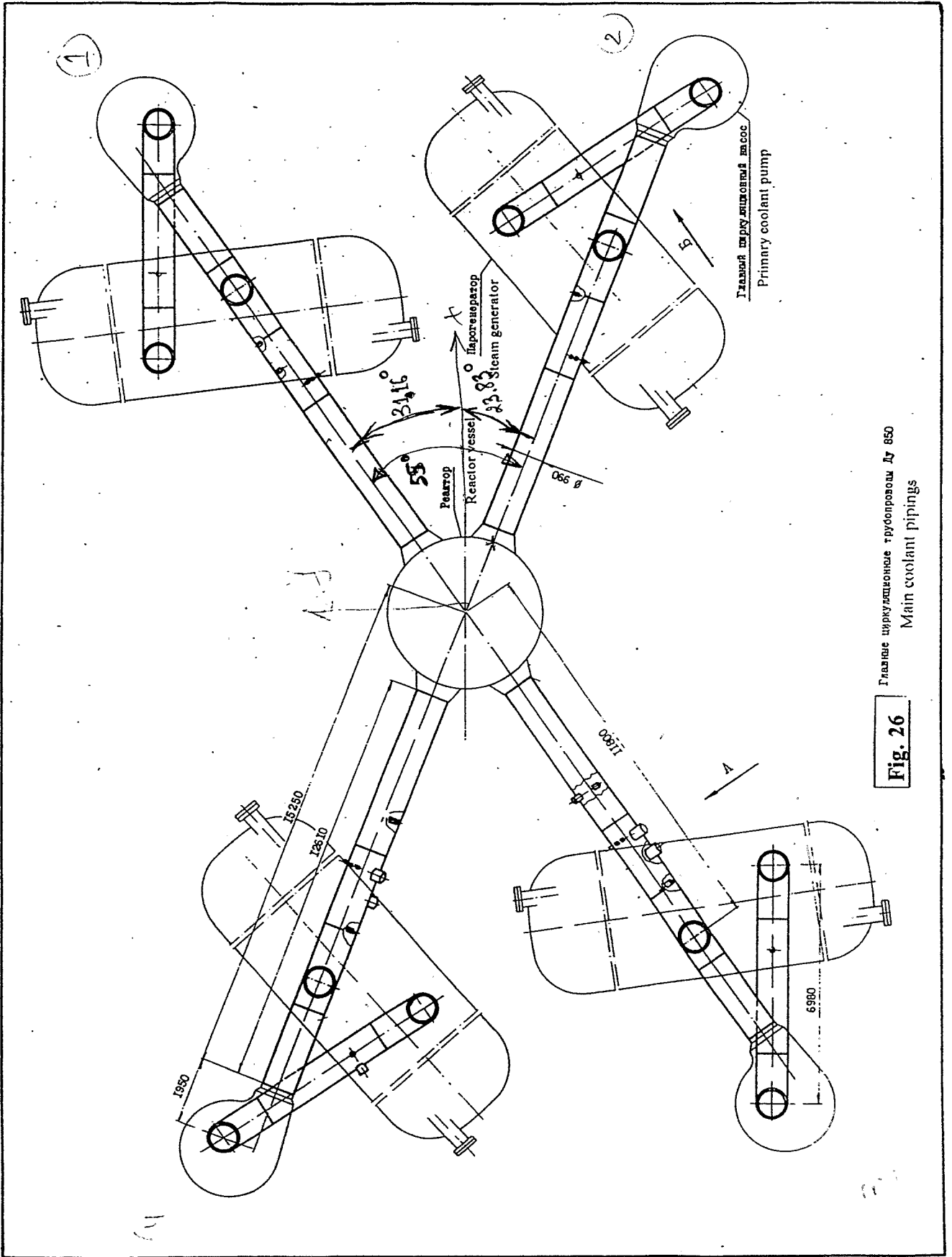
Fig. 23

Паровой коллектор
Main steam collector



Парогенератор
Steam generator

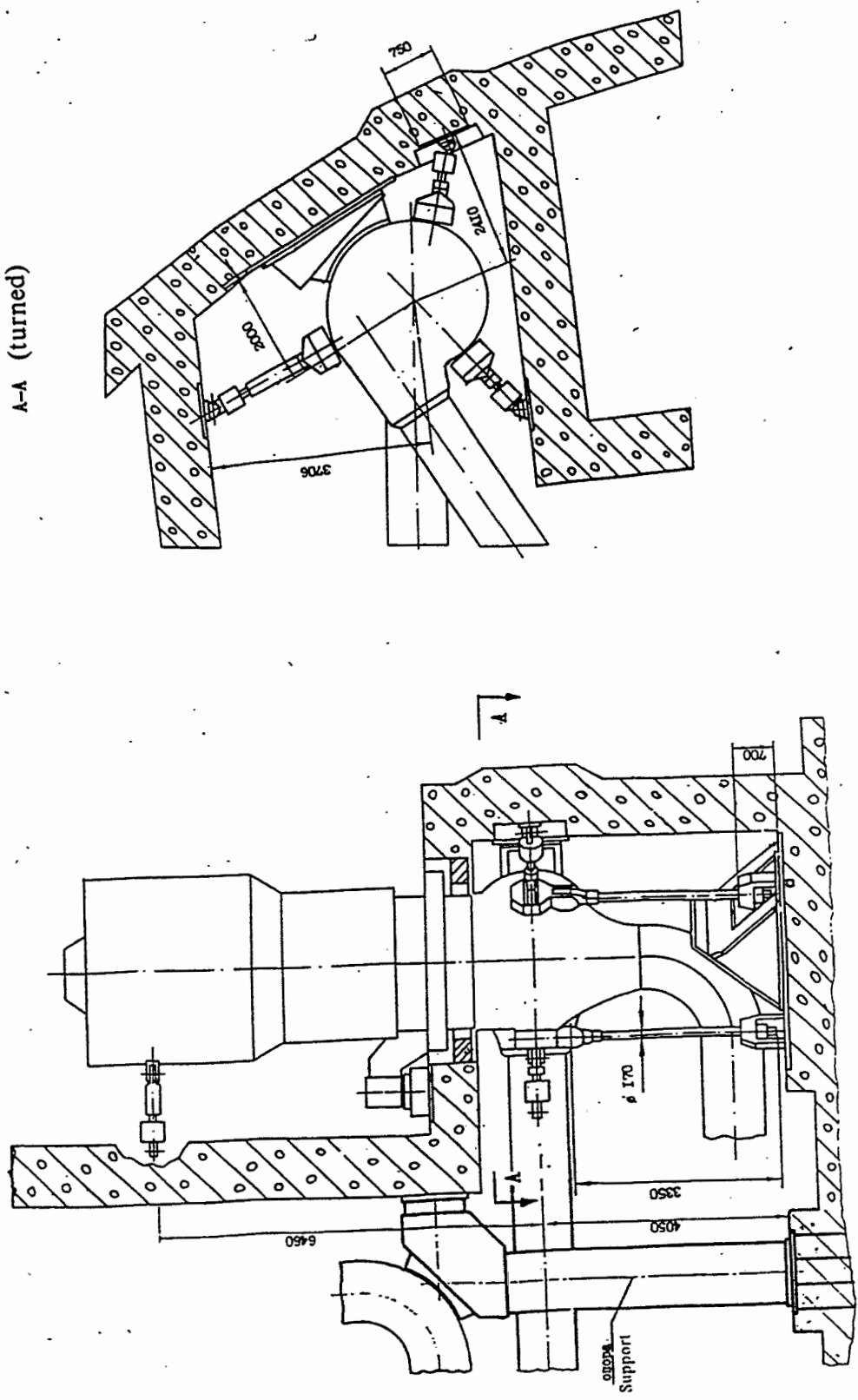
Fig. 24



Главные циркуляционные трубопроводы ДР 650
 Main coolant pipings

Fig. 26

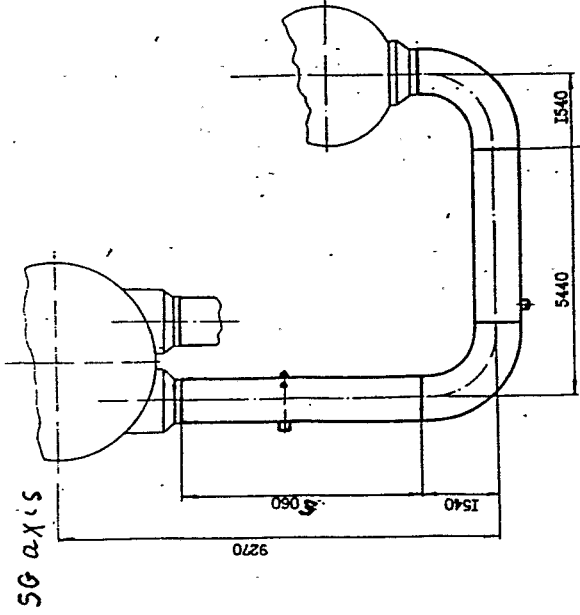
A-A (turned)



Элементы крепления трубопровода ДУ 850

Fig. 27. Primary coolant piping

View B (turned)



View A (turned)

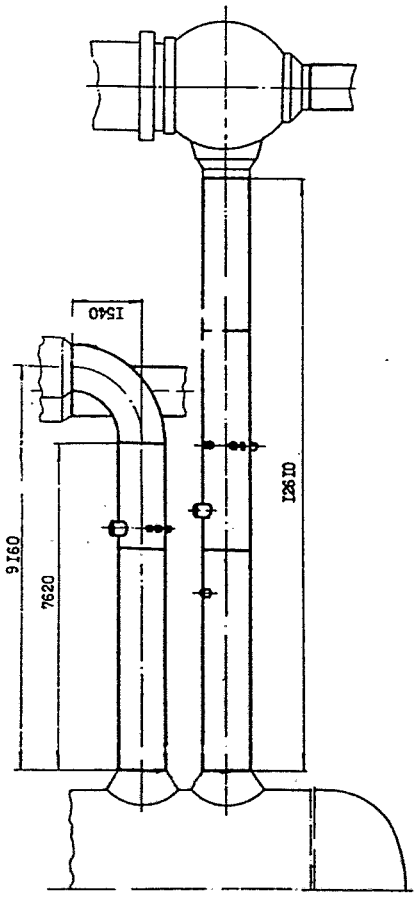


Fig. 28

Инв. № подл.	Подп. и дата	Взам. инв. №	Инв. № дубл.	Подп. и дата
Изм.	Лист	№ докум.	Подп.	Дата

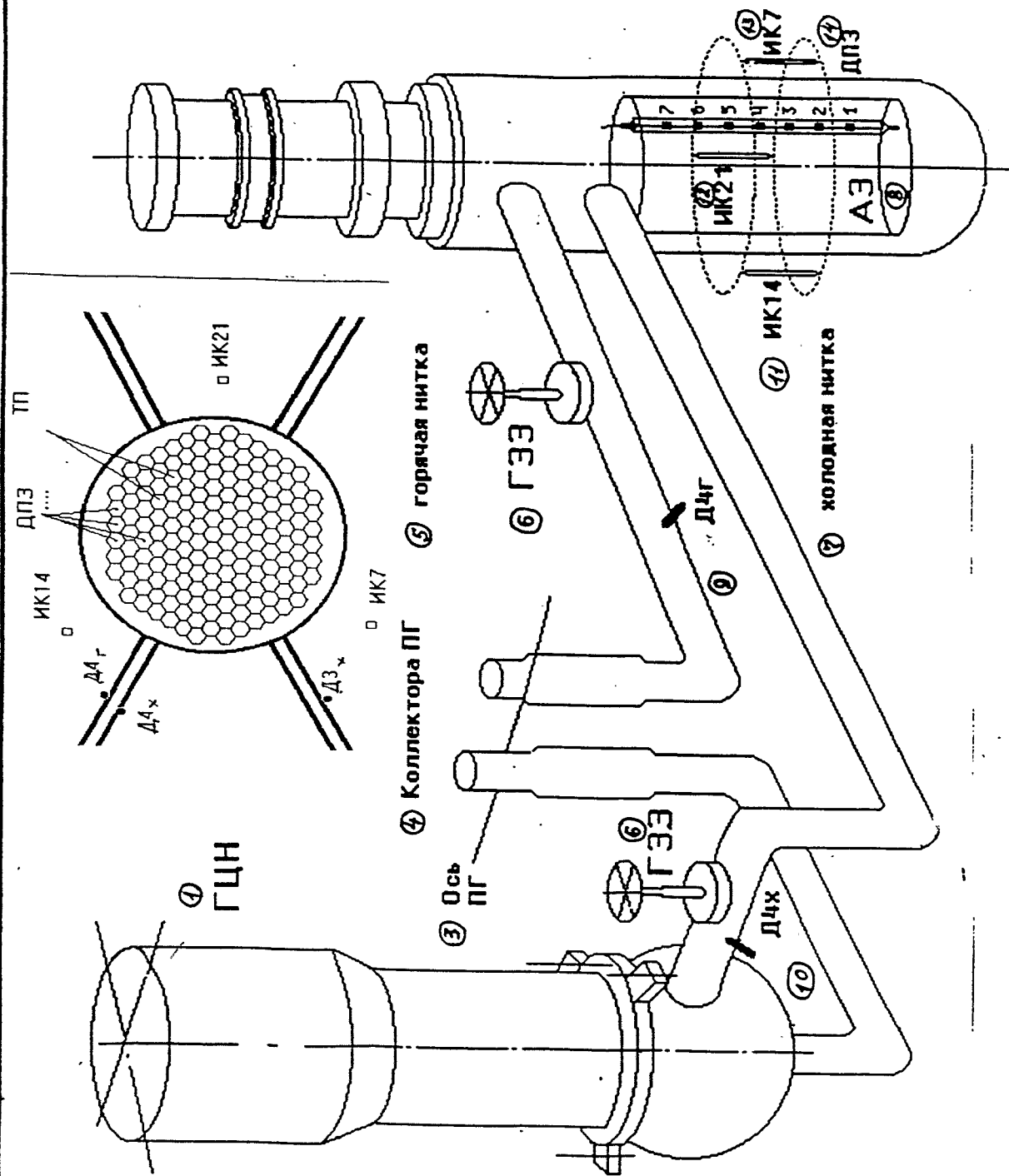


Fig. 29. Detectors arrangement at Kalinin NPP, Unit 1:

- 1. MCP
- 2. Loop No. 4
- 3. SG axis
- 4. SG headers
- 5. Hot leg
- 6. MIV
- 7. Cold leg
- 8. Core
- 9. PPD 4 hot
- 10. PPD 4 cold
- 11. IC 14
- 12. IC 21
- 13. IC 7
- 14. SPD

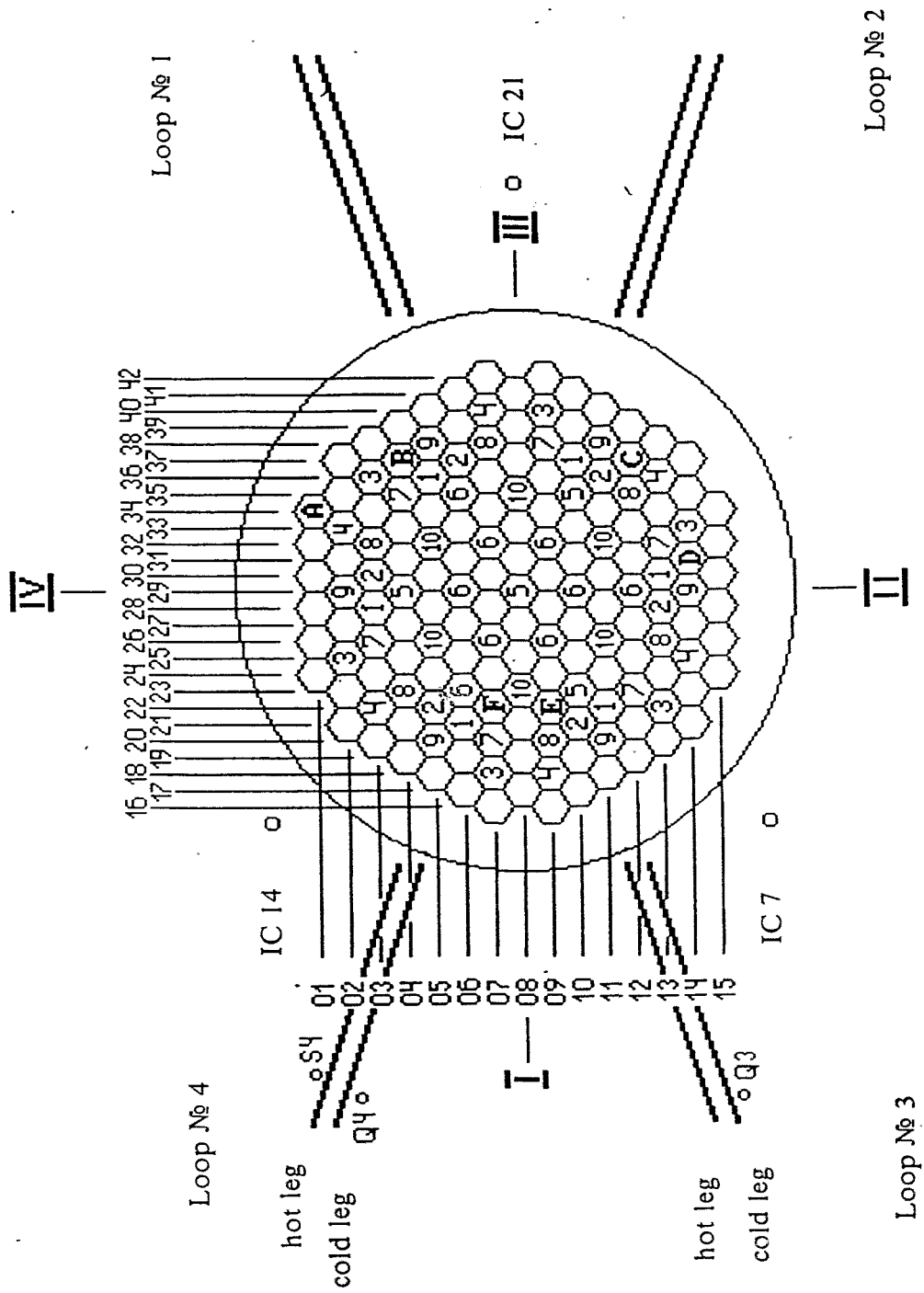


Fig. 30. Location of pressure fluctuation sensors and ionization chambers

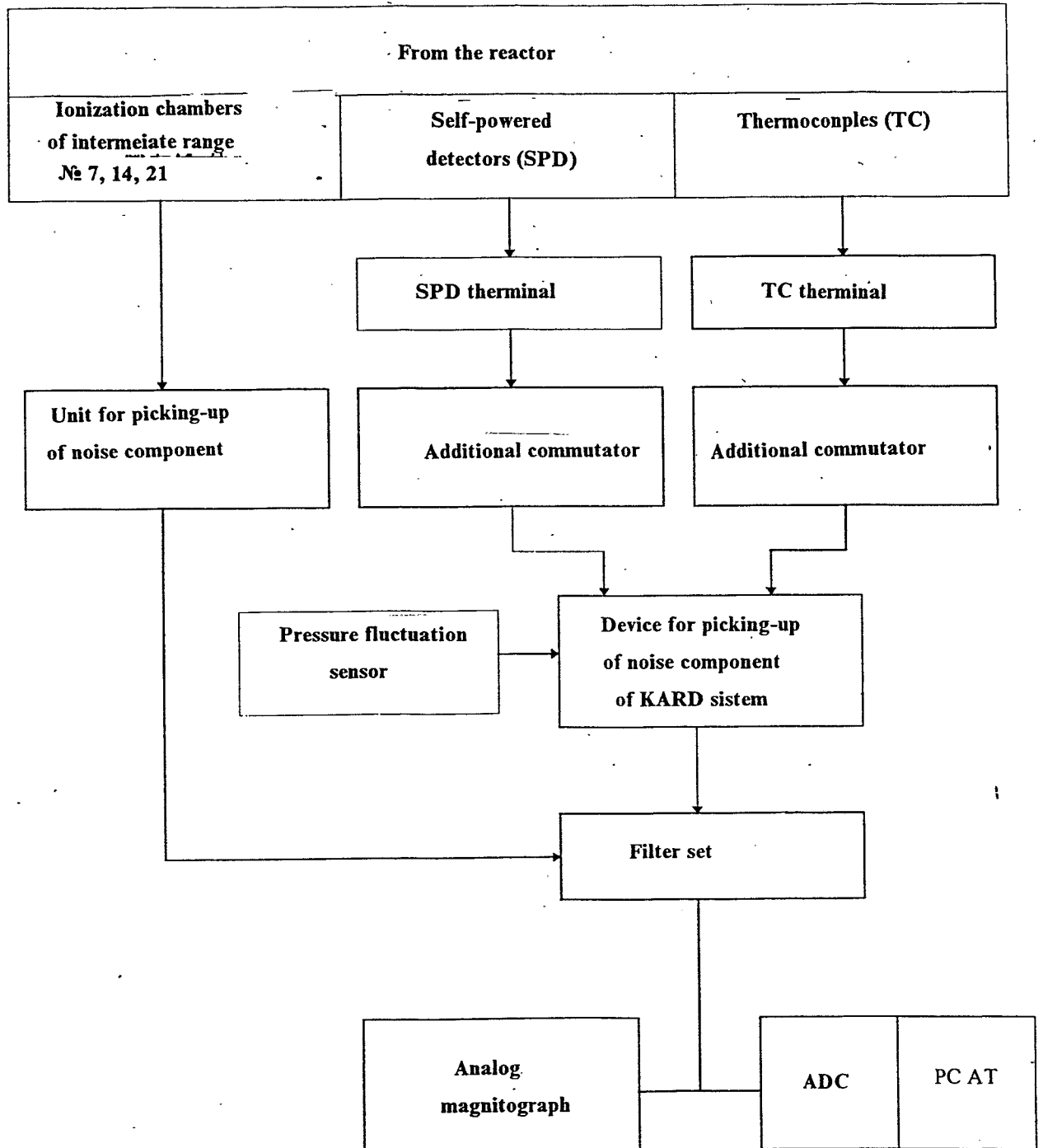


Fig. 31. Measurements scheme

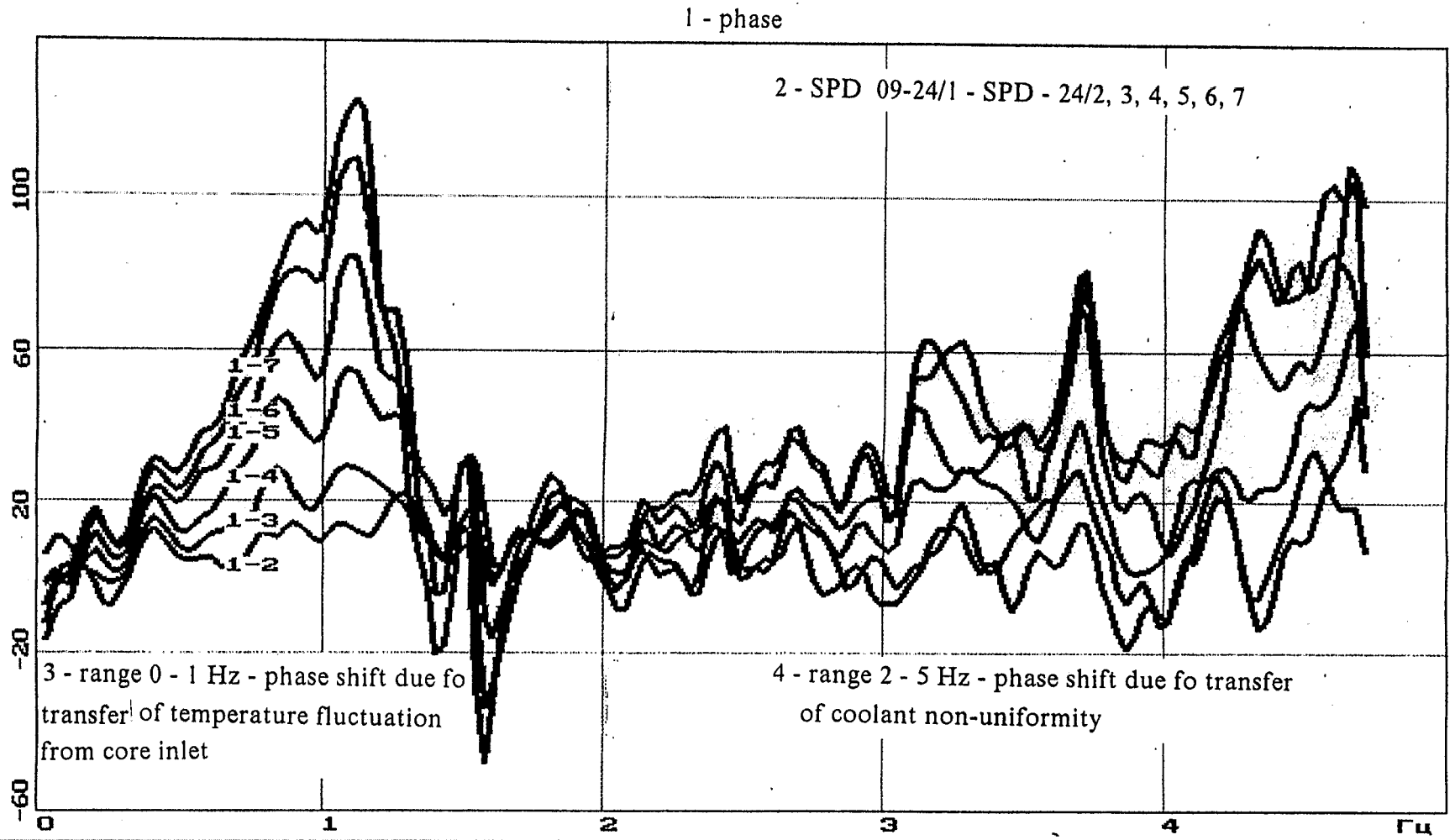


Fig. 33

phase

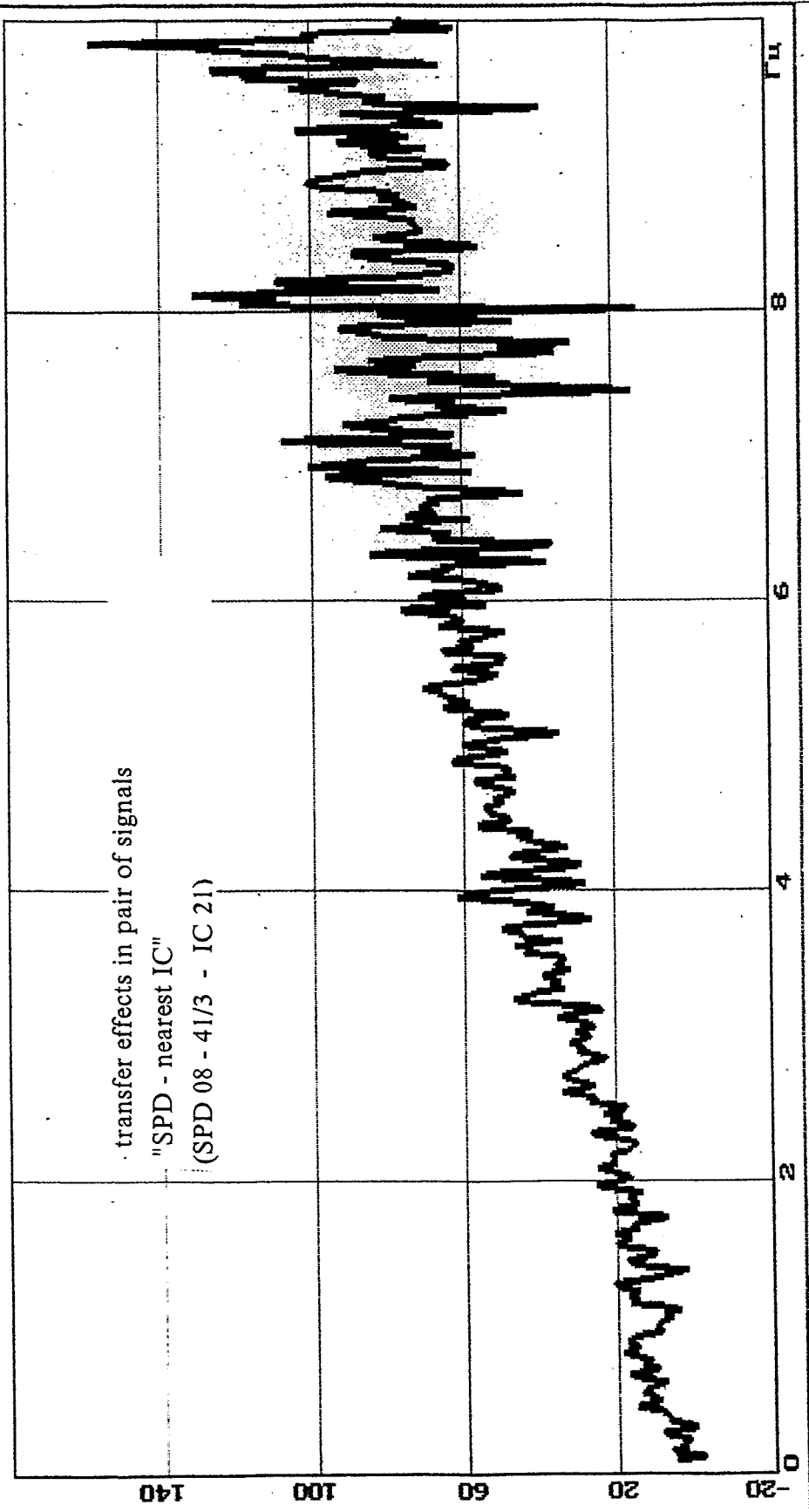


Fig.34

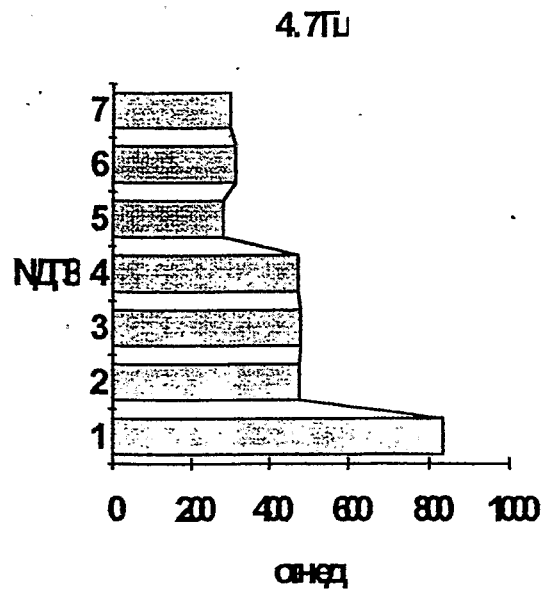
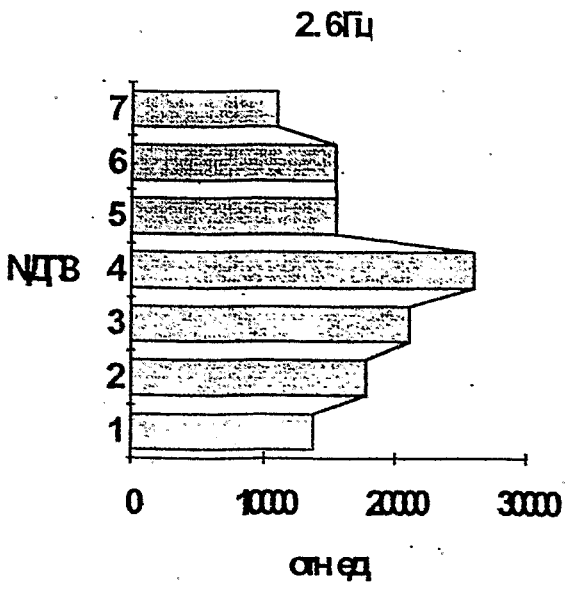


Fig. 35

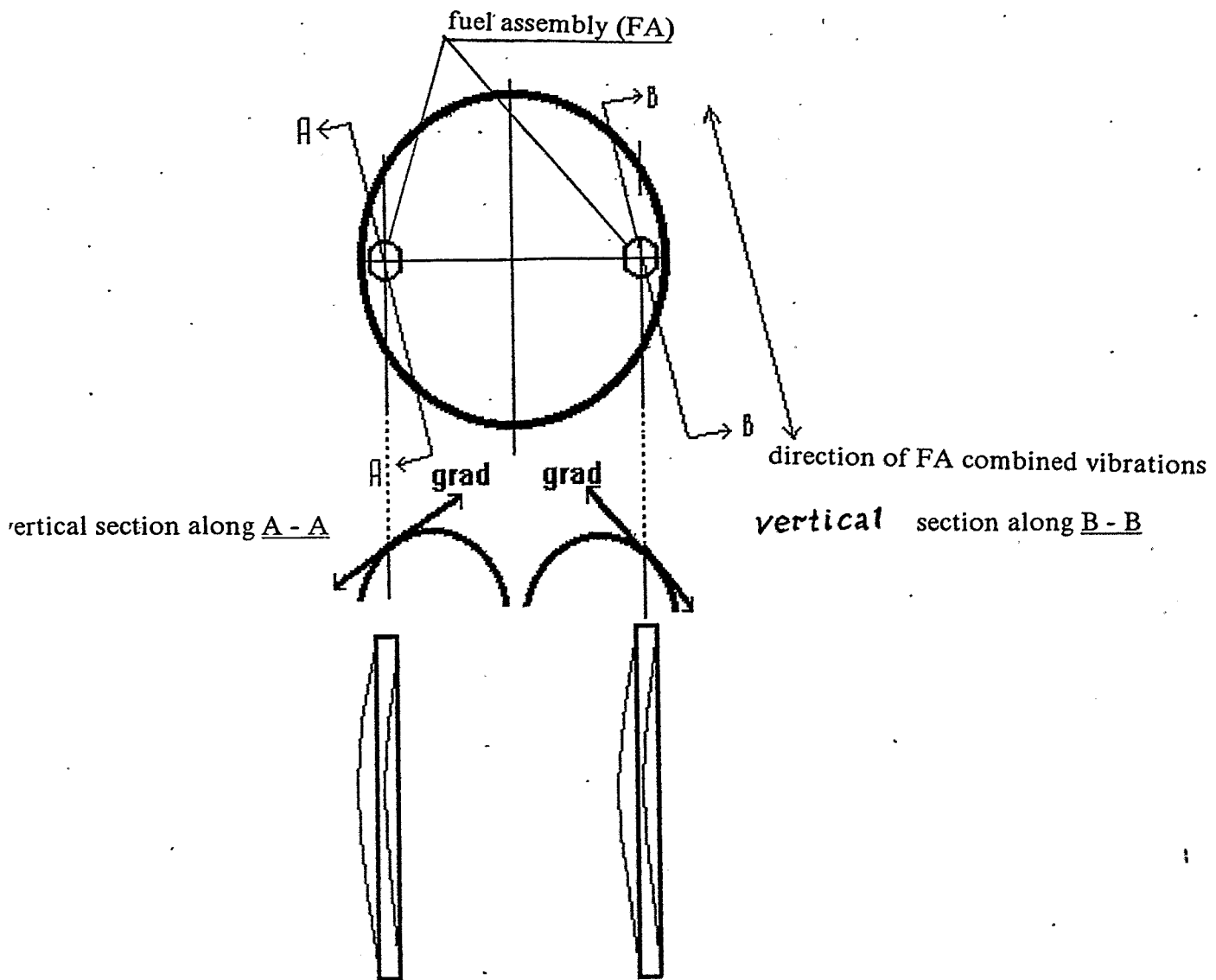


Fig. 36

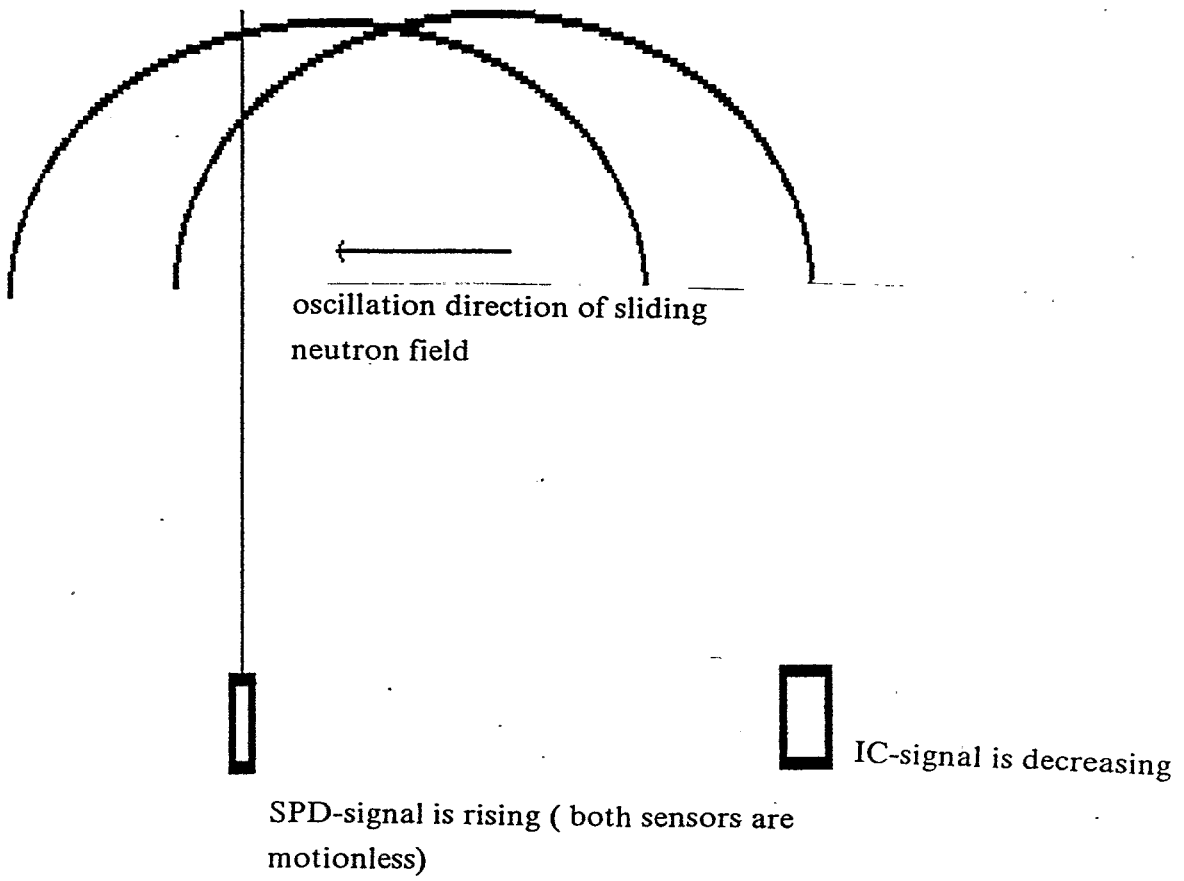


Fig. 37

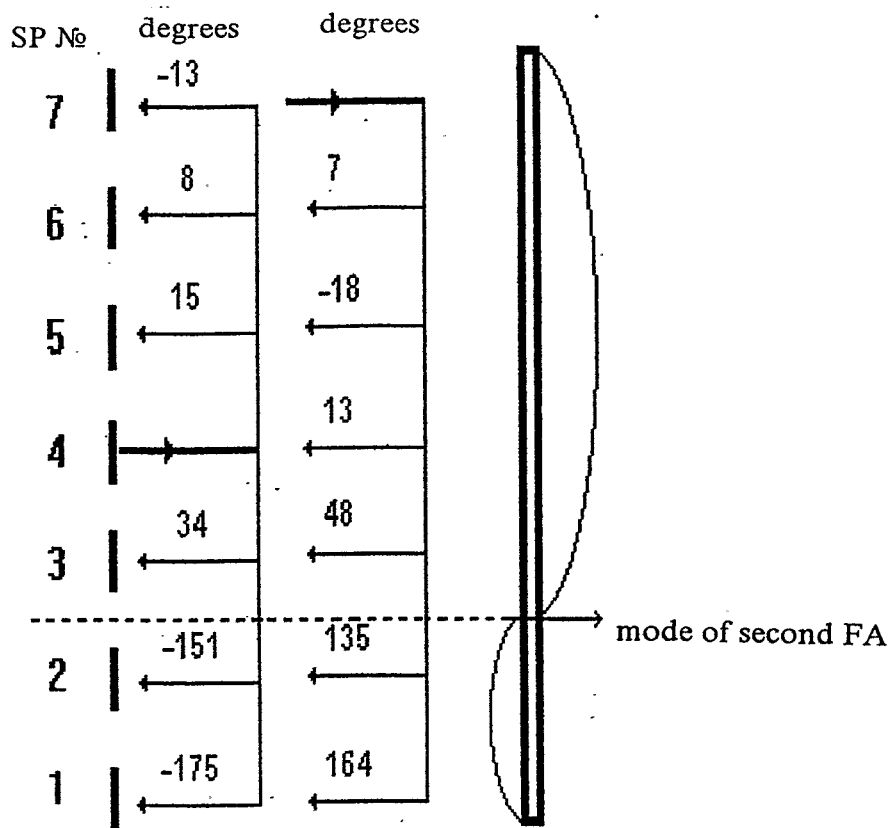


Fig.38

coherence of "SPD - distant IC" signals
(SPD 01-34 - IC7)

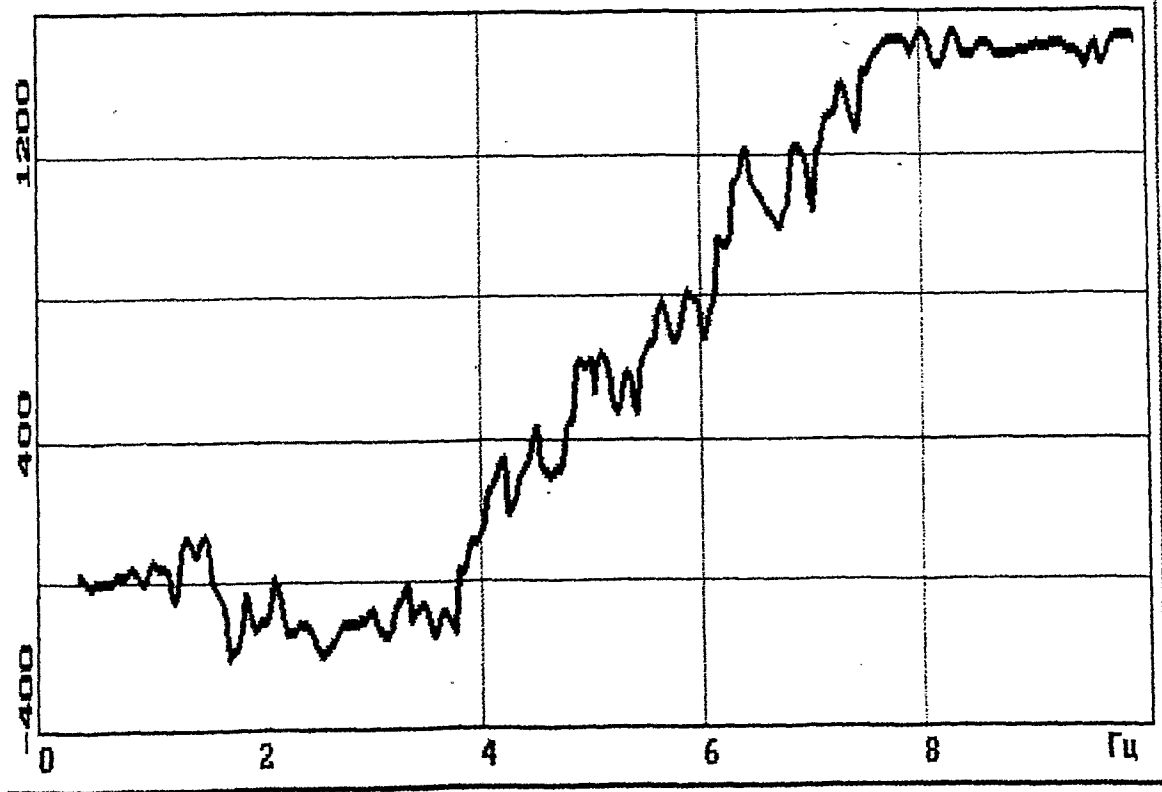
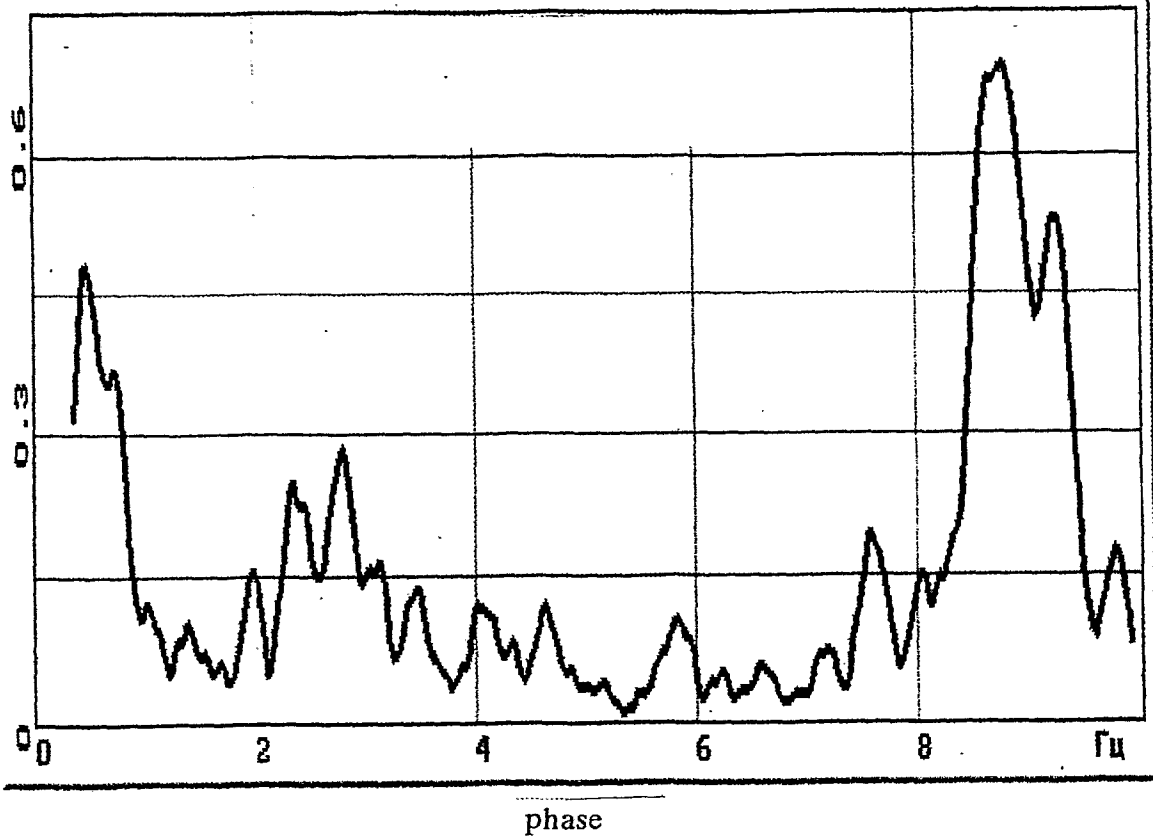


Fig. 39

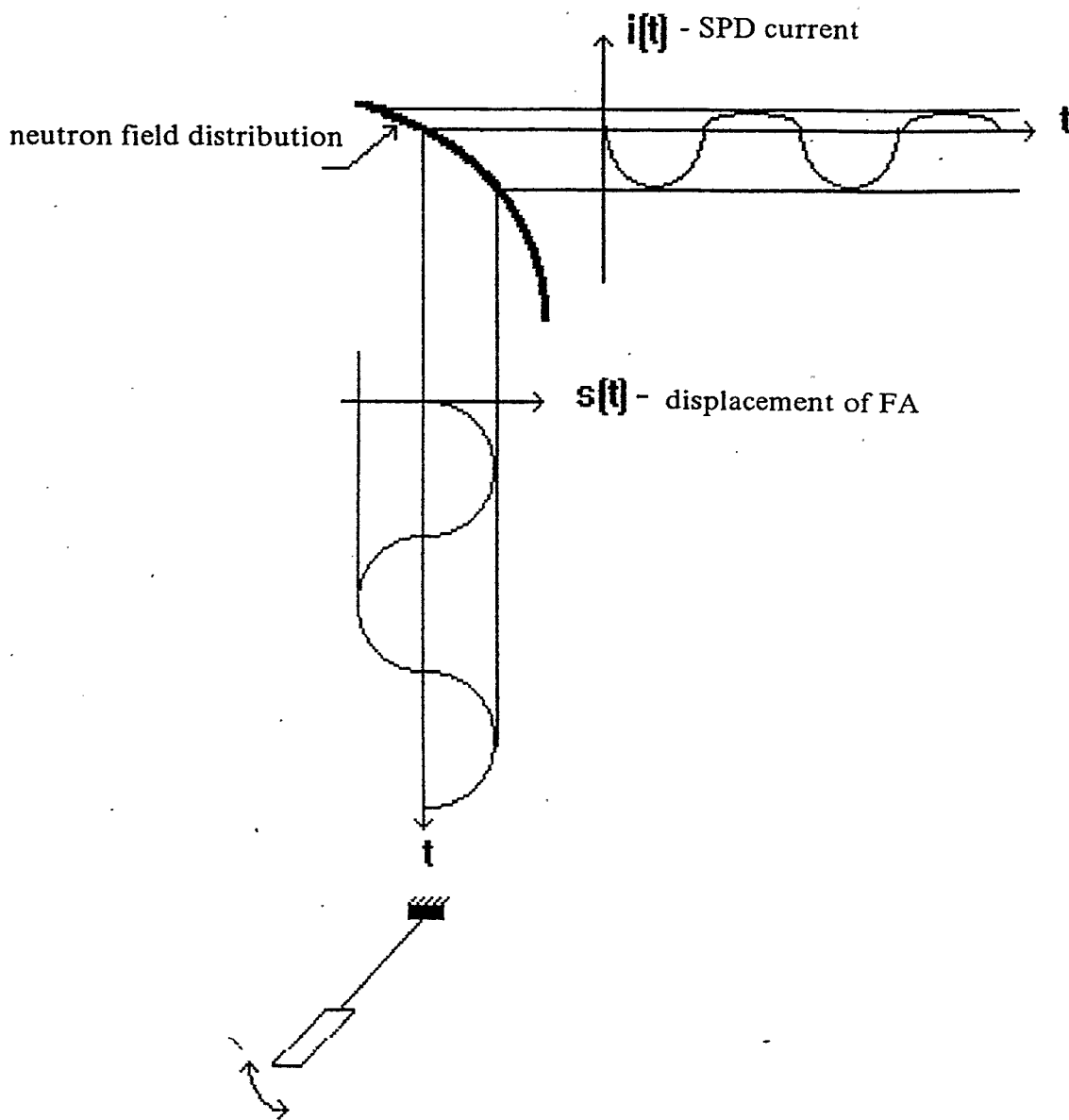


Fig. 40

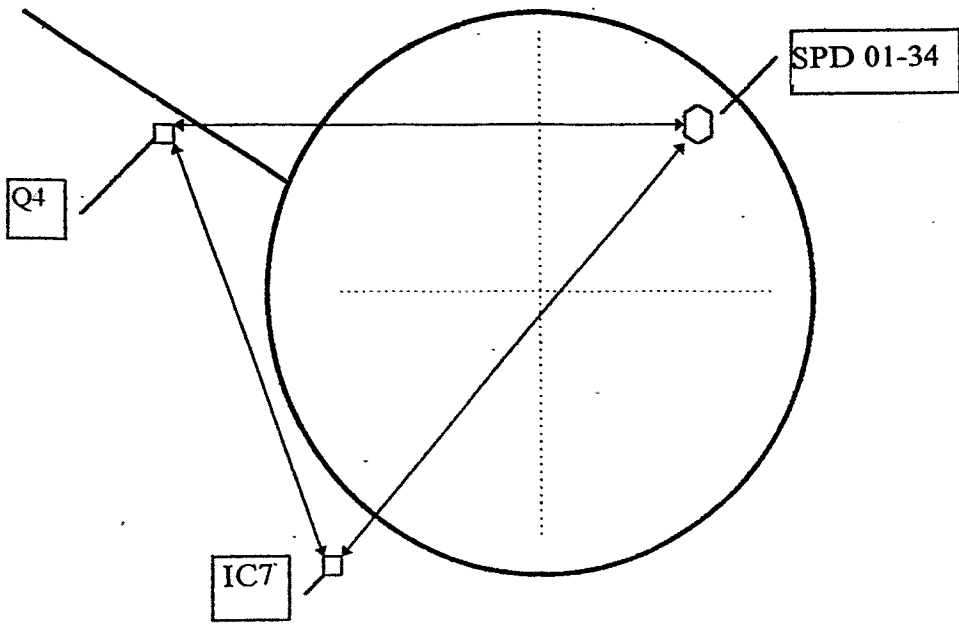


Fig. 41

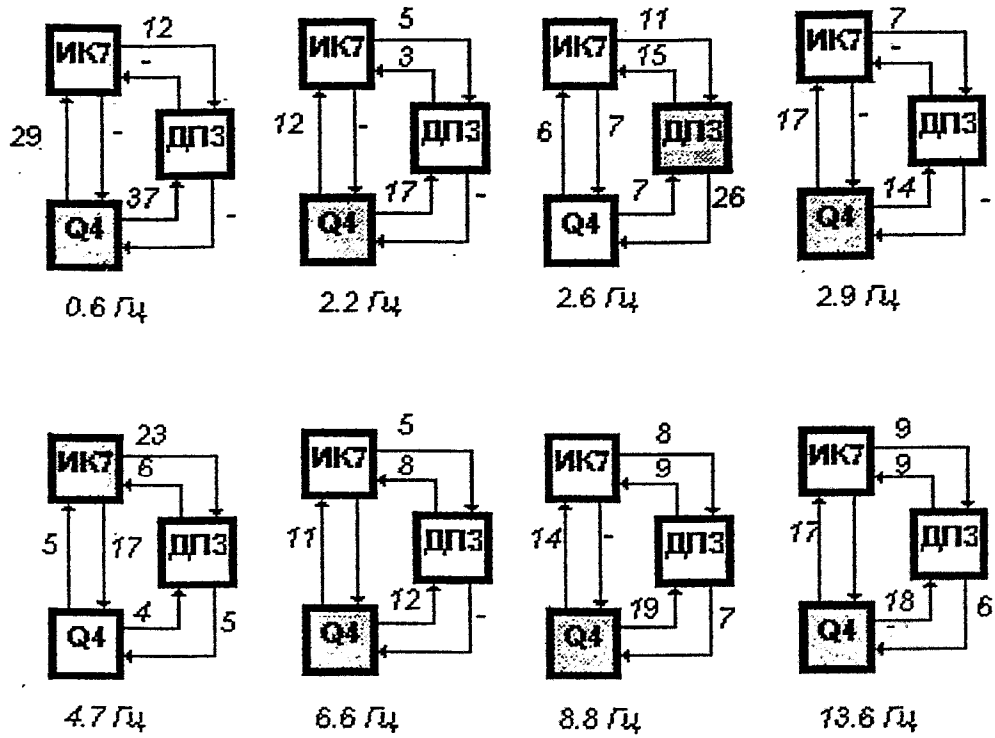


Fig.42

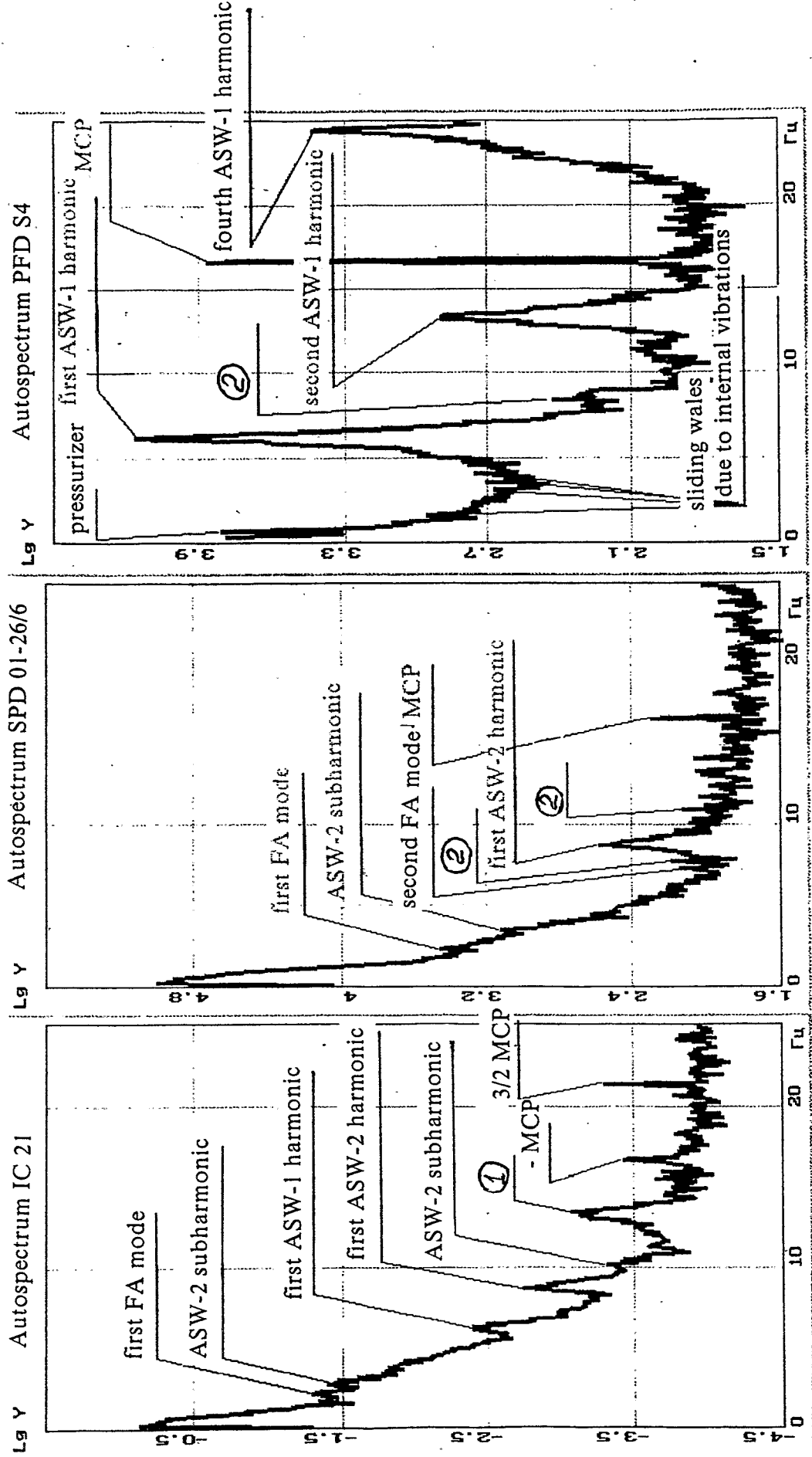
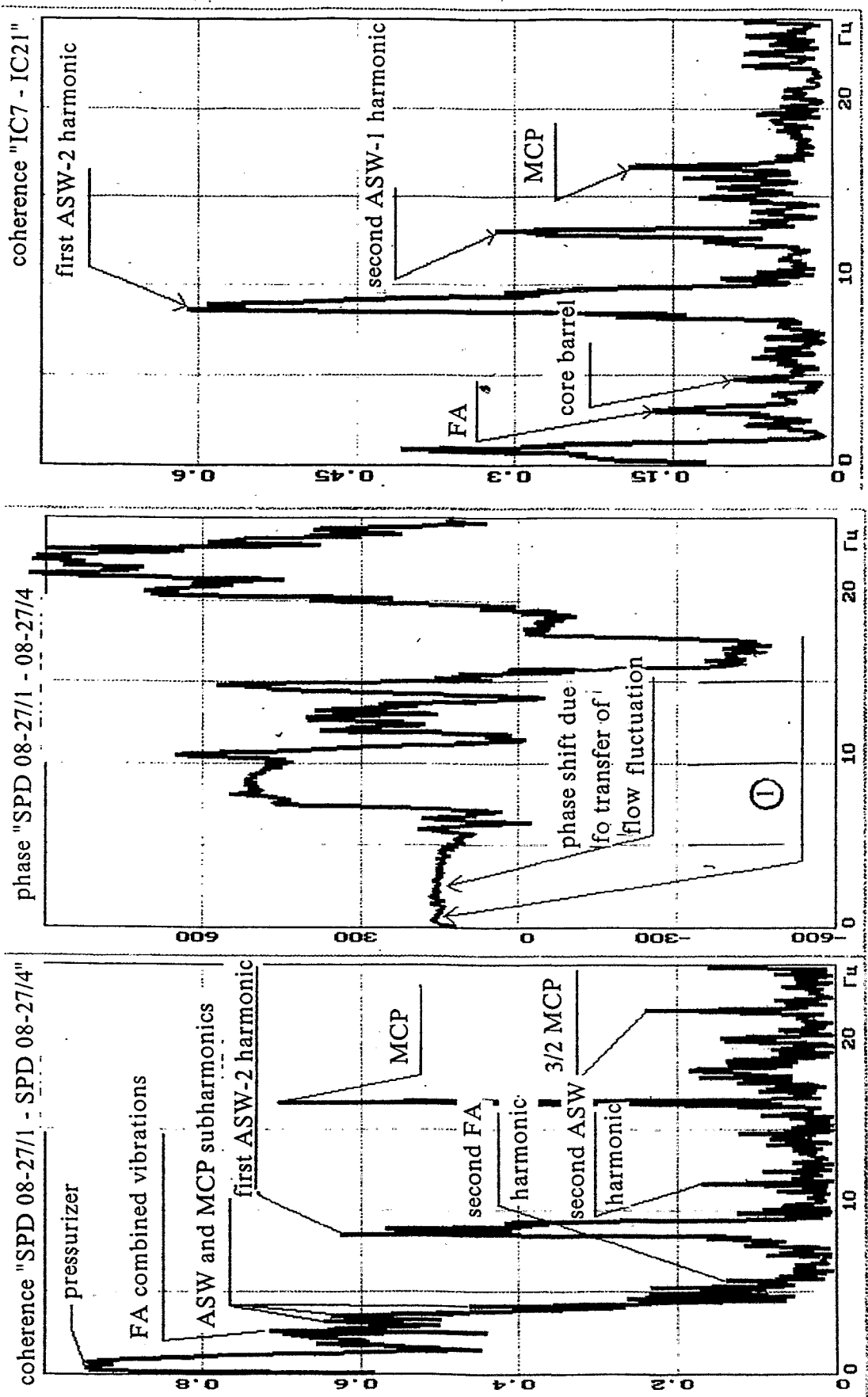


Fig. 43
 ① - second ASW-1 harmonic 2 - MCP subharmonic



① phase shift due to transfer of temperature fluctuation from core inlet

Fig. 44

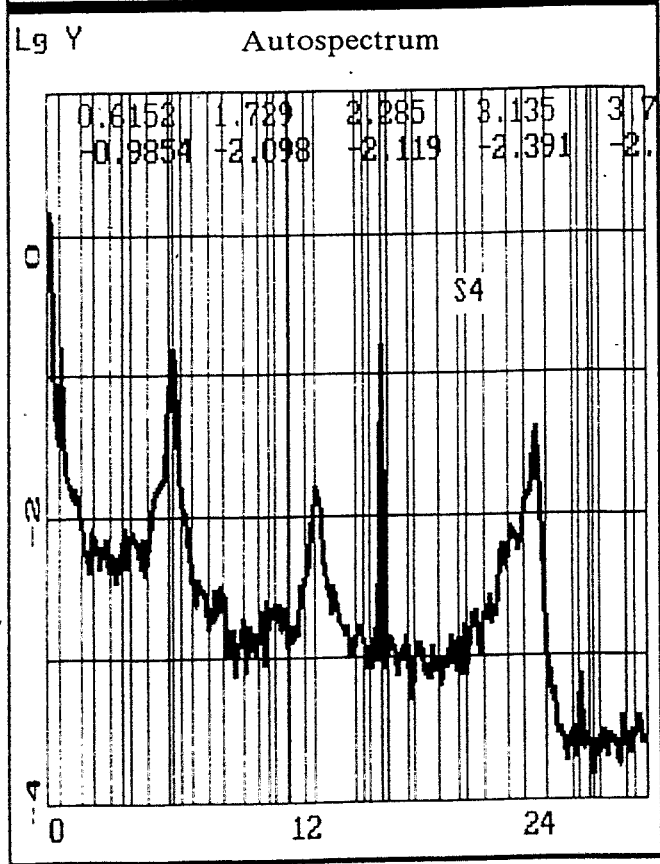
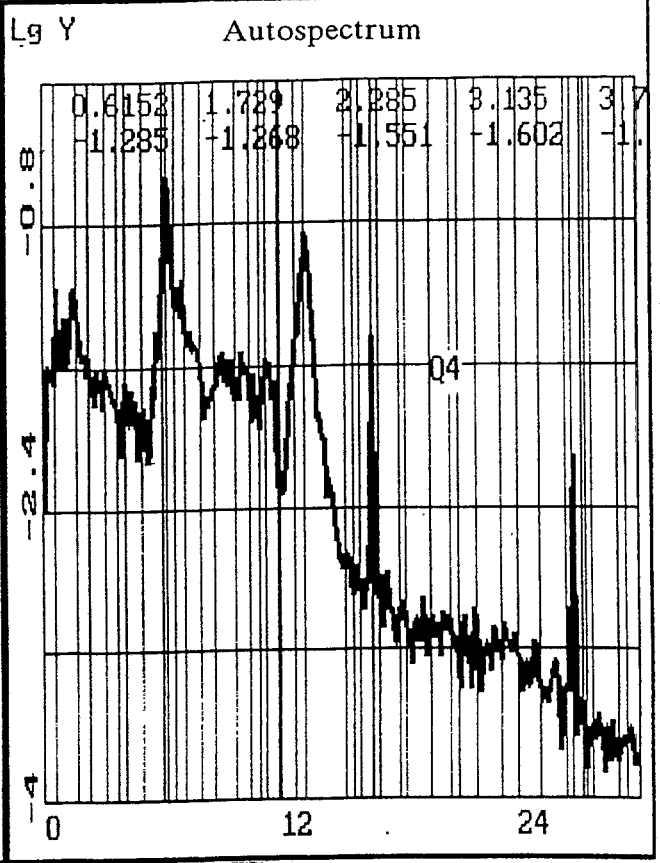
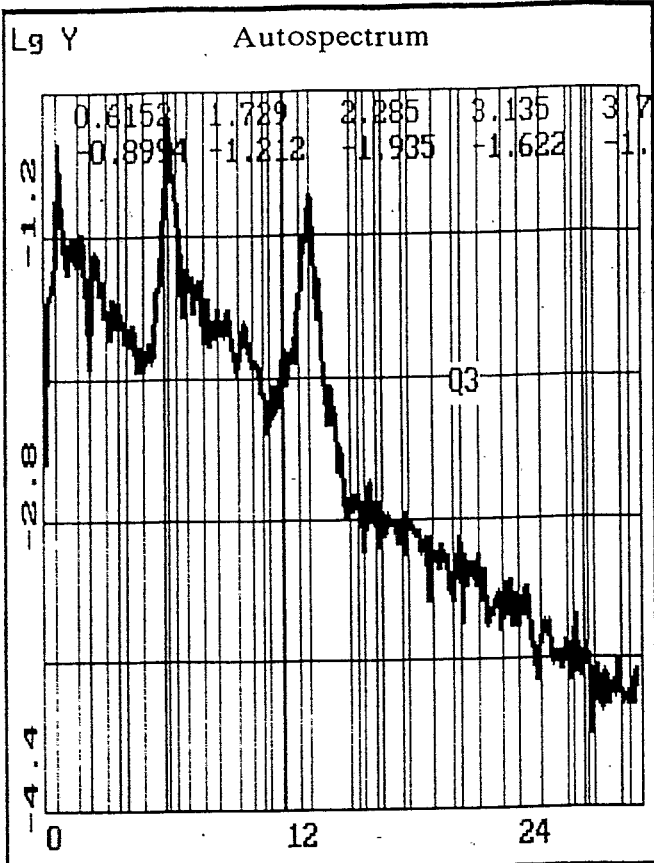


Fig. 45 -

power spectral density of P3, P4, P5
(the mutual frequencies are picked out)

coherence of the pair
of two distant SPD
(SPD 01-34 - SPD 07-22)

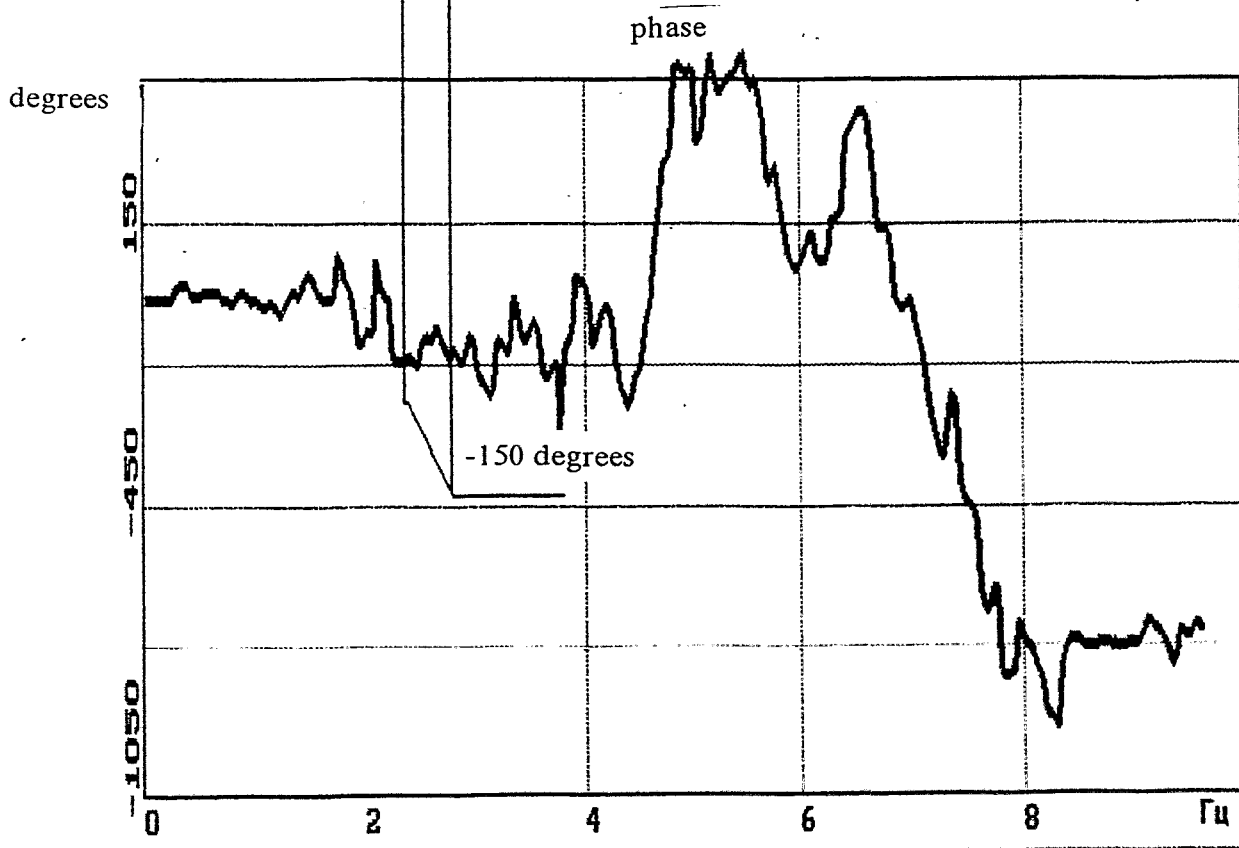
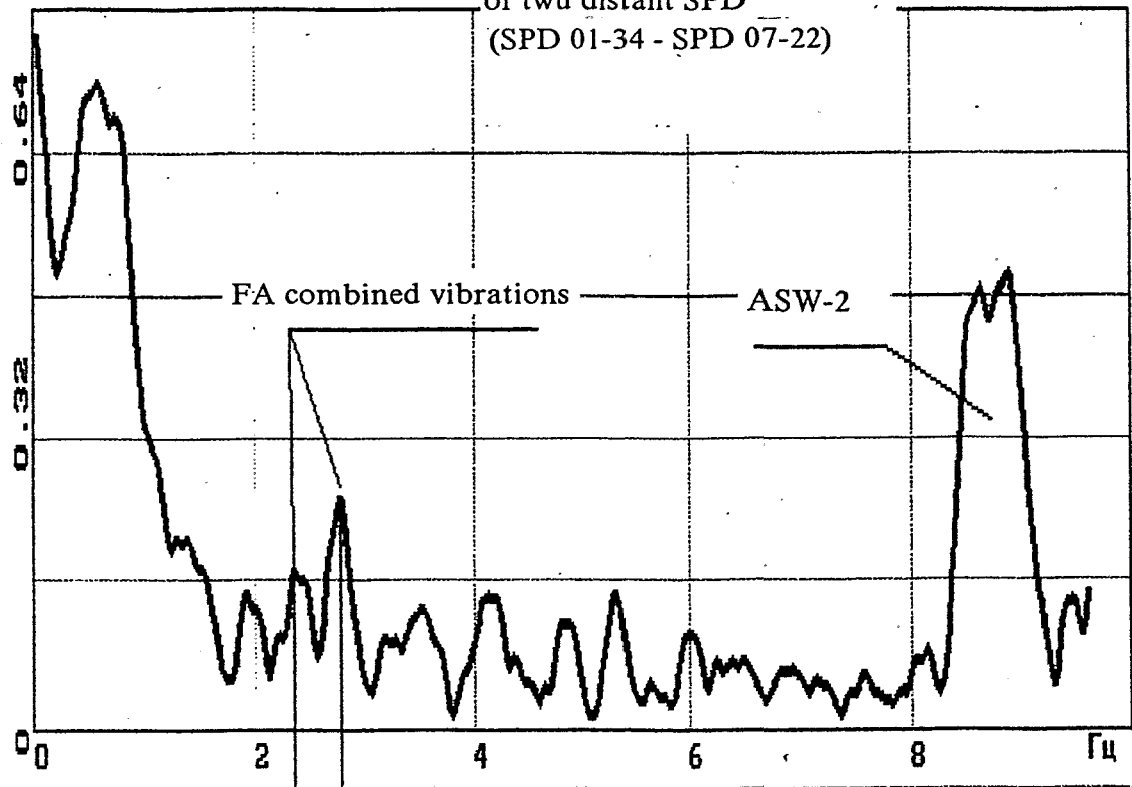


Fig.46

Siemens AG	KWU	KOLA	manual conditions	10/01/93
SUS V 103	BLOK2	PRESSURE	тек. нр. 1/ Рисунок нр. 1	10:43:17

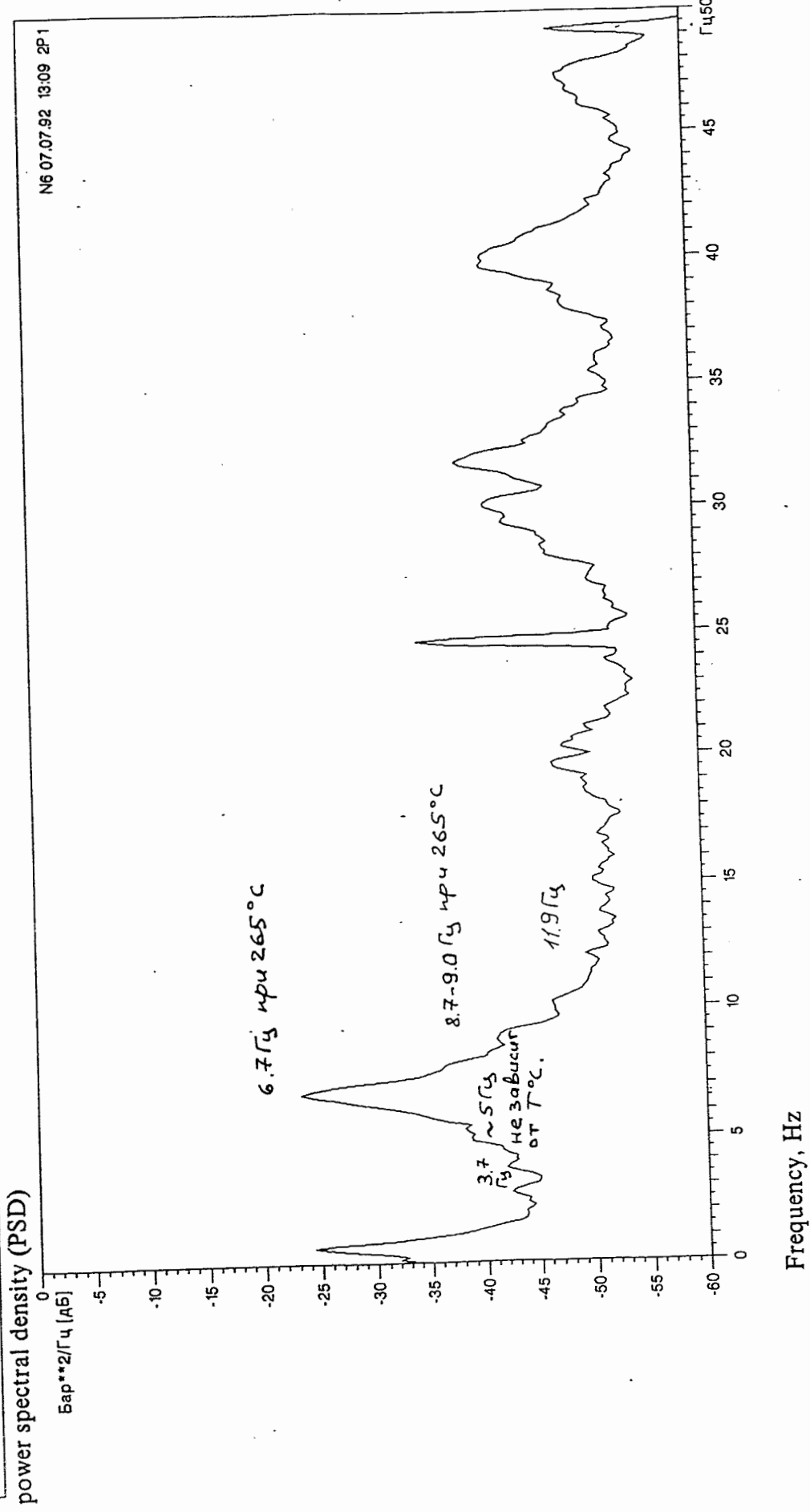


Fig. 47

all MCP are in operation at 265 degrees.
121 bars (pressure fluctuation in the hot leg of

Siemens AG	KWU	KOLA	manual conditions	10/01/93
SUS V 103	BLOK2	PRESSURE	тек. нр. 1 / Рисунок нр. 1	11:32:02

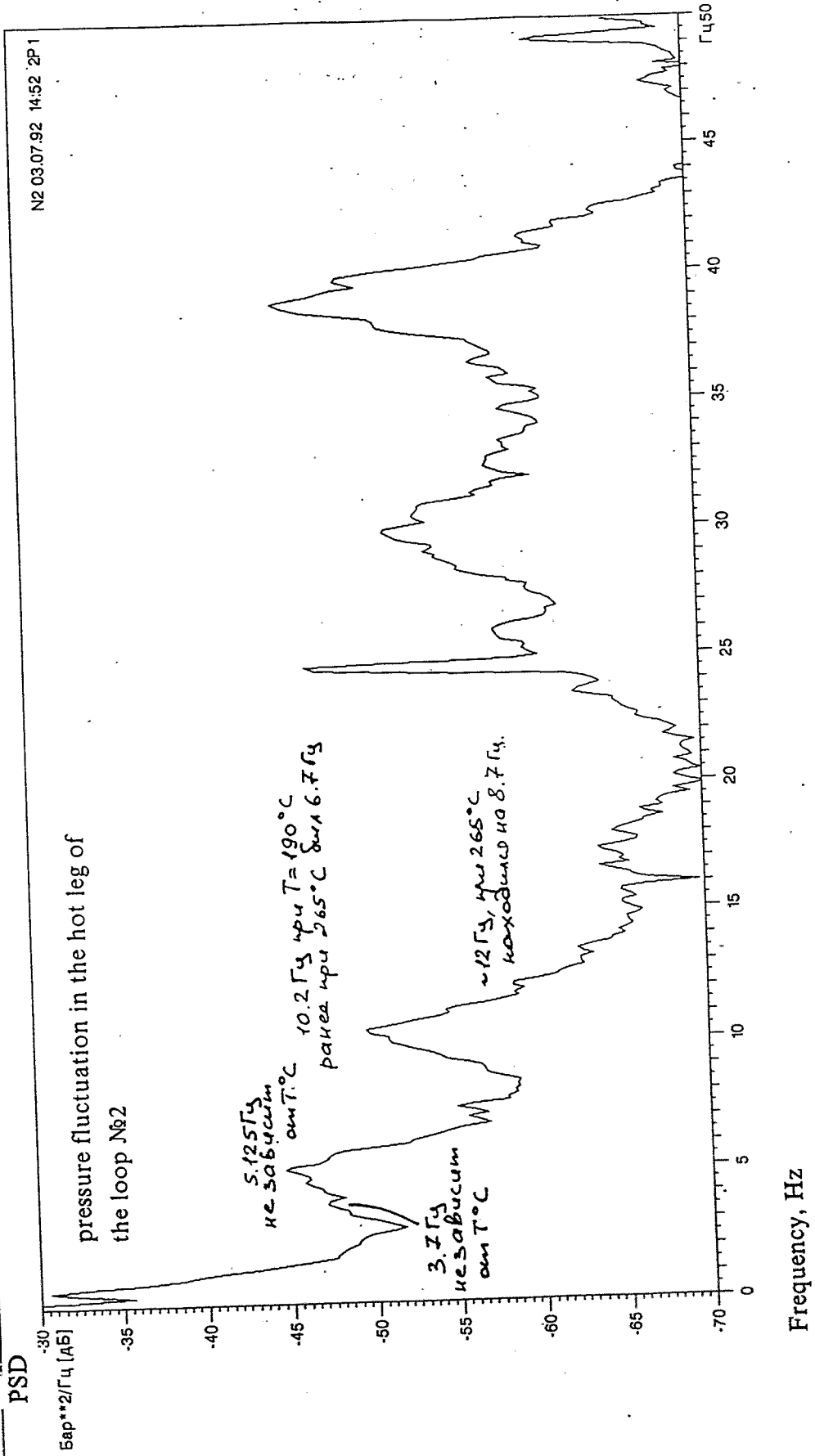


Fig. 48

3 - MCP №1, 2, 3, 4, 5 are in operation at 190 degrees,

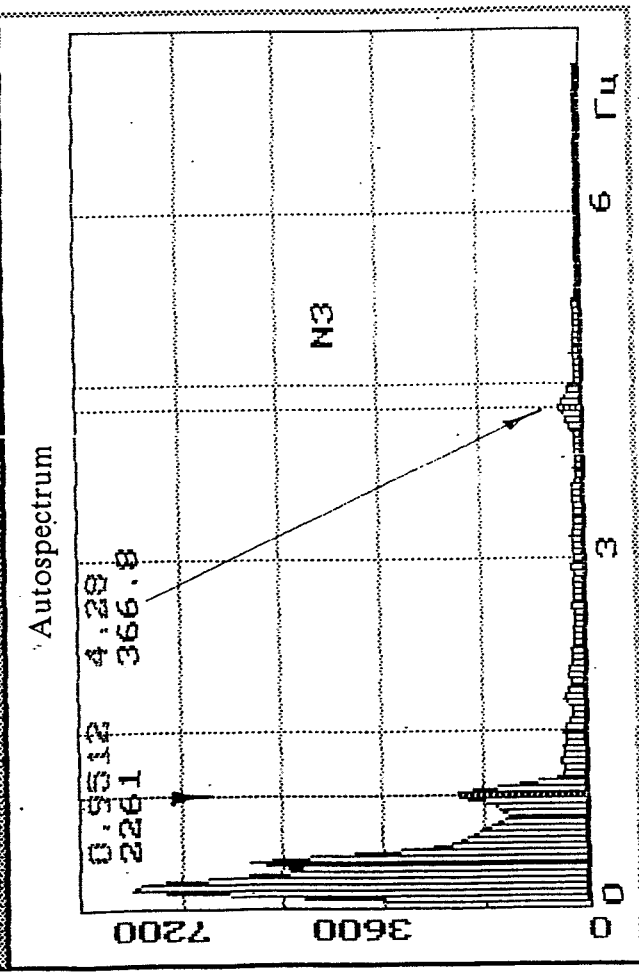
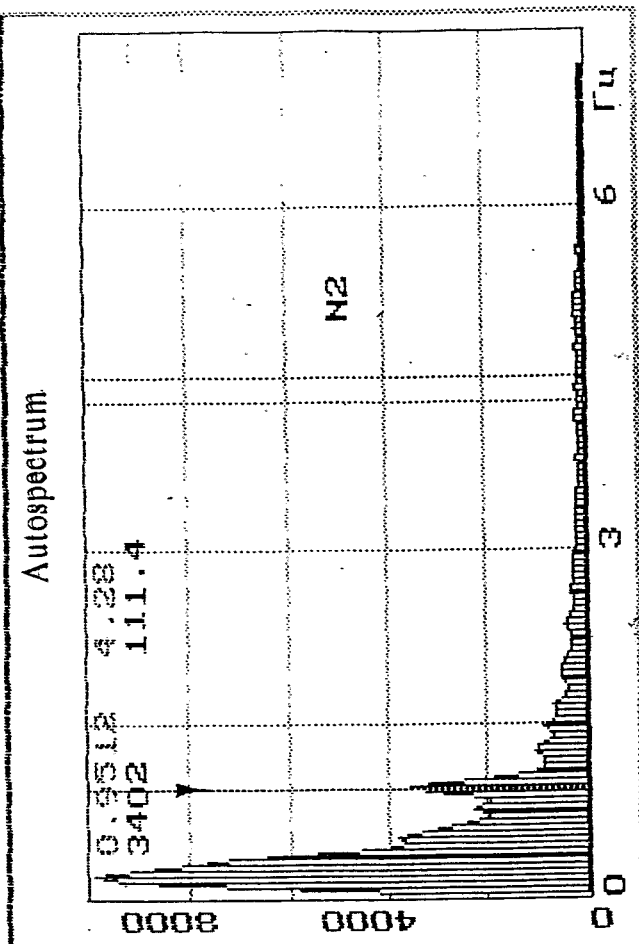
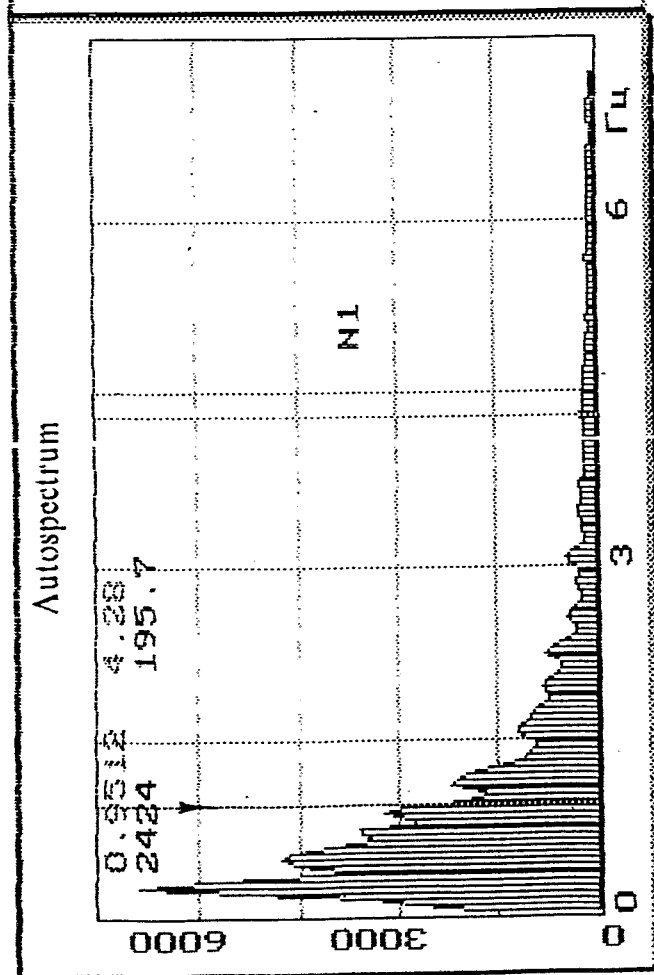


Fig.49 ASPD of the IC noises in low-frequency range

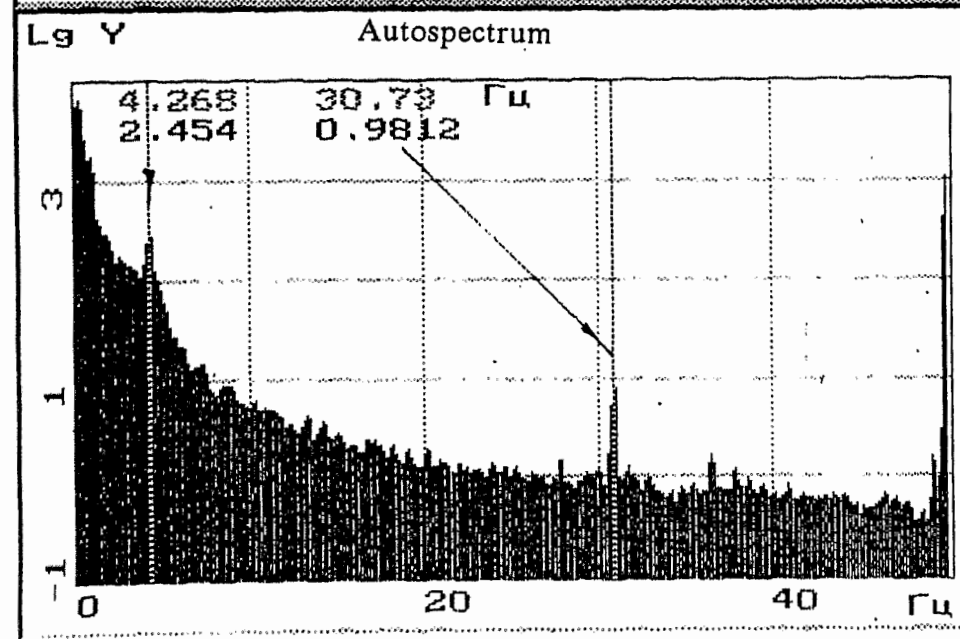
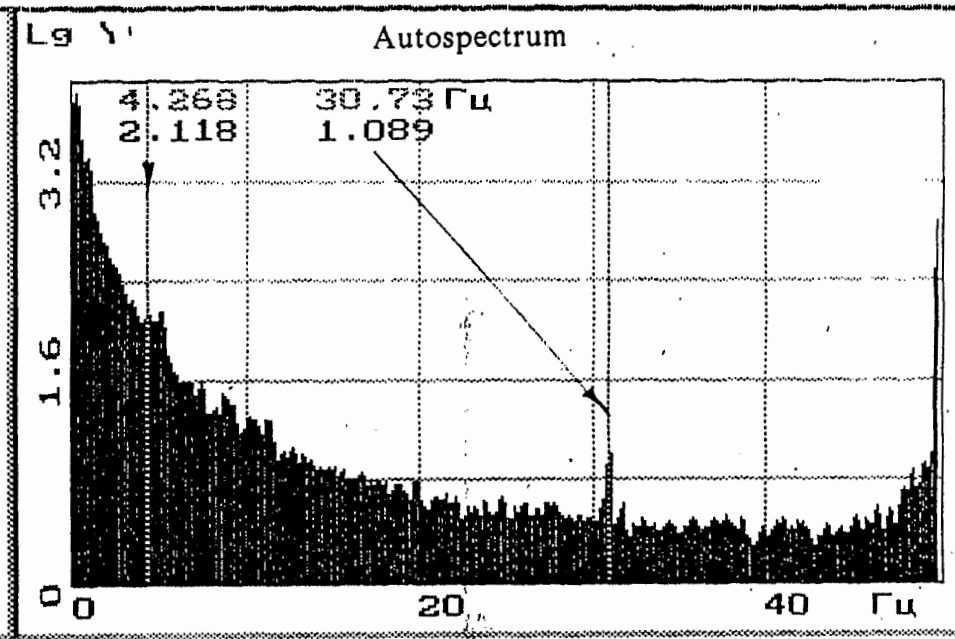
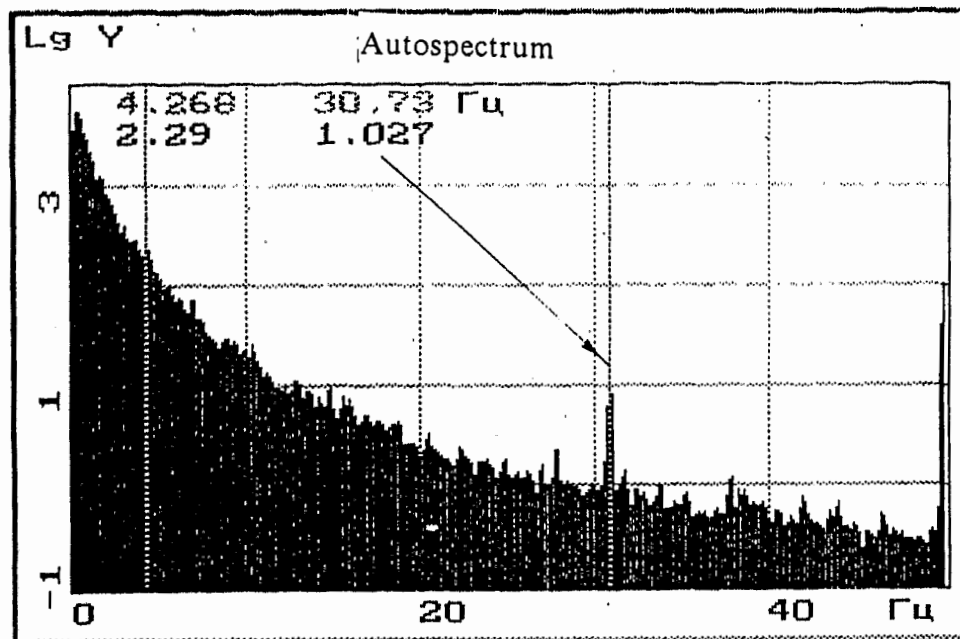
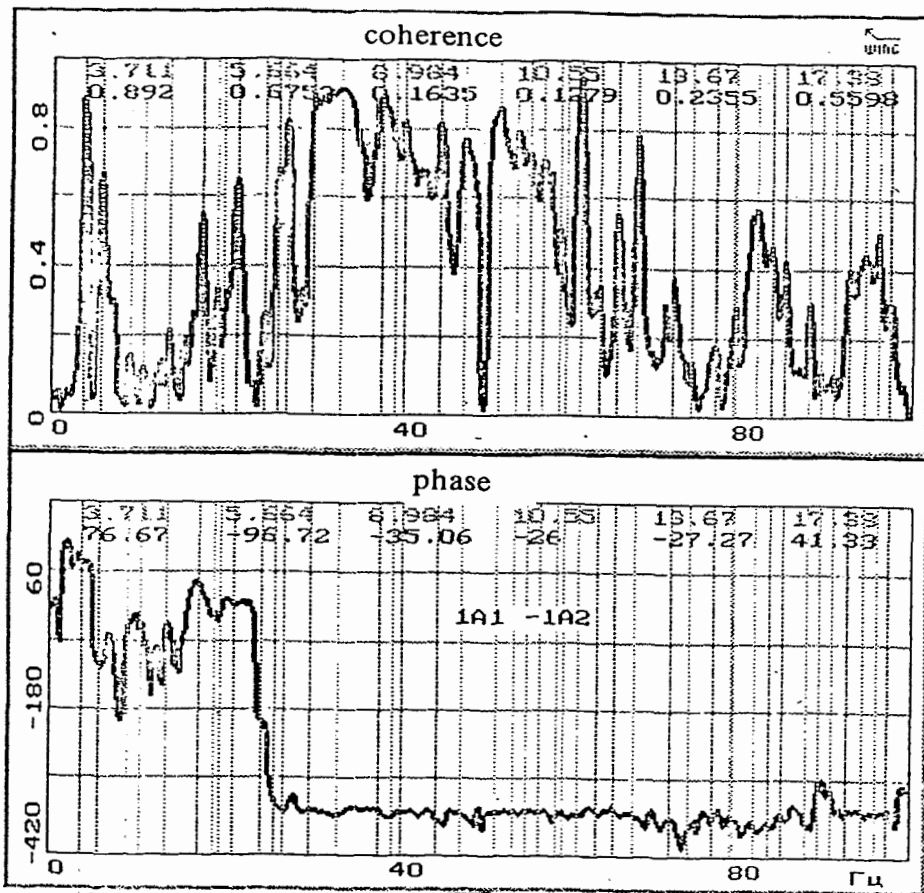
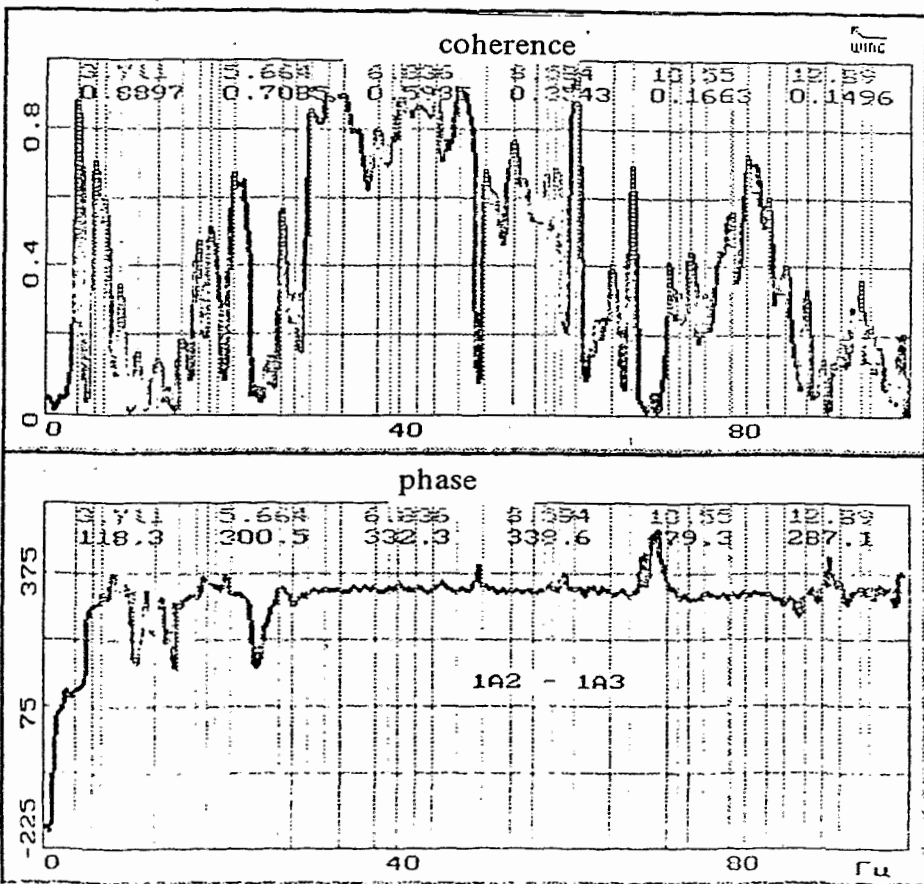


Fig.50 ASPD of the IC noises in the full frequency range



3.711	0.892	76.67
5.664	0.6753	-96.72
8.984	0.1635	-35.06
10.55	0.1279	-26
13.67	0.2355	-27.27
17.38	0.5598	41.33
19.14	0.351	-6.197
21.48	0.6549	4.908
24.61	0.2746	-193.7
25.98	0.6844	-329.8
27.15	0.8287	-346.7
30.27	0.9061	-343.8
33.4	0.924	-355
38.28	0.9019	-345.1
40.82	0.8258	-347.3
44.92	0.8207	-362.8
47.66	0.78	-350.1
51.76	0.8665	-348
53.91	0.7978	-346.9
55.27	0.7375	-345.9
56.84	0.7161	-349.3
58.98	0.5202	-350.6
61.33	0.9509	-353.7
63.67	0.3606	-348.6
65.82	0.5665	-342.4
68.16	0.7926	-354
72.46	0.3894	-363.6
74.8	0.147	-372.9
77.54	0.1934	-359.7
79.69	0.3106	-360.6
82.42	0.5825	-373.1
83.98	0.4812	-365.4
85.74	0.4348	-351.5
88.48	0.3168	-367.4
89.84	0.1172	-299.5
91.41	0.1071	-307.2
93.16	0.4119	-349
94.92	0.4597	-343.7
96.48	0.5167	-348.6
97.85	0.3178	-342.9

Fig. 51 Kola NNP, unit №1



3.711	0.8897	118.3
5.664	0.7085	300.5
6.836	0.5985	332.3
8.594	0.3543	338.6
10.55	0.1663	179.3
12.89	0.1496	287.1
15.62	0.2064	303.3
17.58	0.4855	325
18.95	0.5186	355.9
21.68	0.6811	329.5
27.15	0.5743	345
28.71	0.3288	303.7
30.47	0.8566	331.7
32.42	0.8974	340.7
34.18	0.9024	339
38.28	0.7945	340.2
40.82	0.8963	352.4
42.97	0.8745	344.1
44.92	0.8883	344.3
47.66	0.9159	337.4
50.78	0.6858	346.5
54.1	0.7702	335.6
56.64	0.5974	333.8
57.81	0.6725	341.3
58.98	0.695	339.3
61.33	0.9573	342.3
65.82	0.417	333.7
68.16	0.6991	331.7
72.46	0.4231	344.7
73.63	0.3392	326.7
75	0.4541	319
76.76	0.3316	334.7
79.69	0.5705	323.9
81.54	0.7373	333.4
83.98	0.6134	335.7
86.13	0.4159	308.2
88.67	0.3456	230.1
90.62	0.1495	362
92.77	0.2124	351.1
94.92	0.3726	347.1
96.09	0.2474	341.1

Fig. 52 Kola NNP, unit №1

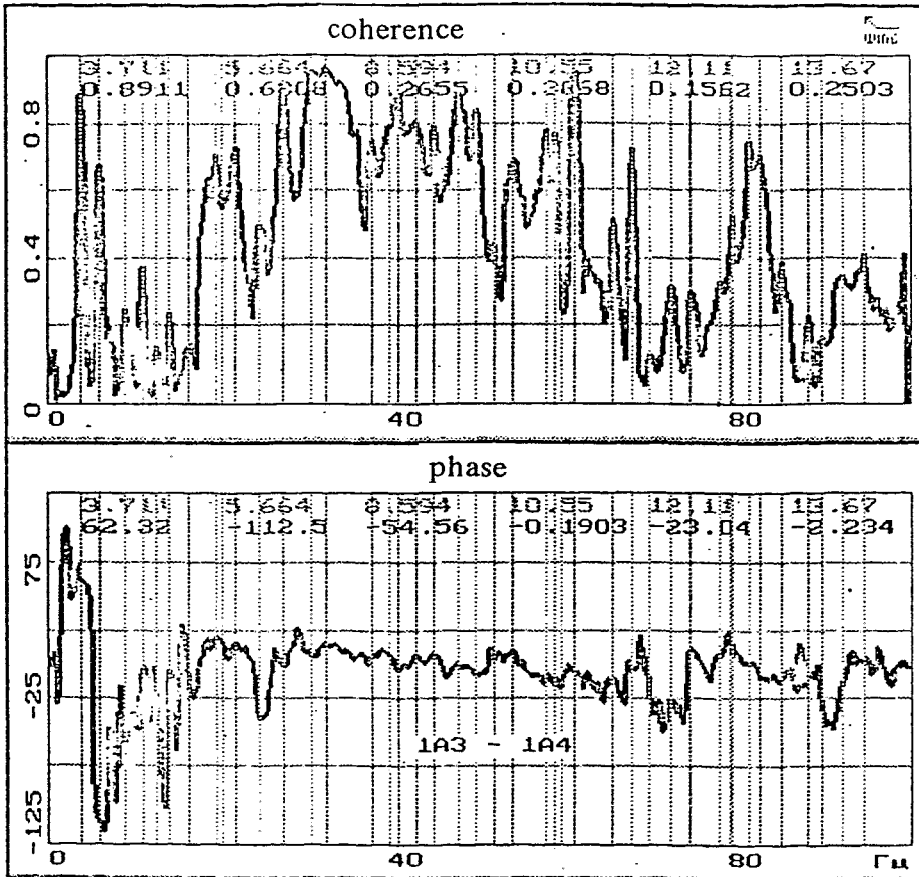


Fig. 53. Kola NNP, unit №1

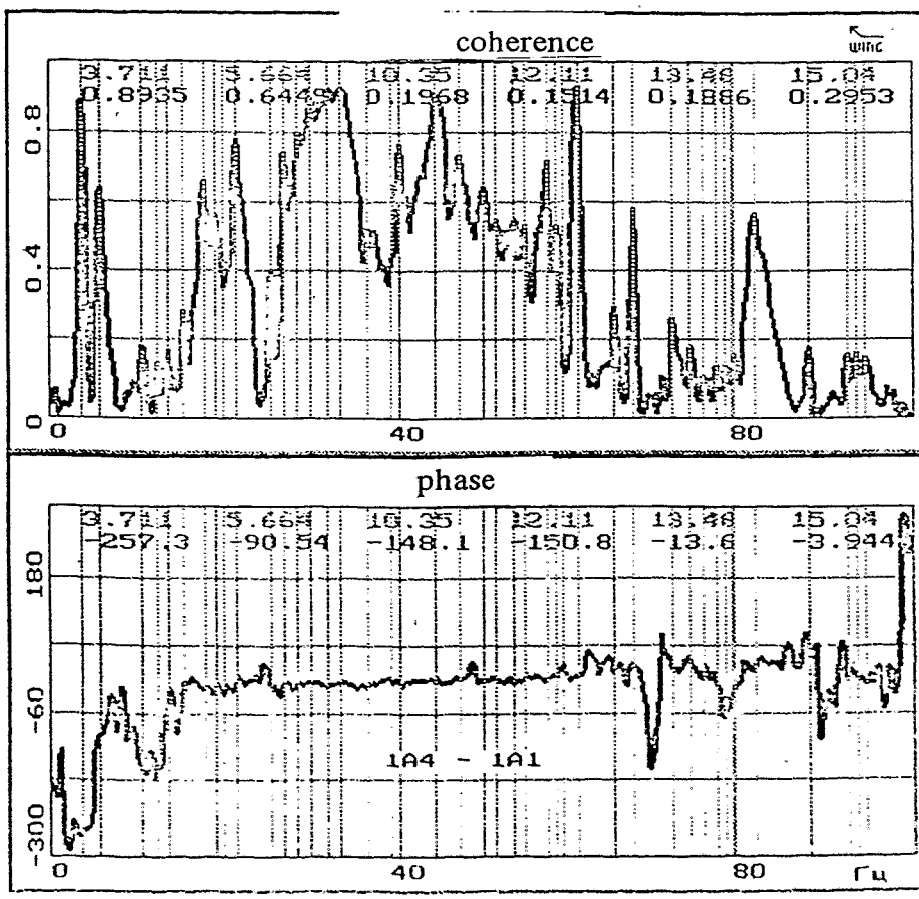


Fig. 54. Kola NNP, unit №1

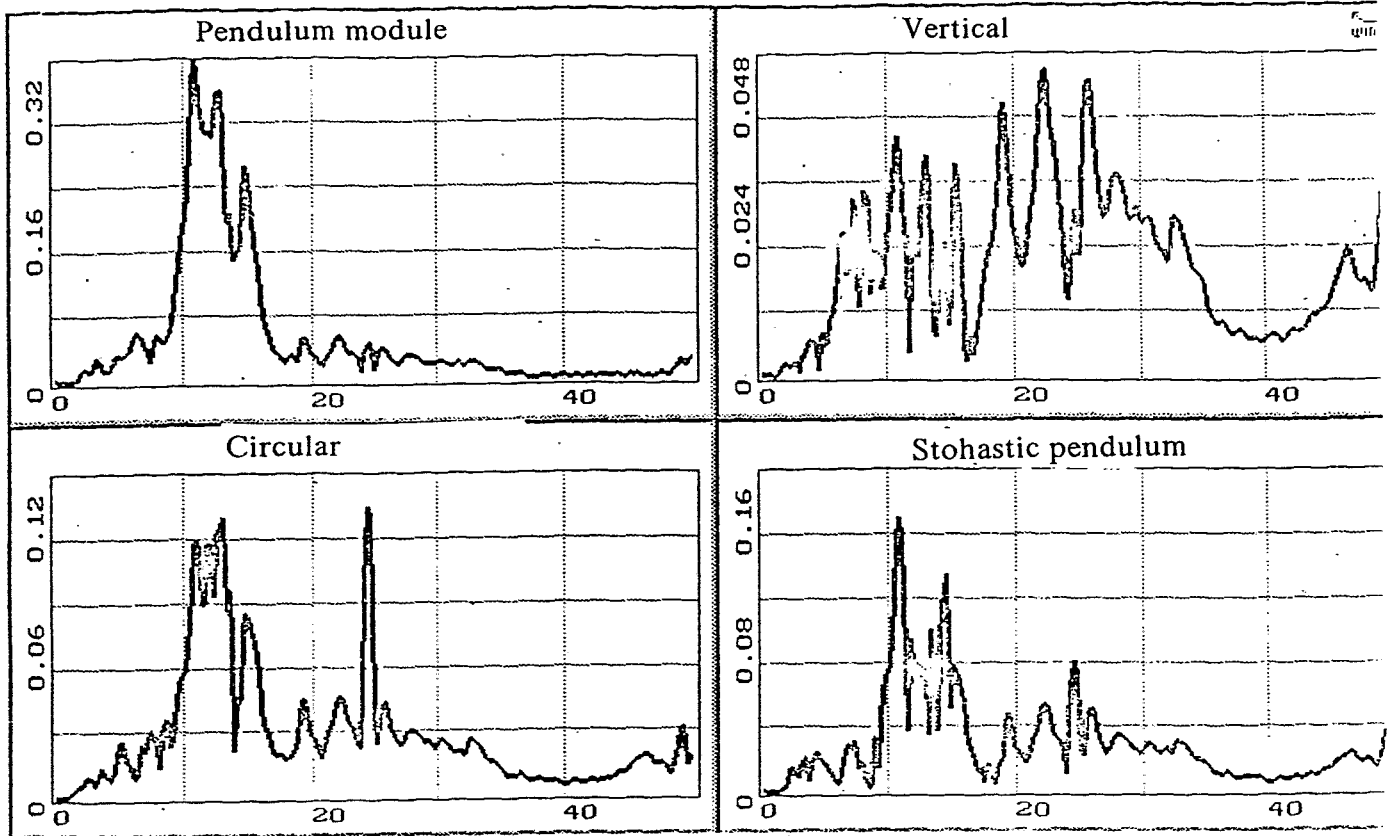


Fig. 55. Decomposition of 2A1, 2A2, 2A3, 2A4 signals

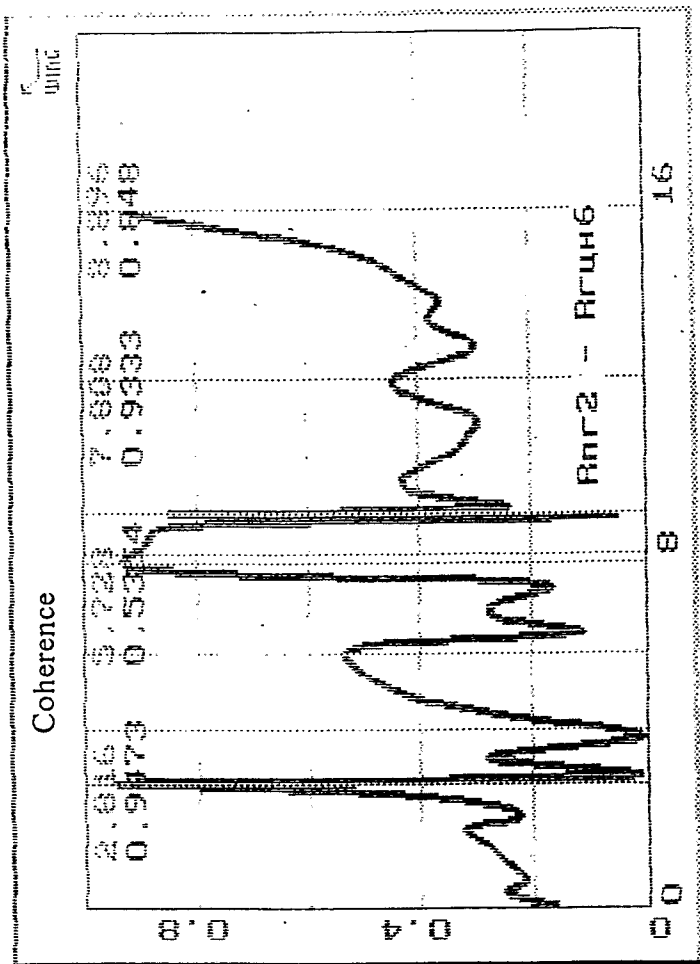
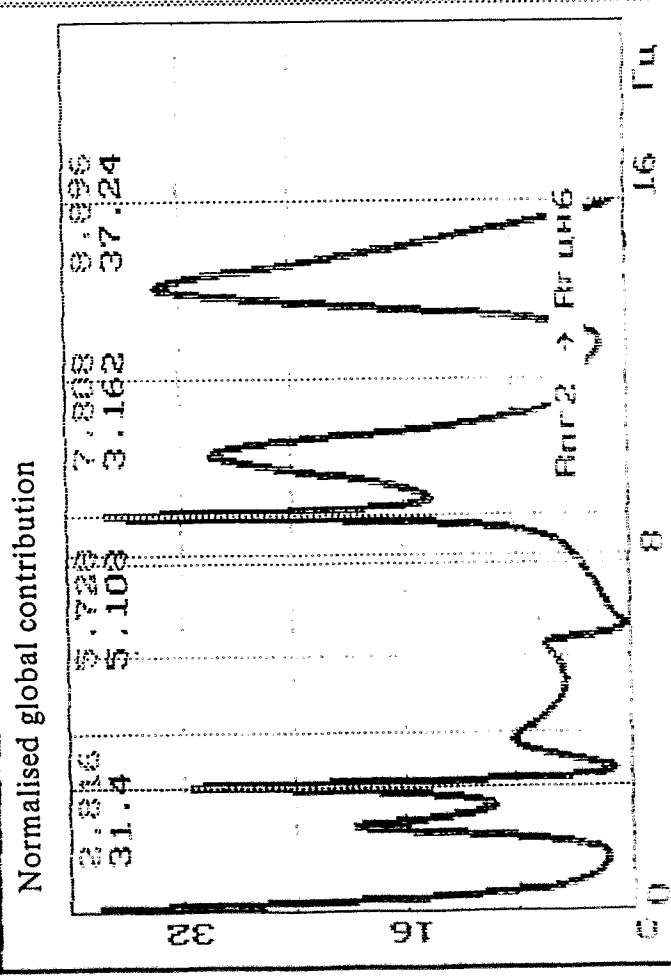
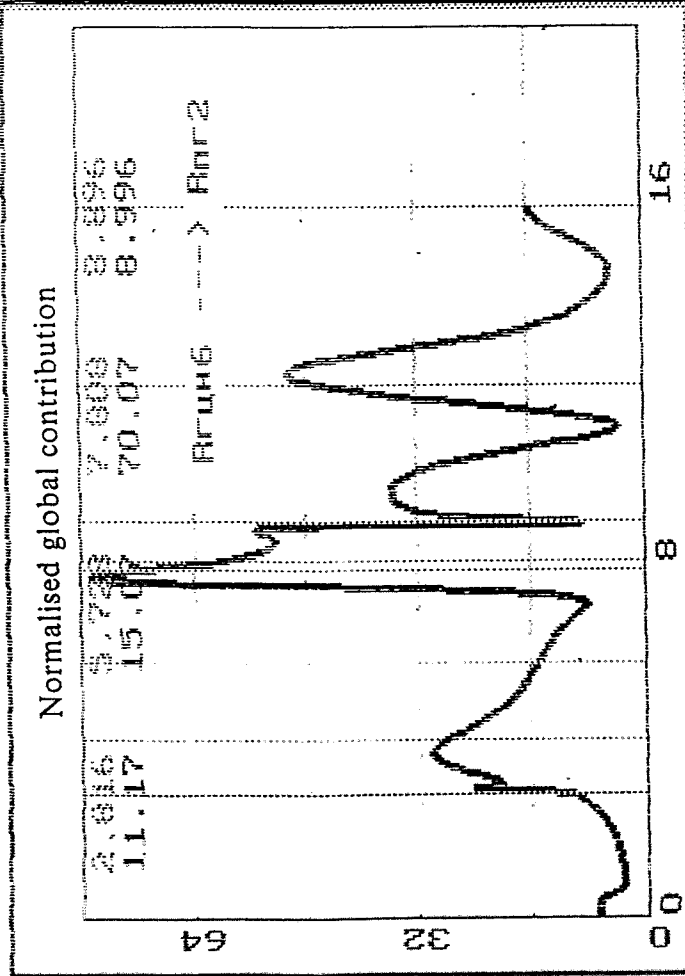


Fig. 56. MAR-model (RSG2, TGMCP4, RMCP6)



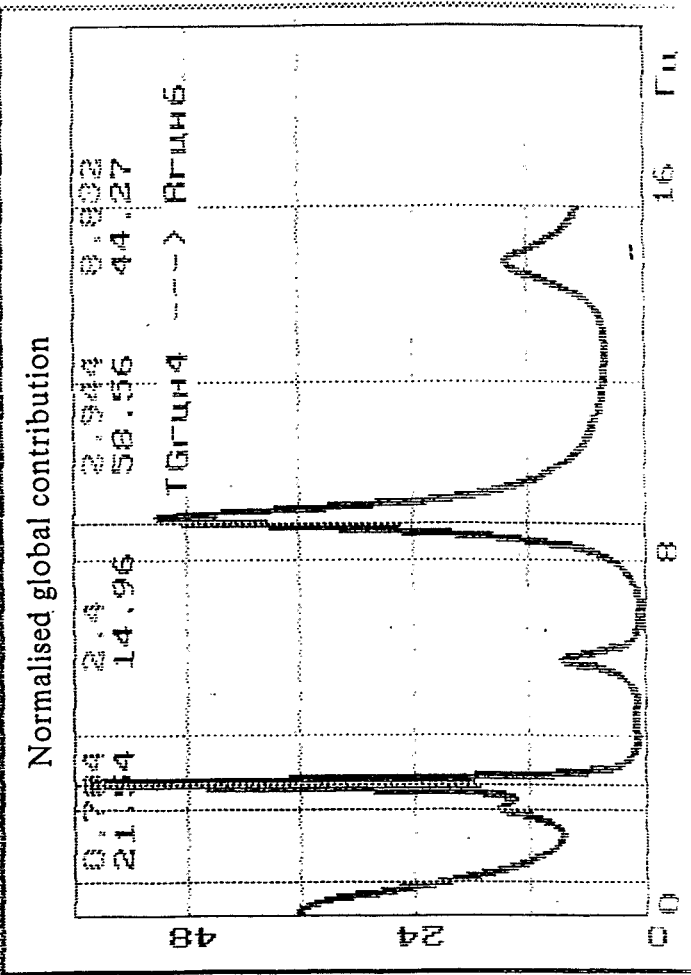
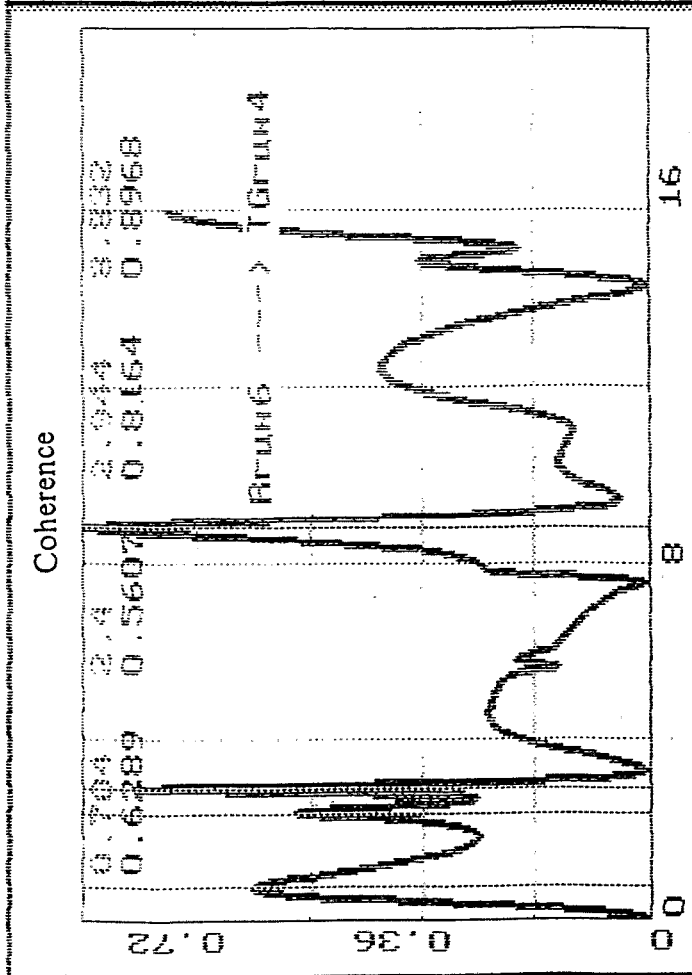
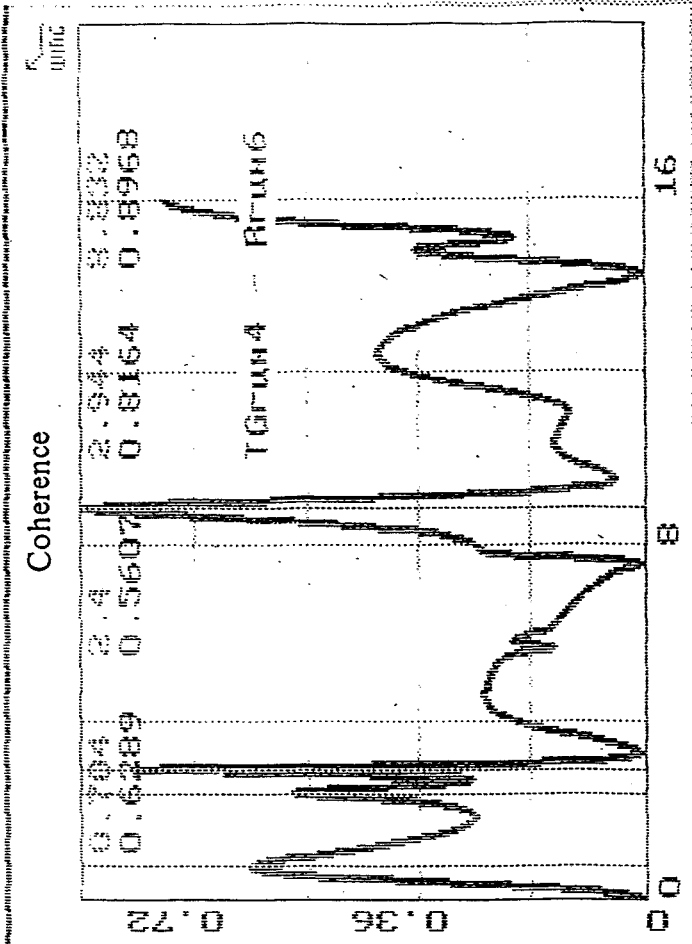


Fig. 57. MAR-model (RSG2, TGMCP4, RMCP6)

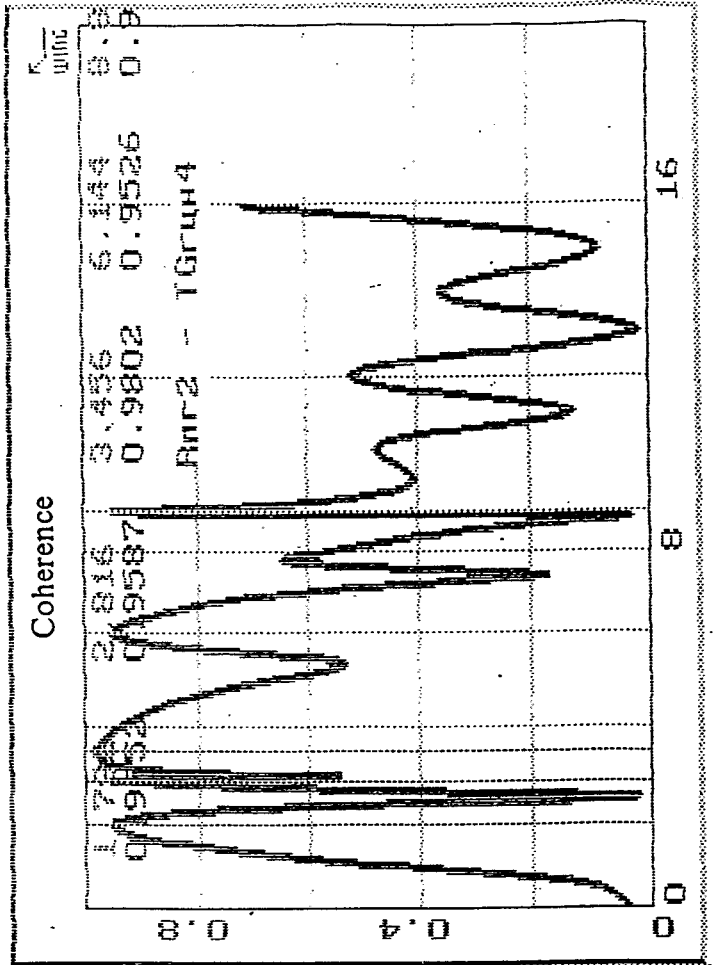
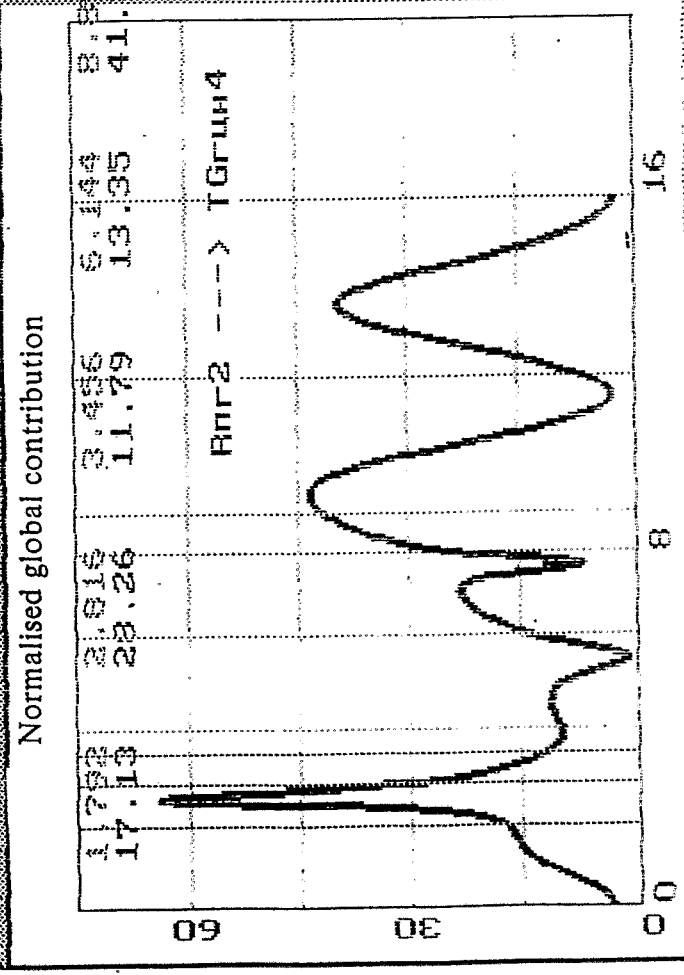
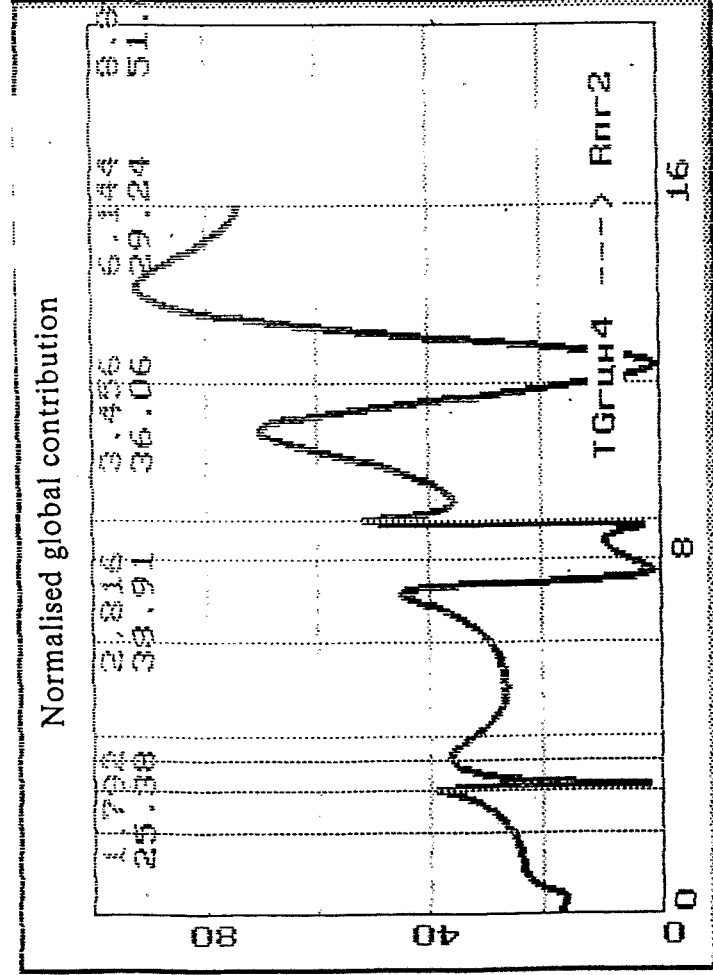


Fig. 58. MAR-model (RSG2, TGMCP4, RMCP6)

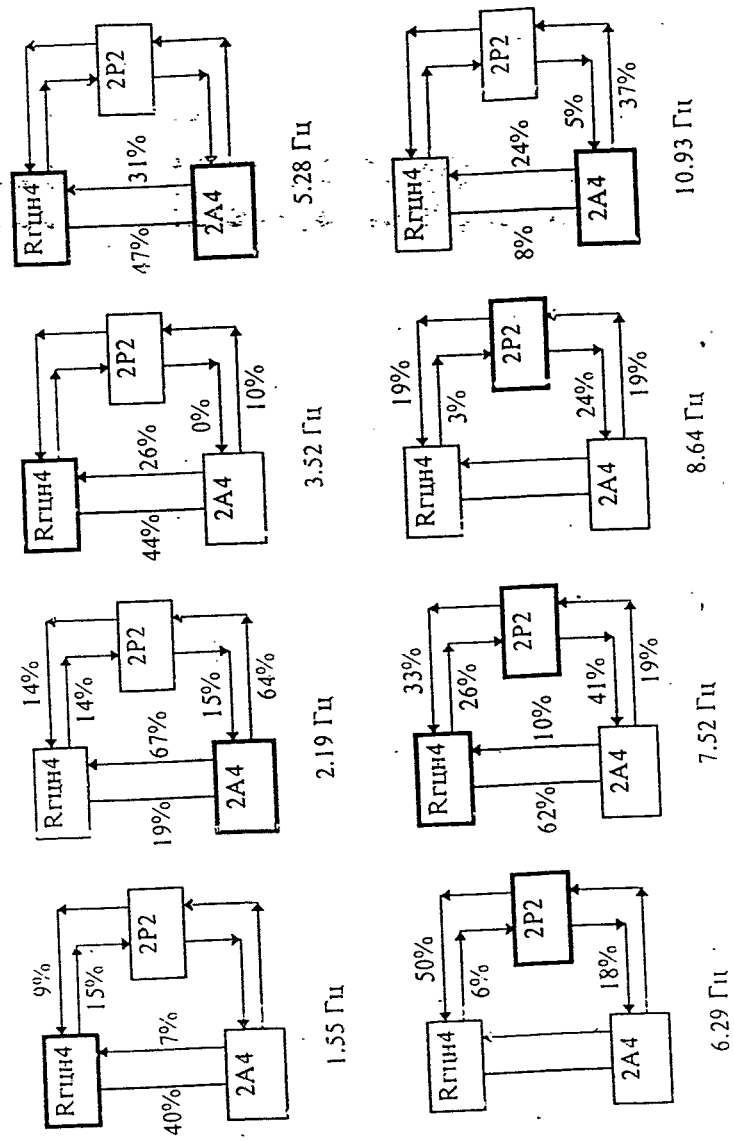
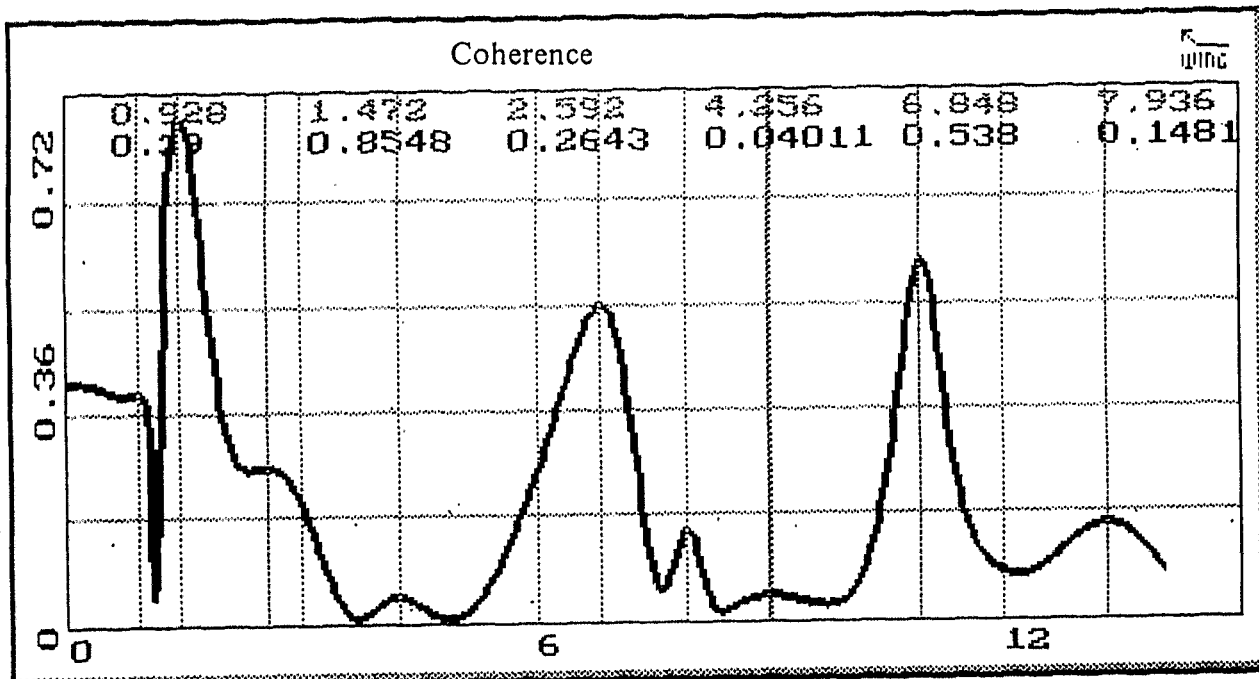
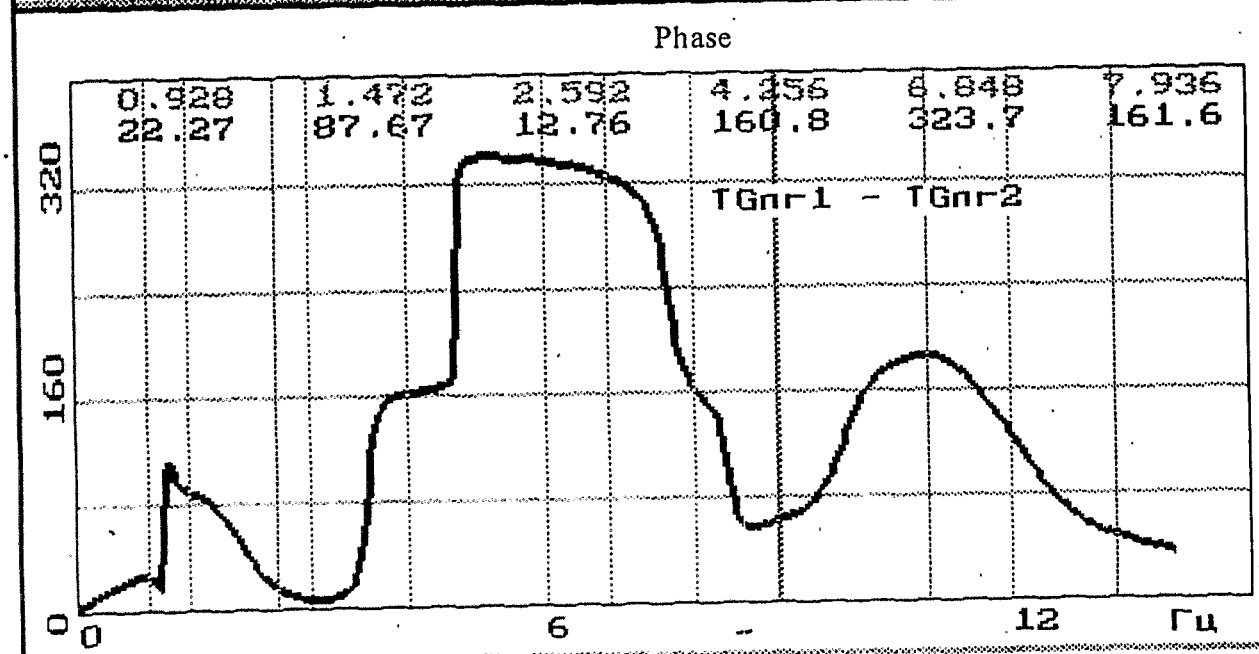
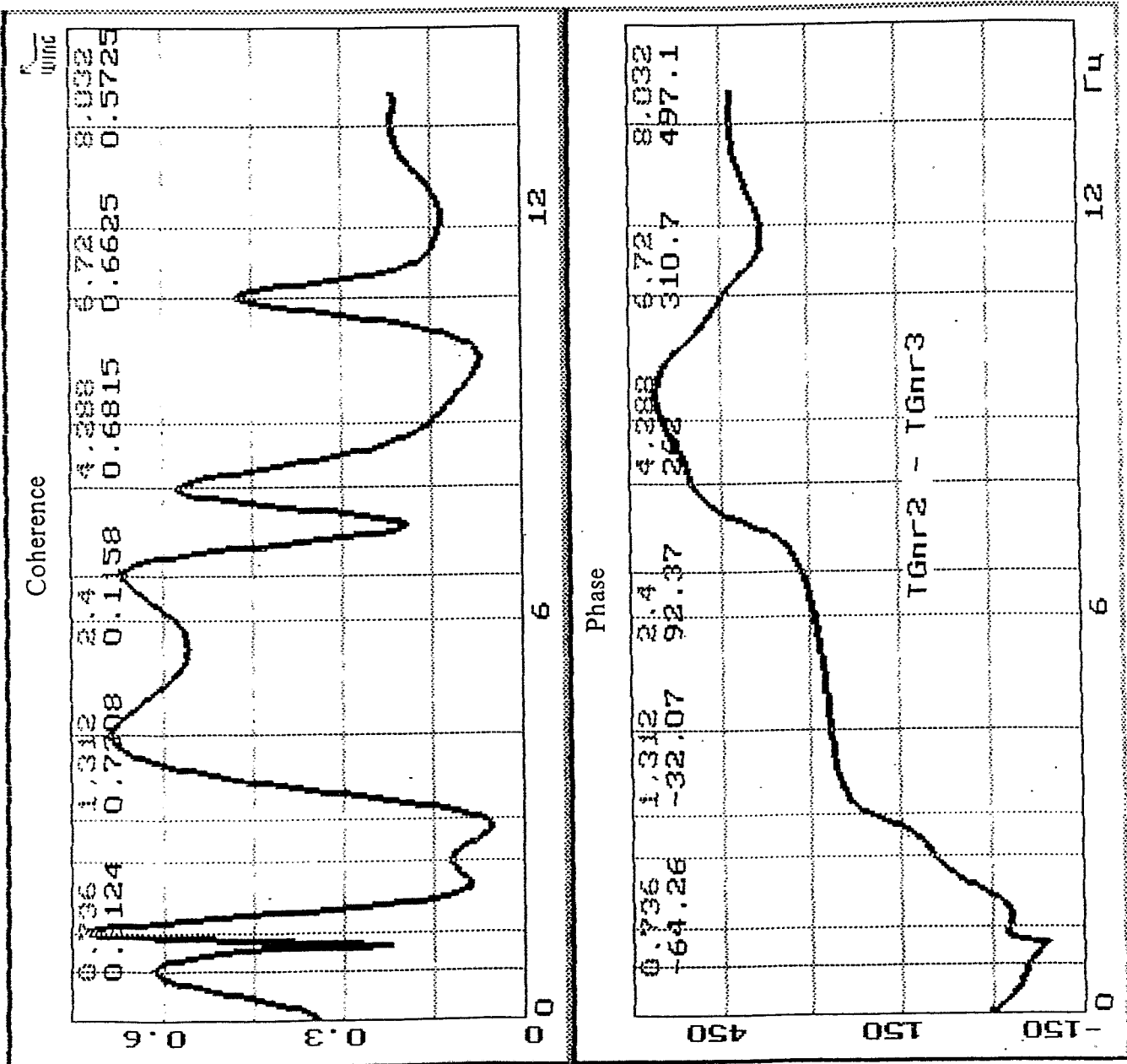


Fig. 59.



0.928	0.39	22.27
1.472	0.8548	87.67
2.592	0.2643	12.76
4.256	0.04011	160.8
6.848	0.538	323.7
7.936	0.1481	161.6
8.992	0.03847	60.23
10.94	0.6075	185.2
13.34	0.1559	45.67





0.736
1.312
2.4
4.288
6.72
8.032
10.94
13.57

0.6124
0.7208
0.1158
0.6815
0.6625
0.5725
0.4733
0.2133

-64.26
-32.07
92.37
262
310.7
497.1
442.3
430.2

Fig. 61. 4 sec. time realization

Thermoconples measurement prosedures

1. Measuring channels PFS № 3, 4, 8 and IC № 7, 14, 21 always in operation
2. In column " № SPD, TC assembly":

T - № SPD, where TC is installed:

7 - SPD № 1 - 7

×4 - SPD № 1 - 4

Table 2

№ SPD, TC assembly		Measurement №														
		60	61	62	63	64	65	66	67	68	69	70	71	72	73	74
07-22	7	x												x4		
09-22	7		x													
14-31	7			x											x4	
01-34	7				x											
04-37	7					x										x4
12-37	7						x									
07-20	T	x	x													
09-20																
14-33	T			x			x								x	
12-35																x
02-33	T				x	x							x			x
04-35															x	
08-31	7							x				x				
05-30	7								x							
04-27	7									x						
08-29	T											x				
07-32							x									
05-32	T							x								
05-28																
04-29	T									x						
04-23																
10-27	7											x				
12-31	7												x			
09-32	T										x					
10-29	T										x		x			
10-25	T											x				
09-28	T											x				
11-28	T											x				
13-32	T												x			
13-28	T												x			
08-23	T													x		

Neutron noise of external IC №1, 2, 3. Peculiarities of APSD

Γ ₁	0.301	0.348	4.22	27.22	33.73	42.50
----------------	-------	-------	------	-------	-------	-------

Matual peculiarities of the spectrums

1) N1 - N2

Γ ₁	0.15	0.27	0.41	0.55	0.68	0.92	2.15	2.22	2.54	3.10	4.22	5.12	5.52	5.71	11.2	11.8	27.7	30.7
Γ	0.16	0.26	0.18	0.16	0.24	0.17	0.11	0.12	0.17	0.09	0.12	0.05	0.07	0.11	0.02	0.07	0.12	0.40
Φ	15	16	16	27	11	250	282	10	113	128	190	173	5	225	223	7	7	5

2) N2 - N3

Γ ₁	0.16	0.28	0.35	0.6	0.70	0.85	0.99	1.07	1.27	1.33	1.46	1.61	1.76	1.9	2.36	2.75	2.87	3.95	5.01	6.43	7.28	9.18	11.5	27.7	30.7	
Γ	0.33	0.35	0.34	0.2	0.25	0.17	0.18	0.24	0.15	0.20	0.25	0.20	0.09	0.1	0.07	0.11	0.14	0.07	0.07	0.18	0.05	0.07	0.14	0.07	0.09	0.56
Φ	12	12	57	40	13	2	115	37	25	13	25	55	92	100	2	2	42	14	191	227	97	117	29	50	14	4

3) N3 - M1

Γ ₁	0.17	0.25	0.29	0.68	0.7	0.85	0.99	1.2	1.3	1.32	1.4	1.5	1.6	1.7	2.0	2.2	2.3	2.7	3.2	3.9	4.3	4.7	5.1	5.5	27.7	30.7
Γ	0.18	0.12	0.15	0.32	0.3	0.05	0.14	0.1	0.1	0.1	0.1	0.1	0.1	0.1	0.1	0.1	0.1	0.1	0.1	0.1	0.1	0.1	0.1	0.1	0.1	0.1
Φ	22	22	51	4	45	17	32	4	26	120	50	75	121	32	52	7	11	32	12	117	97	2	2	2	2	2

Table 8. The frequencies of characteristic phases in ADS signals at Kola NPP, unit №2

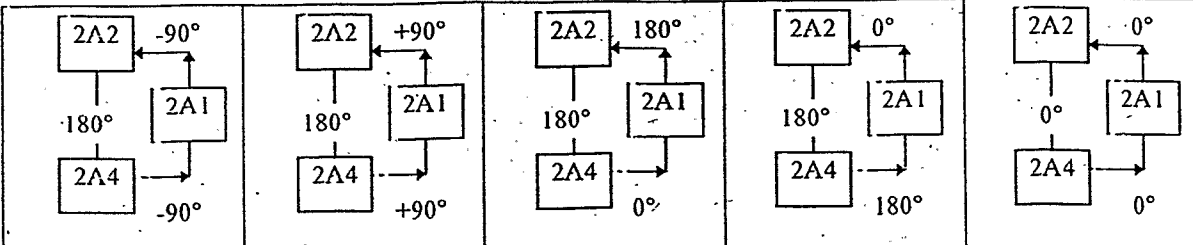
№					
	Rotation motion clockwise	Rotation motion counter clockwise	Pendulum motions from 2 to 4 quadrant	Pendulum motions from 1 to 3 quadrant	vertical motions
1	2.34 Гц	absence			
2	2.78 Гц				
3			3.32 Гц		
4			4.32 Гц		
5	5.13 Гц				
6	5.49 Гц				
7			6.22 Гц		
8			7.80 Гц		
9	8.93 Гц				
10			9.70 Гц		
11		10.70 Гц			
12		11.90 Гц			
13		12.70 Гц			
14			15.62 Гц		
15				19.14 Гц	
16				22.27 Гц	
17				25.59 Гц	
18				30.47 Гц	
19				36.33 Гц	
20				42.58 Гц	
21				43.16 Гц	
22				44.14 Гц	
23				45.92 Гц	
24				48.83 Гц	
25				50.59 Гц	
26				52.73 Гц	
27				57.81 Гц	
28				58.98 Гц	
29			64.26 Гц		
30			73.24 Гц		
31				83.98 Гц	
32				85.55 Гц	
33				89.84 Гц	
34				91.41 Гц	
35				93.55 Гц	

Table 9. The frequencies of characteristic phases in ADS signals at Kola NPP, unit №1

№				
	Rotation motion clockwise	Pendulum motions from 2 to 4 quadrant absence	Pendulum motions from 1 to 3 quadrant	vertical motions
1	4.88 Гц			
2	5.66 Гц			
3			10.35 Гц	
4				17.38 Гц
5				19.14 Гц
6				21.48 Гц
7				25.78 Гц
8				28.71 Гц
9				30.47 Гц
10				32.23 Гц
11				38.28 Гц
12				42.97 Гц
13				44.92 Гц
14				50.78 Гц
15				55.86 Гц
16				57.81 Гц
17				58.98 Гц
18				65.82 Гц
19				72.66 Гц
20				77.54 Гц
21				79.69 Гц
22				83.40 Гц
23				85.35 Гц
24				86.33 Гц
25				87.50 Гц
26				90.43 Гц
27				92.97 Гц

Table 10. Results of decomposition at dominating frequencies

Resonance frequencies, Hz	1.86	2.93	3.71	4.10	4.88	5.08	5.76	10.32	11.13	11.91	12.70	14.26	24.61
Oscillation type													
Pendulum in one direction	0.11	0.10	0.16	-	0.35	0.37	0.27	0.02	-	0.12	0.06	0.05	0.07
Circular	0.02	0.05	-	-	0.57	-	0.37	-	0.02	0.04	0.05	0.03	0.05
Vertical	0.01	0.02	0.05	0.05	0.11	-	0.09	-	-	0.04	0.02	-	0.05
Pendulum stochastic motions	0.12	0.15	-	0.18	0.20	0.20	-	0.03	0.03	0.05	0.04	0.05	0.08

Table 11. Cross characteristics of neutron noise resonances at 100% reactor output

Frequency, Hz	N5 - N13			N13 - N21			N21 - N5			Inherent source in accordance with MAR-mod.	Independence of reactor output
	Cog- ren- ce	pha- se, °	coun- ter- pha- se com- po- nent	Cog- ren- ce	pha- se, °	coun- ter- pha- se com- po- nent	Cog- ren- ce	pha- se, °	coun- ter- pha- se com- po- nent		
0.07-0.08	0.74	30		0.58	13		0.63	10		N13	
0.14	0.70	23		0.76	-17		-	-		N21	
0.23	0.82	14	+	0.78	-17	+	0.89	-5		N5	
0.63	0.85	0		0.82	-3		0.90	-3		N5	
1.03	0.67	5	+	0.45	18	+	0.70	13		N13	
1.20	0.30	-13		0.31	-6		0.30	15		N13	
1.63-1.83	0.24	33		0.15	19	+	0.68	24	+	N21	
2.49-2.53	0.49	7		0.21	40		0.10	-32			
2.75	0.37	-4		0.18	-98		0.58	22			
3.00-3.03	0.16	53		0.31	-76		0.10	28			
3.50-3.66	0.24	6		0.17	-39		0.23	41			+
3.88	0.39	77		0.17	1		0.11	119			
4.00	0.14	15		0.20	176	+	0.39	128	+		
4.24-4.50	0.14	48		0.15	145	+	0.16	143	+		+
4.76-4.84	0.23	28		0.10	-124		0.11	161			+
5.20-5.27	0.16	54		0.23	206		0.10	-130			
6.44-6.88	0.10	150		0.14	-46		0.19	-14			+
7.10-7.32	0.12	155		0.19	-101		0.15	-11			+
8.20-8.35	0.34	-40		0.49	22		0.47	13			+
9.89	0.29	115		0.11	100		0.13	94			
9.96	0.40	152		-	-		0.18	-191			
10.25-10.33	0.21	103		0.27	52		0.10	151		N5	+
11.87-12.16	0.09	26		0.07	170		0.14	180			+
12.67-12.89	0.09	-94		0.09	179		0.08	-70			+
13.62-13.99	0.08	-50		0.07	160		0.06	-159			+
14.21	<0.1	10		<0.1	-134		<0.1	107			
15.38-15.97	<0.1	73		<0.1	-150		<0.1	115			
17.36-17.43	<0.1	-		<0.1	-11		<0.1	4			
18.02-18.16	<0.1	2		<0.1	28		<0.1	53			+
19.34-19.48	<0.1	-60		<0.1	60		<0.1	-85			+
21.09-21.53	<0.1	-120		<0.1	-102		<0.1	-29			
24.17	<0.1	95		<0.1	-43		<0.1	100			
24.60-24.72	0.3	20		0.23	-7		0.17	-5			+
25.34	<0.1	13		<0.1	-20		<0.1	-41			
26.51	<0.1	-12		<0.1	-56		<0.1	26			
27.54	<0.1	-39		<0.1	-20		<0.1	123			
28.56	<0.1	11		<0.1	-172		<0.1	-146			
29.59-29.88	<0.1	-109		<0.1	-196		<0.1	45			
30.91	<0.1	149		<0.1	165		<0.1	-10			+
31.93-32.37	<0.1	39		<0.1	-18		<0.1	73			
34.57-34.72	<0.1	108		<0.1	-159		<0.1	8			+
35.60	<0.1	90		<0.1	47		<0.1	60			
36.62-36.77	<0.1	21		<0.1	-27		<0.1	61			
39.70-39.99	<0.1	65		<0.1	-170		<0.1	100			+
41.60-42.04	<0.1	82		<0.1	-153		<0.1	87			+
44.24	<0.1	46		<0.1	-131		<0.1	84			
46.14	<0.1	77		<0.1	-167		<0.1	70			+
47.31	<0.1	82		<0.1	-168		<0.1	89			

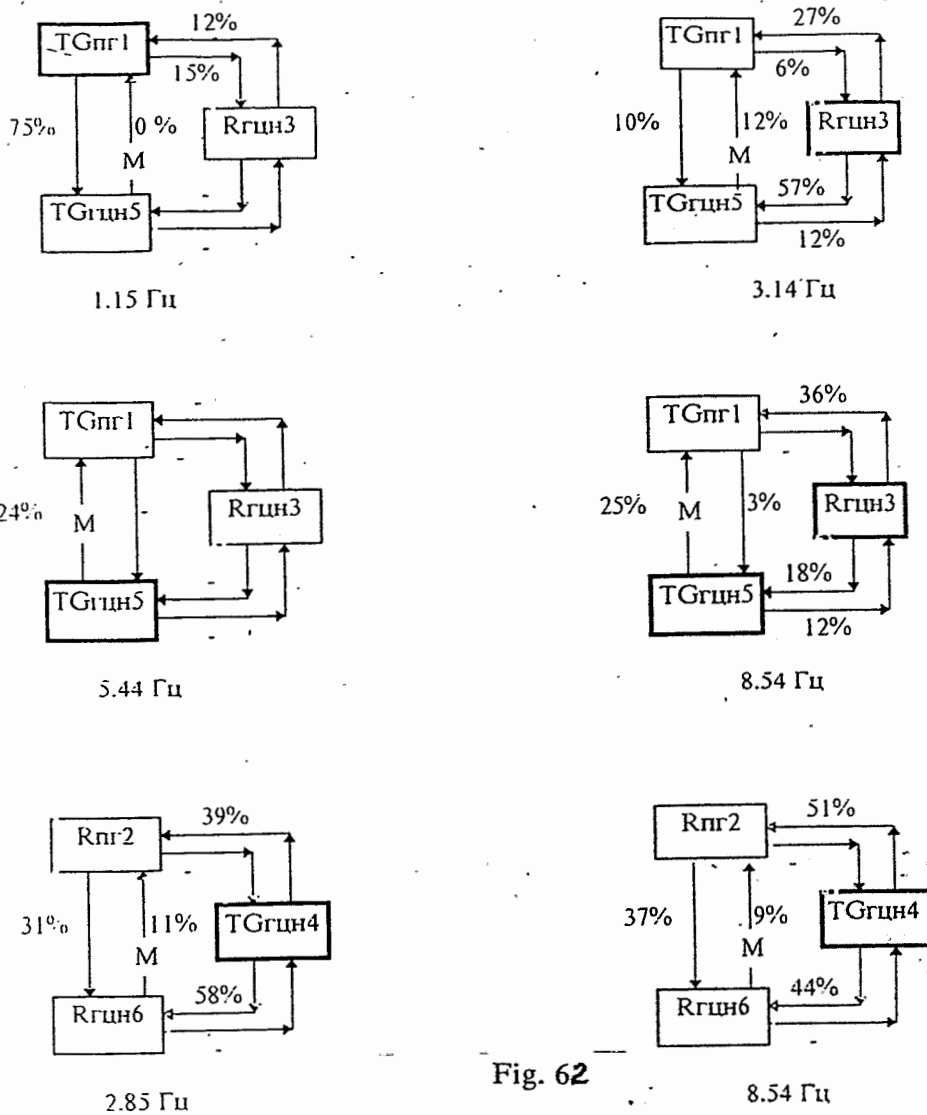


Fig. 62

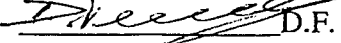
Table 12. Summary table of MAR-analysis

MAR- модель	TG _{пг4} R _{гцн4} P2	TG _{пг1} TG _{гцн1}	R _{гцн1} R _{пг1} TG _{гцн1}	TG _{пг4} R _{пг4} R _{гцн4}	TG _{пг5} R _{пг5} R _{гцн5}	R _{пг2} TG _{гцн4} R _{гцн5}	TG _{пг1} R _{гцн3} TG _{гцн5}	Эле- мент, явление, возбуж- дающее ГЦК	Домини- рующее направ- ление колеба- ний	Нали- чие харак- терных фаз	Предпола- гаемая мода колебаний
Гц											
0.90- 1.50	TG _{пг4}	TG _{пг1}	R _{пг1}	TG _{пг4} R _{пг4}	TG _{пг5}	-	TG _{пг1}	ПГ	T _{пгг}	0° TG _{пг1} - TG _{гцн1}	Маятниковые колебания ПГ вокруг вертикальной оси реактора
1.80	-	-	-	-	R _{пг5}	-	-	ПГ	R _{пгг}	180° R _{пгг} - R _{гцн1}	Маятниковые колебания ПГ вокруг собственной вертикальной оси
2.78- 3.40	-	TG _{пг1} TG _{гцн1}	TG _{гцн1}	-	-	TG _{гцн4}	TG _{гцн5} R _{гцн3}	ГЦН	TG _{гцн1}	180° TG _{пг1} - TG _{гцн1}	Маятниковые колебания ГЦН вокруг оси трубопровода
5.44	-	-	-	-	-	-	TG _{гцн5}	ГЦН	TG _{гцн1}	0° R _{пгг} - R _{гцн1}	
6.28- 6.45	P2	-	-	-	-	-	-	АСВ	-	-	
8.70- 9.00	-	TG _{пг1} TG _{гцн1}	TG _{гцн1}	-	-	TG _{гцн4}	TG _{гцн5}	ГЦН	TG _{гцн1}	-	

Teil 2

APPROVED

Director General of Diagnostic
Center "DIAPROM"

 D.F. Gutsev
"27" мая 1996 г.

VIBRATION MODELLING of VVER TYPE REACTORS

**The analysis of the design characteristics and
experimental data for
adjustment of the VVER-1000 model**

**The intermediate report
320-O.211-004**

Part 1

1996

CONTENT

1. INTRODUCTION	3
2. ANALYSIS of DESIGN DOCUMENTATION	5
2.1 The upper block.....	5
2.2 The main coolant pump.....	7
2.3 Possible malfunctions of the reactor.....	9
3. THE ANALYSIS of EXPERIMENTAL DATA.....	11
3.1. Composition of experimental investigations of VVER-1000 vibration.....	11
3.2. Pressure fluctuations.....	14
3.3. Parameters of a dynamic response of the equipment.....	19
3.4. The vibrational characteristics of the equipment.....	28
4. THE CONCLUSION and PROPOSALS.....	47
List of adopted abbreviations.....	48

1. INTRODUCTION

1.1. The interpretation of signals in the system of vibrational diagnostics VVER-1000 plant should be founded on detail knowledge of the vibrational characteristics of the equipment depending on conditions of its manufacture, assembly and maintenance.

The most optimal tool of definition of the vibrational characteristics of the equipment is vibration modelling.

1.2. Necessary stages of creation of a vibrational model are:

a) Development of input datas at the mass-inertia and elastic characteristics of the equipment because of of design documentation;

b) The analysis and registration in a model of the most probable not design states (malfunction), which can take place in a construction and which can be fixed on a dynamic response of the equipment: a wear of support structures, weakening of a rigidity of a fasteners, not design conditions of manufacture or assembly and etc.;

c) Set-up and verification of a computational model by results of experimental researches of parameters of vibration of actual plant.

1.3. In the present report data on three above-stated directions of development of a vibrational model of vver-1000 are represented.

In section 2 of the report, in addition to data of the report on the previous stage, analysis of design documentation under the elastic and mass characteristics of the upper block and MCP for the more detailed schemes in a structure of a global plant model is given.

In the same section on the basis of the analysis "The Descriptions of VVER-1000 reactor " a list of possible malfunctions in conditions of internals fastening is given which were observed or can take place at maintenance of a reactor. The computational model PY should provide the registration and study of influence of these malfunctions on the vibrational characteristics of the equipment. In consequent (after realization of preliminary calculations under the program) experimental data on quantitative influence of those not design condition will be shown which managed to be fixed at vibrational measurements during VVER-1000 comissioning.

The section 3 of the present report contains the experimental information on eigen frequencies and modes of plant equipment for adjusting of vibrational model. In the basis of the shown data results of vibrational starting-up and adjustment measurements of VVER-1000 plant lie. The value of such experimental data for adjusting of model is stipulated by the following circumstances:

The starting-up and adjustment measurements were conducted at all 20 NPP with VVER-1000, entered in maintenance to the present of time, that provides a completeness of the information on possible vibrational condition of the plant;

Such measurements were conducted at various operational condition of the equipment (at various temperatures of the coolant and conditions of internals fastening, at various quantities

and combinations of working MCP etc.), that allows to estimate influence of the similar factors to parameters of the dynamic response of a design;

As the development of the programs of starting-up and adjustment measurements, and analysis of the obtained data were conducted with engaging of vibrational researches of scale models of VVER-1000 plant, that increases reliability of the experimental information.

1.4. In addition to the data, necessary for direct adjusting of vibrational model, in section 3 of the report the analysis of hydrodynamic instability of the coolant is described. Such analysis is necessary as for obtaining a more full picture on possible plant vibrations, and definition of hydrodynamic forces at consequent calculations of forced vibration of the plant equipment.

2. THE ANALYSIS of the DESIGN DOCUMENTATION

2.1. The upper unit

2.1.1. The upper unit (the fig. 2.1) consists of the following main units: cover (1), control rod drives (2), traverse (3) in the assembly.

Overall dimensions of the upper unit:

Altitude at transporting	- 8285 mm;
Diameter outside on a flange	
Cover of the upper unit	- 4580 mm;
Altitude from a reference surface	
Cover up to connectors of branch nozzles	- 2634 mm;
Altitude of a cover of the drive	- 2874 mm;
Outside diameter of a cover of the drive	- 120 mm;
Step between branch nozzles	- 236 mm;
Weight of the upper unit	- 158 t

Material of the upper unit:

Cover - 15X2HMΦA

Metal construction - BCт3

Weight of the main(basic) constituents of the upper unit is adduced in tab..2.1.

2.1.2. The cover of a reactor has the bearing form(shape) and represents a welded design, consisting of a "truncated" ellipsoid and a flange.

On a cover there are 61 branch PEM nozzles, 14 branch TI nozzles (9), 16 branch NMC nozzles (10), 1 branch blast nozzle and 6 cylindrical lugs with threaded sockets for the installation of bars (6) of metal design of the upper unit.

2.1.3. The CR drive is the executive gear of CPS and is intended for launch, regulation of power and shut down of a nuclear reactor by introduction in an active zone or ascent from its control organ.

2.1.4. The metal design of the upper unit includes:

6 Bars, installed in lugs on an outside surface cover, connected with two spacing grids (7,8);

Air collector (4) with removing chests.

The plate upper (7) provides a centre-of-gravity position of PEM drives, the contraction of hexahedral tubes (11) and serves as the limiter of movement of drives in a horizontal direction at seismic effects.

The collector (4) serves for a tap of a cooling air from drives.

2.1.5. The traverse (3) consists of the lower page, to which ring-type lip, edge and eye is welded. During reactor operation the traverse is installed on the construction of the upper unit.

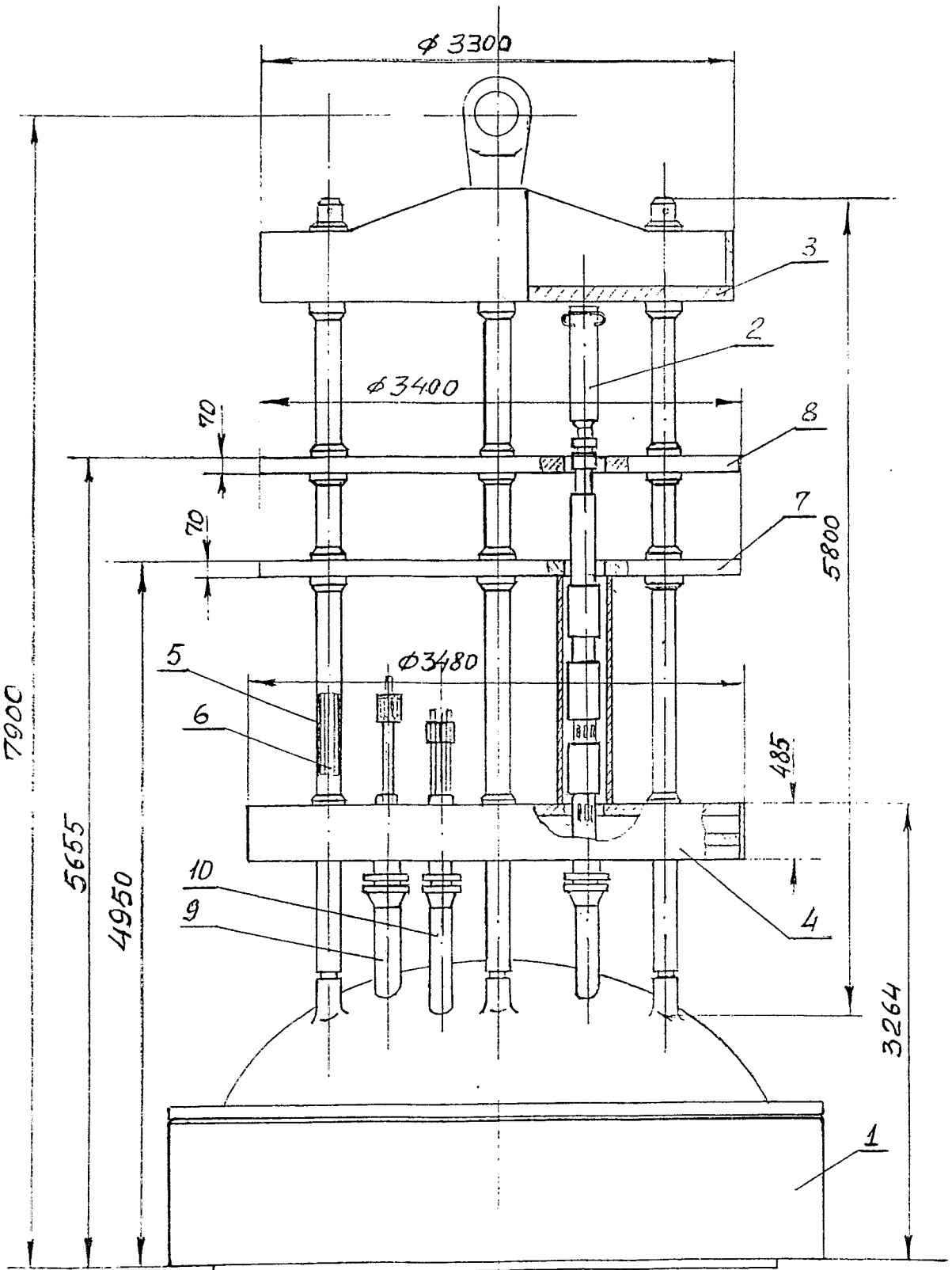


Fig. 2.1

Таблица 2.1

Составные части блока верхнего (рис. 2.1)
Upper unit components

Поз. Pos.	Наименование Name	Кол-во Quant	Масса, 1шт.кг 1ps.kg
1	Крышка Top head	1	90300
2	Привод ШЭМ PEM drive	61	550
3	Траверса Traverse	1	11570
4	Коллектор Header	1	5242
5	Труба $\varnothing 133 \times 12$ Tube	6	132
6	Штанга $\varnothing 80$ Mast	6	220
7	Плита верхняя Top plate	1	2100
8	Решетка дистанционирующая Spacing grid	1	2100
9	Патрубок ТК Nozzle TI	14	-
10	Патрубок КНИ Nozzle NMC	16	-
11	Труба шестигранная Hexahedral tube	61	16

2.2. The main circulating pump

The main circulating pump ГЦН-195М type is intended for creation of circulation of the coolant in a closed loop of VVER-1000 .

ГЦН-195М (fig. 2.2) represents the vertical, centrifugal pump with the unit of the shaft seal cantilever driving wheel, axial bring of a water and the asynchronous motor (1).

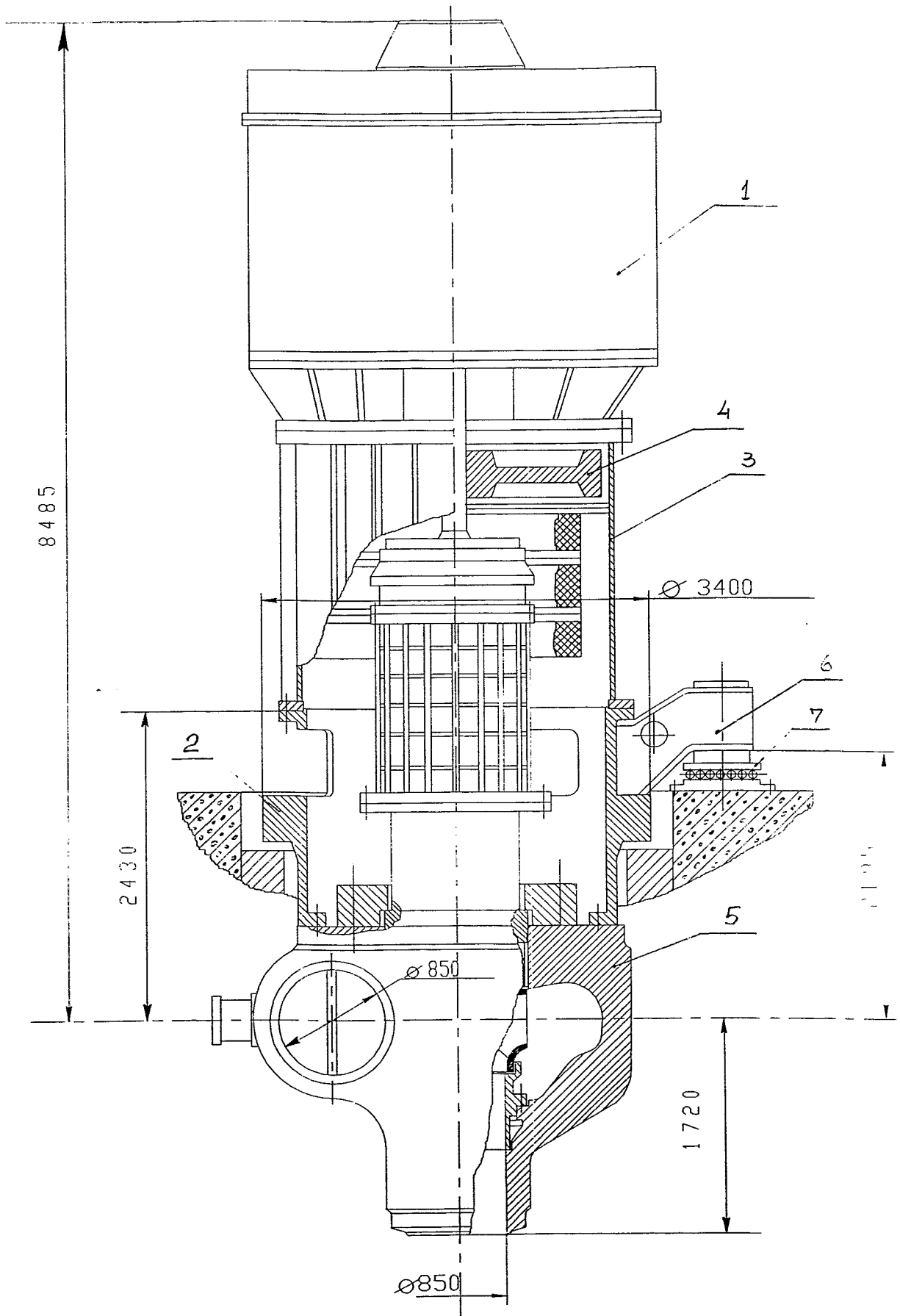


Fig. 22.

A main bearing construction of the pump is weld-cast lower drum element (2) with three brackets (6). On the upper flange of lower the drum element is installed welded upper element (3), on which fastens the motor with the fly-wheel (4). By the lower flange lower element incorporates by bolts with a limaçon of the pump (4). The brackets of lower element lean on reference hinged devices (7), installed on overlap, that allows MCP to move, following for temperature deformations of primary circuit pipes. The connection of MCP limaçon with MCC pipes implements by welding.

MCP weight (195M type) with a limaçon no more than 131,5 т,

Including motor - no more than 48 т,

Purely the pump with a limaçon - no more than 61 т.

2.3. Possible malfunctions of the reactor

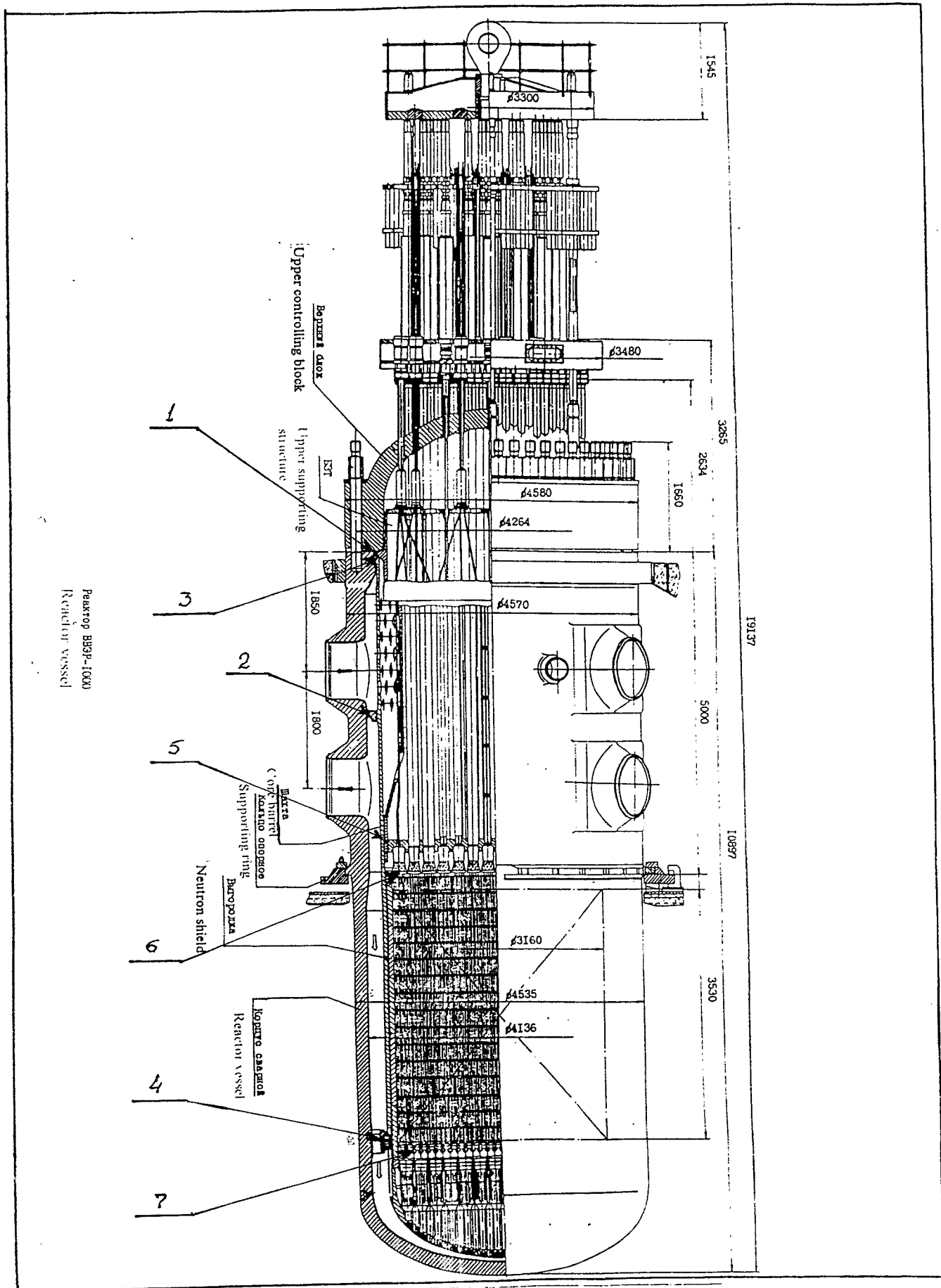
2.3.1. The list of possible malfunctions in conditions of internals fastening, which should be discounted in a computational model of a reactor, is shown in tab. 2.2.

On fig. 2.3. a label of zones of a reactor is given, where there are the above-stated malfunctions.

Table 2.2

Possible malfunctions (damages) in internals fastening conditions

Reactor element	Destination of zone in accordance with fig.2.1.	Malfunction description
Core barrel	1	Relaxation of clasp tubes 63x5 with slackening of core barrel claspings from reactor cover
	2	Exceeding of design gaps at separating ring
	3	Breaking or wear of contact surfaces of keys and key grooves
	4	
PTU	5	Exceeding of design gaps in key junctions of PTU lower plate with core barrel
FA	6	Relaxation of spring units in FA heads
Supporting tubes of reactor bottom	7	Disturbance of wholeness of welding of supporting tube



Peaktrop BB3P-1000
 Реактор vessel

Fig. 2.3

3. THE ANALYSIS OF EXPERIMENTAL DATA

3.1. The composition of VVER-1000 plant vibration investigations

~~3.1.1.~~ The experimental vibration of VVER-1000 plant, which had been carrying out at the design stage, included:

a) vibration investigations of simplified 1:50, 1:44 and 1:10 scaled models. These models simplified to approximate design schemes were used to study modes and eigenfrequencies of reactor internals and aimed at both assessment of dependency on fastening state and equipment composition and justification of technique for calculating dynamic behaviour of reactor internals in operating and emergency conditions.

b) hydrodynamic and vibration study of the one fifth scale model of primary circuit comprising reactor model, as well as main equipment of the primary circuit.

c) hydrodynamic and vibration study of full-scale models of 7-FA rigs.

In absence, the above models represented a sector of real reactor since they had fragments of the real equipment and its full-scale models approximating real ones as far as possible, on both equipment composition, and coolant velocities and flow rates through the model, and fastening reactor internals.

~~3.1.2.~~ Preoperational full-scale (field) measurements of vibration parameters are the following and the most important stage in investigating vibrations and justifying vibration strength of reactor internals and fuel assemblies. Such measurements are performed at any reactor when running equipment and are mandatory.

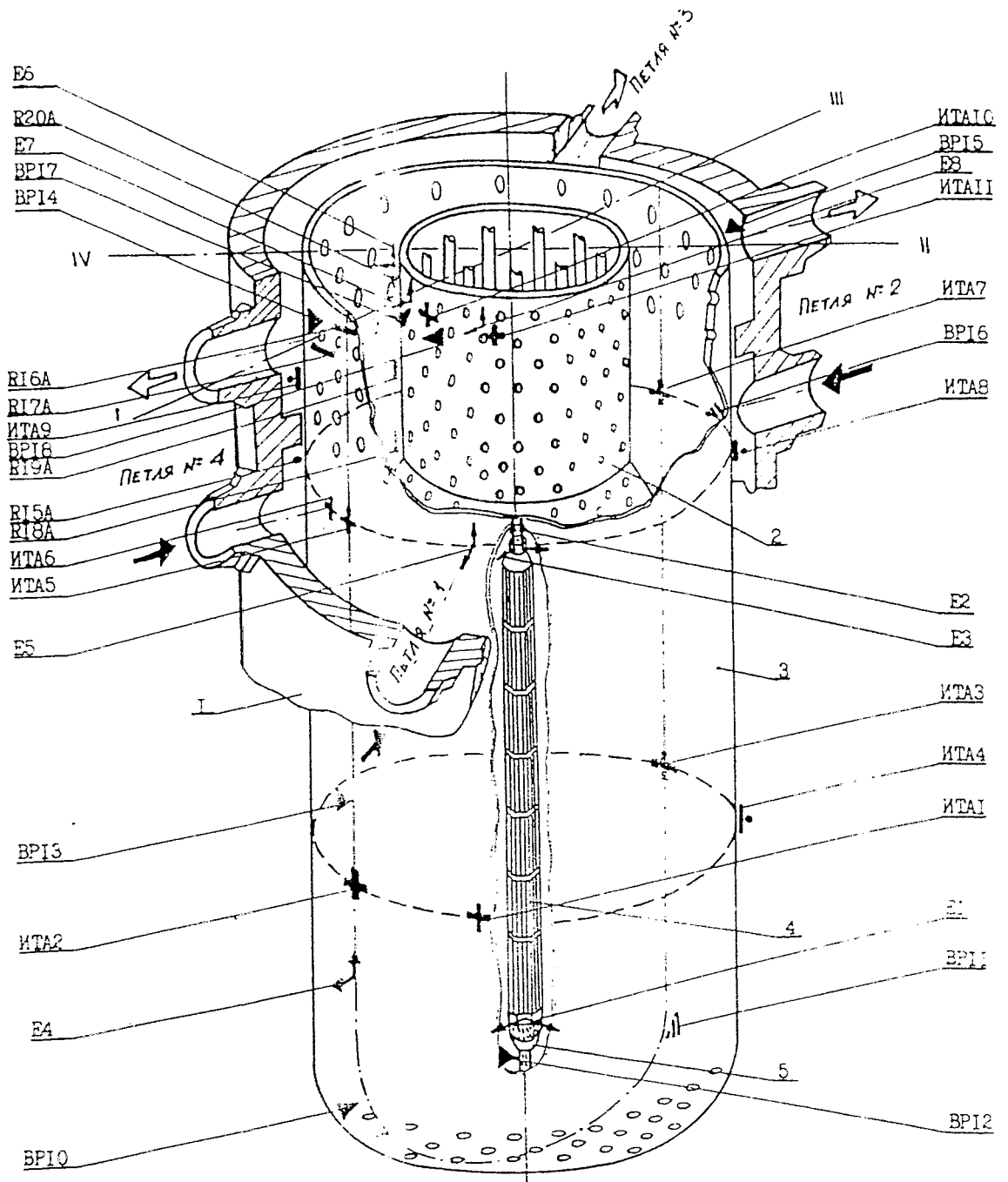
Measurement of vibration parameters at the forerunner VVER-1000 reactor of Novo-Voronezh-5 was performed on the basis of broadened programmes and was directed to confirm adopted design solutions based on conditions of vibration strength. Sufficiently large number of transducers installed on components of reactor internals was applied to provide measuring pressure pulsations, dynamic stresses and vibrations in all characteristic points of reactor internals, and to obtain representative data to estimate strength and lifetime of reactor internals.

Scope of tests and number of metering aids are decreased for the rest of reactors in the series as compared to Novo-Voronezh-5. The measurements are used as basis for inspection and first of all are intended for confirming vibration similarity of the reactor being tested to the forerunner, and otherwise they should reveal and eliminate likely technological deviations in conditions of manufacturing and assembly of reactor components.

The scheme in fig. 3.1 and 3.2 are used for all VVER-1000 reactors in the commissioning stage and comprises 34 sensors at internals and 28 measurement points at MCC.

Preoperational measurements are conducted at both initial stage of reactor running when the reactor is cold, and at rated parameters of hot running ($P=15.7$ MPa, $T=280^{\circ}\text{C}$) at various

Scope of full-scale measurements at serial VVER-1000 reactor

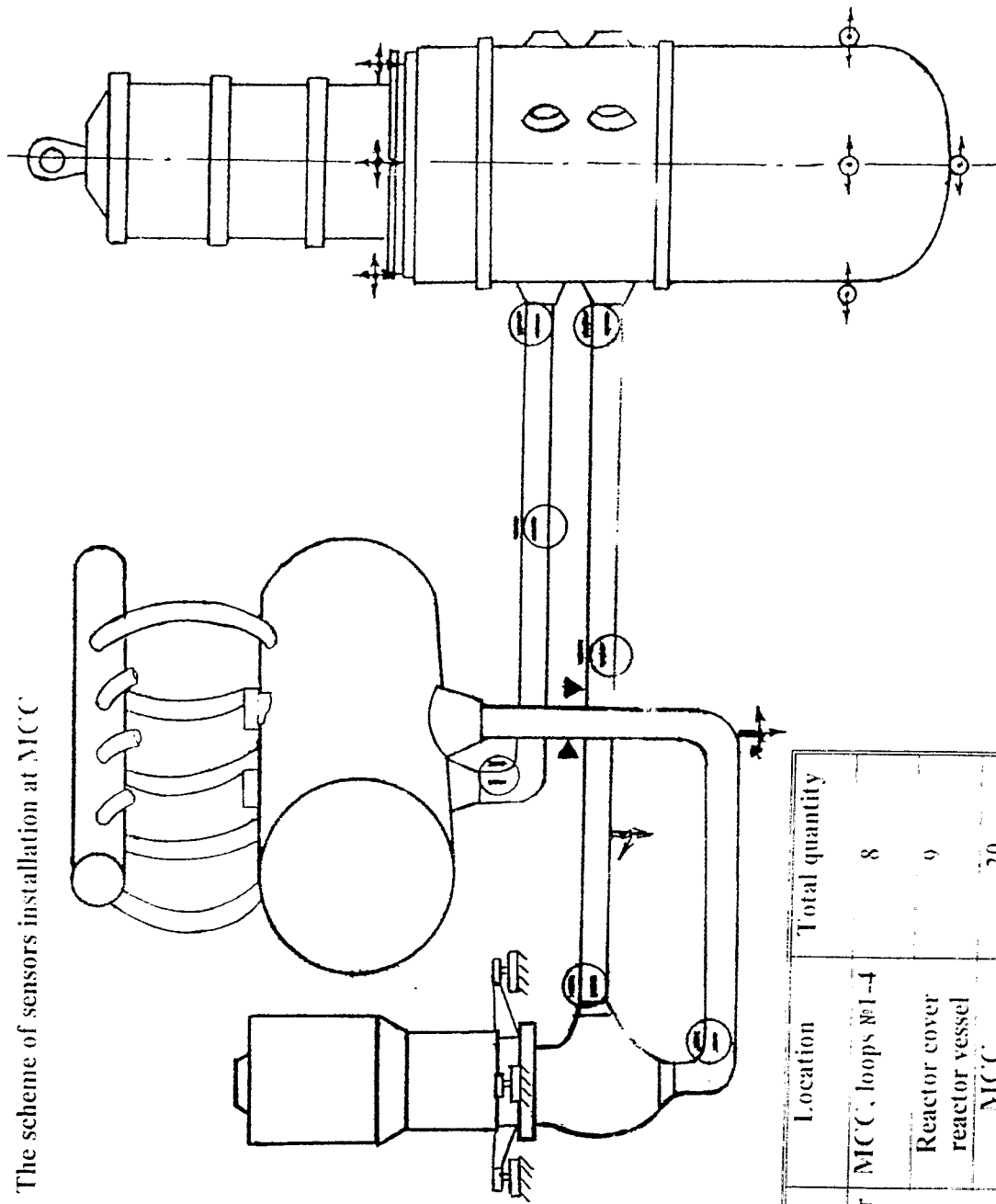


1- reactor vessel; 2- STA shell; 3- core barrel;
 4- central dummy FA; 5- suport tube

- ▷ - PT
- + — Resistance strain gage
- ↗ - Vibration detector

Fig.3.1.

The scheme of sensors installation at MCC



Designation	Sensors type	Location	Total quantity
▲	Pressure transducer	MCC, loops №1-4	8
⊕	Two-component accelerometer	Reactor cover reactor vessel	9
↑	Vibration displacement transducer	MCC, 1 loop №1-4	20
⊖	Strain-gage transducer	MCC, Loops №1-4	20

Fig. 3.2

number and combination of operating MCPs. Besides, loading level of reactor internals is recorded in transients related to start-up and de-energizing MCPs.

Schemes for concurrent data recording sensors of different types (thermostable strain gages, pressure gages and two-component accelerometers (of strain gage type) are composed to perform measurements.

3.1.3: The main purpose of a complex of experimental investigations was confirmation of strength and longevity of the equipment of the plant.

At the same time significant number of applied sensors and diverse ways of energization of oscillations allow to use the obtained information and for the analysis of the vibrational characteristics of the equipment of the VVER-1000 plant.

Such analysis is executed within the framework of the present activity and has two following problems:

a) definition of frequency range, describing vibrations of the plant equipment. With this purpose in section 3.2 and 3.3 a general picture of pressure fluctuations and dynamic response of the equipment is given;

b) the analysis of eigen frequencies and modes of the equipment in detected frequency range.

3.2. Pressure fluctuations

3.2.1: A significant part of the full-scale investigations of internal vibrations of VVER-1000 reactors was aimed at establishing the main pressure pulsation sources; at analysing the conditions of their propagation along the reactor hydraulic path, as well as at assessing a controllability of the intensity of these or those pressure pulsation components. Such analysis was necessitated by the fact that pressure pulsations were the root causes of vibrations, and it was precisely the understimation of the disturbing hydrodynamic forces that the main cause for reactor equipment damage at the initial stage of operation of the first NPPs operation.

3.2.2: The main sources of pressure pulsations in the coolant flow may be considered using the spectral density curves of pressure pulsation intensity in the pressure pipeline of the forerunner VVER-1000 reactor of the Novo-Voronezh-5 (Fig. 3.3) which were derived at the running stage.

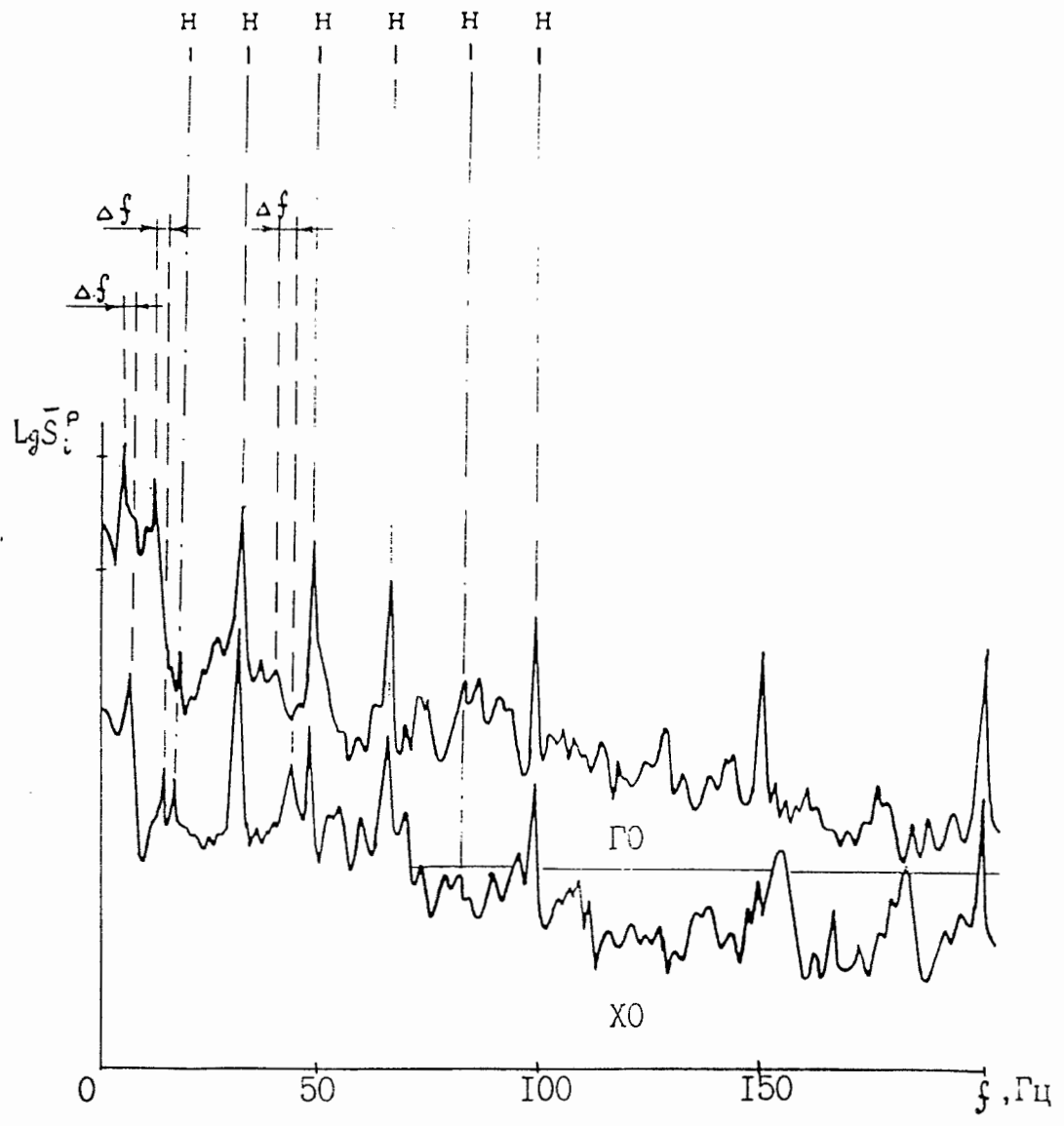
The presented data show that the most intensive frequency components are as follows:

16.5; 33.0; 49.5; 66.0 and 99.0 Hz;

1.3; 9.0; 13.8 Hz for the cold reactor state, as well as 0.8; 7.0; 9.2 Hz for the hot running parameters.

The first set of frequency components is related to the MCP operation and is caused by the hydraulic unbalances resulting from the varying gaps between the shaft of the MCP and mating structural components, as well as by the interaction of impeller vanes and coolant flow.

Results of pressure fluctuations measurements in MCC during cold (XO) and hot (ГО) tests



H - frequencies component deal with MCP
Δf - ASW frequencies shift because of temperature changes

Fig. 3.3

Ив. № подл.	Подп. и дата
Влам. инв. №	Ивв. № дубл.
Подп. и дата	Подп. и дата

Ивв. № подл.	Ивв. № дубл.	Влам. инв. №	Подп. и дата
--------------	--------------	--------------	--------------

The second group can be identified as a set of frequencies of coolant natural acoustic oscillations which follows from the following indications:

the values of these frequencies depend on coolant temperature and sound velocity in liquid is related to temperature;

these components are present in different points of the reactor flow path which shows to the all-system generic nature of these pressure pulsations;

phase angle equals 0 or 180° which is specific for pressure standing waves.

The above sources act on the background of broadband noise whose power decreases monotonically as frequency increases.

Its source is the flow turbulence, as well as vorticities in the location of the change of flow sections and flow directions.

3.3. Pressure pulsations in the flow path of the serial V-320 reactor are of similar nature (Fig. 3.4, the data on the Kozloduy-6), though the values of coolant natural oscillation frequency may differ from the above data by 20% maximum. The latter is explained by a different configuration of circulation loops in V-320 reactor and a different volume of coolant as compared with Novo-Voronezh-5 reactor.

In addition to the analysis of pressure pulsation sources in the reactor flow path the data shown in fig. 3.4, also contain information about the pulsation levels in the characteristic points of the reactor.

The highest pressure pulsations (RMS pressure is up to 4.2 kPa) were measured in the main circulation pipeline at the MCP suction. Practically the same value (4.0 kPa) was measured in the pressure pipeline. The closeness of the pressure pulsation levels at the MCP inlet and outlet is explained by the fact that coolant flow instability is formed in these zones due to the MCP pulsations which propagate over the circuit in two directions.

As regards other zones, the most interesting ones include:

zone of coolant flow inlet into the core where pressure pulsations do not exceed 1.5 kPa;

zone of coolant flow outlet from the reactor (sensor BP15) where pressure pulsations reach 4.0 kPa.

It is worth noting that when all MCPs are in operation an elevated pulsation level in the latter zone is related to a broadband noise whose occurrence is explained by the throttling of the flow when it passes through the perforated section of the CB (see fig. 3.5). When the MCP of loop No.2 (opposite which the sensor is installed) is switched off, pulsation spectrum changes notably and primarily consists of discrete components, related to the MCP operation and coolant natural oscillations. In this case the pulsation level decreases 2 - 3 times.

Exactly the same nature of variations of pressure pulsation frequency components in this zone was also recorded when performing measurements in other reactors. It is necessary to add that a reverse coolant flow of a sufficiently low rate is formed in the loop being switched off.

Distribution of pressure fluctuation APSD over reactor V-320 primary circuit at plant full power

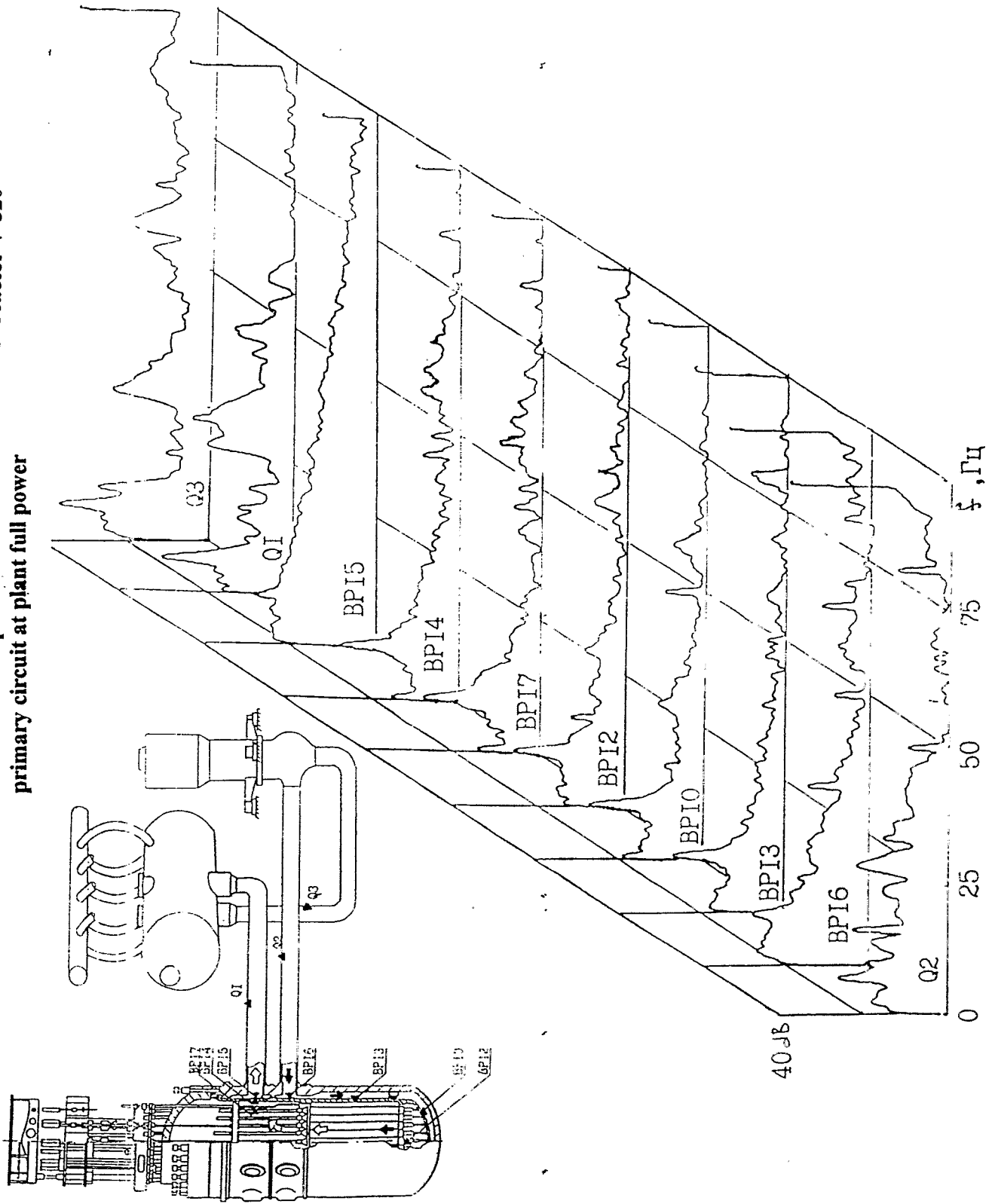


Fig. 3 4

Pressure fluctuations characteristics according to operation conditions (combination of the operating MCP), data on Kosloduy-6

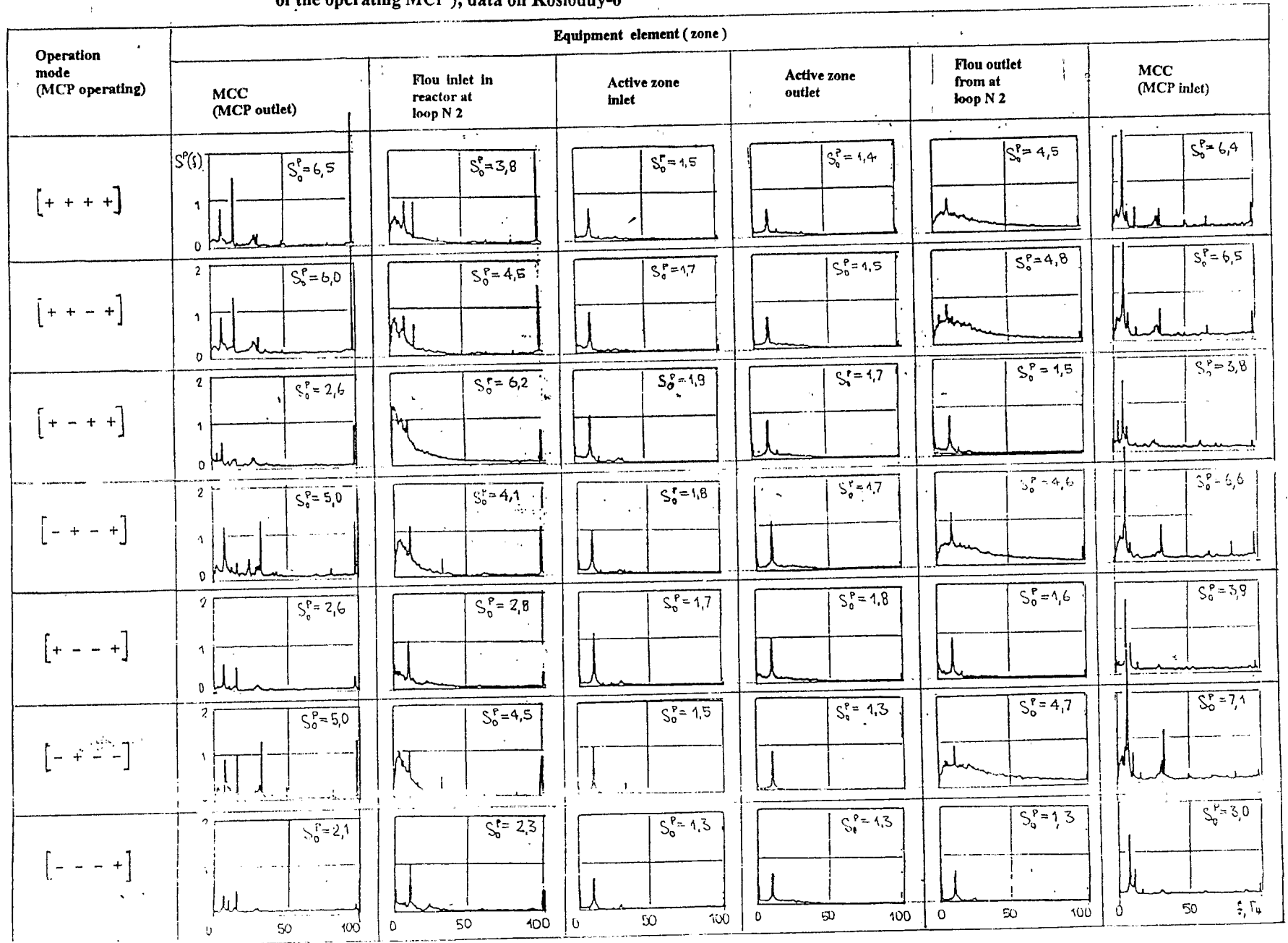


Fig. 3.5

All-system generic pressure oscillations shall dominate in such a flow, and this is really the case.

We should note that the above example of vorticity in the zone of flow outlet from the reactor is the most prominent manifestation of flow disturbances caused by the equipment configuration. In the remaining controlled zones of the flow path the manifestation of this source is less prominent. This is one of the results of the large-scale efforts undertaken at the VVER-1000 design stage to improve the hydrodynamics of the flow path.

3.2.4. Let's consider further the dependence of the pulsation level on the reactor operation conditions. The data presented in Fig. 3.5 attest that the pressure pulsation level is ambiguously related to the reactor running mode in terms of the number and combination of the operating MCPs. So, at the reactor flow inlet the highest pressure pulsations occur when three MCPs are in operation and coolant flow through reactor is not maximum. Similar effects are explained by the superposition of pressure waves which results in a higher asymmetric operation of the loops.

The comparison of the measurement results of reactor running and reactor operation at nominal power level (Fig. 3.6, the data on Balakovo-4) attests that coolant temperature increase from 280°C to 320°C (in hot lines of the main circulation pipeline) results in a certain redistribution of the level of pulsations generated in the main circulation pump: pulsation intensity on the reverse side decreases, while on the vane side it, on the contrary, increases. The values of frequencies, related to the coolant natural oscillations, also decrease by 10% maximum. As it has been already noted, the latter is related to the dependence of sound velocity on temperature.

When reactor is at power, the frequency composition of pressure fluctuations is qualitatively similar to the composition during the startup measurements.

3.3. Parameters of the dynamic response of the equipment.

3.3.1. Some results of measurement of parameters of the dynamic response of the plant equipment is shown on fig. 3.7 - 3.14

From the shown data follows, that the primary oscillations of the equipment are forced. So, in spectrums of vibration stresses predominate frequent components, connected with activity of MCP (16,5; 33,0; 49,5 and 99,0 Hz) and own oscillations of the coolant (0,8; 8,0; 10,5 Hz).

As well as in case of pressure oscillations, vibration of internals elements is a little bit higher for modes with asymmetrical arrangement of working loops. The most sensing to change of a combination of working MCP there are the sensors, located in a mean part of the core barrel (see fig. 3.7, " a zone of input nozzles"). This fact indicates on the fact, that the conditions of energization of low-frequency oscillations of the core barrel immediately depend on distribution of hydrodynamic loads on its surface.

Ивв. № посл.	Подп. и дата	Взам. инв. №	Ивв. № дубл.	Подп. и дата

Results of pressure fluctuations measurements at plant full power, data on Balakovo-4

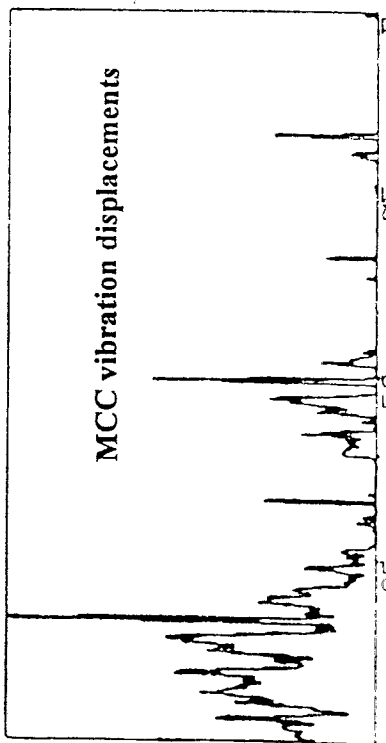
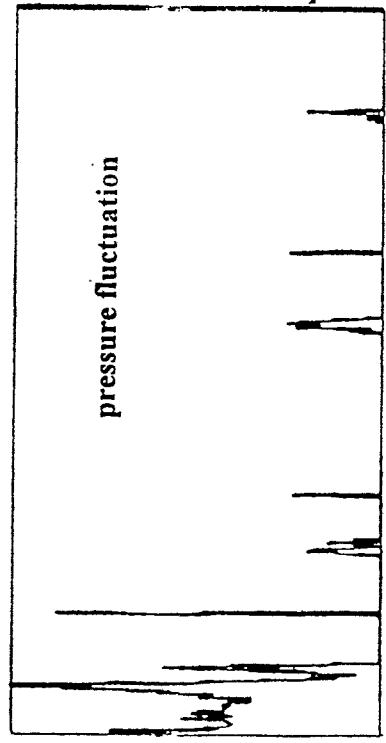
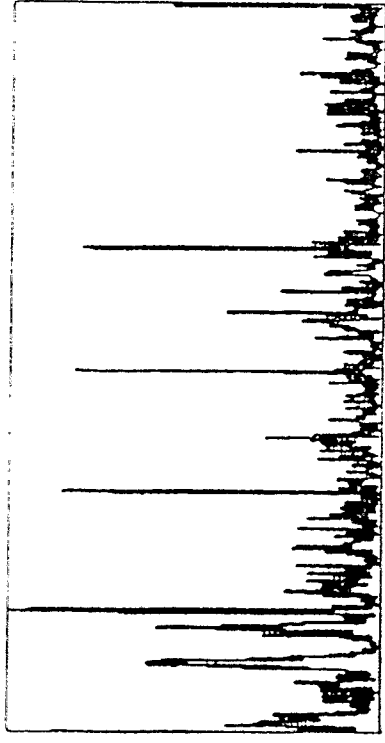
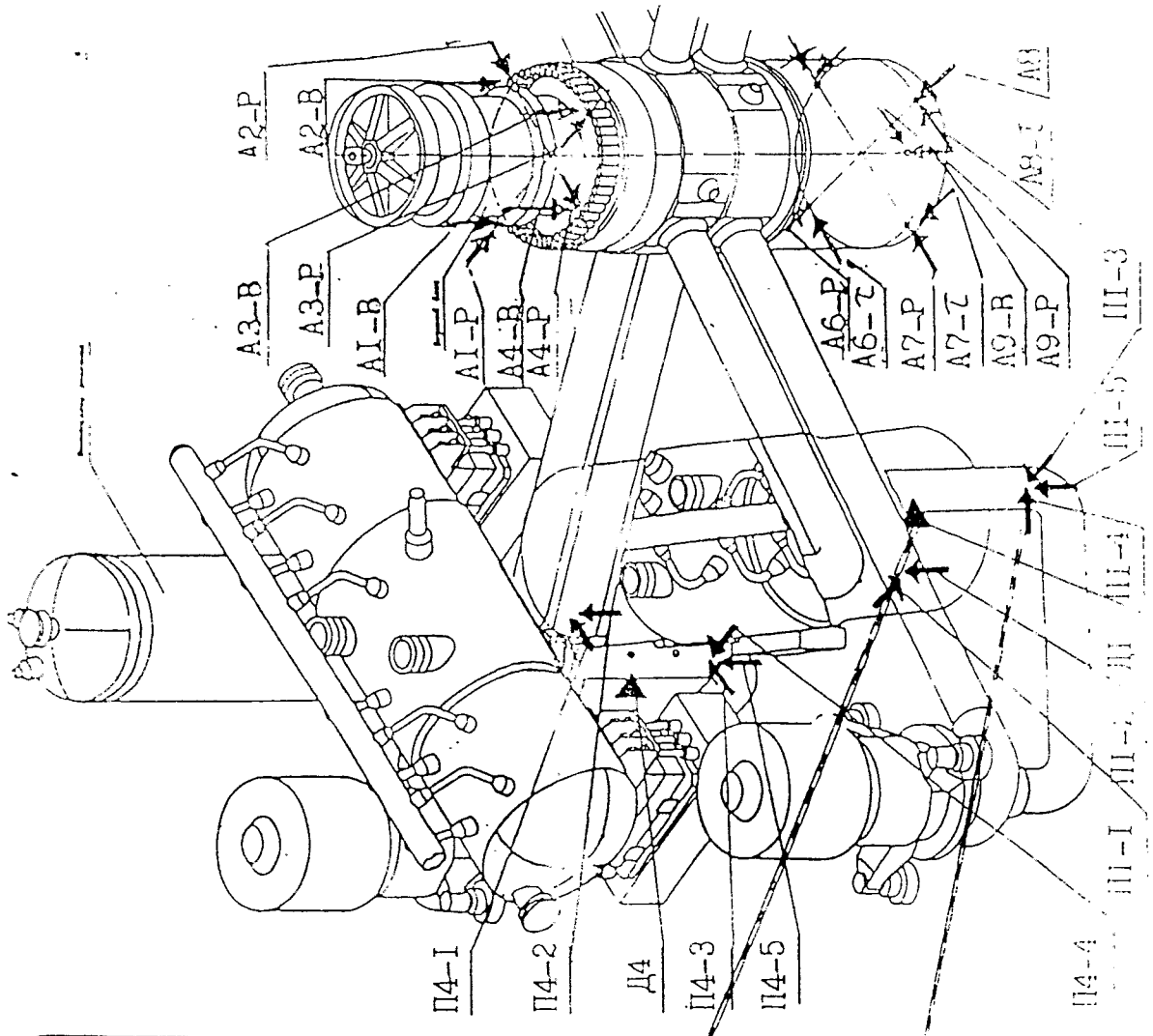
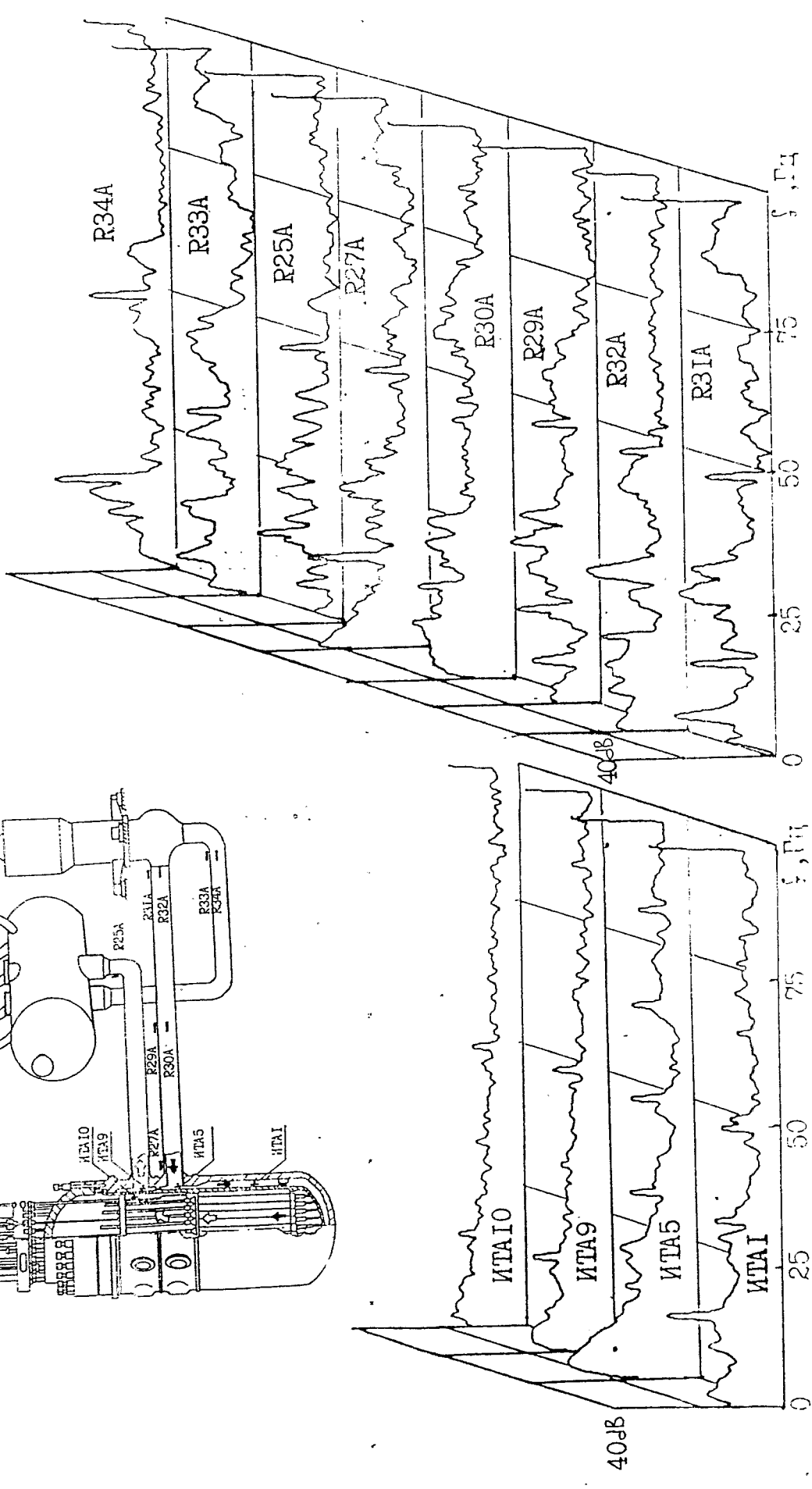
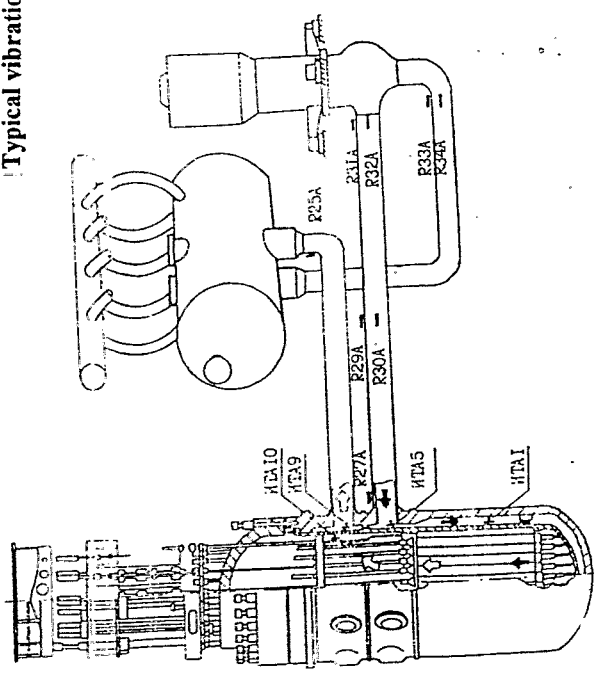


Fig. 3.6

Vibration stresses characteristics according to operation conditions (combination of the operating MCP), data on Kozioduy-6

Operation mode (MCP operating)	Equipment element (zone)					
	Core barrel			MCC		
	lower section	Inlet nozzle zone	Outlet nozzle zone	PTU vessel	MCP outlet	MCP inlet
[+ + + +]	 $S_0^{\sigma} = 0.08$	 $S_0^{\sigma} = 0.14$	 $S_0^{\sigma} = 0.06$	 $S_0^{\sigma} = 0.06$	 $S_0^{\sigma} = 0.04$	 $S_0^{\sigma} = 0.06$
[+ + - +]	 $S_0^{\sigma} = 0.08$	 $S_0^{\sigma} = 0.17$	 $S_0^{\sigma} = 0.07$	 $S_0^{\sigma} = 0.06$	 $S_0^{\sigma} = 0.05$	 $S_0^{\sigma} = 0.11$
[+ + - -]	 $S_0^{\sigma} = 0.08$	 $S_0^{\sigma} = 0.11$	 $S_0^{\sigma} = 0.06$	 $S_0^{\sigma} = 0.6$	 $S_0^{\sigma} = 0.04$	 $S_0^{\sigma} = 0.03$
[+ - - +]	 $S_0^{\sigma} = 0.10$	 $S_0^{\sigma} = 0.22$	 $S_0^{\sigma} = 0.07$	 $S_0^{\sigma} = 0.06$	 $S_0^{\sigma} = 0.07$	 $S_0^{\sigma} = 0.05$
[+ - - -]	 $S_0^{\sigma} = 0.08$	 $S_0^{\sigma} = 0.14$	 $S_0^{\sigma} = 0.05$	 $S_0^{\sigma} = 0.04$	 $S_0^{\sigma} = 0.05$	 $S_0^{\sigma} = 0.03$
[- - - +]	 $S_0^{\sigma} = 0.07$	 $S_0^{\sigma} = 0.15$	 $S_0^{\sigma} = 0.09$	 $S_0^{\sigma} = 0.05$	 $S_0^{\sigma} = 0.07$	 $S_0^{\sigma} = 0.12$
[- + - -]	 $S_0^{\sigma} = 0.06$	 $S_0^{\sigma} = 0.06$	 $S_0^{\sigma} = 0.05$	 $S_0^{\sigma} = 0.05$	 $S_0^{\sigma} = 0.04$	 $S_0^{\sigma} = 0.05$

Typical vibration stresses APSD in internals and MCC at the hot tests conditions



3.3.2. At spectra of the dynamic response are present also frequent components with more wide-band maxima of spectral density, characteristic of damped oscillations at own frequencies. For the core barrel to such frequent component concern 5; 10, 14, 19, 24 Hz.

At accelerometers installed on heads of FA, is present powerful wide-band a resonance at frequency 2.5 Hz. In the indications of sensors, installed at MCC, to such characteristic frequent components are 3, 6, 13, 23 and 25 Hz for cold loop and 3, 6, 9, 18, 23 Hz - for hot loop.

However conventional forms of the analysis of the shown data it appear unsufficiently for unambiguous identification of indicated frequencies as of own frequencies of oscillations of the equipment for the following reasons:

a) the analysis of APSD of signals allows only presumably to specify frequencies of own oscillations, but does not allow to restore the mode of oscillations;

b) the conventional analysis of phase ratios of pairs of signals is also hindered, as the low-frequency oscillations (lifting the most valuable diagnostic information) are not dominating and mask as by hydrodynamic resonances, and non resonant character by hydrodynamic noise. For example, on parameters cold tests by activity of MCP under the scheme [+ ---] (fig. 3.9) spectral components of range 10 - 20 Hz of a signal of the sensor 7p(ИТА 7П) are minimum on a comparison with other schemes of actuation of MCP (sensor 7p is located between cold loop 2-nd and 3-d of closed loops). A resonant composition of APSD is sharp enriches at actuation third MCP (see the same fig. 3.8). The bottom of the core barrel in a smaller degree is subject to influence of the schemes of MCP actuation.

On fig. 3.10 in the same conditions are shown APSD of a signal of the sensor 3p(ИТА 3П), located under the sensor 7p. Thus masking of own styles of oscillations of the core barrel depends on frequency and has variable in space character and is a function of number of MCP operating.

It is necessary also to mark, that at the analysis of the data, obtained at starting-up and adjustment measurements, fact has come to light, that the masking of internals at vibrations own frequencies has yet and correlated character. On fig. 3.11 functions of a coherence for the same pair of signals 1к(ИТА 1К)-4к(ИТА 4К) at cold and hot tests shown at different temperatures of the coolant and different number of MCP operating. From them follows, that does not exist steady, reproduced from a mode to a mode of a picture of internals vibrations. Thus the mutual characteristics, except uncorrelated components, nevertheless leave a set of other correlated sources. From here follows, that the same variability have and phase characteristics of strain-gage signals, will be inconvenient. Really, if to select only anti-phase components (are designated by arrows on the schedules and table at the bottom fig. 3.12) for a pair of signals 3p - 7p, it appear, that, at first, they have a low coherence and, secondly, the phase portraits are not reproduced from a mode to a mode. We shall remark, that the pair of signals 3p - 7p is located

Lg Y

APSD of the sensor in the point HTA-7II

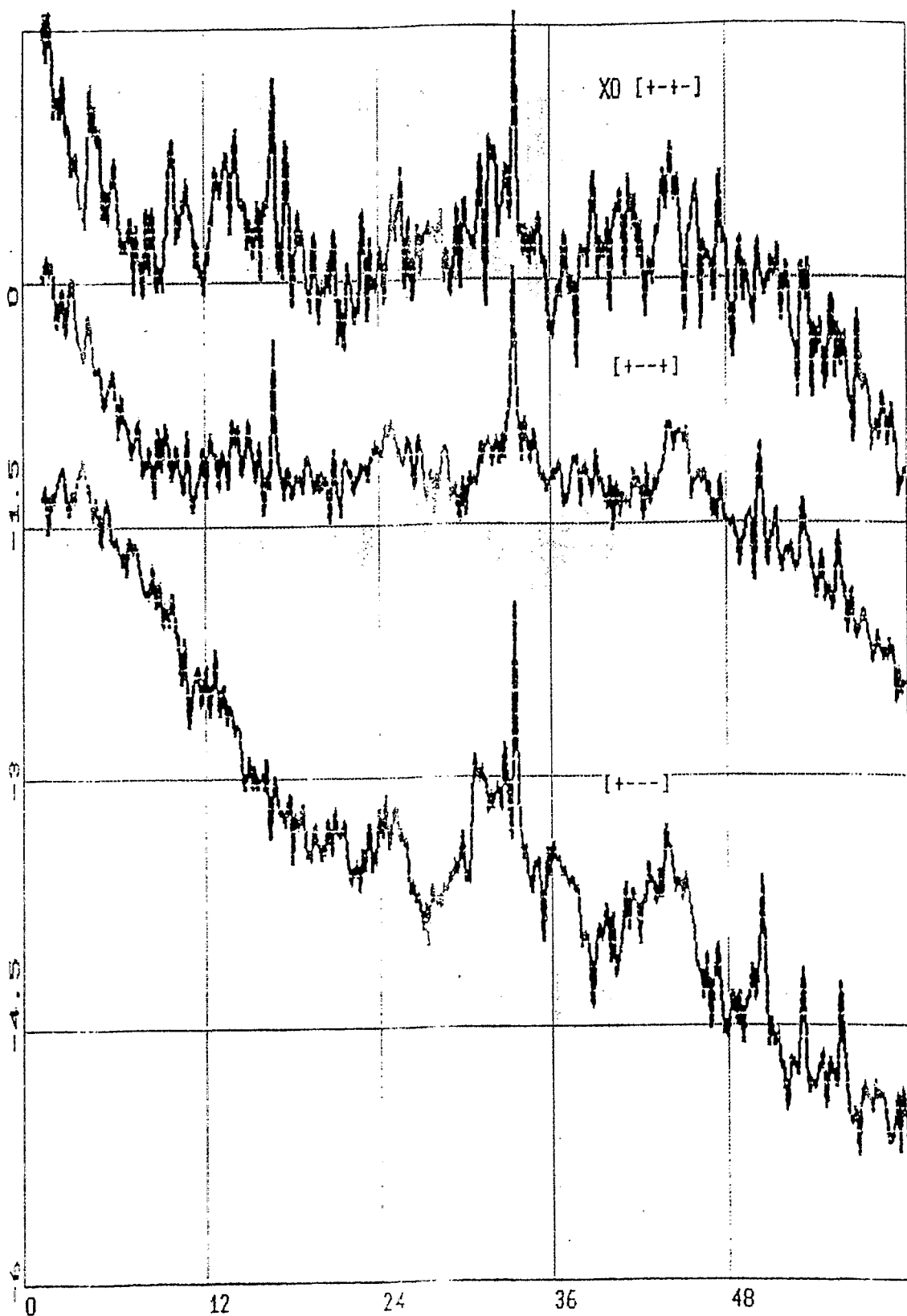


Fig 3.9
6

Lg Y

APSD of the sensor in the point ИТА-3П

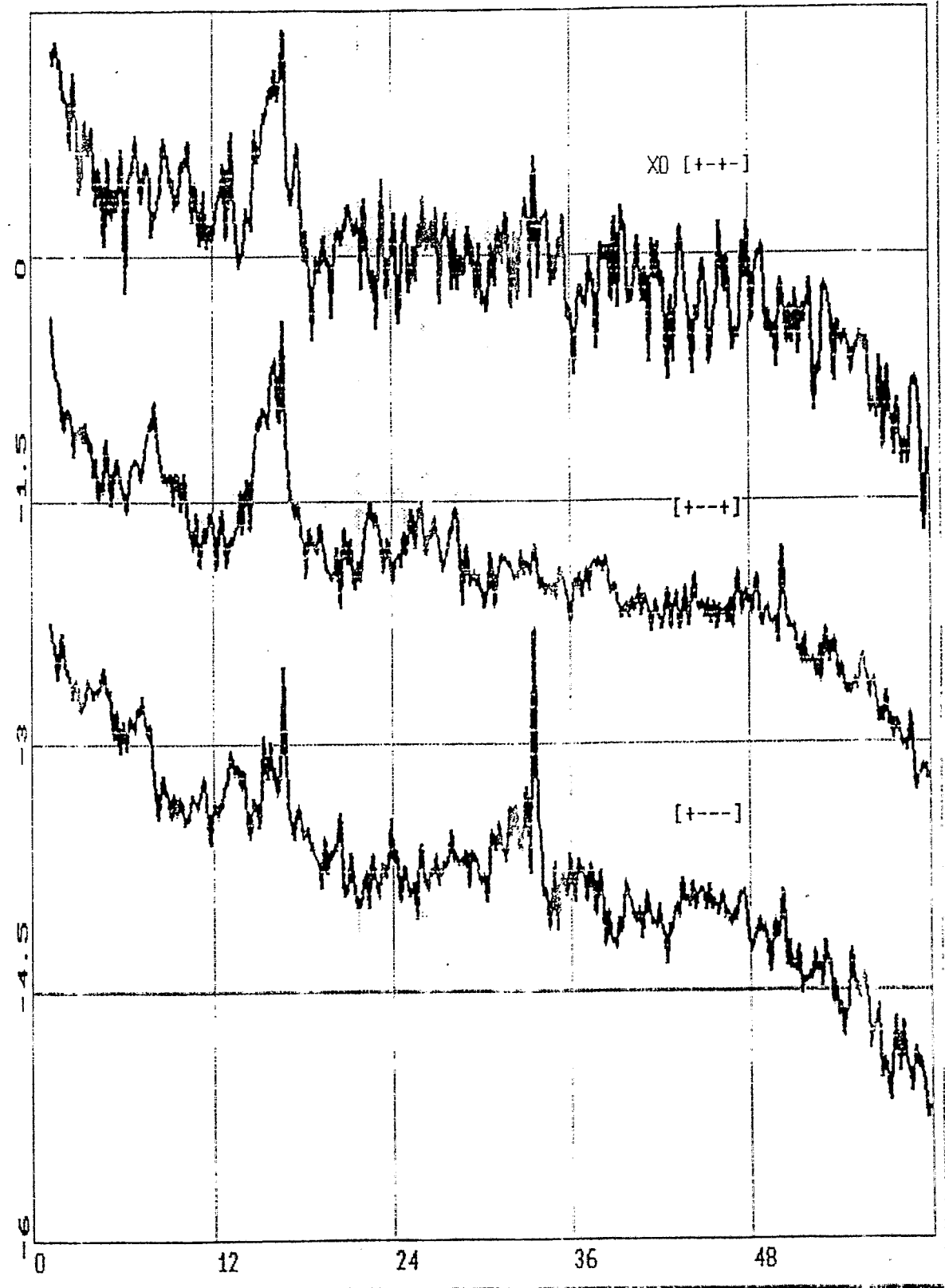


Fig. 3.10

The coherence of the signals ИТА1к- ИТА4к

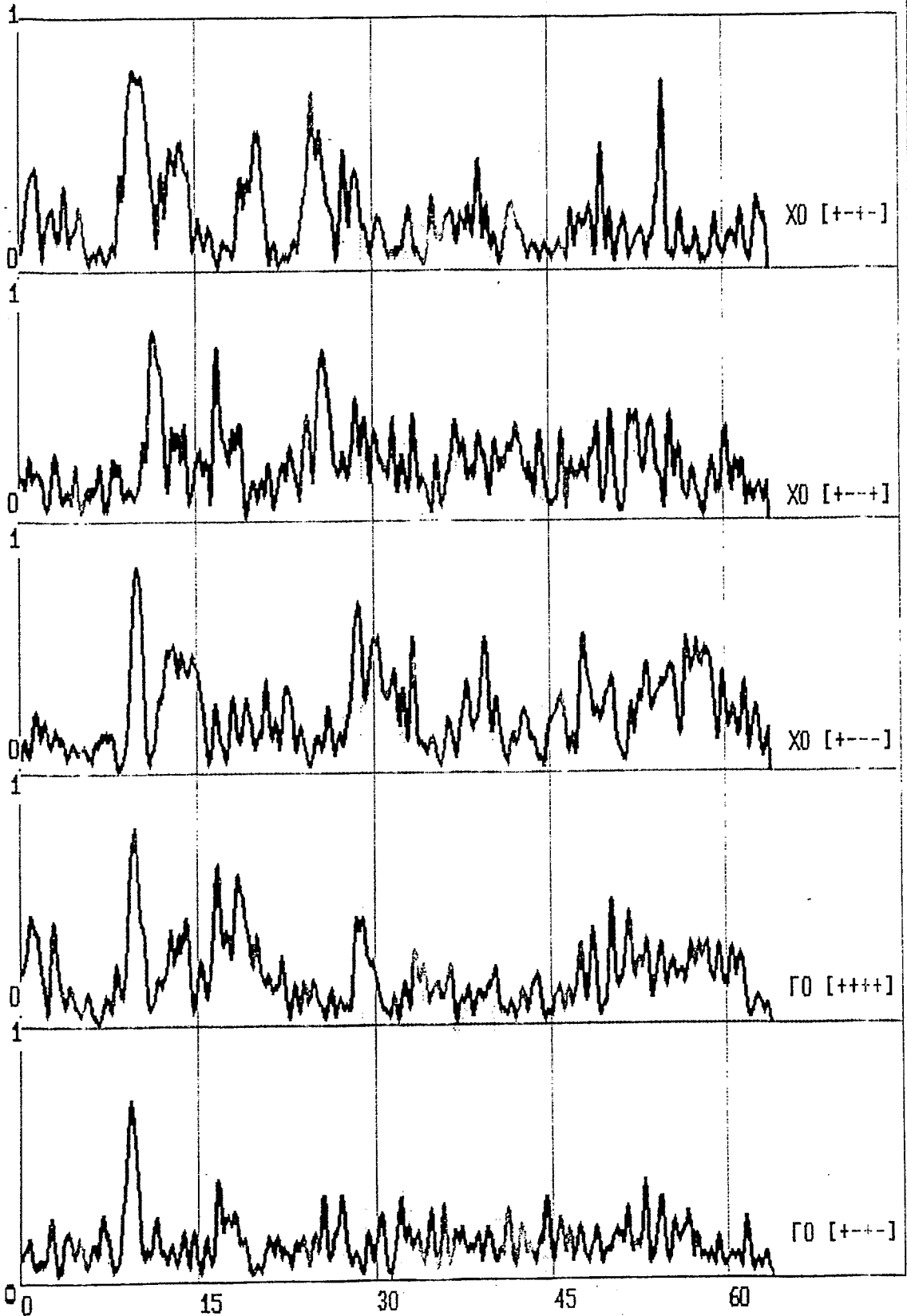
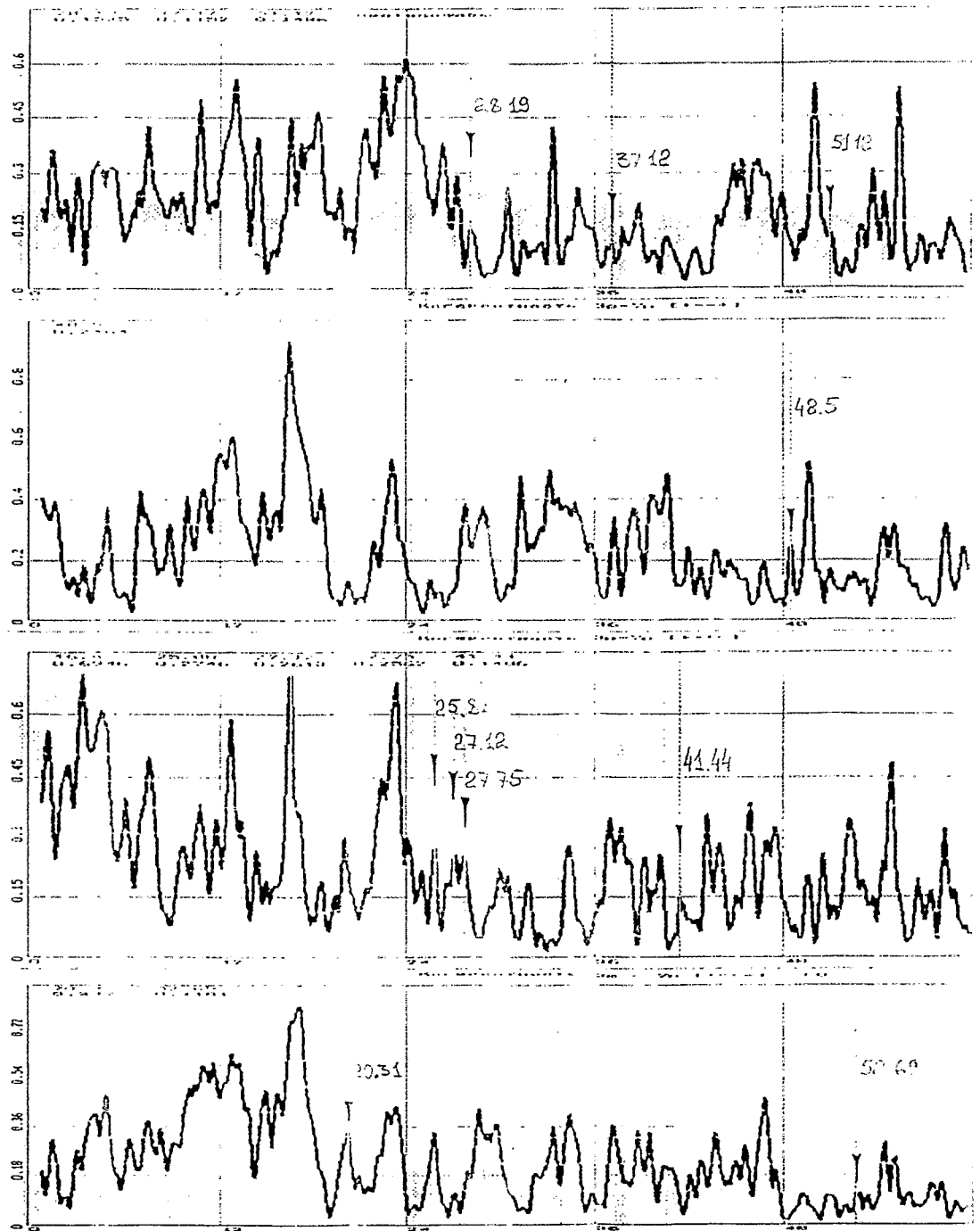


Fig. 3.11

Mutual analysis of the signals ИТА3 П - ИТА7 П



16. 62	254.9	-41.6	140.0	-44.34
20. 31	428	69.86	849.2	-176.49
25. 80	321.0	305.5	359.7	-133.7
27. 12	330.2	215.4	358.8	-93.34
27. 75	428.3	304.5	376.6	-109.47
28. 19	535.4	295.3	346.1	-51.07
37. 12	518.8	343.9	636.5	73.7
41. 44	515.7	354.8	074	302.4
48. 5	242.1	548.1	702.1	109.6
51. 12	204.1	326.8	518.9	503.4
52. 69	226.9	335.3	475.4	525.3
61. 19	11230	457	782.5	51.41
63. 44	547.8	427.2	014.8	161
И	[++++]	[+---]	[+---]	[+---]

Fig. 3.12

on vertical forming of the cylinder and is the most sensitive to lowest pendulum oscillations of the core barrel.

In connection with above-stated for identification of frequencies shown in the given section it was necessary to enlist results of researches of scale models of VVER-1000 plant, and also additional methods of the analysis of random processes. The results of such analysis are shown in section 3.4

3.3.3. From the data, shown on fig. 3.13 - 3.14, it is possible to estimate frequency range, characteristic of vibration of VVER-1000 plant.

The main power of pressure fluctuations is concentrated in frequency range up to 100 Hz. The greatest power of the dynamic response is observed in frequency range up to 15 Hz. In formal speaking, last value can be limited and frequent area of the analysis of the vibrational characteristics of the equipment.

However it is necessary to mark, that depending on means, used for VVER diagnosing, the indicated frequency range can appear insufficient for obtaining the complete information on vibrations of the equipment.

In particular, from the analysis fig. 3.13 with the data on vibration accelerations and estimation of internals displacements follows, that the indicated range does not envelop a series of characteristic frequent components. Similarly, data fig. 3.14 (vibration displacements and estimation of MCC accelerations) show, that for the analysis it is required, as a minimum, frequency band 0 - 25 Hz completely to use the indications of accelerometers (in case of their application in systems of diagnosing).

Accordingly to this, it is expedient ^{to} and analysis of the vibrational characteristics of the equipment to conduct in frequency range 0 - 25 Hz.

3.4. Vibrational characteristics of the equipment

3.4.1. The core barrel.

3.4.1.1. As already was marked, the modal analysis of signals with use of phase ratios appear inconvenient because of effects of masking, and because of a variability of phase characteristics from a mode to a mode.

This fact has required the additional analysis of tests results of simplified models of a reactor to realize main regularities of vibrations of equipment complex in the design relation.

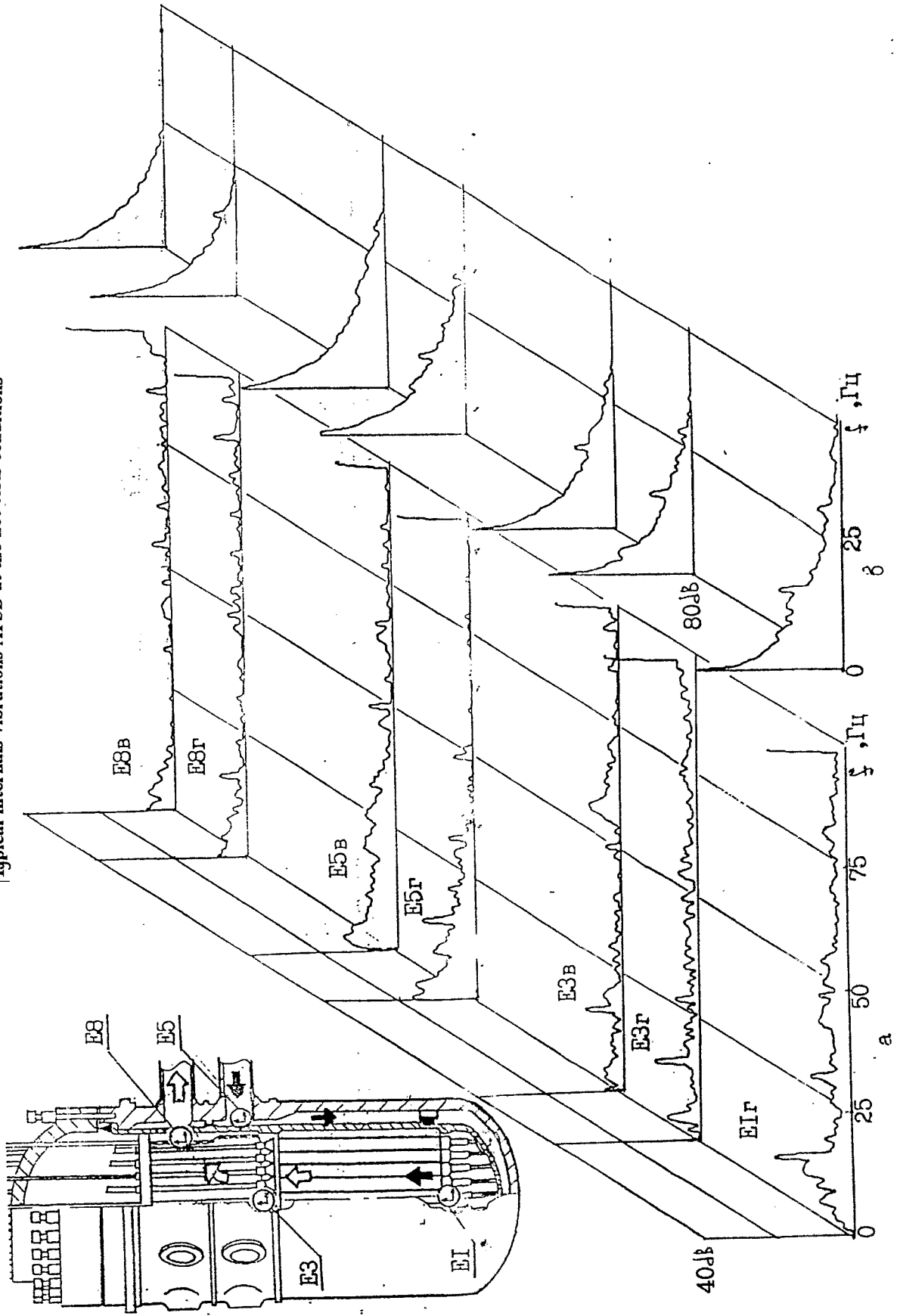
The results of such analysis can be shown to following:

a) the Classical modes of oscillations with full number of half-waves in ^{circumferential} envioning and longitudinal directions are excited in the CB only for idealized cases of its fastening: full absence of keys or, on the contrary, full fixing of the CB in the lower keys (fig. 3.15).

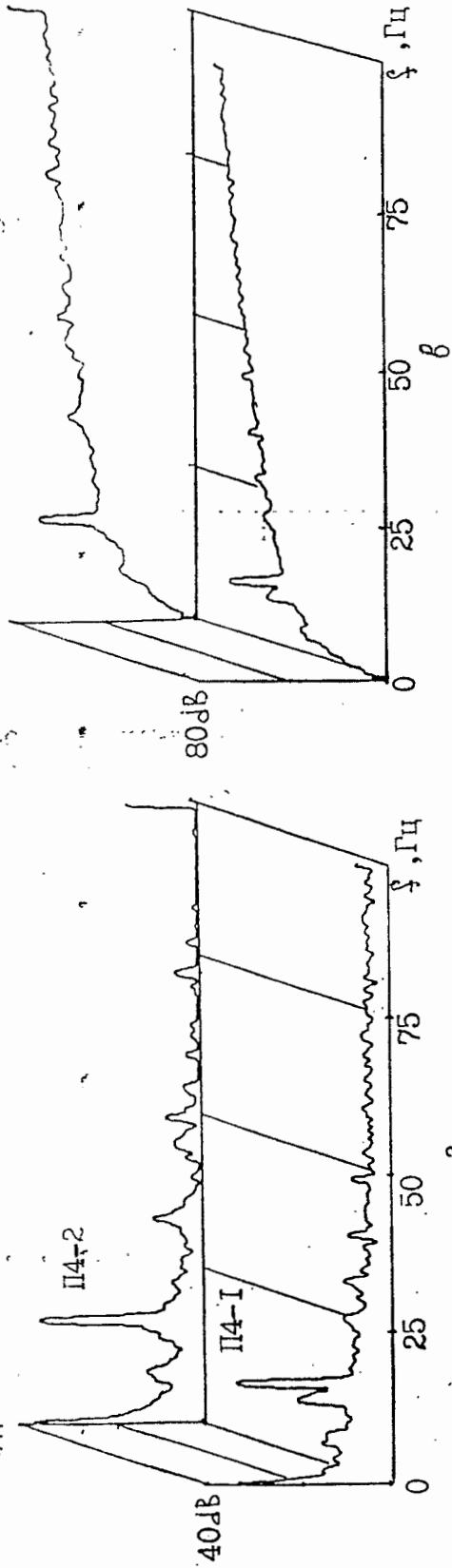
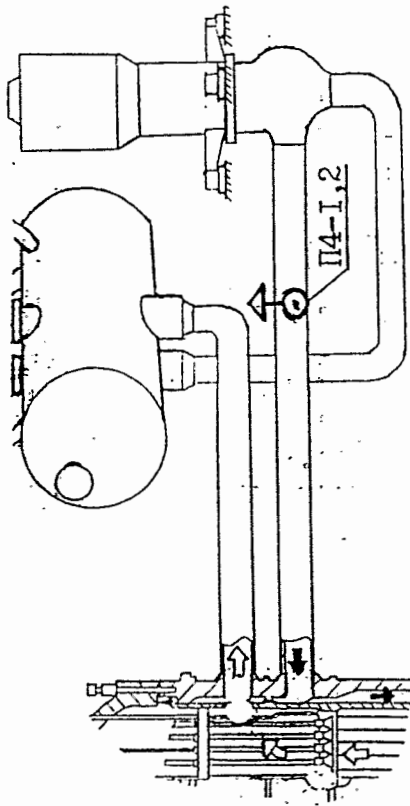
We shall mark, that in this case a phase ratios of strain-gage signals, installed at model, also allow to restore the classical modes of own oscillations of CB (see fig. 3.15).

↑
oscillations

Typical internal vibrations APSD at the hot tests conditions

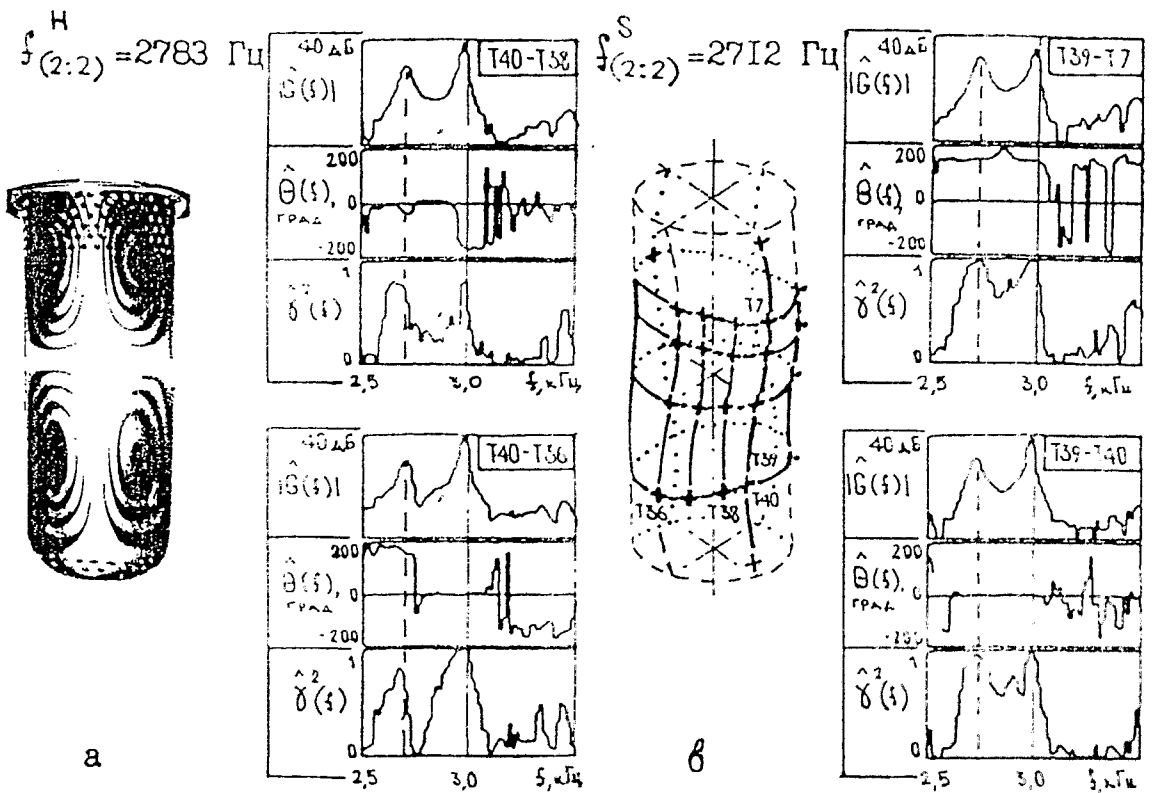


Typical MCC vibration APSD at the hot tests conditions



a - vibration displacements b - accelerations estimation

Fig. 3.14



**a - vibration hologram
 harmonic loading**

**b - mutual spectral analysis of strain gage
 signals at shock tests**

Fig. 3.15

Similarly, the filing of phase ratios of sensors of vibration displacement, installed on large-scale model of reactor without the lower keys, allows steadily to restore pendulum mode of oscillations of CB at frequency 22 Hz (fig. 3.16). The recalculation on a full-scale design gives value of ~~4.7 Hz~~ as frequency of these oscillations.

b) the Introduction of asymmetrical conditions of fastening of small-scale model of the CB gives essential distortion of a picture of the modes of own oscillations (fig. 3.17).

Is probable, as in a full-scale design for such conditions will not be classical (and steady) phase ratios of strain-gage signals, which do not give an integral picture of vibration conditions.

Thus, the representation on vibrations of the CB as combination of free oscillations of a thin cylindrical shells at own frequencies, is rather rough model. The external cylindrical surface of CB in three horizontal planes with a various degree of rigidity is connected to an internal surface of a vessel of a reactor. It is upper and lower series of keys and separating ring. The free vibrations of CB at internal surface are limited in four horizontal planes: two series of PTU keys, series of the baffle keys and lower fixity ring for the baffle. The rigidity of internal key connections is in many respects determined by a vertical effort from PTU. Listed seven horizontal planes, obviously, superimpose serious limitations on a capability of origin of the lowest styles of shell oscillations of the CB. On the other hand, the fact of appearance of lowest modes and, in particular, pendulum modes as well as increasing of their amplitude in operational conditions testifies to process of a wear of key connections or on decreasing of PTU effort, that is is the important diagnostic indication.

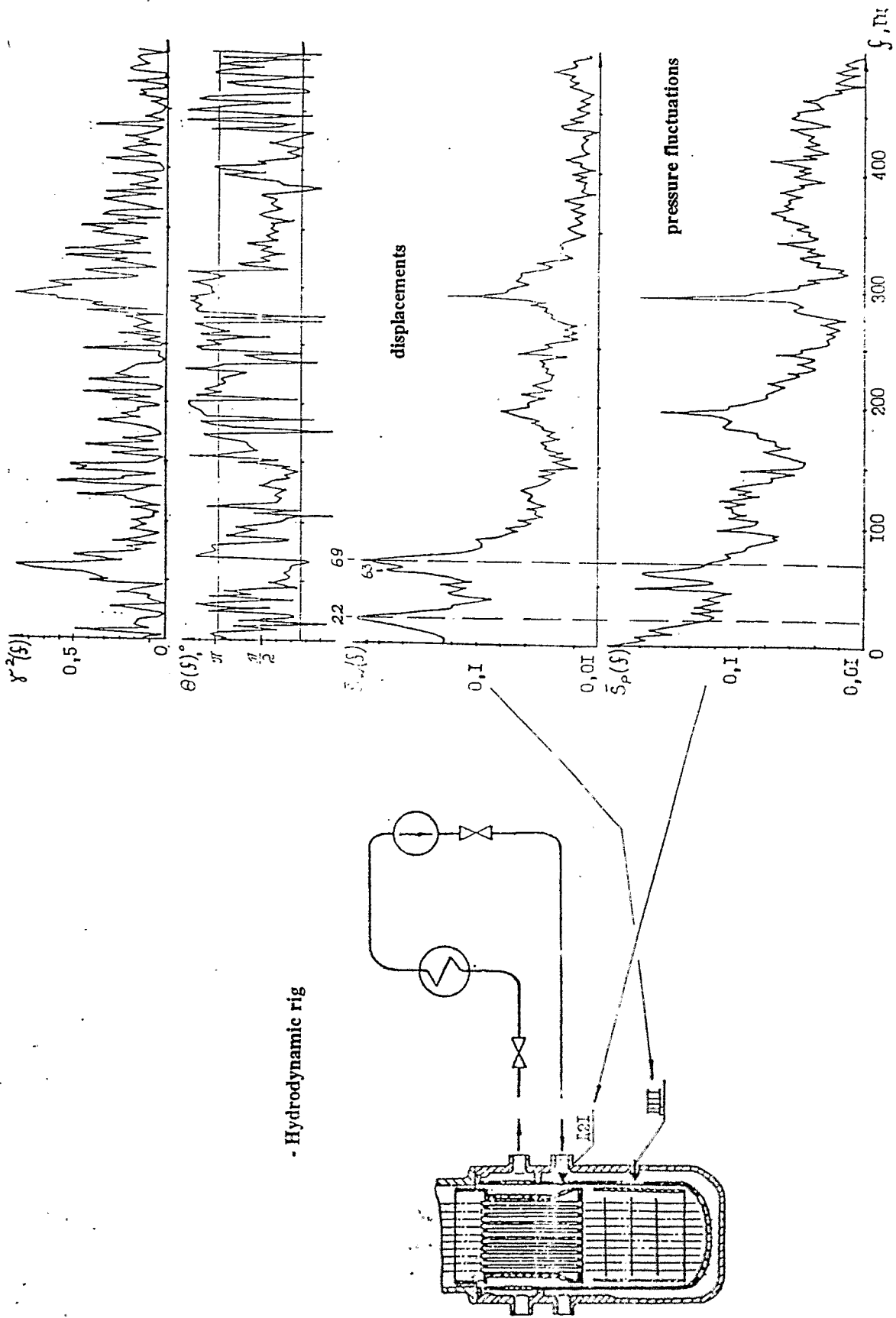
c) In a reality (taking into account, that the CB can be installed with a gap rather some of keys, and remaining keys will have some pliability) it is necessary to expect simultaneous energization as pendulum and beam modes of the CB.

Is real, in the indications of accelerometers, installed at real CB (see fig. 3.13) 10 Hz is observed as well as frequency about 5 Hz. The first is identified as beam mode of the CB with lower keys.

3.4.1.2. Limited capabilities of the modal analysis for identification of the modes of oscillations of the CB expediently to supplement by the MAA-analysis. In model (PT, strain gage at CB, strain gage at PTU lip) = [59(Q3), 16к(ИТА 16К), 11п(ИТА 11П)] low-frequency resonances are well divided under the primary sources which are hardly interpreted at phase portraits. Under the schedules on fig. 3.18, 3.19, 3.20 a table 3.1 normalized global contributions of every possible signal to each another is composed.

Limiting while by consideration of component 4,51 Hz, from табл 3.1 are possible to make a conclusion, that its primary source are oscillations of the CB.

In each column table 3.1 in the greasy fout are given chosen maximum values of the normalized global contributions.

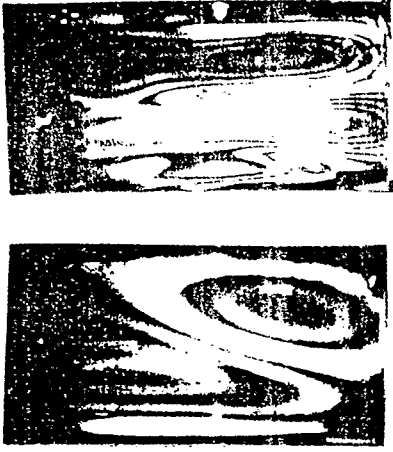


- Hydrodynamic rig

Mutual spectral analysis of pressure fluctuations and vibration displacements in core barrel model (m 1:5)

Fig. 3. 16

b - asymmetric fixing and irregular external and inner fluid gaps



a - classic boundary conditions

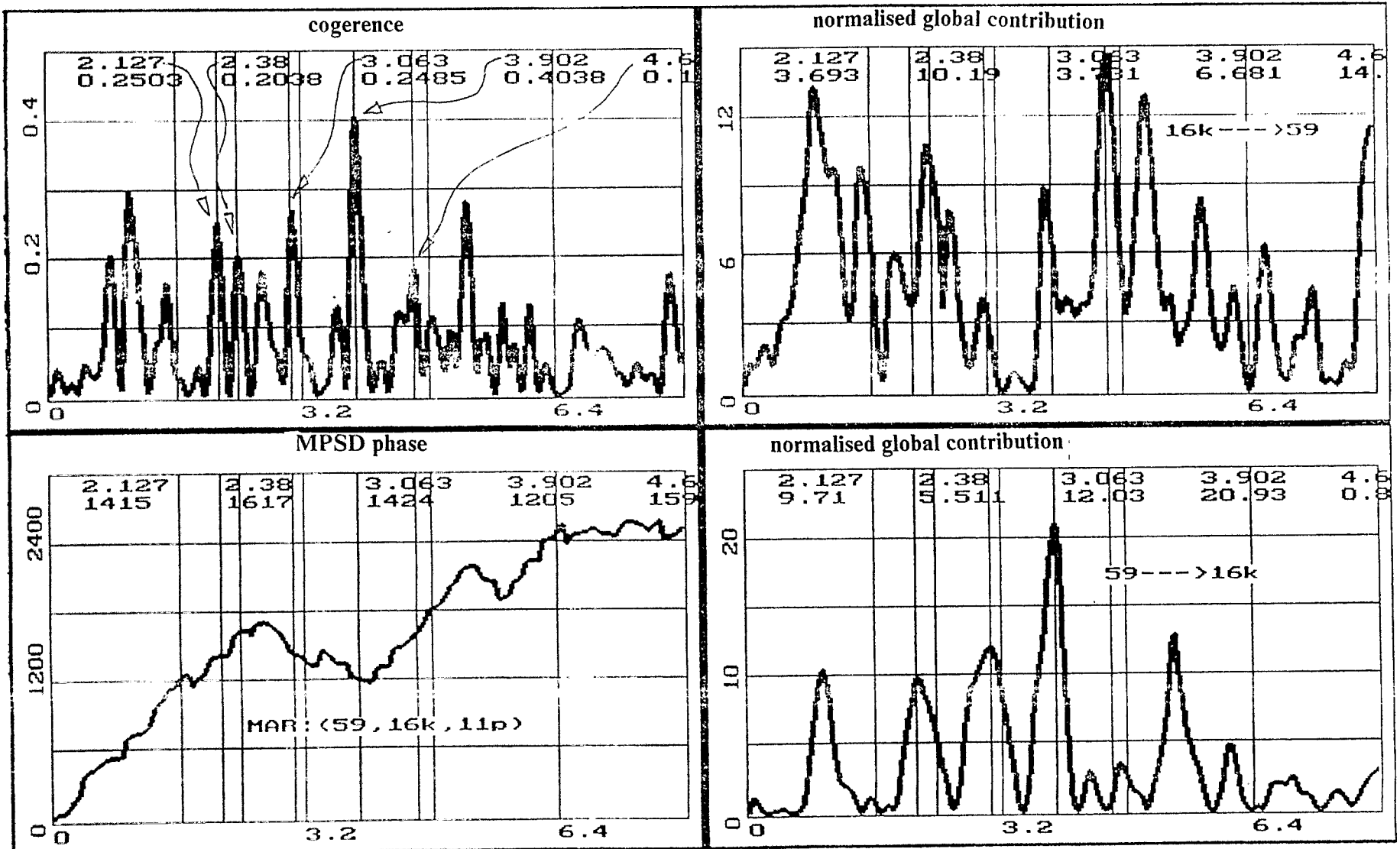


Modes oscillations of the core barrel model at the different boundary conditions
(Results of holographic investigations of small-scale models)

Fig. 3.17

MAA results of signals of 59, 16k, 11p sensors

Fig. 3.18



MAA results of signals of 59, 16k, 11p sensors

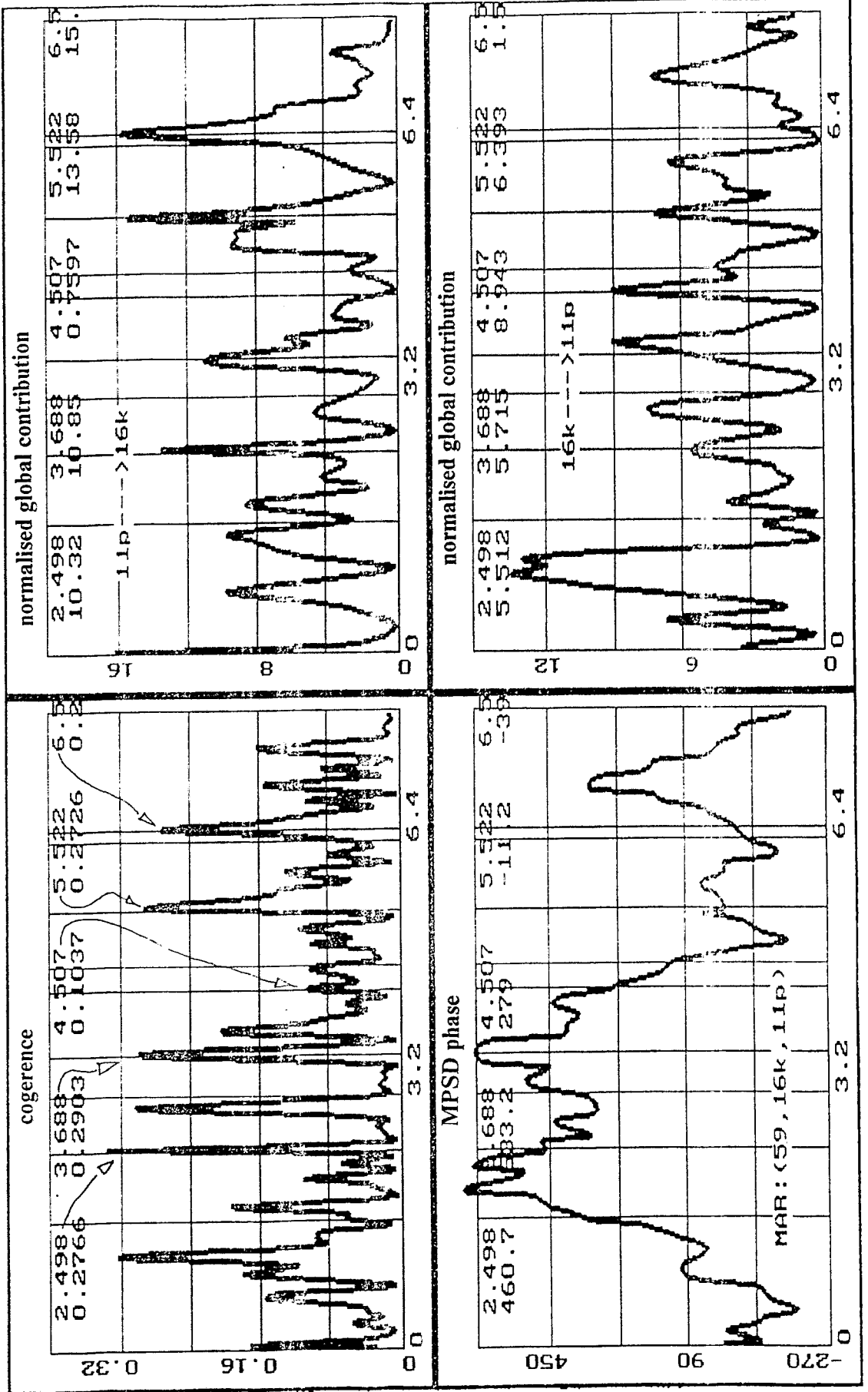


Fig. 3.19

MAA results of signals of 59, 16k, 11p sensors

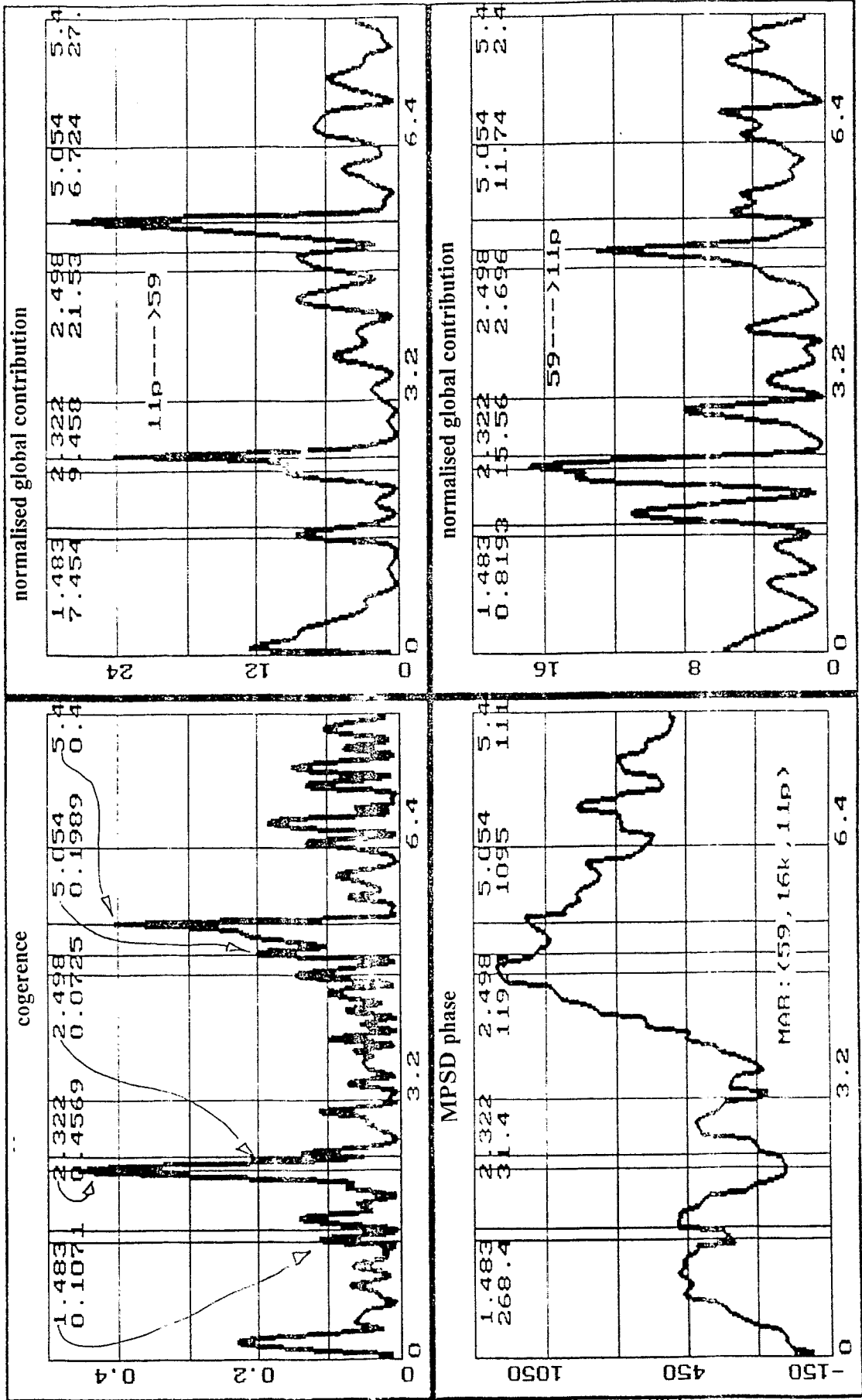


Fig. 3 20

Таблица 3.1

Frequency[Hz]	2.38	2.50	3.08	3.69	3.90	4.51	5.00	5.52	6.50
Contribution									
11p-->16k	-	10.3	-	10.8	-	0.8	-	13.6	15.0
16k-->11p	-	5.5	-	5.7	-	8.9	-	6.4	1.5
16k-->59	10.1	-	3.7	-	6.7	14.0	-	-	-
59-->16k	5.5	-	12.0	-	20.9	0.8	-	-	-
11p-->59	9.4	21.5	-	-	-	-	6.7	27.0	-
59-->11p	15.5	2.7	-	-	-	-	11.7	2.4	-

Similarly, combining the MAA-analysis, results of tests of scale models and results of full-scale measurements, it is possible to confirm, that earlier mentioned frequencies 14, 19, 24 Hz are also frequencies of own oscillations of the CB under the mode 2:1, 1:2, 3:1.

The totals of definition of eigenfrequencies of the CB by various methods are shown in tab. 3.2.

3.4.2. Fuel assembly:

3.4.2.1. In starting-up and adjustment measurements of FA vibration are investigated with the help of of the full scale FA simulator, equipped with accelerometers. A seven-channel record, consisting of the following of signals (fig. 3.21), will below be considered.

59(Q3) - installed in MCP junction of the loop No.3,

E1 (1), E1 (2) - tenzoaccelerometers installed in one point at the FA socket (the point E1), sensing to vibrations in radial co-perpendicular directions,

E3g, E3v - tenzoaccelerometers installed in one point at the FA head, sensing accordingly to vibrations in radial and vertical directions,

E5g, E5v - tenzoaccelerometers installed in one point at the CB, sensing accordingly to vibrations in radial and vertical directions.

Is thus available three classes of processes:

a) A signal of PT, in spectral reflectance of which frequencies, identifiable with Pr, MCP, ASW, are known, and, generally speaking, unknown frequencies of internals vibrations. Basically, the PT signal can contain the information on vibrations any of elements of MCC and internals. Thus the phase characteristics of such vibrations depend on an installation point of sensors, that is in a way are arbitrary, as vibrations are defined by the coolant as damping traveling waves of density.

Auto-spectrum of 59, E1(1), E1(2), E3r, E3b, E5b, E5r sensors

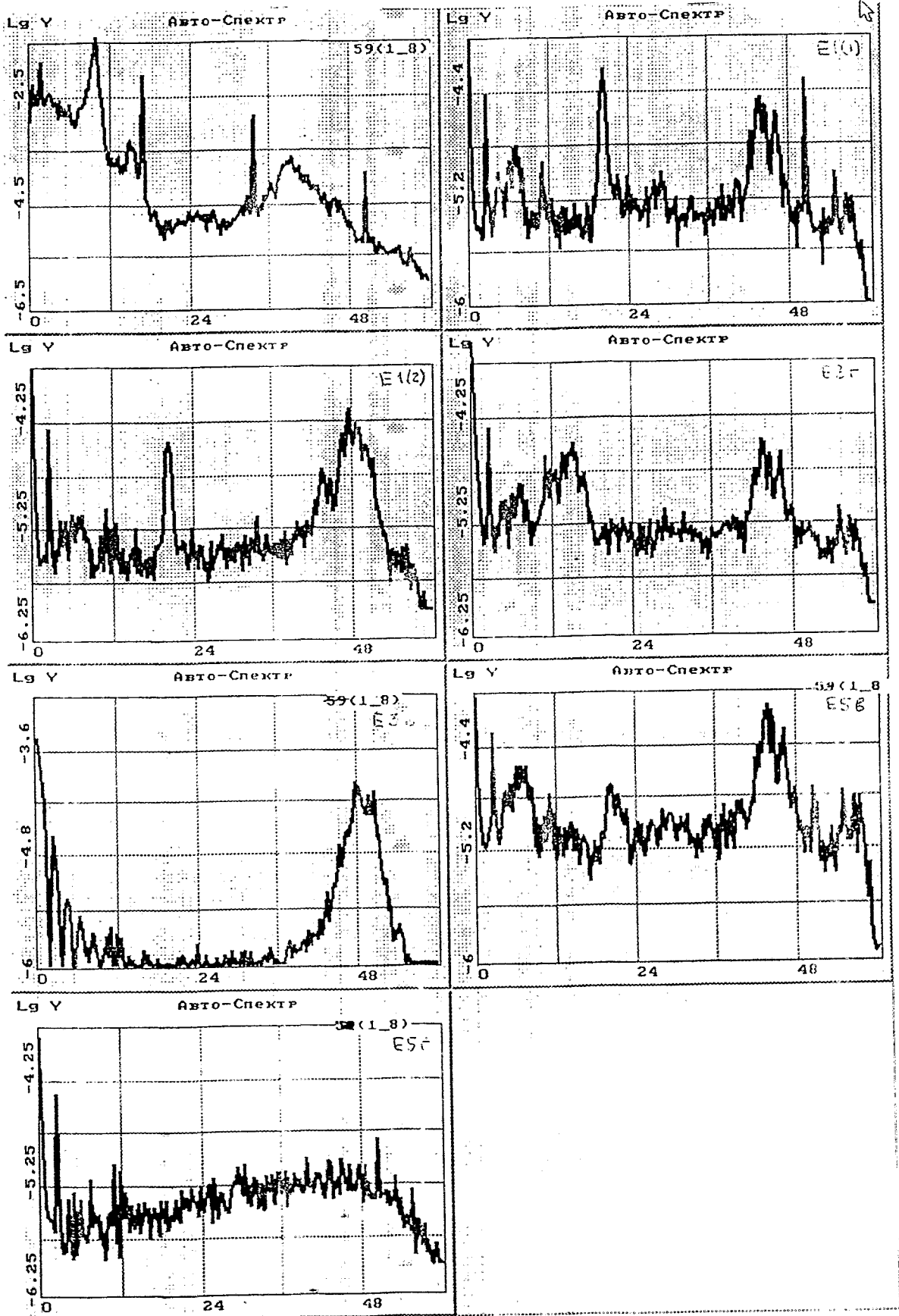


Fig. 3.21

b) Four signals of tenzoaccelerometers installed at FA, in which, doubtlessly, unknown characteristic frequencies of FA vibrations are contained, presence of known frequencies of ASW, MCP, Pr and also unknown frequencies of collective internal vibrations is possible.

c) Two signals of tenzoaccelerometers installed at the CB, for which reasoning of the previous items from that only by a difference are fair, that the data signals doubtlessly contain frequencies of CB vibrations on various modes.

In typical spectral reflectance (APSD, coherence, the phase) mentioned above signals shall mark the following singularities;

In all accelerometer APSD (fig. 3.21) is present powerful wide-band a resonance at frequency 2.5 Hz;

In APSD of signals E1 (1), E1 (2), E5v (that is at the FA socket and CB only in a vertical direction) there is the resonance in region of 20.5 Hz;

In APSD of signals E1 (1), E3g, E5v is present powerful narrow-band a resonance at region of 43.5 Hz;

In APSD of sensors, installed at FA socket, FA head and CB are present narrow-band resonances at frequencies 6.6 and 54 Hz;

APSD of signals E3g, E5v are rather close to each other at the dominating resonances;

All listed above singularities at frequencies 2.5, 6.6, 20.5, 43.5, 54 Hz dominate in functions of a coherence of pairs of signals E1 (1) -E1 (2), E1 (2) -E3g, E1 (1) -E5v (fig.3.22, 3.23, 3.24)

As a rule, at these frequencies happen inphased oscillations asept of the following cases of nonphase at frequencies 20.38 Hz for a pair E1 (1) -E5v and 53-60 Hz for pairs E1 (1) -E5v and E1 (1) -E1 (2).

Thus, on the listed above frequencies take place collective FA oscillation and CB.

To identification of the primary sources of detected above resonances the vehicle MAA-analysis is applied. Any two-dimensional MAA-model, one of components of which is a signal, and other - any accelerometer signal is correct. We shall remind, that a condition of a correctness of MAA-model is a mutual noncorrelatedness of external sources of each signals. The external source, determining the contribution of pressure oscillations in a function of a coherence of any pair of signals "PT-accelerometer" in frequency range 0 - 0 60 Hz consist of harmonices of ASW and MCP (fig. 3.25).

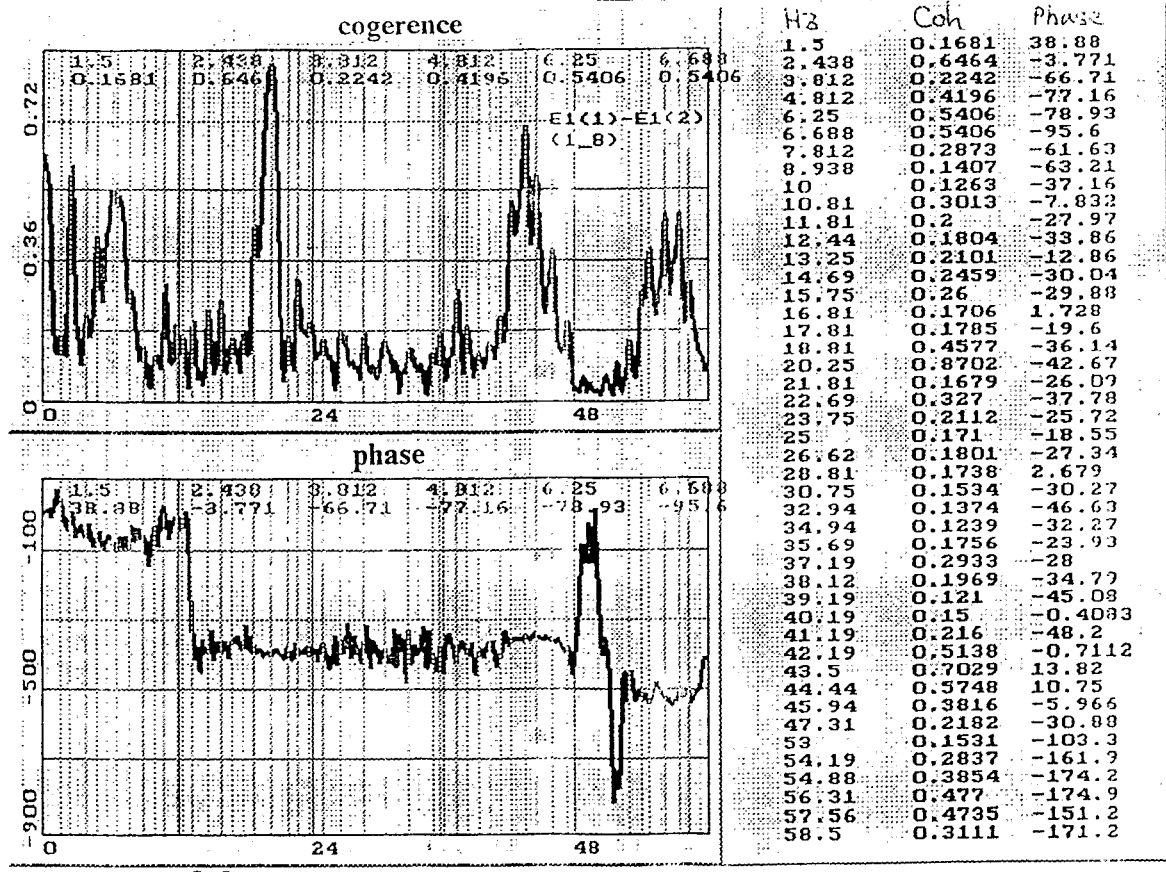
By results of the MAA-analysis it is possible to make the following conclusions:

Collective forced vibrations TBC of FA and CB happen at frequencies at Pr (0.8 Hz), ASW-1 (7.8 Hz), ASW-2 (10.5 Hz) и MCP (16.6, 33.2, 49.8 Hz);

Collective vibrations of FA and CB happen at own frequencies of CB vibration (21.0, 38.9, 43.3 Hz);

Collective vibrations of FA and CB happen at frequencies, identified with FA (2.5, 3.4, 4.4, 4.8, 6.2, 45.9, 52.1, 54.7, 57.6 Hz). Among them the resonance at frequency 2.5 Hz is a

Mutual spectral analysis of signals of E1(1)-E1(2) sensors

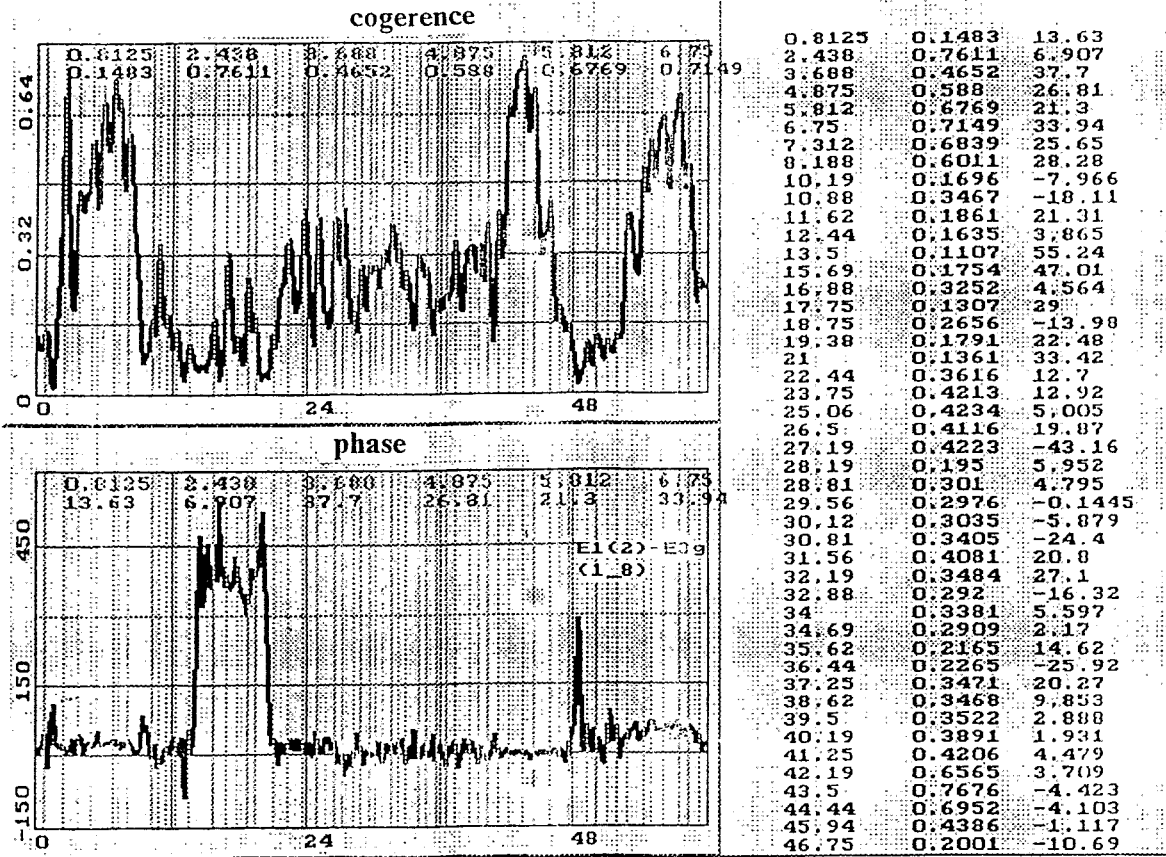


резонансы 2-3
 нулевая фаза с2-3
 противофаза с2-3
 гармоники 2-3

1.5	2.438	54.19	1.5
2.438	10.81	54.88	12.44
3.812	13.25	56.31	13.25
4.812	16.81	57.56	15.75
6.25	17.81	58.5	17.81
6.688	25		18.81
7.812	28.81		20.25
8.938	40.19		21.81
10	42.19		23.75
10.81	43.5		25
11.81	44.44		26.62
12.44	45.94		28.81
13.25			30.75
14.69			32.94
15.75			34.94
16.81			35.69
17.81			37.19
18.81			38.12
20.25			39.19
21.81			40.19
22.69			41.19
23.75			42.19
25			43.5
26.62			44.44
28.81			45.94
30.75			
32.94			
34.94			
35.69			
37.19			
38.12			
39.19			
40.19			
41.19			
42.19			
43.5			
44.44			
45.94			
47.31			
53			
54.19			
54.88			
56.31			
57.56			
58.5			
60.88			
62.94			

Fig. 3.22

Mutual spectral analysis of signals of E1(2)-E3r sensors

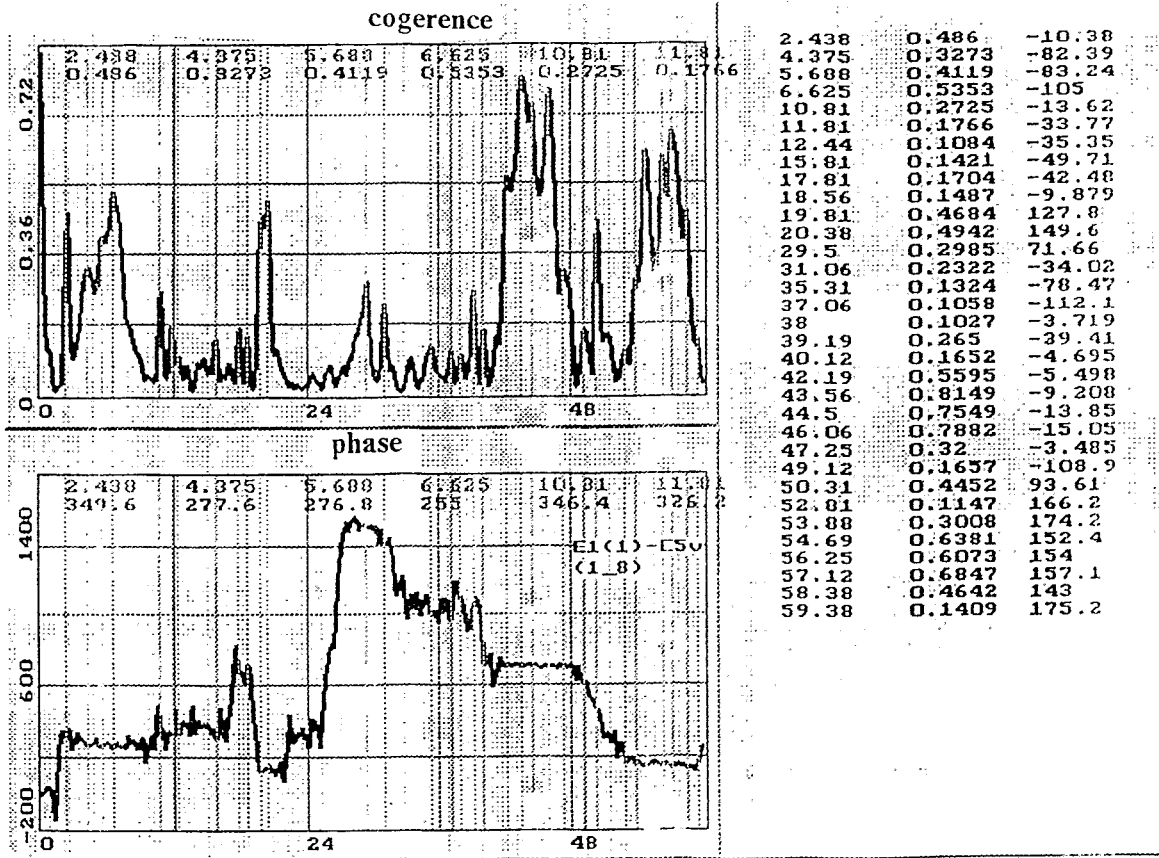


резонансы 3-4
нулевых фаз с3-4
противофаз с3-4
гармоники 3-4

0.8125	0.8125	0.8125
2.438	2.438	2.438
3.688	10.19	4.875
4.875	10.88	7.312
5.812	12.44	7.312
6.75	16.88	11.62
7.312	18.75	13.5
8.188	22.44	19.38
10.19	23.75	25.06
10.88	25.06	27.19
11.62	26.5	28.81
12.44	28.19	30.81
13.5	28.81	31.56
15.69	29.56	32.88
16.88	30.12	34
17.75	32.88	34.69
18.75	34	35.62
19.38	34.69	36.44
21	35.62	37.25
22.44	38.62	38.62
23.75	39.5	40.19
25.06	40.19	41.25
26.5	41.25	42.19
27.19	42.19	43.5
28.19	43.5	44.44
28.81	44.44	46.75
29.56	45.94	47.62
30.12	46.75	50.12
30.81	47.62	51
31.56	60.62	52.94
32.19		54.31
32.88		56.19
34		57.56
34.69		59.44
35.62		60.62
36.44		62.94
37.25		
38.62		
39.5		
40.19		
41.25		
42.19		
43.5		

Fig. 3.23

Mutual spectral analysis of signals of E1(1)-E5B sensors



резонансы 2-6
нулевая фаза с2-6
противофаза с2-6
гармоники 2-6

2.438	2.438	20.38	2.438
4.375	10.81	52.81	19.81
5.688	18.56	53.88	35.31
6.625	38	54.69	37.06
10.81	40.12	56.25	43.56
11.81	42.19	57.12	47.25
12.44	43.56	58.38	53.88
15.81	44.5	59.38	59.38
17.81	46.06	63.31	
18.56	47.25		
19.81			
20.38			
29.5			
31.06			
35.31			
37.06			
38			
39.19			
40.12			
42.19			
43.56			
44.5			
46.06			
47.25			
49.12			
50.31			
52.81			
53.88			
54.69			
56.25			
57.12			
58.38			
59.38			
63.31			

Fig. 3.24

MMA results of signals of 59 - E3B sensors

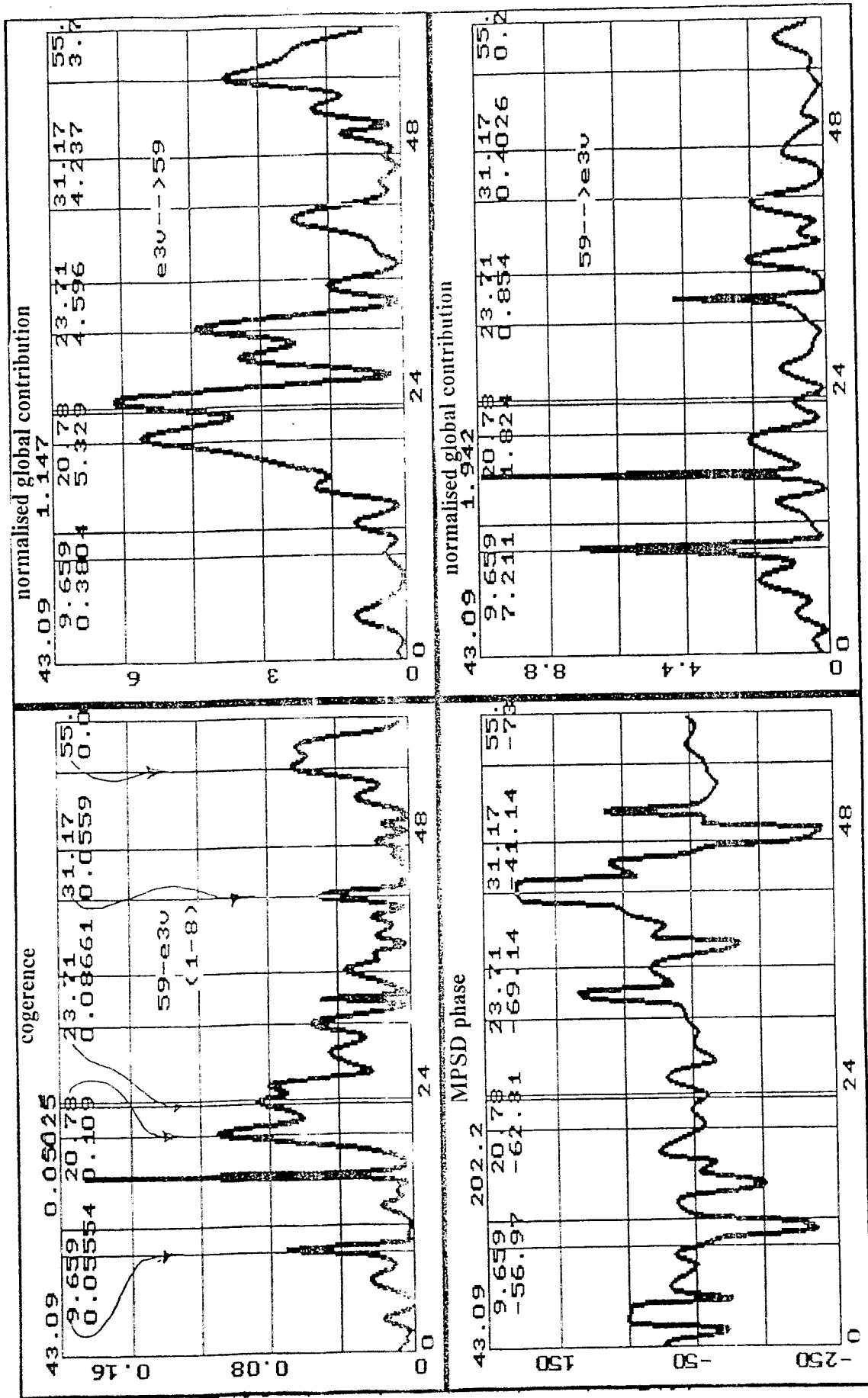


Fig. 2.5

base frequency (first harmonics) of FA vibration . This resonance was observed also in operational conditions at measurements at the unit №1 of Kalinin NPP (see the report for the previous stage).

3.4.3. Protective tube unit

Frequencies 2.5, 3.7, 5.5 and 6.5 Hz, referred to the PTU lips, already were mentioned in a course of realization MAA-analysis (see section 3.4.1 and 3.4.2). Was shown, that all of them arise because of FA vibrations. Own PTU oscillations in indicated frequency range is not detected.

Recalculation at a full-scale design of research results of large-scale model of a reactor gives for the PTU lip eigenfrequency of 43 Hz.

3.4.4. Main coolant circuit

MAA-analysis, the scheme of which is similar applied at the analysis of the indications of internal sensors , confirms, that indicated in section 3.3 frequencies are MCC eigenfrequencies.

Table 3.2

The totals of eigenfrequency estimation of VVER-1000 plant

Equipment Element	Mode		Frequency, Hz		
	n	m	Modelling (Recalculation)	Field Measurements	MAA- analysis
Core barrel	1	0.5	4.7	4.5	4.5
— " —	1	1	-	10.5	-
— " —	1	2	-	20	20-22
— " —	2	1	13	14	-
— " —	3	1	19	24	-
FA	-	1	-	2.5	2.5
PTU	2	1	43	-	-
MCC (cold loop)	-	-	-	3 6 13 23 25	-
MCC (hot loop)	-	-	-	3 6 9 18 23	-

CB - boundary conditions

 $m = 1$

4. CONCLUSIONS And PROPOSALS

4.1. By results of measurements of vibration parameters at serial VVER-1000 plant the vibrational characteristics of the main equipment, including lowest eigenfrequencies and modes of the CB, are determined.

The analysis of the vibrational characteristics is executed with engaging of researches results at scale models of VVER -1000 plant.

4.2. The shown data on the vibrational characteristics of the equipment can be the basis for adjusting of computational vibrational model of VVER-1000.

4.3. Data on the lowest modes of the CB shown in section 3, indicate on the fact, that at operational hydrodynamic loading two modes of oscillations with one half-wave in a longitudinal direction can simultaneously be realized: beam mode for the CB with two fixed ends, and also pendulum mode, appropriate to console fixed CB without lower keys.

The last kind of oscillations can be realized in two cases: at presence of gaps in lower key unit of CB, and also in the event when stiff characteristic of brackets of lower key unit are significantly less then bending stiffness of the CB.

4.4. For elimination of detected uncertainty in boundary conditions of CB attachment the following activities should be sequentially carry out:

a) adjusting of a computational model on ~~on~~ using highest shell modes of CB, also shown in section 3, with consequent introduction in a computational model of those values of a pliability of key unit, which correspond to experimental values of frequencies of pendulum oscillations of the CB;

b) computational determination of the stiff characteristics of lower key unit;

c) experimental determination of lower key unit stiffness.

Measurement on item 4.4.c can be executed at one of VVER-1000 reactors after reactor check assembling. In case of a capability of their realization in the first half of 1996 results of such measurements can be presented in the following report on the theme "Vibration Modelling of VVER Type Reactors".

List of adopted abbreviations

- APSD - auto power spectral density;
- ASW - acoustic standing wave;
- CB - core barrel;
- FA - fuel assembly;
- MAA - multichannel autoregression analysis;
- MCC - main coolant circuit;
- MCP - main circular pump;
- NMC - neutron measurement channel;
- NPP - nuclear power plant;
- NV NPP - Novovoronezh NPP;
- PEM - Control rod drive;
- Pr - pressurizer;
- PT - pressure transducer;
- PTU - protective tube unit;
- TI - thermocouple instrumentation;
- VVER - water cooled and water moderated energetic reactor.

Teil 3

APPROVED
Director General of Diagnostic
Center "DIAPROM"
~~_____~~ D.F. Gutsev
"27" мая 1996 г.

VIBRATION MODELLING of VVER TYPE REACTORS

**The analysis of the design characteristics and
experimental data for
adjustment of the VVER-1000 model**

**The intermediate report
320-O.211-004**

Part 2

1996

CONTENT

1. Acoustic standing waves.....	1
2. Vibrations of fuel assemblies.....	14
3. Common oscillations of core barrel (CB) and shells of the upper supporting structure.....	32

Results of equipment vibration and pressure oscillations measurements on RPV type
VVER-1000 during hot and cold try with use of incore detectors.

1. Acoustic standing waves

During hot try signals of the following pressure fluctuation transducers (PFT) were registered: BP12, BP14, BP15, BP16, 55, 56, 59 (further everywhere for a simplicity PFT will be designated only in digits) in a seven-channel mode. First four PFTs are located inside reactor vessel, 55 and 59 - on MCP inlet according to 1-st and 3-rd loops, transducer 56 - on MCP outlet of the 1-st loop. The exact PFTs location is represented on fig. 1, 2. Six seven-channel records, produced at different coolant temperatures and different number working MCPs according to the following table, will be considered below.

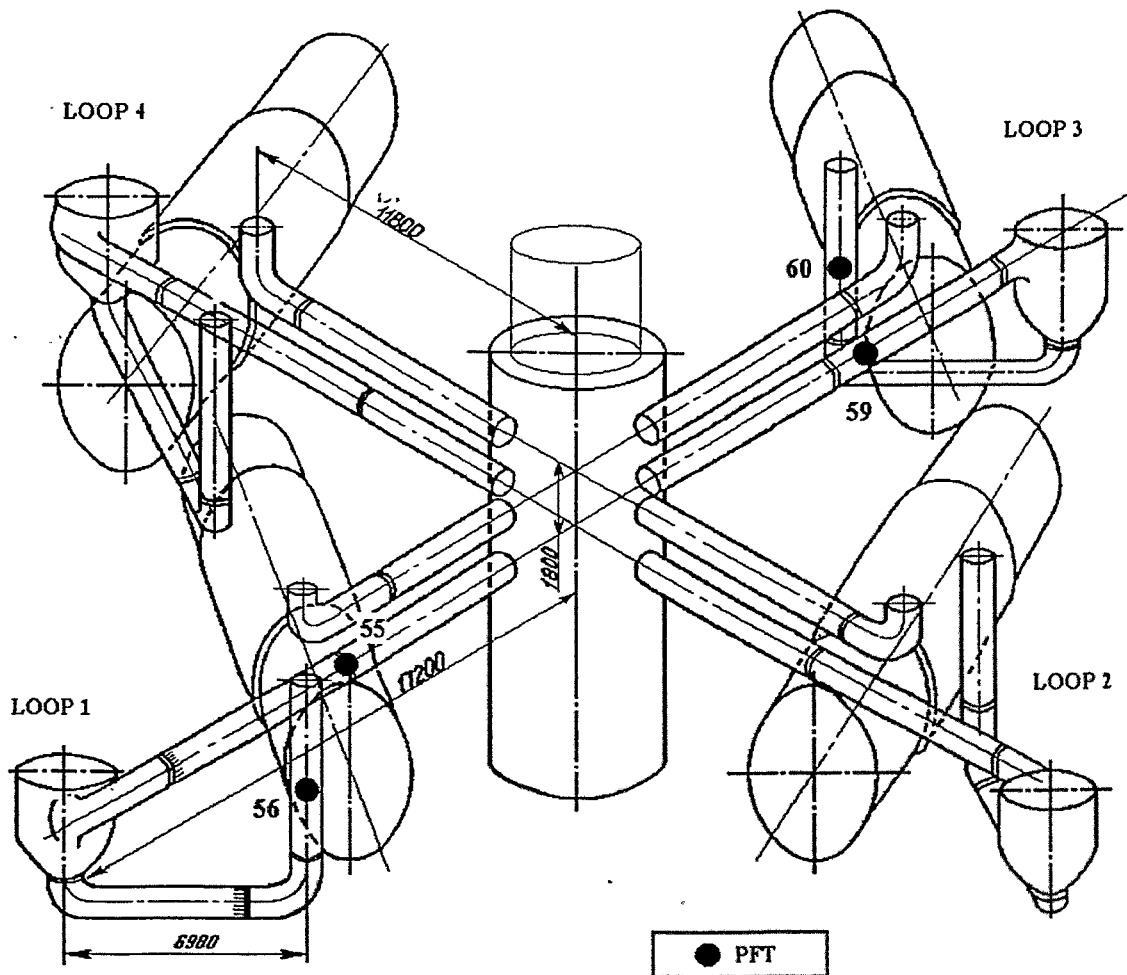
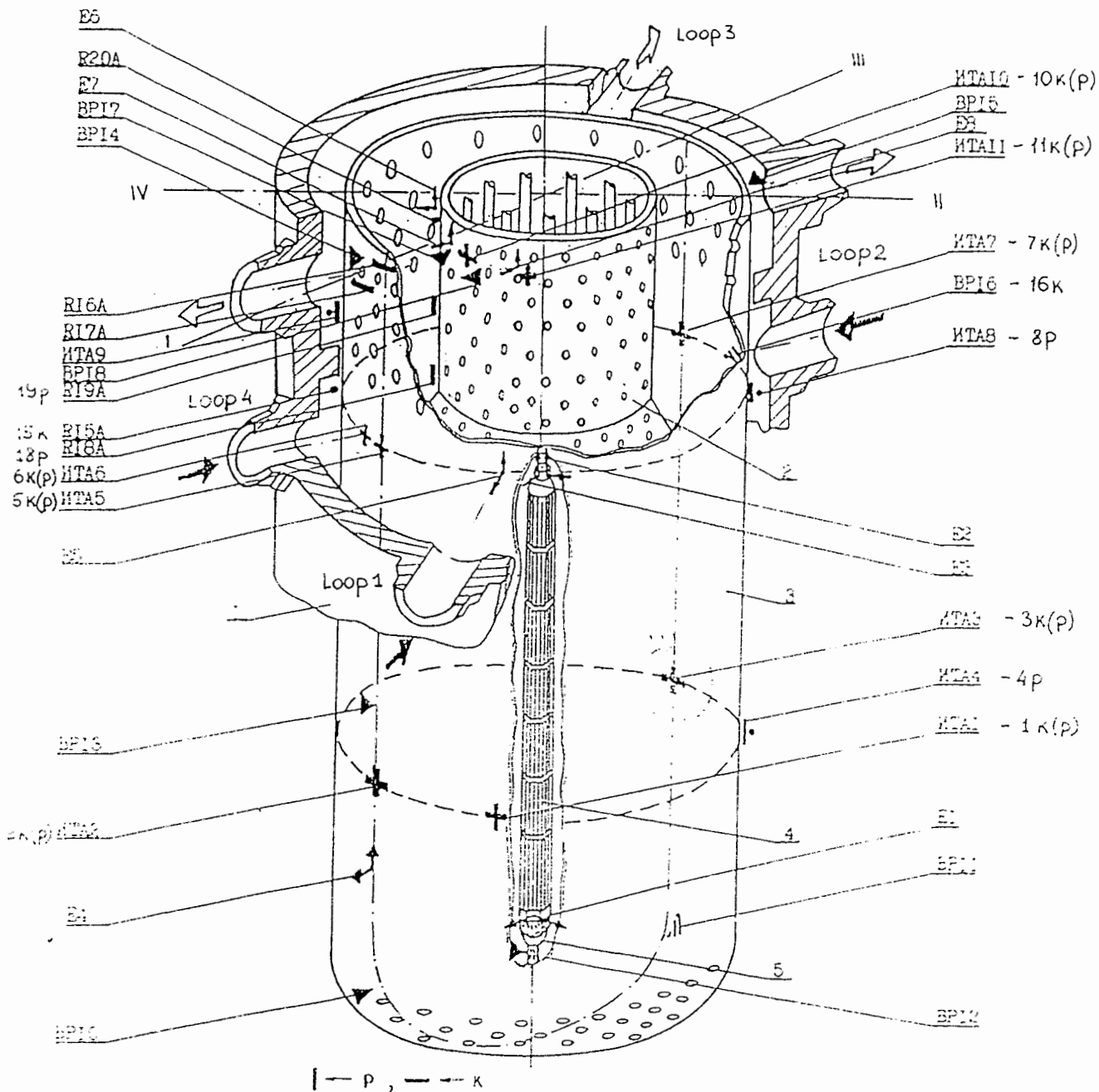


Fig. 1



1- reactor pressure vessel 2- shield of USS 3- core barrel
 4- central simulator of the fuel assemblies 5- support tube

Fig 2

Table 1

T [°C]	240	256	263	268	280	280
Working (+) and disabled (-) MCPs	[+ ---]	[- + --]	[- +++]	[- ++ -]	[+-+ -]	[+++++]
Number of record	1	2	3	4	5	6

The auto power spectral densities (APSD) of PFT signals (so-called "waterfalls of spectra") assembled on one axes give visual representation about temperature dependences of frequencies of various resonances. In particular, all acoustic standing waves (ASW) with their harmonics are characterized by monotonically decreasing dependences $f^{(n)}_{ASW} = F^{(n)}(T)$, where n - number of ASW harmonics.

In APSD of PFT signals, installed in loops, two resonances appropriate to the first harmonics ASW-1 and ASW-2 dominate. Waterfall of PFT spectra with number 55 and various fragments of this set curve in integrated scales are represented on fig. 3. As follows from the first fragment on fig.4, the changes of the pressurizer resonance location with coolant temperature have not a monotone character and are in frequency band [0.58 - 0.81] Hz (see marks of resonances frequencies in upper numerical line on the graphics). It is possible to make the similar conclusion for the resonance from frequency band [3.2 - 4.2] Hz (fig.5), which is generated by vibrations of internals reducing to progressive waves of coolant density. On the consequent two graphs (fig. 6, 7) resonances of the first harmonics ASW-1 and ASW-2 with obvious monotone dependences $f^{(n)}_{ASW} = F^{(n)}(T)$ are presented. The following two graphics (fig. 8, 9) are resonances of ASW higher harmonics also with monotone temperature dependences.

In APSD of internal PFTs signals only one resonance appropriate ASW-2 (fig. 10, 11, 12) dominates. As is known, the amplitude ASW-1 inside reactor vessel falls down up to zero on the reactor vertical axe of symmetry, and the space allocation of its nodes represents a complex picture, but it is essential, that the maximas (antinodes) ASW-1 are in loops. From the same graphs it is follows that the amplitude of resonance ASW-2 in region of exit pipe of the reactor pressure vessel (transducer 15) is in strong dependence on number of working MCPs.

Frequencies of resonances ASW and their harmonics (in Hz) selected on APSD signals of all PFTs are shown in the following table:

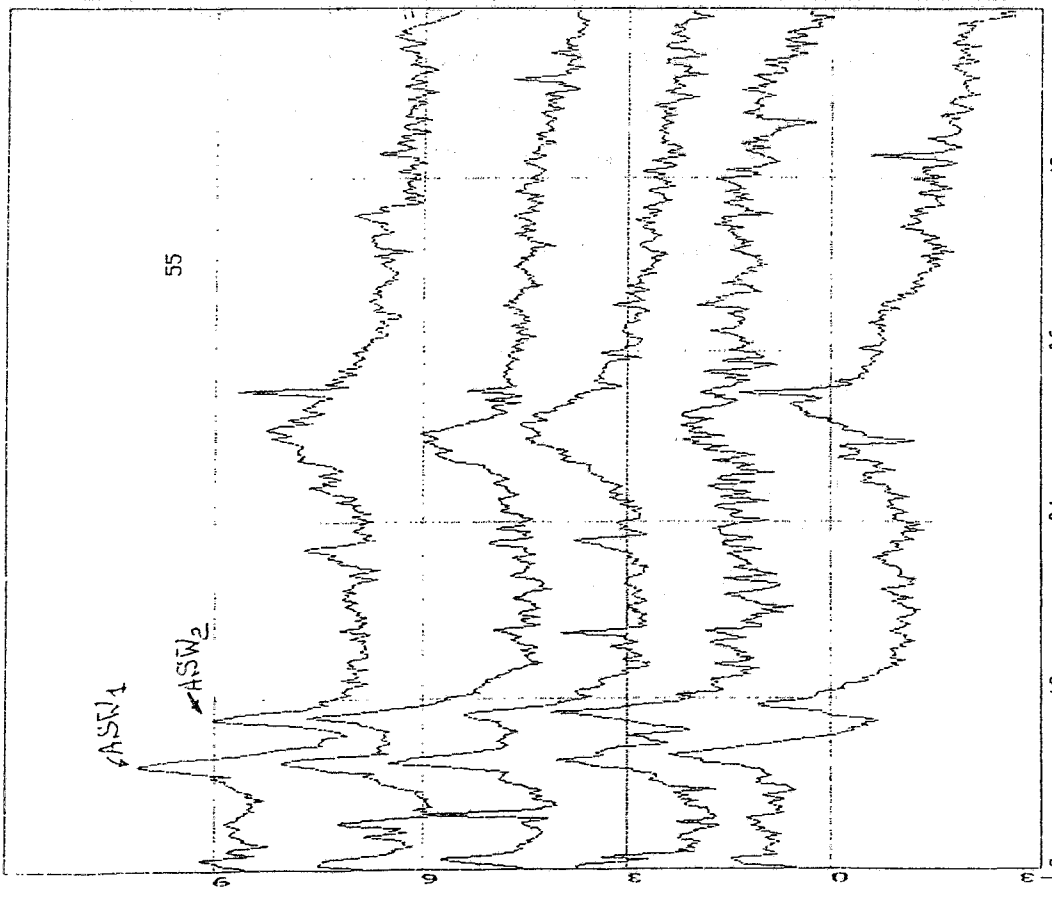
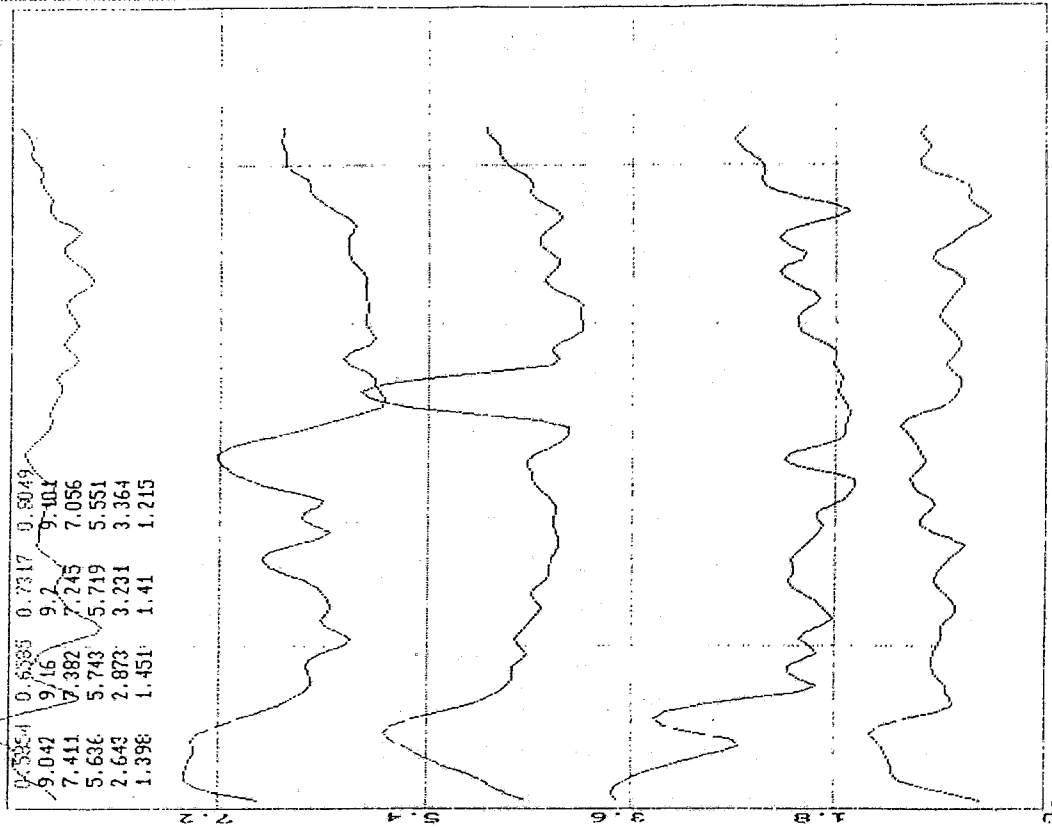


Fig. 4

Fig. 5

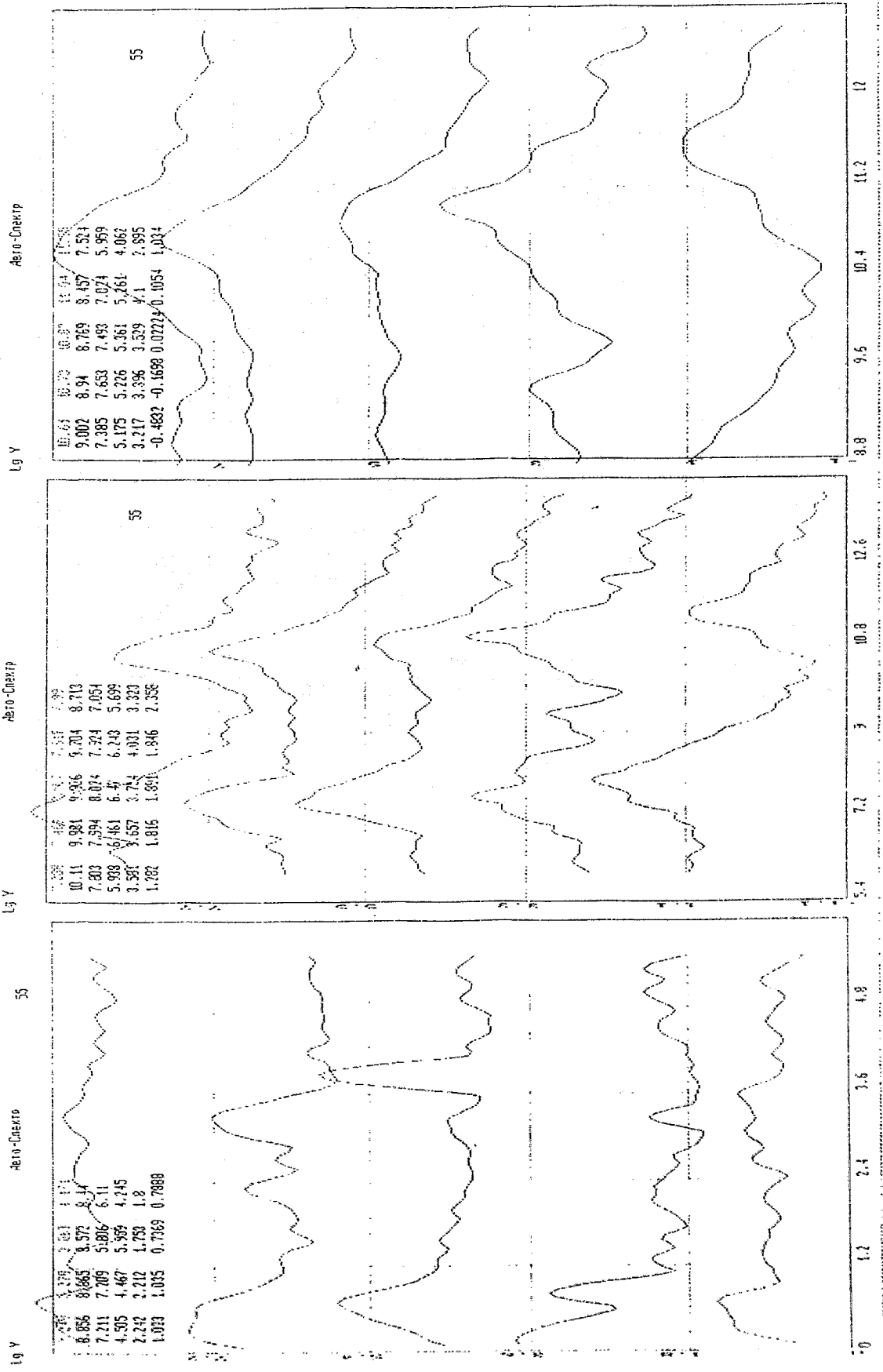


Fig. 5

Fig. 6

Fig. 7

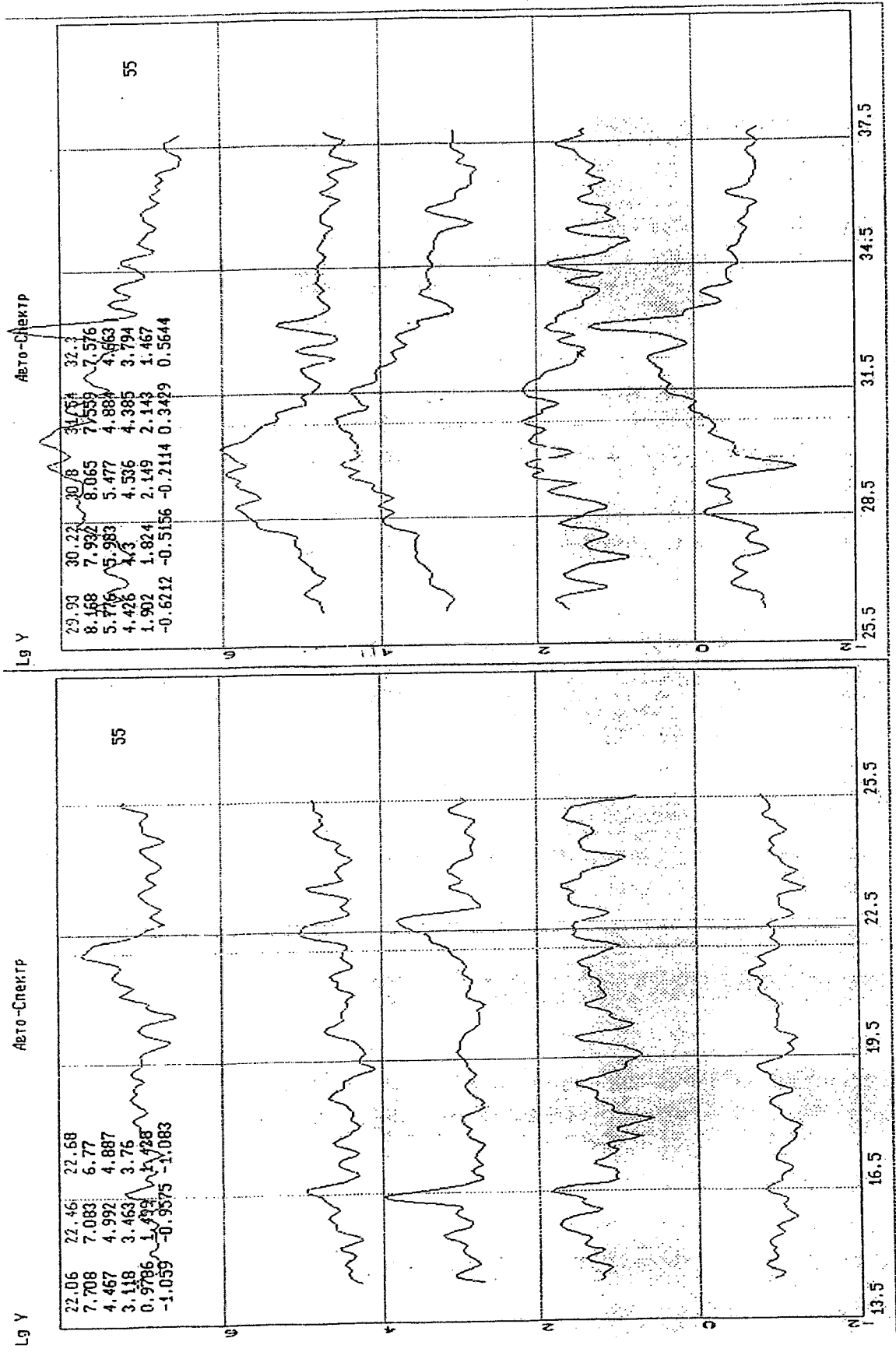
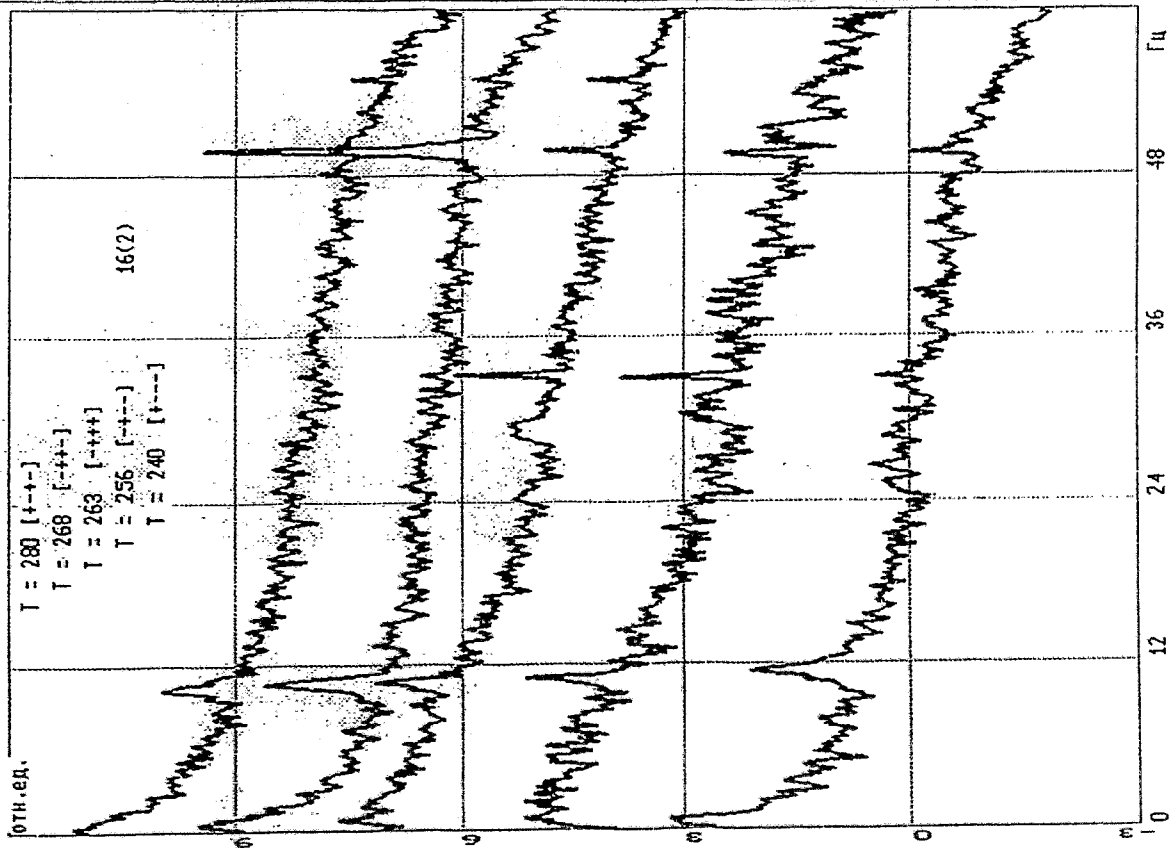


Fig. 8

Fig. 9

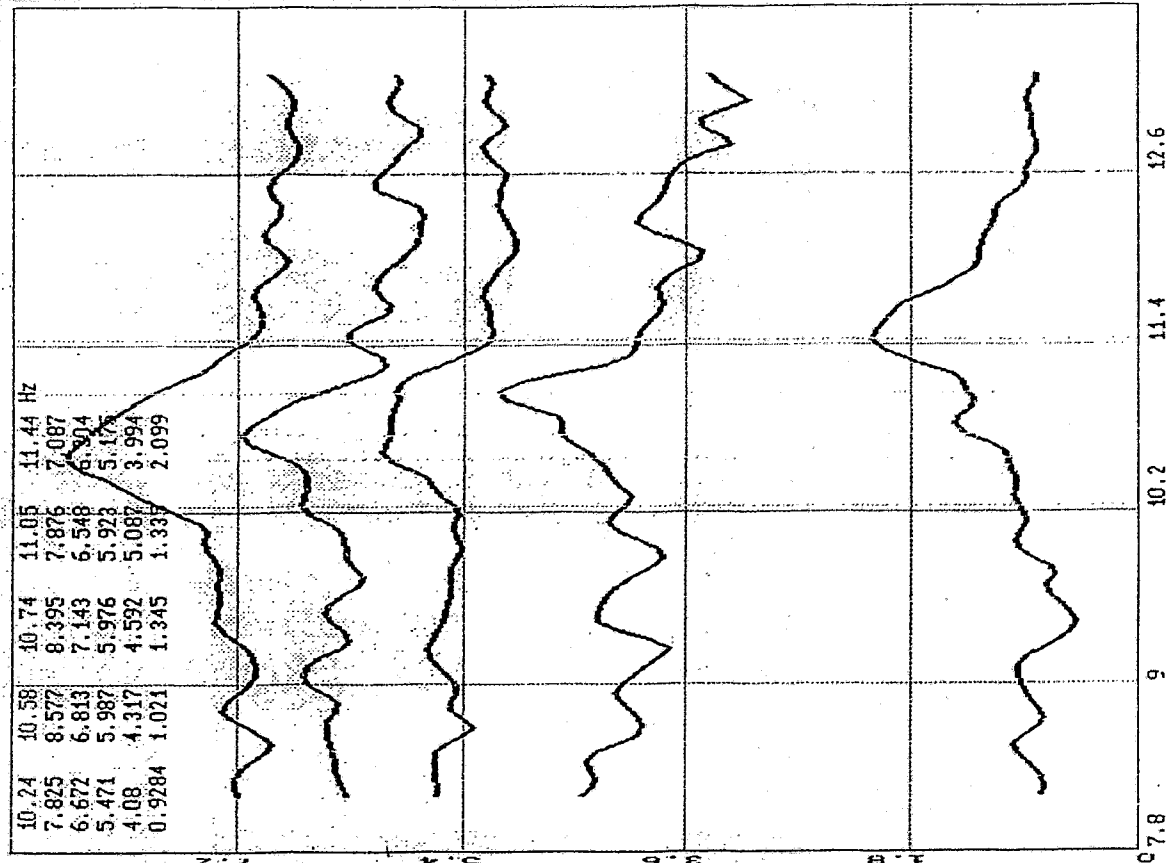
Lg Y

Авто-Спектр



Lg Y

Авто-Спектр



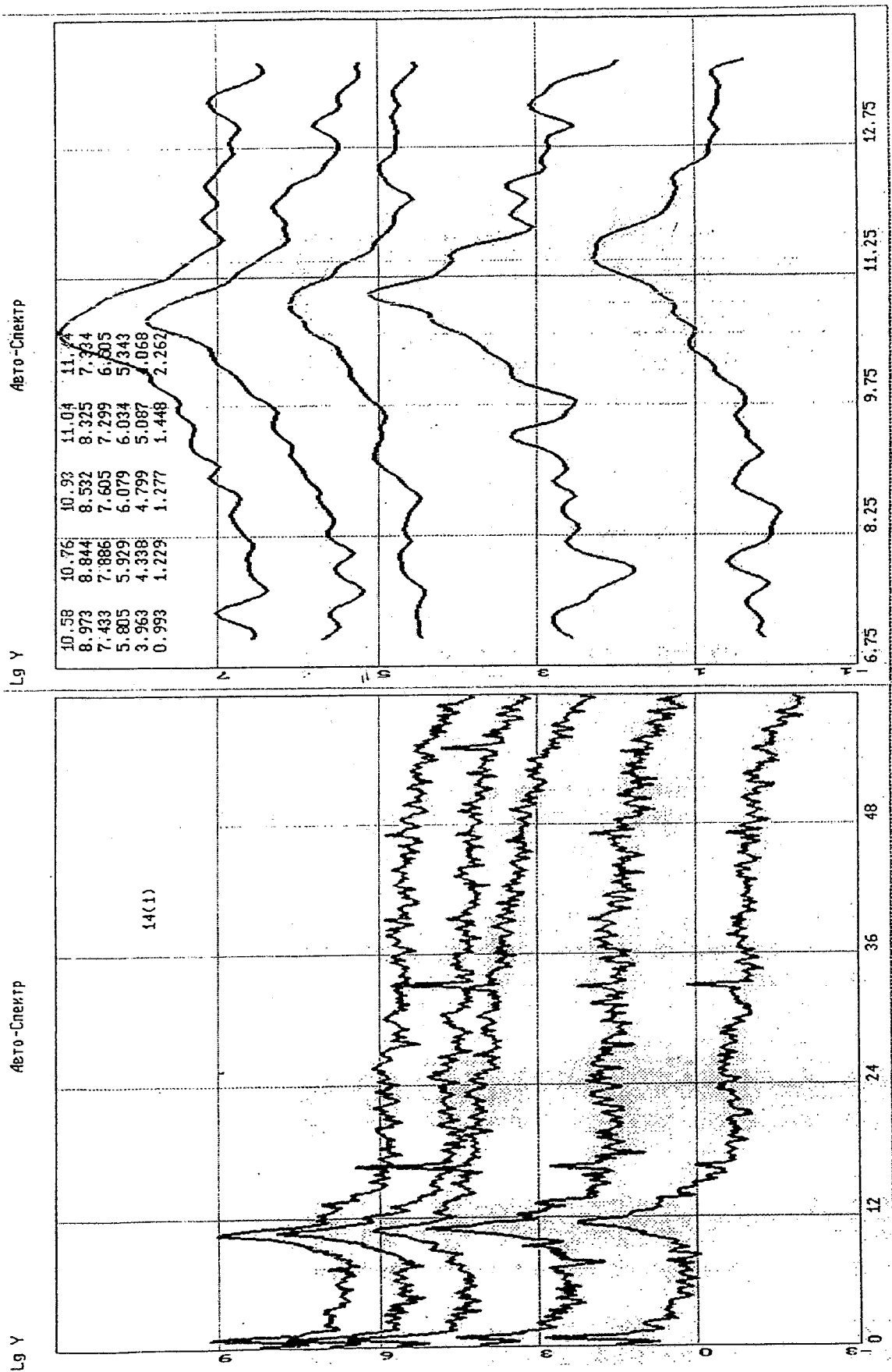


Fig. 11

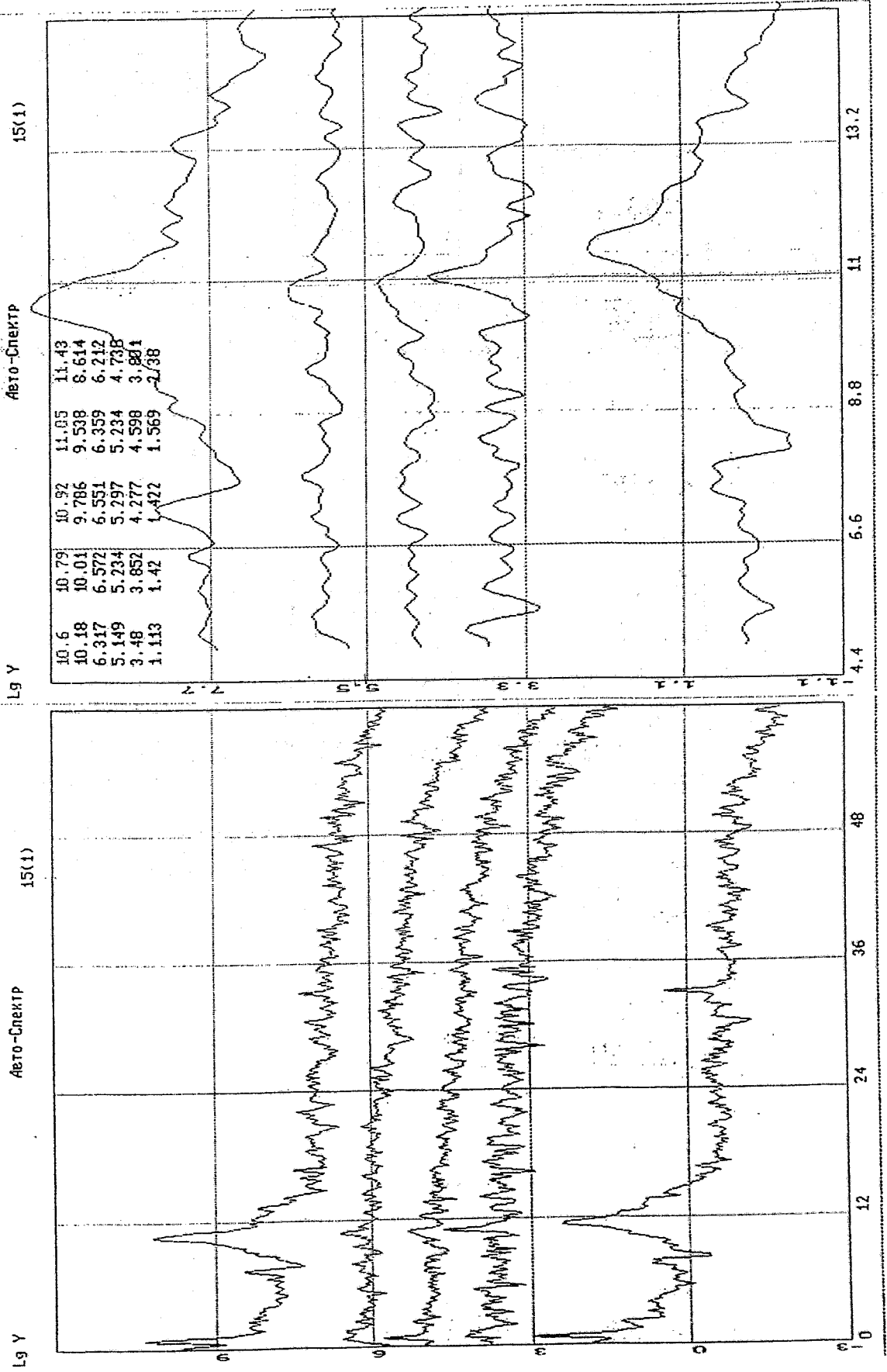


Fig. 12

Table 2

T [°C] PFT	280	268	263	256	240	Harmonics ASW
55	7.29	7.46	7.51	7.62	7.99	ASW ⁽¹⁾ -1
	10.61	10.73	10.87	11.04	11.55	ASW ⁽¹⁾ -2
	-	-	22.06	22.46	22.68	ASW ⁽³⁾ -1
	29.93	30.22	30.80	31.54	32.30	ASW ⁽⁴⁾ -1
56	7.32	7.46	7.48	7.61	8.01	ASW ⁽¹⁾ -1
	10.54	10.74	11.02	11.05	11.32	ASW ⁽¹⁾ -2
	14.93	15.40	-	15.66	15.78	ASW ⁽²⁾ -1
	29.56	29.96	30.70	31.48	32.23	ASW ⁽⁴⁾ -1
	36.22	36.77	37.26	37.99	38.78	ASW ⁽⁵⁾ -1
59	7.30	7.46	7.57	7.81	7.88	ASW ⁽¹⁾ -1
	10.58	10.74	10.87	11.02	11.46	ASW ⁽¹⁾ -2
	28.98	29.63	30.00	30.29	31.57	ASW ⁽⁴⁾ -1
12	-	-	10.88	11.05	11.46	ASW ⁽¹⁾ -2
	-	-	30.06	31.59	32.20	ASW ⁽⁴⁾ -1
14	10.58	10.76	10.93	11.04	11.44	ASW ⁽¹⁾ -2
15	10.60	10.79	10.92	11.05	11.43	ASW ⁽¹⁾ -2
16	10.24	10.58	10.74	11.05	11.44	ASW ⁽¹⁾ -2

The numerical data listed in the table enable to make approximations dependences $f^{(n)}_{ASW} = F^{(n)}(T)$, useful in practical applications. So, for example, ASW-1 and ASW-2 in temperature range [240-280] °C are described satisfactorily by the following linear dependences:

$$F_{ASW-1} = -0.0175T + 12.20$$

$$F_{ASW-2} = -0.0215T + 16.60$$

[°C] f_2

From the linear extrapolation of the last dependence in a zero follows, that at low coolant temperatures, for example in the beginning of reactor pressure vessel heating, F_{ASW-2} is rather close to F_{MCP} . Such coincidence of frequencies of two external driving forces can reduce to increase of internal vibrations level. The similar conclusion follows and for harmonics ASW⁽⁴⁾-1: at coolant temperature close to 220 °C its frequency coincides the second harmonics F_{MCP} (see also fig. 3). The coincidence of frequencies of various harmonics MCP and ASW is inevitable

during reactor pressure vessel heating, it is important that these resonance appearances did not reduce in anomalous vibrations. The great experience of starting-up and adjustment measurements on large number of Units VVER-1000 accumulated by the General Designer, testifies that the similar resonance appearances do not reduce to anomalous internals and PCC equipment vibrations.

In the previous table not every possible harmonicses ASW are represented and only those of them, which are significant mapped in APSD. This conclusion is important for creation of right representation about dominating sources of internals forced oscillations. In this case the first harmonicses ASW do not concede to progressive waves of coolant density on MCP back frequency. As follows from spectral reflectance reduced in the previous sections amplitude of vibrations of various units internals on frequencies of forced oscillations (pressurizer, MCP, harmonicses ASW) frequently much exceed on the value of amplitude of vibrations of units on own frequencies. Because of such masking the detection of characteristical space modes of vibrations on own frequencies represents a challenge.

Just on APSD amplitude it is possible to judge the value of driving force, though for detection of every possible harmonicses ASW and the making of space allocations of amplitudes ASW are necessary for applying the mutual spectral analysis. From functions of coherence, presented it on fig. 13 is visible, that ASWs represent common-circuit phenomenon. Coherence of signals PFT located in opposite loops, are rather close to "one" on frequencies of the first harmonicses ASW-1 and ASW-2. On definition the harmonicses ASW appear in mutual spectral reflectance only as synphasae or anti-phase components. On fig. 14 evaluations of phase and coherence for pair of signals PFT (55-56) located in one loop are represented. In the tables on these figures frequencies of synphase and anti-phase resonances together with appropriate values of the function of coherence are assembled only. Among them it is possible to select high-frequency harmonics ASW-1, which in APSD 55 and APSD 56 is not observed. At $T=263^{\circ}\text{C}$ its frequency of 50,62 Hz, at $T=256^{\circ}\text{C}$ - 54,06 Hz.

Thus inside reactor pressure vessel it is important to take into account ASW-2 as an external driving force, which covers the cross-section of the reactor vessel by its antinode. Registration of ASW-1, and ASW-2 is necessary in loops.

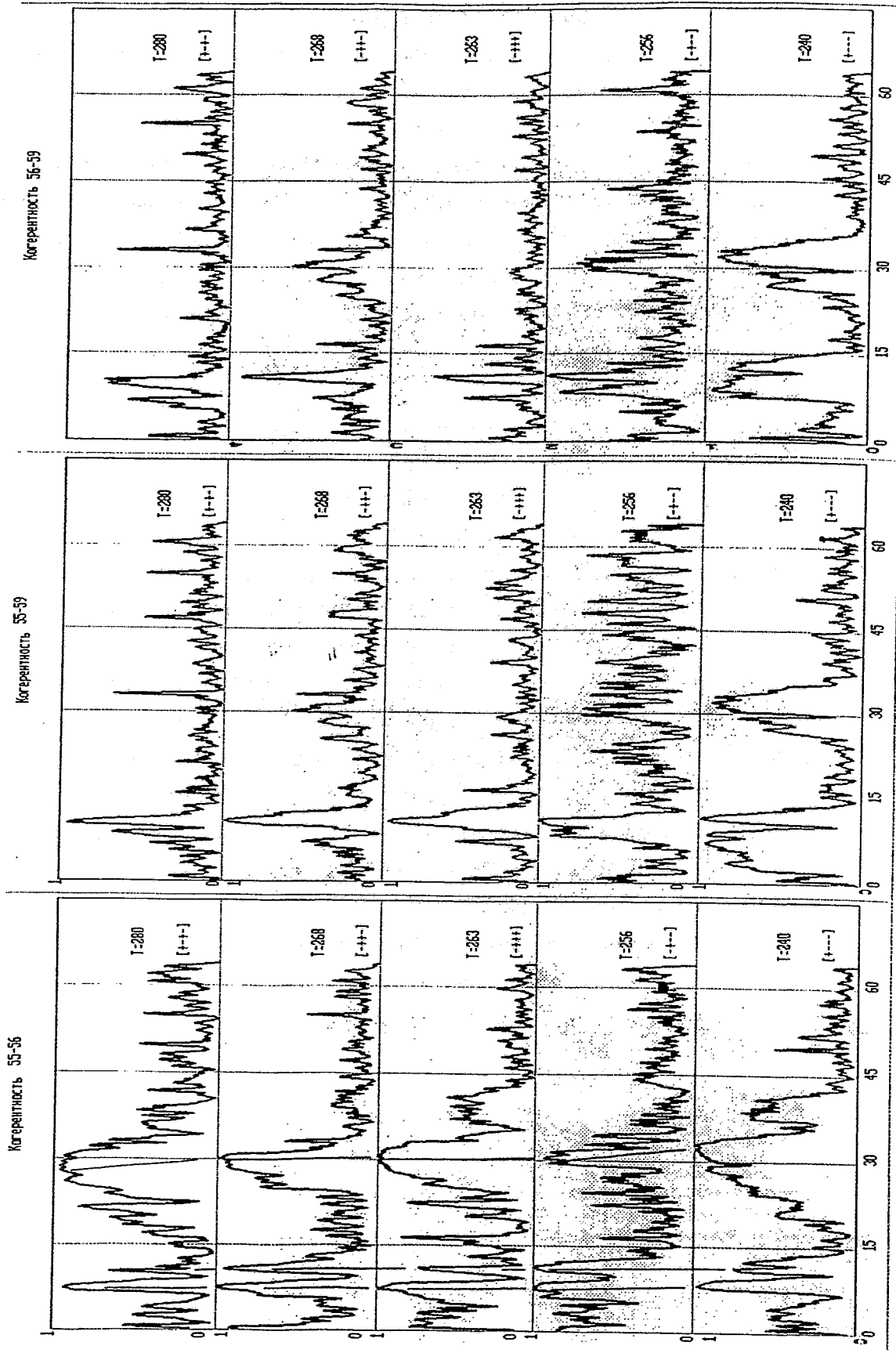
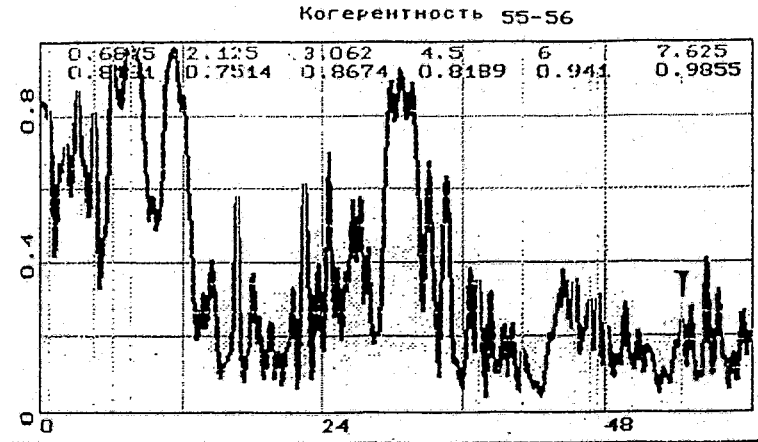
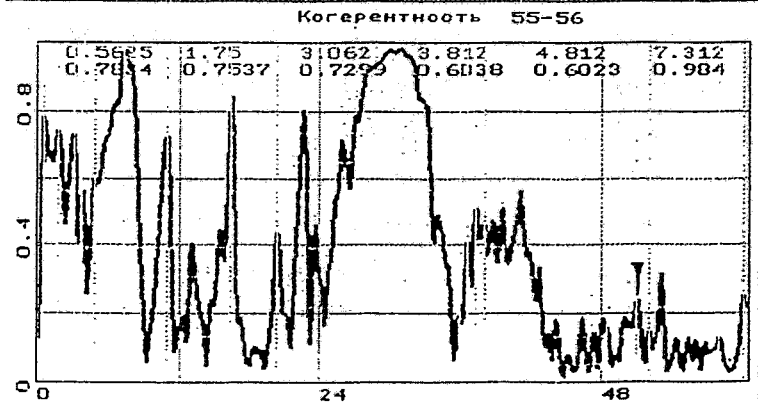
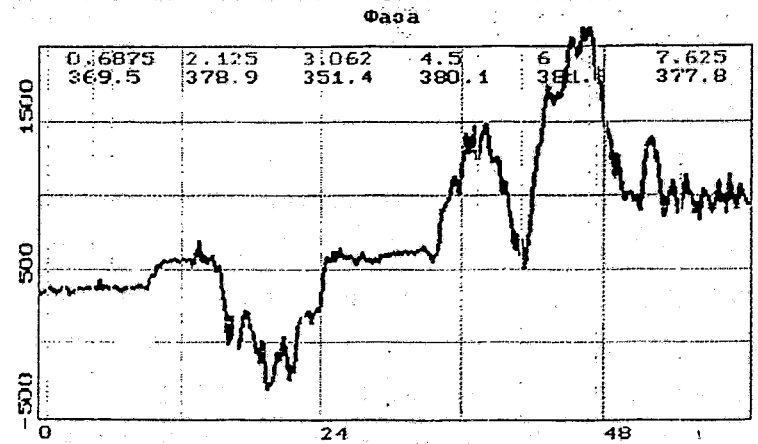


Fig. 13



0.6875	0.8181	9.543
2.125	0.7514	18.93
3.062	0.8674	-8.64
4.5	0.8189	20.13
6	0.941	21.32
7.625	0.9855	17.8
16.5	0.5808	26.02
22.38	0.6384	-174.3
37.19	0.3838	162.8
40.88	0.1675	-175.7
45.12	0.3757	-165.2
46.44	0.3009	-23.15
47.12	0.3287	-22.11
47.88	0.2355	-2.788
54.06	0.2413	-169.6

[---] Γ0
T = 256



0.5625	0.7834	-14.86
1.75	0.7537	-13.16
3.062	0.7299	7.218
3.812	0.6038	-161.8
4.812	0.6023	-9.023
7.312	0.984	19.13
10.94	0.7337	-165.1
16.31	0.8603	13.55
20.25	0.4411	168.8
35.75	0.2025	26
36.44	0.4227	11.92
37.25	0.5398	-27.74
37.88	0.4634	-16.34
50.62	0.2401	-176.2
51.62	0.1475	171.3
57.62	0.1373	4.655
59.75	0.2547	7.546

[---] Γ0
T = 263

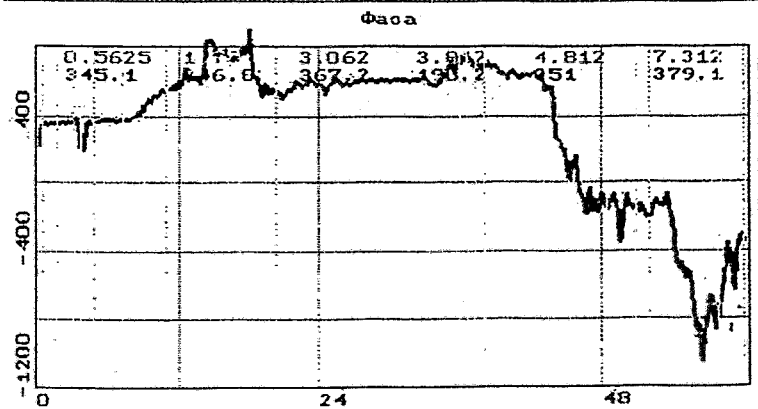


Fig. 14

2. Vibrations of fuel assemblies

In starting-up and adjustment measurements of fuel assemblies vibration are investigated with the help of the full scale fuel assembly simulator equipped with tenzoaccelerometers. Seven-channel record, consisting of the following signals (fig. 2), will be considered below:

BP59 - PFT installed on MCP inlet of 3-rd loop,

e1 (1), e1 (2) - tenzoaccelerometers installed practically in one point on fuel assembly tail, sensing to vibrations in radial mutual perpendicular directions,

e3g, e3v - tenzoaccelerometers installed practically in one point on the fuel assembly head, sensing accordingly to vibrations in radial and vertical directions,

e5g, e5v - tenzoaccelerometers installed practically in one point on core, sensing accordingly to vibrations in radial and vertical directions.

There are thus available three classes of processes:

1. Signal PFT in spectral characteristics of which frequencies, identified with pressurizer, MCP, ASW are known, and generally speaking frequencies of vibrations every possible internals are not known. Basically, the PFT signal can be contained the information on vibrations of any units PCC and internals. Thus the phase characteristics of such vibrations depend on installation site of transducers, that is in a way arbitrary because vibrations assimilated by coolantas as damping progressive waves of density.
2. Four signals of tenzoaccelerometers installed on fuel assembly, in which, doubtlessly, unknown characteristic frequencies of fuel assemblies vibrations are contained, presence of known frequencies of ASW, MCP, pressurizer and also unknown frequencies of collective vibrations of internals is possible.
3. Two signals of tenzoaccelerometers installed on core barrel, for which reasonings of the previous item are fair from that only by a difference, that in data signals doubtlessly to be contained the frequency of core barrel vibrations on various modes.

In everyknown spectral characteristics (APSD, coherence, phase) of mentioned above signals we shall mark the following features:

- In APSD of all tenzoaccelerometers (the fig. 15) powerful high quality resonance on frequency of 2.5 Hz is present,
- In APSD of signals e1 (1), e1 (2), e5v (that is only on fuel assemblies tail and on core barrel only in a vertical direction) there is the resonance in region of 20.5 Hz,
- In APSD of signals e1 (1), e3g, e5v powerful low quality resonance at region of 43.5 Hz is present,
- In APSD of transducers installer on fuel assemblies tail, head and on core barrel low quality resonances of 6.6 Hz and 54 Hz are present,

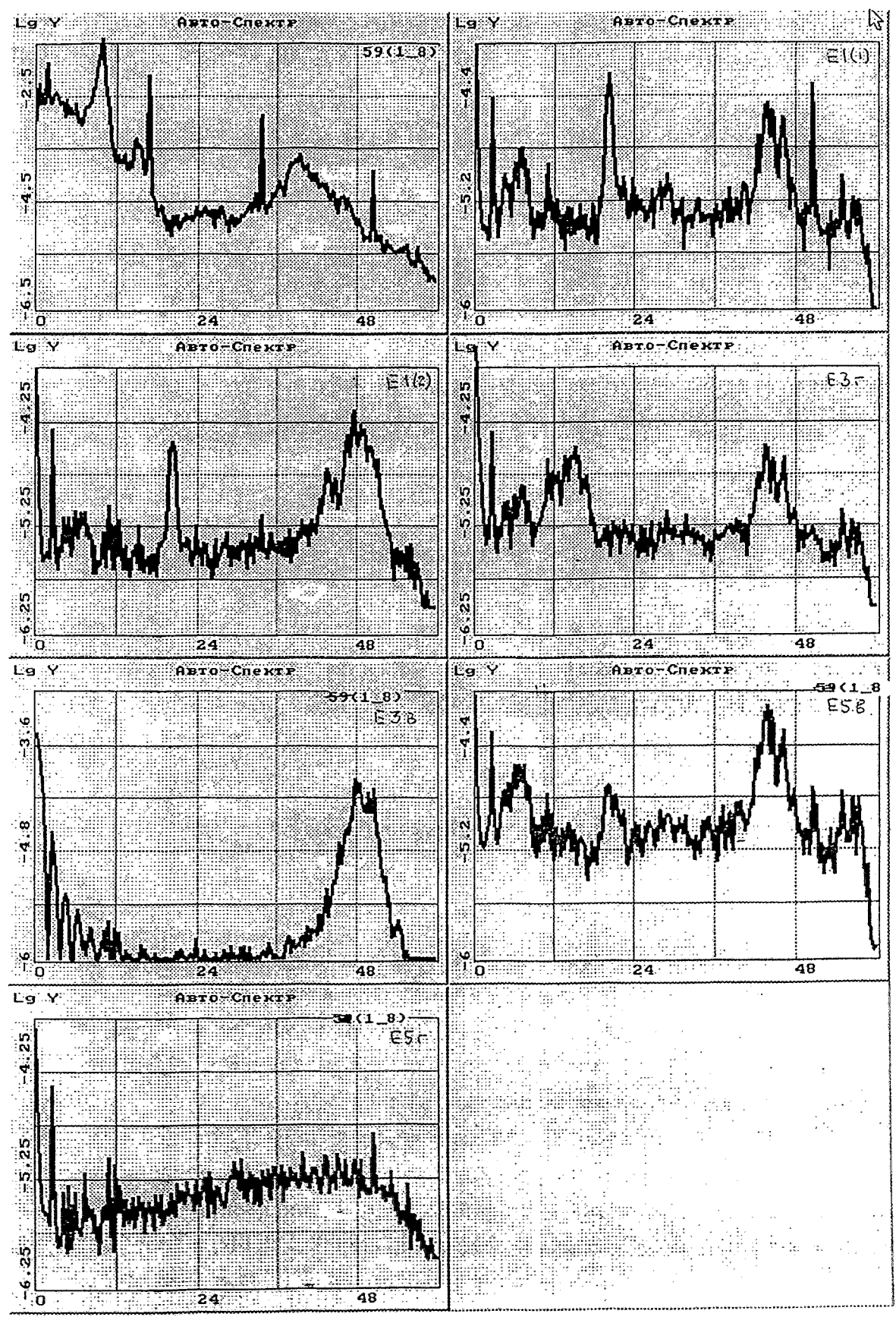


Fig. 15

- APSD of signals e3g, e5v (on fuel assembly and on core barrel) are rather close to each other on the dominating resonances,
- All listed above features (2.5 Hz, 6.6 Hz, 20.5 Hz, 43,5 Hz, 54 Hz) dominate in functions of signals pairs coherence e1 (1) -e1 (2), e1 (2) -e3g, e1 (1) -e5v (fig. 16, 17, 18).
- As a rule, on these frequencies happen synphase oscillation except for the following cases of anti-phase: 20.38 Hz for the pair e1 (1) -e5v, (53-60) Hz for pairs e1 (1) -e5v and e1 (1) -e1 (2).

Thus on the listed above frequencies take place collective oscillation of fuel assemblies and core barrel. Here collective forced oscillations, happening for the known reasons (MCP, pressurizer, ASW) are not deliberately considered.

We apply means of the MAR-analysis for identification of the primary sources, listed above resonances. Any two-dimensional MAR-model, one of components of which is the signal PFT and other - any signal tenzoaccelerometers is correct. We shall remind, that the condition of MAR-model correctness consists in the mutual noncorrelatedness of external sources each of signals. An external source, defining the contribution of pressure fluctuations in the function of coherence of any pair signals PFT- tenzoaccelerometer in frequency band (0 -60) Hz any time consisted of harmonicses ASW and MCP. The vivid example is represented on fig.19. The dominating resonances of the function of coherence e3v-PFT59 are divided as follows on external sources:

PFT: 9.66 Hz - ASW-1, 16.60 Hz and 33.2 Hz - MCP (see normalized global contribution 59 - > e3v in a right lower corner fig. 19),

e3v: 20.78 Hz, 23.71 Hz, 55.00 Hz (see the upper graph in the right corner on the same fig. 19).

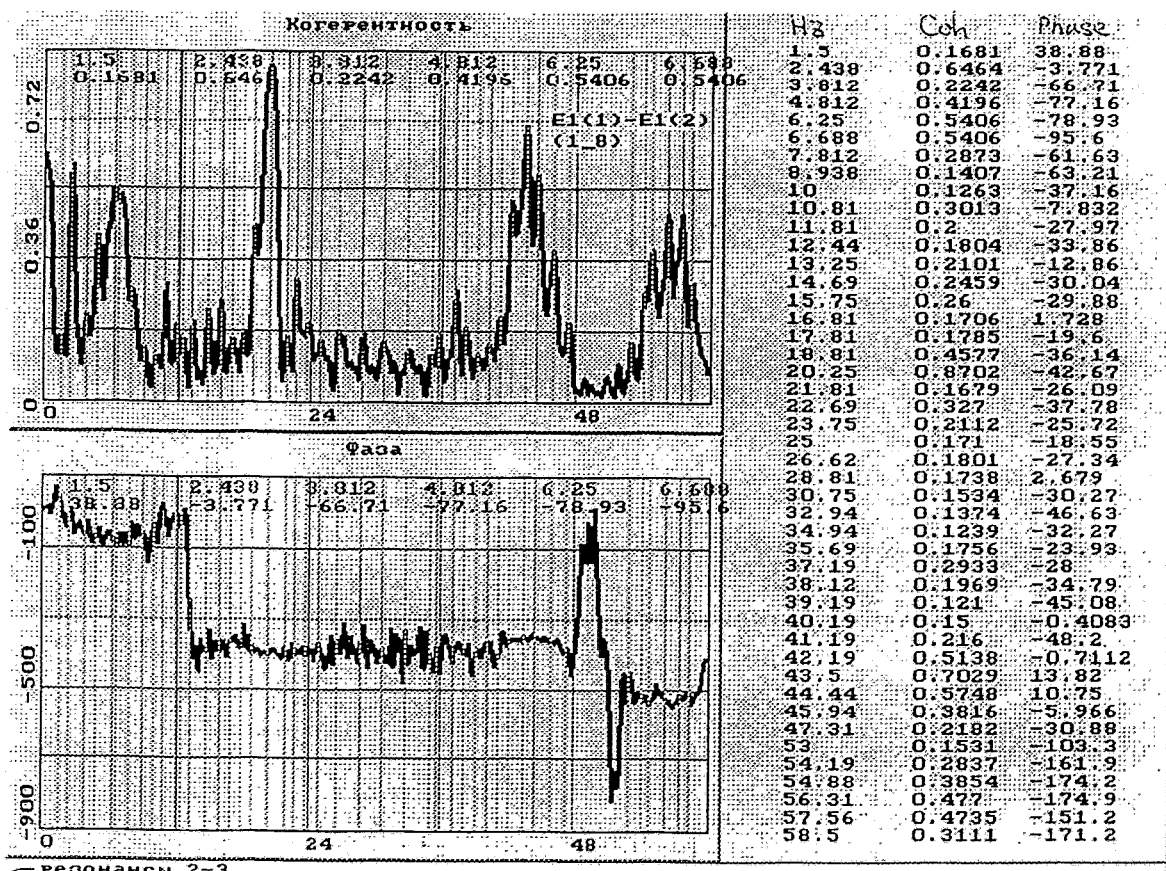
In a low-frequency range (0 - 6) Hz for this pairs of signals we have(fig. 20):

PFT: 1.6 Hz,

e3v - 2.50 Hz, 2.93 Hz, 3.43 Hz, 4.74 Hz, 6.80 Hz.

Thus researched row of frequencies of fuel assemblies collective vibrations (2.5 Hz, 6.6 Hz, 20.5 Hz, 43,5 Hz, 54 Hz) is not introduced of outside of progressive waves of coolant density. There is only one such resonanc on frequency of which vibrations of fuel assemblies and core barrel happen, but which cannot be interpreted as own vibration frequency of fuel assemblies, core-barrel, it is only the resonance on frequency 1.6 Hz.

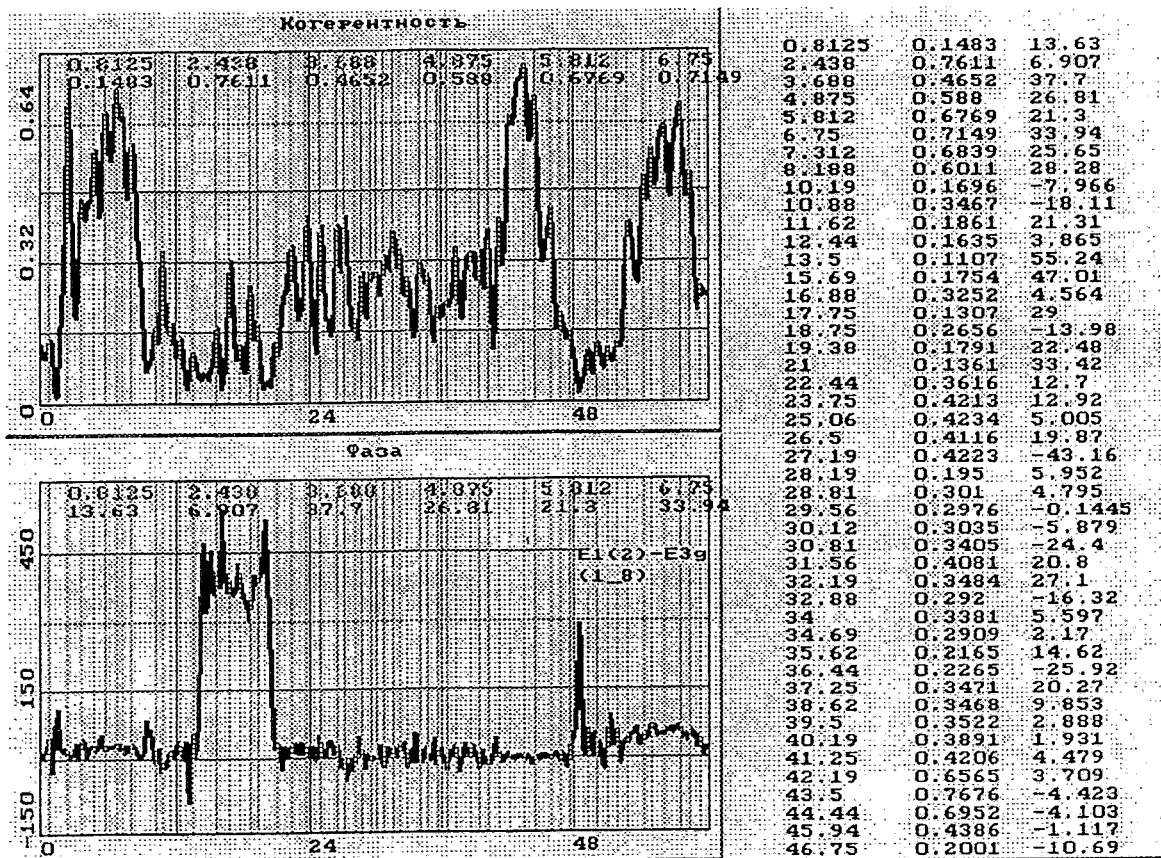
We shall increase dimension of MAR-model so that correlare the researched number of resonances with fuel assemblies or with core barrel considering a vector (PFT, tenzoaccelerometer on fuel assembly, tenzoaccelerometer on core barrel). Among every such MAR-models it was possible to select one correct model (PFT 59, e3g, e5v) in frequency band (0 - 60) Hz (fig. 21, 22, 23). The reason of it in the following. An apart from of the known requirement to components of MAR-models, consisting that the transducers of signals were



резонансы 2-3
нулевая фаза с2-3
противофаза с2-3
гармоники 2-3

1.5	2.438	54.19	1.5
2.438	10.81	54.88	12.44
3.812	13.25	56.31	13.25
4.812	16.81	57.56	15.75
6.25	17.81	58.5	17.81
6.688	25		18.81
7.812	28.81		20.25
8.938	40.19		21.81
10	42.19		23.75
10.81	43.5		25
11.81	44.44		26.62
12.44	45.94		35.69
13.25			37.19
14.69			39.19
15.75			40.19
16.81			43.5
17.81			44.44
18.81			47.31
20.25			53
21.81			54.19
22.69			56.31
23.75			58.5
25			60.88
26.62			62.94
28.81			
30.75			
32.94			
34.94			
35.69			
37.19			
38.12			
39.19			
40.19			
41.19			
42.19			
43.5			
44.44			
45.94			
47.31			
53			
54.19			
54.88			
56.31			

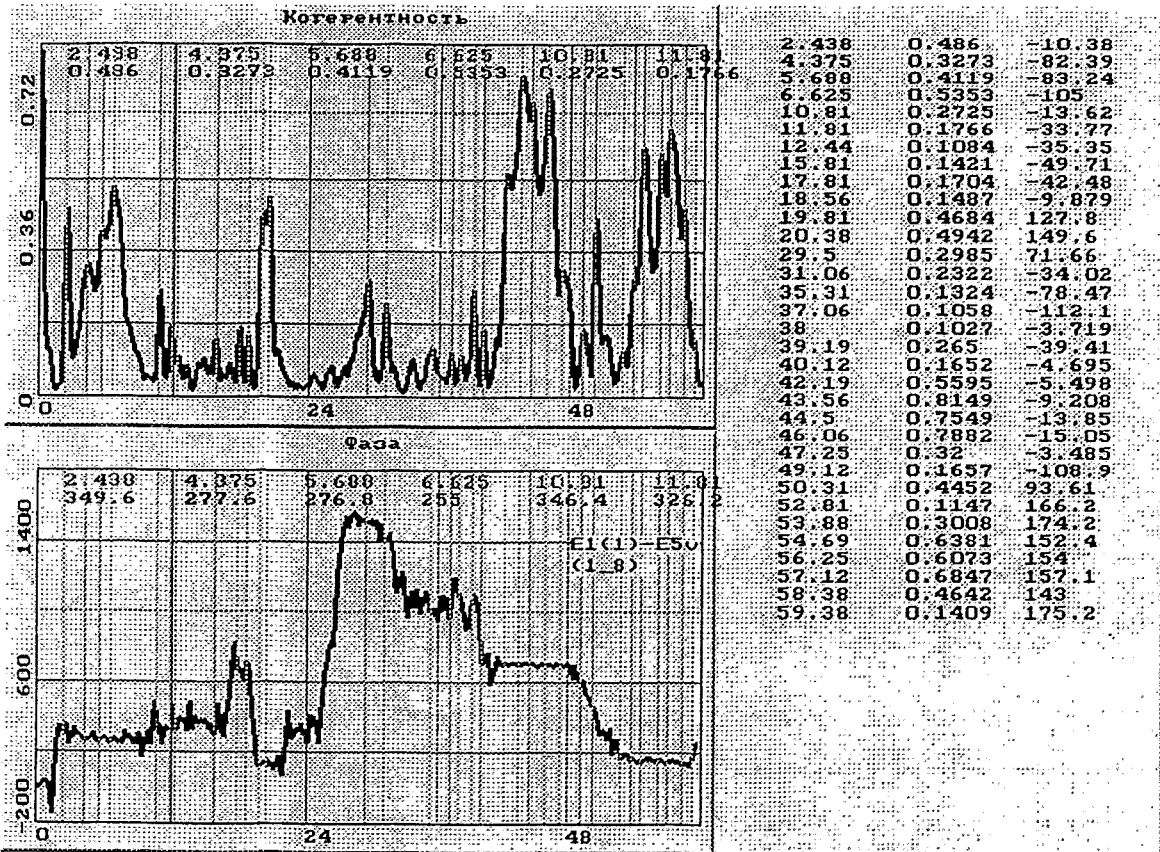
Fig. 16



резонансы 3-4
нулевая фаза с3-4
противофаза с3-4
гармоники 3-4

0.8125	0.8125	0.8125
2.438	2.438	2.438
3.688	10.19	4.875
4.875	10.88	7.312
5.812	12.44	7.312
6.75	16.88	11.62
7.312	18.75	13.5
8.188	22.44	19.38
10.19	23.75	25.06
10.88	25.06	27.19
11.62	26.5	28.81
12.44	28.19	30.81
13.5	28.81	31.56
15.69	29.56	32.88
16.88	30.12	34
17.75	32.88	34.69
18.75	34	35.62
19.38	34.69	36.44
21	35.62	37.25
22.44	38.62	38.62
23.75	39.5	40.19
25.06	40.19	41.25
26.5	41.25	42.19
27.19	42.19	43.5
28.19	43.5	44.44
28.81	44.44	46.75
29.56	45.94	47.62
30.12	46.75	50.12
30.81	47.62	51
31.56	60.62	52.94
32.19		54.31
32.88		56.19
34		57.56
34.69		59.44
35.62		60.62
36.44		62.94
37.25		
38.62		
39.5		
40.19		
41.25		
42.19		
43.5		

Fig.17



Резонансы 2-6
 нулевая фаза с2-6
 противофаза с2-6
 гармоники 2-6

2.438	2.438	20.38	2.438
4.375	10.81	52.81	19.81
5.688	18.56	53.88	35.31
6.625	38	54.69	37.06
10.81	40.12	56.25	43.56
11.81	42.19	57.12	47.25
12.44	43.56	58.38	53.88
15.81	44.5	59.38	59.38
17.81	46.06	63.31	
18.56	47.25		
19.81			
20.38			
29.5			
31.06			
35.31			
37.06			
38			
39.19			
40.12			
42.19			
43.56			
44.5			
46.06			
47.25			
49.12			
50.31			
52.81			
53.88			
54.69			
56.25			
57.12			
58.38			
59.38			
63.31			

Fig. 18

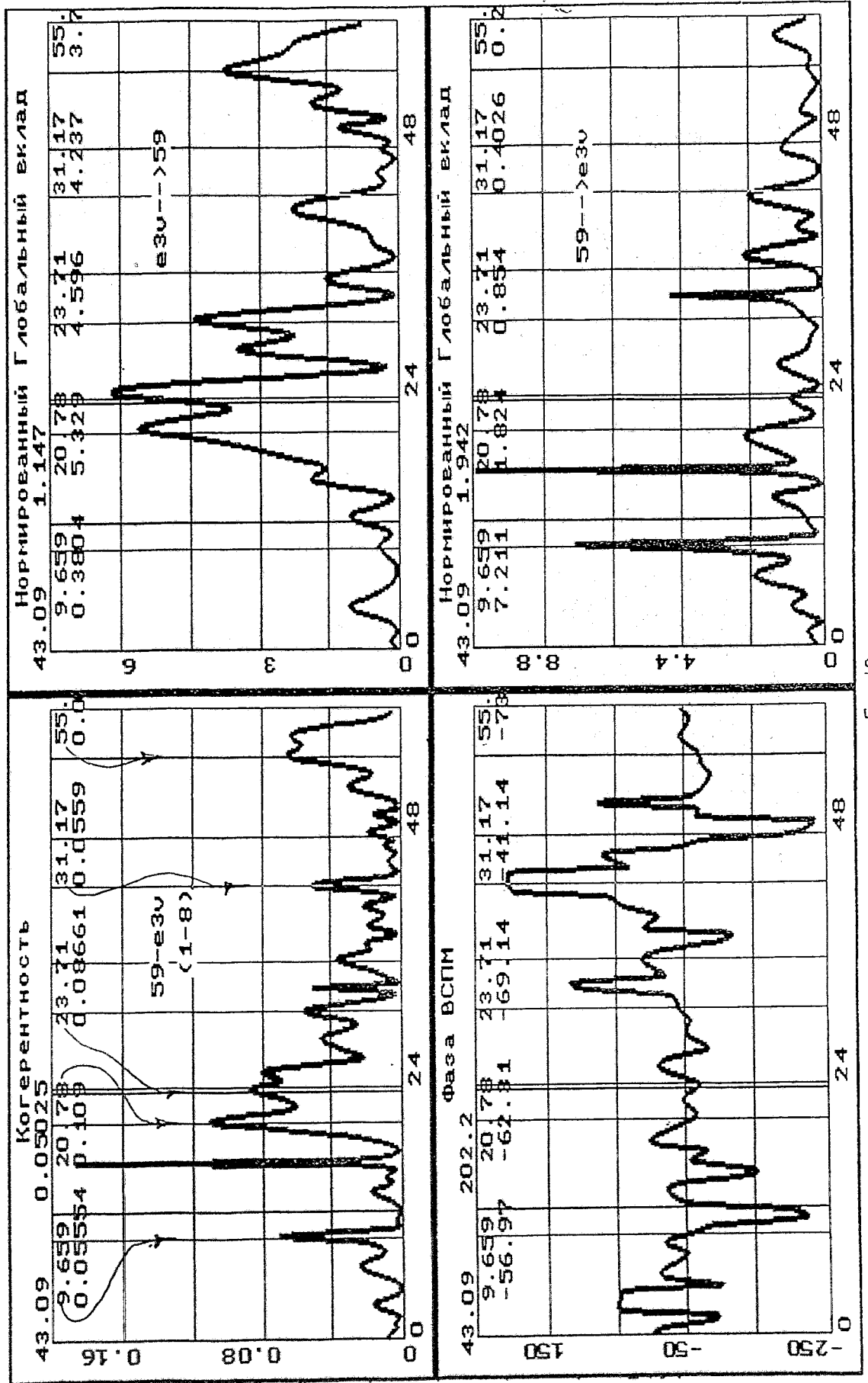


Fig. 19

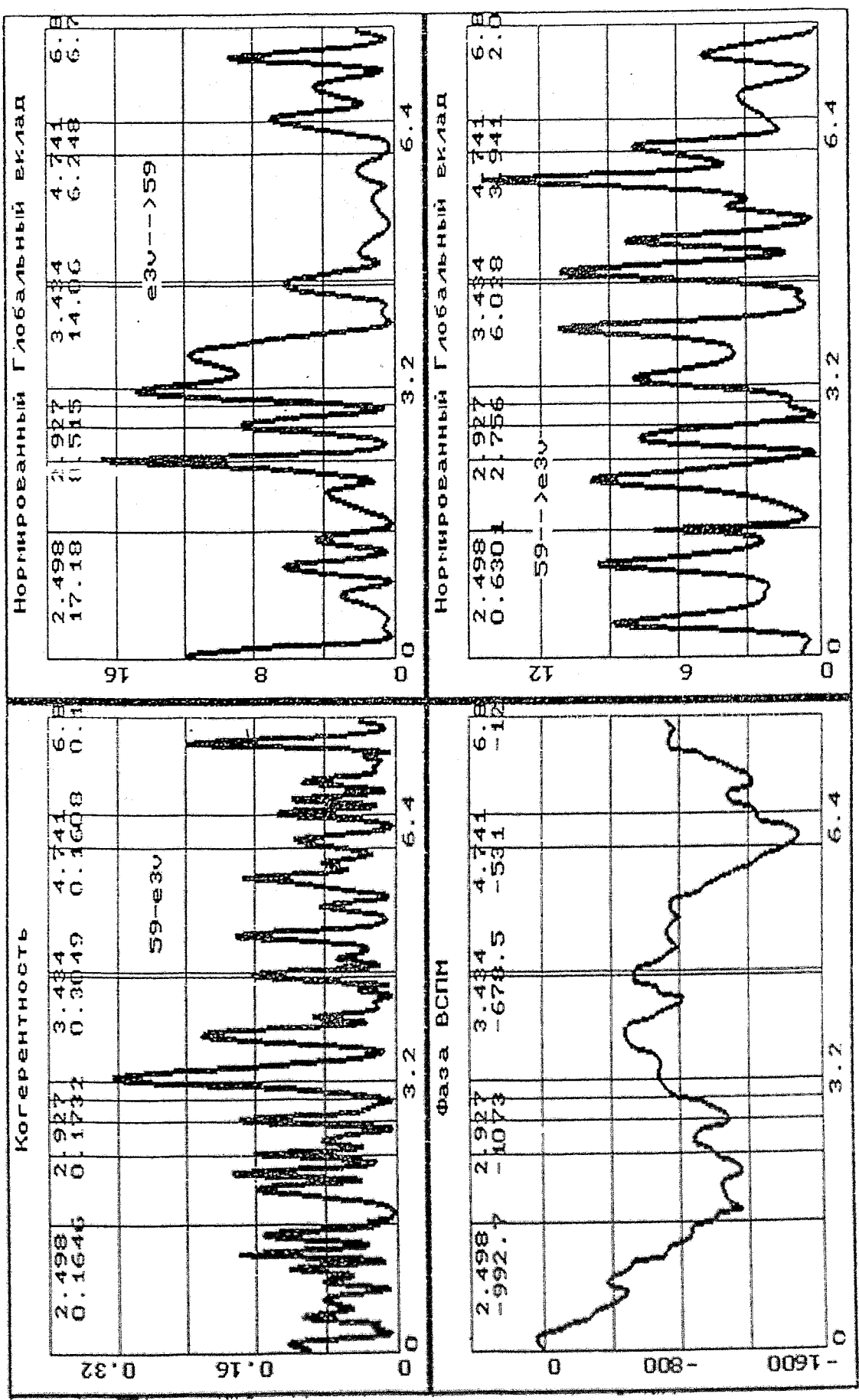


Fig. 20

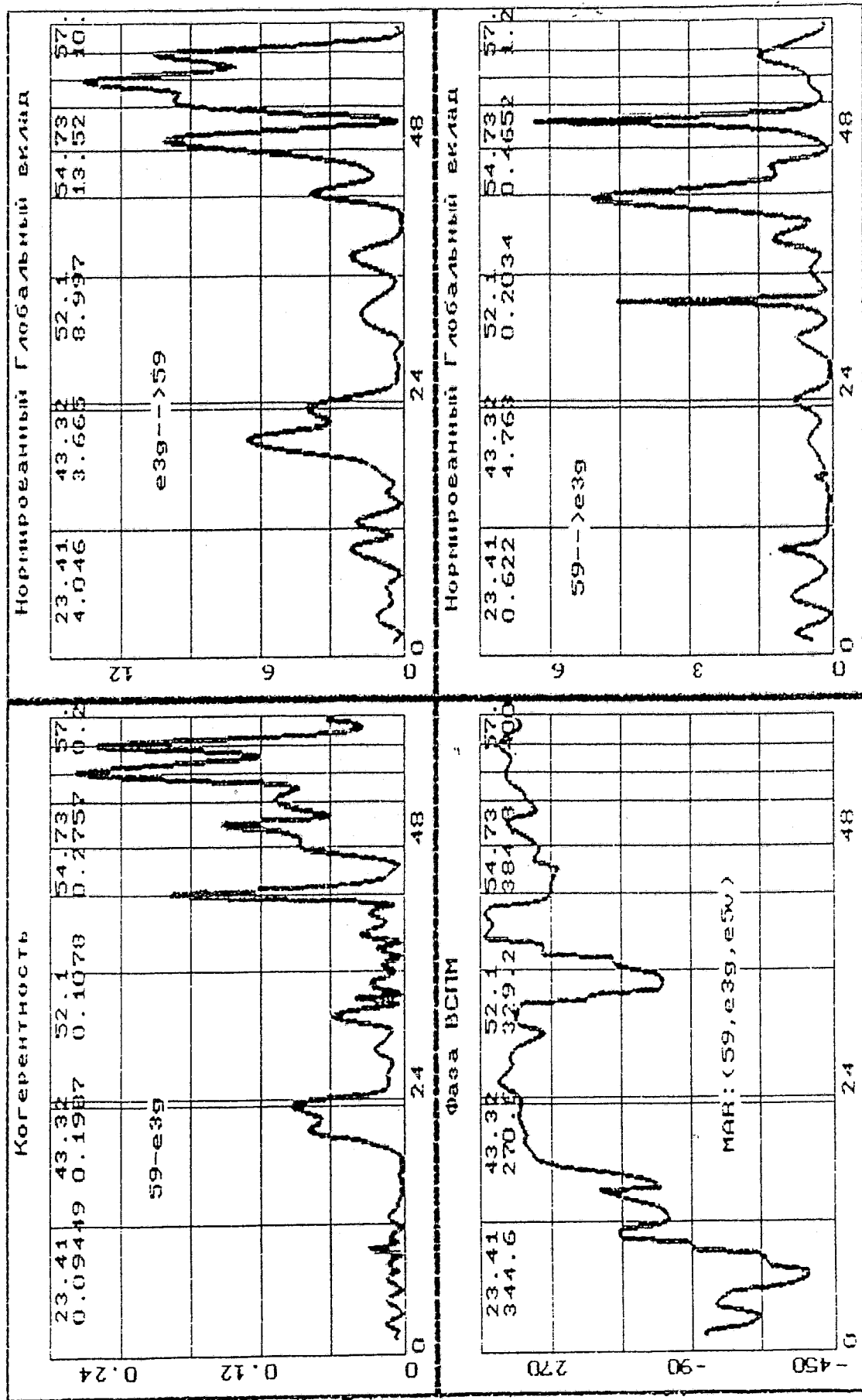


Fig. 21

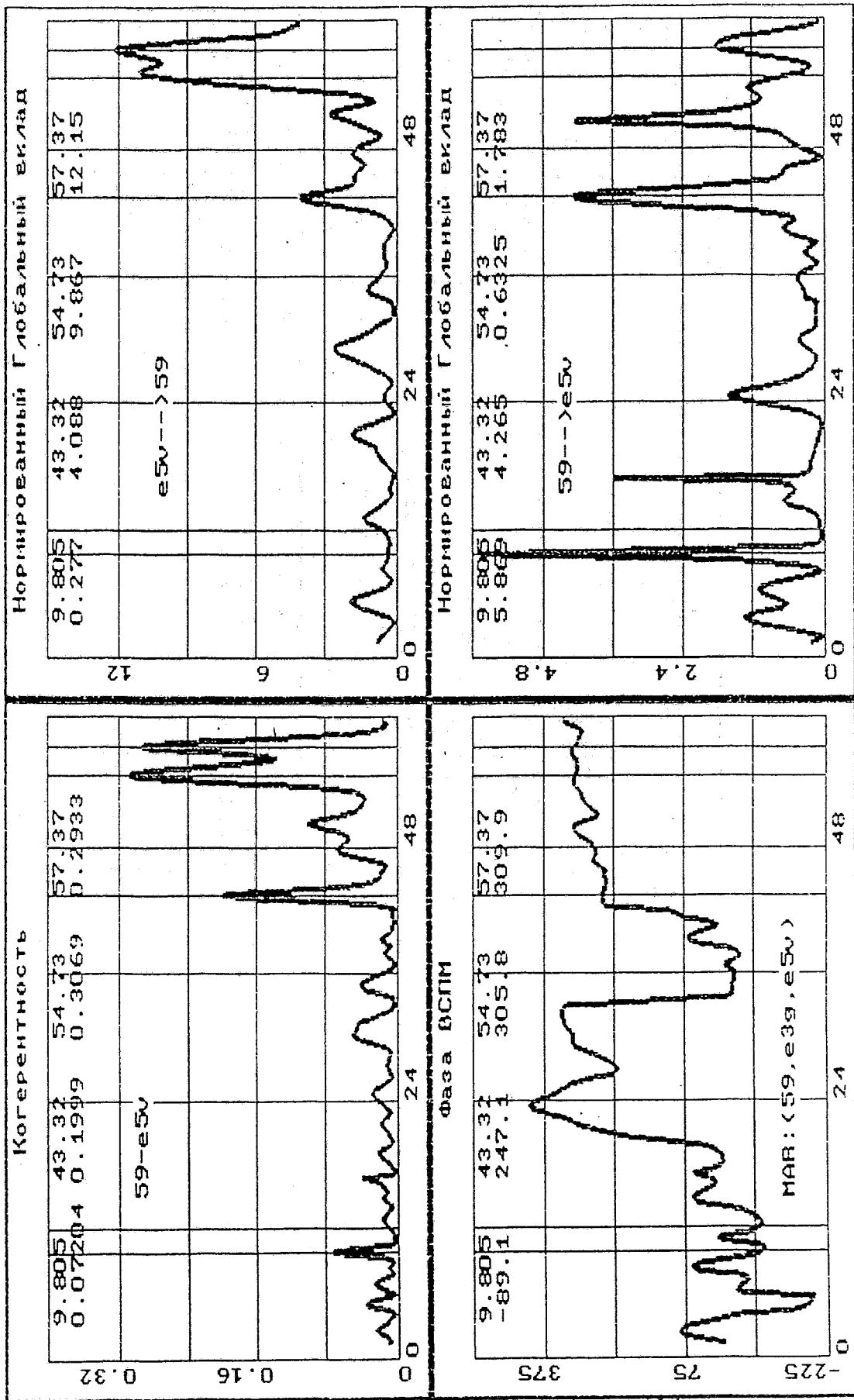


Fig. 22

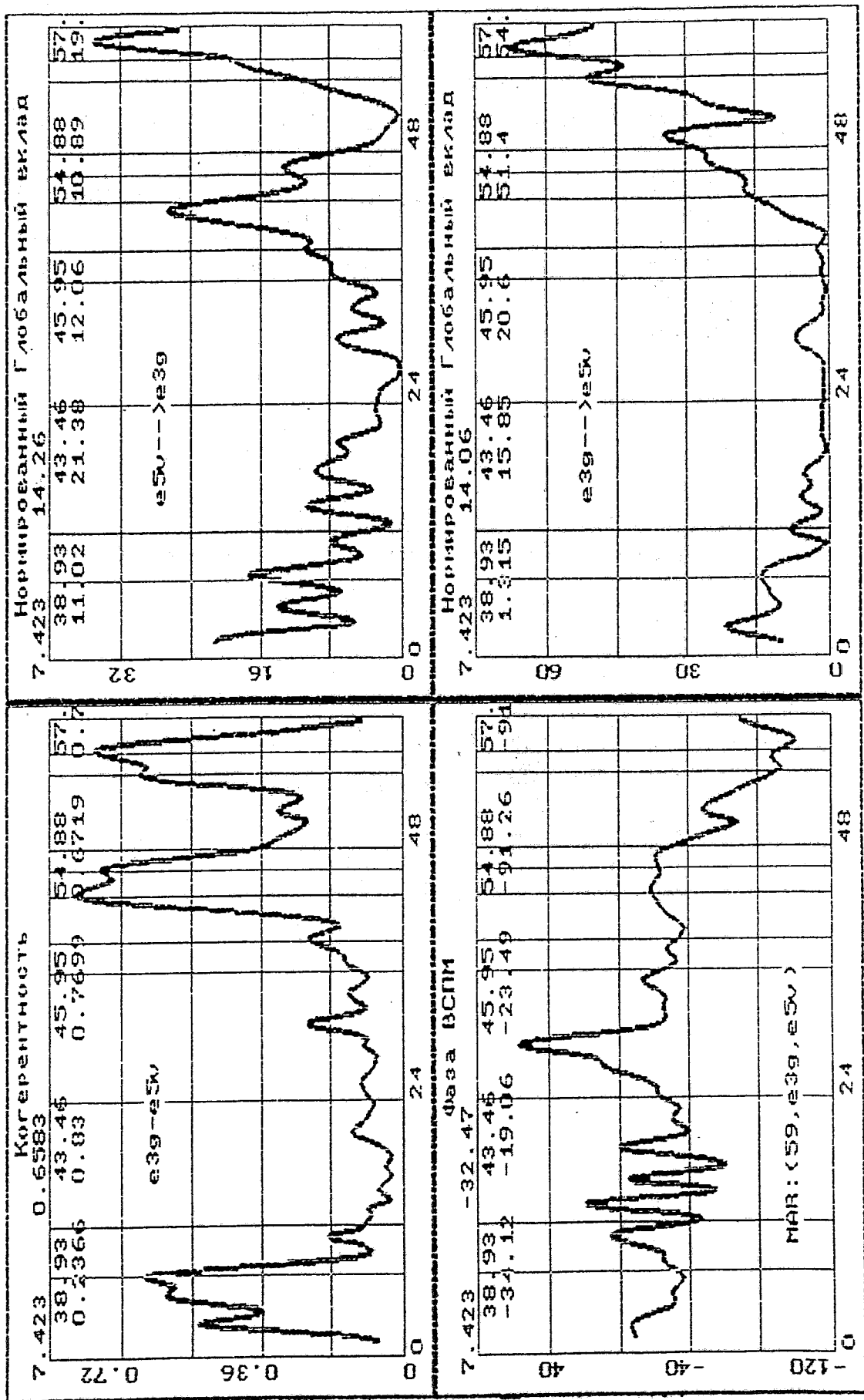


Fig. 23

spatially carried, the important factor of a correctness of model has appeared an incongruity of directions of tenzoaccelerometer sensitivity. On each of the represented graphs in upper numerical line frequencies of resonances and in the following numerical line value of the appropriate function on these frequencies are given.

In a low-frequency range correct there was the model (PFT 59, e1 (1), e3v), where the deviding under the primary sources happens on directions of tenzoaccelerometer sensitivity installed only on fuel assembly (fig. 24, 25, 26).

In the following tables on two mentioned above three-dimensional MAR-models the every possible normalized global contributions (in %) on frequencies of dominating resonances are represented. The primary source of that or other resonance is discovered on their maximum value.

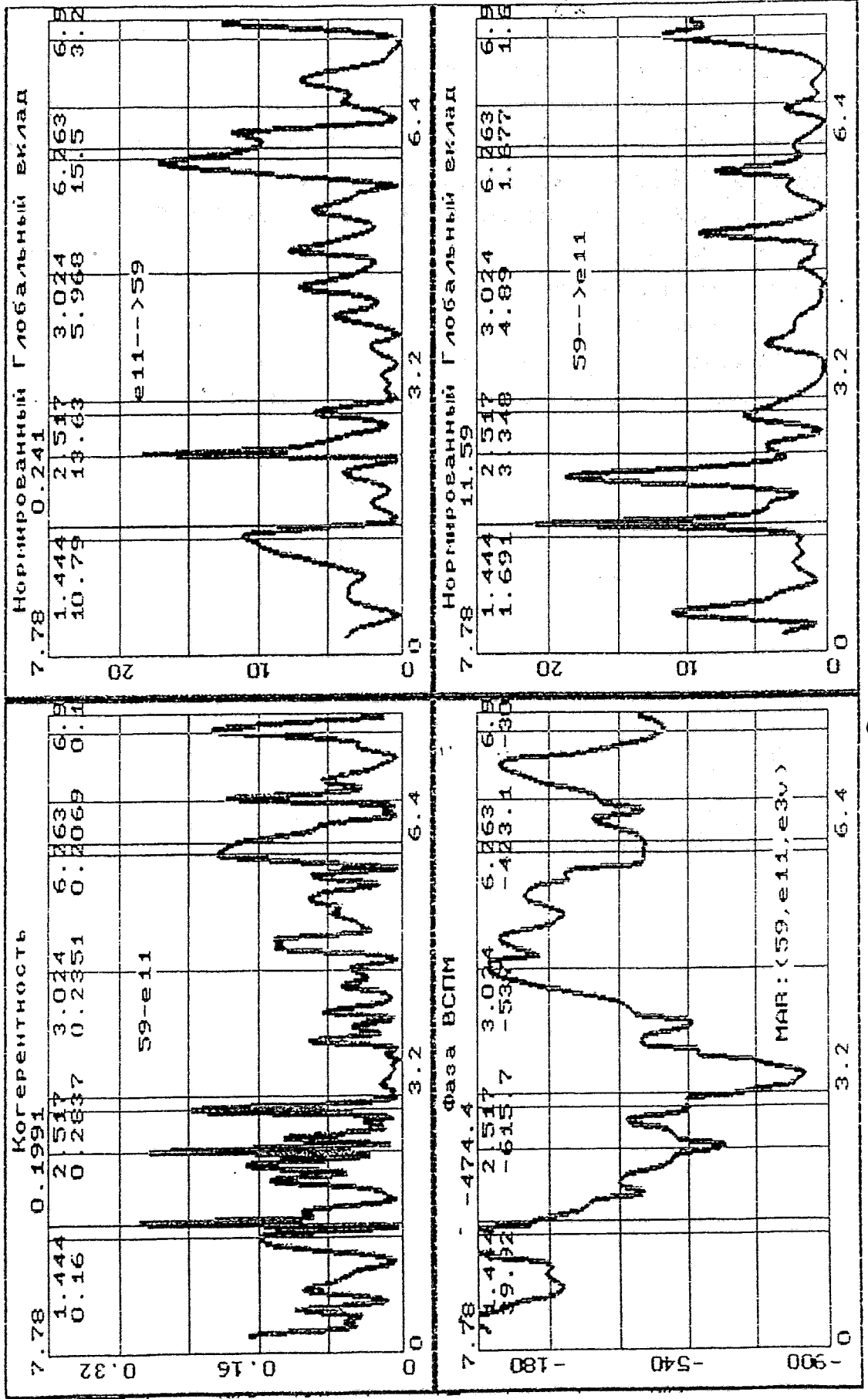


Fig.24

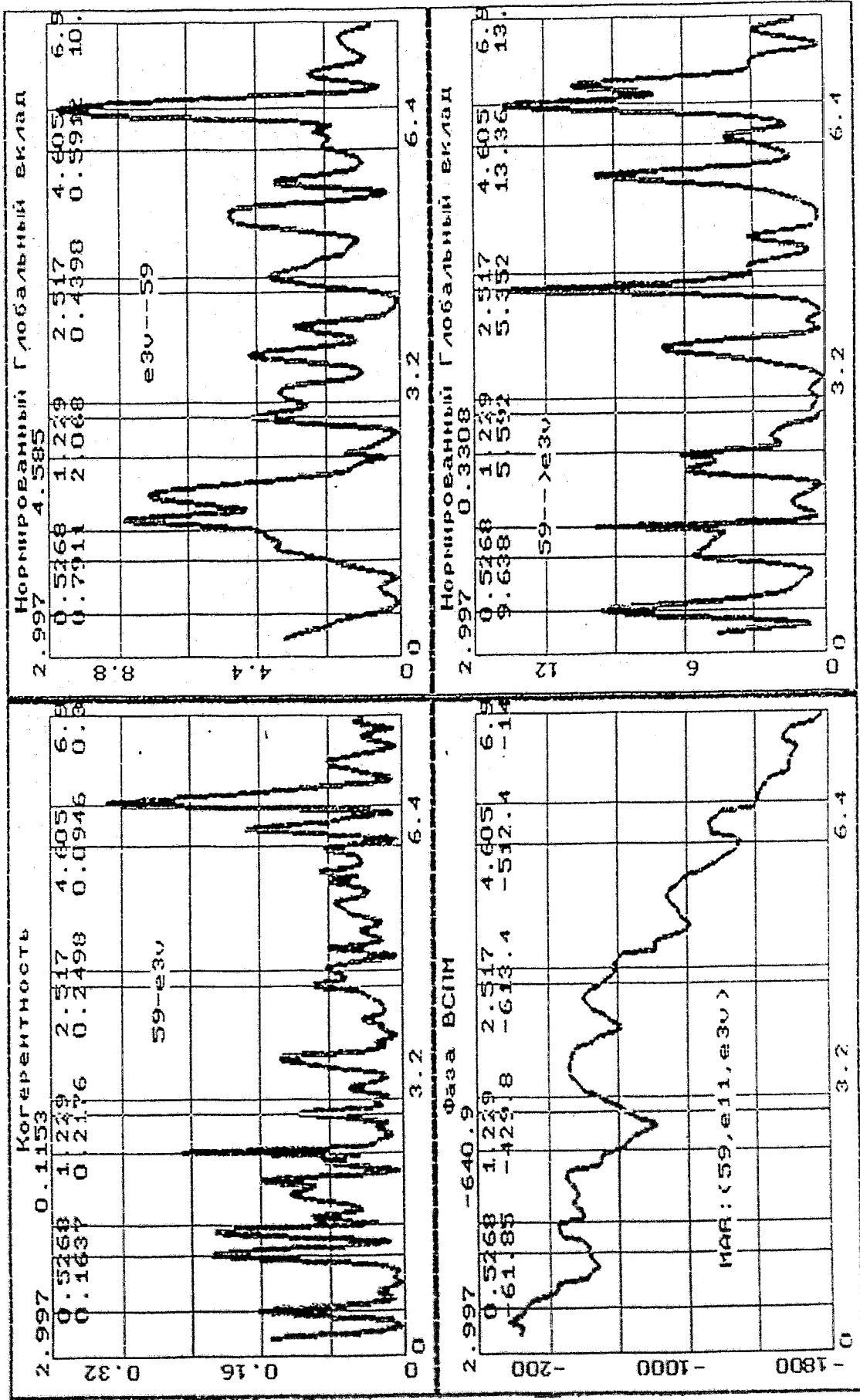


Fig. 25

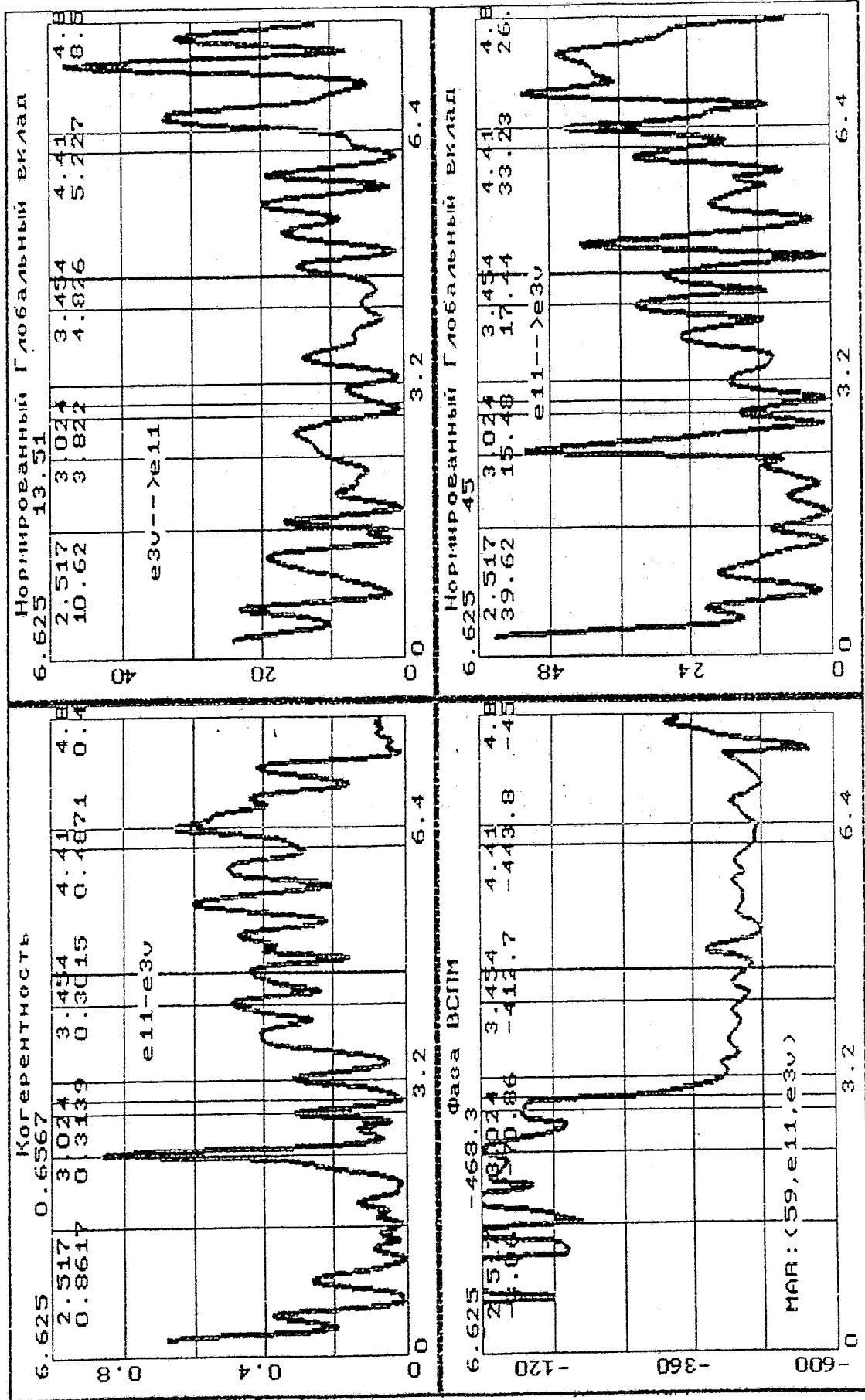


Fig.26

Table 3

Frequency of a resonance [Hz]	9.81	16.6	21.0	33.2	38.9	43.3	45.9	49.8	52.1	54.7	57.6
The mutual contribution [of %]											
E3g --- > 59	-	-	4.1	0	-	3.7	-	0	9.0	13.5	10.0
59 --- > e3g	-	-	0.6	4.5	-	4.8	-	6.5	0.2	0.5	1.2
E5v --- > 59	0.3	0	-	-	-	4.1	-	-	-	9.9	12.1
59 --- > e5v	5.7	3.0	-	-	-	4.3	-	3.5	-	0.6	1.8
E5v --- > e3g	-	-	7.0	-	11.0	21.4	12.1	-	-	10.9	19.0
E3g --- > e5v	-	-	0	-	1.3	15.9	20.6	-	-	51.4	54.0
The primary source	ASW	MCP	Core barrel	MCP	Core barrel	Core barrel	fuel ssemblies (FA)	MCP	FA	FA	FA

Table 4

Frequency of a resonance [Hz]	0.53	1.4	1.6	2.5	3.4	4.4	4.8	6.2	6.9	7.8
The mutual contribution [of %]										
E11 --- > 59	-	10.8	5.0	13.6	6.0	-	-	15.5	3.2	0.2
59 --- > e11	-	1.7	22.0	3.3	4.9	-	-	1.7	1.6	11.6
E3v --- > 59	0.8	2.1	4.0	0.4	-	0.6	-	-	10.0	-
59 --- > e3v	9.6	5.6	10.0	5.3	-	13.4	-	-	13.0	-
E5v --- > e11	-	-	-	10.6	4.8	5.2	8.5	-	13.5	-
E11 --- > e5v	-	-	-	39.6	17.4	33.2	26.0	-	45.0	-
The primary source	Pressurizer	Bottom FA	PFT	Bottom FA	Bottom FA	Bottom FA	Bottom FA	Bottom FA	Bottom FA	ASW-1

In each tables column maximum values of the normalized global contributions are selected by bold font. It is possible to make the following conclusions on them:

- Collective forced vibrations of fuel assemblies and the core barrel happen on frequencies pressurizeer (0.53 Hz), ASW-1 (7.8 Hz), ASW-2 (9.81 Hz) and MCP (16.6ГЦ, 33.2 Hz, 49.8 Hz),
- Collective vibrations of fuel assemblies and core barrel happen on own frequencies of vibrations of core barrel (21.0 Hz, 38.9 Hz, 43.3 Hz),
- Collective vibrations of fuel assemblies and core barrel happen on frequencies, identified with fuel assemblies (2.5 Hz, 3.4 Hz, 4.4 Hz, 4.8 Hz, 6.2 Hz, 45.9 Hz, 52.1 Hz, 54.7 Hz, 57.6 Hz). Among them the resonance on frequency of 2.5 Hz is a base frequency (first harmonics) of fuel assemblies vibrations. This resonance was observed and under operation conditions on neutron noise in experiments on the Kalinin NPP Unit 1 (see also the report for the previous stage). Four high-frequency resonances in region of 50 Hz are close on the value to own frequency of fuel assembly vibrations.

For interpretation of resonances on frequencies in range (4 - 8) Hz we shall consider harmonic and subharmonic rows of resonances of various functions of coherence at high spectral precession. In the tables on fig. 27 obtained automatically at processing of resonances of any spectral functions, harmoniceses and subharmoniceses for coherence of signals e1 (2) - e3g are represented. It is possible to make the following rows on them:

Number of MCP back frequency

Number of a harmonics or subharmonics	1/4	3/4	1	4/3	3/2	2	3
Frequency of resonance [Hz]	4.188	12.44	16.88	22.44	25.06	34.00	50.12

Number of the first harmonics of fuel assemblies vibrations:

Number of a harmonics or subharmonics	1	3/2	2	3
Frequency of resonance [Hz]	2.438	3.688	4.875	7.322

The subharmonic rows are already interpreted by us on results of experiments at Kalinin NPP (see the previous report), here we shall mark, that resonances of 3.6 Hz, 4.2 Hz, 4.8 Hz, 7.3 Hz, observable in spectral characteristics of tenzoaccelerometers signals installed on fuel assemblies are corollary only of two resonances - resonance on MCP circle frequency and resonance of the first mode of fuel assemblies oscillations.

	Fu	2	3	4	5
0.8125	0.8125		2.438		
2.438	2.438	4.875	7.312		
3.688	3.688			19.38	28.81
4.875	4.875	11.62			34
5.812	5.812	13.5		27.19	36.44
6.75	6.75				41.25
7.312	7.312			32.88	51
8.188	8.188		30.81		54.31
10.19	10.19		32.88	43.5	57.56
10.88	10.88		34.69	46.75	
11.62	11.62		37.25	50.12	
12.44	12.44	25.06	40.19	54.31	
13.5	13.5	27.19	46.75	62.94	
15.69	15.69	31.56	50.12		
16.88	16.88	34	52.94		
17.75	17.75	35.62	56.19		
18.75	18.75	37.25	57.56		
19.38	19.38	38.62	62.94		
21	21	42.19			
22.44	22.44	44.44			
23.75	23.75	47.62			
25.06	25.06	50.12			
26.5	26.5	52.94			
27.19	27.19	54.31			
28.19	28.19	56.19			
28.81	28.81	57.56			
29.56	29.56	59.44			
30.12	30.12	60.62			
30.81	30.81	61.38			
31.56	31.56	62.94			
32.19					
32.88					
34					
34.69	a12-e3g				
35.62	(1-8)				
36.44					
37.25					
38.62					
39.5					
40.19					
41.25					
42.19					
43.5					
44.44					
45.94					
46.75					

	Fu	4/3	3/2	8/3	6/2
0.8125	0.8125		3.600		2.438
2.438	2.438		7.312		7.312
3.688	3.688	4.875			
4.875	4.875		10.19		
6.75	6.75		10.88	19.38	
7.312	7.312				
8.188	8.188	10.88		27.19	30.81
10.19	10.19	13.5		28.81	32.88
10.88	10.88			30.81	34.69
11.62	11.62			32.88	37.25
12.44	12.44		18.75	32.88	40.19
13.5	13.5			42.19	46.75
15.69	15.69	21	23.75		50.12
16.88	16.88	22.44	25.06	47.62	52.94
17.75	17.75	23.75	26.5	50.12	56.19
18.75	18.75	25.06	28.19	51.88	57.56
19.38	19.38		28.81	56.19	62.94
21	21	28.19	31.56	56.19	
22.44	22.44	30.12		59.44	
23.75	23.75	31.56	35.62	62.94	
25.06	25.06		37.25		
26.5	26.5	35.62	39.5		
27.19	27.19	36.44			
28.19	28.19	37.25	42.19		
28.81	28.81	38.62	43.5		
29.56	29.56	39.5	44.44		
30.12	30.12	40.19			
30.81	30.81	41.25	45.94		
31.56	31.56	42.19	47.62		
32.88	32.88	43.5	49.25		
34	34		51		
34.69	34.69	45.94	51.88		
35.62	35.62	47.62	52.94		
36.44	36.44		54.31		
37.25	37.25	49.25	56.19		
38.62	38.62	51	57.56		
39.5	39.5	52.94	59.44		
40.19	40.19		60.62		
41.25	41.25	55	61.38		a12-e3v
42.19	42.19	56.19	62.94		
43.5	43.5	57.56			
44.44	44.44	59.44			
45.94	45.94	61.38			
46.75	46.75	62.94			
47.62	47.62	62.94			

Fig. 27

3. Common oscillations of core barrel (CB) and shells of the upper supporting structure

The consideration about of core barrel vibrations, as population of free oscillations of a thin cylindrical shell on eigenfrequencies, is a rather rough model. The exterior cylindrical surface of core barrel in three horizontal planes with various degrees of a rigidity is connected to an interior surface of RPV by means of upper and lower dowels serieses and separating ring. On an interior surface the free vibrations of core barrel are limited in four horizontal planes: two dowels serieses of upper supporting structure (USS), dowels series for neutron shield of CB and lower supporting ring for same neutron shield. The rigidity of interior dowel connections is in many respects determined by a vertical pressing force of USS. Enumerated seven horizontal planes, obviously, superimpose serious restrictions on a possibility of appearance of the lowest modes of radial oscillations of core barrel. On the other hand, the fact of appearance of a lowest shell modes of oscillations of core barrel and, in particular, of the pendulum modes of oscillations, the growth of their amplitude in operation conditions gives evidence the process of a wear out of dowel connections or decreasing of pressing force of USS, that is the important diagnostic indication.

The core barrel and USS shell with respect to each other are demountable coaxial structures. The rigidity of their connection is ensured by two horizontal serieses of dowels and by a vertical pressing force from USS. A wear out of these dowels or insufficient pressing force - two factors, which can lead to specific modes of oscillations of USS shell on eigenfrequencies, independent from core barrel.

In diagnostic applications at a stage of adjustment it is important to define, which modes of vibrations internals were really realized in the nominal operation conditions PP to receive a priori informations for vibromonitoring during nominal maintenance.

The resonances appropriate to vibrations of core barrel and USS shell on eigenfrequencies are not dominating in PSD. They are masked both other resonances phenomena (MCP harmonics, ASW, pressurizer), and by hydrodynamic noise with nonresonance character. The maximum amplitudes of nonresonance noise of vibro transmitters signals, installed on internals, are observed in a low-frequency range (0 - 8) Hz. So especially unfavorable conditions of selection of eigenfrequencies exist for the lowest modes of internals oscillations. Moreover the intensity of masking phenomena, as already shown above, depends essentially on number of working MCPs. For example, on cold try when MCP work under the scheme [+ ---] (fig.28) spectral components of range [10 - 20] Hz of transmitter 7p signal are minimal in comparison with other schemes of MCP turning on (transmitter 7p is located exactly between cold legs of 2-nd and 3-d loops). Resonance structure of PSD is sharply improved with the inclusion of third MCP (see the same fig.28). The bottom of core barrel is subject of influence from the schemes of MCP turning on to a smaller degree: on fig.29 in the same conditions PSD of transmitter 3p,

Lg Y

Авто-Спектр 7p

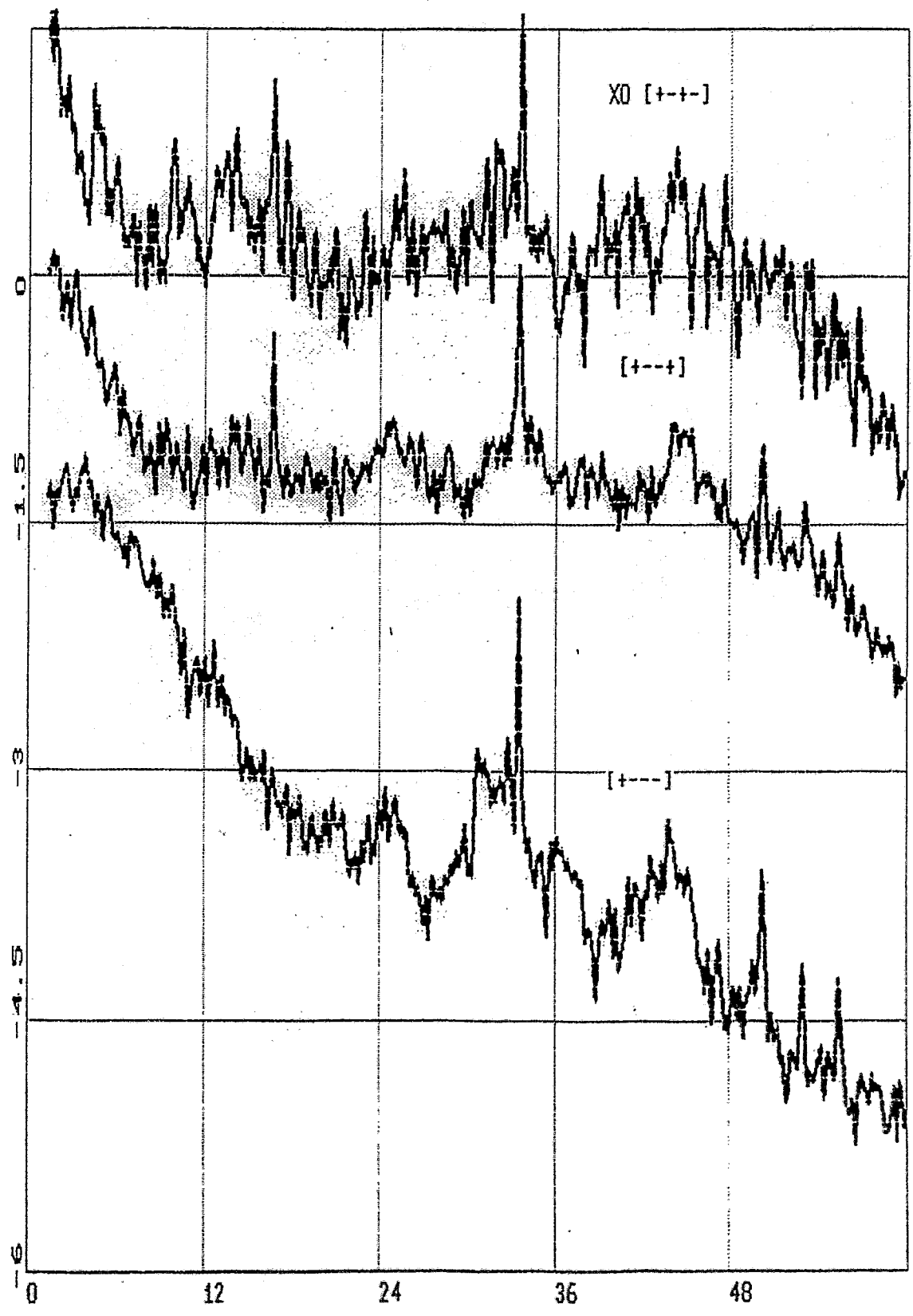


Fig. 28

Lg Y

Авто-Спектр 3p

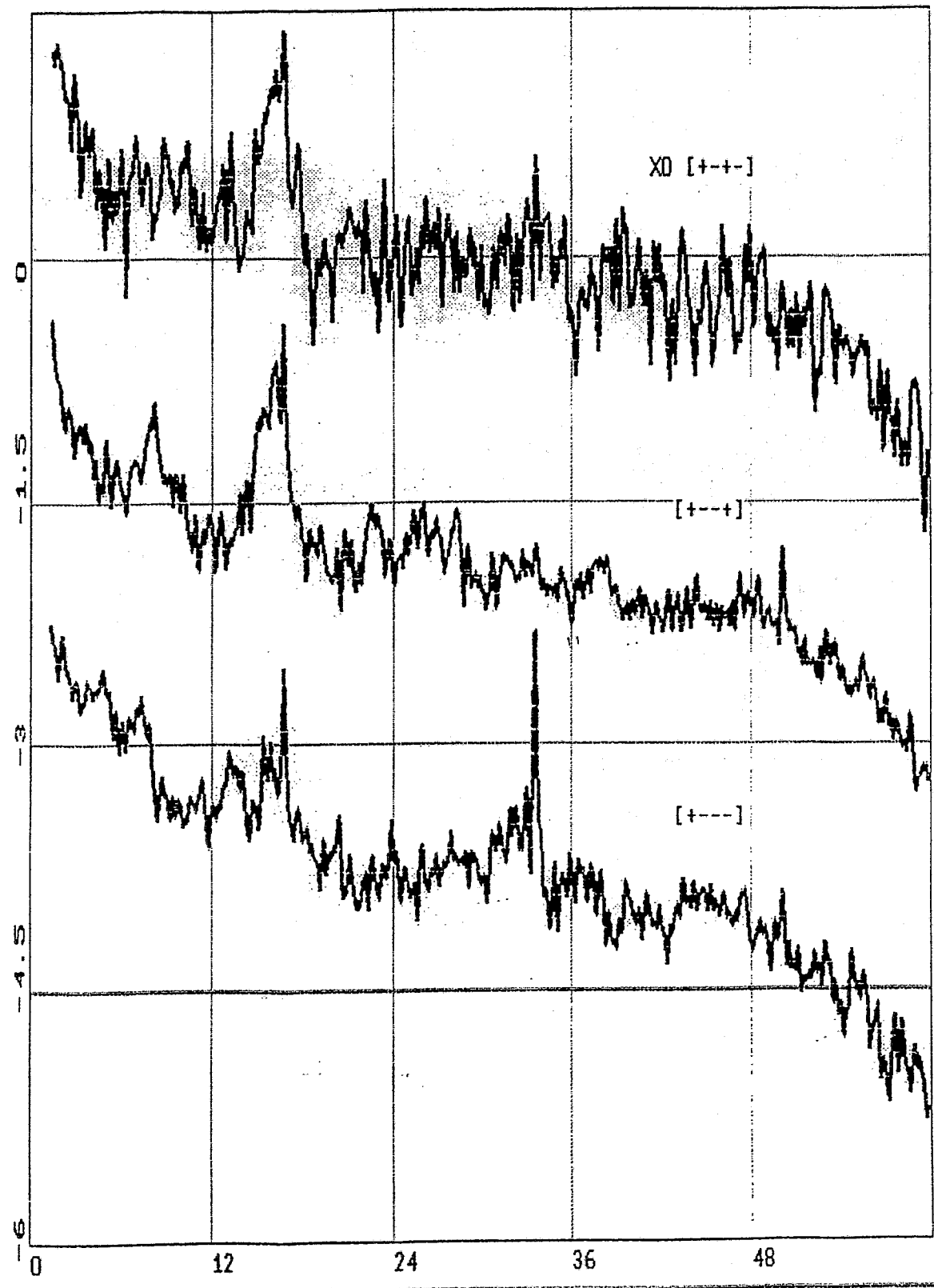


Fig.29

located exactly under transmitter 7p are represented. Thus masking of own modes of core barrel oscillations is the phenomenon depending on frequency, has variable in space character and is function of working MCPs number.

In spectra of tensio-resistors signals (the fig.30), installed directly on USS shell (transmitters 19p, 20k, 10p, 11k, 11p), only one resonance on frequency of 2.5 Hz is selected, which does not coincide with frequencies of driving forces and we already interpreted it as eigenfrequency of fuel assemblies vibrations.

The masking of internals vibrations on eigenfrequencies has also correlated character. On fig. 31 functions of a coherence for the same pair of signals 1k-4k on cold and hot try represented at different temperatures of coolant and with different number of working MCPs. It follows, that steady reproduced from a condition to a condition picture of internals vibrations does not exist. That is the mutual performances, excepting uncorrelated noise components, nevertheless leave a set of other correlated radiants. It follows, that phase characteristics of tensio-resistors signals have the same changeability that so modal analysis of every possible pairs of tensio-resistors signals, installed on internals, will be inconvenient. Really, if only anti-phase components (designated by arrows on the graphs and table at the fig. 32 bottom) are selected for a pair of signals 3p-7p, then, at first, they have a low coherence and, secondly, the phase portraits are not reproduced from a condition to a condition. Note that the pair of signals 3p-7p is located on vertical forming of the cylinder and is the most sensitive to lowest pendulum modes of oscillations of core barrel.

The presence of not absolutely rigid, probably with gaps, dowel limiters of free internals oscillations can transform the lowest form of oscillations in higher. It's easier to show it on an example of forced oscillations of core barrel on ASW-2 frequency. As showed higher, in any point inside RPV of this acoustic standing wave has anti-node, that in the idealized suppositions should lead to the lowest form of oscillations, represented on fig.33. However dowel limiters can "impose" the own nodes and create semblance of a higher mode of oscillations (fig.34).

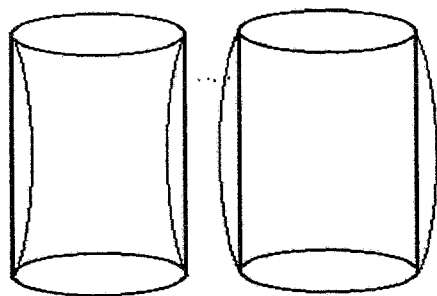


Fig. 33

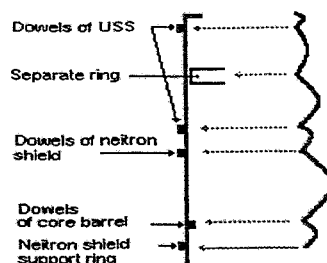


Fig. 34

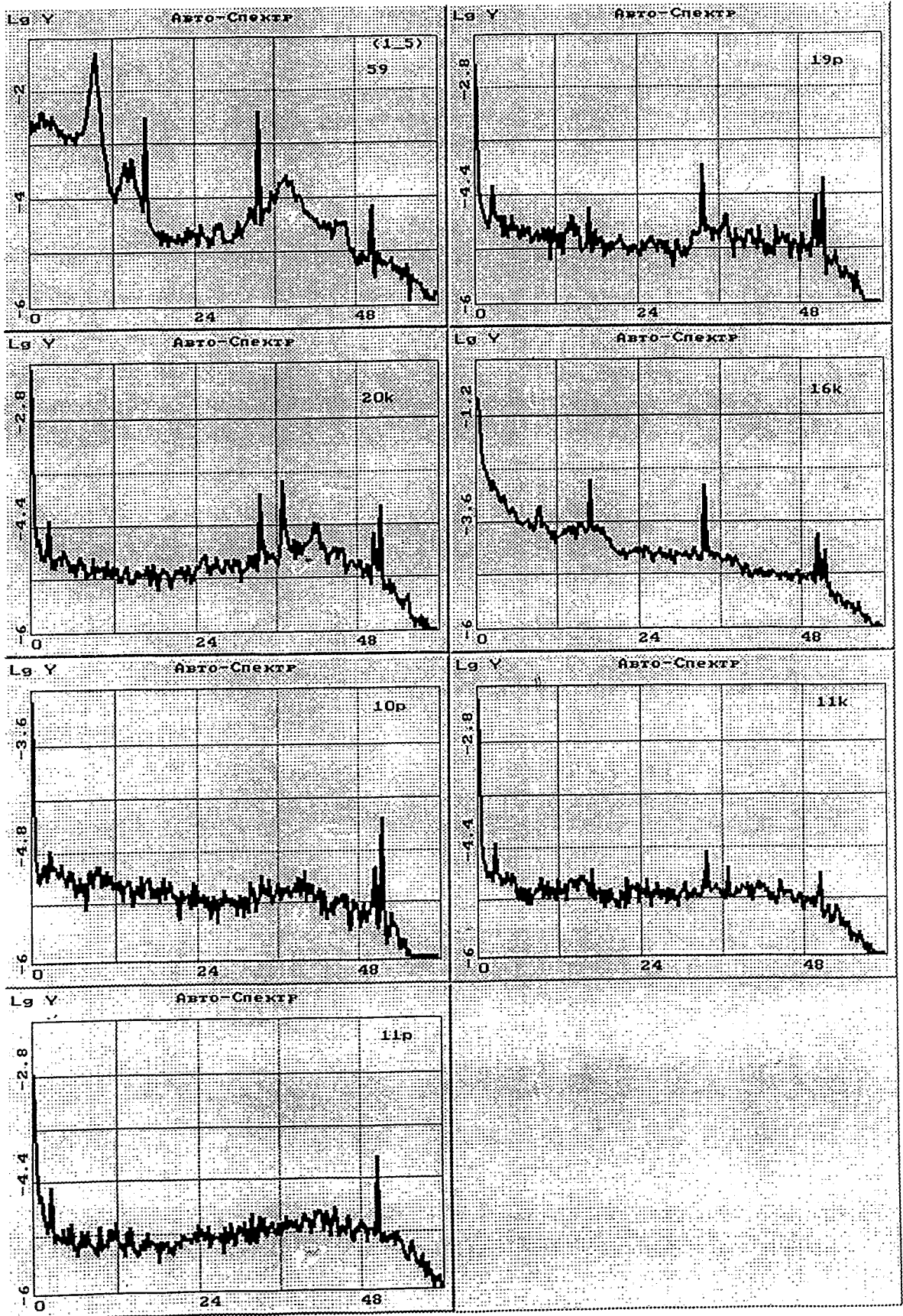


Fig. 30

Когерентность 1к-4к

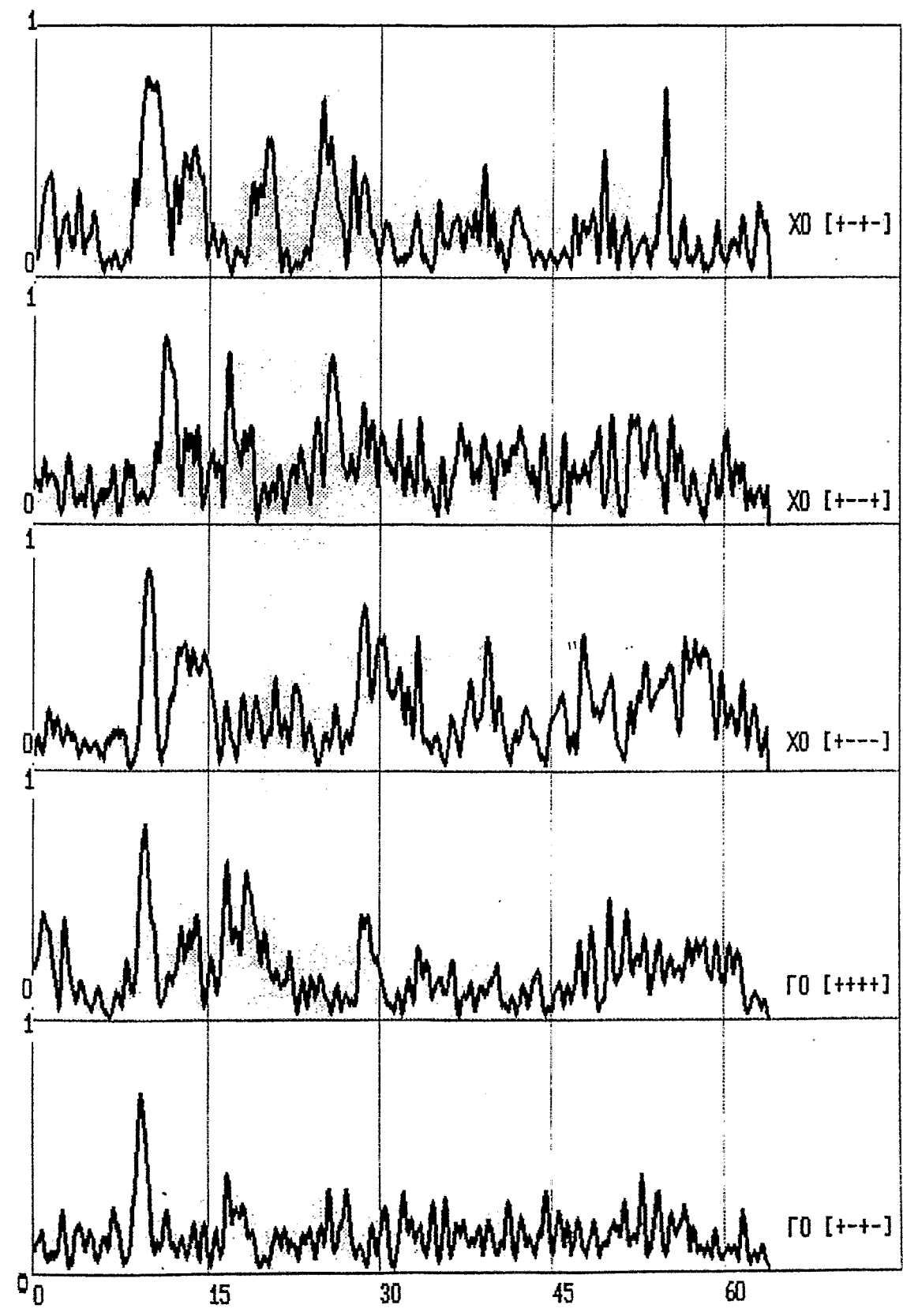
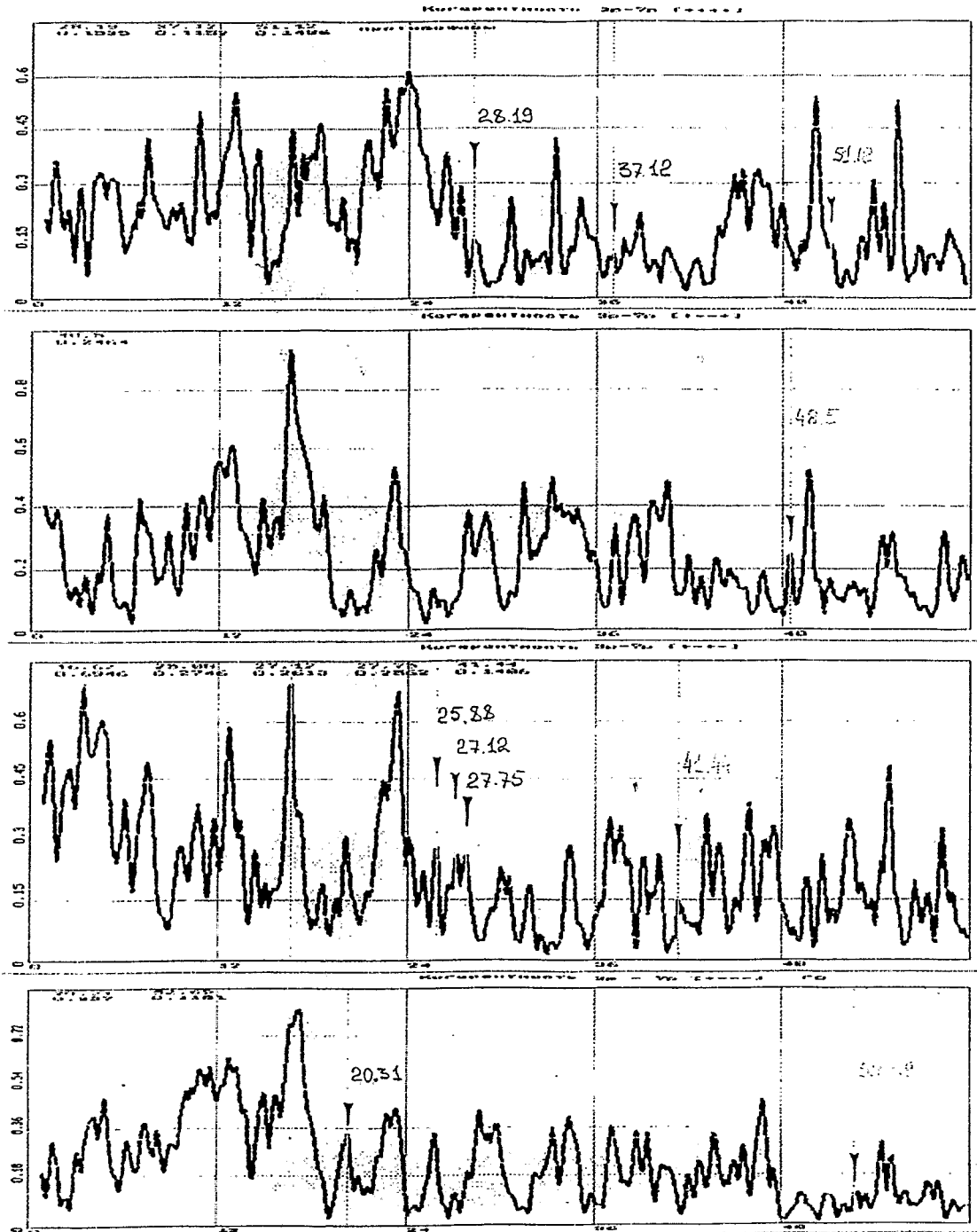


Fig.3i



16.62	22549	25416	17674
20.331	34288	69386	317639
25.98	32288	30555	13333
27.12	33032	21531	33333
27.75	42833	30433	33333
28.19	35533	29333	33333
37.12	34833	33333	33333
41.44	34533	33333	33333
48.5	24233	54833	20233
51.12	20433	32633	31833
52.69	22633	33533	34753
61.19	12503	45733	78233
63.44	54733	42733	36433

Fig. 32

On last figure exaggerated form of core barrel vibrations in one of extreme conditions on frequency ASW-2 is represented. That is instead of the "barrel-type" form it has gained a rather complicated aspect, which can be erroneously interpreted, as the higher mode of oscillations.

To avoid it a priori knowledge about frequencies of various oscillations modes of core barrel, obtained by model calculations and bench experiments is necessary. It will allow purposefully to discover them in experiments data. From fig32. follows that as realized modes of core barrel vibrations it is possible to consider resonances from frequency bands 20.0 - 22.0 Hz, 37.0 - 39 Hz, 48 - 52 Hz.

Limited possibilities of the modal analysis for identification of the oscillations forms of core barrel are expediently to supplement with the MAR-analysis. In a model (pressure fluctuation sensor, tensio-resistors on the core barrel, tensio-resistors on USS shell) = (59, 16к, 11p) low-frequency resonances hardly interpreted on phase portraits are well divided on primary sources. According to the graphs on fig. 35, 36, 37 following table of the normalized global contributions of all possible signals in each other is built.

Thus the following membership of resonances was identified:

USS: 2.50, 3.69, 5.52, 6.50 Hz

Core barrel: 4.51 Hz

Pressure fluctuation sensor (oscillations transmitted from the outside by coolant): 2.38, 3.08, 3.90, 5.00 Hz.

All frequencies, referred to USS, are already interpreted by us, as frequencies, arising from vibrations of fuel assemblies. So the expansion of fuel assemblies vibrations on core barrel happens mainly through USS shell, instead of through coolant. It, in particular, testifies that all connections on a path of distribution of vibrations fuel assembly to core barrel (tail of fuel assembly - USS, dowels of USS - the core barrel) represent rather rigid constructions. Eigenfrequencies of USS shell vibrations in a low-frequency range are not observed. The resonance at the frequency 4.51 Hz with low coherence, referred to core barrel - the lowest mode of core barrel oscillations (pendulum oscillation) - was observed on neutron noise in experiment on Kalinin NPP (see the report on the previous section).

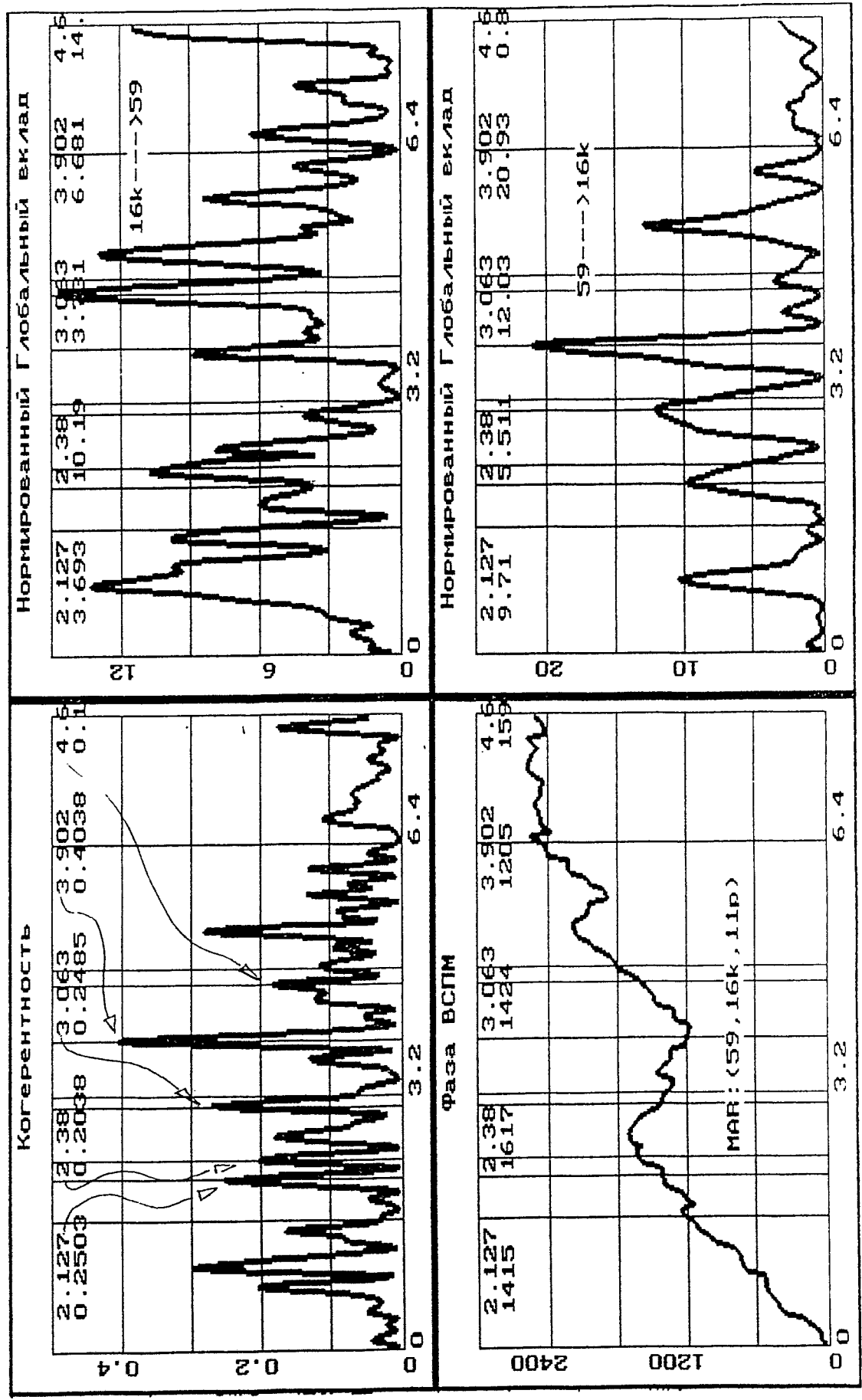
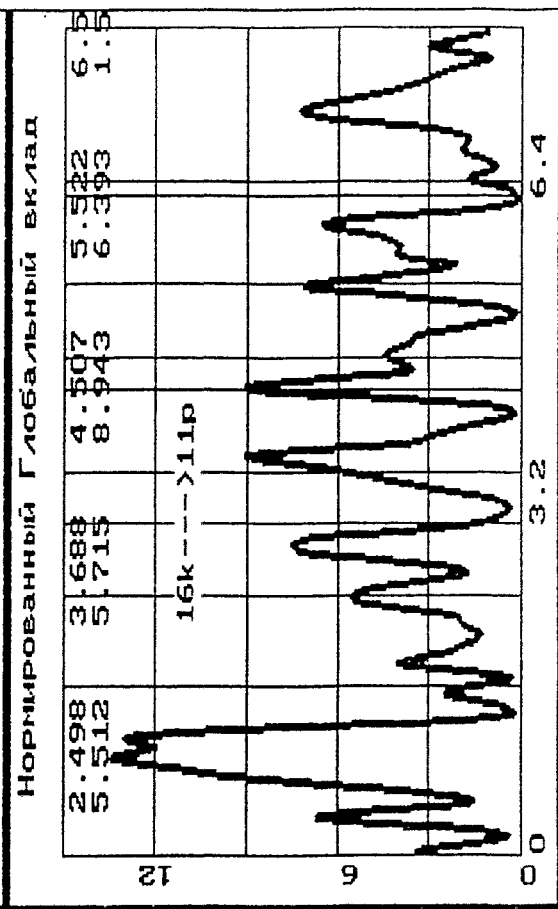
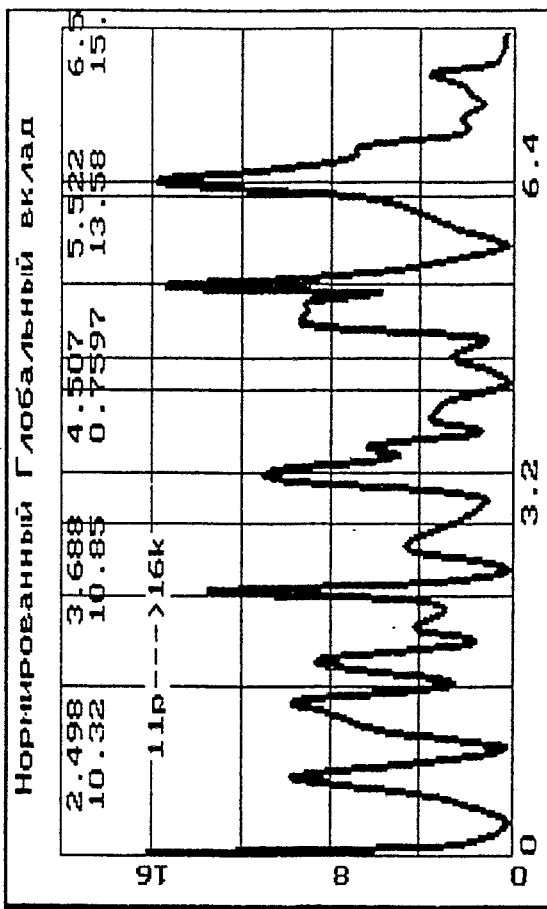
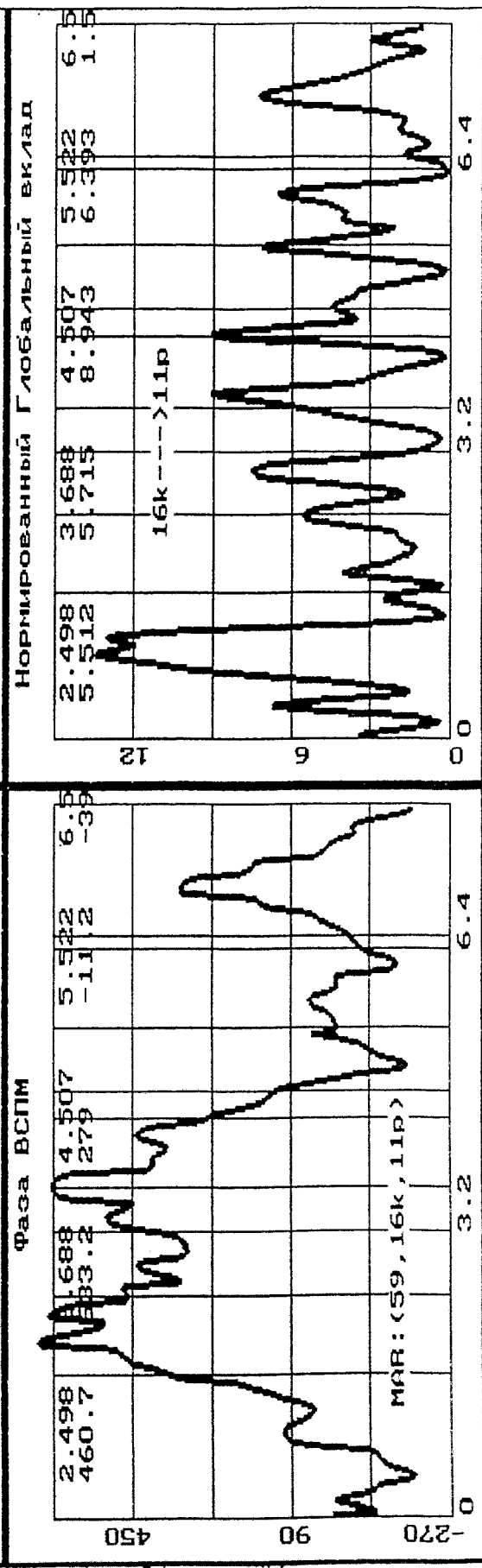
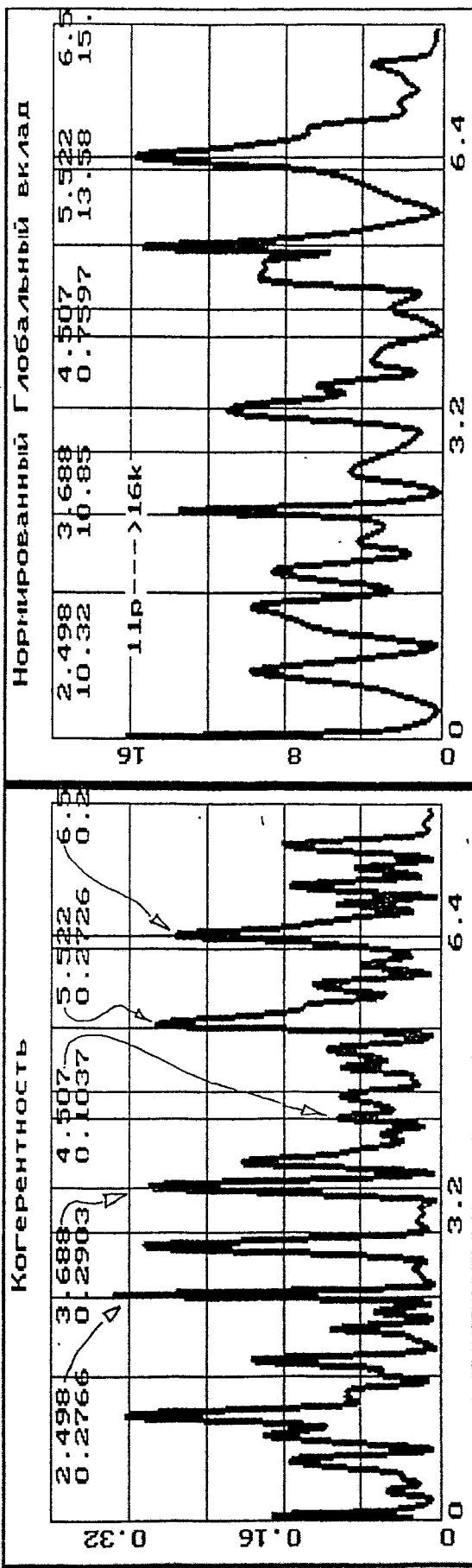


Fig. 3.5



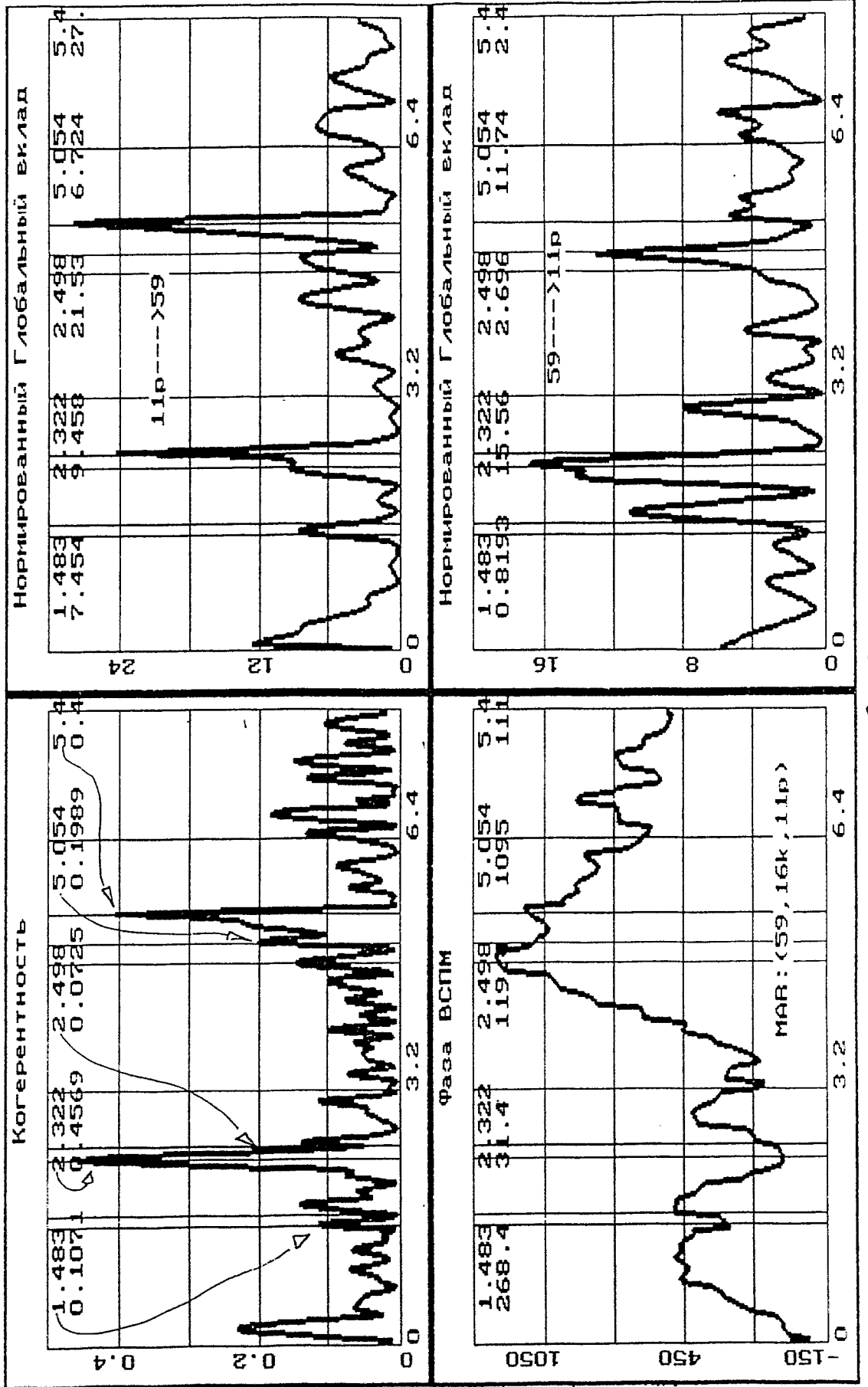


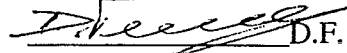
Fig. 37

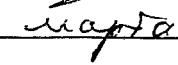
Teil 4

APPROVED

Director General of Diagnostic

Center "DIAPROM"

 D.F. Gutsev

" 27"  1996 г.

VIBRATION MODELLING of VVER TYPE REACTORS

**The analysis of the design characteristics and
experimental data for
adjustment of the VVER-1000 model**

**The intermediate report
320-O.211-004**

Part 3

1996

CONTENT

1.1	Summary.....	1
1.2	Key words.....	2
1.3	Introduction.....	2
1.4	Conditions of pressure fluctuation and neutron noise measurements on the Kalinin NPP Unit 1.....	3
1.5	The analysis of PFT signals noise.....	5
1.5.1	ASW form on frequency 6.2 Hz.....	10
1.5.2	ASW forms on frequencies ~ 13,0 Hz and ~ 18,8 Hz.....	15
1.5.3	The ASW form on Frequency ~ 8,8 Hz.....	17
1.6	The analysis of incore and excore neutron detectors signals noise spectra.....	19
1.6.1	Analysis of phase characteristics of neutron detectors signals on frequency of 9.0 Hz.....	24
1.6.2	Analysis of phase characteristic of neutron detectors signals on frequencies of ~ 6.0 Hz, ~ 13.0 Hz, ~ 19,0 Hz.....	33

Some results of pressure oscillations, incore and excore of neutron noises investigations on reactor plant VVER-1000 of the Kalinin NPP unit 1

1.1 Summary

In this section of the report some results of investigations of pressure fluctuations in the coolant of primary coolant circuit (PCC) VVER-1000 and noises of neutron flux inside core barrel and outside reactor pressure vessel, which were measured on the Kalinin NPP unit 1 (KalNPP), are represented.

The noise analysis of signals of three pressure oscillations transmitters, installed in pipelines of two PCC adjacent loops, allowed to clarify physical nature of resonant peaks with significant amplitude in spectra of indicated signals on frequencies ~ 6.0 Hz, 13.0 Hz, 18.6 Hz and ~ 8.8 Hz. It was shown, that these peaks are stipulated by acoustic standing waves (ASW), excited in the coolant of whole PCC and appropriate to four minimum eigenfrequencies of pressure oscillations in whole PCC. The analysis of experimental results, based on ASW properties, and also on identity of all four circulating loops and symmetry of their arrangement with respect to reactor pressure vessel (RPV) enabled with sufficient completeness to determine the forms of these standing waves (space distribution of amplitude and phase pattern of all four ASWs) in whole PCC volume and three-dimensional space structure of their nodes and antinodes inside RPV (inside core) and outside it. Simultaneously PCC geometric features, causing shaping of mentioned ASWs were established, and reasons of exiting two of them, having principally different forms, on rather close to each other eigenfrequencies ~ 6.0 Hz and ~ 8.8 Hz are determined.

The essential difference between one ASW form from the forms of three others ASWs has stipulated various influence of them on neutron field in reactor vessel (core). The indicated difference defined a various character of each ASW influence as exterior exciting force on the elements of equipment inside reactor pressure vessel and on their forced vibrations due to this oscillating force.

It is shown, that three ASW with practically multiple eigenfrequencies (~ 6.0 Hz, 13.0 Hz and 18.6 Hz) have inside RPV (inside core) a common node, possessing a rather complicated geometric structure. This circumstance does not allow to use them for the experimental definition of coefficient of reactor vessel reactivity on pressure (CRV RP) during NPP operation.

Presence of a node in core at ASWs on frequencies ~ 6.0 Hz, 13.0 Hz and 18.6 Hz gives rise to emerging in some points significant on magnitude space gradients of these standing waves amplitudes in radial and azimuthal directions. It is the reason of forced beam mode oscillations of series of fuel elements, fixed in their upper and bottom parts on indicated above frequencies.

It is shown, that three ASWs similar to ASWs on frequencies ~ 6.0 Hz, 13.0 Hz and 18.6 Hz with respect to their forms, can be formed simultaneously only in PWR with an even number of loops in PCC. In PWR with odd number of loops in PCC ASWs with the forms, similar to forms of ASWs on frequencies ~ 6.0 Hz and 18.6 Hz, will not be formed.

It is established, that fourth ASW on frequency ~ 8.8 Hz has two anti-phase pairs of antinodes, located inside RPV in two various parts of its volume, and one node in region of each steam generator (SG). Two antinodes of this ASW, are in phase to each other, cover core and space above it. Other antinode pair of fourth ASW is in space between RPV and its core barrel. Such ASW with respect to its form can be sometimes used for CRVRP measurement. However it is necessary to do it with large caution to eliminate emerging in some cases of an error result. ASW of the similar form will exist in PWR reactor plant with any number of loops in PCC with the exception of one loop PWR.

The measurement of neutron noise was carried out with use of rhodium self powered neutron detectors (SPND), located in seven various points on a height of large number of fuel elements and three ionization chambers (IC), located outside RPV under an angle approximately 120° to each other on the middle of core height.

The common analysis of noise signals of various SPND inside core, and also SPND noise signals and IC outside RPV has confirmed existence inside PWR (inside core) nodes and antinodes of all four enumerated earlier ASWs with a predicted structures. Moreover this analysis

has confirmed a picture of each ASW phase pattern in core volume, in RPV volume and in total PCC.

Character of a phase shift between noise signals of SPND various pairs in fuel elements on frequencies ~6.0 Hz, 13.0 Hz and 18.6 Hz enabled to identify their forced beam mode vibration on these frequencies.

1.2 Key words

VVER, reactor pressure vessel, fuel assemblies, acoustic standing waves, pressure fluctuations transducers, self powered neutron detectors (SPND/ДПЗ), ionization chambers, auto power spectral densities, cross power spectral densities, coherence function, phase characteristics

1.3 Introduction

In work [1] there were represented results of research of pressure fluctuations in the coolant of reactor plant (RP) VVER-440, having 6 identical coolant loops, symmetrically located around RPV. The measurements, underlying these researches, were carried out on the Unit 2 of Kola NPP in 1992 with aid of four pressure fluctuations transducers (PFT), located directly in pipelines of loops without application of impulse lines.

The analysis of results of these measurements, based on the ASW properties, and also on identity of all six coolant loops and symmetry of the their arrangement around RPV, enabled with sufficient completeness to determine the forms of ASW series, corresponding to four minimum eigenfrequencies of pressure oscillations in the coolant of whole PCC. This analysis has allowed to establish three-dimensional space structure of these ASWs nodes and antinodes inside RPV and outside it, and also phase pattern of each standing wave modification in whole PCC volume. Simultaneously there were defined PCC geometric features, which caused all four ASWs shaping, and reasons of exciting two of them, having basically in essence different forms, on rather close to each other eigenfrequencies are clarified.

In indicated above work it was shown that three ASWs with practically multiple eigenfrequencies have apparently inside RPV (inside core) common node, possessing a complicated geometric structure. The analysis of experimental results has allowed to reach in this work an inference, that three ASW nodes should be located on six vertical planes and on one horizontal plane. Such conclusion is rather convincing. However the PFT lack inside RPV and possibility to measure neutron noise inside core on the Kola NPP Unit 2 has not allowed to check up the given result of researches. For the same reason on the base of measurements, represented in work [1], it was impossible to define inside RPV the position of the horizontal plane, where defined nodes of three mentioned above ASW are located.

In work [1] it was established that fourth ASW has three anti-phase antinodes pairs located inside RPV in two various parts of its volume, and one node in each steam generator (SG) region. First three antinodes of this ASW are in a phase to each other penetrating towards RPV from the side of loops hot legs and cover some core part and space above it. Three other antinodes of fourth ASW are in anti-phase to first three antinodes, penetrating towards RPV from cold legs of all six PCC loops and fill in a defined part of space between RPV and its core barrel. The last result does not cause doubts. Nevertheless it also requires experimental confirmation. Moreover measurements carried out in work [1], could not give the answer to the problem on depth of penetration of two anti-phase antinodes groups of fourth ASW in the core bottom and in the bottom of space between RPV and its core barrel.

Principle of reflection used in work [1] has enabled to show that all four ASWs with the similar forms and similar space structures of nodes and antinodes inside RPV and outside it will be formed simultaneously only in RP as VVER with an even number of loops in PCC. The given circumstance allowed to predict existence of all four ASWs possessing the represented above forms in the VVER-1000 coolant, which has four identical loops in PCC. Such prediction enabled to confirm results of work [1] carried out earlier and to receive the answers to all mentioned problems connected with incompleteness of knowledge of nodes and antinodes of four ASWs inside RPV during corresponding measurements of pressure in coolant, incore and excore neutron noises on the Unit 1 of Kalinin NPP with VVER-1000. Conditions at which measure-

ments of neutron noise and noise of pressure on the Unit 1 of indicated NPP were carried out will be described below and some results of their analysis will be represented explicitly.

It is necessary to mark that the interest to the ASW forms appropriate to minimum eigenfrequencies of pressure oscillations in PCC coolant and structure of their nodes and antinodes inside RPV is caused by two basic reasons.

At first on the ASW form, as an exterior exciting force, depends in particular its influence on the various elements of a technological equipment inside RPV and their forced vibrations due to this oscillating force. Such influence will be especially significant from ASW possessing the least eigenfrequencies and therefore greatest oscillation amplitudes of pressure in coolant.

Besides not any ASW as a natural source of pressure perturbation in coolant it is possible to use for the operating experimental definition in working conditions of such important physical parameter of core barrel, as CRVRP. For CRVRP correct measurement can be suitable only such ASW, which antinode is inside core, and ASW length exceeds greatly its characteristic sizes. It is necessary to search ASW possessing these properties among those several standing waves, which are formed on the lowest frequencies.

ASW on low eigenfrequencies of coolant pressure oscillations in PCC were experimentally identified earlier with various degree of a completeness on some PWRs with an even number of loops [2, 3, 4]. However the level of identification of these ASW forms during the previous measurements and investigations was limited by clearing up of pattern of their behavior in loops pipings and steam generators. Only in works [2, 4] it was exhibited defined interest to ASW having antinode in core region, in connection with the task of a CRVRP measurement. Thus detail investigation of this ASW amplitude and phase inside core and in space between RPV and its core barrel in works [2, 4] was not carried out. Calculations of own frequencies and forms of coolant oscillations in PCC carried out for example in works [3, 5], could not basically give the answer to the problem of three-dimensional space structure of nodes and antinodes, and also about a space picture of distribution of ASW amplitudes and phases on low frequencies inside RPV. The indicated calculations were carried out with use of distributed parametrical one-dimensional model. In such model whole PCC was divided on defined number of the separate functional elements, each of which was considered as one-dimensional in space subsystem.

The experimental definition of three-dimensional space structure of ASW nodes series inside RPV, which are formed on low frequencies, was not realized until emerging work [1].

These circumstances once again underline necessity of detail study of singularities of ASW behavior on low frequencies inside core and inside RPV. As already above was spoken such research is possible to realize at the analysis of results of pressure fluctuations measurement, incore neutron noise and neutron noise outside of RPV on the Unit 1 Kalinin NPP.

1.4 Conditions of pressure fluctuation and neutron noise measurements on the Kalinin NPP Unit 1

The measurement of neutron noise and pressure oscillations was carried out on the Unit 1 of Kalinin NPP in 1994 within the framework of work on vibrational diagnostics of equipment, located inside RPV. These measurements were carried out by group of the "DIAPROM" Diagnostics Center experts under guiding G.G.Anikin. Common guiding connected with preparation, organization and realization of measurements on Kalinin NPP, is realized by "DIAPROM" General Director D.F.Gutsev. The great support at measurements of noises was rendered by Kalinin NPP experts.

Registration of pressure fluctuations was realized with the aid of three PFTs, located in pipelines of two adjacent PCC loops with short impulse lines having length 50 sm. Two PFTs were installed on outlet of main circulating pumps (MCP) in cold legs of third (Q3) and fourth (Q4) loops on a distance 26.5 m from RPV. Third PFT (S4) was in hot leg of the fourth loop on a distance 6.5 m from RPV.

The neutron noise were measured with rhodium SPNDs, located in seven various points on a height of large number of fuel assemblies, and three neutron ionization chambers (IC-7, IC-14 and IC-21), located outside of RPV under angle approximately 120° to each other on core height middle.

The locations of various transmitters are indicated on fig. 1, where the scheme of PCC of VVER-1000 is represented. Scheme of core with the indication of its fuel assemblies coordinates, position of swallowing neutron clusters of reactor regulating rods of ten various groups and installation places of ionization chambers (IC-7, IC-14, IC-21) and location of SPNDs (S4, Q4, Q3) are introduced on fig. 2.

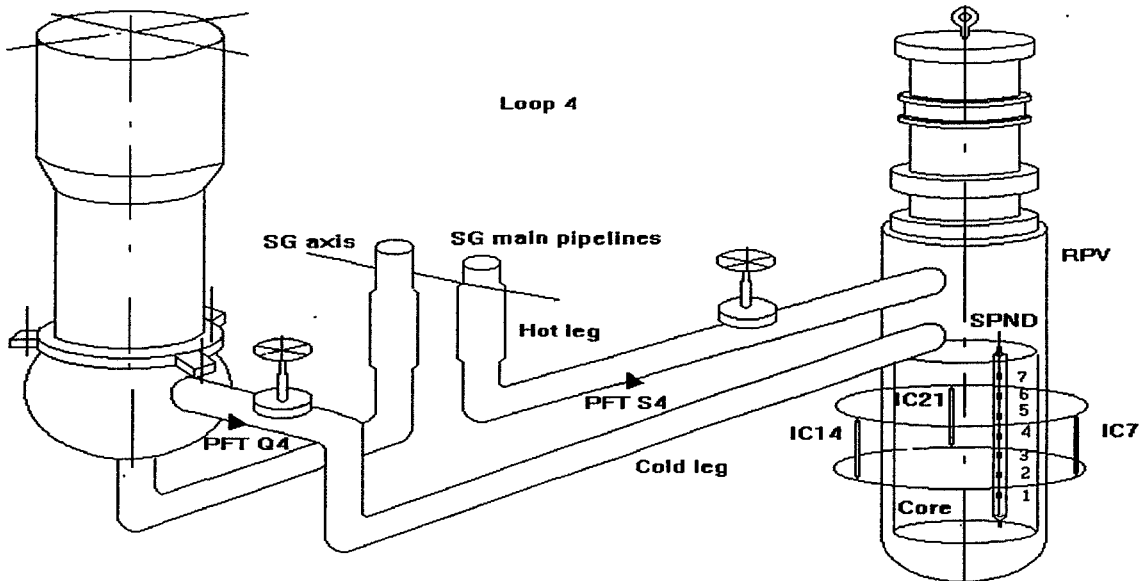


Fig.1

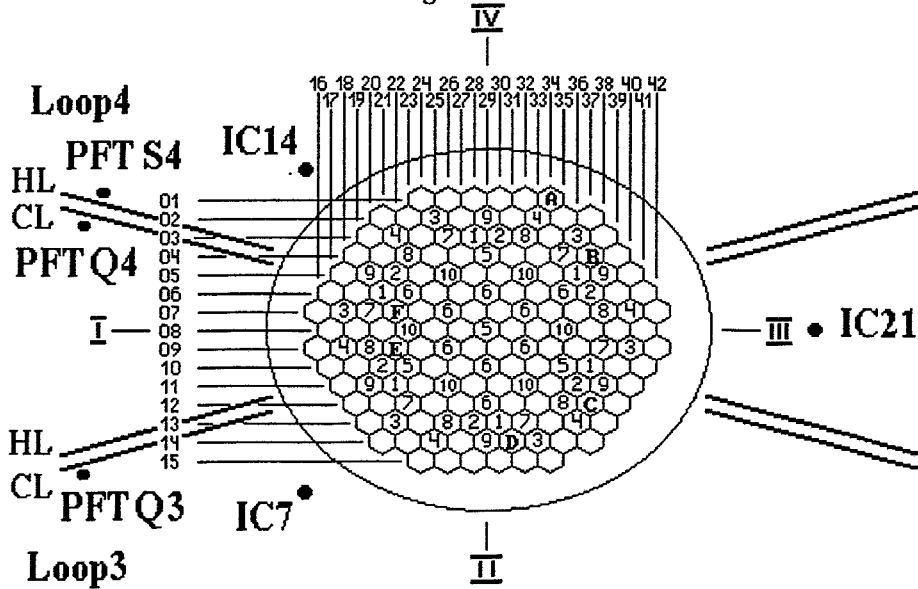


Fig.2

The measurements on the Unit 1 of KalNPP were carried out under following conditions:

- Electric power was 800 MW,
- 4 MCPs were in work,
- Pressure in 1-st circuit was 160 kg/sm²,
- Coolant temperature in cold legs was 288°C,
- Coolant temperature in hot legs was 311°C

- The clusters of all nine groups of control rods are extracted from core
- The clusters of the tenth group are lowered in core on 20 % from there overall height and fulfilled function of automatic power regulators
- Concentration of boric acid is 0.22 g H₃BO₃/kg H₂O

Further we shall use for signals of any transmitter types the same symbols, which were adopted earlier for transmitters themselves.

Whole volume of work connected with various aspects of spectral and multidimensional autoregression processing of measured noise signals has been executed by V.I.Pavelko(RSC "KI") with aid of the programs, created under his guiding has defined auto power spectral densities (APSD) of signals of PFT, SPND and IC, cross power spectral densities (CPSD), coherence function (CF) and phase characteristics (PC) of various pairs of these signals and normalized variances of signals in various frequency bands.

In consequent sections of this part the report is represents analysis of some features in spectra of measured signals, carried out by V.V.Bulavin (RSC "KI"), and their physical interpretation is given.

1.5 The analysis of PFT signals noise

The frequency spectra of noise of three PFT signals have appeared to be rather close to each other. On fig. 3 APSD of a signal S4 for example is represented. In spectra of all PFT signals will pay attention to significant on amplitude resonance peaks on frequencies (6.0 Hz, 13.0 Hz, 18.6 Hz and ~8.8 Hz. For illustration on fig. 4 ..6 CF and PC between signals Q4 and S4, Q3 and S4, and also Q3 and Q4 are shown. Values of CF and PC on frequencies (6.0 Hz, 13.0 Hz, 18.6 Hz and ~8.8 Hz for various pairs of PFT signals are represented in tables 1, 2, 3, 4.

Table 1

Signals	Frequency, Hz	Coherence	Phase shift, °
Q4-S4	6.201	0.9342	6.51
Q3-S4	6.201	0.1443	152.7
Q3-Q4	6.201	0.1583	159

Table 2

Signals	Frequency, Hz	Coherence	Phase shift, °
Q4-S4	12.84	0.8393	174.4
	13.33	0.9109	175.3
Q3-S4	12.9	0.06	164
Q3-Q4	12.9	0.154	16

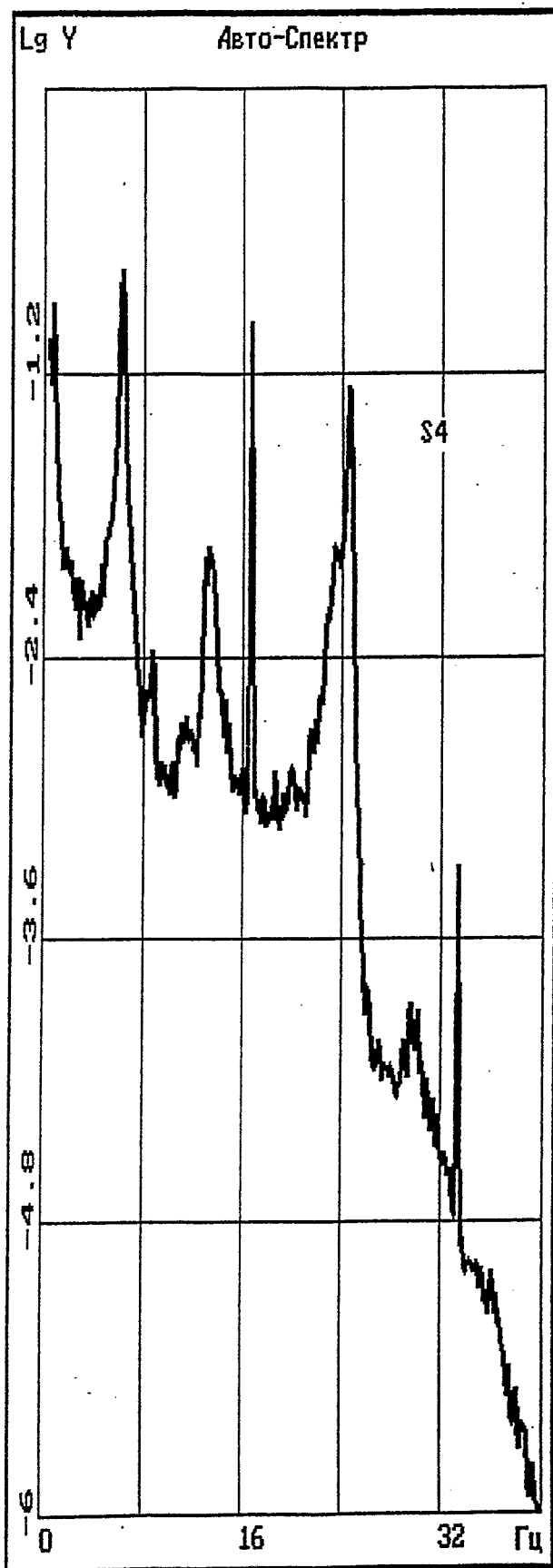
Table 3

Signals	Frequency, Hz	Coherence	Phase shift, °
Q4-S4	18.7	0.28	172
Q3-S4	18.7	0.09	4.3
Q3-Q4	18.7	0.183	148

Table 4

Signals	Frequency, Hz	Coherence	Phase shift, °
Q4-S4	9.0	0.228	140
Q3-S4	9.0	0.111	162
Q3-Q4	9.0	0.110	11

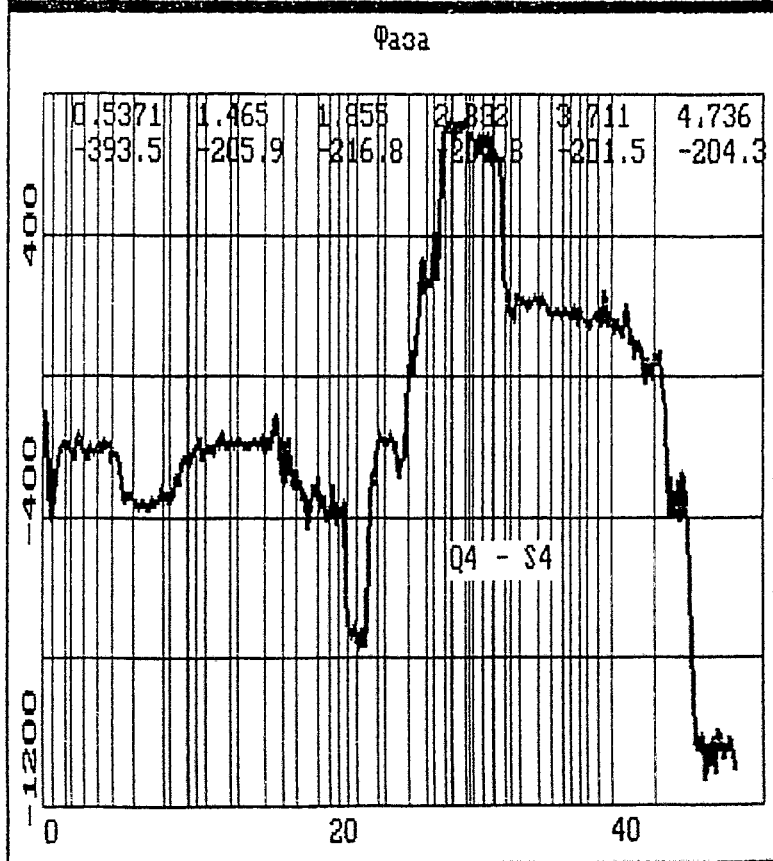
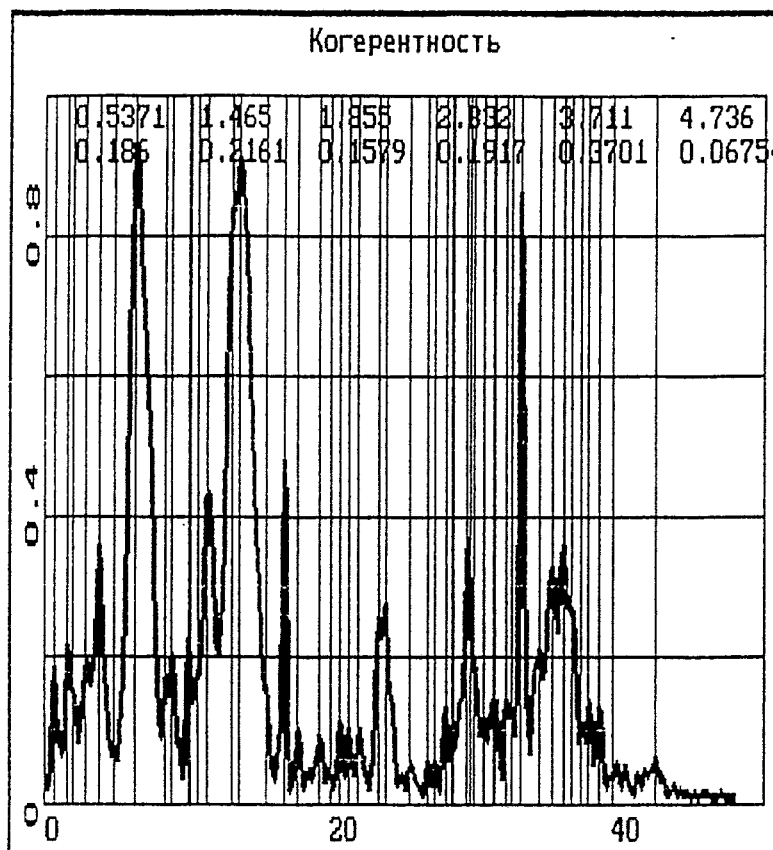
These tables follows, that the phase shift between harmonic components (HC) in signals of each PFT pair on four mentioned above frequencies is equal 0 or 180°, taking into account the error of estimations. This circumstance is an indication that on these four enumerated frequencies we deal with four types of ASWs, corresponding to four minimum eigenfrequencies of pressure oscillations in coolant of whole volume PCC, including incore RPV part.



1.611	-1.922
2.1	-1.996
2.637	-2.074
3.711	-2.095
6.152	-0.712
8.74	-2.317
9.326	-2.832
10.3	-2.811
10.99	-2.672
11.43	-2.649
11.87	-2.72
13.28	-1.9
15.48	-2.892
15.97	-2.869
16.65	-0.9808
17.72	-2.981
18.6	-2.877
19.24	-2.969
19.87	-2.811
20.56	-2.947
23.44	-1.912
24.56	-1.254
27	-4.016
27.59	-4.122
27.98	-4.081
29.05	-4.011
29.49	-3.872
30.13	-3.899
31.35	-4.269
33.3	-3.297
34.18	-4.95
34.91	-4.936
35.99	-4.994
37.55	-5.398
38.04	-5.5
38.57	-5.603
39.45	-5.809

Гц

Fig. 3



Гц	Coherence	Град
0.5371	0.186	-33.48
1.465	0.2161	154.1
1.855	0.1579	143.2
2.832	0.1917	152.2
3.711	0.3701	158.5
4.736	0.06754	155.7
6.201	0.9342	6.51
8.301	0.1762	19.39
8.691	0.2058	2.191
9.814	0.2275	139.2
10.45	0.1788	169.8
11.18	0.4324	148
12.84	0.8393	174.4
13.33	0.9109	175.3
15.28	0.1622	141.5
16.6	0.493	61.57
17.53	0.1003	77.88
19.09	0.09281	43.26
20.51	0.1162	-10.78
21.14	0.1014	20.94
21.88	0.1023	-56.32
23.19	0.2568	152.7
23.73	0.2776	171.5
25.49	0.05417	26.33
26.76	0.05638	-103.5
27.29	0.05817	37.5
28.03	0.1278	-11.03
28.42	0.06889	-5.024
28.61	0.07644	-69.98
29.54	0.3857	-30.59
29.98	0.1944	-44.59
30.62	0.1164	-69.23
31.3	0.1396	-102.2
31.49	0.1447	-89.85
32.23	0.1496	-107.9
32.62	0.1303	-168.3
33.25	0.8606	-147.4
34.57	0.2171	-156.5
35.45	0.3266	-174.4
36.23	0.3594	-178.7
36.82	0.2676	172
37.5	0.111	166.3
37.99	0.1388	142.5
38.77	0.1325	152.4
42.68	0.05967	55.06

Fig. 4

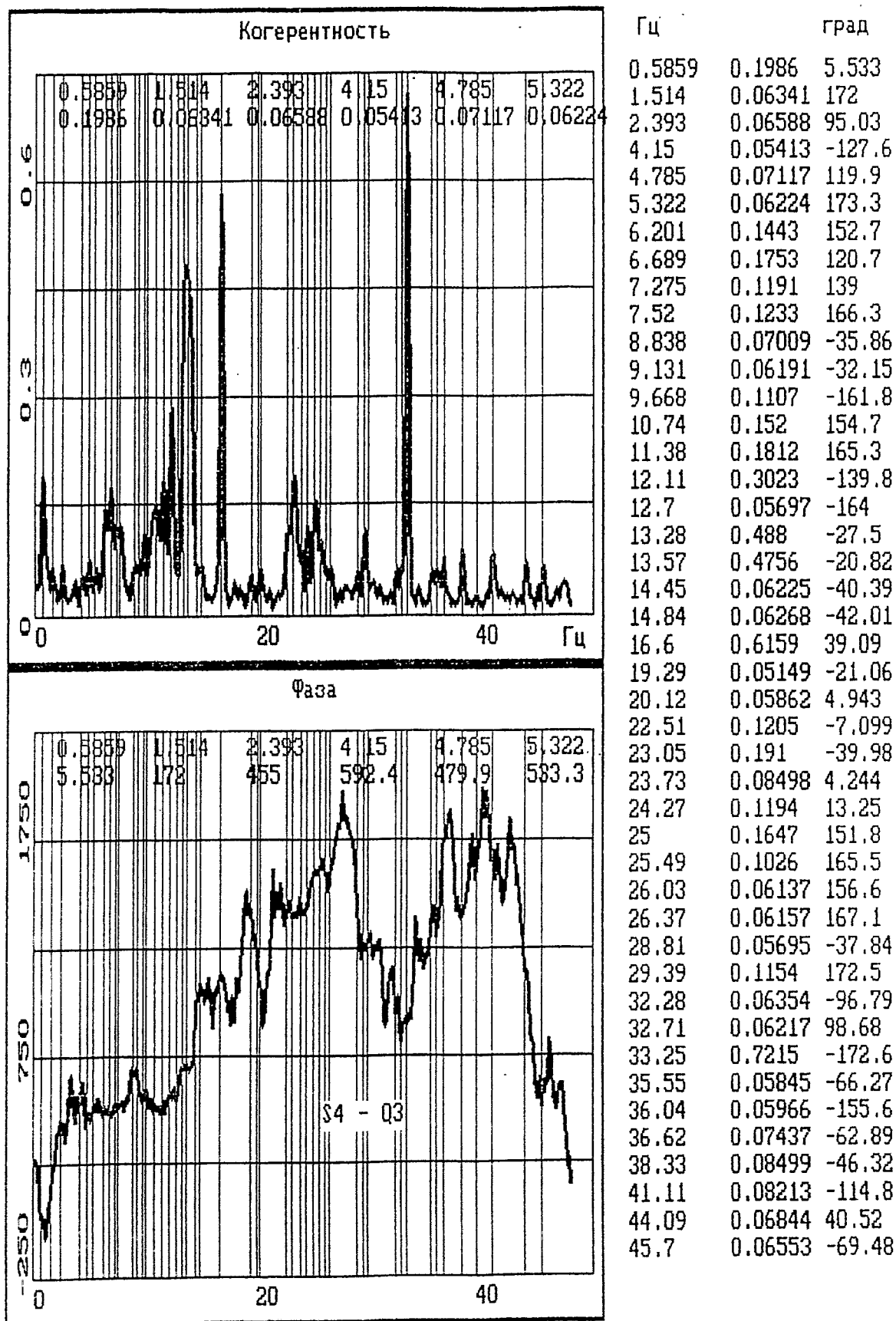
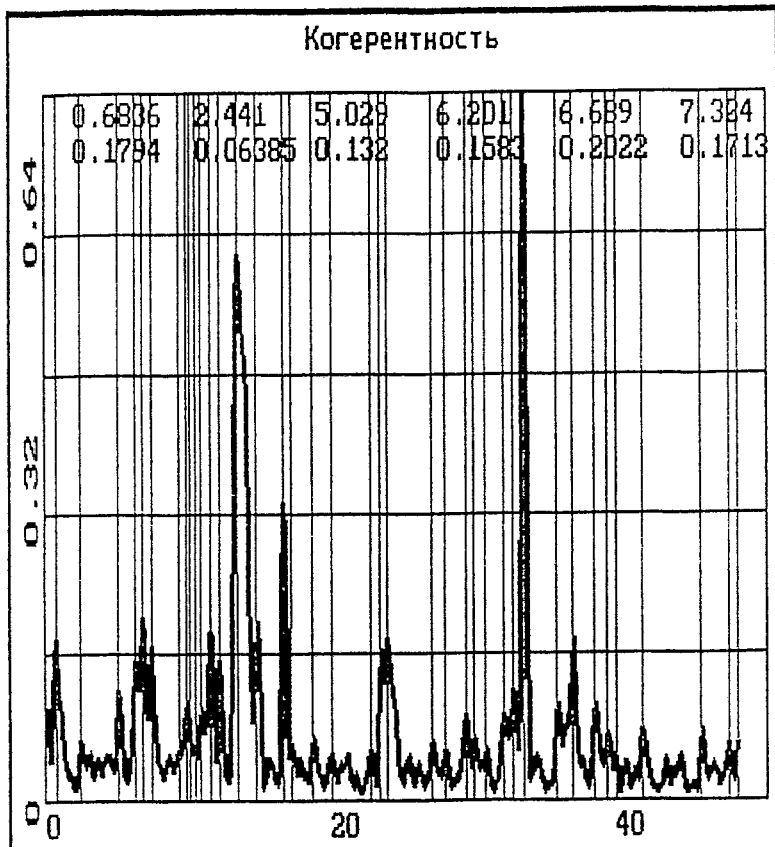


Fig.5



0.6836	0.1794	-1.994
2.441	0.06385	106.4
5.029	0.132	47.63
6.201	0.1583	-159
6.689	0.2022	-128.3
7.324	0.1713	-144.2
9.131	0.05138	-31.84
9.766	0.11	11.13
10.3	0.05868	56.65
10.79	0.101	61.34
11.43	0.1878	43.23
12.06	0.1541	-49.29
13.33	0.615	-153.8
14.7	0.2003	-146.9
16.6	0.3356	-99.28
17.09	0.05952	-81.61
18.55	0.06663	108
22.61	0.05539	-81.65
23.29	0.1687	-153.4
23.78	0.1834	-147.5
26.95	0.06521	-125.7
27.78	0.05007	49.88
29.2	0.09063	-167.3
29.74	0.06444	176.9
30.57	0.05192	-61.22
31.84	0.09301	34.45
32.47	0.1206	82.63
33.25	0.7997	-39.24
35.55	0.1069	-138.7
36.57	0.1805	-165.6
38.13	0.1066	-116.9
39.01	0.07004	56.42
41.5	0.07821	34.19
45.56	0.07591	119.8
47.41	0.05869	100.5
48.14	0.05901	-102.5

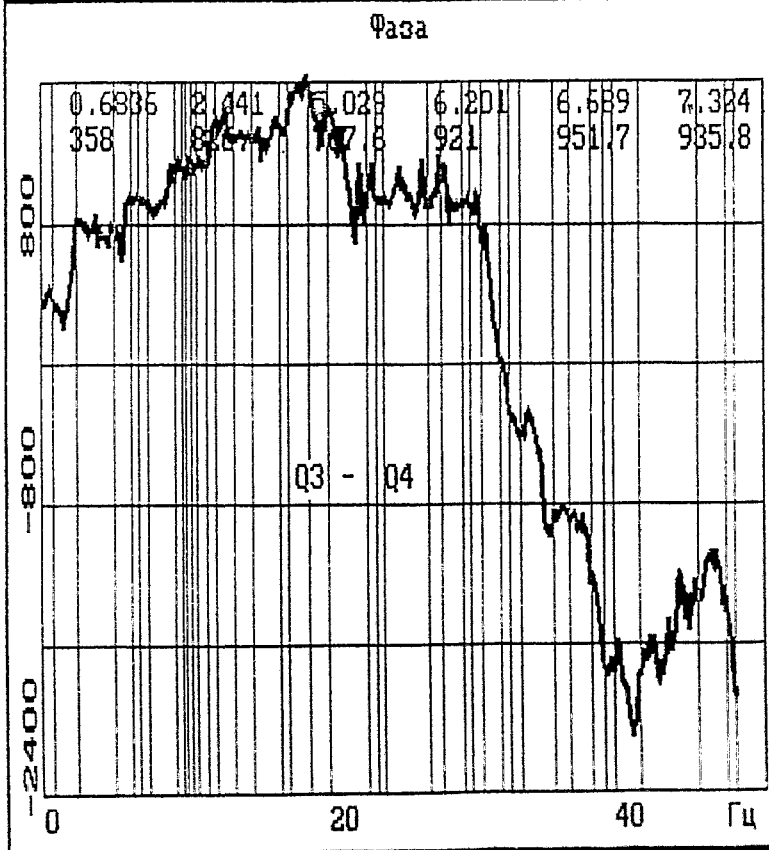


Fig. 6

1.5.1 ASW form on frequency 6.2 Hz

To define the form ASW on frequency 6.2 Hz in separate loops and in whole volume of PCC we need return to table 1. It follows, that on this frequency HC in PFT signals Q4 and S4, installed in cold and hot legs of 4-th loop, are in a phase at very high CF value. The full identity of all 4 loops and arrangement rather close to symmetry with respect to RPV allow to state, that in other loops a similar picture will be observed, if similar measurements will be performed.

Fact of phase shift on 180° between HC in pair of signals Q3 and S4, and in pair of signals Q3 and Q4 on frequency of 6.2 Hz at rather high values of coherences (0.144 and 0.158, accordingly) is essential. Obviously, that such situation will take place in any two adjacent loops at realization of appropriate measurements. It indicates, that in whole PCC volume on the given frequency uniform ASW is formed, and its separate parts are in pipelines of various loops and inside RPV. We execute a round estimation of wavelength of this standing wave with aid of simple one-dimensional model, which is true to a sufficient degree only in limits of pipelines of loops. Within the framework of such model length ASW λ is connected to its frequency f by the formula $\lambda=v/f$, where v - speed of a sound in the coolant. At temperature of coolant $\sim 300^\circ\text{C}$, obtained as a simple average of temperatures in hot and cold legs, and pressure 160 kg/sm^2 the speed of a sound is equal $v=1000\text{m/s}$. It follows, that length of ASW on frequencies of 6.2 Hz is approximately 170 m. This value will be close to actual, as the pipelines of each loop play a defining role at shaping of given ASW.

Overall length of a loop, in which coolant circulates in VVER-1000 RP type on the Unit 1 of Kalinin NPP, is equal approximately 86 m. It includes pipelines of hot and cold legs of separate loop, and also appropriate sites inside stream generator and RPV. A total sum of experimental results represented in a table 1, conclusions and estimations mentioned above, allows to conclude, that on length of each closed circuit, connected to any loop, half of length of ASW on frequency 6.2 Hz with two nodes concurrent in space, and one antinode is formed. These nodes are located in some part of one plane in perpendicular direction to stream of coolant flowing, and will conditionally organize the first group of nodes.

It is obvious, that two halves of uniform ASW, formed by two adjacent loops and being in anti-phase can be united with each other only inside RPV through their common nodes, which we shall conditionally refer as the second group of nodes.

It is easy to see, that the nodes of the second group, common for the two ASW parts, formed in any two adjacent loops, will be placed on that part of a vertical plane, which is shaded on Figure 7. Inside RPV it will be four such vertical planes, similarly completed by nodes of a similar type. The segment of a vertical axis RPV will be common for all these planes, joining them. Nodes will be located on it, simultaneously belongs to all ASW parts, generated by various loops. An angle between any two adjacent planes, on which nodes of the second group are located, will be 90° . Four such planes divide whole volume of coolant inside RPV into four parts, each of them will adjoin to an appropriate loop.

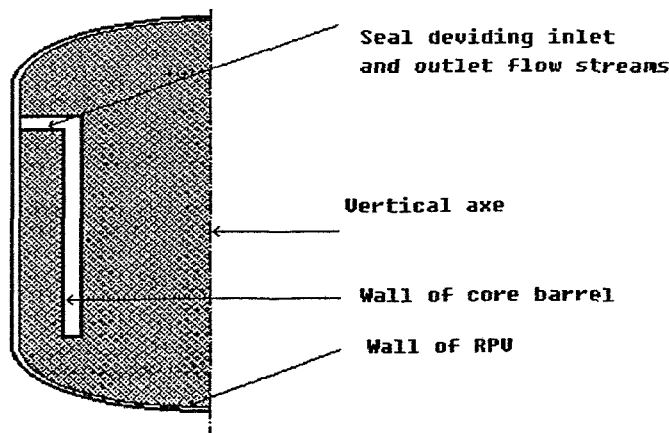


Fig.7

Four indicated planes for ASW on frequency 6.2 Hz will form finally inside RPV the boundaries of all four closed circuits, generated by various loops outside PVR. In some sense such planes for this standing wave are possible to be considered as absolutely rigid walls, the thickness of which is equal to zero. They as though isolate one loop from other and form inside RPV four channels, each of them continues the pipeline of cold leg (CL) of any loop and connects it to the pipeline of hot leg (HL) of same loop. However, it does not mean, that the separate parts of ASW, generated in each loop, will be independent. Four vertical planes - walls with nodes of the second group will provide their mutual and appropriate synchronization.

In a space node structure, formed by four vertical planes inside RPV, it is logical also to include nodes, entering in a structure of the first group. Then these nodes will fill inside RPV some two-dimensional area on one horizontal plane, perpendicular to its vertical axes. It follows, that in SG region of each loop antinodes of ASW on frequency 6.2 Hz will locate. Thus the ASW form on the given frequency and geometric structure of its node inside RPV are almost completely defined.

Only PFTs cross spectral analysis does not allow to determine precisely inside SG or its neighborhoods, points with maximum amplitude of pressure oscillation on frequency of 6.2 Hz. It, in turn, does not give a possibility to determine precisely inside RPV a position of that horizontal plane, on which nodes of the first group are placed. The character of their arrangement on it will depend on the place with respect to inside RPV direction of coolant slow where indicated nodes are located.

Space pressure oscillations amplitude distribution in coolant of VVER-1000 PCC on frequency of 6.2 Hz is schematically represented on fig. 8.

The picture of ASW phase behavior on frequency of 6.2 Hz and arrangement of its nodes of the first and second groups inside RPV in a crosssection which is made by a horizontal plane with nodes of the first group, in part where inlet coolant flows down in space between the cylindrical surface of RPV and its core barrel is represented on fig. 9. The filled part of a plane on this Figure shows, where nodes of the first group will be placed in this case. On this Figure also a mutual disposition of pipelines of hot and cold legs of each loop is schematically represented.

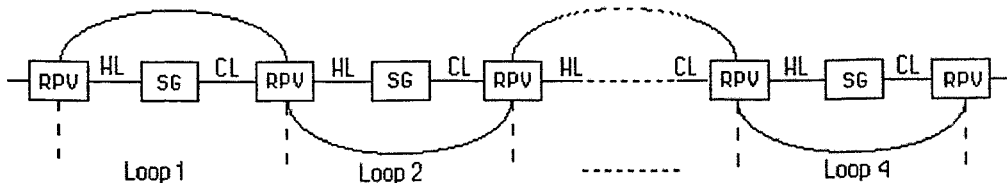


Fig. 8

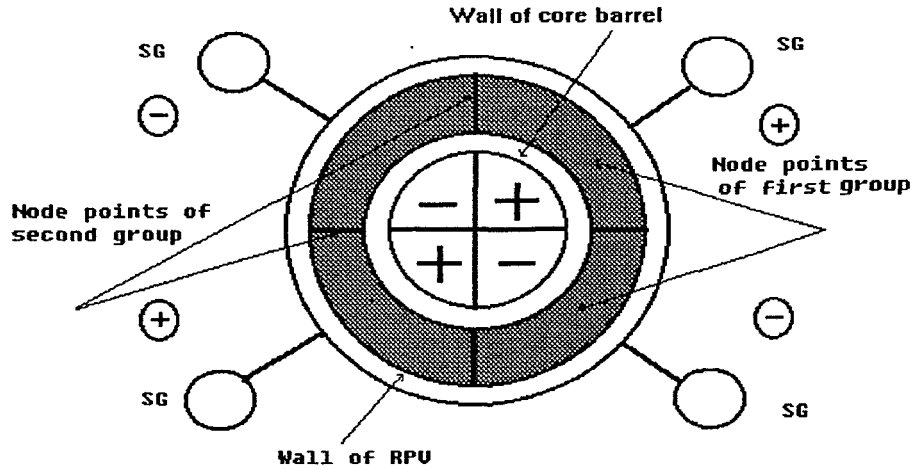


Fig. 9

If any area of space inside RPV is marked with +, and other area with -, in two these areas ASW on frequency of 6.2 Hz oscillations will be in anti-phase. The same labels will be applied for illustration of phase relations between separate parts of any ASW, formed in two elements of RP equipment outside RPV.

For example, other variant is possible, when the nodes of the first group, lying in a horizontal plane, will be in limits of core volume. Then they will fill in that part of this plane, which is shaded on fig. 10. On it distribution of ASW phase on frequency of 6.2 Hz and location of its nodes of both groups inside RPV in crosssection carried out by that horizontal plane, in which nodes of the first group are located is shown.

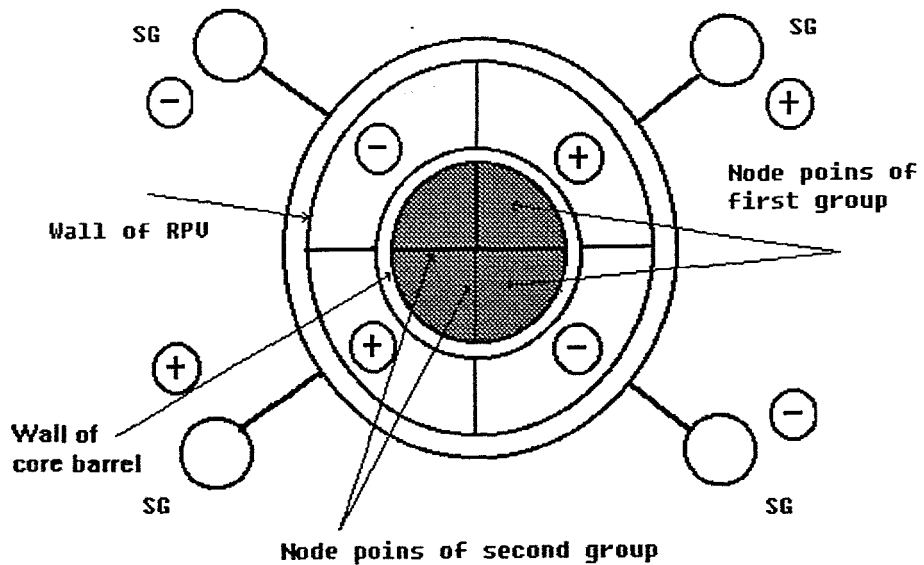


Fig. 10

The picture of the second group nodes arrangement and behavior of ASW phase on frequency ~ 6.2 Hz inside RPV in two various horizontal crosssections, not coincide with that horizontal plane, in which nodes of the first group are located is schematically represented on fig. 11 (a, b). The picture on fig. 11 (a) is observed in a horizontal crosssection, made above the obtruding ring, separating output stream of coolant from an entering stream. The picture on fig. 11 (b) takes place in a horizontal crosssection, spent below obtruding ring - stream separators at the core level. On two Figures 11 (a, b) the arrangement of pipelines of hot and cold legs of each loop with respect to RPV is schematically shown.

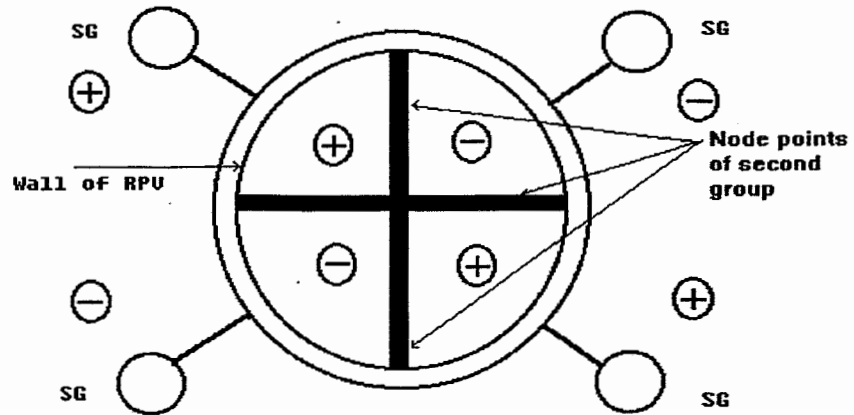


Fig. 11a

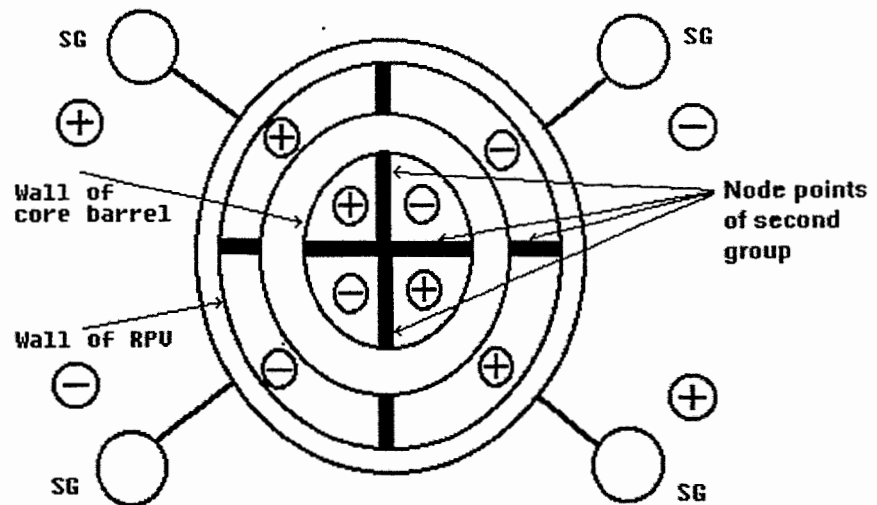


Fig. 11b

In moving on a circle inside RPV in both indicated above horizontal crosssections the ASW phase on frequency of 6.2 Hz four times jumps each 90° angular degrees on 180°.

Thus in hot and cold legs of the first and third loops ASW pressure oscillation on frequency of 6.2 Hz, generated in whole volume PCC, are in phase to each other and in anti-phase to oscillations of pressure on this frequency in hot and cold legs of the second and fourth loops. This ASW has 4 antinodes, located in the SG region, and a unique node, which is inside RPV and has a rather complicated three-dimensional space structure, described above in detail. The order of an azimuthal symmetry of geometric structure of this node coincides an order of azimuthal symmetry of VVER-1000 RP PCC. The responsibility for forming ASW of indicated shape on frequency of 6,2 Hz is on the first basic group of PCC elements symmetry, which consists of four identical circulating loops, symmetrically located around RPV and acoustically connected them. It is necessary to mark, that a principle of reflection allowed to predict existence of such ASW form for VVER-1000 RP and to determine a space structure of its node inside RPV without realization of any measurements and calculations.

The form of such ASW and space structure of its node will not depend on temperature of coolant. With changing of temperature only frequency of this ASW will vary. Obviously, that ASW of the similar form and with a similar space structure of node inside RPV will exist only in RP with an even number of loops. It allows without difficulties to generalize an obtained result on RP VVER-440, having six loops in PCC. ASW of such form cannot exist in RP of VVERs with odd number of loops in PCC, otherwise an azimuthal space symmetry of a picture of its phase changing will be broken. The shape of this standing wave and space structure of its node inside RPV can be used for quality check of theoretical model, which is applied for calculation of frequent ASW spectrum and their forms.

It is impossible to use ASW on frequency of 6,2 Hz for measurement of CRVRP. It is connected with perturbation of coolant density on ASW frequency of such shape in two adjacent core areas, contiguous to any two adjacent PCC loops, will be in anti-phase. Perturbations of coolant density in two appropriate areas outside core in parts where inlet coolant flows down between RPV and its core barrel will be under influence of indicated ASW similarly, that is in anti-phase. It will reduce to leakage of neutrons outside RPV on some two various sites of its surface will vary in anti-phase on ASW frequency of such type.

The three-dimensional structure of ASW node on frequency 6,2 Hz described above will create inside RPV rather significant gradients at its amplitude in radial, azimuthal and vertical directions in space between any two vertical planes, on which nodes of the second group are located. It will reduce to emerging of exciting force, causing, for example, FA beam oscillations of some fuel assemblies of core on frequency of this ASW.

The mentioned here effects by defined image will exhibit themselves in signals noise of excore neutron detectors, located outside RPV, and incore neutron detectors, located in core. Thus location of each IC rather circulating PCC loops and position of each SPND inside core will have an essential value.

The experimental check of obtained results will be represented below during the analysis of SPND and IC signals noises.

It is necessary to mark in an inference the fact of existence of rather low values of coherence functions between PFTs signals located in various loops on frequency of 6,2 Hz. It is impossible to tell about value of coherence function on the given frequency for two PFTs signals, located in one loop. It is clearly visible at reviewing of table 1. Such situation most likely develops for the reason of existence of significant on amplitude, uncorrelated and wide-band on frequency pressure oscillations in each four loops. These fluctuations being in various loops, including frequencies close to frequency 6,2 Hz, are caused by running acoustic waves, the amplitudes of which damp in accordance with deleting from pumps. Such waves are generated by uncorrelated vibrations of pumps configuration items at their independent work. Emerging of indicated vibrations is connected with lack of full identity between all pumps, that is stipulated by reasons of technological character, accompanying the process of their manufacture. Moreover all pumps have various degree of the unbalance and centre-of-gravity position with the shaft of the drive.

The situation, similar to that, about which was spoken above, takes place also on frequencies of ~13,0 Hz, ~18 Hz and ~9,0 Hz. Figures in tables 2, 3, and 4 are testify that.

1.5.2 ASW forms on frequencies $\sim 13,0$ Hz and $\sim 18,8$ Hz

The results, obtained in the previous section 1.4.1 of analysis of experimental data entitle to make the following supposition.

In all four closed circuits formed by various loops and four vertical planes inside RPV, on which nodes of the second group for ASW on frequency of $\sim 6,2$ Hz are located, some number of ASWs will be formed on frequencies, practically multiple frequency $\sim 6,2$ Hz.

Resonance peaks on frequencies of $\sim 13,0$ Hz and $\sim 18,8$ Hz were really detected in APSD of all PFT signals and in CF of their various pairs (see Figures 3, 4, 5 and 6) at measurement of pressure noise. The CF and PC analysis on indicated frequencies for various pairs of PFT signals allowed to make tables 2 and 3. From these tables, as was already spoken earlier, followed that on frequencies of $\sim 13,0$ Hz and $\sim 18,8$ Hz yet two ASW types are formed.

Thus in each loop on frequency of $\sim 13,0$ Hz ASW with length ~ 82 meters with two nodes and two anti-nodes will be formed. Anti-nodes of this ASW will be accordingly in pipelines of hot and cold legs of each loop in anti-phase to each other. Thus in hot leg of all four loops, as follows from table 2, ASW on frequency of $\sim 13,0$ Hz will be in a phase. One node of this standing wave will be located inside RPV, and other - in SG region on a distance ~ 41 meters from the first node, if to measure this distance at moving at closed circuit.

On frequency of $\sim 18,8$ Hz in each loop ASW with length of ~ 57 meters will be generated. Three halves of such standing wave with three anti-nodes and three nodes will be formed in it. One of these nodes will be evidently inside RPV. Two other nodes of this ASW will be located then accordingly in pipelines of hot and cold legs of each loop.

It is natural, that the nodes of the second ASW group on frequency of $\sim 6,2$ Hz, located inside RPV on four vertical planes, will be simultaneously nodes for ASW on frequencies of $\sim 13,0$ Hz and $18,8$ Hz. The nodes of this type will integrate separate parts of two indicated ASW, generated in various closed circuits and provide an appropriate synchronization of pressure oscillations on frequencies of $\sim 13,0$ Hz and $\sim 18,8$ Hz. The results of measurements, represented in tables 2 and 3, confirm existence of connection between separate ASW parts on these two frequencies, formed in various loops. In each closed circuit ASW on frequencies of $\sim 13,0$ Hz and $\sim 18,8$ Hz will have moreover nodes of other type, which were named earlier as nodes of the first group for ASW on frequency of $\sim 6,2$ Hz. They will be placed in planes, perpendicular direction of coolant flux moving. For ASW on frequency of $\sim 13,0$ Hz one horizontal plane with such nodes will be inside RPV. Nodes of the first ASW group on frequency of $\sim 18,8$ Hz will also fill on some part of one horizontal plane inside RPV. It is reasonably to assume, that for all three ASWs on frequencies of $\sim 6,2$ Hz, $\sim 13,0$ Hz and $\sim 18,8$ Hz nodes of the first group, located inside RPV, will be located in one horizontal plane and, therefore, will fill on it the same area. In this case all three indicated ASW will have one common node inside RPV.

The given supposition does not contradict to experimental results and is not deprived of foundations. Nevertheless it requires in additional experimental check, which, as already was spoken above, it is possible to realize with use of neutron detectors, located in the various points of core. Space expansion of pressure oscillations amplitude in PCC coolant of VVER-1000 RP on frequencies $\sim 13,0$ Hz and $\sim 18,8$ Hz accordingly is schematically represented on Figures 12 and 13. Moreover position of PFTs S4 and Q4 in pipelines of 4-th PCC loop, and also position PFT Q3 in the pipeline of the third loop are shown on Figure 13.

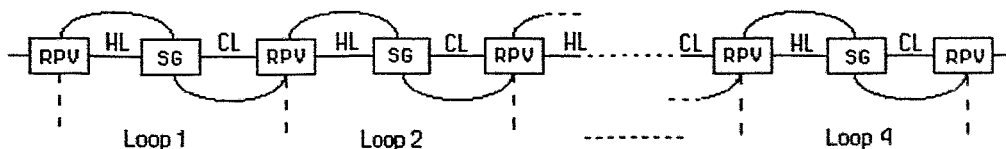


Fig. 12

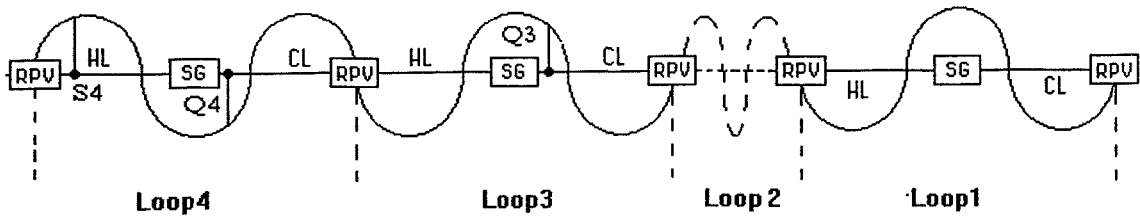


Fig. 13

Picture of ASW phase behavior on frequency ~ 13.0 Hz and arrangement of its nodes of the second group inside RPV in a horizontal cross section at core level in the supposition, that the horizontal plane with nodes of the first group is under core, is represented on Figure 14.

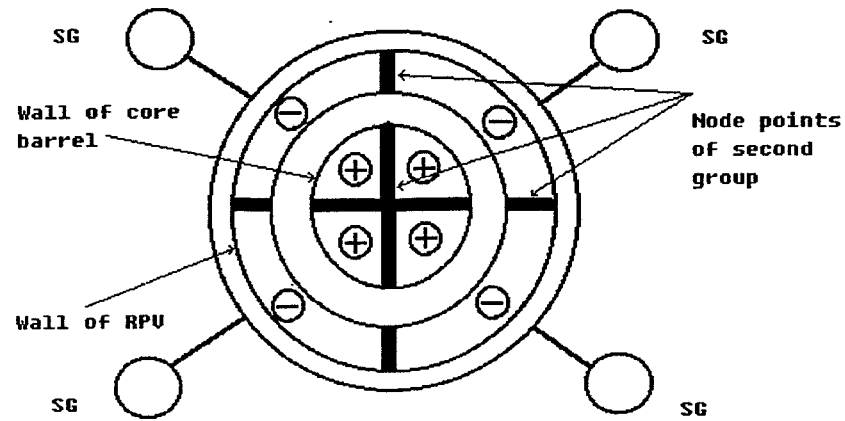


Fig. 14

Picture of ASW phase behavior on frequency ~ 18.8 Hz and arrangement of its nodes of the second group inside RPV in horizontal cross section at core level in the supposition that its nodes of the first group are under core is represented on Fig.15.

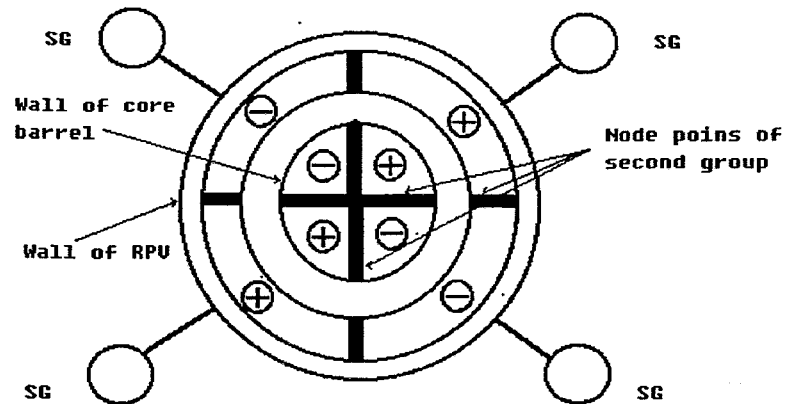


Fig. 15

1.5.3 The ASW form on frequency ~8.8 Hz.

Let's return again to results of measurements, represented in tab. 4. It follows, that harmonic components on frequency ~9.0 Hz in PFT signals Q3 and S4, located in cold and hot legs of the fourth loop, are in anti-phase to each other at coherence value equal 0.228. On this frequency HC in signals PFT Q3 and S4, located accordingly in cold and hot legs of adjacent third and fourth loops are also in anti-phase. At the same time harmonic components on frequency ~9.0 Hz in PFT signals Q3 and Q4, located in cold legs of two adjacent loops (3-rd and 4-th), are in phase.

If we again take into account identity of all PCC loops, symmetrically located around RPV, the noticed above regularity can be generalized on all remaining loops and their legs. In result there is the possibility to make the following statement.

In hot legs of all four PCC loops pressure oscillation in coolant on frequency ~9.0 Hz are in phase. Precisely also in phase on this frequency pressure in all cold PCC legs oscillates. However in arbitrary selected cold and hot legs of one loop or different loops pressure oscillation on frequency ~9.0 Hz are in anti-phase.

Obtained results indicate on the fact, that the ASW phase, formed in PCC coolant on frequency ~9.0 Hz, changes the value on 180° in limits of each loop between its hot and cold legs. It gives foundation to conclude, that its nodes are inside of all four loops somewhere in their SG region. To find the form of such standing wave, we shall estimate its length, assuming, that sound velocity in coolant $V=1000$ m/s. This velocity value was defined in corresponding with temperature and pressure in coolant during measurements. It follows, that on frequency ~9.0 Hz ASW length should be equal $\lambda=110$ meters.

We shall assume now, that in each loop given ASW node is precisely on middle of that loop site length, which is located inside SG. Then the distance from one node in which loop up to other node in an opposite (or adjacent) loop on path, taking place along their hot legs, will be ~ 50 meter, if length of some path site inside RPV will be subtracted from it. Similar distance between indicated above points along the path along cold legs, will be ~ 68 meters, if length of defined path site, on which ASW exists inside RPV in it is not take into account. The given evaluations give foundation to consider, that half of ASW on frequency ~9.0 Hz with antinode inside RPV is formed in each pair of hot legs. The similar situation will take place in each pair of cold legs, where on indicated frequency other half of ASW, antinode of which located in space be-

tween RPV and its core barrel, will be formed. Thus the separate parts of given ASW, formed in all hot legs, will be in anti-phase to those its parts, which are located in two pairs of cold legs.

Thus two groups of standing half-waves, being in anti-phase to each other, penetrate inside RPV from different sides and seize there some areas. One group does it from side of coolant outlet from RPV, other group - from side of its input in RPV. In pressure oscillation in coolant on frequency of such standing wave in two various volumes of fluid, located inside RPV, will be with phase shift, equal 180° .

It is essential here, that length of cold leg of each loop exceeds length its hot leg. The difference in lengths these legs becomes even more significant, if in structure of each cold leg of part where inlet coolant flows down between RPV and its core barrel will be included. For this reason the penetration degree inside RPV of two standing half-waves located in anti-phase will be not identical. Great influence to it temperature of coolant in hot and cold legs of PCC will be rendered.

It is possible to tell, that all 4 hot legs will form one group of the symmetry elements, and 4 cold legs - other group. Both these groups differ from that first basic group of the symmetry elements, which is formed by 4 PCC loops. Therefore two such groups jointly form on frequency ~ 9.0 Hz ASW of completely other form, power of which there is less ASW power on frequency ~ 6.2 Hz.

We shall assume that length of half ASW on frequency ~ 9.0 Hz, formed in two hot legs, is equal to length of half of indicated standing wave, generated in two cold legs. It will take place in case of PVR operation at zero or such small level of power, when temperature of coolant in cold and hot legs is identical. Then, proceeding from made earlier estimations, those two halves ASW, which were formed in hot legs, will capture majority of volume inside RPV together with core. Thus antinodes of these two half-waves will cover whole core volume of the RPV and will revolt density of coolant in phase in all its points with practically identical amplitude. The standing wave of such form can be used for CRV RP measurement.

In case, when temperature of coolant in hot legs exceeds temperature in cold legs, the situation can become worse with respect to ASW on the given frequency use for measurement of an indicated parameter. Under such condition depth of penetration downwards between RPV and core barrel of those parts of given ASW which were generated in cold legs will apparently increase. This circumstance is necessary to take into consideration at measurement of CRVRP, and if necessary to introduce to correct the results. The last reason however requires additional experimental check.

The picture of ASW phase behavior on frequency ~ 9.0 Hz inside RPV in horizontal cross-section below then obturating ring - inlet and outlet coolant streams separator on level of core top - is represented on fig. 16.

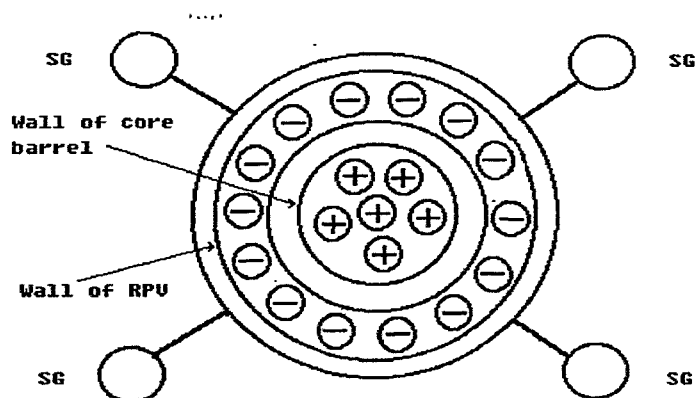


Fig. 16

1.6 The analysis of incore and excore neutron detectors signals noise spectra

We shall consider APSDs of signals of neutron detectors IC-7, IC-14, and IC-21 located outside RPV. They are represented on fig. 17 in frequency band 0 - 25 Hz. In these APSDs brightly expressed peaks on frequencies ~ 9.0 and ~ 13.0 Hz attract the attention. No doubt these peaks are caused by influence of two ASWs on indicated frequencies on a neutron field in vicinity of IC-7, IC-14 and IC-21 and, therefore, on current noise of these neutron chambers. It is transmitted through perturbation of coolant density on these frequencies inside core and in space between RPV and its core barrel.

Fig. 3 follows, that the amplitude of coolant density oscillation, caused by ASW on frequency ~ 6.2 Hz, exceeds greatly both density oscillations frequencies, caused two by ASWs on two frequencies ~ 9.0 and ~ 13.0 Hz. However ASW on frequency ~ 6.2 Hz does not render such influence on neutron field near the arrangement of neutron ionization chambers, which is brightly and strongly exhibited itself in APSD of signals IC-7, IC-14 and IC-21. As follows from fig. 17, influence of ASW on frequency ~ 6.2 Hz on neutron field near IC appeared on level of other numerous influences in this frequency region, which are caused by other radiants and, in this case, can be considered as background.

Enumerated experimental facts indirectly confirm the facts:

- The picture of ASW phase behavior on frequency ~ 6.2 Hz inside core and in space between RPV and its core barrel differs greatly from phase portraits of ASWs on frequencies ~ 9.0 Hz and ~ 13.0 Hz in indicated areas of space inside RPV (compare pictures of a behavior of a phase inside RPV on fig. 11b, 14 and 16);
- Oscillation of coolant density on frequency 6.2 Hz in two adjacent sectors inside RPV (each sector includes a definite part of core and some part of space between RPV and its core barrel), contiguous to two adjacent loops are in anti-phase (see. Fig. 11b);
- ASWs on frequencies ~ 9.0 and ~ 13.0 Hz have inside RPV identical phase portraits and, for example, in a phase disturb density of the coolant in all points of core (compare pictures of a behavior of a phase inside RPV on fig. 14 and 16).

The last circumstance was the reason of influence on a reactivity of the reactor and, therefore, on its neutron stream from ASW on frequencies ~ 9.0 and ~ 13.0 Hz. Moreover these two ASWs on the frequencies in a phase will disturb density of the coolant in whole volume of space between RPV and its core barrel (see. Fig. 14 and 16). Such perturbations will lead to significant on amplitude oscillations of current of all three neutron ionization chambers on frequencies ~ 9.0 and ~ 13.0 Hz.

Results of the APSD analysis on fig. 17 rather transparently (though indirectly) indicate, that for all three ASWs on frequencies ~ 6.2 , ~ 13.0 and ~ 18.8 Hz nodes of the first group, which have to be located inside RPV on defined part of one horizontal plane will be outside core limits and outside part where inlet coolant flows down located in space between RPV and its core barrel. Really the ASW phase on frequency ~ 13.0 Hz has 180° shift at crossing inside RPV through that part of the horizontal plane, on which nodes of the first group for three ASWs on frequencies ~ 6.2 Hz, ~ 13.0 Hz and ~ 18.8 Hz are located.

If, for example, the nodes of the first group were in limits of core on any horizontal plane, then summarized effect of influence from ASW on frequency ~ 13.0 Hz on neutron field in a neighborhood of ionization chambers would be significantly less, as the oscillations of density of coolant on frequency of this ASW in upper and bottom of core would be in anti-phase. The similar situation would have place also in case when the nodes of the first group are somewhere in parts where inlet coolant flows down between RPV cylindrical surface and its core barrel.

Influence on neutron field in a neighborhood of excore IC from ASW on frequency ~ 18.6 Hz, as expected, has appeared very weak. It was connected with small its amplitude, and with the circumstance, that the oscillations of coolant density on frequency ~ 18.6 Hz, caused by this ASW in two adjacent sectors inside RPV, contiguous to two adjacent loops, happen in anti-phase (see. Fig. 15 and 17).

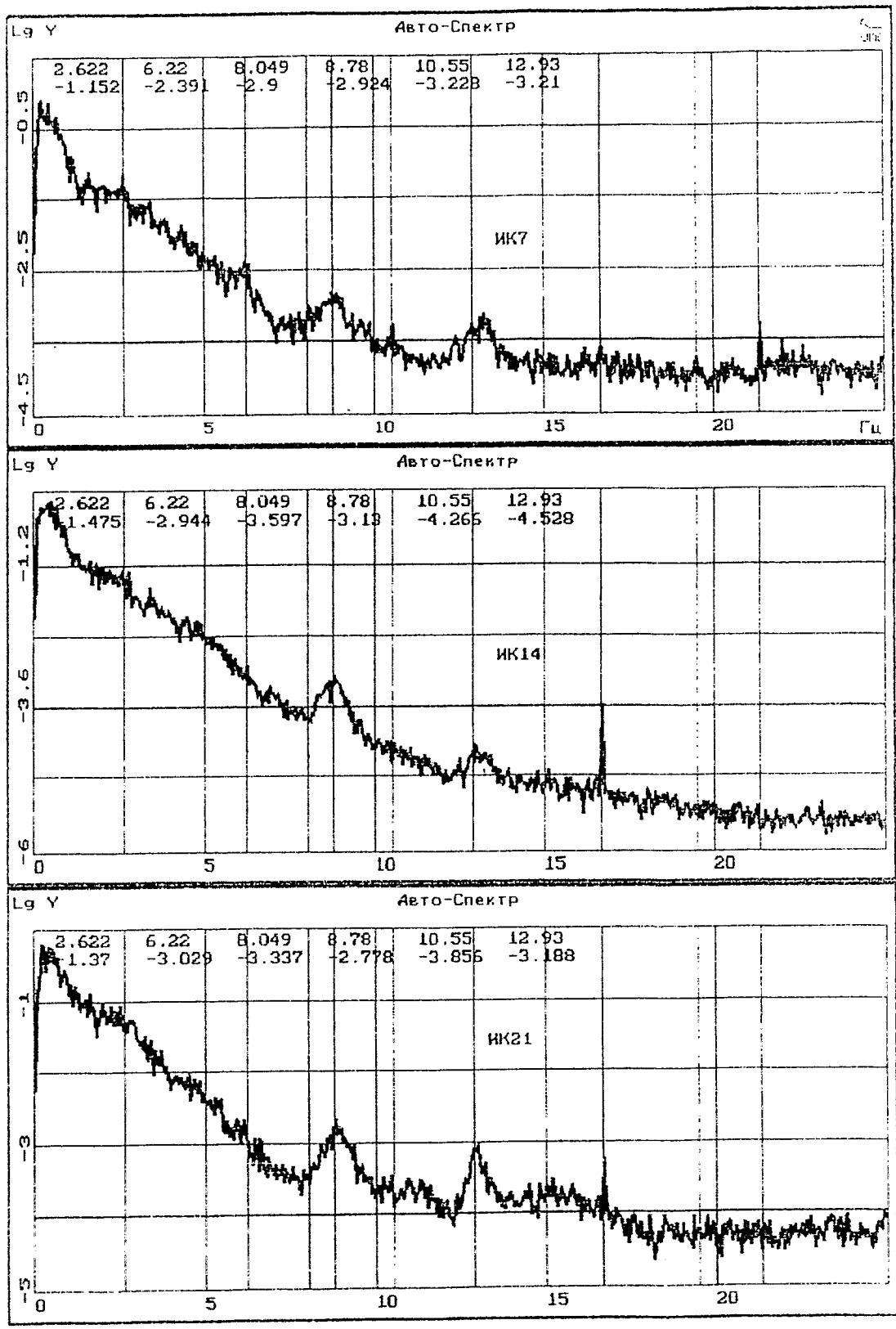


Fig.17

As an example APSD signals of all seven neutron SPNDs located in the fuel assembly, which has in core coordinates 10-27 are represented on fig. 18 (a, b). We shall remind to the reader, that SPND-1 is at the core bottom, and SPND-7 - in its top.

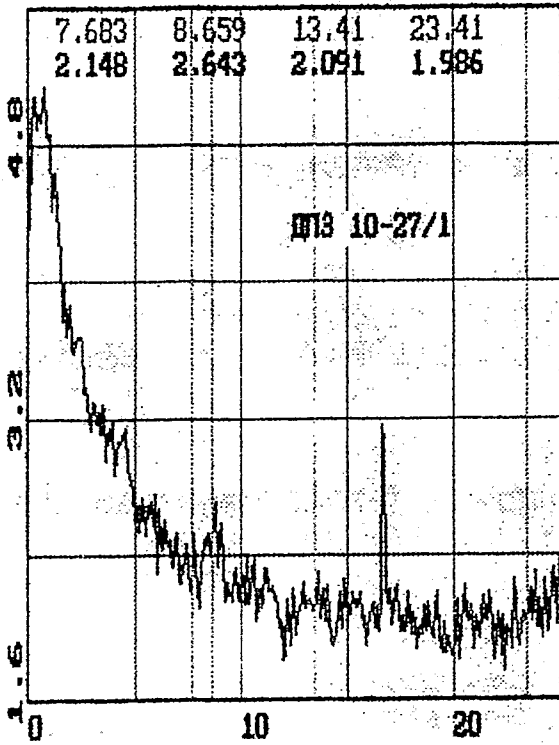
At reviewing APSD on fig. 18 (a, b) it is possible to reach an inference that the resonance peak on frequency ~ 9.0 Hz is very precisely selected in APSD of signals of all seven SPNDs, in 10-27. It means that antinodes of two ASW half-waves on frequency ~ 9.0 Hz generated in two pairs of PCC hot legs, cover whole core volume.

Absolutely in different way peak on frequency ~ 13.0 Hz in APSD represented on fig. 18 (a, b) behaves. So in APSD of signals SPND-1 and SPND-2, located in the bottom of FA 10-27, and also SPND-7, located in a top FA 10-27, peak on frequency ~ 13.0 Hz is selected rather clearly. In APSD of signals SPND-3, SPND-4, SPND-5 and SPND-6, located in middle part of FA 10-27, peak on frequency ~ 13.0 Hz is practically not recognized its amplitude is small. Such situation first can be shown surprising, because of conclusions, made in sections 1.5.2 and 1.5.3 of given reports that on frequencies ~ 9.0 Hz and ~ 13.0 Hz ASWs have inside RPV and inside core identical phase portraits (see fig. 14 and 16). However ASW on frequency ~ 9.0 Hz has not nodes inside core, and ASW on frequency ~ 13.0 Hz has inside core a node of a rather complicated geometric structure. This circumstance is the reason of indicated above effect.

Let's realize now more careful analysis of various spectral characteristics of noise signals of incore and excore neutron detectors on frequencies ~ 6.2 Hz, ~ 9.0 Hz, ~ 13.0 Hz and ~ 18.6 Hz. It is necessary for study of four ASWs phase portraits, definition of geometric structures of their nodes and anti-nodes inside RPV and its core, and also for detection of additional physical processes, which are stipulated by these ASW.

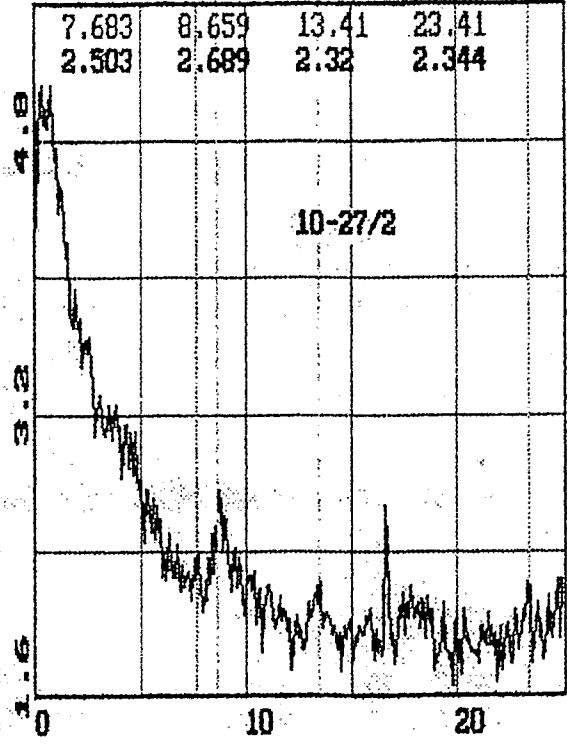
Lg Y

Авто-Спектр



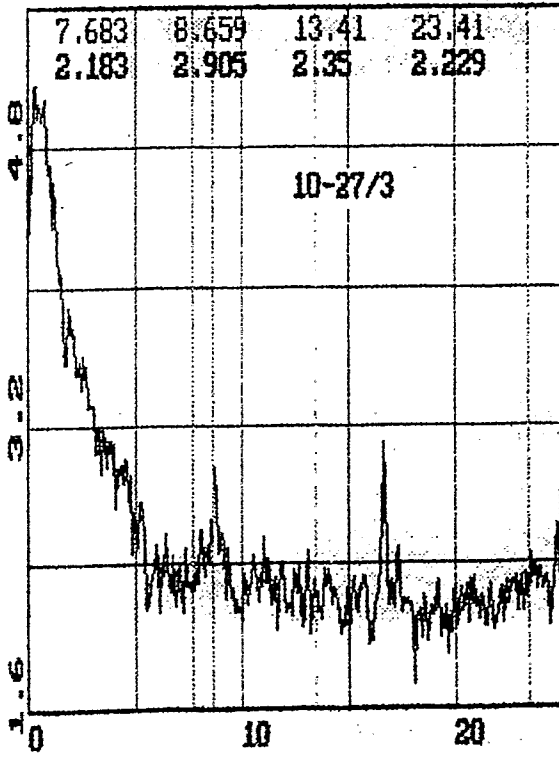
Lg Y

Авто-Спектр



Lg Y

Авто-Спектр



Lg Y

Авто-Спектр

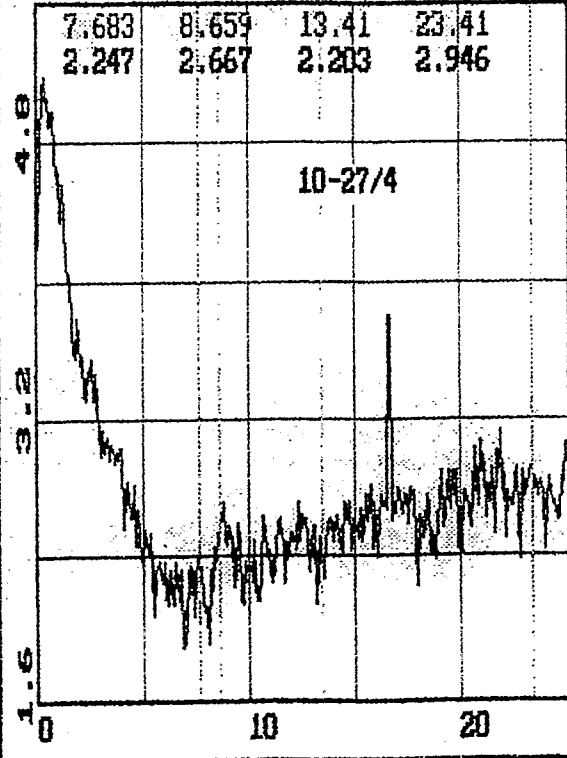
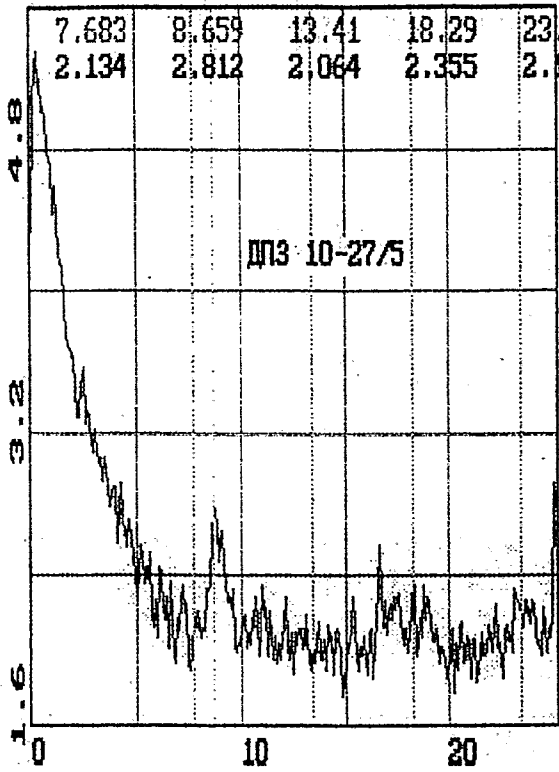


Fig. 18a

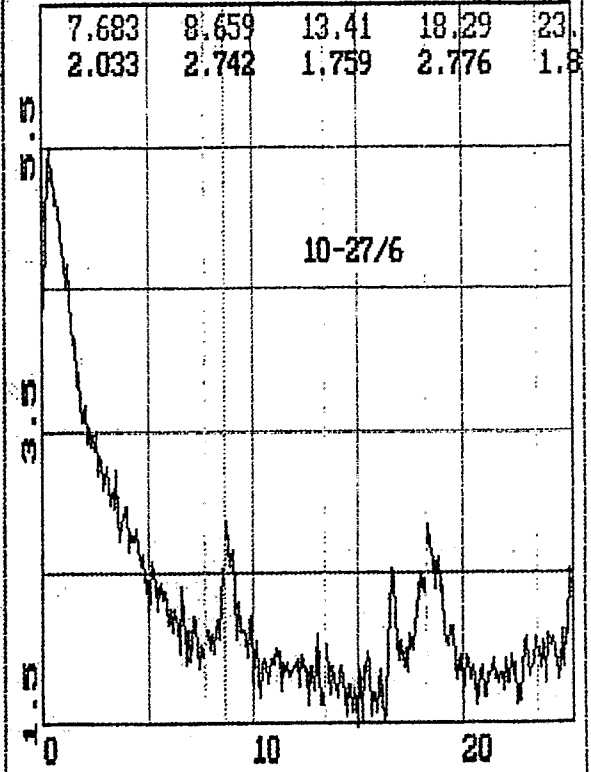
Lg Y

Авто-Спектр



Lg Y

Авто-Спектр



Lg Y

Авто-Спектр

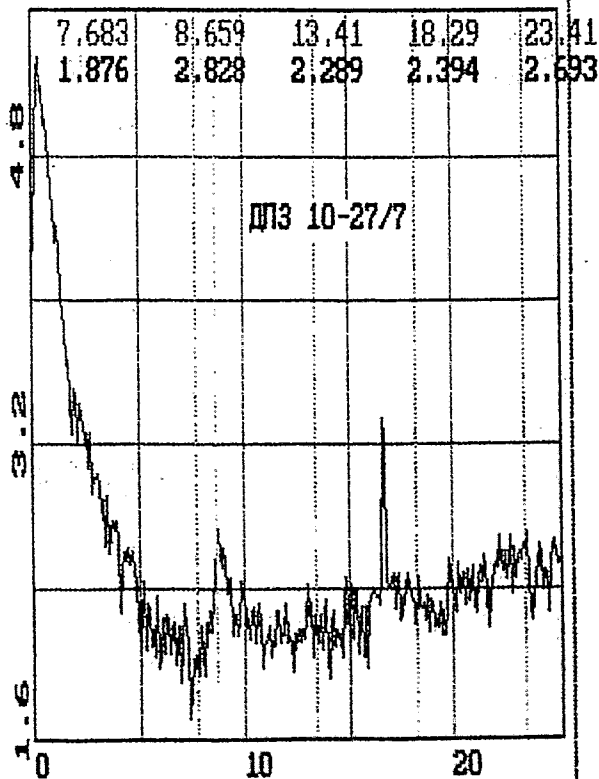


Fig 18b

1.6.1 Analysis of phase characteristics of neutron detectors signals on frequency of 9.0 Hz.

On Figures 19 (a, b, c) functions of coherence and phase characteristics between pairs of signals of incore neutron detectors (1 - 2), (1 - 3), (1 - 4), (1 - 5), (1 - 6), (1 - 7) located in the fuel assembly (10-27) are represented. On each of these Figures from each side from the graphs (curves), representing behavior of coherence function and the phase characteristics for any pair of signals in an association from frequency are reduced three columns of figures. In the first column frequencies of significant resonance peaks in coherence function of defined pair of signals are indicated. In the second and third columns according to value of coherence and phase for each frequency from the first column are represented. The representation of indicated cross spectral characteristics as such tables - columns will always be used hereinafter.

The analysis of results represented on Figures 19 (a, b, c) shows, that the phase shift on frequency of ~ 9.0 Hz between signals of any pair SPND located in FA (10-27) is equal to zero. The similar result took place at realization similar measurements in large number fuel assemblies, installed in various parts of core.

The phase shift on frequency of ~ 9.0 Hz between signals any two SPND located in any two FA of core is equal to zero. As one example on Fig. 20 functions of coherence and phase characteristics between pairs of signals SPND (1-1) and (1-3) located in fuel assemblies (04-37) and (12-37) are represented. Other example is represented on Fig. 21, in which coherence functions and phase characteristics between pairs of SPND signals (5-5) and (7-7) located in fuel assemblies (07-22) and (07-24) are represented.

Above mentioned results definitely indicated on the fact that ASW on frequency of 9.0 Hz generated in PCC of reactor plant in phase revolts density of coolant in whole volume of core.

Interesting is the experimental fact consisting that variance of any SPND signal, measured in narrow frequency band near frequency ~ 9.0 Hz and normalized on quadrate constant component of this SPND signal, does not depend on position of incore neutron detector in core of the reactor pressure vessel. This experimental fact shows that the ASW amplitude on frequency ~ 9.0 Hz does not practically depend on coordinate in limits of whole core volume. This circumstance simultaneously indicated that the nodes of this standing wave are away inside core of the reactor pressure vessel.

These results completely agreed with conclusion which was made in section 1.5.3 of given report. This conclusion shows that the nodes ASW on frequency of ~ 9.0 Hz are in SG region of each loop and one of anti-nodes of this ASW is inside RPV and covers whole core and space above it.

Given ASW has too large length ($\lambda = 110$ meter) considerably exceeding characteristic core sizes. Therefore the amplitude of this standing wave practically does not change in everything its volume. And pressure oscillations in coolant on frequency ~ 9.0 Hz, being in phase with identical amplitude in all core points, cannot excite in particular FA beam oscillation of core fuel assembly.

Thus given ASW produces in core limits only perturbations of coolant density, which reduce to oscillations of neutron flux on frequency ~ 9.0 Hz. This circumstance explains stability, with which the peak on frequency ~ 9.0 Hz exhibits itself in APSD of signals of all seven neutron detectors in FA (10-27), represented on Figures 18 (a, b). As already was mentioned amplitude of peak on the frequency ~ 13.0 Hz, connected with other ASW has not such stability in APSD of signals same seven SPND, located in various points on height of FA (10-27). The reason of such position will be discussed hereinafter.

In section 1.5.3 of given report there was made the conclusion that second ASW anti-node on frequency ~ 9.0 Hz is between RPV and core barrel in part where inlet coolant flows down below separator of streams. For check of this conclusion it is necessary jointly analyze PFT S4 signals, incore and excore neutron detectors on frequency ~ 9.0 Hz from point of view of phase shift between them.

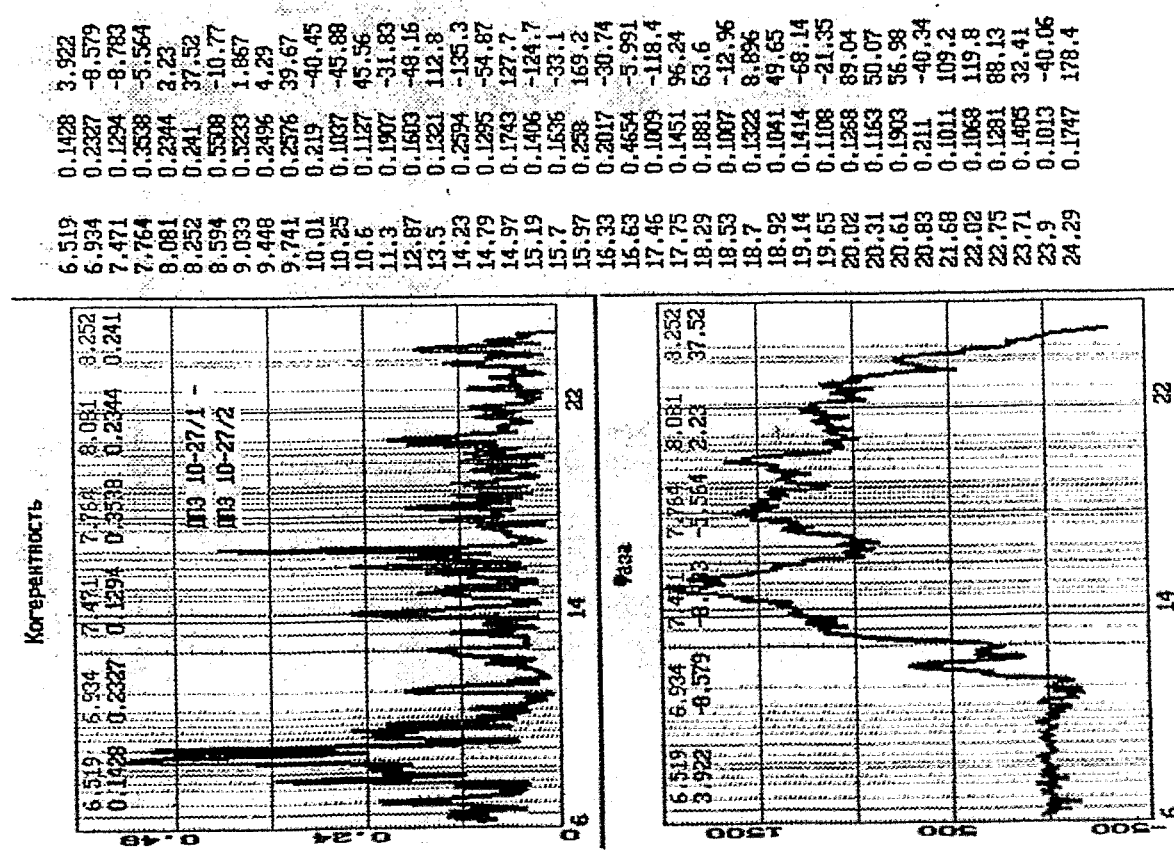
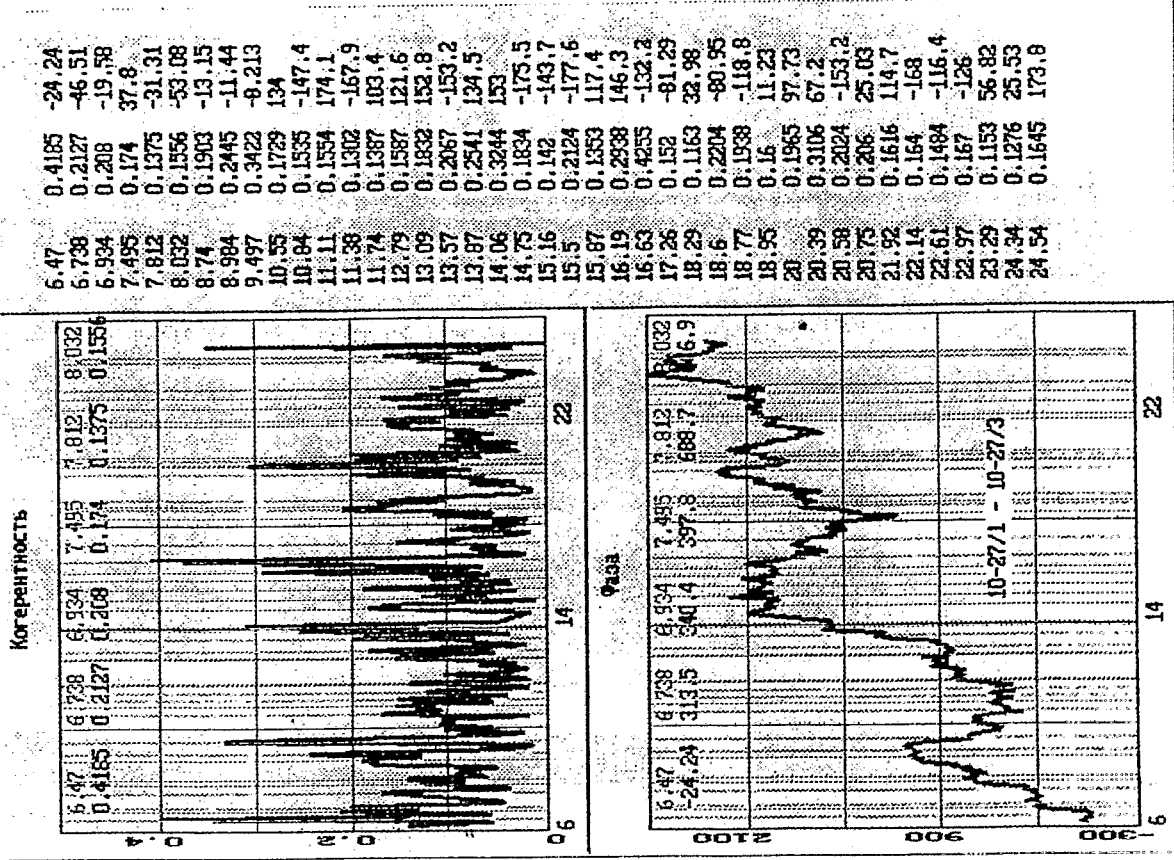


Fig. 19a

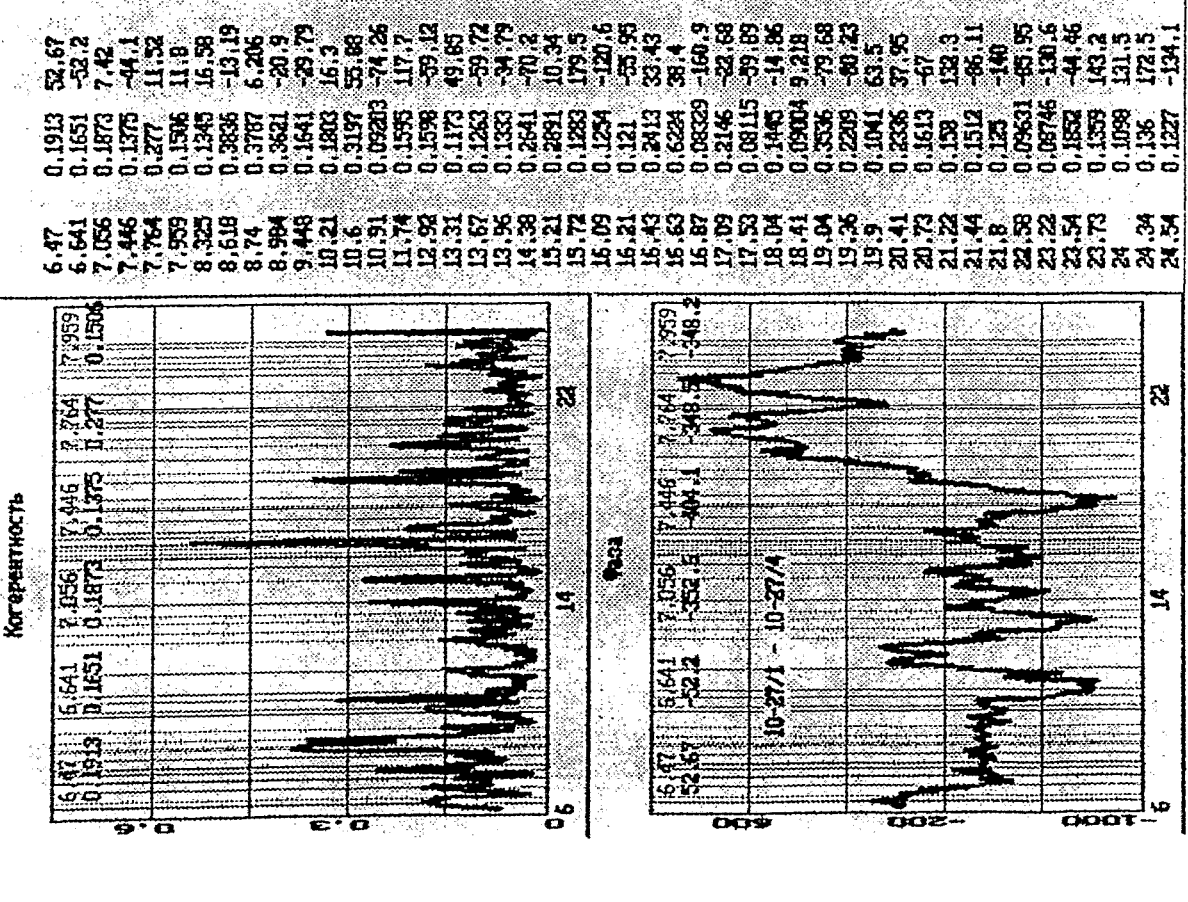
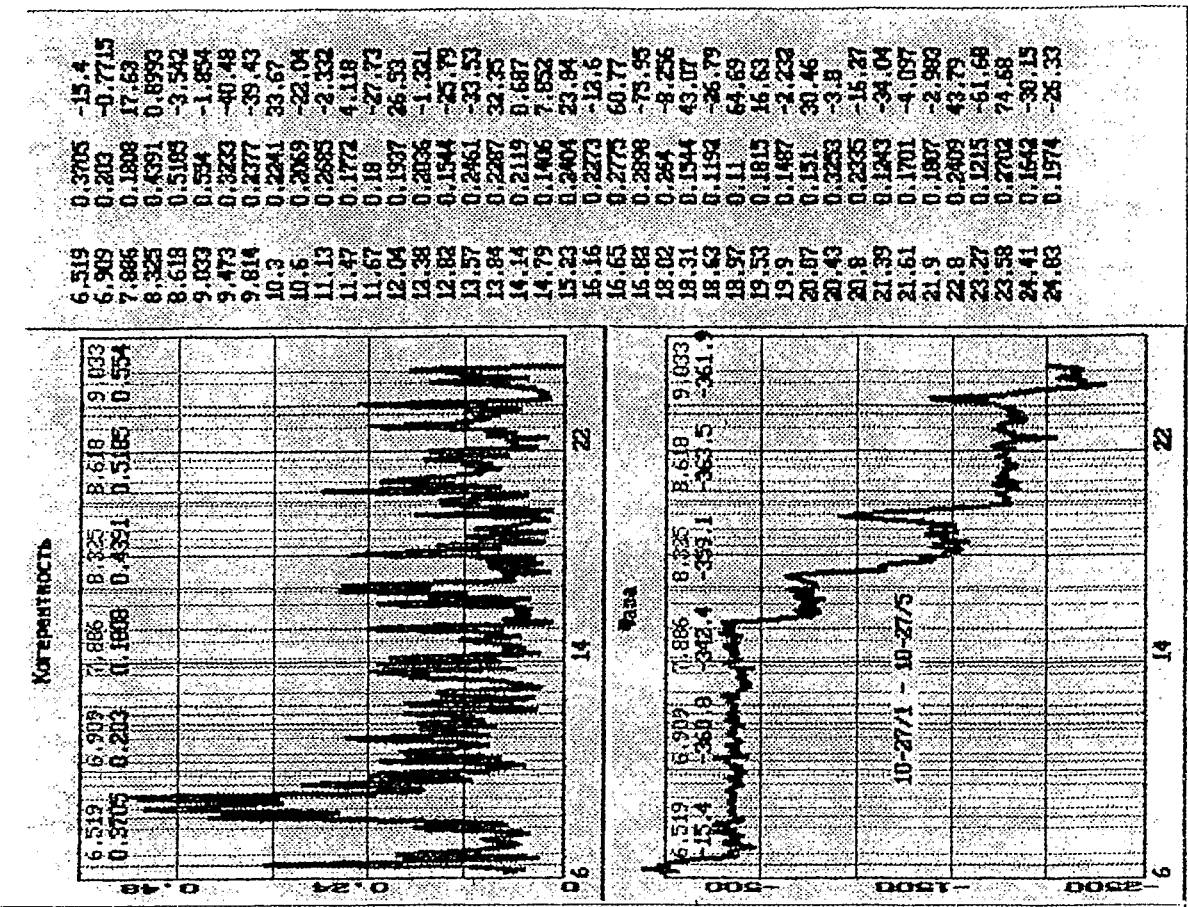
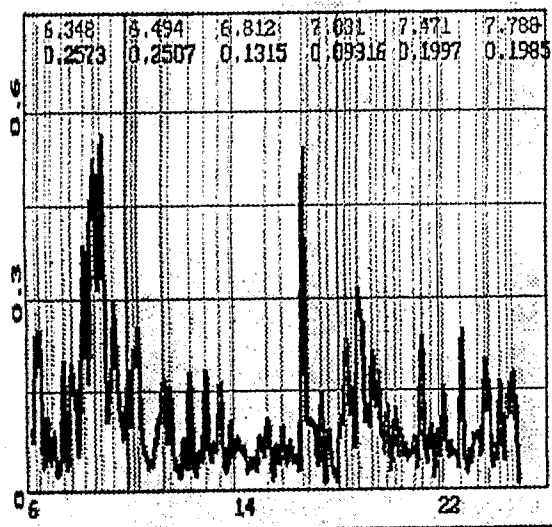
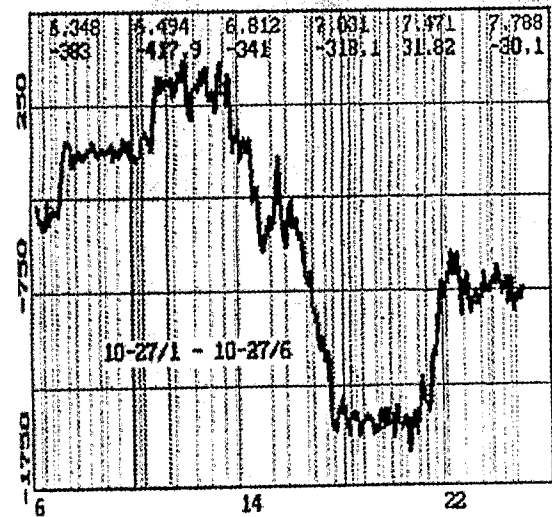


Fig. 19b

Когерентность

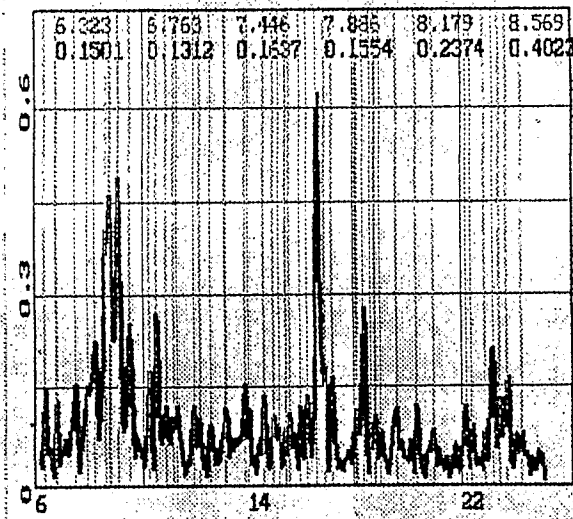


Фаза

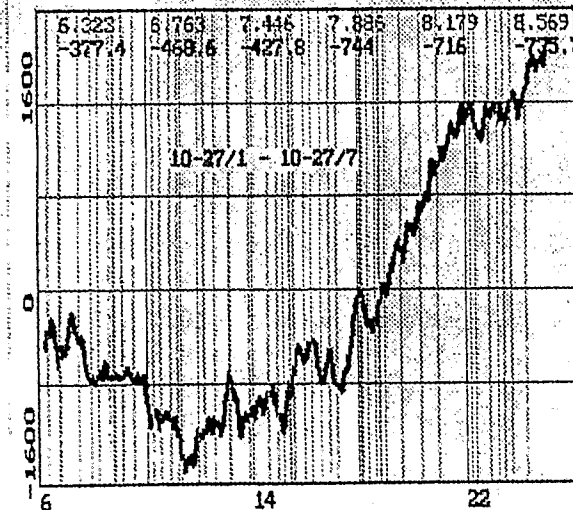


6.348	0.2573	-23
6.494	0.2507	-57.91
6.812	0.1315	19.04
7.031	0.09316	41.92
7.471	0.1997	31.82
7.789	0.1985	-30.1
8.35	0.3963	13.95
8.74	0.5271	4.173
9.033	0.5833	-0.1377
9.473	0.2931	-19.65
10.06	0.1839	-37.18
10.25	0.2207	-34.65
10.42	0.2564	80.54
11.38	0.1783	20.4
11.62	0.157	-60.06
12.35	0.18	-22.93
12.92	0.1844	-86.77
13.48	0.1702	-85.81
13.87	0.1035	85.77
15.23	0.1075	3.608
15.82	0.1014	-156.8
16.63	0.6247	3.623
16.85	0.1105	-119.3
17.31	0.1489	-16.76
17.6	0.09133	-35.22
18.02	0.112	29.32
18.29	0.2453	48.62
18.48	0.1559	40.85
18.73	0.3168	17.3
19.26	0.2177	-33.52
19.51	0.1941	-0.1378
19.87	0.1398	-23.52
20.21	0.1294	-15.66
20.41	0.09051	45.15
20.97	0.09141	87.44
21.24	0.2397	98.92
21.61	0.05854	-10.85
22.09	0.1603	60.86
22.8	0.2587	25.79
23.46	0.1025	-49.46
23.71	0.2018	-32.81
23.88	0.1658	39.81
24.32	0.1734	-1.24
24.58	0.1611	31.57
24.78	0.1877	-40.94

Когерентность

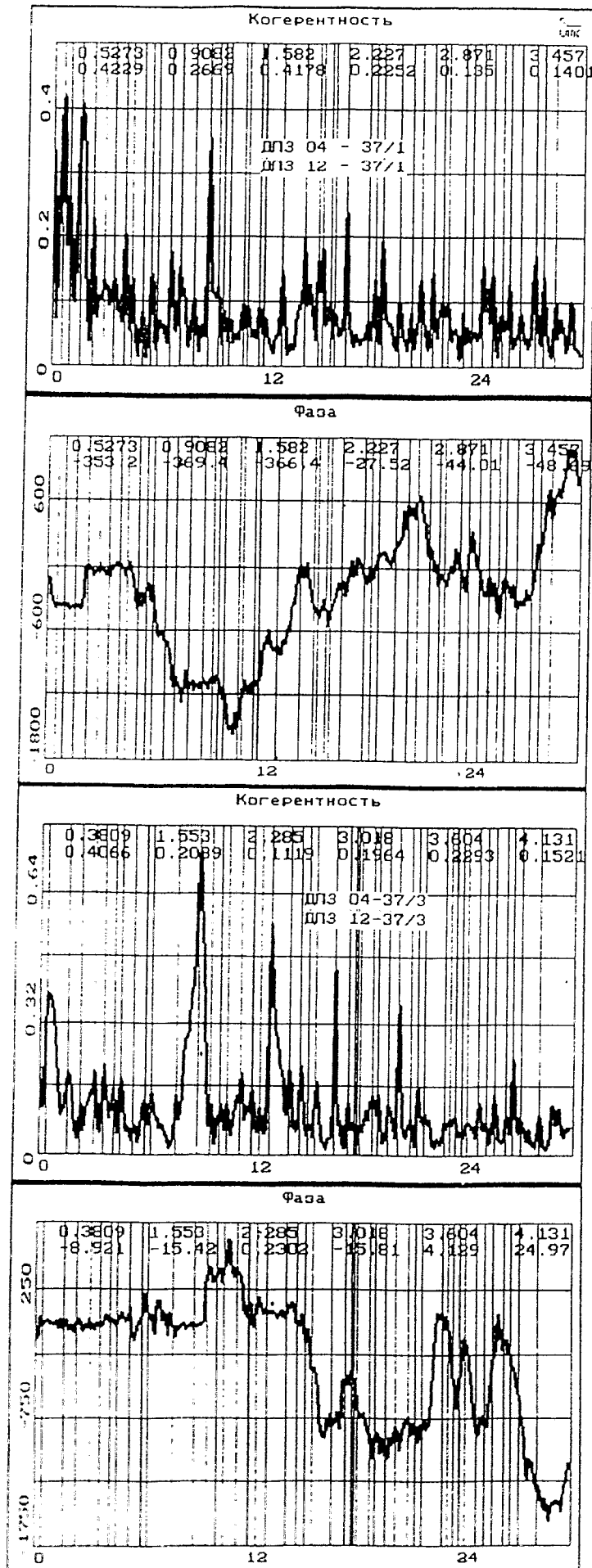


Фаза



6.323	0.1501	-17.38
6.763	0.1312	-108.6
7.446	0.1637	-67.8
7.886	0.1554	-23.99
8.179	0.2374	4.043
8.569	0.4023	-15.69
8.74	0.462	-1.708
9.058	0.4879	16.39
9.473	0.2539	-39.83
10.23	0.1882	49.68
10.5	0.2831	14.24
10.84	0.1211	-2.528
11.08	0.1034	-118
11.25	0.122	31.33
11.87	0.122	-113.4
12.11	0.1047	-82.81
12.5	0.08825	-11.71
13.11	0.118	-67.56
13.82	0.1554	22.77
13.99	0.1215	2.827
14.55	0.1366	-141.1
14.94	0.1101	-1.738
15.11	0.08508	-124.3
15.38	0.08738	-131.2
15.55	0.1085	41.83
15.97	0.1202	106.1
16.24	0.1437	-83.63
16.63	0.7228	-55.4
16.89	0.1809	-154.4
17.16	0.168	-81.63
18.04	0.1118	-11.33
18.33	0.2817	50.95
18.6	0.093	66.31
18.73	0.1088	-74.19
18.97	0.08131	-37.29
19.53	0.1153	-58.85
20.29	0.1247	-62.59
20.87	0.08066	2.959
22.09	0.1208	156.7
22.31	0.08996	-103.1
22.8	0.08542	47.38
23.07	0.2132	73.97
23.34	0.1335	-6.797
23.63	0.1702	-179
24.15	0.08046	-97.87

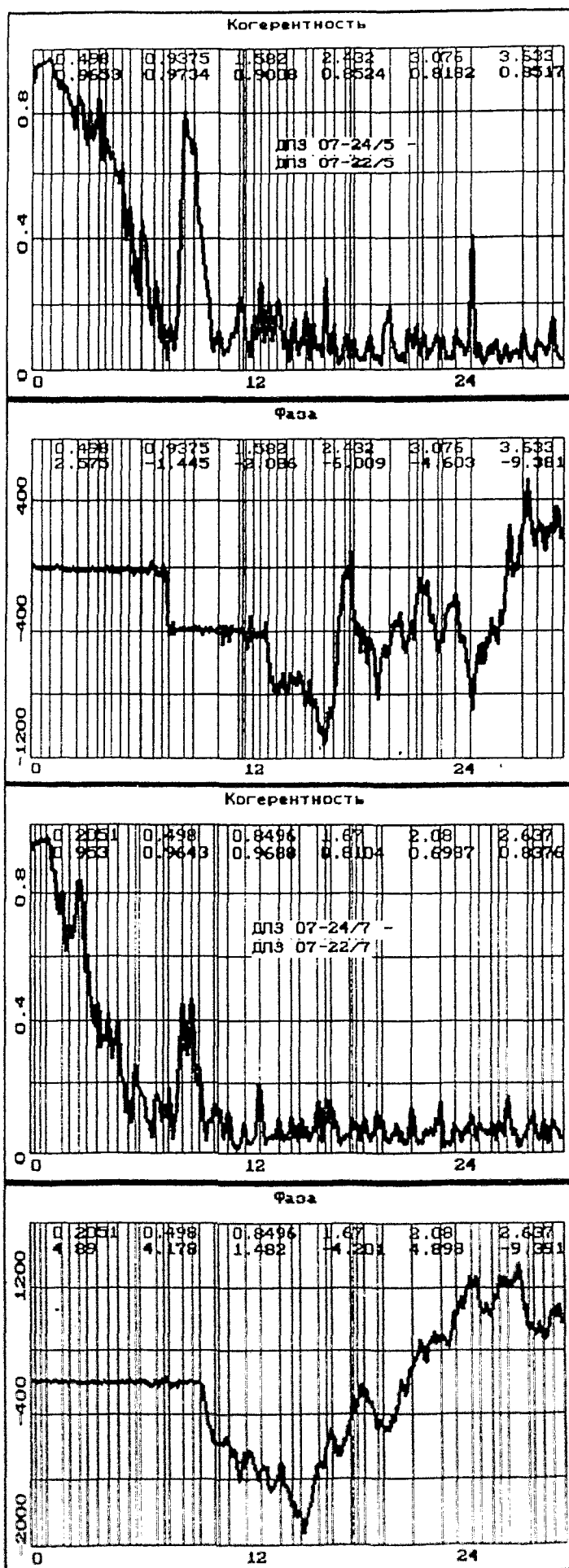
Fig. 19c



0.5273	0.4229	6.768
0.9088	0.2669	-9.436
1.582	0.4178	-6.401
2.227	0.2252	-27.52
2.871	0.135	-44.01
3.457	0.1401	-48.43
4.072	0.2109	-5.61
4.512	0.1394	-8.553
5.068	0.08363	-16.15
5.596	0.1529	-178.3
6.709	0.1918	-1.831
7.207	0.1541	-16.5
8.027	0.112	-60.34
8.848	0.3775	-3.069
9.346	0.1236	10.6
9.697	0.0892	-56.4
10.05	0.07565	-100.2
10.78	0.09564	-61.21
11.04	0.1026	-62.31
11.69	0.09424	-57.09
11.95	0.07483	16.85
12.95	0.1571	-26.35
14.18	0.2002	20.18
14.97	0.1652	-23.63
15.23	0.1863	-103.9
15.67	0.09729	-27.95
15.97	0.08501	-44.92
16.61	0.2451	-144.5
18.22	0.1362	-28.55
18.63	0.195	125.2
19.63	0.111	-174.3
20.27	0.0827	-156.3
20.86	0.1374	-123.9
21.53	0.1474	121.1
22.12	0.1083	-114.4
22.41	0.0992	-105.7
23.29	0.00505	15.24
24.43	0.1632	-10.23
24.99	0.1475	-72.79
25.49	0.07957	-40.9
25.9	0.129	-95.57
26.57	0.08225	24.92
27.39	0.173	135.7
27.92	0.1429	-151.7
28.56	0.1024	117.7

0.3809	0.4066	-8.921
1.553	0.2039	-15.42
2.285	0.1119	0.2302
3.018	0.1964	-15.81
3.604	0.2293	4.129
4.131	0.1521	24.97
4.57	0.1922	2.952
5.303	0.06182	-10.83
5.889	0.1237	58.97
6.328	0.1502	69.19
7.705	0.1363	-23.39
8.936	0.7516	-22.91
9.639	0.1219	-22.71
10.2	0.113	31.5
10.55	0.1123	21.07
11.31	0.1945	-2.477
11.95	0.149	159.4
12.36	0.1021	116.8
12.92	0.5599	92.69
14	0.2186	73.12
14.62	0.2225	-11.18
15.12	0.06796	-82.98
15.5	0.1794	-11.71
16.61	0.4704	-99
17.37	0.1196	-74.14
17.67	0.06627	-25.16
17.99	0.06502	33.84
18.72	0.1411	175
19.04	0.1479	-175.2
19.6	0.1227	53.85
20.16	0.3706	-142.7
20.83	0.08091	-22.23
21.27	0.1615	-101.4
21.68	0.09445	-27.96
22.82	0.07296	85.02
23.14	0.09001	29.35
23.47	0.08796	109
24.11	0.08325	-124.2
24.76	0.1227	-144.6
25.2	0.07199	-97.59
25.66	0.1404	32.56
26.34	0.08586	-138.4
26.69	0.2294	13.66
27.22	0.08217	140.2
28.18	0.08763	103.5

Fig. 20



0.498	0.9653	2.575
0.9375	0.9734	-1.445
1.582	0.9008	-2.086
2.432	0.8524	-6.009
3.076	0.8182	-4.603
3.633	0.8517	-9.381
4.014	0.723	-6.39
4.365	0.6735	7.073
4.951	0.6405	-15.01
5.42	0.4952	-23.7
6.094	0.4519	-27.84
6.855	0.281	16.48
7.324	0.1351	-0.1696
7.705	0.135	-19.74
8.496	0.806	-11.61
9.082	0.7146	-11.09
10.49	0.1257	-6.133
11.63	0.2256	-27.42
11.87	0.1932	-21.86
12.48	0.1667	-39.49
12.89	0.2803	-63.25
13.33	0.2114	-134.8
13.83	0.2307	-38.22
14.36	0.08826	-66.43
14.79	0.1661	29.43
15.47	0.182	-146
15.88	0.1415	-140.7
16.58	0.2858	-17.03
17.08	0.136	-143.7
17.75	0.1096	-42.13
18.31	0.09937	57.5
19.22	0.09821	-101.4
20.27	0.192	165.5
21.36	0.122	-106.5
21.83	0.137	137
22.21	0.1097	-121.2
23	0.09945	-173.1
23.26	0.09654	-89.2
24.05	0.1208	-161.3
24.93	0.4121	-165.7
27.8	0.1173	-110.2
28.62	0.08614	-155.4
29.5	0.1566	-157.1

0.2051	0.953	4.89
0.498	0.9643	4.178
0.8496	0.9688	1.482
1.67	0.8104	-4.201
2.08	0.6987	4.898
2.637	0.8376	-9.391
3.105	0.6085	-7.004
3.633	0.4661	-3.209
4.248	0.4312	5.501
4.805	0.4061	-15.35
5.42	0.1509	-4.717
5.801	0.2628	3.906
6.973	0.1697	-53.77
7.383	0.142	24.05
7.705	0.1959	-53
8.437	0.4495	-3.728
8.994	0.4722	7.77
9.404	0.2582	-34.87
10.22	0.1332	-20.24
10.46	0.1264	-31.94
11.04	0.1126	-57.25
12.86	0.2041	-20.9
13.97	0.09193	76.55
14.71	0.1066	-37.49
15.18	0.105	50.66
16.2	0.1533	66.71
16.61	0.1535	-49.4
16.93	0.1508	95.25
18.16	0.09372	-165.6
18.43	0.08316	130.7
18.84	0.09947	-124.1
19.6	0.1233	126.9
19.89	0.09028	129.3
21.53	0.1258	153.8
23.14	0.1405	-168.2
24.9	0.1096	176.3
25.37	0.08018	-157.6
26.04	0.08036	-139.9
26.46	0.09471	-106
26.95	0.1782	167.3
28.12	0.08679	-13.86
28.39	0.1155	-47.16
28.97	0.09384	-128.3
29.5	0.09814	162

Fig 21

In the Table 5 values of phases shifts on frequency ~ 9.0 Hz between signals of PFT S4 and signals of various SPNDs located in FA (08-17) are represented.

Table 5

Types of two signals	S4-SPND 1	S4-SPND 2	S4-SPND 3	S4-SPND 4	S4-SPND 5	S4-SPND 6	S4-SPND 7
Phase shift on frequency 9.0 Hz	- 105°	- 100°	- 95°	- 114°	- 101°	- 107°	- 111°
Coherence of signals on frequency 9.0 Hz	0.23	0.25	0.29	0.27	0.28	0.25	0.37

It follows from tables, that on frequency ~ 9.0 Hz the signal of each SPND in FA (08-17) is shifted concerning the signal of PFT S4 on magnitude 100° . The magnitude of phase shift between the signal S4 and signals of all SPNDs, located in other fuel assembly, on frequency ~ 9.0 Hz will have the same value. This phase shift is stipulated only by phase characteristic of transfunction of the reactor vessel, defining character of pressure influence in core coolant through reactivity on neutron flux. Really, the pressure oscillations on frequency ~ 9.0 Hz in core coolant of the reactor vessel and hot leg of fourth loop pipeline in installation site of PFT S4 are in phase and density oscillation of coolant on this frequency in space between RPV and its core barrel is lower streams separator do not render the influence on neutron flux in any core point. Thus, harmonic component on frequency ~ 9.0 Hz in signal of any incore neutron detector is stipulated only by one physical process, connected with perturbation of coolant density in core on this frequency. Other situation takes place for signals of excore neutron ionization chambers IC-21, IC-14 and IC-7 located outside RPV. The harmonic component in them on frequency ~ 9.0 Hz is stipulated by two physical processes. Each of them with appropriate amplitude and phase will give the contribution to the full harmonic component of any ionization chamber signal on frequency ~ 9.0 Hz.

The first process is connected with perturbation of coolant density on frequency ~ 9.0 Hz in core of the reactor vessel. Therefore one component in signal of any IC current on frequency ~ 9.0 Hz stipulated by such process will be shifted on phase on an angle 100° rather harmonic component in the signal PFT S4 on indicated frequency.

The second process is connected with perturbation of coolant density on frequency ~ 9.0 Hz in space between RPV and its core barrel below streams separator. The second process can be in anti-phase or in phase in relation to the first process. Therefore other component in signal of any IC current on frequency ~ 9.0 Hz stipulated by the second process, will be shifted on phase on 180° or on 0° rather harmonic component in signal S4 on this frequency. Our task is to determine, which of these two mutually eliminating each other variants is realized actually.

Before results of measurements reviewing it is necessary to pay attention to one extremely important circumstance.

The full harmonic component on frequency ~ 9.0 Hz in the current signal of any IC formed by two separate harmonic components, will be certainly shifted on phase of rather harmonic component in signal PFT S4 on this frequency. The magnitude of such phase shift will be determined not only by value of phase at each of two components, which will form this harmonic component. This phase shift will also depend on amplitudes of two indicated components, forming the full harmonic component, with respect to their ratio to each other. For this reason such phase shift can accept any value, different from 0° , 90° and 180° , and continuously change in case of relation modification between amplitudes of two harmonic components on any defined frequency, which form on this frequency the resulting signal. The given feature in behavior of harmonic signal phase stipulated by two various physical processes, will be used hereinafter at identification FA beam oscillations of fuel assemblies under operation of ASW series.

We shall return to results of our measurements. Values of phase shifts on frequency ~ 9.0 Hz between signals of three various excore neutron IC (IC-21, IC-14 and IC-7) and signals of various incore detectors (SPND) installed in FA (08-31) are represented in tables 6, 7, 8.

Table 6

Types of two signals	<u>IC-21</u> 1(08-31)	<u>IC-21</u> 2(08-31)	<u>IC-21</u> 3(08-31)	<u>IC-21</u> 4(08-31)	<u>IC-21</u> 5(08-31)	<u>IC-21</u> 6(08-31)	<u>IC-21</u> 7(08-31)
Shift of phase on frequency ~9.0 Hz	85°	79°	86°	81°	83°	87°	78°

Table 7

Types of two signals	<u>IC-14</u> 1(08-31)	<u>IC-14</u> 2(08-31)	<u>IC-14</u> 3(08-31)	<u>IC-14</u> 4(08-31)	<u>IC-14</u> 5(08-31)	<u>IC-14</u> 6(08-31)	<u>IC-14</u> 7(08-31)
Shift of phase on frequency ~9.0 Hz	25°	21°	31°	19°	27°	20°	26°

Table 8

Types of two signals	<u>IC-7</u> 1(08-31)	<u>IC-7</u> 2(08-31)	<u>IC-7</u> 3(08-31)	<u>IC-7</u> 4(08-31)	<u>IC-7</u> 5(08-31)	<u>IC-7</u> 6(08-31)	<u>IC-7</u> 7(08-31)
Shift of phase on frequency ~9.0 Hz	53°	58°	55°	56°	52°	55°	55°

Phases shifts closed on values on frequency ~ 9.0 Hz were observed also between signals of three various IC and signals of various SPNDs located in other fuel assemblies. Results represented in tables 6, 7, 8, are obtained at high values of coherence, which varied in range from 0.3 till 0.8.

Values of phase shifts on frequency ~ 9.0 Hz between signals of various IC at rather large value of coherence (~ 0.5) on this frequency are represented in the Table 9

Table 9

Types of two signals	<u>IC-21</u> IC-14	<u>IC-14</u> IC-7	<u>IC-21</u> IC-7
Shift of phase on frequency ~ 9.0 Hz	50°	30°	14°

The share analysis of phase shifts values represented in tables 6, 7, 8, 9 indicates, that ASW anti-node on frequency ~ 9.0 Hz is in space between RPV and its core barrel below streams separator. This anti-node is in anti-phase to other anti-nodes of this ASW, covering core and space above it. It penetrates downwards between RPV and its core barrel on the whole core height. Apparently both anti-phase anti-nodes form horizontal plane with nodes ASW on frequency ~ 9.0 Hz in place of their touch under core. The behavior pattern of ASW phase on frequency ~ 9.0 Hz inside RPV in cross-section, made by vertical plane, made through RPV vertical axes, is schematic represented on fig. 22.

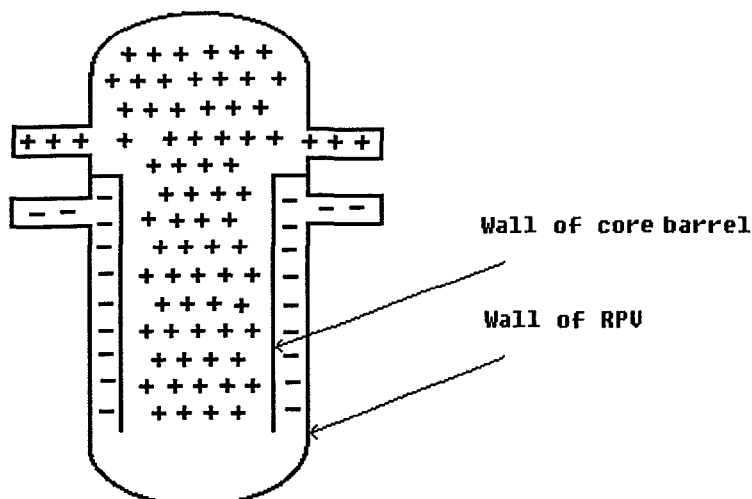


Fig. 22

Values of phase shifts between various signals represented in tables 6, 7, 8, 9 shows that the ASW amplitude on frequency ~ 9.0 Hz is not constant in space between RPV and its core barrel. The pattern of amplitude modification of this ASW at moving on a circle in horizontal plane between RPV and its core barrel is qualitatively represented on fig. 23. The character of ASW amplitude modification on frequency ~ 9.0 Hz represented on fig. 23 is possible to explain by lack of full azimuthal symmetry at pipelines mounting of various loops to RPV.

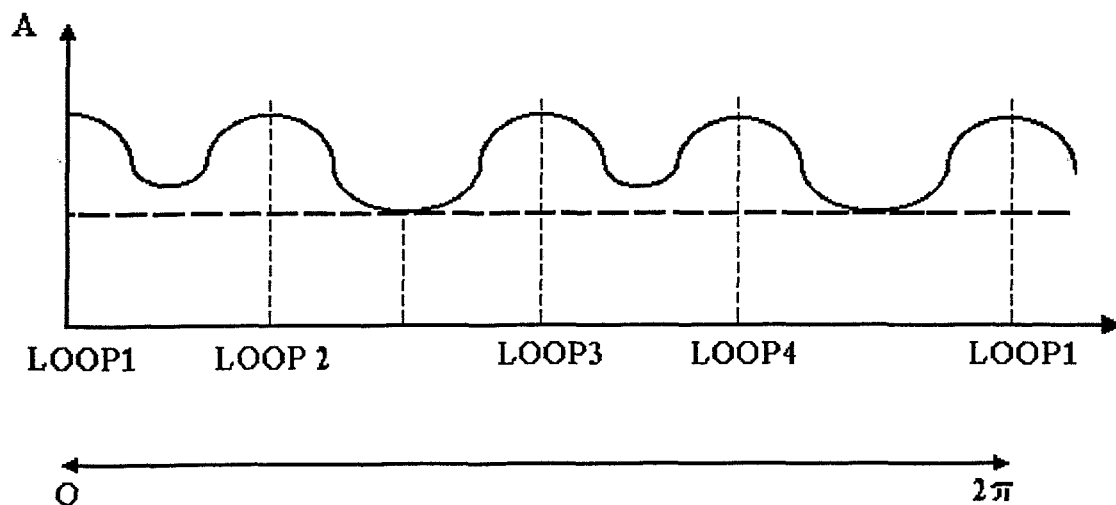


Fig.23

1.6.2 Analysis of phase characteristic of neutron detectors signals on frequencies of ~ 6.0 Hz, ~ 13.0 Hz, ~ 19.0 Hz.

In section 1.5 of given report it was made conclusion that ASW on frequencies of ~ 6.0 Hz, ~ 13.0 Hz, ~ 19.0 Hz have inside RPV a common node, possessing a rather complicated three-dimensional geometric structure. As affirmed earlier in this section of the report one first group of these ASW nodes, located inside RPV, should be placed on horizontal plane of RPV perpendicular axes. At moving through this horizontal plane only ASW phase on frequency ~ 13.0 Hz changes the value on 180° . Thus the phase of standing waves on frequencies of ~ 6.0 Hz and ~ 19.0 Hz does not change the value. This circumstance should be used hereinafter to place a position of a horizontal plane with nodes of the first group inside RPV on coolant flow direction.

In section 1.5 of the report also affirmed, that second group of nodes for ASW on frequencies of ~ 6.0 Hz, ~ 13.0 Hz, ~ 19.0 Hz will place inside RPV on four vertical planes, which divide whole volume inside RPV and its core on four identical sectors, contiguous to various RP loops. At moving through any such vertical plane from one sector in an adjacent sector the ASW phase on frequency ~ 13.0 Hz should not change the value (see Figure 14), and the ASW phase on frequencies of ~ 6.0 Hz and ~ 19.0 Hz should vary on 180° (see Figures 11 (b) and 15).

We shall assume, that four indicated above vertical planes with node points of the second group really exist. Then inside core ASW amplitude on frequency for example ~ 13.0 Hz, will vary identically and greatly in any horizontal crosssection in radial and azimuthal directions in limits of each sector. Such space modification of this ASW amplitude will lead with rise of oscillating force, influencing on each fuel assembly (FA) on frequency ~ 13.0 Hz in horizontal direction, perpendicular of its vertical axes. The given force will oscillate in a phase with pressure (density) oscillation in the core coolant on this frequency and it will be the reason of FA beam vibrations, fixed with two ends, on frequency ~ 13.0 Hz. The vibration of each FA can happen in one, two and three directions, on which the rigidity of FA is minimum. FA displacement from a position of an equilibrium during vibrations on each of these three directions will be shifted on a phase on 180° concerning perturbation of pressure in the core coolant on frequency ~ 13.0 Hz. It is supposed, that the pressure oscillations in the coolant on this frequency are in a phase in whole core volume. This supposition hereinafter will be confirmed experimentally. The amplitude of concrete FA displacement in one of indicated directions under influence of oscillating force will depend on derivative value on this direction at ASW amplitude on the given frequency in a place of this FA arrangement. It will also depend on an axial coordinate and have various values in various points on FA height. The amplitude of its displacement in any direction will be very small or is equal to zero in upper and bottom of FA near to points of its fixing. This circumstance will be used hereinafter at the interpretation of measurements results.

Any FA displacement during its forced vibrations, for example in direction, where its amplitude is maximum, will caused appropriate perturbation in current signals of all seven SPNDs, located in this FA, on frequency ~ 13.0 Hz. This perturbation will define one first harmonic component in full signal of each SPND on frequency ~ 13.0 Hz. In signals of all seven FA SPNDs it will be in a phase or in anti-phase concerning pressure oscillation in the core coolant on frequency ~ 13.0 Hz. The neutron flux derivative sign in a place of the FA arrangement in direction of its displacement will determine a concrete value of first harmonic phase component among those two values (0° or 180°), which were indicated above. In a series of cases an elimination is possible. It will arise, when the neutron flux derivative in a place of the FA place on direction of its displacement will change the sign at moving from one any SPND to following on FA height. However given circumstance will not have an essential value and will not affect on results of our consequent reasoning.

Other second harmonic component in full current signal of each SPND, located in FA, on frequency ~ 13.0 Hz will be stipulated by pressure (density) perturbation of the coolant on this frequency. This perturbation is in phase in all core points. In signals of seven SPNDs second harmonic component will be in a phase, shifted on some angle \ominus° concerning pressure oscillation in the core coolant on frequency ~ 13.0 Hz.

The magnitude of this phase shift will be determined by a phase characteristic of reactor vessel transfunction on the given frequency, quantitatively describing perturbation transposition from pressure to neutron flux through a reactivity. The phase of full harmonic component on frequency ~ 13.0 Hz in signal of each SPND, formed by two harmonic components on indicated frequency rather basic harmonic signal, connected to pressure perturbation in the core coolant on frequency ~ 13.0 Hz, will depend not only from a value of phase shift each of them separately. The value of this phase will be determined also by amplitudes ratio of two harmonic component, forming a full component in SPND signals on this frequency.

The amplitude of first harmonic component will have various value in signals of seven various SPNDs, located in FA. It is connected to various magnitude of its displacement in various horizontal crosssections on core height. Only in signals of incore neutron detectors SPND-1 and SPND-7, located in region of the lower and upper FA mountings, the magnitude of first harmonic component will be very small or is equal to zero, and the full harmonic component on frequency ~ 13.0 Hz in signals of these SPND will be determined extremely by second harmonic component on this frequency. For this reason the signals SPND-1 and SPND-7 in any FA will be in phase on frequency ~ 13.0 Hz, if horizontal plane with nodes of the first group for ASW on frequencies ~ 6.0 Hz, ~ 13.0 Hz, ~ 19.0 Hz will be placed outside core. Only the signals of these two extreme SPNDs can be used for check of ASW phase portraits on frequencies ~ 6.0 Hz, ~ 13.0 Hz, ~ 19.0 Hz inside core and for evaluation of their nodes position.

The amplitude of second harmonic component in a full signal of SPND, located in any FA on frequency ~ 13.0 Hz will depend also on its height position. Therefore at moving up inside some FA and moving from SPND -1 to SPND-2 and further sequentially to other SPNDs, located on its height, phase of full harmonic component on frequency ~ 13.0 Hz in signals of these incore neutron detectors will vary under complicated law and accept values, distinguished from values of phases, equal 0° , 90° and 180° , which traditionally used for interpretation of results of noise signals measurement. The given situation is similar to that, which was observed earlier in signals excore neutron IC on frequency ~ 9.0 Hz and was described in the previous section of the given report.

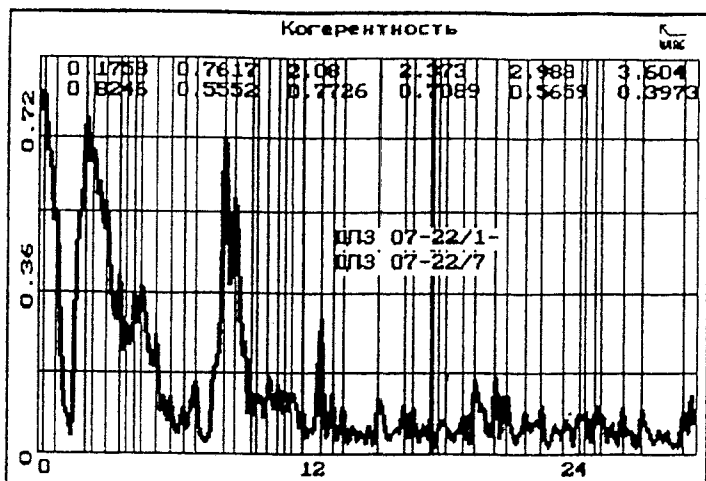
The similar character of action on all SPND signals, located in FA will take place from ASW on frequencies ~ 6.0 Hz and ~ 19.0 Hz. It can be shown with the help of reasoning, similar themes, which were described above on the example of ASW action on frequency ~ 13.0 Hz on these signals. It is necessary to take into consideration, that oscillations of pressure in the core coolant on frequencies ~ 6.0 Hz ~ 19.0 Hz in two adjacent sectors happen to a shift of a phase, equal 180° .

We shall pass now to show the experimental measurements. Function of a coherence and phase characteristic of SPND (7-1) and (7-3) signals, located in FA 07-22 are represented on fig. 24. Values of a coherence and phase for various frequencies are represented on the same figure. Equality to zero of phase shift on frequency ~ 12.92 Hz at a value of a coherence 0.3 between SPND 1 and 7 signals, located in various ends of FA 07-22, indicates on the fact, that the horizontal plane with nodes of the first group is outside of limits core. This result is confirmed also by results of similar measurements, carried out with use upper and lower SPND, located in other fuel assemblies.

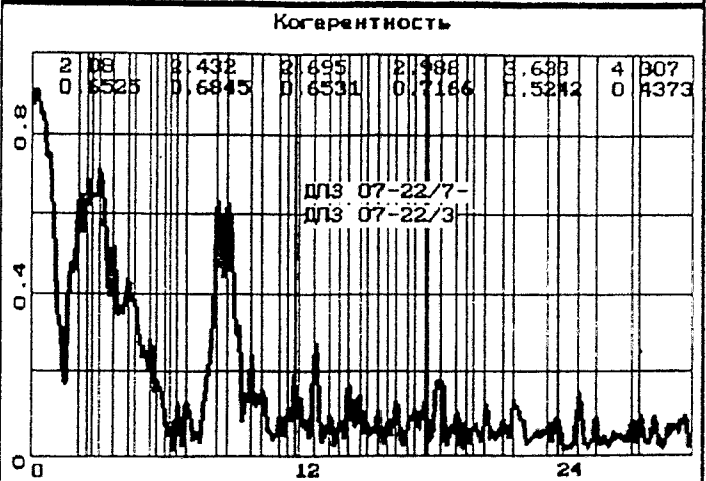
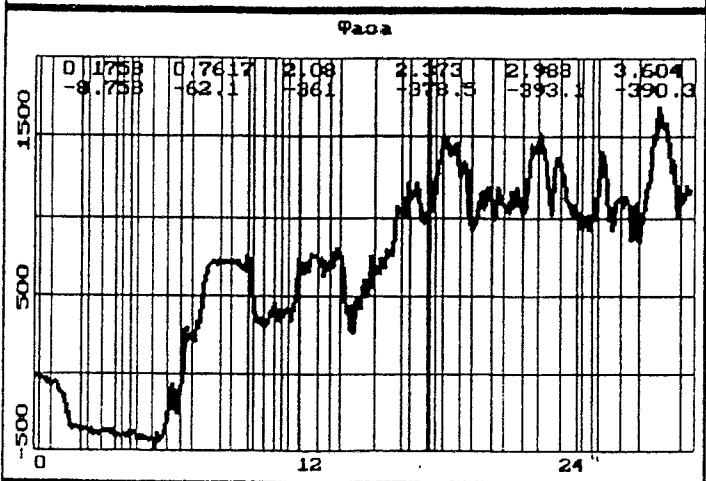
As one more example we shall describe a result, represented on fig. 19 (c), where is shown, that a phase shift on frequency ~ 13.0 Hz between signals SPND 1 and 7, located in FA 10-27, is equal to zero.

Represented results allows us to assume, that the horizontal plane with nodes of first group is located under core and coincides with a horizontal plane under core, on which ASW nodes on frequency ~ 9.0 Hz, formed during interaction of two anti-phase anti-nodes this ASW.

We are converted again to results, represented on fig. 24. They indicate on the fact, that the signals SPND 1 and 7, located in FA 07-22, are also in a phase on frequencies ~ 6.0 Hz and ~ 18.5 Hz. It confirms an earlier made conclusion that the full harmonic component in signals SPND 1 and 7, located in any FA, on frequencies ~ 6.0 Hz, ~ 13.0 Hz and ~ 19.0 Hz will be determined only by second harmonic component on these frequencies.



0.1758	0.8246	-8.758
0.7617	0.5552	-62.1
2.08	0.7726	-0.9686
2.373	0.7089	-18.49
2.988	0.5659	-33.08
3.604	0.3973	-30.29
3.926	0.3005	-41.12
4.277	0.3563	-40.19
4.629	0.3954	-75.28
5.303	0.2674	-65.29
6.006	0.1219	-29.9
6.621	0.09974	-123
7.178	0.1583	-106.8
8.496	0.7195	-2.902
8.965	0.5698	12.21
9.727	0.1373	22.28
9.99	0.132	22.86
10.49	0.1846	-28.97
10.93	0.1619	61.49
11.25	0.1444	14.84
11.54	0.1416	29.53
12.07	0.09636	-30.11
12.92	0.3056	-6.8
13.45	0.1294	-30.33
13.92	0.1004	55.86
15.5	0.1248	-37.2
16.67	0.1049	-28.22
17.02	0.0968	34.85
17.81	0.07123	-45.95
18.25	0.07486	158
18.54	0.07358	12.13
19.34	0.08177	-164.9
19.86	0.1632	-127.5
20.8	0.1825	-53.95
21.36	0.128	-29.49
22.18	0.08945	-54.13
22.91	0.1061	76.09
24.73	0.08437	-82.05
25.02	0.092	-121.4
25.49	0.105	-97.11
25.78	0.08699	164.7
26.75	0.09996	44.48
27.63	0.09353	146.5
29.5	0.0926	36.07



2.08	0.6525	5.524
2.432	0.6845	-0.4922
2.695	0.6531	-17.56
2.988	0.7166	-23.02
3.633	0.5242	-36.51
4.307	0.4373	-22.54
4.629	0.391	-60.62
5.303	0.2807	-56.94
5.654	0.1828	-52.32
6.24	0.07626	-15.24
6.562	0.1255	-112.9
7.031	0.1278	-105.9
8.467	0.6301	-1.381
8.936	0.6383	12.83
9.961	0.2403	44.68
10.46	0.1682	-6.898
11.22	0.09063	30.43
11.6	0.1076	-21.29
11.89	0.1889	165
12.19	0.1415	-7.393
12.89	0.2763	-8.356
13.56	0.09239	105.5
14.03	0.08423	82.09
14.44	0.1727	-139.4
14.94	0.1383	-65.89
15.26	0.07637	-97.06
15.7	0.1026	161.7
16.14	0.08112	162.9
16.52	0.1412	-18.96
17.08	0.08917	-27.72
17.37	0.1193	-51.69
17.81	0.1256	166.1
18.54	0.2083	-125.3
19.25	0.09903	1.563
19.69	0.07518	-13.22
20.04	0.07318	78.75
20.6	0.1106	127.1
21.42	0.09347	147.2
21.88	0.1428	93.49
23.47	0.07949	131.5
23.88	0.09092	15.42
24.93	0.1529	-21.22
25.75	0.09086	-150.7
27.36	0.07945	-43.6
27.74	0.09826	-108.3

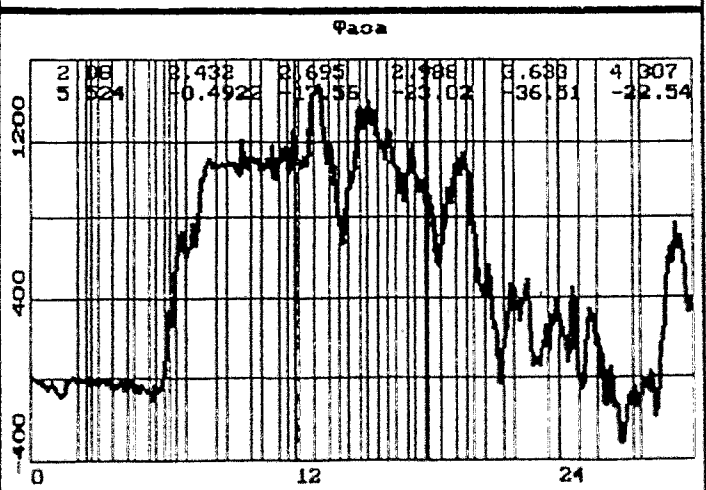


Fig 24

One example of existence two harmonic component, shifted on a phase and which have various amplitudes, in a full harmonic component of signals SPND-2, SPND-3, SPND-4, SPND-5 and SPND-6, located in FA 10-27, on frequency ~ 13.0 Hz is represented in the Table 10.

Table 10

Types of signals in FA (10-27)	SPND (1) 1-2 SPND (2)	SPND (1) 1-3 SPND (2)	SPND (1) 1-4 SPND (2)	SPND (1) 1-5 SPND (2)	SPND (1) 1-6 SPND (2)	SPND (1) 1-7 SPND (2)
Phase shift on frequency 13.0 Hz	+ 48°	+ 134°	+ 59°	+ 33°	+ 85°	+ 22°
Coherence on frequency 13.0 Hz	0,16	0.25	0.13	0.24	0.17	0.16

This table is composed by results of signals SPND in FA (10-27) noise measurement, which are represented on Figure 19 (a, b, c). Phases shifts, represented in it for various pairs of SPND signals on frequency 13.0 Hz, definitely indicate existence of forced beam oscillations FA (10-27) under influence of ASW, generated on this frequency. However such beam oscillation of FA are possible only at presence of gradients inside core at amplitude ASW on frequency 13.0 Hz in radial and azimuthal directions, that indirect on existence inside core of four vertical planes with nodes of the second group for given ASW in its turn.

Other example of a similar type, verifying existence of FA beam oscillation on frequency 6.0 Hz, listed in the Table 11.

Table 11

Types of signals in AF (10-27)	SPND (1) 1-2 SPND (2)	SPND (1) 1-3 SPND (2)	SPND (1) 1-4 SPND (2)	SPND (1) 1-5 SPND (2)	SPND (1) 1-6 SPND (2)	SPND (1) 1-7 SPND (2)
Phase shift on frequency of 6.0 Hz	+ 1.0°	+ 7.5°	+ 92°	+ 117°	+ 116°	+ 4.1
Coherence on frequency of 6.0 Hz	0,19	0.17	0.20	0.20	0.20	0.12

Results, represented in this table, also indirectly indicate on existence inside core of four vertical planes with nodes of the second group for ASW on frequency of 6.0 Hz.

We are converted now to Fig. 20. Results, represented on it show, that a phase shift a between a signal SPND-1 in FA (04-37) and signal SPND-1 in FA (12-37) makes 180° on frequencies of 6.0 Hz and 19.0 Hz, and on frequency 13.0 Hz this shift is equal to zero.

The FA (04-37) and (12-37) are in adjacent core sectors of the reactor vessel, contiguous to two adjacent loops.

The analysis of results, represented on Figure 21, shows that in difference from the previous case phase shift between signal SPND-7 in FA (07-22) makes approximately 0° on frequencies of 6.0 Hz and 13.0 Hz. The disposition of FA (07-24) and FA (07-22) in one core sector, contiguous to one loop, is the reason of this difference.

Two last results directly and finally confirm a behavior pattern of ASW phase on frequencies of 6.0 Hz, 13.0 Hz and 19.0 Hz inside RPV represented on Figures 11 (b), 14 and 15 and prove existence of four vertical planes with nodes of the second group, which are represented on these three Figures.

We shall say in summary a few words about a character of phase shift in signals of various SPNDs rather signal SPND-1 in FA (10-27) on frequency 13.0 Hz. The values of these phase shifts are represented in the Table 10. They indicate that the amplitudes ratio of two various harmonic components, shifted on phase from each other and forming a full harmonic component on frequency 13.0 Hz in signal of any SPND, is essential vary at move from SPND-2 to SPND-3 and further to other SPND on height of FA (10-27). It is possible the case, when the amplitude of full harmonic component of signal SPND on frequency, for example, 13.0 Hz, formed by two

mentioned above harmonic components, will be small than amplitude of each in individuality. Behavior character of peak amplitude on frequency 13.0 Hz in APSD of various SPND signals in FA (10-27) which are represented on Figure 18 (a, b) it is follows to explain just by this circumstance.

Conclusions

Some results of pressure oscillations, incore and excore of neutron noises investigations on reactor plant VVER-1000 of the Kalinin NPP unit 1 were represented in this part of the report.

The analysis of signals noise of three pressure fluctuation transducers (PFT), installed in pipelines of two adjacent PPC loops, allowed to determine the forms of ASW series, corresponding to four minimal eigenfrequencies of pressure oscillations in coolant and determine three-dimensional space structure of their nodes and anti-nodes inside RPV and its core.

The analysis of pressure noises in pipelines has enabled to look inwards RPV and define a pattern of phase modification for all four ASW inside core and in space between RPV and its core barrel below streams separator.

The space form ASW node on frequencies of 6.0 Hz, 13.0 Hz and 19.0 Hz reduces to emerging of space gradients at amplitudes of these standing waves in radial and azimuthal directions inside core. It was the reason of forced beam oscillations of fuel assemblies, fixed in their upper and lower sides, under influence of ASW on indicated above frequencies.

All obtained results were confirmed by measurements of noise of incore and excore neutron detectors.

References

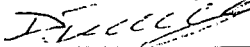
1. Bulavin, V.V., D.F. Gutsev and V.J. Pavelko (1995). The experimental definition of the acoustic standing waves series, formed in the coolant of the primary circuit of VVER-440 type reactor. *Progr. Nucl. Energy*, 29, n 3/4, 153-170.
2. Turcan E. (1982). Review of Borssele PWR noise experiments, analysis and instrumentation. *Progr. Nucl. Energy*, 9, 437-452.
3. Grunwald, G., Junghanss and P. Lievers (1985). Investigation of pressure oscillations in a PWR primary circuit. *Progr. Nucl. Energy*, 15, 651-659.
4. Valco, J., G. Por, T. Czibok, E. Tzak, E. Hallo and P. Syklossy (1985). Experiences with noise analysis at Paks Nuclear Power Plant. *Progr. Nucl. Energy*, 15, 403-412.
5. Nagy, J. and T. Katona (1985). Theoretical investigation of the low-frequency pressure fluctuation in PWRs. *Progr. Nucl. Energy*, 15, 671-683.

Teil 5

Nondestructive Examination and Diagnostics Centre
DIAPROM

APPROVED

DIAPROM Director General

 D. F. Gutsev

" 16 " 10 1996

ELABORATION of NUMERICAL VIBRATION
MODELS of the VVER TYPE REACTORS

Additional Analysis of Experimental Data at the Normal Condition of the
VVER Type Reactor and Analysis of the Data at the Anomalous Condition of
the VVER-1000 Type Reactor

Intermediate Report

0018.04.01-96 OT

Contents

1. THE ADDITIONAL ANALYSIS OF SPATIAL STRUCTURE OF NODES AND ANTINODES OF ACOUSTIC STANDING WAVES IN THE COOLANT INSIDE THE REACTOR VESSEL OF VVER-1000 REACTOR TYPE AND FORCED VIBRATIONS OF FUEL ASSEMBLIES	3
1.1 ABSTRACT	3
1.2 INTRODUCTION	3
1.3 MEASUREMENT OF NOISE ON REACTOR VVER-1000 OF KALININ NPP UNIT 1	4
1.4 THE ANALYSIS OF PRESSURE NOISE	5
1.4.1 The ASW forms on frequencies 6.2 Hz, 12.8 Hz and 18.7 Hz.....	5
1.4.2 The form of ASW on frequency 9.0 Hz.	9
1.5 THE ANALYSIS OF INCORE AND EXCORE NEUTRON DETECTORS SIGNALS NOISE	10
1.6 CONCLUSION	13
2. THE REACTOR ANOMALOUS VIBRATION STATE ANALYSIS OF 1 UNIT OF HMELNITSKAYA NPP	14
3. FURTHER ANALYSIS OF FULL-SCALE VIBRATION MEASUREMENTS RESULTS.....	22

1. The additional analysis of spatial structure of nodes and antinodes of acoustic standing waves in the coolant inside the reactor vessel of VVER-1000 reactor type and forced vibrations of fuel assemblies

1.1 Abstract

In the given section of the report new representation about the form of an acoustic standing wave (ASW) on frequency 9,0 Hz for reactor as VVER-1000 is given and proved. The mechanism of its formation is presented also.

Analysis of incore and excore neutron detectors signals measurements results, carried out taking into account characteristic sizes of separate parts of closed circulating circuit, location of pressure transducers (PT) in various parts of loops and their data, have allowed with sufficient completeness to determine the form ASW on frequency 9,0 Hz and location of two its nodes and two antinodes in a main circulating circuit of reactor. The phase of this ASW has the same value in whole volume of a core and in space between the reactor pressure vessel (RPV) and its core barrel. Its amplitude will be practically constant in limits of the whole core. Therefore such ASW cannot be the reason of forced beam mode vibrations of fuel assemblies (FAs). 3-dimensional spatial effects inside RPV are of large significance in formation ASW on frequency 9,0 Hz. Neglecting of such effects has not allowed to obtain in work [1] correct representation about the ASW form of a similar type in reactor VVER-440. The analysis of results of measurements on reactor VVER-1000 of Kalinin NPP Unit 1, carried out earlier, also suffered by this lack.

It is shown, that ASWs on frequencies 6.0 Hz, 13.0 Hz and 19.0 Hz are formed practically according to 1-dimensional model. These three ASWs with practically multiple eigenfrequencies have inside RPV (inside core) one common node, having rather complex geometrical structure, and various phase portraits. The spatial structure of this node results in occurrence in some parts of core gradients with significant amplitudes of these three ASWs in radial and azimuthal directions. The last circumstance was the reason of forced beam mode fluctuations of FAs on frequencies 6.0 Hz, 13.0 Hz and 19.0 Hz.

The analysis of neutron noise inside core and outside of RPV has confirmed presence inside it (inside core) nodes and antinodes of all four mentioned above ASWs with predicted spatial structures and has determined their details. It has confirmed also picture of each ASW phase shift inside RPV, received on the basis of pressure noise analysis. Common research of noise signals of all seven neutron detectors in some of FAs has allowed to identify forced beam mode fluctuation of them on frequencies 6.0 Hz, 13.0 Hz and 19.0 Hz under influence of appropriate ASW.

1.2 Introduction

In the work [1] results of measurements of pressure noise in pipelines of loops of reactor VVER-440 on the 2-nd Unit of Kola NPP were submitted. Their analysis has allowed with sufficient completeness to determine the forms of a sequence of acoustic standing waves, corresponding to four minimum eigenfrequencies oscillations of pressure in the coolant of such type reactor. The form of ASW determines, for example, character of its influence on various elements of the equipment inside the reactor vessel and their forced vibrations. Such influence will be especially significant from the ASW, having the least eigenfrequencies and, hence, greatest amplitudes of fluctuations of pressure in the coolant. The analysis of measurements, carried out in the specified above work, has shown, that three ASW with practically multiple eigenfrequencies (6.7 Hz, 12.8 Hz and 20.1 Hz) have inside RPV various phase portraits and one common node, having complex 3-dimensional structure. The formation of fourth ASW on frequency 9.0 Hz was determined by other acoustic and geometrical peculiarities of a main circulating circuit (MCC). However experimental data have not allowed to create precise picture of this ASW form. Four

ASW of a similar type with respect to their form will be formed simultaneously only in reactor VVER (PWR) with even number of loops. ASW, having similar to 6.7 Hz and 20.1 Hz ASWs form, should be absent in reactors with odd number of loops in MCC.

These important conclusions gave the basis to extend received results on reactor VVER-1000, having four loops in MCC. Absence of conditions for measurement of neutron noise inside core on the 2-nd Unit of Kola NPP has not allowed to check up and correct the results of the specified above work. The attempt to some extent to liquidate this lack was undertaken during the analysis of measurements results of pressure, incore and excore neutron noise on reactor VVER-1000 of 1 Unit of Kalinin NPP.

1.3 Measurement of noise on reactor VVER-1000 of Kalinin NPP Unit 1

Fluctuation of pressure and neutron noise were measured in conditions, when the electrical capacity of 1 Unit of Kalinin NPP was equal to 800 MW, in work there were four main circulating pumps (MCP), and pressure in the coolant was 160 kg/cm². Temperatures of the coolant in hot and cold legs were equal accordingly 311 and 288 degrees. Fluctuations of pressure were measured by three transducers of pressure, placed in pipelines with application of short impulse lines with length 50 sm. Two PT were installed on MCP inlet in cold legs of third (Q3) and fourth (Q4) loops on distance 26.5 m from RPV in the direction of coolant flow. Third PT (S4) was in hot leg of the fourth loop on distance 6.5 m from RPV.

Incore neutron noise was measured by rhodium self-powered neutron detectors (SPND), located on identical distance from each other in seven various points on height of large number of fuel assemblies, which was equal to 3.5 m. Three ionization chambers (IC-7, IC-14 and IC-21), placed outside RPV under a corner approximately 120 degrees to each other on middle of core on its height, provided measurement of excore neutron noise. On Fig. 1 the draft of an arrangement of four loops with respect to RPV of VVER-1000 and its main axes I-III and II-IV are submitted, co-ordinates of fuel assemblies in core, and also placement of ICs and PTs are specified.

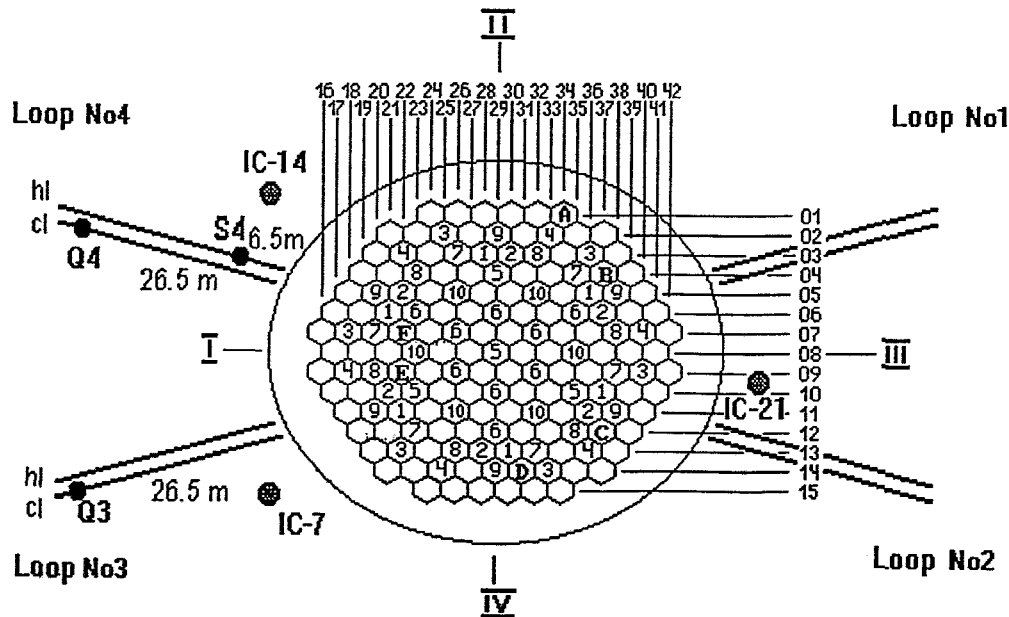


Fig. 1 The arrangement of four MCC loops with respect to RPV of VVER-1000 and its main axes I-III and II-IV; co-ordinates of fuel assemblies in core, and also place of PT and IC location.

Hereinafter the signal of the transducer of any type will have a designation, which was accepted earlier for the transducer himself.

1.4 The analysis of pressure noise

At frequency spectra of signals of all PT there were significant on amplitude resonant peaks on frequencies 6.0 Hz, 13.0 Hz, 19.0 Hz and 9.0 Hz. The values of coherence functions (CF) and phase characteristics (PC) on the specified frequencies for various pairs of PT signals are submitted in tables 1, 2, 3 and 4.

Table 1 Phase shifts between different PT on 6.2 Hz

Sensors	Frequency, Hz	Coherence functions	Phase shift
Q4 - S4	6.2	0.93	6,5°
Q3 - S4	6.2	0.14	153°
Q3 - Q4	6.2	0.16	159°

Table 2 Phase shifts between different PT on 12.8 Hz

Sensors	Frequency, Hz	Coherence functions	Phase shift
Q4 - S4	12.8	0.84	174°
Q3 - S4	12.9	0.06	164°
Q3 - Q4	12.8	0.15	16°

Table 3 Phase shifts between different PT on 18.7 Hz

Sensors	Frequency, Hz	Coherence functions	Phase shift
Q4 - S4	18.7	0.28	172°
Q3 - S4	18.7	0.09	4,3°
Q3 - Q4	18.8	0.18	148°

Table 4 Phase shifts between different PT on 9.0 Hz

Sensors	Frequency, Hz	Coherence functions	Phase shift
Q4 - S4	9.0	0.23	140°
Q3 - S4	9.0	0.11	162°
Q3 - Q4	9.0	0.11	11°

Data of these tables specified the fact, that the shift of a phase between components in signals of each pair of PTs on four listed above frequencies accurate to an error of evaluation is equal to 0 or 180 degrees. This circumstance is an attribute of existence of four types ASWs in the coolant of primary loop.

1.4.1 The ASW forms on frequencies 6.2 Hz, 12.8 Hz and 18.7 Hz.

Set of results, submitted in tables 1, 2 and 3, give us the possibility to investigate data with use of that logic reasoning, which were applied in work [1] during the analysis of similar experimental data, received on reactor VVER-440. Such research has allowed to determine the forms of ASWs on frequencies 6.2 Hz, 12.8 Hz and 18.7 Hz in whole volume of primary circuit, 3-dimensional

spatial structure of their common node and picture of behaviour of phase of each ASW inside RPV.

Spatial distributions of amplitude and the phases in VVER-1000 on frequencies 6.2 Hz, 12.8 Hz and 18.7 Hz are schematically submitted accordingly on Fig. 2 - Fig. 4, where a location of PT S4, Q4 and Q3 is specified also.

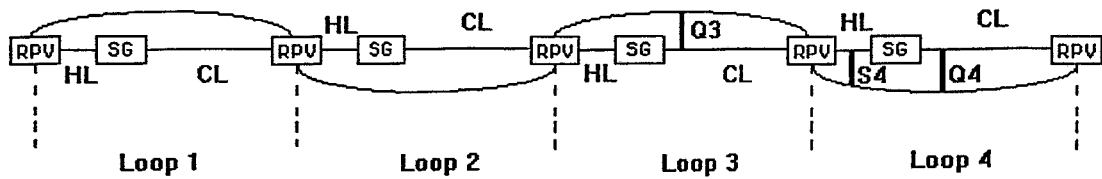


Fig. 2 Spatial distribution of amplitude and phase of pressure oscillations in the coolant in MCC of VVER-1000 on frequency 6.2 Hz

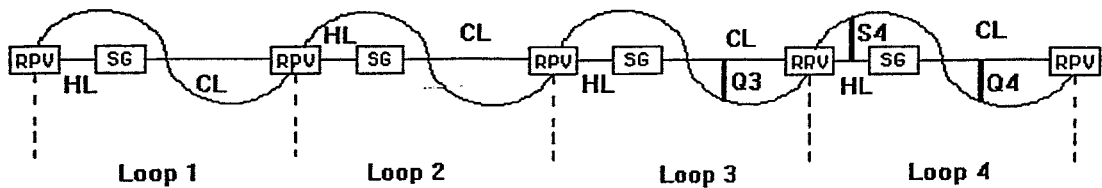


Fig. 3 Spatial distribution of amplitude and phase of pressure oscillations in the coolant in MCC of VVER-1000 on frequency 12.8 Hz

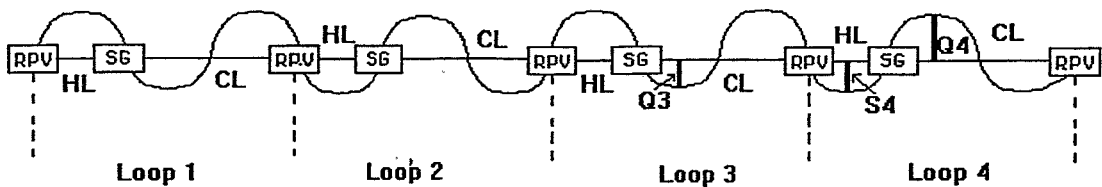


Fig. 4 Spatial distribution of amplitude and phase of pressure oscillations in the coolant in MCC of VVER-1000 on frequency 18.7 Hz

Complete length of a closed coolant circulation loop in reactor VVER-1000 on the first block of Kalinin NPP is equal to 86 m. It includes pipelines of hot and cold legs of a separate loop, and also appropriate parts inside steam generator (SG) and RPV. The estimation of these three ASWs lengths was made with application of simple 1-dimensional model, in which length of

ASW is connected to its frequency f by the formula $l=V/f$, where V - speed of a sound in the coolant which is temperature and pressure dependent. In our case it was equal to 1100 m/s. According to the specified above formula ASWs have lengths 177 m, 86 m and 59 m.

The analysis of experimental results has enabled to reach the conclusion, that first (conventionally) group of node points of these three ASW should be located inside RPV on one horizontal plane, and other second (conventionally) group of their node points should be placed inside RPV on four identical vertical planes. They will fill in that part of each vertical plane, which is shaded on Fig. 7 of the mentioned above work. Part of a vertical axis of RPV will be common for all these planes direct, which is the top of the corner between any two adjacent planes, on which node points of the second group are located, the corner will be 90 degrees. Four such planes will divide whole volume of the coolant inside RPV into four identical sectors, each of them will adjoin to the appropriate loop. Both groups of node points form inside RPV one common node for three ASWs on frequencies 6.2 Hz, 12.8 Hz and 18.7 Hz.

Four specified above vertical planes will finally form inside RPV the border of all four closed circuits, caused by various loops outside RPV limits. In some sense such planes for these three ASW are possible to consider as absolutely rigid walls, the thickness of which are equal to zero. They form inside RPV four channels, each of them continues the pipeline of cold leg of any loop and connects it to the pipeline of hot leg of the same loop, and to certain degree isolate one closed circuit from other. It, however, does not mean, that the separate parts of these three ASWs, generated in each closed circuit, will be independent. Four vertical planes - the walls with node points of the second group will provide their mutual and appropriate synchronization.

Here it is necessary to note, that the formation ASWs on frequencies 6.2 Hz, 12.8 Hz and 18.7 Hz occurs practically under the simple 1-dimensional model despite the complex geometry of primary loop and 3-dimensional spatial structure of their node inside RPV. Such model strictly speaking will be fair only in limits of loops pipelines. However multiple frequencies of these ASWs, ratio between their lengths and length of one closed circuit are arguments for the benefit of justice of 1-dimensional of model. Length of pipelines in one loop is equal to 68 m and in them the main part of complete power of all three ASWs is concentrated. Therefore the pipelines of each loop play a determining role in their formation, and RPV carries out only acoustic connection between various loops. Four vertical planes - the walls with node points of the second group inside RPV also create the appropriate conditions for realization 1- dimensional model.

The pictures of second group node points location and behaviour of a phase for ASWs on frequencies 6.2 Hz, 12.8 Hz and 18.7 Hz inside RPV at a level of core in a horizontal plane, where the node points of the first group are absent, are submitted accordingly on Fig. 5 - Fig. 7. Signs (+) and (-) on these drawings specify existence of contrphase at specific ASW in the appropriate areas of space inside RPV and other parts of MCC.

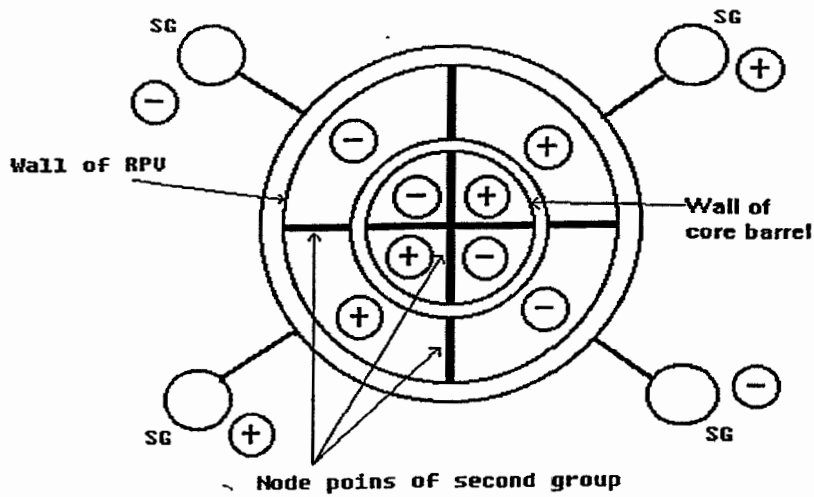


Fig. 5 The picture of 2-nd group node points location and behaviour of phase for ASW on frequency 6.2 Hz inside RPV at a level of core in a horizontal plane where node points of 1-st group are absent.

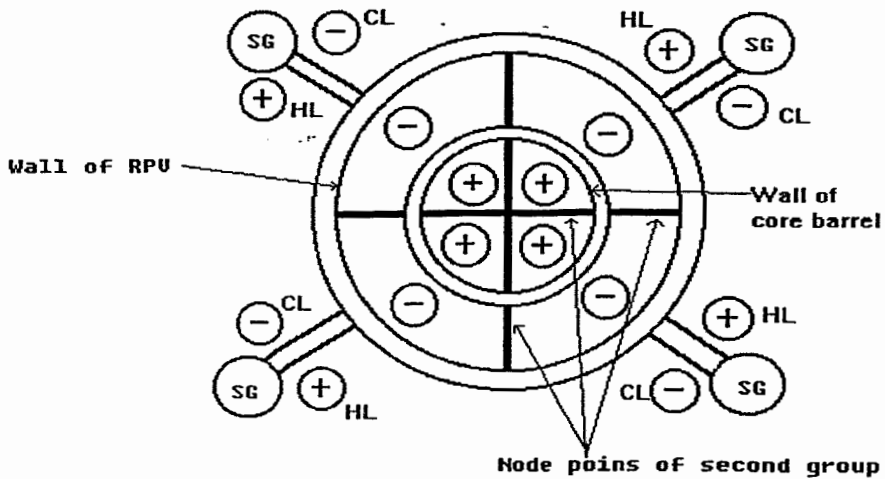


Fig. 6 The picture of 2-nd group node points location and behaviour of phase for ASW on frequency 12.8 Hz inside RPV at a level of core in a horizontal plane where node points of 1-st group are absent.

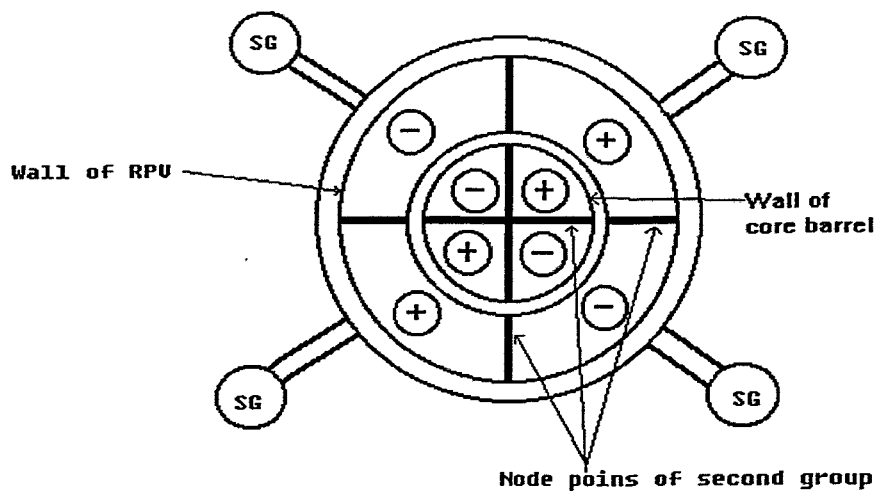


Fig. 7 The picture of 2-nd group node points location and behaviour of phase for ASW on frequency 18.7 Hz inside RPV at a level of core in a horizontal plane where node points of 1-st group are absent

3-Dimensional structure of common node of three ASWs inside RPV will result in occurrence in some places of core significant amplitudes gradients of these standing waves in radial and azimuthal directions in areas between any two vertical planes, on which node points of the second group are located. It should be by the reason of forced beam mode vibrations of large number of fuel assemblies, fixed in their top and bottom parts, on the specified above frequencies. The listed here effects in a determined way will manifest themselves in noise of incore neutron detectors signals.

1.4.2 The form of ASW on frequency 9.0 Hz.

The results, submitted in Table 4 entitle to approve that pulsations of pressure in the coolant on frequency 9.0 Hz in hot legs (MCP) of all four loops MCC occur in phase. Oscillations of pressure on this frequency in all cold legs also occur in phase. However in arbitrary chosen hot and cold legs of one loop or different loops oscillations of pressure on frequency 9.0 Hz occur in contrphase. It gave the basis to approve, that ASW of this type has node in a vicinity of steam generator in each loop and antinode inside RPV. Limited number of PT has not allowed to determine a location of other nodes and antinodes of this ASW in pipelines of MCC. The possible and the most probable form of it is represented on Fig. 8, where spatial distribution of amplitude and phase of this ASW in MCC is schematically shown. ASW of such form has in each closed circuit two nodes and two contrphase antinodes. One of its nodes is close to SG from the side of MCP, and other node - near RPV. One antinode of such form ASW should be inside RPV, and other antinode - in each loop. The antinodes group of this ASW, formed in four closed circuits, will disturb density of the coolant in phase in all points inside RPV. The amplitude of such disturbances will be maximum and practically constant in whole core volume. Its value will decrease during a transition upwards from the bottom part of core in space between RPV and its core barrel in a direction of pipelines of all loops, where close RPV the nodes of this ASW will be. In reactor core, in space between RPV and its core barrel, and also in place of PT S4 installation the fluctuations of pressure on frequency 9.0 Hz will occur in phase. This ASW will be formed not in accordance with 1-dimensional model. The formula V/f is not fair here. Large participation in formation of this ASW belongs to RPV, where a significant part of its complete

power is concentrated and role of 3-dimensional spatial effects is great. The given circumstance was not accepted in attention in the specified above work. It was not allowed to create of precise and correct representation about the form ASW of a similar type in reactor VVER-440.

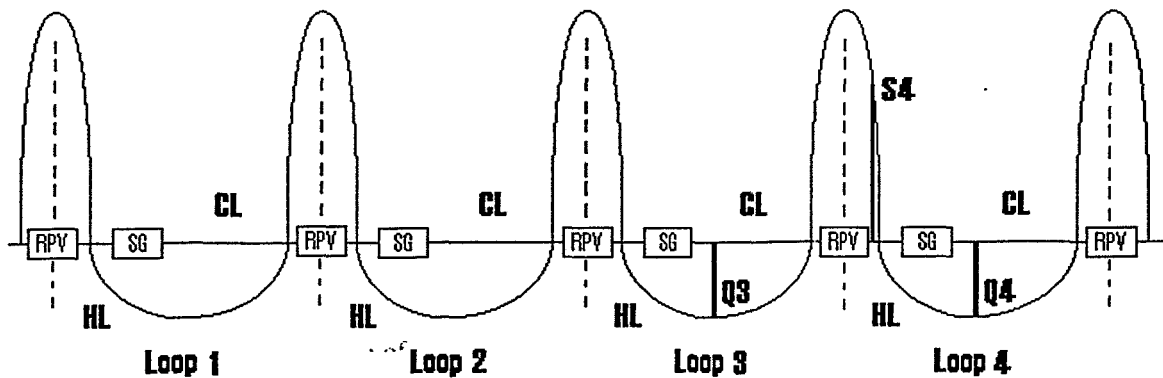


Fig. 8 Spatial distribution of amplitude and phase of ASW on frequency 9.0 Hz

ASWs on frequencies 9.0 Hz and 12.8 Hz had in each closed loop of reactor VVER-1000 an identical number of nodes and antinodes. However the forms of these ASWs differ essentially due to the specified above reasons.

1.5 The analysis of incore and excore neutron detectors signals noise

The auto power spectral density (APSD) of signals IC-7, IC-14 and IC-21 are submitted on Fig. 9. In these frequency spectra peaks on the frequencies 9,0 Hz and 13,0 Hz, caused by action of two ASWs on density of the coolant inside core and in space between RPV and its core barrel attract attention. ASW on frequency 6.0 Hz also disturbs density of the coolant in the specified areas of space inside RPV. The amplitude of pressure disturbance on frequency of this ASW considerably surpasses amplitudes of fluctuations of pressure on frequencies 9.0 Hz and 13.0 Hz. However the signals of excore neutron detectors reacted differently to three kinds of these ASWs. Only the various phase portraits of ASWs on frequencies 6.0 Hz, 13.0 Hz and 9.0 Hz inside RPV and core could explain such result.

ASW on frequency 13.0 Hz changes the phase on 180 degrees at transition inside RPV through such part of horizontal plane, on which node points of the first group of ASW on frequencies 6.0 Hz, 13.0 Hz and 18.8 Hz are placed. The shift of a phase on frequency 13.0 Hz between signals of first (bottom) SPND and seventh (top) SPND in the fuel assemblies with coordinate (07-22) was equal to zero at coherence 0.3. The similar situation took place during measurement of phase shift between signals of bottom and top incore neutron detectors on this frequency in other FAs. These results pointed, that the horizontal plane with node points of the first group is outside core and is located, apparently, in the bottom part of RPV. The given circumstance strengthened effect of influence of this ASW on IC signals.

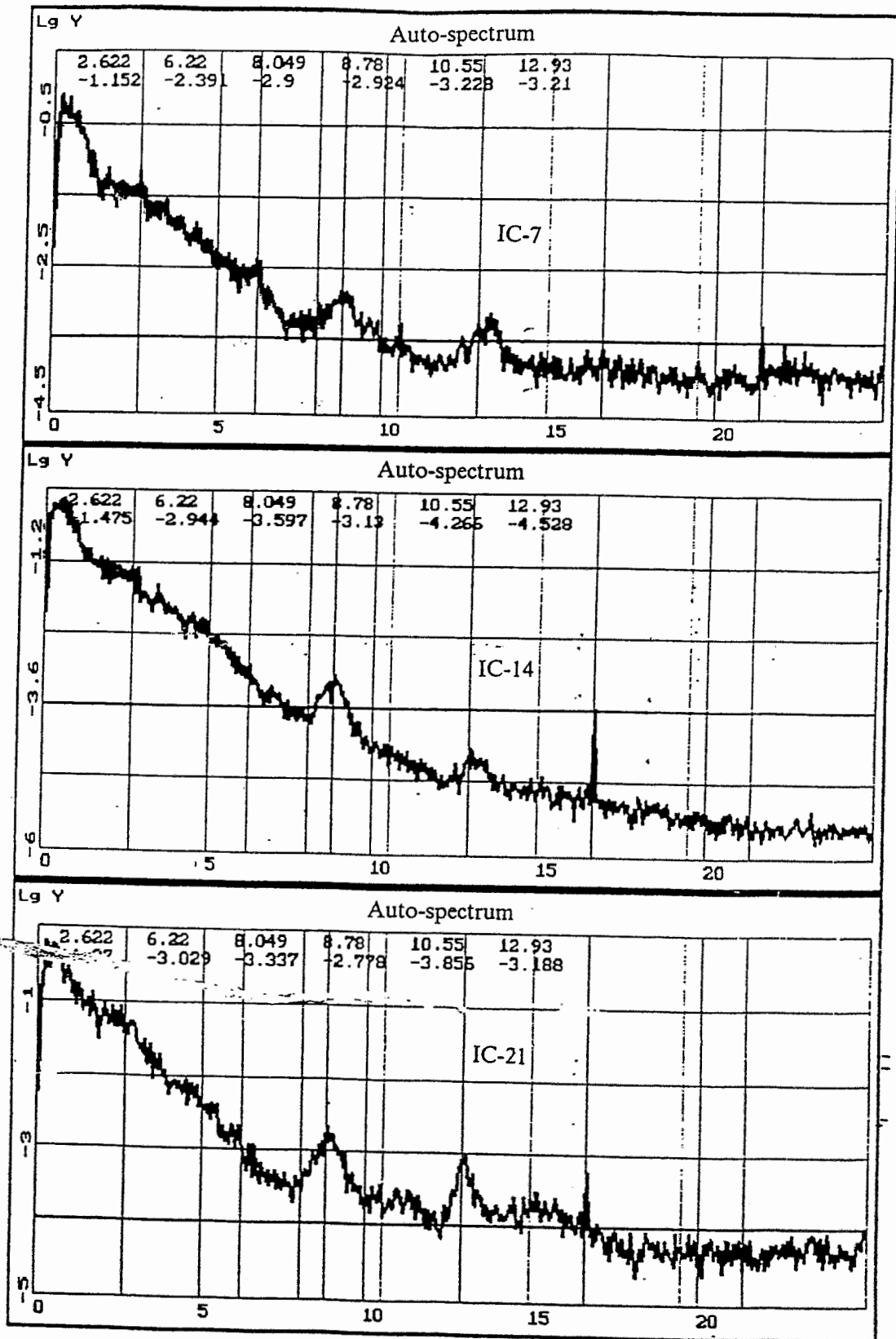


Fig. 9 APSD of signals IC-7, IC-14 and IC-21

The phase shift on frequency 9.0 Hz between signals of any two SPNDs, located in core, was equal to zero, ASW on this frequency disturbs density of the coolant in whole volume of core in phase. Deviation of SPNDs signal, measured in a narrow band of frequencies in vicinity of frequency 9.0 Hz and normalized on square of its constant part, did not depend on a location of neutron detector in reactor core. This fact tells that the amplitude of ASW on frequency 9.0 Hz does not practically depend on coordinate in limits of whole core volume, where it has the maximum value. The characteristic sizes of this ASW let us approve that its phase will not change at transition from core in area of space between RPV and its core barrel. Such ASW will disturb density of the coolant in core only. It could not be the reason of forced beam mode FA vibrations.

ASW on frequency 13.0 Hz also disturbs in a phase pressure of the coolant in whole volume of core. However it has inside core four vertical planes with node points of the second group. It should excite forced beam mode of FA fluctuation in core of reactor. Such fluctuations of each FA could occur in one, two and even three directions, on which the rigidity of FA is minimum. The occurrence of the second physical process, connected to vibration of FA, has determined character of phase shift on frequency 13.0 Hz between signals of various pairs of SPNDs, located in one FA.

As an example in Table 5 values of phase shifts on frequency 13.0 Hz between signals of various pairs incore neutron of detectors (SPNDs), located in FA with coordinate (10-27) are given.

Table 5 Values of phase shifts on 13.0 Hz frequency between different SPNDs pairs in FA (10-27)

Types of signals in FA (10-27)	SPND(1)- SPND(2)	SPND(1)- SPND(3)	SPND(1)- SPND(4)	SPND(1)- SPND(5)	SPND(1)- SPND(6)	SPND(1)- SPND(7)
Phase shift on 13.0 Hz frequency	+48°	134°	59°	33°	85°	22°
Coherence on frequency 13.0 Hz	0.16	0.25	0.13	0.24	0.17	0.16

For FA, located in the other place of core, the phase shifts between various pairs of neutron detectors will have other values, different from that, which were resulted in Table 5 for FA with coordinate (10-27). The values of these shifts will depend on character and amplitudes of forced vibrations of specific FA in the appropriate place of core under influence of ASW on frequency 13.0 Hz.

The similar influence on signals of all SPNDs, located in FA, will take place from the ASW on frequencies 6.0 Hz and 19.0 Hz. Thus, certainly, it is necessary will be considered, that the fluctuations of pressure in the coolant core on frequencies 6.0 Hz and 19.0 Hz in the next sectors occur with phase shift, equal to 180°. The example, confirming existence of beam mode vibrations of FA on frequency 6.0 Hz, is submitted in Table 6.

Table 6 Values of phase shifts on 6.0 Hz frequency between different SPNDs pairs in FA (10-27)

Types of signals in FA (10-27)	SPND(1)- SPND(2)	SPND(1)- SPND(3)	SPND(1)- SPND(4)	SPND(1)- SPND(5)	SPND(1)- SPND(6)	SPND(1)- SPND(7)
Phase shift on frequency 6.0 Hz	+1,0°	+7,5°	+92,0°	+117°	+116°	+4,1°
Coherence on frequency 6.0 Hz	0.19	0.16	0.20	0.20	0.20	0.12

Only signals of SPND-1 and SPND-7, located accordingly in the bottom and top parts of FA near to places of their fastening can be possibly used for check of phase portraits of ASWs on frequencies 6.0 Hz, 13.0 Hz and 19.0 Hz and structure of their common node inside core. Amplitudes and the phases of signals of two specified SPNDs on these three frequencies will be determined only by fluctuations of pressure in the coolant in places of their installation. Their amplitudes and the phases will not be deformed by effects, caused by forced beam mode fluctuations of fuel assemblies under influence of ASWs on three listed above frequencies. It was the reason that shift of a phase between a signal SPND-1 in FA (04-37) and signal SPND 1 in FA (12-37) was 180° on frequencies 6.0 Hz and 19.0 Hz, and on frequency 13.0 Hz this shift was equal to zero. The fuel assemblies (04-37) and (12-37) are, as known, in the adjacent sectors of reactor core, contiguous to two adjacent loops. Unlike the previous case shift of phase between signal SPND-7 in FA (07-24) and signal SPND-7 in FA (07-22) is 0° on frequencies 6.0 Hz and 13.0 Hz. The location of FA (07-24) and FA (07-22) in one sector core, adjacent to one loop, is the reason of such difference.

Two last results confirm pictures of behaviour of phases ASW on frequencies 6.0, 13.0 and 19 Hz inside RPV, represented on Fig. 5, Fig. 6 and Fig. 7, prove existence in it four vertical planes with node points of the second group.

1.6 Conclusion

In this part of the report results of pressure fluctuations investigations in the coolant of VVER-1000, and also incore and excore neutron noises, measured on the 1 Unit of Kalinin NPP were submitted. The analysis of noise of signals of three pressure sensors, located in pipelines of two adjacent MCP loops, has allowed to determine the forms of ASW sequence, corresponding to four minimum eigenfrequencies of pressure oscillations in the coolant, and to determine 3-dimensional spatial structure of their nodes and antinodes inside core and RPV. The analysis of pressure noise in pipelines of loops has enabled to make a look inside RPV and to determine a picture of phase shifts for all four ASWs inside core and in space between RPV and core barrel below separator of flows.

It was shown, that in formation of ASW on frequency 9.0 Hz RPV participate greatly, and a significant part of this ASW complete power is concentrated inside RPV and role of 3-dimensional spatial effects is great. According to this circumstance for MCC of VVER-1000 reactor the form of this ASW was supposed, receiving certain confirmations during the analysis of ex- and incore neutron noises measurements results.

In the mentioned above work at attempt to determine the ASW form of a similar type for MCC of reactor VVER-440 the influence of 3-dimensional structure on its formation was not taken into attention. It has resulted in faulty result and essential difference of its form from the form of ASW, offered here. Spatial structure of ASWs nodes on frequencies 6.0, 13.0 and 19.0 Hz results in occurrence inside core the spatial gradients at amplitudes of these standing waves in radial and azimuthal directions. It was by the reason of forced beam mode fluctuations of FA, fixed in their top and bottom parts, under influence of ASWs on the specified above frequencies. These fluctuations of FA can be used for supervision of the conditions of their fastening, probably, with higher efficiency, than fluctuation FA on eigenfrequencies.

The received results were confirmed by measurements of incore and excore neutron detectors noise.

The noise measurements of PT, SPNDs and IC signals on reactor VVER-1000 on the 1 Unit of Kalinin NPP were carried out by the experts of DIAPROM.

2. The reactor anomalous vibration state analysis of 1 Unit of Hmelnitskaya NPP

Firstly the internals vibration parameters measurements at the 1 Unit of HML NPP have been planned according to the typical program of start and setting up tests (SST) for VVER-1000 type of reactors. In these tests the following parameters should be monitored: pressure oscillations in reactor flow passage, vibration stresses and vibration accelerations in the main elements of internals (Fig. 10). SST results were approved on the basis of recommended control values of vibration parameters. These values have been worked out on the basis of SST results for headquarters VVER-1000 reactors.

The raised internals vibration levels have been observed during hot test runs of the 1 Unit of Hmelnitskaya NPP. These vibrations were higher than corresponding control values. More over the hydrodynamical conditions in the unit flow passage were normal (

Fig. 11). This made it necessary to carry out special complex of arrangements. These arrangements are as follows:

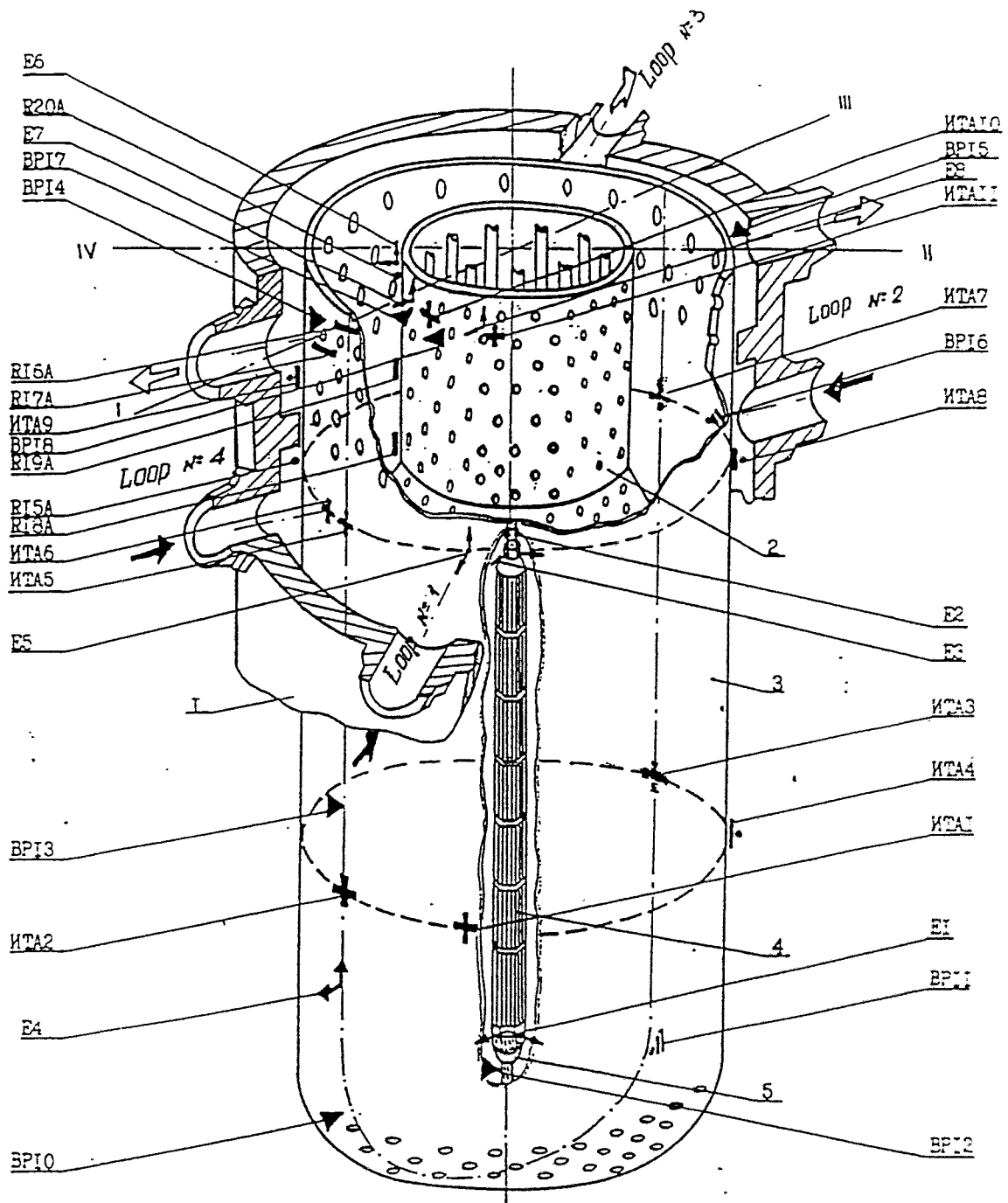
- the reactor disassembly with extra visual inspections and measurements of fastening internals elements;
- repairing works to recover the design conditions of internals fastening;
- reconditioning of the vibration control system;
- repeated measurements of internals vibration parameters.

Visual inspection and measurements after the reactor disassembly revealed the increased gaps between the core barrel and flow splitter. These gaps were of different size along the perimeter. The inspection also revealed noncomplete core barrel upper flange fit to the support vessel clamp. On the basis of the revision results the recovering of designed core barrel fastening conditions including metal built up on the fitting surfaces have been done.

The typical anomalous feature of the 1 Unit of Hmelnitskaya NPP reactor vibration state is high vibrations level of core barrel at frequencies near 5.0 and 10.0 Hz. As it was shown in previous report the frequency of 5.0 Hz corresponds to the lowest waveshape of beam mode vibrations of core barrel girder with fixed upper end. The frequency of 10 Hz corresponds to the oscillations with two waves in circumferential direction ($m=2$). The fact that the last mentioned waveform of oscillations in resistance strain gage data displays itself in strain gauges records mounted near the flow splitter is evidence of noncomplete core barrel draft by the splitter. The loosening of core barrel fastening in support assembly also changes the static internals loading that is it changes the vertical holding down force. The internals oscillations damping changes as a result that is the internals system quality changes as a whole. The cross spectral characteristics obtained at SST for the 1 Unit of Hmelnitskaya NPP is shown in figs. 14, 16, 17, 18, 19. Figs. 12, 13, 15 represent the corresponding characteristics obtained at the Kozlodyi NPP. Table 1 depicts the behaviour of typical spectral salient features.

Insufficient vertical holding down force on internals doesn't provide the necessary fixity of the following key joints:

- core barrel - reactor vessel,
- core barrel - STA shell, core
- core barrel - neutron shield...

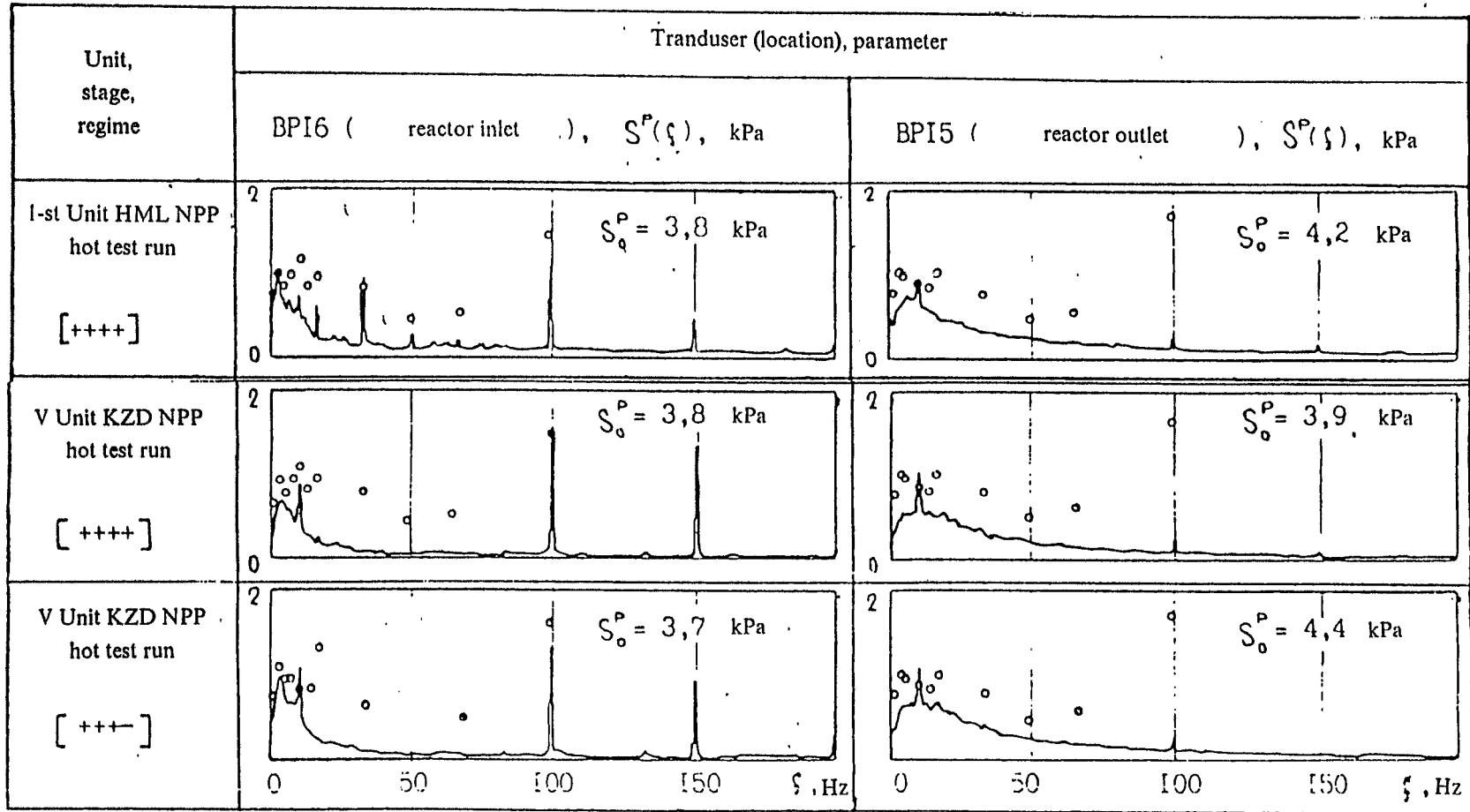


- | | | |
|-------|--------------------------|--------------------------|
| ▷ | - PT | 1 - reactor vessel |
| + - | - resistance strain gage | 2 - STA shell |
| ↑ → | - vibration detectors | 3 - core barrel |
| | | 4 - the central dummy FA |
| | | 5 - support tube |

Fig. 10 A body of measurements for VVER-1000 type of reactors

limits were determined by comparison with units already running

Fig. 11 Comparative spectral records of pressure transducers in main regimes for different units and test stages.



Note: The estimated values of frequency components standards (o) shown in spectral records are obtained by the general analysis of measured data obtained at V Unit of Novovoronezhskaya NPP and At 1-st Units of South-Ukrainian and Kalininskaya NPP.

The designed holding down force on fuel assemblies (FAs) also is not achieved. The following phenomena are eventually possible:

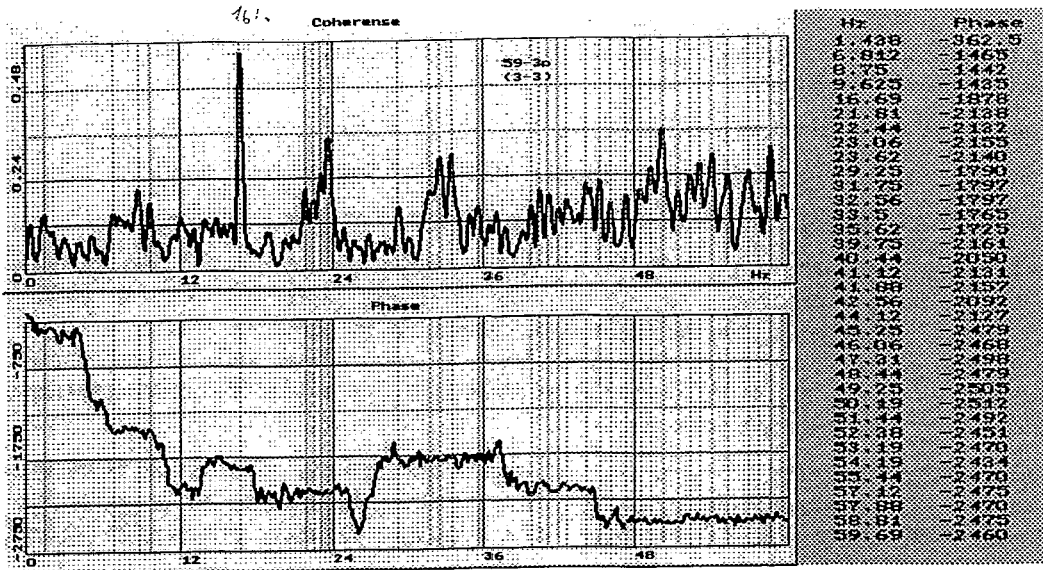
- 1) impact interactions in the core key joints;
- 2) impact interactions in FAs locations (subharmonics of MCP rotational frequency);
- 3) the key joints gaps increasing that makes the core barrel lowest waveforms possible.

The nonrigid FAs fastening leads to the loss of main design oscillation mode at the frequency of 2.5 Hz. The core barrel compliance to the external excitation forces increases at ASW, pressurizer and MCP frequencies. The nontight core barrel fit to the flow splitter leads to broadband phase opposite core barrel vibrations both in longitudinal and circumferential directions between its upper and lower parts. These vibrations are caused by countercurrent coolant flow in downflow and upflow passages.

The repeated measurements after the repair showed significant decrease of internals vibration loading. All of the control values appeared to be within the limits determined by the vibration standards (fig.11). At the same time the core barrel vibrations have not been observed at typical frequencies of 5.0 and 10.0 Hz.

Table 7 The comparison of internals vibration conditions characteristics in normal and anomalous state.

	Normal vibration conditions	Anomalous vibration conditions at the 1 Unit of Hmelnitskaja NPP
The relation between the PT signals and signals of strain gauge mounted at core barrel.	The absence or very low coherent relationships at frequencies of the lowest core barrel vibration modes (5.0 Hz, 10.0 Hz) (figs. 14, 13). The resonance predominating at first MCP rotational frequency (figs. 12,13).	High coherent low quality resonance at first ASW -2 harmonic frequency. Series of high quality resonances within low frequencies range; resonance at pressurizer frequency (0.75 Hz), resonance at core barrel vibration frequency of 5.0 Hz. High coherent resonances frequencies at harmonics and subharmonics of MCP rotational frequency (fig.14)
The relation between the signals of strain gauges mounted at core barrel (3p - 7p, 3k - 7k).	Phase coincident resonances within the wide range of frequencies (0 - 60 Hz) between the signals of the longitudinally oriented transducers in upper and lower parts of core barrel (fig.15)	Phase opposite resonances within the wide frequency range (0 - 60 Hz) between the signals of longitudinally oriented transducers and transducers oriented in circumferential direction (18 - 60 Hz). The existence of high coherent resonances at frequencies higher than 25 Hz (fig.16,17).
The relation between the signals of strain transducers mounted at the core barrel and strain transducers mounted on FA.	High coherent resonance at the first mode of frequency of FA oscillations (2.5 Hz).	The resonance absence at 2.5 Hz. The significant influence of the core barrel vibrations at 5.0 Hz on the FA vibrations. The significant ASW-2 effect on the FA vibrations (fig. 18, 19).



normal
Koslovici

Fig. 12

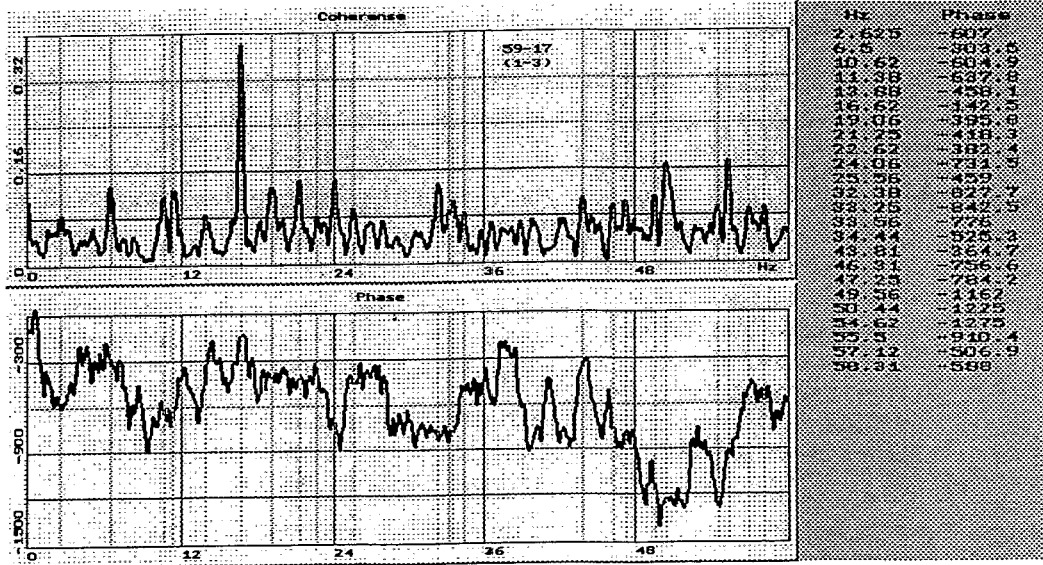
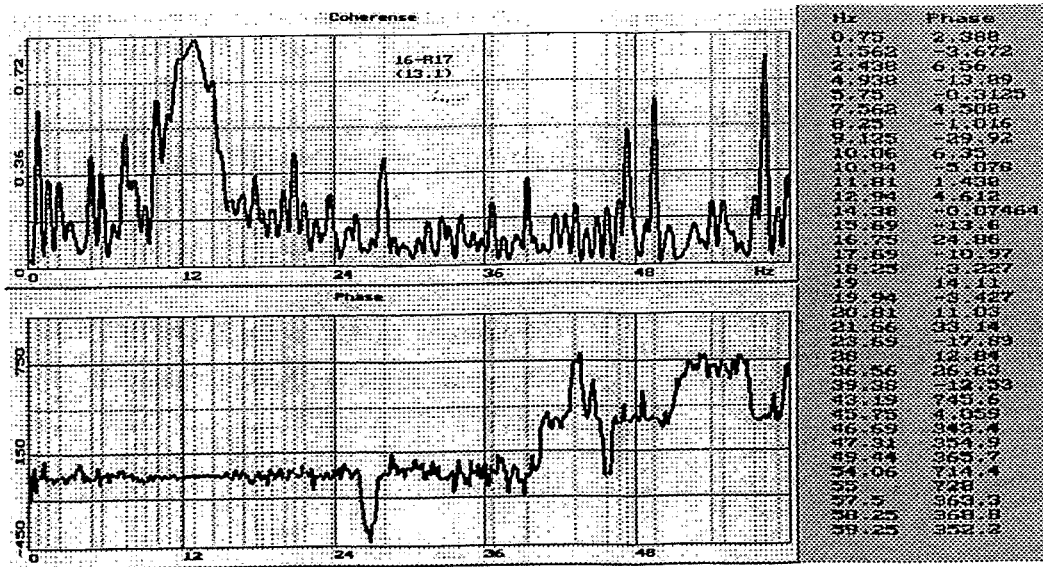


Fig. 13



abnormal
Hmel.

Fig. 14

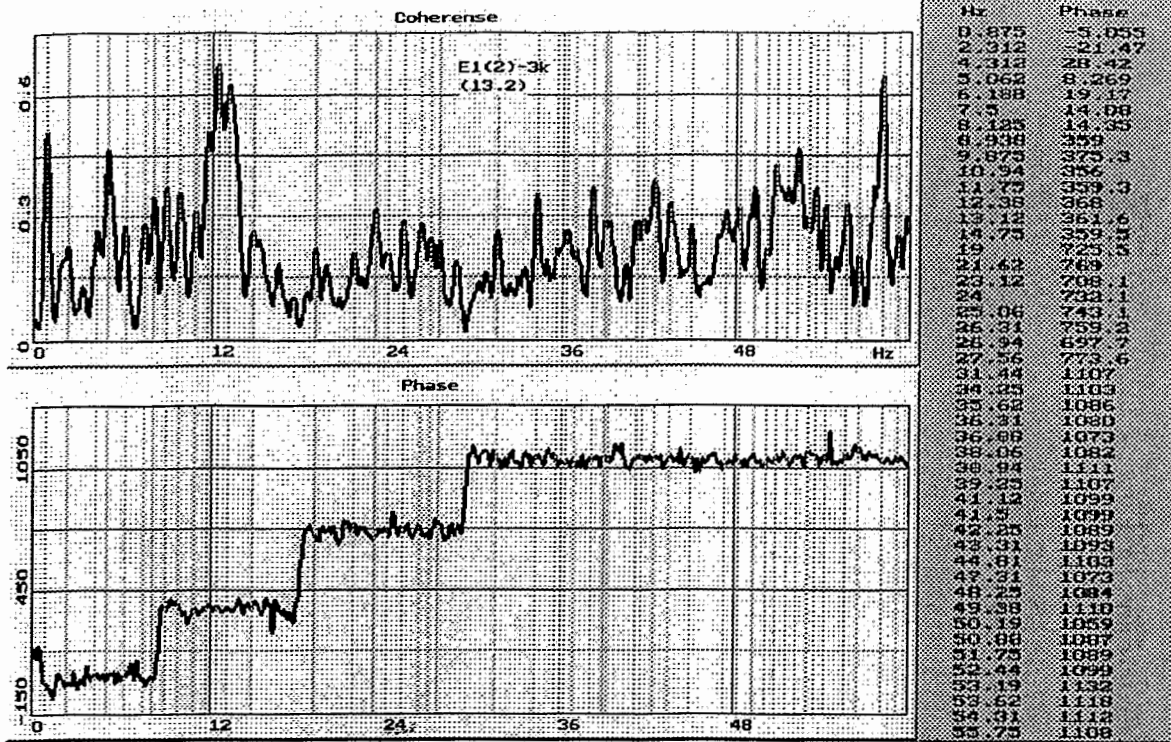


Fig. 18

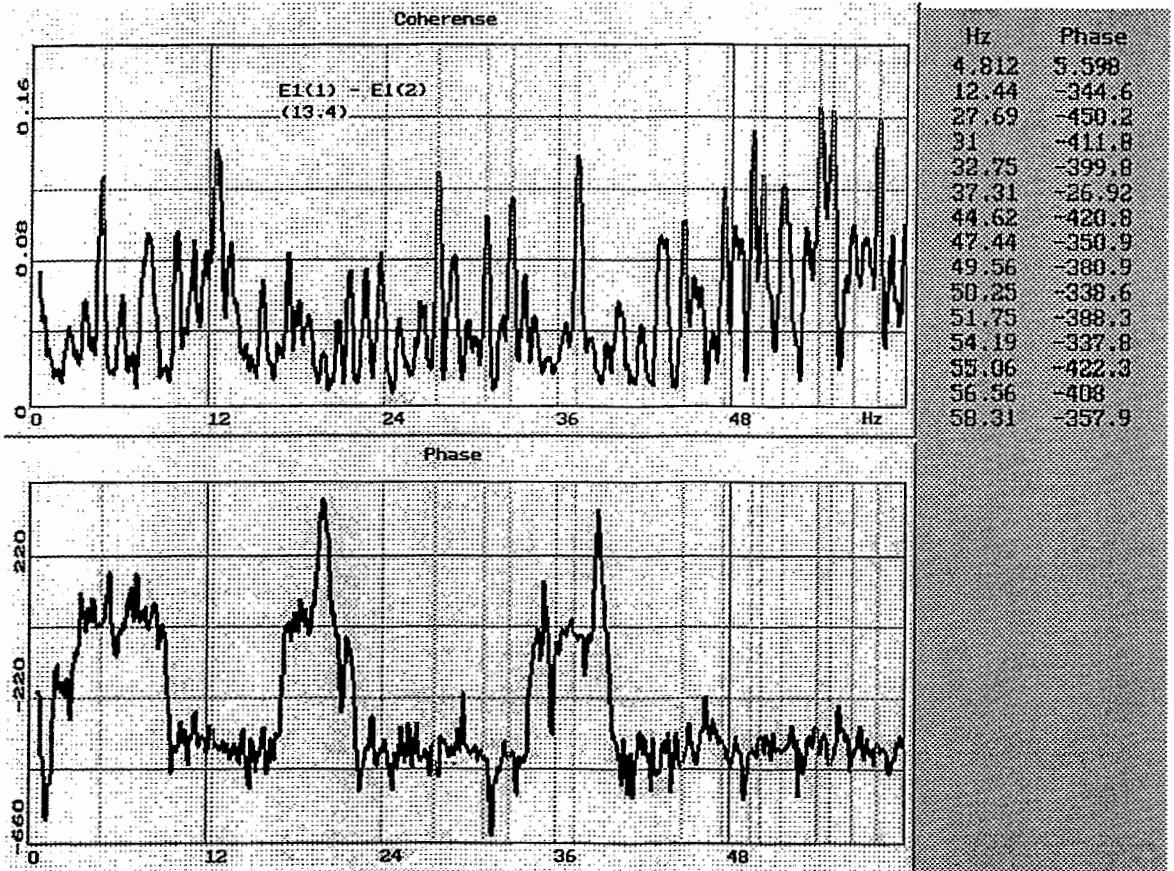
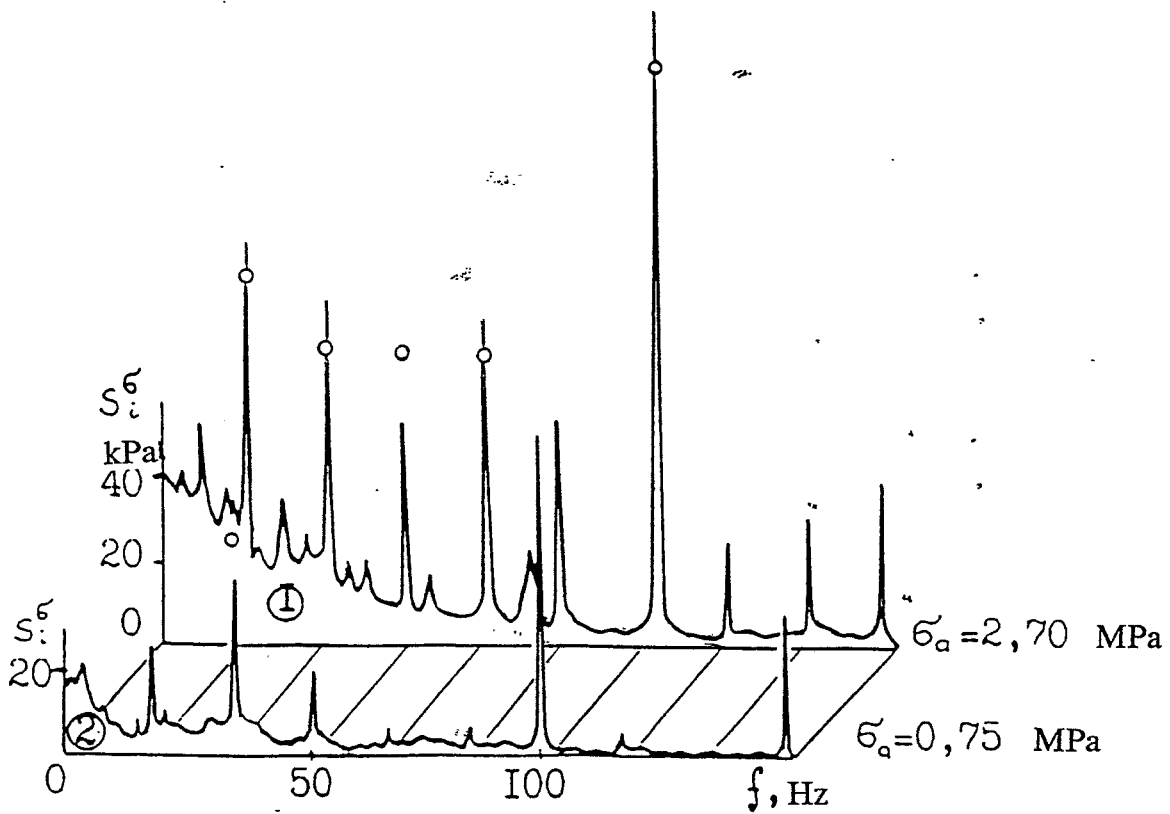


Fig. 19



1 - equipment test runs measurements

2 - start up measurements

Fig. 20 Spectral records of dynamic stresses in reactor core barrel of the Hmel'nitskaja NPP 1-st generating unit

3. Further analysis of full-scale vibration measurements results.

Previous report [2] contains some of the vibration measurements results obtained at reactor start up. The dynamical response spectra analysis made it possible to extract supposedly a series of frequency components as a natural reactor coolant pipe (MCC) frequencies. The Internals and fuel assemblies (FA) natural frequency values have been confirmed by the results of plant measurements on the simplified and scaled models. However it was not sufficient within previous analysis to identify definitively the natural frequencies for oscillation tones connected with RCP loops. Besides the natural waveform have not analysed for these tones. At the same time the natural frequencies determination without information about the waveform leads to difficulties in calculation model adjustment because of rather dense MCC natural frequencies spectrum.

The present report contains further analysis of preoperating stage measurements directed to natural waveforms identification for some oscillation tones connected with MCC loops. The measured data obtained at start up of unit №6 at Kozłodyi NPP have been used in present analysis.

The vibration measurements at pipelines have been carried out by strain transducers. The schematic of their locations is shown in Fig.21. The measurement conditions and list of parameters being measured were typical for tests of all of the VVER-1000 reactors to be put into operation [2].

The phase spectra and coherent structures at different locations of RCP have been used for waveform identification. The lowest oscillation tones are most interesting for calculation model adjustment because the effect of unreliable parameters (stiffness characteristics of elastic relations, support structures etc.) is most displayable at these tones. The lowest natural waveforms in MCC loops are usually characterised by the shift of MCC loops equipment (MCP, SG) in horizontal plane. This shift occurs as the result of support structures absence of loops equipment because of the necessity to provide pipelines thermal expansion. That's why the information about phase spectrum and coherent functions at different locations of MCC in horizontal plane is most interesting for natural waveforms identification of lowest tone oscillations.

The vibration measurements at generating unit start up are directed first of all to justification of the reactor equipment vibration strength. Interests connected with natural tones identification have not been taken into account. That's why unfortunately we couldn't obtain complete data on phase spectra and coherent functions including pairs of most interest.

Another disadvantage of the discussed experimental results is the lack of information about vibration accelerations for MCP and SG vessel. The point is that the MCP is the most compliant and SG is the most heavy element of MCC loop and it's their motion that causes a series of lowest natural tones.

As the result of experimental data analysis it became possible to obtain phase spectra and coherent functions for the following pairs of detectors: R32-R30, R29-R31, R29-R25, R29-R33, R25-R33, R29-R34, R34-R33. These spectra are shown in Fig.22 - Fig.28. In the spectra on can extract a series of components (spikes) of rather high value of coherent function or a series of spikes which repeat themselves in a number of spectra. These components are given in table X.1 for the range of frequencies up to 15 Hz. The phase coincide oscillations are marked by "f" symbol and phase opposite oscillations are marked by "af" symbol.

It should be noted that in general the coherent function levels is not high. There are several intensive spectral components of high coherent function value in spectra at 7.3, 10.8 and 14.8 Hz which correspond to the acoustic waves and for this reason can be excluded from the analysis. Unfortunately they mask spikes of closely spaced frequencies in some of the spectra. These frequencies are 6.5, 8.0, 8.6, 10 Hz.

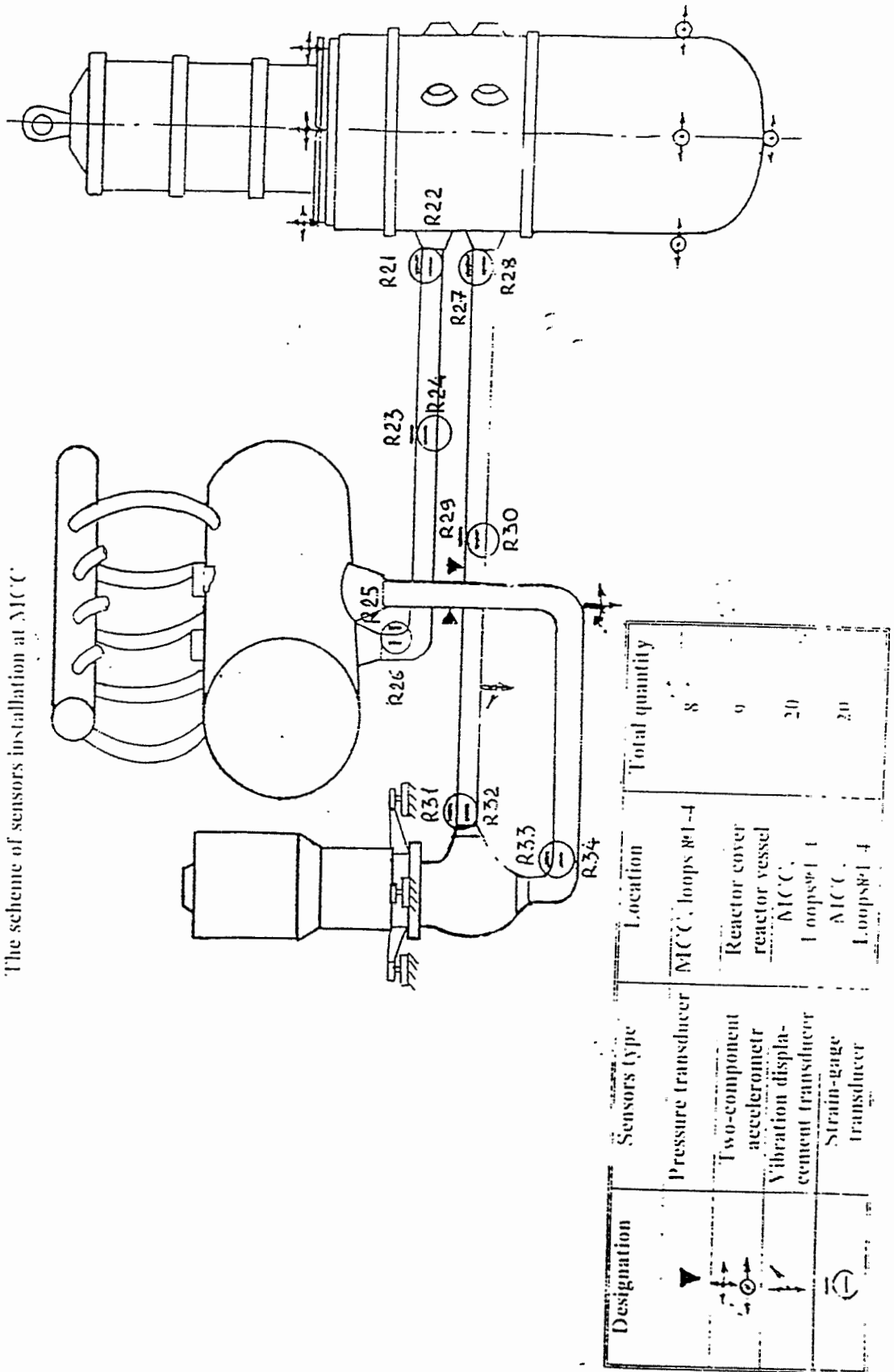
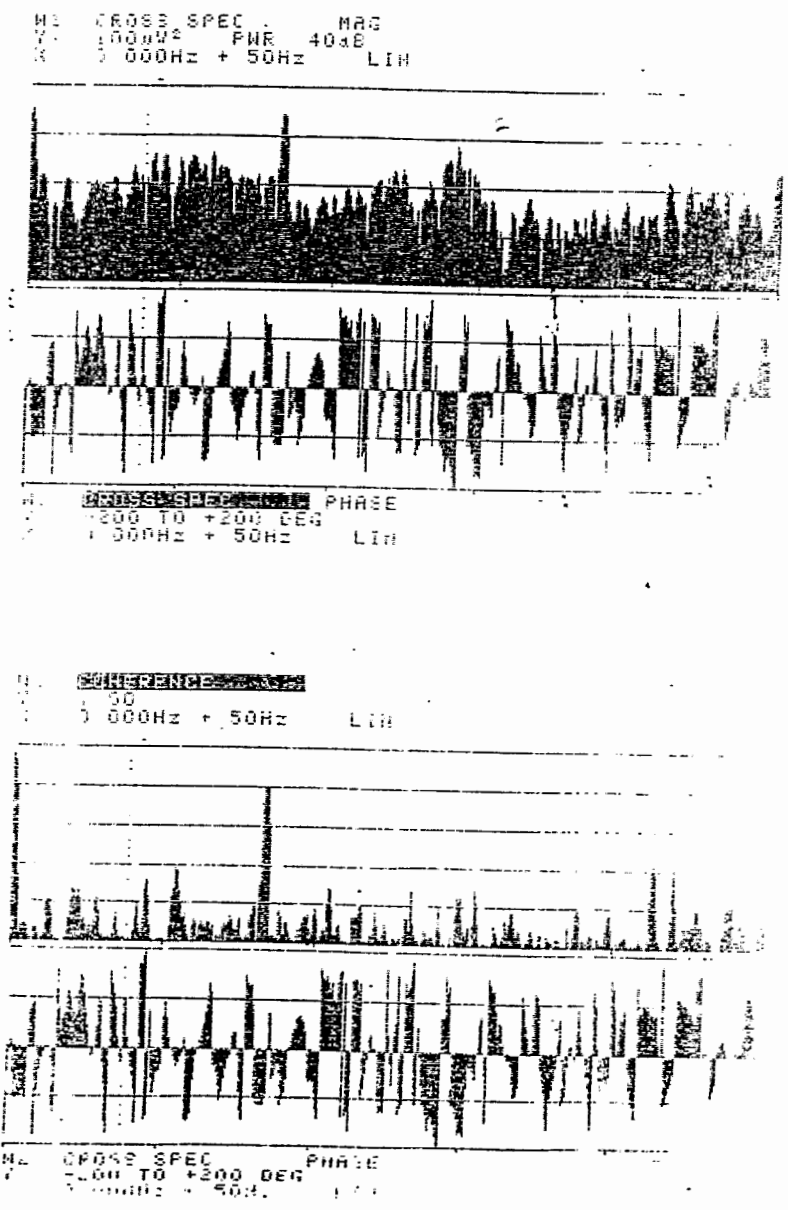


Fig. 21

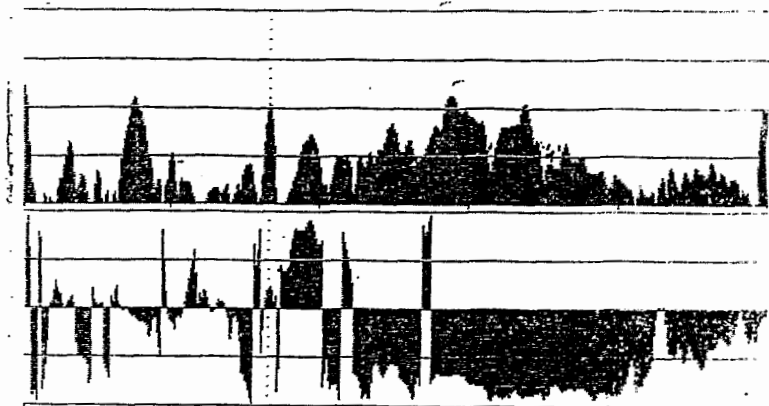


Ch.A - R32
Ch.B - R30

Fig. 22

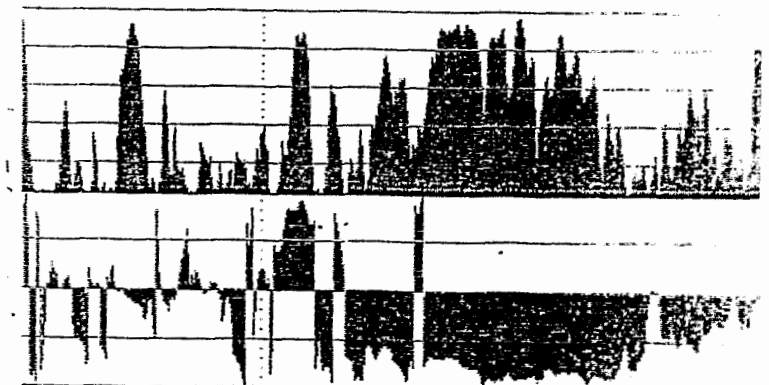
W1 CROSS SPEC MAG
Y: 1.00mV² PWR 40dB
X: 0.000Hz + 50Hz LIN

Ch. A - R29
Ch. B - R31



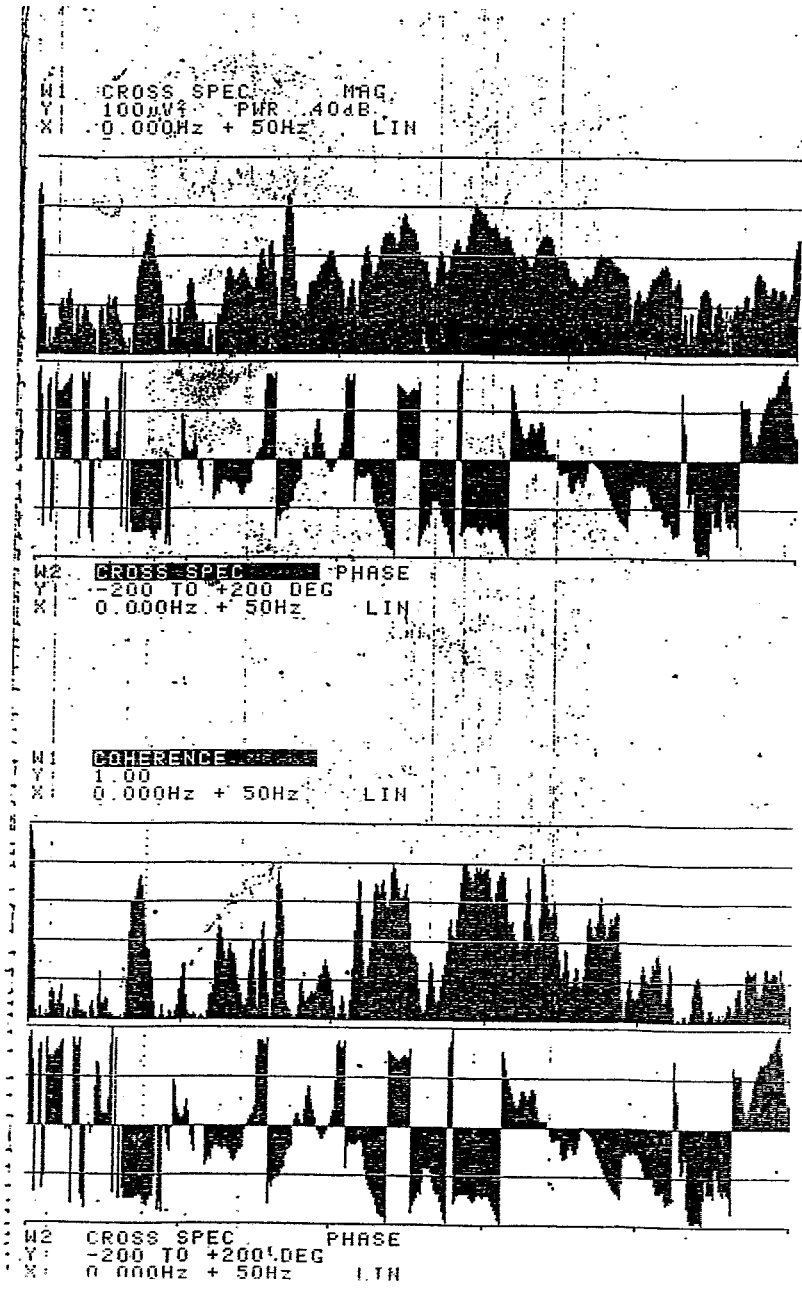
W2 CROSS SPEC PHASE
Y: -200 TO +200 DEG
X: 0.000Hz + 50Hz LIN

W3 COHERENCE
Y: 1.00
X: 0.000Hz + 50Hz LIN



W4 CROSS SPEC PHASE
Y: -200 TO +200 DEG
X: 0.000Hz + 50Hz LIN

Fig. 23



Ch. A - R29

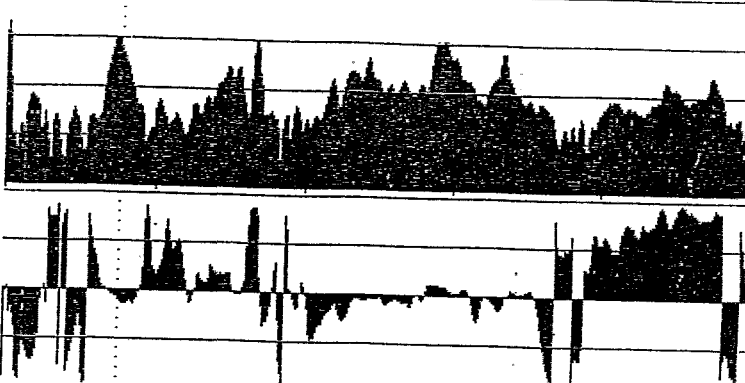
Ch. B - R25

Fig. 24

M1 CROSS SPEC MAG
Y: 100 μ V² PWR 40dB
X: 0.000Hz + 50Hz LIN

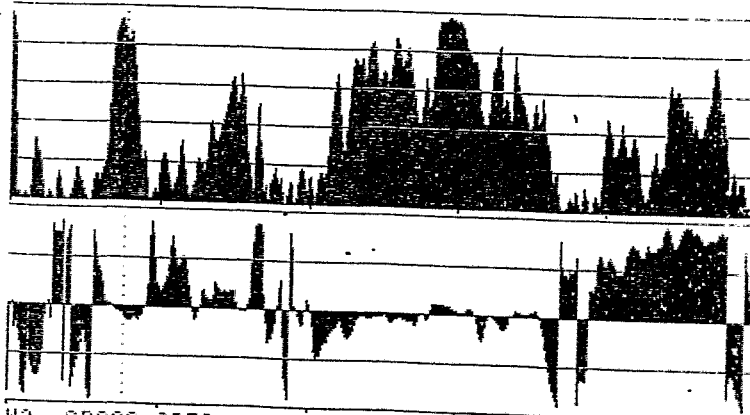
Ch. A-R29

Ch. B-R33



M2 CROSS SPEC PHASE
Y: -200 TO +200 DEG
X: 0.000Hz + 50Hz LIN

M1 COHERENCE
Y: 1.00
X: 0.000Hz + 50Hz LIN

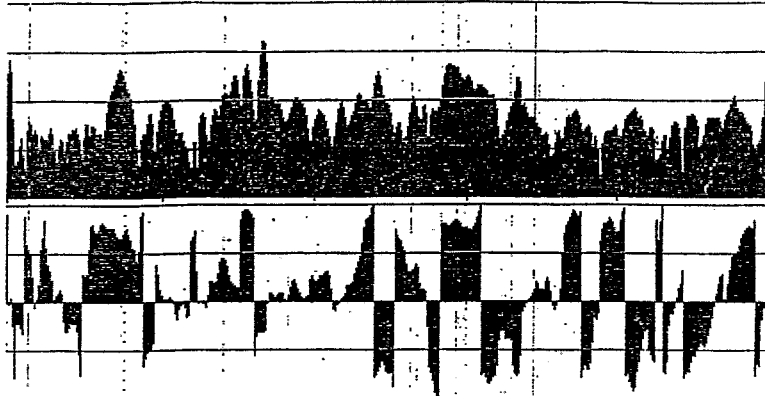


M2 CROSS SPEC PHASE
Y: -200 TO +200 DEG
X: 0.000Hz + 50Hz LIN

Fig. 25

M1 CROSS SPEC MAG
Y: 100µV² PWR 40dB
X: 0.000Hz + 50Hz LIN

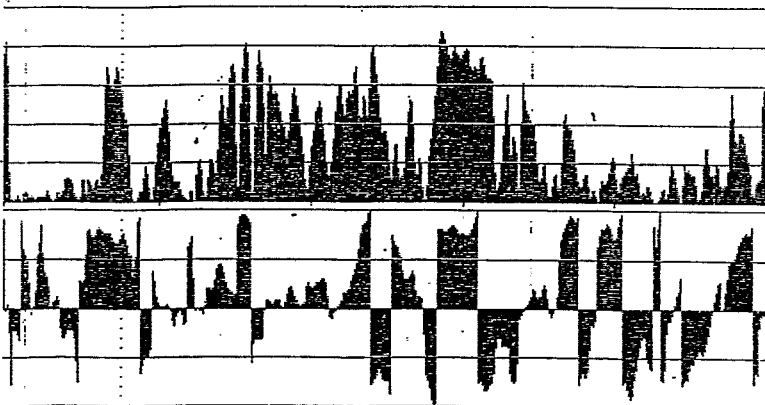
Ch.A - R25
Ch.B - R33



M2 CROSS SPEC PHASE
Y: -200 TO +200 DEG
X: 0.000Hz + 50Hz LIN

X: 7.625Hz
ΔX: 100.000Hz
16

M1 COHERENCE
Y: 1.00
X: 0.000Hz + 50Hz LIN



M2 CROSS SPEC PHASE
Y: -200 TO +200 DEG
X: 0.000Hz + 50Hz LIN

Fig. 26

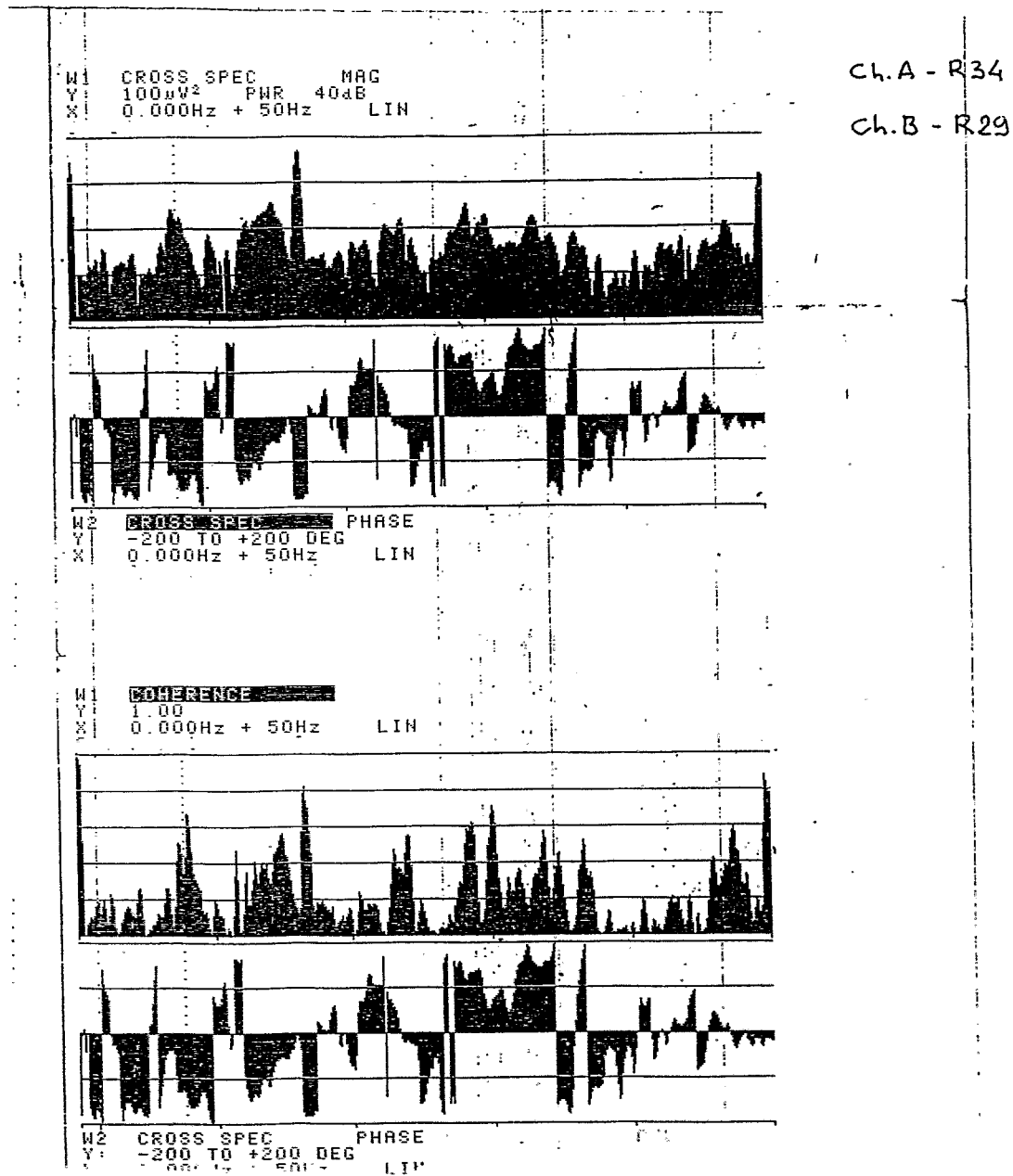
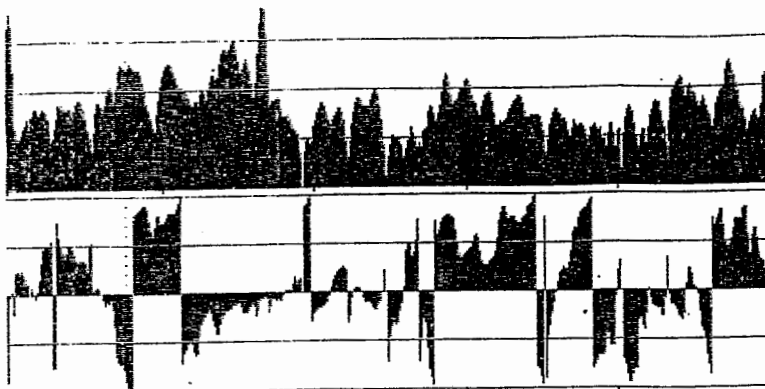


Fig. 27

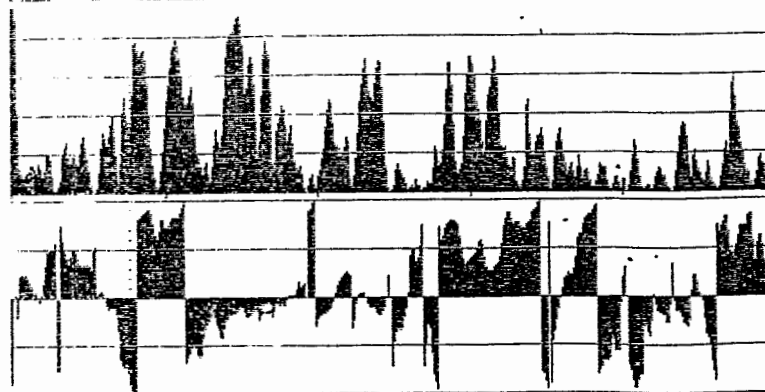
M1 CROSS SPEC MAG
Y: 1000W² PNR 40dB
X: 0.000Hz + 50Hz LIN

Ch.A-R34
Ch.B-R33



M2 CROSS SPEC PHASE
Y: -200 TO +200 DEG
X: 0.000Hz + 50Hz LIN

M1 REFERENCE
Y: 1.00
X: 0.000Hz + 50Hz LIN



M2 CROSS SPEC PHASE
Y: -200 TO +200 DEG
X: 0.000Hz + 50Hz LIN

Fig. 28

The presented phase spectra and coherent functions doesn't carry enough information for definitive conclusions on natural RCP frequencies. That's why power autospectra of the above pointed out detectors have been included into analysis. These autospectra are shown in Fig.29 - Fig.31.

Natural oscillation tones for frequencies more than 15 Hz are characterised by a complex waveshape and it's impossible to recover their waveform on the basis of available information. So the discussion is limited to spectral components analysis of Table 8.

Table 8 Values of frequency and coherent functions

f, Hz	R32-R30	R29-R31	R29-R25	R29-R33	R25-R33	R29-R34	R34-R33
1.9				0.3 (f)			
2.5	0.22 (f)					0.22 (f)	0.2
3.0		0.5 (f)					
3.4				0.15 (af)		0.17 (af)	0.25
4.7		0.35 (f)	0.23	0.18 (af)		0.25 (af)	0.3
5.6	0.22 (f)			0.15 (af)			0.3 (f)
6.5					0.7 (af)	0.28 (af)	0.4 (f)
7.3		0.93 (f)	0.75 (af)	0.95 (f)	0.7 (f)	0.5 (af)	0.5 (af)
8.0				0.87 (f)		0.67 (f)	0.8 (f)
8.6	0.2 (f)			0.23 (f)			0.75 (f)
9.0	0.3 (af)				0.2		
10.0		0.58 (f)	0.3 (f)			0.2	
10.8	0.4 (f)	0.39 (f)		0.23 (f)	0.5 (f)		0.8 (af)
11.5				0.3 (f)		0.5 (af)	0.55
12.5		0.3 (f)	0.5	0.2 (f)	0.2 (f)		0.18
13.4		0.2 (f)	0.4	0.4 (f)	0.2 (f)	0.4	0.4
14.8		0.22 (af)	0.4 (f)	0.65 (f)	0.7 (f)	0.58 (f)	0.9 (f)

The spike at 1.9 Hz appears only in a single spectrum of coherent function for R29-R33 detectors. This spike is absent in autospectra including R29 and R33 detectors. There are also no components at 3.4, 6.5 and 11.5 Hz in autospectra. The spectral component at 3.0 Hz is observed only in autospectrum for R31 detector and more over not in all of the realizations. That's why further in the analysis these spectral components were excluded from the consideration.

The rest of spectral components at 2.5, 4.7, 5.6, 8.0, 8.6, 9.0, 10.0, 12.5 and 13.4 Hz are observed in a series of coherent function spectra their values being rather high. They also appear in the most of autospectra. The origin of these frequency components in spectra of dynamic response are not explained by the known induced actions, that's why they can be considered as possible natural RCP frequencies.

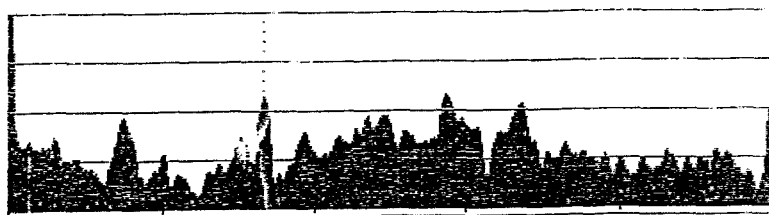
The further analysis was carried out on the basis of phase relations, components values in autospectra, calculated results and modern view on natural waveforms. The MCP and SG support structures analysis, the analysis of their inertia characteristics and pipelines configuration analysis allow one to suppose that among the lowest natural tones of oscillations

there must exist ones with the waveforms that in general is characterised by the following kinds of motion (the list of motions is given in the order of frequency increase):

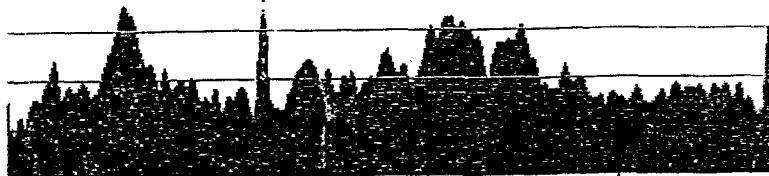
- translational MCP motion in horizontal plane in the direction perpendicular to the cold pipe axis;
- translational SG motion in horizontal plane in the direction perpendicular to the hot (cold) pipe axis;
- rotary SG motion around vertical axis;
- rotary MCP motion around horizontal axis perpendicular to the cold pipe axis;
- rotary MCP motion around horizontal axis parallel to the cold pipe axis;
- translational SG motion in horizontal plane in the direction parallel to the hot (cold) pipe axis;
- vertical translational MCP motion (vertical MCP vibration on the support);
- the combination of the above listed simplest motions.

There also can exist tones among the lowest ones that are connected with the reactor vessel motion and upper block motion. However it's impossible to identify these tones by the detectors mounted on the pipelines. Natural tones connected with the wave origin on the pipes are estimated to be within the frequency range higher than 15 Hz.

M: AUTO SPEC CH. A
Y: 1.00mV² PHR 40dB
X: 0.000Hz + 50Hz LIN



CH. A - R29

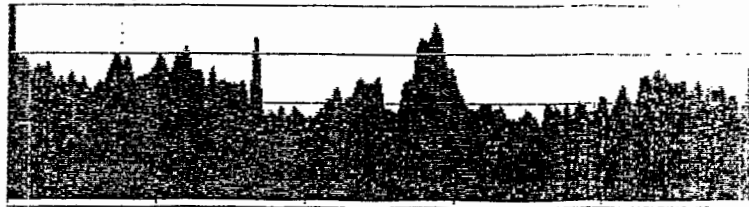


CH. B - R31

M2: AUTO SPEC CH. B []
Y: 10.0mV RMS 40dB
X: 0.000Hz + 50Hz LIN

Fig. 29

M1 AUTO SPEC CH A
Y: 100.0mV RMS 40dB
X: 0.000Hz + 50Hz LIN



CH.A - R32



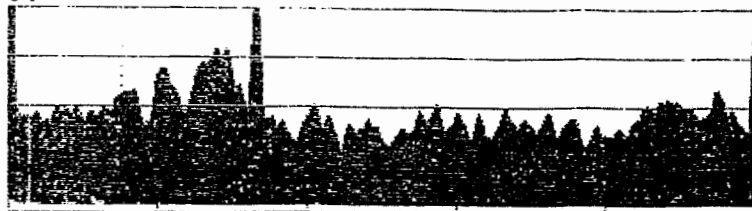
CH.B - R30

M2 AUTO SPEC CH B
Y: 10.0mV RMS 40dB
X: 0.000Hz + 50Hz LIN

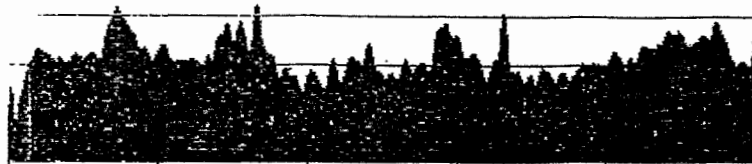
30

Fig. 30

M1 AUTO SPEC CH A
Y: 10.0mV RMS 40dB
X: 0.000Hz + 50Hz LIN



CH.A - R34



CH.B - R33

M2 AUTO SPEC CH B
Y: 10.0mV RMS 40dB
X: 0.000Hz + 50Hz LIN

Fig. 31

Let's discuss spectral components that can be considered as natural tones of oscillations. The spectral components with frequency of 2.5 Hz display themselves first of all in flexural cold pipe vibrations for phase in horizontal plane, the oscillation intensity being higher near MCP. The oscillations of this frequency have been observed also for the U-shaped tube. These observations and calculated estimates make it possible to suppose this tone to correspond in waveform to the natural vibrations typical for translational MCP motion as a solid body motion on roller supports in horizontal plane in the direction perpendicular to the cold pipe axis. This waveform is presented in Fig. 32 where the upper view of the reactor facility is shown. (The waveforms visualization was carried out with finite element model.)

The spectral component with frequency of 4.7 Hz exists in general in R25 detector records which provides data on hot pipe bending. In less extent this component exists in the records of R33 and R34 detectors providing data on U-shaped tube motion. The waveforms of this tone can be considered as translational SG motion on roller supports in horizontal plane in the direction perpendicular to the cold pipe axis. The waveshapes being discussed is shown in Fig. 33.

It's rather difficult to interpret the spectrum component of 5.6 Hz because of weak displaying itself in autospectra. More over the R27-R29 detectors records are out of phase. Such kind of waveshapes can realize themselves only when there is a wave on the cold pipe with the knot between the detectors. The calculated estimates show that this phenomenon can take place only for frequencies higher than 20 Hz. That's why the waveshapes for this frequency have not been analysed.

The spectral component for frequency of 8.0 Hz in coherent function spectra and in autospectra masks itself to great extent by the acoustic wave component with frequency of 7.3 Hz. So it's difficult to recover the waveform for this component too.

The component with frequency of 8.6 Hz is characterised by horizontal and weak vertical motions of cold and U-shaped pipes. Amplitude and phase functions analysis and calculated estimates allows one to suppose the waveshape of this tone to be connected with rotary MCP motions around horizontal axis parallel to the cold pipe axis. The waveshape of this type is shown in Fig. 34.

In autospectra the component with frequency of 9.0 Hz manifests itself very weakly. Besides as in the case of component with 5.6 Hz it's very difficult to explain the existence of phase opposition in R32-R30 detectors records. That's why the waveform for this frequency have not been analysed.

The spectral component for frequency of 10.0 Hz displays itself mainly in coherent functions spectra of R27, R29, R31 and R25 detectors records. These detectors give information about cold and hot pipes bending in vertical plane. But this component practically doesn't manifest itself in spectra obtained from the records of detectors mounted on U-shaped pipe. Such kind of motion can take place when the reactor vessel vibrates in vertical direction. However the amplitude ratio in autospectra of R27, R29 and R31 detectors records doesn't allow one to draw such a conclusion. More over the intensive spectral acoustic wave component with frequency of 10.8 Hz masks essentially the spike being discussed. So it's difficult to recover the waveform for this spectral component.

The spectrum component for frequency of 12.5 Hz exists mainly in the R25 detector record. This detector indicates the hot pipe bending. The above named component in less extent is observed in the record of R33 detector which indicates the U-shaped tube motion in vertical plane. So one can consider this tone to be connected with translational SG motion in horizontal plane in the direction parallel to the hot (cold) pipe axis. The waveshape for this tone is shown in Fig. 35.

The spectral component for frequency of 13.4 Hz is observed practically in autospectra of all of the detectors. That's why it's impossible to interpret this waveform as one of the discussed above simplest motions.

Among the discussed spectral components there have not been discovered tones connected with rotary MCP motion around horizontal axis perpendicular to the cold pipe axis and there have

not been discovered tones connected with the vertical MCP vibrations. These tones are characterised by the cold and U-shaped pipes bending in vertical plane. May be the natural frequencies of these tones are higher than the discussed frequency range or may be spectral components of these tones are masking themselves in spectrum by other lines. The tone, connected with the SG rotation around vertical axis also have not been discovered. It should be noted that it's rather difficult to discover this tone by the available detectors because the rotation axis is situated between the cold and hot headers and bending strain of hot and U-shaped pipes is negligible for this kind of motion at the detectors location.

Thus one can draw the following conclusions:

1. The list of frequencies that can be interpreted as natural frequencies connected with the RCP loops of VVER-1000 is refined in the range of frequencies up to 15 Hz. These frequencies are 2.5, 4.7, 5.6, 8.0, 8.6, 9.0, 10.0, 12.5 and 13.4 Hz.
2. The waveshapes have been proposed for spectral components for frequencies 2.5, 4.7, 8.6 and 12.5 Hz.
3. The presented results can't be considered as final ones because the available information is not enough for natural frequencies and vibration forms definitive identification.

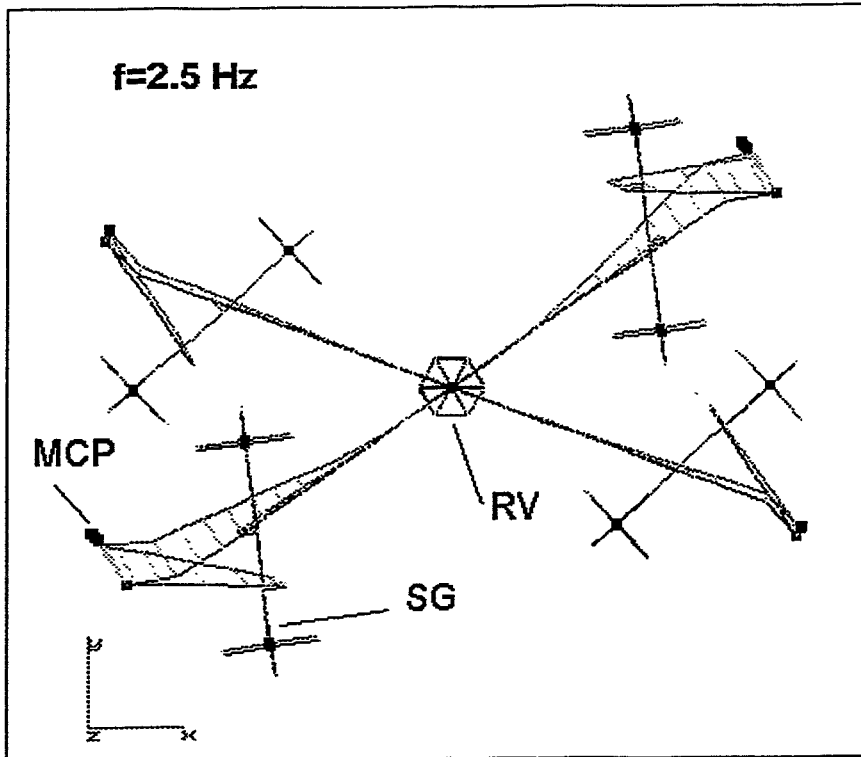


Fig. 32 Shape of mode (top view)

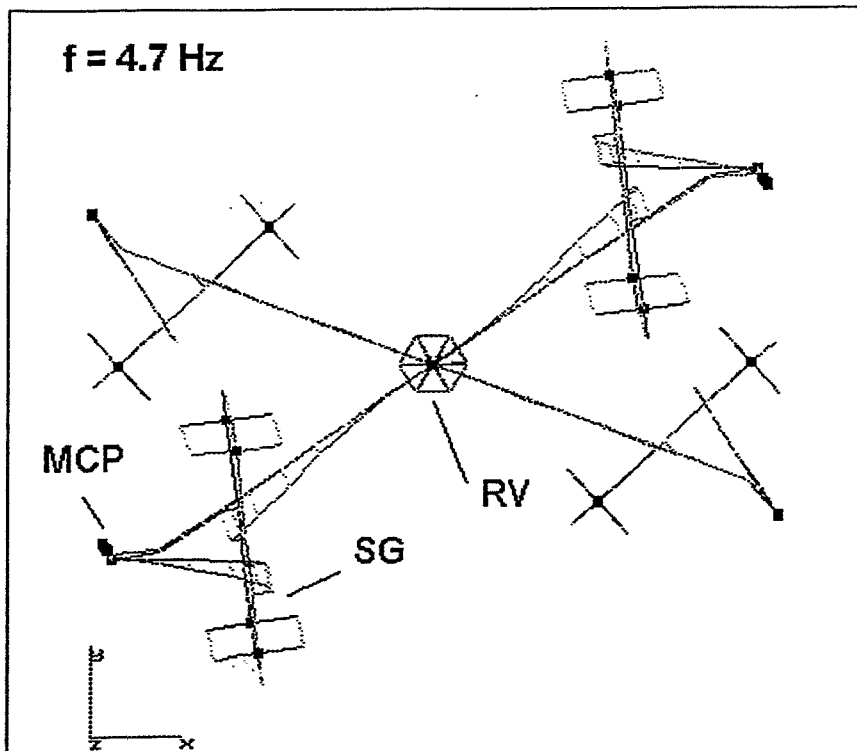


Fig. 33 Shape of mode (top view)

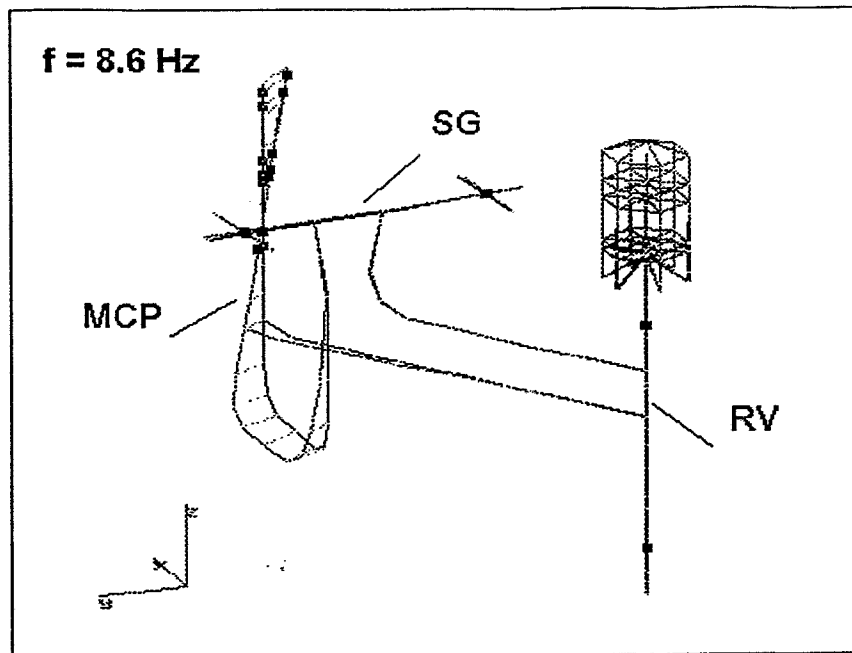


Fig. 34 Shape of mode (spatial view of one loop only)

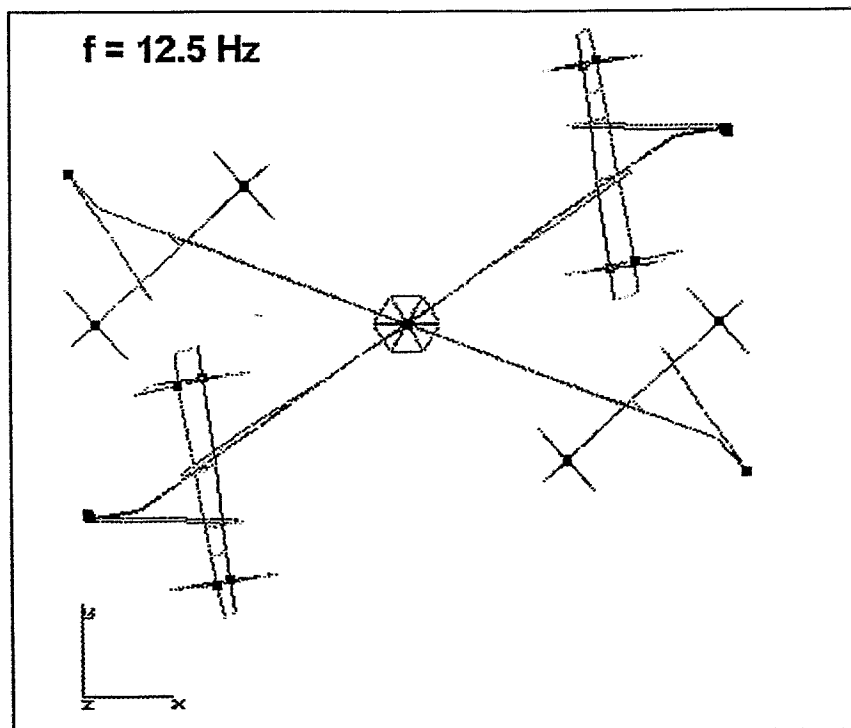


Fig. 35 Shape of mode (top view)

Reference

- [1] V.V.Bulavin, D.F.Gutsev and V.I.Pavelko. The experimental definition of the acoustic standing waves series shapes, formed in the coolant of the primary circuit of VVER-440 type reactor. Progress in Nuclear Energy, Volume 29, Number 3/4, 1995, p.p 153-170.
- [2] Vibration modelling of the VVER type reactors. The analysis of the design characteristics and experimental data for adjustment of the VVER-1000 model. The intermediate report. 320-O.211-004

Teil 6

Theoretical Modelling of VVER-1000 Primary Circuit Vibrations

S. Perov

First version of a global vibration model of the
VVER-1000 primary circuit
based on the finite element code ANSYS®

1996

Content

1. LOCAL MODELS OF THE VVER-1000 UNITS

- 1.1. The model of the CB guide lugs
- 1.2. Local model of RPV
- 1.3. Local model of MCP support.
- 1.4. Local model of steampipe.
- 1.5. Local model of Upper Block (UB)

2. GLOBAL MODEL OF WWER-1000 PRIMARY CIRCUIT

- 2.1. Models of RPV, internals and upper structures
- 2.2. Models of the WWER-1000 loop
- 2.3. Global model of the primary circuit on the whole

3. CONCLUSIONS AND PROPOSALS

- 3.1. Modelling of RPV with internals
- 3.2. Loop models
- 3.3. Forced vibration
- 3.4. Testing and tuning models
- 3.5. Diagnostics

Theoretical Modelling of WWER-1000 Primary Circuit Vibrations

S. Perov

Abstracts

The finite-element models and computational results obtained by use of the ANSYS code are shortly represented in this paper. The local models of separate units are described in the first section. The simplified models of units have been built on base of these local models to use them in global model of primary circuit on the whole. The global model and appropriate results are represented in the second section. Conclusions and proposals for future steps are in the third section.

1. LOCAL MODELS of the WWER-1000 UNITS

The main object of this part of the work is building of accurate models of separate units and than the development of simplified models on base of computing investigation of units mechanical features (deformations, eigenfrequencies, e.t.c). This approach makes it possible both to analyse the separate units in all details and to build global model of WWER-1000 primary circuit on the whole.

The local models of core barrel (CB) guide lugs, reactor pressure vessel (RPV), main coolant pump (MCP) supporting structure, steampipe, upper block (UB) are considered in this paper.

1.1 The model of CB guide lugs

The CB is connected to RPV in the lower part by means of 8 identical guide lugs. In normal condition each guide lug admits free CB movement in axial and radial directions and prevent free one in tangential direction. Therefore, the CB has additional support in lower part for nonaxisymmetric vibrations.

The model of guide lug (GLUG.MAC) includes the guide lug itself and holder for connection guide lug to the RPV. Solid finite elements are used for modeling. Discretisations are choosen so that there are three layers at least in each part of structure.

The main aim of modelling is to define stiffness characteristics of guide lugs as support of the CB. Therefore, a static analysis is used. Two kinds of loads are applied: pointed force and distributed forces (pressure) in tangential direction. The pointed force is imposed in the centre of the guide lug, the distributed forces are in approximatly one-third area of side surface of the guide lug that is in correspondance with real conditions.

Discuss briefly main results.

Case one (pointed force). Maximal displacement is in a load point equal $1.0e-9$ m/N. It corresponds to stiffness of guide lugs $1.0e+9$ N/m. These results coincide with

experimental ones for real guide lug structure under pointed load.

Case two (distributed forces). Maximal displacement is equal $0.48e-9$ m/N and equivalent stiffness is $2.1e+9$ N/m. This case is more close to real condition and this result is used further.

In the global model of WWER-1000 (beam model) it is possible to use one elastic support with stiffness characteristics calculated by formulas:

$$c_{xx} = c_0 \cdot \sum_1^8 A_i \sin^2(\varphi_i)$$

$$c_{yy} = c_0 \cdot \sum_1^8 A_i \cos^2(\varphi_i)$$

$$c_{xy} = -c_0 \cdot \sum_1^8 A_i \sin(\varphi_i) \cos(\varphi_i)$$

where x, y - are two axis perpendicular to symmetry axis of CB, A - coefficients equal 0 or 1 in dependence on clamping state each guide lug, φ - is angle between x -axis and each guide lug.

1.2 Local model of RPV

In the global model the RPV is considered as a beam (pipe) structure, but really RPV is a shell (or solid in some tasks) structure. Therefore the local model of RPV (RPVSHELL.MAC) has been developed to take into account local shell (or solid) effects in the global model.

The RPV is modeled as shell structure in all details. Additional constraints are applied to define shell effects only. The nodes located in vertical plane ($xz, y=0$) is fixed additionally, that corresponds to fixation symmetry axis of beam. Pointed or distributed loads are applied in x, y, z directions to define local shell effects in connection places RPV with guide lugs and main pipes.

The main results are following.

Connection RPV-guide lug. Pointed force (F_x) and moment (M_z) equal force on length of guide lug holder are imposed in node corresponding to location of one guide lug. The equivalent stiffness of the RPV is equal to $2.0e+10$ N/m. This value is 1 power more than stiffness of guide lug itself and this local effect is neglectable. Small influence of local shell effects on guide lug stiffness characteristics is explained by closeness of RPV bottom - strong part of RPV.

Connection RPV-Cold Leg (CL). Three types of load are applied for modelling of this connection F_x, F_y, F_z . In each case the distributed forces are imposed in the

nodes of RPV model corresponding to location of RPV-CL connection and the displacements of these nodes are computed. On base of these results it is possible to define stiffness characteristics of equivalent beam to model connection between RPV axis and CL. Such beam has following stiffness parameters:

$$EA=6.9 \cdot 10^{10} N, \quad EI_{yy}=1.5 \cdot 10^{12} N \cdot m^2, \quad EI_{zz}=1.3 \cdot 10^{11} N \cdot m^2.$$

For comparison, the stiffness characteristics of main pipes are:

$$EA=3.9 \cdot 10^{10} N, \quad EI_{yy}=4.2 \cdot 10^9 N \cdot m^2, \quad EI_{zz}=4.2 \cdot 10^9 N \cdot m^2.$$

So, connective beam has tension stiffness the same order as main pipe and bending stiffness one-two powers more. The strong stiffness of the connecting beam results from the small distance of the RPV-CL connection to the supporting ring of the RPV, which has a rather large thickness (0.29 m).

Connection RPV-Hot Leg (HL). The same types of loads are used in this case and only location of loads corresponds connection RPV-CL. The equivalent beam has following stiffness parameters:

$$EA=3.7 \cdot 10^{10} N, \quad EI_{yy}=6.2 \cdot 10^{10} N \cdot m^2, \quad EI_{zz}=1.8 \cdot 10^{11} N \cdot m^2.$$

The tension stiffness is the same as for main pipes and bending stiffness one power more.

It should be pointed out, because of length of connective beam three-five times less than length of main pipes and of tension stiffness has less influence on vibration of primary circuit than bending stiffness, the influence of local shell effects are rather small.

1.3 Local model of MCP support.

The MCP supporting structure consists of three legs installed on rollers and admits free displacement in horizontal plane. Each leg is complex structure including shell and solid elements. In the finite-element model (MCPSUP.MAC) the shell elements are represented only and the solid elements are modeled by imposing additional constraints. So, supporting cylinders of legs and supporting ring of MCP vessel are considered as rigid bodies.

The loads are applied to an additional central node and constraint equations are used to connect this node to legs. Three types of loads are used: force in vertical direction (F_z) and moments around axis in horizontal plane (M_x , M_y). On the base of computing of central node displacements under each kind of loads it is possible to define stiffness matrix of equivalent one-node support.

Under normal conditions the MCP supporting structure is symmetric one. Therefore all nondiagonal elements of stiffness matrix are close to null. The nonequal to null elements have the following values:

$$C_{zz}=7.63 \cdot 10^9 N/m$$

$$C_{rot_x rot_x} = C_{rot_y rot_y} = 1.49 \cdot 10^{10} N \cdot m$$

This model can also be used for computing of stiffness parameters of MCP support under abnormal conditions too if there are damages in MCP legs. In these cases we have nondiagonal stiffness matrices.

1.4 Local model of steampipe.

The WWER-1000 steam generator (SG) is installed on roller supports which allow free displacements in the horizontal plane. However, such displacements are associated with deformations of the steampipe which is equivalent to additional support of SG in horizontal plane.

The finite-element model of steampipe (SECCON.MAC) has been developed to define stiffness characteristics of additional support. It includes steampipe itself and steam collector as elastic beams and SG vessel as a rigid beam. The loads are applied in one node located in the centre of the SG. Three types of loads are used: forces in x and y directions, moment around z-axis. It is used local coordinate system where x-axis coincides with SG symmetry axis. The displacements of central node are computed in each case and then stiffness parameters are defined.

The stiffness matrix of additional support located in central node has following elements:

$$C_{xx}=3.85 \cdot 10^5 N/m$$

$$C_{yy}=1.95 \cdot 10^5 N/m$$

$$C_{xy}=-0.70 \cdot 10^5 N/m$$

$$C_{\theta\theta}=7.38 \cdot 10^6 N \cdot m$$

$$C_{x\Theta} = 2.47 \cdot 10^6 N$$

$$C_{y\Theta} = -3.34 \cdot 10^6 N$$

where Θ - is rotational degree of freedom around z-axis.

It should be pointed out that the additional SG support is rather weak in comparison with the stiffness of main pipes and it has small influence on eigenfrequencies of primary circuit.

1.5 Local model of Upper Block (UB)

The UB consists of a traverse and 6 rods for lifting of RPV cover, collector, three horizontal plates and set of vertical tubes between all horizontal structures (plates, collector). The rods are arranged inside of the tubes. In the finite-element model of the UB (UPBLOCK.MAC) the rods and the tubes are represented by beam (pipe) elements, the collector and the plates are modeled as shells. In view of the fact that the plates and the collector have a lot of holes, reduced material properties are used which are calculated by use of total mass of each unit. The collector tubes are modeled by one beam (pipe) with reduced material properties too.

The main goal is to compute eigenfrequencies of UB. In view of some simplifications are used in finite-element model, it is necessary to define influence of ones on calculation accuracy. So, it was obtained that collector tubes have weak influence on eigenfrequencies and it is possible to use a simple model of ones. On the other hand, the plates are insufficient strong and it is necessary to use precise their models.

Here the main results of eigencharacteristics computing are presented.

Eigenfrequency, Hz	Shape of mode
0.54	Rotation (1-st shape)
4.4	Bending of all structure (1-st shape)
5.3	Rotation (2-nd shape)
16.6	Bending of internal rods only (1-st shape)
20.6	Bending of all structure (2-nd shape)
25.2	Rotation (3-rd shape)
29.1	Bending of all structure (3-rd shape)
32.5	Rotation (4-th shape)
45.6	Bending internal rods only (2-nd shape)

It is an interesting fact that one eigenfrequency coincide with the frequency of

MCP rotation (16.6 Hz) and resonance effects can take place.

The simplified beam model of UB (MDLUB.MAC) has been developed on the base of these results for using in the global model. It contains five nodes only. The tension and bending stiffness of each beam element is equal to 6 times of those of tubes and rods jointly. The plates and the collector are modeled by pointed masses. Additional constraints are imposed to get bending shape of modes of all structure similar to same shape of modes of complex model. By use such approach it is possible to get the same eigenfrequencies for both bending modes of all structure and axial modes. Small adjusting of bending stiffness is applied to take into account flexibility of the plates. In view of considered model is very simple it is possible to tune two first eigenfrequencies only for bending modes. The simplified model has following eigenfrequencies.

Eigenfrequency, Hz	Shape of mode
4.4	Bending of all structure (1-st shape)
20.5	Bending of all structure (2-nd shape)
25.2	Bending of all structure (3-rd shape)

2. GLOBAL MODEL OF WWER-1000 PRIMARY CIRCUIT

The global model of WWER-1000 can be conventionally divided into two part. The first is the RPV including internals and upper structures, the second consists of 4 identical loops. At first consider these two separately.

2.1 Models of RPV, internals and upper structures

Pipe elements are used for modeling of RPV, internals and upper structures.

The model of RPV together with cover (MDLRPV.MAC) has 16 nodes. Elliptical parts of cover and bottom are modeled stepwise. Reduced material properties are used for nozzles above cover and elliptical parts. The RPV is considered as structure filled by frozen liquid.

The core barrel (CB) model (MDLCB.MAC) has 13 nodes. Reduced material properties are used for the CB above the separating ring (in view of a lot of holes) and for the CB bottom.

The model of thermal shield (TS) (MDLTS.MAC) has 3 nodes only because it is a rather strong structure. In view of it has a lot of internal channels for coolant flow, reduced material properties are used.

The core is modeled as sum of fuel assemblies (MDLCORE.MAC), because boundary conditions of each fuel assembly are close to free support (hinge). The tension stiffness (EA) take into account tension stiffness of directing tubes only, and bending stiffness (EI) take into account bending stiffness of tubes and fuel pins jointly. It follows from the structure of fuel assembly, because fuel pins don't connect to a fuel assembly head and can not be loaded by axial force. Small tuning of bending stiffness is used to have the same first bending eigenfrequency as the real fuel assembly.

In the model of upper supporting structure (internal unit) (MDLUSS.MAC) the shell of USS is modeled as a pipe, supporting plates as pointed masses, all supporting tubes as one pipe element with reduced material properties.

The model of upper block (MDLUB.MAC) was describe above.

The model of control power structure (MDLCPS.MAC) is very rough, because inertial characteristics only are modeled correctly.

In the full model of RPV including internals and upper structure (REACMOD.MAC) connections between separate units are carried out by means of coupling of nodes (CPL.MAC) or by use of stiffness matrices between nodes (SPRING.MAC). Coupling is used for connection of UB and CPS to RPV, of TS to CB bottom. The stiffness matrices are used for modeling of upper CB support, separating ring (at two levels), guide lugs, upper keys of TS, supporting cups of core, spring block of core, keys between CB and USS, upper support of USS.

Because up to now there are no local models of all connective units, it is assumed the following:

- upper CB support - full clamping,
- separating ring - fixation of side displacements at two levels,
- guide lugs - from local model,
- upper keys of TS - free,
- supporting cups of core - free support (hinge),
- spring block of core - sum of stiffnesses of fuel assemblies spring blocks,
- keys CB-USS - free,
- upper support USS - full clamping.

The RPV has one support (supporting ring) which is modeled by one stiffness matrix. Because there is no local model of supporting ring, the approximate values from previous models are used.

Under these assumptions, the following results on eigencharacteristics of reactor without loops are obtained.

Eigenfrequency, Hz	Shape of mode
2.3	Bending of core (1-st shape)
3.9	Bending of UB (1-st shape)+RPV (in phase)
5.9	RPV (pendular)+UB (in antiphase)
9.3	Bending of core (2-nd shape)
20.6	Bending of UB (2-nd shape)
21.3	Bending of core (3-rd shape)+UB (2-nd shape)
25.2	Bending of UB (3-rd shape)
28.6	Axial CB, core
33.8	Bending CPS (1-st shape)
37.9	Bending CB+USS
38.4	Axial RPV, USS, CB, core
42.2	Bending CB
49.9	Axial RPV, USS, CB, core
53.1	Axial UB + RPV (in phase)
53.2	Bending USS

This model doesn't take into account fluid-structure interaction. Therefore, all eigenfrequencies associated with CB bending movements are not valid. The model of core is tuned one first mode only. The last core modes are not correct.

2.2 Models of the WWER-1000 loop

Each loop of WWER-1000 consists of steam generator (SG), main coolant pump (MCP), hot leg (HL), cold leg (CL) and U-shape leg (UL). Pipe elements are used for modelling.

The model of SG (MDLSG.MAC) includes SG vessel and supporting structure. The model has 21 nodes. Elliptical ends are modeled as a stepwise pipe. Hot and cold collectors are modeled by pointed masses. Two strong beam elements without mass are used for connection SG to HL and UL. The SG model has 4 main supports which have fixation in vertical direction only, and 1 additional support from steampipe (see above). The SG is considered as a structure filled by frozen liquid.

The model of MCP (MDLMCP.MAC) includes MCP vessel and MCP shaft. It has 18 nodes. The MCP vessel is modeled as a number of pipes (vertical shells) and pointed masses (horizontal plates), the MCP shaft as pipes (shaft itself) and one pointed mass (flywheel). Connections between vessel and shaft (shaft bearings) are modeled by stiffness matrices. It is supposed a very strong connection like a hinge. Two strong beam elements are used for connection MCP vessel to the CL and the UL. The model of MCP support see above.

Straight and elbow pipe elements are used in the models of HL, CL, UL (MDLHL.MAC, MDLCL.MAC, MDLUL.MAC). All these models include frozen liquid inside.

The eigencharacteristics of one loop only (LOOP1COM.MAC) are presented in next table (nodes of connections to RPV are full fixed). Local x-axis coincides with CL.

Eigenfrequency, Hz	Shape of mode
0.7	SG(y, rotz), MCP(y) (in phase)
1.8	SG(y, rotz)
2.5	MCP(y), SG (y, rotz) (in antiphase)
7.4	SG(x)
8.0	MCP(bending in x-direction)
11.2	MCP(bending in y-direction), UL
12.7	MCP, CL, UL
17.2	UL (in hor. plane)
26.1	CL (1-st wave)
27.8	CL, MCP(vessel and shaft in phase)
33.2	MCP shaft
34.5	MCP(vertical), CL
37.9	CL, UL, MCP
38.0	CL, HL
40.0	HL (in hor. plane)
43.4	HL (in vert. plane), SG (bending)
45.5	U (wave with node)
49.0	HL (in vert. plane)
53.1	CL (2-nd wave), HL, UL, MCP
58.3	UL, MCP
61.3	SG(bending)
64.1	CL(2-nd wave)

As follows from this table a lot of eigenfrequencies are associated with MCP movements because it is rather flexible unit.

2.3 Global model of the primary circuit on the whole

The global model of the WWER-1000 primary circuit (PRIMCOM.MAC) includes RPV with internals and upper structure and 4 identical loops. Because this structure is regular (has identical loops), it has multiple modes with close eigenfrequencies and with different phase only.

The most part of modes is the sum of RPV (with internals and upper structure) and one loop modes. The lowest modes of loop have the same eigenfrequencies as for one loop only. The same results for internals and upper structures modes were obtained.

The pendular mode of RPV has two different eigenfrequencies in x- and y-directions (5.2 Hz and 5.7 Hz) in view of nonsymmetrical arrangement of loops to x and y axis. The modes associated with waves on CL and HL interact with bending of RPV. Therefore the eigenfrequencies splits of these modes are occurred, especially above 40 Hz.

A set of new modes appear in this model. They are associated with interaction of

the RPV and loops. This modes are presented in next table.

Eigenfrequency, Hz	Shape of mode
8.5	RPV(pendular around x-axis), CLs, Hls
10.4	RPV(pendular around y-axis), CLs, Hls
31.8	RPV(rotation around z-axis), CLs, Hls
49.9	RPV(rotation around z-axis), CLs, Hls

3. CONCLUSIONS AND PROPOSALS

3.1 Modelling of RPV with internals

The model of RPV with internals which have to be considered is too simple for investigations of internals vibrations. It can be sufficient for loop vibrations because it has accurate stiffness and inertial characteristics of RPV on the whole. For investigation of internals vibrations it is necessary to develop the local models. For the CB it must be a hydroelastic shell model that take into account fluid-structure interaction in narrow channels between RPV and CB and especially between CB and TS. This model has to take into account interaction between CB and TS-core too, especially in case of free guide lugs, because the mass of core is very large, larger than mass of CB itself. It should be pointed out that this interaction is strong for axisymmetric and beam CB modes only, because for shell modes there is clamping in the lower end of CB in view of strong CB bottom. However, the beam modes of CB are of special interest for diagnostics problems.

The next problem for internals modelling is local model of core, because it is a rather flexible structure and a lot of lowest modes are associated with movements of core. As first step it is necessary to build the model of fuel assembly. The most difficult problem for this model is interaction between directing tubes (load-bearing structure) and fuel elements. The fluid-structure interaction is a problem too. The next step is building of model for cooperative vibrations all fuel assemblies.

The final step is development of new simplified model of RPV with internals that take into account all above mentioned features.

One of another problem is building of local model of RPV supporting ring. This model is needed for determination of stiffness matrix elements for RPV support both in global and local models.

3.2 Loop models

As follows from computing results a lot of eigenmodes are associated with MCP movements. Therefore it is necessary to develop an accurate model of MCP vessel. It must be shell model with all details. On base of this model it will be possible to build the simplified model. One problem more is modeling of MCP shaft bearings, because it is one of diagnostics problems.

The local model of MCP support is not full, because it doesn't take into account elasticity of vessel supporting ring and rollers. It is one of future problems.

The SG moves as rigid body for lowest modes. Therefore it is sufficient to have simple model of SG. But the occurrence of local shell effects is possible like ones were described in the first section for RPV. Moreover the SG vessel is less strong than RPV. One problem more is interaction SG vessel with hot-cold collectors, also with filling fluid and heat exchanging tubes. Therefore it is necessary to develop more

complex local model of SG including supporting structure.

The SG and the MCP have special hydroshock-absorber systems that is used to induce horizontal seismic loads. These systems cause damping effects that affect on vibration frequencies. So it is needed to evaluate this effect.

The next interesting problem is interaction main pipes with fluid flow inside, because in this case Coriolis's, inertial and hydrodynamic forces affect on eigenfrequencies.

3.3 Forced vibration

Theoretical investigations of forced vibrations are important, because in this case it is possible to make direct comparison with experimental data and to use amplitudes as diagnostic attributes, not frequencies only. There are two difficult problems in this way. The first is model of exciting forces, the second is damping model.

All exciting forces can be conventionally divided in three parts: mechanical one caused by disbalance of MCPs (or another pumps) shafts, hydrodynamical ones associated with acoustic waves and other hydrodynamical forces. For first two ones it is possible to develop theoretical models, which need minimum experimental data (in some points of primary circuit only). The third part - hydrodynamical forces itself - is the most difficult theoretical problem. Now, the only experimental way is possible, but it is necessary to have a sufficient amount of pressure sensors over loops and RPV.

The same problem is for damping model - the only experimental way is possible now.

3.4 Testing and tuning models

All developed models are needed to test by use of experimental data obtained during NPP test or on scale models. Then, in view of all NPP units have small differences each other, it is necessary to tune models specially for each NPP unit by variations of initial data. It is promising to use for this purpose the optimization technique and appropriate software.

3.5 Diagnostics

The final object of theoretical modeling is diagnostic support. Therefore it is necessary to define influence of possible anomalies on vibrational parameters. The other problem is in return to identify anomaly by use abnormal experimental spectra and theoretical models. In this way it is useful to apply special algorithm and software like mentioned above.

Teil 7

Protocol of the Workshop on Vibration Modelling of VVER Type Reactors

held at the Research Center Rossendorf, Institute for Safety Research,
Dec. 12-16 1994

Participants:

Dr. V. V. Bulavin, Kurchatov Institute Moscow, Russia
Dr. A. I. Usanov, OKB Hidropress Podolsk, Russia

Dr. G. Pór, Technical University of Budapest, Hungary
Dr. I. Józsa, Nuclear Power Plant Paks Ltd., Hungary

Prof. Dr. F.-P. Weiß, Research Center Rossendorf, Germany
Dr. E. Altstadt, Beyer (translator), Dr. G. Grunwald, G. Hessel, Dr. F. Hollstein,
M. Scheffler, Dr. W. Schmitt, K. van der Vorst, R. Weiß, J. Zoller (all from
Research Center Rossendorf = RCR)

1. The aim of the workshop was the preparation of the German-Russian-Hungarian project "Investigation of Mechanical Accident Scenarios at VVER Type Reactors Using the Finite-Element-Method for Vibration Modelling". The project is explicitly mentioned in the 1995 schedule for German-Russian Scientific Technological Cooperation on the Peaceful Use of Nuclear Energy under issue III/4: safety of water cooled reactors.
2. The German, Russian and Hungarian participants gave an overview about the state of art of VVER-vibration modelling and vibration monitoring (see the programme appended). Finite element models for the VVER-440, experimental vibration investigations, noise measurements and analysis at VVER-440 and VVER-1000, the theoretical modelling of fluid-structure-interaction and fluid flow excitation of the structure were reported on.
3. The common project (see point 1.) was introduced in detail to the Russian and Hungarian partners (aims, working programme).
4. The suggested working programme (see attachment 1) is to be realized as a common project (see point 1.). Based on this protocol an application will be directed to BMBF (Bundesministerium für Bildung und Forschung) to establish the project as a WTZ (WTZ = Scientific Technological Cooperation with Foreign Institutions) activity and to achieve financial support. Moreover the RCR is looking for opportunities to support the Russian and Hungarian partners by temporarily making available to them hardware and software on a cost free lending base.

5. Comments to the working programme:

In general, the envisioned project partners agreed with the working programme proposed by RCR and declared their willingness to take part in it. During discussion the following supplements were discussed and agreed on:

Working programme point A1.2: The Russian side confirmed its readiness to take part in the calculations of the initial parameters of the finite element model (masses, momenta of inertia) of certain components of the VVER-1000 reactor. In addition, the partners expressed the necessity to perform separate finite element calculations for the guide lugs of the VVER-1000.

Working programme point A2: The Russian partners offered to perform measurements during operation at several reactors. Emphasis shall be put on measurements at Balakovo NPP unit 2. These measurements can take place in the period June 1995 to December 1996, when the diagnostic instrumentation is available. The instrumentation for these measurements will be as follows (see also in the attachment 3):

- 4 absolute displacement sensors at reactor pressure vessel head
frequency range ... 2 to 100 Hz
- 2 relative displacement sensors at each steam generator
frequency range ... 0 to 100 Hz
- 2 relative displacement sensors at each coolant pump
frequency range ... 0 to 100 Hz
- 8 ionization chambers 90 deg. (each four in two elevations)
frequency range ... 0 to 50 Hz
- 14 SPNDs in two freely chooseable fuel assemblies
frequency range ... 0 to 30 Hz
- 5 pressure fluctuation sensors
frequency range ... 0.5 to 100 Hz
- additional accelerometers at the pressure vessel (2 x 4 in two different elevations)
frequency range ... 2 to 100 Hz

Supplementary measurements at other VVER-1000 reactors should be performed to validate the Balakovo measurements. In general that instrumentation shall be used there, which has already been available. If necessary and possible additional transducers will temporarily be installed.

Measurements at VVER-440 reactors should be carried out at unit 4 of the Novovoronezh NPP using the following instrumentation (see also attachment 4):

- 4 absolute displacement sensors at reactor pressure vessel head
frequency range ... 2 to 100 Hz
- 2 relative displacement sensors at each steam generator
frequency range ... 0 to 100 Hz
- 2 relative displacement sensors at each coolant pump
frequency range ... 0 to 100 Hz
- 3 ionization chambers in one plane
frequency range ... 0 to 50 Hz
- 4 pressure fluctuation sensors
frequency range ... 0.5 to 100 Hz

The Russian side proposed to perform modal analysis experiments at running VVERs during outage times to the possible extent. External excitation shall be used but no incore vibration transducers. In case of the excitation has necessarily to be made with a servohydraulic shaker such a device must be made available.

The representative of Paks NPP handed over written material about the features and capabilities of the diagnostics instrumentation available at all four units of Paks NPP. This instrumentation has been and can be used for measurements. Technical University of Budapest expressed its interest to take part in the measurements necessary for the given project and in the work of inter-comparison of calculated and measured data. Hungarian side will check the possibility to contribute to further measurements when all information is available to calculate the costs of its participation.

All partners are ready to make available the results of former measurements at any of the reactors for the adjustment of the theoretical models.

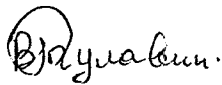
Working programme point A3: The Russian side announced that during commissionings of VVER-1000 reactors incore vibration measurements were performed. An instrumentation, as indicated in attachment 5, had been used. No artificial vibration excitation had been applied. These experiences are a good base for future incore vibration measurements.

The partners agreed that RCR will provide a proposal containing the measuring positions and signals (including incore vibration signals) as well as excitation positions and mechanisms. The Russian and Hungarian sides will respond to this proposal and check the feasibility. In addition to that, the Russian side agreed to perform vibration experiments at laboratory setups especially at a full scale fuel assembly model and at a 1:5 scaled VVER-1000 model. The 1:5 model should especially be utilized to develop an on-line procedure for condition monitoring of the core barrel guide lugs.

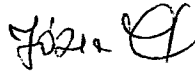
Working programme point A5: The representative of the Paks NPP initiated to add issue A5.6 :

A5.6 Accomplishment of stress calculations to provide information on high-cyclic stress changes as possible input to fatigue and lifetime assessments (responsibility still open).


6. The final version of the application for the project, that will be directed to BMBF, will be adjusted with all participants. Immediately after getting a confirmation of the support through the BMBF, the partners will have a second meeting to specify the project realization in detail.



Dr. V.V. Bulavin
KI Moscow
Nuclear Reactor 's Institute



Dr. I. Jozsa
Paks NPP

15.12.94 F-P. Weiß

Prof. Dr. F.-P. Weiß
RC Rossendorf
Institute for Safety Research

Dr. A.I. Usanov
OKB Gidropress



Dr. G. Por
TU Budapest

Attachments

1. Working programme
2. Programme of the workshop
3. Sensor arrangement of the Balakovo NPP unit 2
4. Sensor arrangement of the Novovoronesh NPP unit 4
5. Location of experimental check transducers on the primary circuit equipment

Working Programme

- A1 Elaboration of a numerical vibration model for the primary circuit of VVER-1000 type reactors using the finite-element-code ANSYS® (RCR)
 - A1.1 Structural design of the finite-element-model evaluating the construction drawings (RCR, Russian partners)
 - A1.2 Calculation of an initial parameter set for the finite-element-model based on masses, momenta of inertia, stiffness matrices etc. gained from the construction drawings (RCR)
 - A1.3 Generation of input files for the finite-element-code for all main components of the primary circuit: reactor pressure vessel, core barrel, core, main coolant legs, main coolant pumps, steam generators (RCR)
 - A1.4 Coupling of the main components
 - A1.5 Consideration of the flowing coolant by fluid-structure-elements
 - A1.6 Calculation of eigenfrequencies and mode shapes in the frequency range up to 50 Hz (RCR)
 - A1.7 Modelling of the excitation forces due to the flowing coolant (RCR)
 - A1.8 Calculation of spectral responses to the excitation (RCR)

- A2 Realization of measurements at Russian, Ukrainian and Hungarian VVERs during operation (measurement of neutron noise, pressure fluctuations, accelerations and displacements), depending on the opportunities given by the utilities (Russian and Hungarian partners)
 - A2.1 Elaboration of measurement programmes for VVER-1000 and VVER-440 (Russian and Hungarian partners, RCR)
 - A2.2 Preparation and realization at selected VVERs. The following NPPs are taken into consideration:
 - Unit 1/2 of Kola NPP (VVER-440) (Russian partners)
 - Unit 3/4 of Novovoronezh NPP (VVER-440) (Russian partners)
 - Unit 6 of Zaporoshie NPP (VVER-1000) (Russian partners)
 - Unit 1 of Kalinin NPP (VVER-1000) (Russian partners)
 - Unit 1-4 of Paks NPP (VVER-440) (Hungarian partners)

- A3 Realization of vibration experiments at selected VVERs during refueling or during commissioning, depending on the opportunities given by the utilities (Russian and Hungarian partners)
 - A3.1 Selection of one individual VVER-440 and one VVER-1000, where the measurements should take place (Russian and Hungarian partners)
 - A3.2 Selection of well suited mechanisms, positions and signals of excitation (RCR, Russian and Hungarian partners)
 - A3.3 Selection of measurement positions and measurement signals (including signals of vibrations of the reactor pressure vessel internals) (RCR, Russian and Hungarian partners)
 - A3.4 Technical preparation of the experiment (Russian and Hungarian partners)
 - A3.5 Performing the experiment (Russian and Hungarian partners)

- A4 Adjustment of the numerical finite-element-models for the VVER-440 and for the VVER-1000 (RCR, Russian and Hungarian partners)
- A4.1 Processing, analysis and selection of the experimental data for the adjustment (RCR, Russian and Hungarian partners)
- A4.2 Comparison of eigenfrequencies and mode shapes from the measurement with those obtained by the numerical vibration models (ref. A1) (RCR)
- A4.3 Updating the finite-element-model parameters to get an agreement between measurement and calculation (ref. A1) (RCR)

- A5 Investigation of the influence of mechanical failures on the vibration behaviour based on the adjusted finite-element-models. (VVER-440 and VVER-1000) (RCR)
- A5.1 Table of mechanical damages to be analyzed (RCR, Russian and Hungarian partners)
- A5.2 Variation of finite-element-model parameters according to the various mechanical failures (RCR)
- A5.3 Calculation of eigenfrequencies, mode shapes and spectral responses with the models of the damaged structure (RCR)
- A5.4 Evaluation of the early detectability of certain mechanical failures from the vibration signals during operation (RCR)
- A5.5 Recommendations for on-line vibration monitoring (limits for frequency shifts, amplitude increase etc.) (RCR, Russian and Hungarian partners)

Workshop on Vibration Modelling of VVER Type Reactors

December 13 - 16 1994

Programme

Tuesday, 13-Dec

- 09.00 Prof. F.-P. Weiß
Welcome address, organization
Presentation of the Institute for Safety Research
- 10.00 Dr. E. Altstadt
Modelling of primary circuit components of the VVER-440 type reactor using
the finite-element-method
- 12.00 Lunch
- 13.00 Dr. G. Pór, Dr. I. Józsa
Calculation of the modes of the main isolating valves of the Paks NPP with
finite elements and comparison with experimental results obtained during the
maintenance period
- 14.30 R. Weiß
Experimental modal analysis at a VVER-440 coolant loop of NPP Greifswald
- 15.30 Dr. V. Bulavin, Dr. A. Usanov
The experience of vibro condition determination of the reactor plants
VVER-440 and VVER-1000 (Russian language with translation)

Wednesday, 14-Dec

- 09.00 Dr. G. Pór, Dr. I. Józsa
Some results of noise measurements in Paks NPP and in Kalinin NPP
- 10.00 Dr. G. Grunwald, J. Zoller
Theoretical and experimental investigation of fluid-structure-interaction in the
downcomer
- 11.00 Dr. F. Hollstein
Nodal model for the calculation of neutron noise due to stochastic control ele-
ment vibrations

12.30 Lunch

13.15 Dr. G. Grunwald, M. Scheffler
Modelling of the excitation of RPV and internals by the flowing coolant

14.00 Prof. F.-P. Weiß
Introduction of the German-Russian-Hungarian project "Investigation of Mechanical Accident Scenarios at VVER Type Reactors Using the Finite-Element-Method for the Vibration Modelling"

15.00 Discussion of the project

Topics:

- * which individual VVERs are available for vibration experiments
- * which individual VVERs will be chosen for measurements during operation
- expected time periods for measurements and experiments
- * Draft of a measurement program for VVER-440 for measurements during operation (measurement positions, measurement signals, data acquisition, sampling rates, filters etc.)
- Technical preparation of the VVER-440 measurements
- * Draft of a measurement program for VVER-1000 for measurements during operation (measurement positions, measurement signals, data acquisition, sampling rates, filters etc.)
- * Technical preparation of the measurements
- * Survey of required hardware, specification of necessary investments
- * data processing

Thursday, 15-Dec

09.00 Discussion of the project (continuation)

Topics:

- * Draft of a measurement program for VVER-1000 vibration experiments (measurement positions, measurement signals, data acquisition, sampling rates, filters etc.)
- * Determination of excitation positions, excitation mechanisms and excitation signals
- * Technical preparation of the excitation
- * Technical preparation of incore signals
- * Survey of required hardware, specification of necessary investments
- * data processing
- * specification of construction drawings needed for finite-element-modelling
- * transfer of the ANSYS-code

Protocol of the Work Meeting "Vibration Modelling of VVER Type Recators"

held at the Research Center Rossendorf (RCR), 01.-03.November 1995

Participants:

DIAPROM: Dr. D. Gutzev, Dr. V Bulavin, Dr. A. Usanov, Dr. V. Dodonov,
Dr. S. Perov, Dr. V. Pavelko

RCR: Prof. F.-P. Weiß, Dr. E. Altstadt, Dr. G. Grunwald, J. Zoller, S. Kliem, M.
Beyer, Dr. F. Hollstein

1. The meeting was held in the frame of the cooperation agreement for the project no. 1500999 sponsored by the BMBF.
2. In addition to the first interim report DIAPROM presented the current state of work according to the scientific work programme. RCR confirmed the first milestone of the work programme to be fulfilled.
3. With respect to the following steps of the work programme (point A3: vibration experiments at a VVER-1000 during commissioning), DIAPROM explained that such an experiment probably cannot be performed within the next two years. There is no VVER-1000 to be put into operation in Russia during that period. A possible alternative is the cooperation with the Ukrainian utilities of NPP Khmelnitzkij but for that an additional financial support (for example from the EU) would be necessary.
4. Due to the situation as stated in point 3 of this protocol DIAPROM and RCR agreed to examine whether the existing basis measurements at VVER-1000s are sufficient to adjust the finite-element-model.
5. The finite-element-model which is to be developed for the VVER-1000 should have an analogous structure like the existing model of the VVER-440. Especially it is recommended to assemble the FE-model from 1D-pipe or beam elements. Calculations with shell elements are only necessary to determine the parameters of the beam elements of the global model. Fracture mechanical investigations of the CB and for of the RPV based on shell or volume elements are not envisaged within the frame of this project.

6. The next interim report to be supplied in January 1996 should give amongst others information on the following issues:
- A description of existing measurements from experiments during commissioning of VVER-1000s (which NPP, measurement locations, frequency range, experimental conditions etc.). An evaluation of whether or not the concerned measurements can be used to update the FE-model should be given.
 - A description of the mechanical damages and scenarios to be investigated with the FE-model
 - More detailed initial mass parameters for the MCP (motor mass, shaft mass, center of gravity) and for the upper block.
7. DIAPROM and RCR agreed to proceed the cooperation in the field of vibration modelling after the successful conclusion of this project in the end of 1996. In that context RCR hints at the fact, that the continuation of its engagement in FE-modelling of VVER-1000 reactors in the framework of BMBF project funding sensitively depends on the accomplishment of modal analysis experiments at an original reactor during refueling or commissioning.
8. With respect to the delivery of the hardware according to the cooperation agreement the partners agreed on the following procedure at the request of DIAPROM: The personal computer including printer and monitor (see attachment 3, Pos. 3 and 4 of the cooperation agreement) is handed over to DIAPROM during this meeting. DIAPROM is exclusively responsible for transport according to the customs regulations.

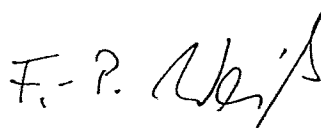
DIAPROM hereby confirms the receipt of the PENTIUM-PC including monitor and color desk jet printer.

The remaining equipment (positions 1 and 2 of attachment 3 of the cooperation agreement) will be sent directly to Moscow by the deliverer.

Rosendorf, 03.11.1995



Dr. D. Gutzev
Director
DIAPROM



Prof. Dr. F.-P. Weiß
Director of the Institute
for Safety Research of RCR

Protocol of the Work Meeting "Vibration Modelling of VVER Type Reactors"

held at the Research Center Rossendorf (RCR), 05.-07.November 1996

Participants:

DIAPROM: Dr. D. Gutzev, Dr. V. Hayretdinov, Dr. A. Usanov,
Dr. V. Dodonov, Dr. S. Perov, Dr. V. Pavelko

RCR: Prof. F.-P. Weiß, Dr. E. Altstadt, S. Kliem, Dr. U. Rohde,
R. Weiß, Dr. M. Werner

1. The meeting was held in the frame of the cooperation agreement for the project no. 1500999 sponsored by the BMBF.
2. The second and third interim reports were presented in detail by the Russian representatives. These reports contain an extensive overview about experimental results which were obtained at VVER-1000 reactors during commissioning and during operation. Both sides agreed that the available experimental data are sufficient for the adjustment of the finite element model to be developed. Thus the work plan of the project will probably successfully be fulfilled until December 1996.
3. The RCR representatives reported on their activities concerning
 - * vibration modelling of BWRs and
 - * consideration of prestressed thermal shock scenarios (during LOCA and transients) using detailed finite element models of LWR structures and inputs from thermalhydraulic calculations

In that context the RCR engagement in the ATHLET verification for VVERs has briefly been presented. The delegates of OKB Gidropress will check the possibility to make available the results of VVER thermalhydraulics tests for the ATHLET verification.

4. The Russian side declared its interest to develop a reliable method for the on-line monitoring of the moderator temperature coefficient (MTC) from temperature fluctuations and neutron noise. This method would offer a very comfortable approach to a highly safety relevant reactor parameter and particularly is an appropriate means to prevent unintentional boron dilution. The Problem is that 3-dimensional reactor simulations are needed

to assess the capability of the method, specifically to quantify the dependence on local effects and coolant mixing.

RCR presented the capabilities of the 3D neutron kinetics code DYN3D for VVERs and proposed to synthesize signals of neutron noise and temperature fluctuations that can be used for the development and testing of the MTC monitoring procedure.

Both sides agree that this idea should further be pursued and that funding should be found to start a common complementary initiative.

5. It was agreed that Dr. Perov will stay for two months at RCR as a guest scientist. During the guest stay he will elaborate a first version of a global vibration model of the VVER-1000 primary circuit based on the finite element code ANSYS (working plan point A1.3, A1.4).
6. In order to make the developed VVER-1000 and VVER-440 vibration model available to the Russian partners, RCR will check the possibility to place a license for a full ANSYS version to DIAPROM's disposal.
7. DIAPROM and RCR agreed to try to proceed the cooperation in the field of vibration modelling after the successful conclusion of this project in the end of 1996 in the frame of a BMBF sponsored project. This envisaged project should be part of the Scientific-Technological Collaboration Program between Russia and Germany. The main topics of the work program will be:
 - * Finishing of the global vibration model for the VVER-1000
 - * Adjustment of the vibration model basing on the experimental data made available through the current project and by data from an experiment which is to be performed at the Balakovo NPP in 1997
 - * Elaboration of detailed local FE-models of reactor internals which are endangered by forced vibrations (e. g. fuel elements)
 - * Integration of fluid-structure interaction into the FE-model
 - * Modelling of the excitation forces during normal plant operation
 - * Simulation of mechanical damages based on the global vibration model
 - * Transfer and validation of the vibration model for the VVER-440 developed by the RCR

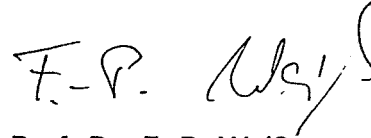
A project description will be elaborated by RCR as soon as possible for application at BMBF. The duration of such a project should be two years in minimum.

8. RCR will check the possibility to extend the cooperation in the framework of BMBF TRANSFORM projects.

Rosendorf, 07.11.1996



Dr. D. Gutzev
General Director
DIAPROM



Prof. Dr. F.-P. Weiß
Director of the Institute
for Safety Research of RCR

Berichtszeitraum/Period 01.01.95 -31.12.95	Klassifikation/Classification	Kennzeichen/Project Number 1500999
Vorhaben/Project Title Entwicklung von theoretischen Schwingungsmodellen für VVER-Reaktoren auf der Grundlage der Finite-Elemente-Methode und Justierung dieser Modelle mit Schwingungsmessungen von Originalanlagen		Land/Country
Development of theoretical vibration models for VVER type reactors based on the finite element method and adjustment of these models by vibrations measurements at original nuclear power plants		Fördernde Institution/Sponsor BMBF
		Auftragnehmer/Zuwendgempf./ Contractor Forschungszentrum Rossendorf e. V. PF 510119 01314 DRESDEN
Arbeitsbeginn/Initiated 01.11.1994	Arbeitsende/Completed 31.10.1996	Leiter des Vorhabens/Project Leader Prof. Dr. F.-P. Weiß
Stand der Arbeiten/Status continuing	Berichtsdatum/Last Updating Februar 1996	Bewilligte Mittel/Funds

1. General Aim

The project aims to support 6 Russian scientists from three different institutions, who otherwise might become unemployed. Their work on plant diagnostics/early failure detection significantly contributes to the increase of the safety of VVER reactors. The operational experience of these reactors has revealed that the reactor pressure vessel internals can be damaged by flow induced mechanical vibrations. Therefore, vibration monitoring systems had been installed at many VVERs.

Up to now, vibration monitoring has suffered from the lack of a theoretical model, which permits the physical interpretation of the measurements. In the framework of a former project (registr.-No. 1500916) which was funded by BMFT, the Research Center Rossendorf developed a theoretical finite elements (FE) based vibration model for VVER-440 reactors. This model and probably an analogous one for VVER-1000 reactors require adjustment and verification with data from vibration measurements performed at the original facilities in Eastern Europe.

The accomplishment and processing of vibration measurements during commissioning and normal operating conditions by the Russian partners are content of this project.

It is intended finally to transfer the adjusted and validated vibration models to the Eastern European partners for application in Russia, in order to make available the scientific base for a sensitive on-line vibration monitoring. This could improve the operational safety of VVERs.

2. Particular Objectives

- 2.1 - Preparation of VVER-1000 modeling with finite elements to calculate the mechanical vibration with consideration of fluid-structure interaction
- 2.2 - Accomplishment of operational measurements at VVER-440 and VVER-1000 reactors; processing of the measurements
- 2.3 - Accomplishment of vibration investigations at a VVER-1000 during commissioning; processing of the measurements
- 2.4 - Further adjustment of the FE model for VVER-440s; preparation of the adjustment of the VVER-1000 model using the experimental data.

3. Research Programme

- 3.1 Elaboration of a structural model for the VVER-1000 primary circuit using the FE code ANSYS®. This step of work is mainly based on a review and evaluation of the construction drawings. Calculation of the initial parameters of the FE model based on masses, momenta of inertia and stiffnesses as they can be estimated from the construction specification. Generation of an ANSYS® input file for all primary circuit main components: RPV, core barrel, core, main coolant pump, coolant loops, steam generators.
- 3.2 Performing of operational measurements at Russian and Ukrainian VVERs (neutron noise, pressure fluctuations, accelerations, displacements). The volume of the measurements depends on the restrictions imposed by the concerned utilities.
Schedule of a measuring programme for VVER-1000 and VVER-440 reactors.
Preparation and accomplishment of measurements at selected VVERs.
- 3.3 Realization of base-line vibration measurements at one selected VVER-1000 either during commissioning or exceptionally during refueling. Selection of appropriate types, positions, and signals for vibration excitation. Selection of measuring positions and types of measuring signals (including signals from RPV and internals). Technical preparation and accomplishment of the experiment.
- 3.4 Adjustment of the VVER-440 FE-model and qualification of the measuring data from VVER-1000s for the adjustment of the model, which might later be available.
Processing, analysis and selection of the experimental data that are useful for adjustment purposes.
Comparison of experimentally and numerically obtained eigenfrequencies and eigenmodes of the VVER-440.
Review of available data (earlier measurements); check of their relevance and quality. Correction of the VVER-440 FE parameters to achieve agreement between measurement and calculation.
- 3.5 Preparative work for damage simulations and sensitivity studies. Elaboration of a catalogue of relevant mechanical damages to be investigated. Setting-up of recommendations for on-line vibration monitoring.

4. Experimental Facilities, Computer Codes

- FE-code ANSYS® (Rev. 5.2) running on a workstation HP 9000/735
- Computer code NLSYS (Rev. 4.0; developed by FZR) running on a workstation HP 9000/720, needed to implement fluid-structure-interaction and to solve unsymmetric eigenvalue problems
- MACET (FE-code of Baumann-Institute Moscow)
- 32 measuring channels for accelerations (accelerometers, charge amplifiers, amplifiers, and power supply)
- PC Pentium-90, 17" monitor, 16 MB RAM, 850 MB HDD, ink jet printer

5. Progress to Date

- rel. 3.1
- Survey of the most important construction drawings and specifications (report)
 - Calculation of masses and momenta of inertia for VVER-1000 components using drawings and specifications

- rel. 3.2 - Analysis of available measurements from VVER-440s (Kola 1/2, Novovoronezh) obtained with SÜS and unit specific diagnostic instrumentation (excore ionization chambers, SPNDs, pressure sensors)
- Analysis of available measurements from a VVER-1000 (Kalinin) obtained with unit specific diagnostic instrumentation
- rel. 3.3 - No work was done relating to this item of the work programme. During the meeting in November 1995 the Russian partners declared, that the items A2 and A3 of the work programme cannot be fulfilled as scheduled. The FZR participants emphasized, that the realization of vibration measurements is an essential of the project. Consequently the partners agreed (see attached protocoll), that the 2nd interim report (due date 15.01.1996) should provide a detailed list of all measurements earlier performed at VVER-1000s during operation and/or commissioning and should give an assessment of the experimental data regarding their quality and relevance for model adjustment (3.4).
- rel. 3.4 - Consideration of the experimental data from VVER-440s in the theoretical FE model of FZR

6. Results

- rel. 3.1 - Construction description, main measures, masses, and mechanical parameters of RPV, core barrel, steam generator, main coolant pump, and main coolant loop are available now
- rel. 3.2 - Identification of the driving forces of peaks in the neutron noise frequency spectra (pump rotation frequencies and their subharmonics, fluid resonances)
- Identification of the driving forces of peaks in the frequency spectra of SÜS signals and of signals from unit specific instrumentation of VVER-440s; assignment to fluid resonances and to components vibration modes (RPV and core barrel pendulum motions, pendulum motion of the main coolant pump).

7. Next Steps

The project will be continued.

8. Relations with other Projects

Project: "Analytical modelling of mechanical vibrations of VVER-440 primary circuit components using finite elements", Reg.-No. 1500 916, finished.

9. Literature

- /1/ Anikin, G.G., V. V. Bulavin, D. F. Gutsev, V. A. Dodonov, V. I. Pavelko, A. I. Usanov
Elaboration of Numerical Vibration Models of the VVER Type Reactors. 1st interim report according to the collaboration agreement of this project.

10. Reports available with

GRS-Forschungsbetreuung, Köln

01.01.96 - 30.06.96	01.1.4	1500999
Entwicklung von theoretischen Schwingungsmodellen für WWER-Reaktoren auf der Grundlage der Finite-Elemente-Methode und Justierung dieser Modelle mit Schwingungsmessungen von Originalanlagen		— BMBF
Development of theoretical vibration models for VVER type reactors based on the finite element method and adjustment of these models by vibrations measurements at original nuclear power plants		Forschungszentrum Rossendorf e. V. (FZR)
		01314 Dresden
01.11.1994	31.10.1996	Prof. Dr. F.-P. Weiß
wird fortgesetzt	September 1996	DM 163.176,—

1. Übergeordnete Zielsetzung

Dieses Vorhaben zielt auf die Unterstützung von 6 russischen Wissenschaftlern aus drei unterschiedlichen Institutionen ab, deren Arbeitsplätze bedroht sind. Ihre Arbeiten zur Anlagen-diagnostik / Schadensfrüherkennung sind ein wichtiger Beitrag zur Erhöhung der Sicherheit von WWER-Reaktoren. Die Betriebserfahrung dieser Reaktoren zeigt, daß die Einbauten der Reaktordruckbehälter durch strömungsinduzierte mechanische Schwingungen beschädigt werden können. Deshalb wurden an vielen WWER-Anlagen Monitore zur on-line Schwingungsüberwachung installiert. Ein entscheidender Mangel der Schwingungsüberwachungssysteme ist zum gegenwärtigen Zeitpunkt noch das Fehlen eines theoretischen Schwingungsmodelles, welches die physikalische Interpretation der Messungen gestattet. Im Rahmen eines vom BMFT geförderten Vorhabens (Förderkennzeichen: 1500916) entwickelte das Forschungszentrum Rossendorf ein theoretisches, auf finiten Elementen (FE) basierendes Modell für den WWER-440. Dieses Modell und u. U. auch ein analoges für den WWER-1000 bedürfen allerdings der Justierung und der Verifikation mit Daten aus Schwingungsmessungen an den Originalanlagen in Osteuropa. Die Durchführung und Auswertung von Schwingungsmessungen bei Inbetriebnahmen und normalem Anlagenbetrieb durch die russischen Partner ist Inhalt des Vorhabens. Es ist ein generelles Ziel, die justierten und verifizierten Schwingungsmodelle zur Nutzung an die osteuropäischen Partner zu übergeben, um damit die wissenschaftliche Grundlage für eine empfindliche on-line Schwingungsüberwachung zur Verbesserung der Anlagensicherheit von WWER-Reaktoren bereitzustellen.

2. Einzelzielsetzung

- 2.1 - Vorbereitung der Modellierung des WWER-1000 mit finiten Elementen zur Berechnung des mechanischen Schwingungsverhaltens unter Einbeziehung der Fluid-Struktur-Wechselwirkung
- 2.2 - Durchführung von Betriebsmessungen an WWER-440 und WWER-1000 und Auswertung dieser Messungen
- 2.3 - Durchführung experimenteller Schwingungsuntersuchungen an einem WWER-1000 während der Inbetriebnahme und Auswertung dieses Experimentes
- 2.4 - Weitere Justierung des FE-Modells für den WWER-440 und Vorbereitung der Justierung des FE-Modells für den WWER-1000 anhand der experimentellen Daten.

3. Arbeitsprogramm

- 3.1 Erarbeitung eines Strukturmodelles für den Primärkreislauf des WWER-1000 unter Verwendung des FE-Codes ANSYS® basierend auf der Sichtung und Bewertung der Konstruktionsunterlagen. Berechnung der anfänglichen Parameter für das FE-Modell auf Grundlage der sich aus den Konstruktionsunterlagen ergebenden Massen, Trägheitsmomente, Steifigkeiten. Generierung der Eingabefiles für den FE-Code für alle Hauptkomponenten des Primärkreislaufes: RDB, Kernbehälter, Kern, Hauptkühlmittelleitungen, Hauptumwälzpumpen, Dampferzeuger
- 3.2 Realisierung von Betriebsmessungen an russischen und ukrainischen WWERs (Neutronenrauschen, Druckschwankungen, Beschleunigungen und Verschiebungen) in Abhängigkeit davon, welche Möglichkeiten von den jeweiligen Betreibern eingeräumt werden. Erstellung von Meßprogrammen für WWER-1000 und WWER-440. Vorbereitung und Durchführung der Messungen an den ausgewählten WWER-Anlagen.
- 3.3 Realisierung von Schwingungsexperimenten an einem ausgewählten WWER-1000 während der Inbetriebnahme oder im Ausnahmefall während der Umladung. Auswahl geeigneter Typen, Positionen und Signale für die Erregung. Auswahl von Meßpositionen und Meßsignalen (einschließlich von Signalen des RDB und seiner Einbauten). Technische Vorbereitung und Durchführung des Experimentes.
- 3.4 Justierung des Modells für den WWER-440 und Aufbereitung der Meßdaten vom WWER-1000 für eine spätere Justierung nach Vorliegen des Modells. Verarbeitung, Analyse und Auswahl der experimentellen Daten für die Justierung. Vergleich der Eigenfrequenzen und Schwingungsformen aus der Messung mit denen der numerischen Rechnung zum WWER-440. Sichtung von vorhandenem Datenmaterial (ältere Messungen) und Prüfung der Verwendbarkeit. Korrektur der Parameter des FE-Modells des WWER-440, um Übereinstimmung zwischen Experiment und Berechnung zu erhalten.
- 3.5 Vorbereitende Arbeiten zur Durchführung der Schadenssimulation und der Sensitivitätsstudien. Erstellung eines Kataloges der zu untersuchenden mechanischen Schäden. Erarbeitung von ersten Empfehlungen für die on-line Schwingungsüberwachung.

4. Versuchseinrichtungen, Rechenprogramme

- FE-Programm ANSYS Rev. 5.2) auf einer Workstation HP 9000/735
- Programm NLSYS (Rev 4.0, FZR-Entwicklung) auf der Workstation HP 9000/720 zur Einbindung der FSE und zur Lösung unsymmetrischer Eigenwertprobleme
- MACET (FE-Code am Baumann-Institut Moskau)
- Meßketten für Beschleunigungsmessungen (Beschleunigungssensoren, Ladungsverstärker sowie Stromversorgungs- und Verstärkereinheiten, insgesamt 32 Kanäle)
- PC Pentium-90 mit 17" Monitor, 16MB RAM, 850 MB HDD und Farbtintenstrahldrucker

5. Durchgeführte Arbeiten

- Zu 3.1 - Zusammenstellung der wichtigsten Konstruktionsunterlagen in Berichtsform
- Berechnung von Massen und Trägheitsmomenten der WWER-1000 Komponenten aus den Konstruktionsunterlagen

- Zu 3.2 - Auswertung von vorhandenen Messungen an WWER-440 (Kola 1/2, Novovoronesh) mit SÜS-Instrumentierung und blockspezifischer Diagnoseinstrumentierung (excore Ionisationskammern, incore Neutronendetektoren, Drucksensoren)
- Auswertung von vorhandenen Messungen an WWER-1000 (Kalinin 1, Kosloduj 6 sowie Novovoronesh 5) mit blockspezifischer Diagnoseinstrumentierung
- Zu 3.3 - Es wurden keine Schwingungsexperimente an einem WWER-1000 durchgeführt. Auf dem im November 1995 in Rossendorf durchgeführten Arbeitstreffen wurde von den russischen Partnern dargelegt, daß die Arbeitsplanpunkte A2 und A3 nicht wie vorgesehen realisiert werden können. Vom FZR wurde darauf hingewiesen, daß die Realisierung von Schwingungsmessungen ein wesentlicher Punkt für die Zielstellung des Vorhabens ist. Gemäß der im Protokoll zum Arbeitstreffen getroffenen Vereinbarung liegt statt dessen ein Zwischenbericht vor, der eine detaillierte Auflistung der bereits durchgeführten verfügbaren Betriebs- und Inbetriebnahmemessungen an WWER-1000 enthält sowie Experimente an maßstäblichen Versuchsmodellen in der Designphase /1/. Dieser Bericht umfaßt die Untersuchung der Fluidresonanzen im Primärkreislauf, das Schwingungsverhalten der Brennelemente sowie die Untersuchung von Schalenschwingungen des Kernbehälters (KB).
- Zu 3.4 - Einarbeitung der Meßergebnisse von den WWER-440 in das FE-Model des FZR
- Zu 3.5 - Erarbeitung einer Aufstellung von möglichen mechanischen Schädigungen an RDB-internen Komponenten

6. Erzielte Ergebnisse

- Zu 3.1 - Konstruktive Beschreibung, Hauptabmessungen und Massenparameter sowie die Materialparameter von RDB, Kernbehälter, Dampferzeuger, Hauptkühlmittelpumpe und Hauptumwälzleitung liegen vor.
- Zu 3.2 - Lage der Peaks in den Spektren der SÜS-Signale und der Signale der Diagnoseinstrumentierung beim WWER-440 mit Zuordnung zu Fluidresonanzen und teilweise zu Komponentenschwingungen (RDB-Pendelbewegung, Kernbehälterpendelbewegung, Pendelbewegungen der Kühlmittelpumpe)
- Lage der Peaks in den Spektren der Neutronensignale des WWER-1000 mit Zuordnung zu Subharmonischen der Pumpendrehzahl und zu Subharmonischen von Fluidresonanzen
 - Frequenzen und Moden der stehenden akustischen Wellen im Primärkreis des WWER-1000
- Zu 3.3 - Eigenfrequenzen und Schwingungsformen eines Kernbehältermodells (Maßstab 1:5) bei verschiedenen Lagerungsvarianten
- Eigenfrequenzen der Biegeschwingungen von Brennelementen (aus 1:1 Versuchsmodell)
- Zu 3.5 - Festlegung von 7 zu untersuchenden möglichen Schäden: Federrohrsegmente, Dichtungsring zwischen RDB und KB, obere KB-Verstiftung, KB-Führungskeile, Verbindung oberes Kerngitter - KB, Federelemente der Brennelemente, Stützrohre

der Brennelemente (unteres Kerngitter)

7. Geplante Weiterarbeit

Die Arbeiten werden fortgesetzt.

8. Beziehung zu anderen Vorhaben

Abgeschlossenes Vorhaben Nr. 1500916: "Analytische Modellierung mechanischer Schwingungen von Primärkreis-Komponenten des Druckwasserreaktors WWER-440 mit finiten Elementen"

9. Literatur

- /1/ D.F. Gutsev et al.: Vibration Modelling of VVER Type Reactors - The analysis of the design characteristics and experimental data for adjustment of the VVER-1000 model. Zweiter Zwischenbericht (Nr. 320-O.211-004) gemäß Kooperationsvereinbarung zu diesem Vorhaben.

10. Zugänglichkeit der Berichte

GRS-Forschungsbetreuung, Köln.